National Research Council Canada

Conseil national de recherches Canada

NRC·CNRC

Canadian Journal of Fisheries and Aquatic Sciences

Journal canadien des sciences halieutiques et aquatiques

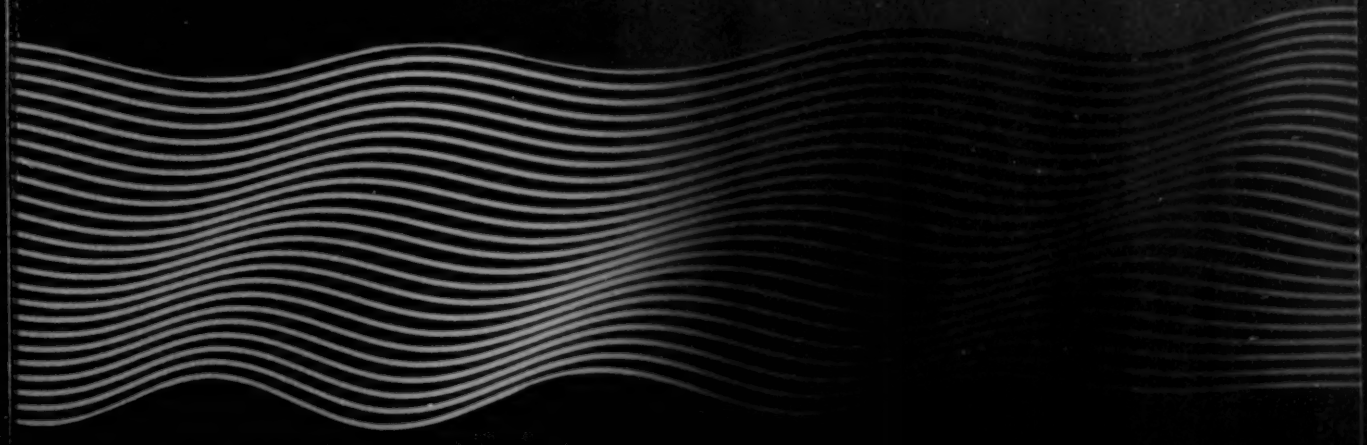

http://www.nrc.ca/cisti/journals

ISSN 0706-652X / CJFSDX 57(6) 1113–1319 (2000)

The *Canadian Journal of Fisheries and Aquatic Sciences*, previously published as *Contributions to Canadian Biology* 1901–1925, *Contributions to Canadian Biology and Fisheries* 1926–1934, *Journal of the Biological Board of Canada* 1934–1937, and *Journal of the Fisheries Research Board of Canada* 1938–1979, is issued monthly to form annual volumes of 12 numbers plus supplements.

Editorial policy: The Journal publishes original research articles, perspectives (syntheses, critiques, re-evaluations), discussions (comment and reply), and rapid communications. Manuscripts may concern cells, organisms, populations, communities, ecosystems, or processes that affect aquatic systems. They may cover a range of disciplines including biology and ecology of marine and freshwater organisms, limnology, oceanography, physiology, toxicology, genetics, economics, disease, and management. Preference will be given to manuscripts that emphasize understanding of observed phenomena and interpretation of experimental results. The Journal encourages papers that lead from clearly stated purpose or rationale and from testable hypotheses, concepts, or questions to identifiable conclusions or syntheses. Such papers may amplify, modify, question, or redirect accumulated knowledge embodied in contemporary perceptions of a particular state of aquatic sciences. The Journal discourages papers that are essentially descriptive, except in emerging disciplines; have only site-specific or local applications (a certain year, place, taxon, chemical compound, etc.); only confirm previously established principles; or apply standard techniques without breaking new methodological ground.

Manuscripts for publication should be submitted to the Editors, Canadian Journal of Fisheries and Aquatic Sciences, Department of Zoology, University of Guelph, Guelph, ON N1G 2W1, Canada (519-824-4120 ext. 2646; fax: 519-767-9798; e-mail: cjfas@uoguelph.ca).

Submissions in either English or French are acceptable. The information must be original, that is, not copyrighted, published, or submitted elsewhere except in abstract form or unless by written consent of the Editor. NRC accepts no responsibility for statements or opinions expressed by a contributor. Acceptance of an advertisement, announcement, or other material does not imply endorsement by either the *Journal*'s Editors or NRC. The use of proprietary names does not imply endorsement of the product or company.

Correspondence concerning accepted manuscripts and corrected proofs should be sent to NRC Research Press, National Research Council of Canada, Ottawa, ON K1A 0R6, Canada.

Instructions to Authors are published once a year in the first issue of each volume. Copies are available from NRC Research Press or from our Web site. The **Publication Policy** of NRC Research Press is also available at our Web site:
http://www.nrc.ca/cisti/journals/rj.html

Microfilm: Issues from 1934 through the current volume can be purchased on 16- or 35-mm microfilm. Photocopies of individual articles or issues can be purchased from University Microfilms International, 330 North Zeeb Road, Ann Arbor, MI 48106, U.S.A.

U.S. periodical postage paid at Champlain, N.Y., and at additional mailing offices. Attention U.S. POSTMASTER: Send address changes to **Canadian Journal of Fisheries and Aquatic Sciences**, c/o USACAN Media Distribution Center, P.O. Box 2888, Plattsburg, NY 12901, U.S.A.

Publié sans interruption depuis 1901, le *Journal canadien des sciences halieutiques et aquatiques* a paru sous plusieurs titres : *Contributions to Canadian Biology* 1901–1925, *Contributions to Canadian Biology and Fisheries* 1926–1934, *Journal of the Biological Board of Canada* 1934–1937, et *Journal of the Fisheries Research Board of Canada* 1938–1979. Le *Journal* paraît tous les mois, formant ainsi un volume de 12 numéros, et offre en plus jusqu'à deux suppléments par année.

Politique éditoriale : On publie, dans le Journal, des articles rendant compte de recherche originale, des perspectives (synthèses, critiques et réévaluations), des discussions (commentaires et réponses) et des communications rapides. Les documents peuvent porter sur les cellules, organismes, populations, communautés, écosystèmes ou processus qui affectent les systèmes aquatiques. Ils peuvent relever de divers domaines y compris la biologie et l'écologie des organismes marins et d'eau douce, la limnologie, l'océanographie, la physiologie, la toxicologie, la génétique, l'économie, la pathologie et la gestion. On accorde la préséance aux articles qui contribuent à la compréhension de phénomènes observés et à l'interprétation de résultats expérimentaux. On invite les auteurs à soumettre des articles ayant des objectifs précis ou relevant d'hypothèses, de concepts ou de questions vérifiables et se terminant par de solides conclusions ou d'utiles synthèses. Ces articles enrichissent, changent, mettent en question ou réorientent les connaissances acquises sur divers aspects des sciences aquatiques. On décourage toutefois la soumission d'articles simplement descriptifs (à moins qu'il ne s'agisse de nouvelles disciplines), d'application très limitée (applicables à une seule année, une seule région ou un seul taxon, portant sur un unique composé chimique, etc.); d'articles qui ne font que reprendre les principes énoncés dans des articles précédents; et d'articles rendant compte de l'application de normes sans gain de méthodologie.

Les auteurs voudront adresser leurs **manuscrits** aux directeurs scientifiques, Journal canadien des sciences halieutiques et aquatiques, Department of Zoology, University of Guelph, Guelph, ON N1G 2W1, Canada (519-824-4120 poste 2646; télécopieur : 519-767-9798; adresse électronique : cjfas@uoguelph.ca).

Les contributions peuvent être en anglais ou en français. Elles doivent être originales, c.-à.-d. qu'elles ne doivent pas avoir fait l'objet d'un copyright, avoir été publiées ou soumises ailleurs, sauf sous forme abrégée ou avec le consentement du rédacteur. Le CNRC ne se tient en aucune façon responsable des opinions exprimées par un collaborateur ou des déclarations qui pourrait faire ce dernier. La publication d'annonces publicitaires, d'avis et autres n'implique pas l'endossement de leur contenu par les directeurs du *Journal* ou du CNRC. L'utilisation des noms de marques de commerce ne signifie aucunement une sanction du produit en question ou de la compagnie qui le fabrique.

La correspondance ayant trait aux manuscrits acceptés et les **épreuves corrigés** doivent être envoyées aux Presses scientifiques du CNRC, Conseil national de recherches du Canada, Ottawa, ON K1A 0R6, Canada.

Recommandations aux auteurs sont publiés une fois par année dans le premier numéro de chaque volume. Des copies, ainsi que la **Politique de publication**, sont disponibles auprès des Presses scientifiques du CNRC ou au site Web :
http://www.nrc.ca/cisti/journals/rj.html

Microfilms : On peut acheter sur microfilms de 16 ou 35 mm tous les numéros depuis 1934. Des photocopies d'articles ou de numéros individuels sont aussi en vente auprès de University Microfilms International, 330 North Zeeb Road, Ann Arbor, MI 48106, É.-U.

This journal is indexed or abstracted in / Ce journal est signalé ou résumé dans
ABSEARCH, Aquatic Sciences and Fisheries Abstracts, Biological Abstracts, Biological & Agricultural Index, CAB Abstracts, Chemical Abstracts, Current Contents, Elsevier BIOBASE, Environmental Abstracts, Environmental Periodicals Bibliography, GEOBASE, GeoRef, Life Sciences Collection, Meteorological and Geoastrophysical Abstracts, Oceanic Abstracts, PASCAL Database, and Science Citation Index.

Volume 57, Number 6, June 2000

Canadian Journal of Fisheries and Aquatic Sciences

Published by the National Research Council of Canada

Volume 57, numéro 6, juin 2000

Journal canadien des sciences halieutiques et aquatiques

Publié par le Conseil national de recherches du Canada

Editors / directeurs scientifiques John C. Roff and Moira M. Ferguson

Assistant to the Editors / adjointe aux directeurs scientifiques **Holly Foster**

Associate Editors / directeurs scientifique associés

D. Boisclair, *Université de Montréal*
U. Borgmann, *Environment Canada, Burlington*
S.E. Campana, *DFO/MPO, Dartmouth*
D.G. Dixon, *University of Waterloo*
A.E. Dizon, *National Marine Fisheries Service, La Jolla, Calif.*
J.J. Dodson, *Université Laval*
J.A. Downing, *Iowa State University*
K.T. Frank, *DFO/MPO, Dartmouth*
D.F. Houlihan, *University of Aberdeen, Aberdeen, Scotland*
F.A. Huntingford, *University of Glasgow*
J.A. Hutchings, *Dalhousie University*
G.S. Jamieson, *DFO/MPO, Nanaimo*
B. Jonsson, *Norwegian Institute for Nature Research, Oslo, Norway*
L. Legendre, *Université Laval*
D.M. Mason, *NOAA-Great Lakes Environmental Research Laboratory, Ann Arbor, Mich.*
A. Mazumder, *University of Victoria*
D.L. Parrish, *Vermont Cooperative Fish and Wildlife Research Unit (USGS/BRD), University of Vermont*
P. Pepin, *DFO/MPO, St. John's*
R.M. Peterman, *Simon Fraser University*
E.E. Prepas, *University of Alberta*
T.M. Powell, *University of California, Berkeley, Calif.*
T.J. Quinn II, *University of Alaska–Fairbanks, Juneau, Alaska*
T.P. Quinn, *University of Washington*
R.D. Robarts, *Environment Canada, Saskatoon*
B. Sainte-Marie, *DFO/MPO, Mont-Joli*
P.F. Sale, *University of Windsor*
D.W. Schindler, *University of Alberta*
S.J. Smith, *DFO/MPO, Dartmouth*
W.G. Sprules, *University of Toronto*
R.J. Thompson, *Memorial University of Newfoundland*
C.J. Walters, *University of British Columbia*
R.D. Ward, *CSIRO Division of Fisheries, Australia*
C.M. Wood, *McMaster University*
B. de Young, *Memorial University of Newfoundland*

NRC Research Press / Presses scientifiques du CNRC

Editor-in-chief / directeur général **Bruce P. Dancik**

Assistant Editor-in-chief / directeur général adjoint **Iain E.P. Taylor**

Journals Program / Programme des revues

(Fax / télécopieur : 613-952-7656; e-mail / adresse électronique : research.journals@nrc.ca;
URL: http://www.nrc.ca/cisti/journals/)

Director / directrice **Aldyth Holmes**

Business Manager / gestionnaire des affaires **Paul McClymont**

Managing Editor / rédactrice administrative **Cecily M. Pearson (613-993-9099)**

Publication Officer / agente de publication **Jennifer McColl**

Advertising / annonces publicitaires **Judy Heyman (613-993-0151)**

Reprints / tirés à part **Roxanne Landriault (613-990-2254)**

Subscriptions / abonnements **Helen Goulet (613-993-9084)**

© National Research Council of Canada 2000. World rights reserved.
No part of this publication may be reproduced, stored, or transmitted in any form or by any means, without the written permission of the publisher, except as stated below.

The National Research Council of Canada grants **permission*** to individuals to make single copies of articles for personal use. Any person may reproduce short excerpts from articles in the journal for any purpose that respects the moral rights of authors, provided that the source is fully acknowledged. As a courtesy, the consent of authors of such material should be obtained directly from the author.

Authorization to reproduce items for other than personal use, as stated above, is granted by the National Research Council of Canada provided that the copyright fee of $7.00 per copy is paid directly to CANCOPY, One Yonge Street, Suite 1900, Toronto, ON M5E 1E5, Canada.

*The above permission does not extend to other kinds of copying, such as copying for general distribution, for advertising, or promotional purposes, for creating new collective works, or for resale. For such copying, arrangements must be made with the publisher, National Research Council of Canada, Ottawa, ON K1A 0R6, Canada.

© Conseil national de recherches du Canada 2000. Tous droits réservés.
Il est interdit de reproduire, de sauvegarder ou de transmettre quelque partie de la présente publication dans quelque format ou de quelque façon sans le consentement écrit de l'éditeur, à l'exception des conditions suivantes.

Le Conseil national de recherches du Canada accorde aux particuliers le droit de faire des copies individuelles pour leur usage personnel. Toute personne peut reproduire de courts extraits des articles de la Revue pour autant que les droits moraux de l'auteur soient respectés et que la mention de provenance soit clairement indiquée. Il est de convenance de demander le consentement de l'auteur avant de faire mention de son travail.

On obtiendra l'autorisation de reproduire des articles à d'autres fins que l'usage personnel (tel qu'on l'a décrit ci-dessus) auprès du Conseil national de recherches du Canada pour autant que des redevances de droits d'auteurs de 7,00 $/copie soient versées au CANCOPY, 1, rue Yonge, bureau 1900, Toronto, ON M5E 1E5, Canada.

*La permission ci-dessus ne s'applique pas à la reproduction à grande échelle, telle que la reproduction aux fins de distribution générale, publicitaire ou promotionnelle, de compilation de nouveaux ouvrages collectifs ou de revente. Dans de tels cas, il faudra ratifier une entente particulière avec l'éditeur, le Conseil national de recherches du Canada, Ottawa, ON K1A 0R6, Canada.

Subscription information

The *Canadian Journal of Fisheries and Aquatic Sciences* (ISSN 0706-652X) is published monthly by the National Research Council of Canada. 2000 annual subscription rates (second class postage) for Canada are $630CAN institutional and $191CAN personal, for US & foreign $630US institutional and $191US personal. For air mail add $150US to foreign rate. Canadian customers please include 7% GST (business no. 12149 1807 RT 0275). Subscriptions are entered for the calendar year. Remittances should be made payable to the Receiver General for Canada credit NRC. Price for regular single issues: institutional, $80.00; personal, $25.00. Supplements will be priced separately. Special rates apply to members of Canadian scientific and engineering societies if they subscribe through their respective societies.

There are no refunds on cancelled subscriptions once delivery has begun. Claims for missing issues should be made within four months (N. America) or six months (outside N. America) following the date of publication. The publisher expects to supply missing issues only when losses have occurred in transit and when the reserve stock will permit. For change of address and subscription enquiries: Subscription Office, NRC Research Press, National Research Council of Canada, Ottawa, ON K1A 0R6, Canada; tel: 613-993-9084; fax: 613-952-7656; e-mail: research.journals@nrc.ca.

Microform backfiles are available from UMI, P.O. Box 1346, Ann Arbor, MI 48106-1346, U.S.A., and Micromedia Ltd., 20 Victoria St., Toronto, ON M5C 2N8, Canada.

All issues of the *Canadian Journal of Fisheries and Aquatic Sciences* since 1996 are available on the Web. Pricing information can be found at

http://www.nrc.ca/cisti/journals/

Renseignements sur l'abonnement

Journal canadien des sciences halieutiques et aquatiques (ISSN 0706-652X) est une publication mensuelle du Conseil national de recherches du Canada. Le prix de l'abonnement annuel au Canada (courrier de deuxième classe) est de 630 $CAN pour les organismes et de 191 $CAN pour les particuliers. À l'étranger (y compris les É.-U.), le prix de l'abonnement est de 630 $US pour les organismes et de 191 $US pour les particuliers. L'expédition par avion exige des frais de 150 $US en sus du prix d'abonnement à l'étranger. Les clients du Canada doivent ajouter la TPS de 7% (numéro d'entreprise 12149 1807 RT 0275). Les abonnements sont pour l'année civile. Tout paiement doit être adressé au Receveur général du Canada, crédit du CNRC. Le prix par numéro est de 80 $ pour les organismes et de 25 $ pour les particuliers. Le prix des hors-série varie. Les membres des sociétés canadiennes de sciences et de génie bénéficient de taux préférentiels en s'abonnant via leurs sociétés respectives.

Aucun remboursement ne sera accordé ni aucune annulation acceptée une fois que les livraisons auront commencé. Les réclamations de numéros manquants devront être soumises dans les quatre mois (Amérique du Nord) ou dans les six mois (à l'extérieur de l'Amérique du Nord) suivant la date de publication. L'éditeur ne fournira de numéros manquants que si le document a été perdu pendant l'expédition et que si le stock le permet. Adressez tout changement d'adresse ou toute question quant à l'abonnement au : Bureau des abonnements, Presses scientifiques du CNRC, Conseil national de recherches Canada, Ottawa, ON K1A 0R6, Canada; téléphone : 613-993-9084; télécopieur : 613-952-7656; adresse électronique : research.journals@nrc.ca.

On peut obtenir les fichiers rétrospectifs sur **microforme** auprès de UMI, P.O. Box 1346, Ann Arbor, MI 48106-1346, É.-U., et auprès de Micromedia Ltée, 20 rue Victoria, Toronto, ON M5C 2N8, Canada.

À partir de 1996, tous les numéros de *Journal canadien des sciences halieutiques et aquatiques* sont accessibles sur le Web. On trouvera des renseignements sur les tarifs à

http://www.nrc.ca/cisti/journals/rjfr.html

Digestive enzyme and gut surfactant activity of detritivorous gizzard shad (*Dorosoma cepedianum*)

James C. Smoot and Robert H. Findlay

Abstract: Measuring digestive enzyme and surfactant activities tested specialization of gizzard shad (*Dorosoma cepedianum*) digestive physiology to a detritivorous feeding strategy. Digestive enzyme activity was measured in adult and larval gizzard shad using fluorescently labeled artificial substrates. Surfactant activity in gizzard shad was measured by comparing gut juice drop diameters over a range of dilutions. Enzyme activity in the ceca region of adult gizzard shad was high for esterase, β-glucosidase, lipase, and protease. Enzyme activity was lower in posterior intestine sections than in anterior intestine sections, although protease activity remained high for the greatest distance in the intestine. Micelles were detected in adult gizzard shad gut juice, and surfactant activity was greatest in the ceca region. Larval gizzard shad protease activity was similar to that of adult fish, and surfactants were below their critical micelle concentration. Gizzard shad coupled digestive physiology with gut anatomy to obtain nutrients from detritus, and these adaptations may explain elevated growth rates observed in these fish when they are planktivorous.

Résumé : En mesurant l'activité des enzymes digestives et des surfactants, nous avons testé la spécialisation de la physiologie digestive de l'alose à gésier (*Dorosoma cepedianum)* dans le sens d'une stratégie d'alimentation détritivore. Nous avons mesuré l'activité des enzymes digestives chez des adultes et des larves d'alose à gésier en utilisant des substrats artificiels à marquage fluorescent. Pour mesurer l'activité des surfactants, nous avons comparé le diamètre des gouttes de sécrétion intestinale à diverses dilutions. Chez les aloses à gésier adultes, dans la région caecale, l'activité enzymatique était élevée en ce qui concerne l'estérase, la β-glucosidase, la lipase et la protéase. Cette activité était plus faible dans les sections de l'intestin postérieur que dans celles de l'intestin antérieur, mais l'activité de la protéase était celle qui demeurait élevée sur la plus grande distance dans l'intestin. Des micelles ont été détectées dans la sécrétion intestinale, et l'activité des surfactants était au maximum dans la région caecale. Chez les larves, l'activité de la protéase était similaire à celle des adultes, et la concentration de surfactants était inférieure à celle qui est critique pour l'apparition de micelles. Les aloses à gésier couplaient la physiologie digestive à l'anatomie de l'intestin pour tirer des matières nutritives des détritus, et cette adaptation peut expliquer les taux de croissance élevés observés chez ces poissons lorsqu'ils sont planctonophages.

[Traduit par la Rédaction]

Introduction

Many detritivores ingest sediment, a nutritionally dilute diet, and glean their metabolic requirements from it. Detritivores have anatomical and physiological adaptations to survive on this low-energy diet by maximizing energy and nutrient recovery while minimizing their losses (Penry and Jumars 1987). Detritivorous fishes have elongated digestive tracts (Stevens 1988) that increase surface area and potentially gut residence time and, subsequently, increase the opportunity for food digestion and assimilation (Penry and Jumars 1987). Adaptation of digestive physiology to diet was described by Diamond (1991) and set forth as the adaptive modulation hypothesis by Karasov (1992). From this hypothesis, digestion of nutrients readily used as energy sources (e.g., simple sugars and lipids) is predicted to be concomitant with their concentration so that a favorable absorption rate is maintained. In addition, enhanced digestion of food containing limited nutrients is predicted to maximize uptake of the limiting nutrients. Polychaete detritivores adapted their digestive physiology compared with their carnivorous relatives to both maximize protein digestion and minimize losses of digestive enzymes to adsorption on sediment mineral grains (Mayer et al. 1997). Protease activities in crustacean larvae support the hypothesis in that the lowest activities were observed in carnivores and the highest in omnivores and herbivores (Jones et al. 1997). However, digestive enzyme measurements in fish with a variety of feeding strategies did not support the hypothesis (Chakrabarti et al. 1995), although diel feeding cycles were not incorporated in the experimental design of this study.

Gizzard shad (*Dorosoma cepedianum*) are often important members of temperate freshwater ecosystems and, due to their high biomass, can influence ecosystem nutrient transport (Schaus et al. 1997). These fish "telescope" the pelagic food web by feeding on detritus (Odum 1970). Although gizzard shad show anatomical features indicating that they are adapted to consuming detritus, including subterminal mouths, pharyngeal organs, and long digestive tracts approximately threefold greater than the body length of the fish

Received May 19, 1999. Accepted February 4, 2000.
J15142

J.C. Smoot[1] **and R.H. Findlay.**[2] Department of Microbiology, 32 Pearson Hall, Miami University, Oxford, OH 45056, U.S.A.

[1]Present address: Rocky Mountain Laboratory, NIAID, NIH, 903 S. 4th Street, Hamilton, MT 59840, U.S.A.
[2]Author to whom all correspondence should be addressed. e-mail: rfindlay@miavx1.muohio.edu

© 2000 NRC Canada

(Schmitz and Baker 1969), adult gizzard shad are known to consume other food items in addition to detritus and are described as omnivores (Bodola 1966; Yako et al. 1996). Feeding plasticity in gizzard shad is controlled by fish population density or abundance of zooplankton (Yako et al. 1996). In a small eutrophic reservoir, when fish biomass was less than 20 kg·ha^{-1}, gizzard shad were planktivorous and grew rapidly, but when fish biomass exceeded 50 kg·ha^{-1}, they fed on detritus and their growth rate slowed (Schaus 1998). However, based solely on stable isotope data, Gu et al. (1996) concluded that adult gizzard shad were planktivorous and consumed a mixture of phyto- and zoo-plankton in a shallow, eutrophic lake with anoxic surface sediment despite a biomass of 363 kg·ha^{-1}. Stable isotope data from Acton Lake supported detritus being the main carbon source for gizzard shad, but $\delta^{15}N$ values indicated that bulk sediment was not the primary nitrogen source (Schaus 1998).

The life history, ecological importance to aquatic systems, feeding preferences, and anatomical features of the digestive system of the gizzard shad are well studied. The understanding of the digestive physiology of this fish is more limited. Bodola (1966) made qualitative estimates of digestive enzyme activity. King et al. (1977) showed chitinase activity in gizzard shad but did not show β-glucosidase activity necessary for a complete chitolytic system. These previous studies, as well as the ontogenetic shift in dietary preference, establish gizzard shad as a useful model system for testing the hypothesis that digestive physiology reflects feeding strategy. To test this hypothesis, we quantitatively measured the digestive enzyme activity and surfactant activity in the gut juice of adult gizzard shad. To compare enzyme and surfactant activities between feeding strategies, we also measured these features in carnivorous larval gizzard shad.

Materials and methods

Collection of fish and gut contents

Adult gizzard shad were collected at 12:00 on September 24, 1998, from Acton Lake, Preble Co., Ohio. This 253-ha, shallow eutrophic reservoir does not stratify except near its dam during summer. Gizzard shad feeding in Acton Lake has been described previously (e.g., Mundahl and Wissing 1987). Fish for this study were collected with an electroshocker (DC mode, 7 A, 120 Hz) mounted on a 6.8-m-long pontoon boat. Fish were collected in a 25-m transect from approximately 1-m-deep water near Marshal Creek's confluence with the reservoir. Fish were dipnetted immediately after being stunned and were placed in a 160-L container that was filled with lake water immediately prior to shocking. Fish were killed within 15 min of capture by severing their cervical vertebrae, measured for standard length, and dissected in the field. The entire digestive tract of each fish was clamped, tied off at the esophagus and anus, removed from the fish, doubled bagged in a Whirl-pac bag and then a Ziplock bag, chilled by placing the bagged digestive tract in a lake water brine solution for 7–10 min, and kept on wet ice until dissected in the laboratory 1–2 h later.

The digestive tract was dissected into six sections (esophagus, gizzard, and four intestinal sections). The most anterior intestinal section was defined by the presence of ceca (referred to as the ceca region); the remainder of the intestine was divided into the fore intestine, midintestine, and hind intestine. Each section was sampled by making a series of longitudinal cuts with a clean scalpel and collecting the contents in preweighed 1.5-mL microfuge tubes. Samples were weighed and centrifuged at 12 000 × *g* for 5 min at 4°C. Gut juice was removed and divided for enzyme analysis and surfactant analysis. Aliquots of 20 µL were used in all enzyme assays, and, where possible, 20 µL was taken for surfactant activity measurements. The surfactant assay samples were immediately frozen and stored at –70°C until assayed (several weeks later). Trace amounts of gut juice were removed from the surface of gut solids with a Rainin P-100 pipetman, and gut solids were weighed, subsampled for enzyme analysis, and weighed again. The esophagus and gizzard were not sampled for enzyme activity due to the small quantities of material available in these organs.

Larval gizzard shad were collected with an ichthyoplankton net (0.75-m-diameter × 2-m conical net; 500-µm mesh) attached to a glass jar. Larvae were collected during midday on June 2, 3, 5, and 10, 1998. Gizzard shad larvae were identified by the position of the anus compared with larval total length (Auer 1982). To be included in enzyme assay samples, larvae were required to be intact and alive at the time of dissection. In the field, larvae were killed and the alimentary canal of each was removed and transferred to a 1.5-mL microfuge tube in 100 µL of a 0.1 M phosphate buffer (pH 8.0). A 100-µL phosphate buffer rinse of the dissection area was also added to the 1.5-mL microfuge tube. This was repeated for each individual. Typically, the alimentary canals of five larvae were pooled and stored on ice until transported back to the laboratory. Samples were mixed for 5 s and centrifuged (3900 × *g* at 4°C) for 1 min. Supernatants were removed and samples rinsed twice with 1 mL of phosphate buffer. Supernatants were brought to a final volume of 6 mL of phosphate buffer, and enzyme activities were measured immediately. Alimentary canal volumes were estimated from published cross-sectional areas (Heinrichs 1982) and lengths of canals.

Larvae for surfactant measurements were collected as described above. Undiluted gut juice was collected either with a capillary tube or by collecting and centrifuging the alimentary canals. Gut juice from two to six larvae was pooled for analysis. Samples were stored on ice (1–3 h) until returned to the laboratory. Gut juice was recovered from alimentary canals by centrifugation (12 000 × *g* at 4°C) for 5 min.

Determination of relative enzyme activity

Enzymatic rates were determined using artificial substrates that consisted of fluorophores covalently bound to different biochemical moieties. Hydrolysis by the digestive enzymes released the fluorophore, and thus, increased fluorescence over time described the relative enzymatic rate for each enzyme class. This approach to measuring enzyme activity provides several advantages. It is sensitive, fast, and can be used to detect very specific enzymes such as β-glucosidases (e.g., King 1986) or general enzyme classes such as protease (e.g., Mayer 1989). The fluorophores used in this study were methylumbelliferone (MUF) and methylcouminamide (MCA) (Sigma, St. Louis, Mo.). The artificial substrates were MUF β-D-glucose, MUF palmitate, MUF butyrate, and MCA alanine (Sigma).

Gut juice enzyme assays were initiated within 4 h and completed within 24 h of fish collection. When samples were not being assayed, they were kept at 4°C in the dark. All enzyme assays were done at room temperature. The activities of four digestive enzyme classes in larval and adult gizzard shad gut juice were assayed as previously described (Mayer et al. 1997). Briefly, gut juice (20-µL samples from adult fish or pooled samples from larvae) was diluted with 6.0 mL of 0.1 M potassium phosphate buffer (pH 8.0). The buffer pH is typical of gut juice (Mayer et al. 1997) and was verified to be appropriate for this study by measuring the pH of pooled samples of ceca region gut juice. The activity of each enzyme class was determined by adding100 µL of 100 µM artificial substrate to 900 µL of diluted gut juice and continuously measuring the release of fluorophore with a Perkin Elmer LS 50B fluorescence spectrophotometer (Ex 340 nm, Em 450 nm) for 12 min. Quenching of the fluorophore was determined by measuring fluorescence of free

© 2000 NRC Canada

MUF and free MCA in diluted gut juice compared with fluorescence of the fluorophores in 0.1 M potassium phosphate buffer (pH 8.0). Background fluorescence from autohydrolysis of the artificial substrate was determined by adding substrate to 0.1 M potassium phosphate buffer (pH 8.0). Some substrates are sensitive to autohydrolysis and break down with repeated freeze–thaw cycles. Thus, aliquots of stock substrate solutions were typically kept at –70°C in the dark until used for enzyme analysis. Concentration of released flourophore was determined using a serial dilution of free MUF and free MCA in 0.1 M potassium phosphate buffer (pH 8.0).

Enzyme activities associated with gut solids from adult fish were measured using previously described methods (King 1986; Mayer 1989). Briefly, aliquots of gut solids were stored at 4°C overnight and immediately prior to enzyme analysis transferred to 50-mL test tubes and diluted with 20 mL of phosphate buffer. Samples were vortexed and 1-mL aliquots were put into 10-mL test tubes (mixed before each 1-mL transfer). A three-point time series was run for 30 min by adding 100 µL of artificial substrate at appropriate intervals. Microwaving for 1 min terminated all reactions. Samples were centrifuged for 5 min at 1500 × *g*; fluorescence of the supernatants was measured as described above.

Acton Lake sediment samples for enzyme analysis were collected within a month of gut enzyme analysis near where fish for this study were collected. Three replicate cores were collected by hand with 6.5-cm (inner diameter) corers, and intact cores were transported to the laboratory. Cores were extruded and the surface 1 cm of sediment was collected, homogenized, and diluted 1:1 with 0.2-µm-filtered lake water collected at the same location as the sediments. Sediment slurry samples (2 cm^3) were put into 10-mL test tubes with a modified syringe. Enzyme activities were determined following the gut solids protocol except that time series were run for 60 min.

Determination of surfactant activity

To detect surfactant activity in gut juice, samples were serially diluted and diameters of triplicate 1-µL drops on a parafilm surface were measured at 40× magnification with an ocular ruler. Surfactants are characterized by their critical micelle concentration (CMC) (the point where a surfactant will form micelles), but in a solution of unknown initial surfactant concentration, CMC cannot be determined through this method. The critical micelle dilution (CMD) is the dilution where a surfactant in solution can no longer form micelles. It is determined as the break point in the dilution series where the drop diameter becomes smaller as the surface tension against the parafilm increases. Using an indicator variable to distinguish between the dilutions greater and less than CMD, the CMD was estimated to be the dilution value at the intersection of two lines made from regression analysis. The dilution nearest to the visually detected break in the dilution series was excluded from analysis so as not to leverage either line. Points that have very large drop diameters (indicative of strong cosurfactancy) that were not sustained during dilution (i.e., the cosurfactants were below their CMD) were not included in the regression analysis.

We tested the accuracy of drop diameter measures with sodium dodecyl sulfate (SDS) (Fig. 1). Indicator variable regression analyses (see below) of dilution series described the dilution of SDS both above and below its CMC; the hinge where the two segments intersect estimated the CMD. Average published SDS CMC was 8.2 mM (n = 12, 20–25°C) (Mukerjee and Mysels 1971). Our average CMD was 6.2 ± 1.34 mM, which was, on average, 76% of the published molar CMC for SDS.

Statistical analyses

SPSS 7.5 for Windows 95 was used for analyses of variance and cluster box plots. All analyses of variance were with $\alpha = 0.05$. Indicator variable regression analyses and calculations of the test statistic used to compare regression slopes ($F^* = SSR(X_1X_2|X_1,X_2)/1 \div SSE(X_1,X_2,X_1X_2)/(n-4)$; Neter et al. 1996) were done with Minitab 12. Plots were made with Microsoft Excel 97.

Fig. 1. Representative drop diameter analysis of SDS. The two lines were produced from indicator regression analysis from the regression equation $y = 1.34 + 0.0859x + 0.670I - 0.0889xI$, where y is the drop diameter, x is SDS concentration, and I is the indicator variable (0 or 1). The partial F test statistic (F^*) was used to determine whether the slopes of the two lines produced from the regression model were different. Symbols represent individual drop diameter measurements.

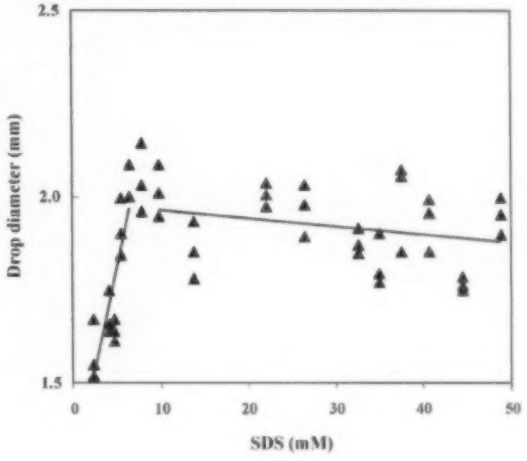

Results

Adult gizzard shad ranged in standard length from 119 to 125 mm. Water content of gut samples ranged from 40 to 80%, varied among fish, and averaged 50% across all individuals for all sections, and statistical analysis failed to reveal any significant trends in water content between anterior and posterior gut sections. Gut juice was very colored in the ceca region and fore intestine and colorless in the hind section with the exception of one fish that had colored gut juice throughout the intestine. The gut contents were amorphous and contained sediments. Larval gut contents consisted of light-brown fluid; occasionally, zooplankton exoskeletons were observed.

Enzyme activity

For all gut sections assayed, the majority of the total esterase activity was always in the gut juice (Fig. 2). β-Glucosidase and lipase activities in the ceca region and fore intestine were substantially higher in gut juice than in gut solids. In the midintestine, the majority of β-glucosidase and lipase activities was in the gut solids. Protease activity was variable among the fish but on average was equivalent for gut juice and gut solids or was higher in gut juice (fore intestine). Uningested sediment showed enzyme activity less than 1% when compared with gut juice and gut solids, indicating that little of the digestive enzyme activity was contributed by bulk sediment.

Gut juice enzyme activities in adult gizzard shad spanned over three orders of magnitude from 5 to 1100 nmol substrate

© 2000 NRC Canada

Fig. 2. Distribution of esterase, β-glucosidase, lipase, and protease activities measured in gizzard shad (*a*) gut juice and (*b*) gut solids. Samples were taken from the ceca region (CR), fore intestine (FI), midintestine (MI), and hind intestine (HI) sections of the intestine. Boxes represent the quartiles and whiskers represent the range of data. Median values are shown as the line across each box. Pairwise comparisons from analysis of variance of activity by gut section are shown (insets). Gut sections that were not significantly different (Tukey's HSD, $p < 0.05$) are connected by bars.

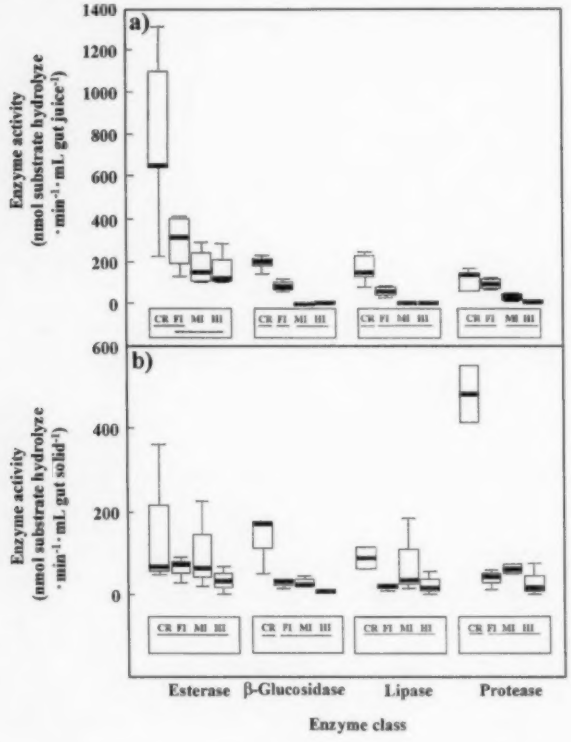

hydrolyzed·min^{-1}·mL^{-1}. Enzyme activity in the gut juice was lower in posterior intestine sections than in anterior intestine sections for all enzyme classes tested (Fig. 2*a*). The ceca region (or the ceca region and fore intestine) was the point of highest enzyme activity per volume of gut juice. Protease activity in the fore intestine was virtually the same as in the ceca region, whereas lipase activity dropped by half in the fore intestine compared with the ceca region, as detected by the decrease in the lipase to protease ratio (Table 1). The last two sections of gut appear to provide a measure of activity lost to the environment in feces in that none of the enzymes showed a significant decrease between the midintestine and hind intestine (Fig. 2).

Enzyme activities in gut solids from adult gizzard shad ranged from 5 to 600 nmol substrate hydrolyzed·min^{-1}·mL^{-1} (Fig. 2*b*). Esterase and lipase activities remained constant throughout the gut, but median β-glucosidase and protease activities dropped from 171 and 484 nmol substrate hydrolyzed·min^{-1}·mL^{-1}, respectively, in the ceca region to less than 60 nmol substrate hydrolyzed·min^{-1}·mL^{-1} for either enzyme in the rest of the gut (Fig. 2).

Table 1. Ratio of gizzard shad gut juice lipase and protease activities.

Gut section	*n*	Lipase to protease ratio
Ceca region	5	1.77 (048–2.28)
Fore intestine	4	0.51 (0.33–1.23)
Midintestine	4	0.15 (0.04–0.22)
Hind intestine	4	0.58 (0.17–1.50)
Entire intestine	4	1.06 (0.84–1.57)
Larvae	6	0.39 (0.23–0.67)

Note: Data are median ration values with ranges in parentheses. Gut sections of adult gizzard shad are described in the text. Values for the entire intestine were calculated from volume-corrected measurements of individual gut sections.

Larval gut enzyme activity was made as one measurement for the entire alimentary canal. Esterase was the enzyme class with the highest activity, and β-glucosidase activity was virtually nonexistent (Fig. 3). When comparing total enzyme activity in the intestine of the larvae to adult fish, larval esterase and protease activities were significantly greater ($p < 0.0002$ and $p < 0.04$, respectively), whereas lipase activity was not significantly different ($p = 0.29$) between larvae and adult fish. In contrast, β-glucosidase activity was significantly lower in the larval intestine compared with adult fish intestine ($p < 0.0001$). Lipase to protease ratios in larval gut juice were less than the median for the entire adult fish intestine and comparable with those in the gut sections distal to the ceca region of the adult fish (Table 1).

Surfactant activity

Adult gizzard shad surfactant activity decreased in posterior intestine sections compared with anterior intestine sections (Table 2; Fig. 4). Except for the midintestine of one fish and the hind intestine of another, all samples had discernable CMD, as shown by the significant change in slopes in the regression analyses (Table 2). In all cases, gut fluid from the ceca region showed the greatest surfactant activity. Gut juice from the ceca region had surfactants at an approximately 10-fold greater concentration than CMD and initial drop diameters that were comparable to SDS (compare Figs. 1 and 4*a*). The fore intestine contained surfactant activity greater than CMD but at two- to three-fold less than the ceca region (Table 2). The remainder of the gut surfactant activity was near CMD. Dilutions of larval gut juice were similar to the dilution of hind intestine gut juice, and regression analysis showed a linear relationship between dilution and drop diameter (H_0: $\beta_1 = 0$, $p < 0.0005$). Slopes of lines generated to estimate breakpoints were not different (H_0: $\beta_3 = 0$, $p > 0.08$). The immediate and continuous decrease in drop diameter indicated that surfactant concentration in larval gut juice was below CMD.

Discussion

We hypothesized that detritivorous gizzard shad, which have been observed to routinely have intestines full of sediment, have special digestive features requisite for obtaining dietary requirements from this dilute food source. We further postulated that larval gizzard shad, which are carnivorous, would have a digestive physiology mirroring that feeding

© 2000 NRC Canada

Fig. 3. Digestive enzyme activity measured in the gut juice of larval gizzard shad (total length ≤25 mm). Boxes and whiskers are as described in Fig. 2 (n = 4 for esterase, n = 5 for β-glucosidase, and n = 6 for lipase and protease). An asterisk shows a datum greater than three times the interquartile range.

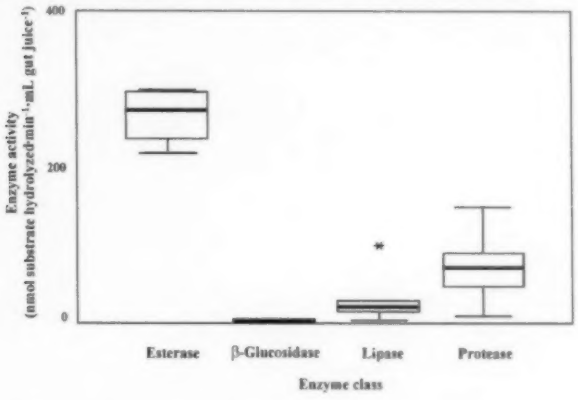

strategy. To test these hypotheses, we measured features of the digestive physiology that were previously shown to be important benchmarks that distinguished detrivores from carnivores, that is, the presence of surfactants at concentrations significantly greater than CMD and a lipase to protease ratio <1.

Mayer et al. (1997) showed that surfactant activity was a crucial component in the digestive physiology of detritivorous marine invertebrates and subsequently a good descriptor of feeding strategy. Bile in fish forms micelles for lipid digestion and is generally composed of bile salts, cholesterol, and pigments (Fange and Grove 1979). Our results showed that gut juice in adult gizzard shad had surfactant CMD similar to detritivorous invertebrates and overall activity comparable with a commercial surfactant (SDS). Surfactant activity in detritivores has been postulated to be not only directly involved with dissolving lipids for assimilation but also indirectly in increasing overall digestion efficiency by preventing digestive enzyme loss to sediment grains (Mayer et al. 1997). The lack of surfactant activity in excess of CMD in the larval gizzard shad may reflect their immature digestive tract and carnivorous diet.

The lipase to protease ratio in gut juice was also reported to be an important distinguishing feature between invertebrate detritvores and carnivores (Mayer et al. 1997). They observed that carnivorous and detritivorous polychaetes had similar lipase activities, while protease activity was lower in the carnivores compared with the detritivores. By linking lipase to protease ratios to feeding strategy, they showed that carnivorous marine polychaetes had high lipase to protease ratios and detritivores had low lipase to protease ratios. In a similar study, B.N. Smith et al. (Miami University, Oxford, Ohio, personal communication) found that two species of detritivorous freshwater mussels (*Elliptio dilatata* and *Ptychobranchus fascioloris*) had lipase to protease ratios of 0.06. These ratios suggest that carnivores eating a protein-rich diet require less enzymatic effort to obtain their nitrogen requirement and that detritivores invest significantly in proteolytic enzymes (or have developed ones with greater efficiency) to digest available proteins from their comparatively nutritionally dilute diet. Lipase to protease ratios in ceca region gut juice from adult gizzard shad were intermediate compared with ratios measured in invertebrate carnivores and detritivores. Due to an abrupt decrease in lipase activity, the lipase to protease ratios in the fore intestine were lower and approached the ratios of invertebrate detritivores. These lower lipase to protease ratios persisted for the remainder of the gut and may reflect longer digestion times required for effective digestion of proteins from detritus. This increased digestive activity is predicted for limiting nutrients by the plug-flow reactor model of digestive optimization theory (Penry and Jumars 1987). The difference between invertebrate and gizzard shad lipase to protease ratios supports the adaptive modulation hypothesis (Karasov 1992) and demonstrates a difference in the overall digestive strategy among these detritivores. Given the role of digestion is to make food available for absorption, two strategies that couple anatomical and physiological features for obtaining daily nutrition rations are demonstrated by gizzard shad and marine invertebrates. Penry and Jumars (1987) predicted that invertebrates with shorter guts and short gut residence times would require high protease activity. The extended gut length of the gizzard shad may provide longer residence times and should allow lower proteolytic enzyme activities to achieve the same digestive output, although these organisms would need to extend protease activity further down the gut.

Table 2. CMD of gizzard shad gut juice surfactants.

Gut section	No. gut sections sampled	No. with a significant break point	Estimated CMD
Ceca region	5	5	9.8±4.0
Fore intestine	4	4	23.8±14.7
Midintestine	3	2	na
Hind intestine	1	0	na

Note: Gut sections of gizzard shad are described in the text. Several fish did not contain sufficient gut fluids to allow a sample from the midintestine or hind intestine regions. CMDs are expressed as the average percentage of original gut juice ± SD; na, calculation not appropriate.

The observed β-glucosidase activity in the adult gizzard shad, coupled with the chitinolytic data reported by King et al. (1977), demonstrated that adult gizzard shad possess the requisite enzymes to utilize chitin as a food resource. Our study does not differentiate autochthonous gut microbes from gizzard shad as the source of the chitinolytic enzymes. The presence of β-glucosidase suggests that digestion of recalcitrant polysaccharides occurs in the ceca region of the gizzard shad. Microbial fermentation of cellulose in the guts of fish has been shown (e.g., Lindsay and Harris 1980), but the importance of fermentation in chitin digestion was questioned (Fange and Grove 1979; Danulat 1986; Lindsay 1987). The strength of microbe–animal symbioses appears dependent on gut architecture and kinematics (Sinsabaugh et al. 1985). Smith et al. (1996) showed virtually no volatile fatty acids in the gizzard shad gut and concluded that, due to high gut throughput, little autochthonous microbial fermentation was possible, although efficient uptake was not ruled out. Further study of the ceca region of the gizzard shad is needed to resolve the source of enzymes utilized for digestion of recalcitrant polysaccharides and if gut residence

© 2000 NRC Canada

Fig. 4. Drop diameter dilution curves of adult gizzard shad gut juice from the (*a*) ceca region and (*b*) hind intestine. Drop diameter analyses of gut juice from the ceca region of the intestine showed the presence of a distinct break point and the presence of a surfactant(s) at greater than CMD, whereas gut juice from the hind intestine did not show a break point or surfactants above CMD. Symbols represent individual drop diameter measurements.

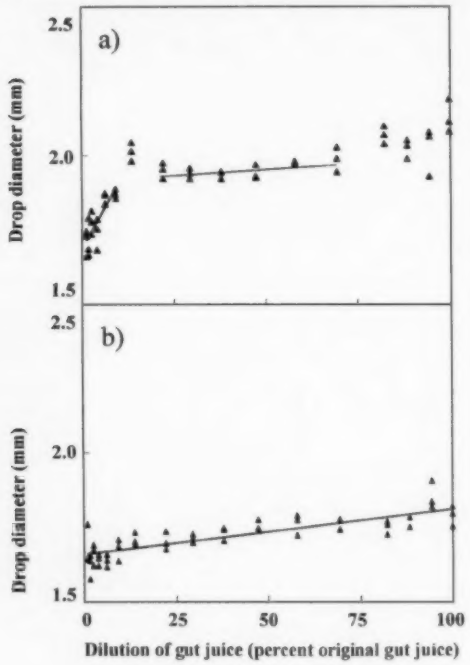

times are sufficient to maintain an effective microbe – gizzard shad symbiosis.

Gizzard shad larvae are carnivores and switch to feeding on detritus when zooplankton become scarce. When fish biomass is low, young-of-the-year gizzard shad sustain their zooplankton diet longer and grow rapidly (Schaus 1998). Bowen et al. (1995) showed a positive correlation between fish growth rate and protein content of their food. Horn and Messer (1992) applied gut chemical reactor optimization theory (Penry and Jumars 1987) to fish digestion and predicted that fish fed a high-quality diet would have an increased digestion efficiency that supported a higher growth rate compared with fish fed a low-quality diet. They also predicted that fish fed a medium-quality diet could obtain the same digestion efficiency with longer gut retention times. Gizzard shad larval intestines extend to 90% of their body length (Auer 1982) and exhibit a median lipase to protease ratio of 0.4. Together, these features (concentrated food, long gut lengths, and high protease activity) may explain the observed accelerated growth rates of these fish when they are feeding on zooplankton.

Quantifying digestive enzyme activity relative to feeding strategy is necessary in understanding and predicting the food resources exploited by fish in their natural environment or in attempting to optimize feeding regimes in aquaculture. Digestion occurs both in the lumen and at the brush border cells of the mucosa of the small intestine (Fange and Grove 1979; Johnson 1987). Studies of digestive enzymes are numerous but often are not directly comparable (Jones et al. 1997). For instance, studies of enzyme activity that use enzyme histochemistry or tissue homogenate methods are useful for describing intracellular and brush border enzymes or the overall presence of enzymes in tissue. However, these techniques may be semiquantitative and inadequate for describing enzyme activities in the lumen. In addition, some studies use assays specific for well-characterized enzymes (e.g., Kuz'mina 1996), whereas others use more generalized substrates (Mayer et al. 1997; this study). Finally, in published enzyme studies, data are typically normalized against different factors such as overall protein content (e.g., Chakrabarti et al. 1995), weight of the homogenized tissue or mucosa (e.g., Kuz'mina 1996), or volume sampled (Mayer et al. 1997; this study). Provided the same or similar enzymes were quantified, these limits in direct comparison can be circumvented by comparing relative activities of different enzymes within data sets (e.g., amylase to protease ratios and lipase to protease ratios (Jones et al. 1997; Mayer et al. 1997)). Thus, the lipase to protease ratio is an important parameter when correlating digestive enzyme activity with feeding strategy in studying detritivorous members of animal phyla.

Detritus has long been cited as a food source for gizzard shad (e.g., Bodola 1965). The combined increased gut length, persistent protease activity, and high surfactant activity provide this species with the physiological traits necessary to survive and thrive on a mud diet. Ironically, the same physiological features used by marine invertebrates feeding on mud have resulted in an effective mechanism for facilitating dissolution of adsorbed hydrophobic pollutants from sediment (Mayer et al. 1996). It remains to be tested whether similar results will occur with gut juice from detritivorous fish such as gizzard shad, although polyaromatic hydrocarbons have been detected in their bile (Metcalfe et al. 1997).

Acknowledgements

We thank L. Schick and L. Mayer, Darling Marine Center, University of Maine, for their technical assistance with enzyme assays and J. Brannock, D. Langworthy, K. Mumy, H. Schran, S. Sutton, Department of Microbiology, Miami University, for their laboratory and field assistance during this study. We thank the Department of Zoology, Miami University, for use of their sampling gear and especially M. Schaus for technical assistance and T. Wissing for providing a critical review of this manuscript. This study was supported, in part, by funding from the Office of Naval Research (N00014-96-1-0185) and the Department of Microbiology, Miami University.

References

Auer, N.A. (*Editor*). 1982. Identification of larval fishes of the Great Lakes basin with emphasis on the Lake Michigan drainage. Gt. Lakes Fish. Comm. Spec. Publ. 82-3.

© 2000 NRC Canada

Bodola, A. 1965. Life history of the gizzard shad, *Dorosoma cepedianum* (Le Sueur), in western Lake Erie. U.S. Fish Wildl. Serv. Fish. Bull. **65**: 391–425.

Bowen, S.H., Lutz, E.V., and Ahlgren, M.O. 1995. Dietary protein and energy as determinants of food quality: trophic strategies compared. Ecology, **76**: 899–907.

Chakrabarti, I., Gani, M.A., Chaki, K.K., Sur, R., and Misra, K.K. 1995. Digestive enzymes in 11 freshwater teleost fish species in relation to food habit and niche segregation. Comp. Biochem. Physiol. A, Comp. Physiol. **112**: 167–177.

Danulat, E. 1986. Role of bacteria with regard to chitin degradation in the digestive tract of the cod *Gadus morhua*. Mar. Biol. **90**: 335–343.

Diamond, J. 1991. Evolutionary design of intestinal nutrient absorption: enough but not too much. News Physiol. Sci. **6**: 92–96.

Fange, R., and Grove, D. 1979. Digestion. *In* Fish physiology. *Edited by* W.S. Hoar, D.J. Randall, and J.R. Brett. Academic Press, New York. pp. 161–260.

Gu, B., Schelske, C.L., and Hoyer, M.V. 1996. Stable isotopes of carbon and nitrogen as indicators of diet and trophic structure of the fish community in a shallow hypereutrophic lake. J. Fish Biol. **49**: 1233–1243.

Heinrichs, S.M. 1982. Ontogenetic changes in the digestive tract of the larval gizzard shad, *Dorosoma cepedianum*. Trans. Am. Microsc. Soc. **101**: 262–275.

Horn, M.H., and Messer, K.S. 1992. Fish guts as chemical reactors: a model of the alimentary canals of marine herbivorous fishes. Mar. Biol. **113**: 527–535.

Johnson, L.R. 1987. Physiology of the gastrointestinal tract. Raven Press, New York.

Jones, D.A., Kumlu, M., Le Vay, L., and Fletcher, D.J. 1997. The digestive physiology of herbivorous, omnivorous and carnivorous crustacean larvae: a review. Aquaculture, **155**: 285–295.

Karasov, W.H. 1992. Tests of the adaptive modulation hypothesis for dietary control of intestinal nutrient transport. Am. J. Physiol. **263**: R496–R502.

King, G.M. 1986. Characterization of β-glucosidase activity in intertidal marine sediments. Appl. Environ. Microbiol. **51**: 373–380.

King, P.A., Wissing, T.E., DeVillez, E.J., Chimney, M.J., and Randall, W.B., Jr. 1977. Nutritional implications of surface feeding by gizzard shad (*Dorosoma cepedianum*) on insect remains in an Ohio reservoir. Can. J. Fish. Aquat. Sci. **34**: 269–273.

Kuz'mina, V.V. 1996. Influence of age on digestive enzyme activity in some freshwater teleosts. Aquaculture, **148**: 25–37.

Lindsay, G.J.H. 1987. Seasonal activities of chitinase and chitobiase in the digestive tract and serum of cod, *Gadus morhua* (L.). J. Fish Biol. **30**: 495–500.

Lindsay, G.J.H., and Harris, J.E. 1980. Carboxymethylcellulose activity in the digestive tracts of fish. J. Fish Biol. **16**: 219–223.

Mayer, L.M. 1989. Extracellular proteolytic enzyme activity in sediments of an intertidal mudflat. Limnol. Oceanogr. **34**: 973–981.

Mayer, L.M., Chen, Z., Findlay, R.H., Fang, J.S., Sampson, S., Self, R.F.L., Jumars, P.A., Quetel, C., and Donard, O.F.X. 1996. Bioavailability of sedimentary contaminants subject to deposit-feeder digestion. Environ. Sci. Tech. **30**: 2641–2645.

Mayer, L.M., Schick, L.L., Self, R.F.L., Jumars, P.A., Findlay, R.H., Chen, Z., and Sampson, S. 1997. Digestive environments of benthic macroinvertebrate guts: enzymes, surfactants and dissolved organic matter. J. Mar. Res. **55**: 785–812.

Metcalfe, C.D., Metcalfe, T.L., Riddle, G., and Haffner, G.D. 1997. Aromatic hydrocarbons in biota from the Detroit River and western Lake Erie. J. Gt. Lakes Res. **23**: 160–168.

Mukerjee, P., and Mysels, K.J. 1971. Critical micelle concentrations of aqueous surfactant systems. Natl. Standards Ref. Data Ser. Natl. Bur. Standards (U.S.), 36.

Mundahl, N.D., and Wissing, T.E. 1987. Nutritional importance of detritivory in the growth and condition of gizzard shad in an Ohio reservoir. Environ. Biol. Fishes, **20**: 129–142.

Neter, J., Kutner, M.H., Nachtsheim, C.J., and Wasserman, W. 1996. Applied linear statistical models. Irwin, Chicago, Ill.

Odum, W.E. 1970. Utilization of the direct grazing and plant detritus food chains by the striped mullet *Mugil cephalus*. *In* Marine food chains. *Edited by* J.H. Steele. University of California Press, Berkeley, Calif. pp. 222–240.

Penry, D.L., and Jumars, P.A. 1987. Modeling animal guts as chemical reactors. Am. Nat. **129**: 69–96.

Schaus, M.H. 1998. Effects of gizzard shad on nutrient cycles and phytoplankton in a reservoir ecosystem: roles of diet, biomass and population size-structure. Ph.D. dissertation, Miami University, Oxford, Ohio.

Schaus, M.H., Vanni, M.J., Wissing, T.E., Bremigan, M.T., Garvey, J.E., and Stein, R.A. 1997. Nitrogen and phosphorus excretion by detritivorous gizzard shad in a reservoir ecosystem. Limnol. Oceanogr. **42**: 1386–1397.

Schmitz, E.H., and Baker, C.D. 1969. Digestive anatomy of the gizzard shad, *Dorosoma cepedianum* and the threadfin shad, *D. petenense*. Trans Am. Microsc. Soc. **88**: 525–546.

Sinsabaugh, R.L., Linkins, A.E., and Benfield, E.F. 1985. Cellulose digestion and assimilation by three leaf-shredding aquatic insects. Ecology, **66**: 1464–1471.

Smith, T.B., Wahl, D.H., and Mackie, R.I. 1996. Volatile fatty acids and anaerobic fermentation in temperate piscivorous and omnivorous freshwater fish. J. Fish Biol. **48**: 829–841.

Stevens, C.E. 1988. Comparative physiology of the vertebrate digestive system. Cambridge University Press, Cambridge, U.K.

Yako, L.A., Dettmers, J.M., and Stein, R.A. 1996. Feeding preferences of omnivorous gizzard shad as influenced by fish size and zooplankton density. Trans. Am. Fish. Soc. **125**: 753–759.

© 2000 NRC Canada

Modelling the probability of salmonid egg pocket scour due to floods[1]

Michel Lapointe, Brett Eaton, Steve Driscoll, and Christian Latulippe

Abstract: Flood disturbance plays a key but complex role in structuring lotic ecosystems. Empirical models proposed here allow salmonid resource managers to quantify the probability of egg pocket scour during floods and to predict how the expected losses vary with flood strength and reach characteristics. The models are based on comparisons between published salmonid egg pocket depth criteria and statistics on the intensity and spatial distribution of scour and fill produced by three flood events of widely different magnitudes in three separate reaches of a gravel–cobble Atlantic salmon (*Salmo salar*) river in the Saguenay region, Quebec. A simple substrate mobility index, based on reach-scale geomorphic characteristics and flood hydraulics, was shown to provide useful predictions (R^2 up to 74%) of the fraction of the area of potential spawning zones undergoing flood scour greater than 30 cm. Any Atlantic salmon egg pockets present in these deeply scoured areas would be destroyed. The models also predict the distribution of fill (net rise in bed) potentially causing fry entombment at redds. The flood disturbance data suggest that average probability of scour of an Atlantic salmon egg pocket in the study reaches ranges from under 5% for frequent-recurrence spring floods to approximately 20% for an extreme, multicentenary-recurrence flood.

Résumé : Les perturbations causées par les crues jouent un rôle clé mais complexe dans la structuration des écosystèmes lotiques. Les modèles empiriques proposés ici permettent aux gestionnaires des ressources de salmonidés de quantifier la probabilité d'affouillement des poches d'œufs pendant les crues et de prédire comment les pertes prévues vont varier en fonction de la force de la crue et des caractéristiques du tronçon. Les modèles se fondent sur des comparaisons entre des critères publiés sur la profondeur des poches d'œufs de salmonidés et sur des statistiques concernant l'intensité et la distribution spatiale de l'affouillement et du colmatage produits par trois épisodes de crue d'ampleur très différente, survenus dans trois tronçons séparés d'un cours d'eau à saumon à fond de gravier et de cailloux de la région du Saguenay, au Québec. Un indice simple de la mobilité du substrat, fondé sur des caractéristiques géomorphologiques à l'échelle du tronçon et sur l'hydraulique de la crue, a fourni des prévisions utiles (R^2 jusqu'à 74%) de la fraction de la superficie des frayères potentielles qui subissait un affouillement sur plus de 30 cm. Toutes les poches d'œufs de saumon atlantique présentes dans ces zones profondément affouillées seraient détruites. Les modèles prédisent aussi la distribution du colmatage (hausse nette du lit), qui risque de causer l'étouffement des alevins prisonniers des nids. Les données sur les perturbations causées par les crues permettent de penser que la probabilité moyenne d'affouillement d'une poche d'œufs de saumon dans les tronçons d'étude va de moins de 5% pour les crues printanières fréquentes à environ 20% pour une crue extrême à récurrence pluricentenaire.

[Traduit par la Rédaction]

Introduction

The physical and spatial complexity of stream microhabitat poses real challenges to the study of running-water ecosystems. However, the paradoxical role of flood disturbance in structuring running-water communities arguably poses even greater challenges to understanding lotic ecosystems. The problem of defining optimum physical disturbance regimes for various lotic communities, raised by several authors (e.g., Resh et al. 1988; Allen 1995; Sparks and Spink 1998), applies in particular to stream salmonid communities. On the one hand, substrate entrainment by flood flows is necessary to maintain the long-term productivity of gravel stream habitat for salmonids. Indeed, the curtailment of regular high-flow events and associated gravel transport (e.g., following reservoir construction) can lead to excess sand encroachment into substrate, resulting in degradation of spawning habitat (e.g., Kondolf and Wilcock 1996; Wilcock et al. 1996; Milhous 1998) and in the displacement of the lithophylous benthic insect populations, a major food source during juvenile salmonid growth (Waters 1995). Conversely, intense and frequent disturbances to gravel substrate may limit salmonid production by destroying fish eggs during incubation (Seegrist and Gard 1972; Holtby and Healy 1986; Lisle 1989), by temporarily decimating benthic insect populations (Elwood and Waters 1969; Milner et al. 1981) or by directly inhibiting foraging by juvenile salmonids.

In particular, flood scour of salmonid eggs in spawning beds can directly affect cohort and population dynamics. Numerous studies have indicated the importance of spawning bed grain size distribution in controlling intergravel flow, egg maturation, and fry emergence (Scrivener and Brownlee

Received June 25, 1999. Accepted January 19, 2000.
J15217

M. Lapointe,[2] B. Eaton, S. Driscoll, and C. Latulippe.
Department of Geography, McGill University,
805 Sherbrooke St. West, Montreal, QC H3A 2K6, Canada.

[1]A contribution to the scientific program of CIRSA (Centre Interuniversitaire de Recherche sur le Saumon Atlantique).

[2]Author to whom all correspondence should be addressed.
e-mail: lapointe@geog.mcgill.ca

© 2000 NRC Canada

1989; Kondolf and Wolman 1993). However, the impact on salmonid reproductive success of flood disturbances to spawning beds has been poorly studied. Payne and Lapointe (1997) showed that, in an unstable gravel–cobble river, high rates of erosion of sand-rich cutbanks during floods did not necessarily lead to enhanced sand encroachment into the spawning substrate in the reach. Their study did not, however, address the possible effects of intense spawning bed disturbance during floods on embryos incubating in such unstable channels.

A variety of flood-related geomorphic processes can directly hinder salmonid incubation and emergence from redds. Sediment fill (i.e., accreting sediment producing a net rise in bed level) over egg pockets during floods may be harmful to fry emergence, particularly if the accreting sediments have a high content of fine sediments. Conversely, substrate mobilization (i.e., scour) down to egg pocket depths can entrain and destroy embryos (DeVries 1997). Allen (1951) and Elwood and Waters (1969) highlighted the transient effects on salmonid communities of the destruction of incubating eggs by strong flood flows. Montgomery et al. (1999) hypothesized that interreach geomorphic contrasts in flood scour patterns constrain salmonid distributions through the requirement that egg burial depth must exceed typical scour depths in spawning beds. In particular, egg loss due to flood scour has also been thought to affect the relative distribution of spring- versus fall-spawning species, depending on the seasonal timing of high flows (Kondolf et al. 1991; Pearsons et al. 1992). Finally, the simple infiltration of fine sediments into egg pockets in fresh redds during high-flow events can also smother incubating embryos (Gibbons and Salo 1973). Lisle and Lewis (1992) presented a model predicting embryo losses due to this latter process. Their model is particularly useful in regions such as northern California where repeated, moderate-winter high flows, capable of mobilizing sands on the river bed, can occur during the period of incubation. The model did not, however, quantify the losses directly due to egg pocket scour during stronger floods, the focus of this paper. For Atlantic salmon (*Salmo salar*) populations in northeastern North America, which spawn mainly in fall and whose fry emerge in late spring, very low winter flows are typical of much of the egg incubation period. In such settings, disturbance to egg pockets during the dominant, gravel-mobilizing, late-winter or spring flood associated with snowmelt is a notable but poorly quantified cause of juvenile loss.

To begin understanding the complex role that floods play in structuring salmonid stream communities, ecologists need analytical methods developed by geomorphologists to model how severely physical disturbances affect stream habitats and organisms at various life stages using those habitats. This study proposes tools to quantify the flood damage to salmonid egg pockets. Based on observations on the Sainte-Marguerite River, Quebec, empirical models are presented that predict the intensity of scour and fill affecting spawning redds as a function of local stream characteristics and flood strength. An unusually broad range of flood intensities during the study period provided a unique opportunity to characterize a response curve for disturbance to spawning beds. Observed scour patterns were then compared with typical salmonid egg pocket depths (DeVries 1997) to estimate probabilities of egg pocket losses due to various flood events.

Materials and methods

Study sites and flood events

The Sainte-Marguerite River drains a catchment of 2135 km^2 into the Saguenay Fjord, Quebec, Canada (Fig. 1). The river supports an Atlantic salmon sport fishery, which plays a prominent role in the local economy. Research was carried out along the upper section of the main branch of the Sainte-Marguerite River, an area draining a 285-km^2 subbasin. In several locations along this section of valley (Fig. 2), meanders were rectified over 35 years ago to facilitate highway construction. This reach displays a general downstream decrease in channel gradient and concomitant substrate sizes, a common pattern along gravel rivers. Atlantic salmon have been observed to spawn on riffles with gravel to cobble substrate at various points along the upper 8 km of the reach shown in Fig. 2.

Three flood events, covering a particularly wide range of magnitudes, occurred during the 1995–1997 study period. The May 1996 and May 1997 events, both generated by spring snowmelt, were moderate (recurrence period 8–10 years) and small (2–3 years) in magnitude, respectively. In contrast, the July 1996 event was a flood event of very large magnitude, the largest on record in the study basin, with a recurrence period measured in centuries. This high-intensity flooding occurred when an extreme frontal precipitation system stalled for 48 h over the entire Saguenay region (Lapointe et al. 1998). Although this July flood did not coincide with a period of salmonid egg incubation, it provided a unique opportunity to assess the level of physical disturbance to spawning habitat corresponding to a very large flood.

For each event, detailed patterns of flood disturbance to the spawning zones were studied in three reaches (Fig. 2). There are no significant tributaries in this section of valley, and the three study reaches share a common discharge regime. These study reaches were selected to represent a range of sedimentological, morphological, and channel slope characteristics (Table 1) typical of the spawning habitat in this section of valley. Within these three reaches, a total of seven separate riffle spawning zones were monitored in detail for flood disturbance. Two potential spawning zones were directly flanked by artificially stabilized banks.

Delimitation of potential spawning zones

Potential spawning zones were carefully identified before each flood event to focus on scour and fill patterns that could affect incubating embryos. The limits of these zones were defined based on generally accepted sedimentological, morphological, and hydraulic criteria for Atlantic salmon spawning habitat (Beland et al. 1982; Gibson 1993). Due to year-to-year variations in spawning pressure, the seven spawning zones monitored in this study were not used by spawners every year. Zone locations are consistent, however, with historical redd location patterns in this reach. Potential spawning zones were operationally defined here as the segments of the low-flow (summer-stage) channel extending one bankfull width upstream of each riffle crest (the latter defined as the local peak in bed elevation between pools) (Fig. 3). In the study reaches, mean flow depths at the lateral edges of these zones would generally be 15–25 cm in October, the usual spawning season. The upstream limit of each zone corresponds to sectors where depths increase rapidly upstream towards the preceding pool. Analysis showed that the statistics on bed disturbance probabilities presented below are not very sensitive to the precise lateral and upstream limits used to delimit potential spawning zones.

During high flows, stronger velocities tend to be concentrated towards the outside of a bend, due to the effects of channel sinuosity (Chang 1992), producing lateral gradients in flood shear

© 2000 NRC Canada

Fig. 1. Location map of the Sainte-Marguerite River study basin.

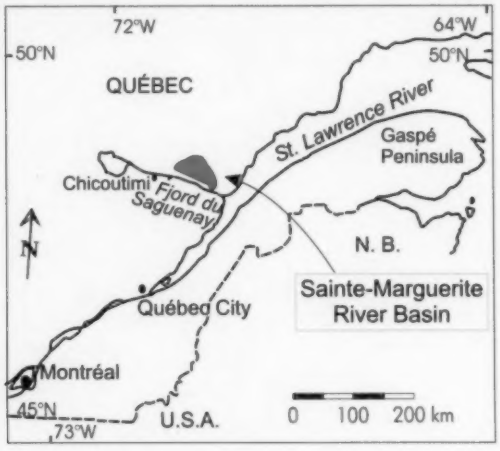

stresses and substrate size distributions at riffle cross sections (Payne and Lapointe 1997). To account for this spatial variation in geomorphic conditions, spawning zones were laterally broken down into three subzones (Fig. 3). The thalweg subzone was defined as a 3-m-wide swath centred on the thalweg within each spawning zone. High-velocity subzones (on the cutbank side with respect to the previous bend) and low-velocity subzones (on the point bar side of the previous bend) were identified on each side of the thalweg subzone.

Observations of scour and fill in potential spawning zones

A key parameter for modelling egg scour is the depth of egg pocket emplacement at redds. In a review of data on egg burial depths for various salmonids, DeVries (1997) proposed scour depth criteria corresponding to the typical levels of the top and the bottom of egg pockets. At Atlantic salmon redds, scour to a depth of 15 cm below the original bed level begins to affect the top of egg pockets, while 30 cm of scour would generally reach the base of egg pockets, causing total egg loss (DeVries 1997). For most other salmonid species, thresholds for the start of egg scour varied from 10 to 15 cm (top of egg pockets below the original bed level), while egg pocket bottom depths varied from 20 to 50 cm. Unfortunately, no study is available yielding precise criteria on thickness of fresh flood fill (i.e., net rise of bed level) over egg pockets leading to inhibition of fry emergence and entombment.

Initially, scour chains were emplaced at riffle sites during the 1995–1996 period. However, floods during the study period were powerful enough to produce easily surveyed net scour or fill with clear implications for egg pocket integrity. Scour chains were not employed after 1996. Between each flood, repeated high-resolution topographic surveys of the bed in the three study reaches were carried out under low-flow conditions. Topographic soundings were collected approximately every 3–4 m (i.e., 500–600 survey points in a 400 × 25 m wetted zone) using 5-mm-precision total station surveys. Analysis of replicate surveys showed that this technique yields digital elevation models with a mean vertical uncertainty of approximately 5 cm (due mainly to interpolation errors between sounding points). All surveys were precisely referenced to permanent benchmarks on the floodplain, allowing for an accurate assessment of net topographic changes caused by intervening flood events. Maps of the topographic changes (net scour and net fill) associated with each flood event were derived by subtracting the preevent topographic model from the postevent model. To the extent that observed net lowering (or raising) of the bed at spawning sites can destroy (or entomb) eggs, these net change maps yield conservative or minimal estimates of embryo loss probabilities. The potential of additional egg losses due to deep scour followed by fill during a single event is addressed in the Discussion.

Predictors of substrate scour and fill depths

Bed scour depths have been empirically correlated with peak flood discharges and associated bed load transport rates in a number of studies (Carling 1987; Ziemer et al. 1991). However, scour depth (and egg pocket integrity) during floods cannot be accurately predicted solely from peak discharge values. The substrate scouring potential of a discharge level in a particular stream reach depends on a number of local geomorphic variables, such as channel cross-sectional geometry and slope, as well as sediment calibre (size) on spawning beds. Erman et al. (1988) argued, for example, that variations in the height of banks along Sagehen Creek (due to differential snow buildup in winter) produced, at the same flood discharges, downstream variations in the bed shear forces, bed scour, and salmonid egg loss. Fluvial geomorphologists model substrate transport intensity using measures such as bed mobility ratios or "Shield's stresses" (Chang 1992; Montgomery et al. 1996). These parameters express the ratio of the hydraulic mobilizing forces of the flood at its peak (shear stresses, τ_o) to the mechanical forces resisting substrate entrainment (critical entrainment stresses, τ_c), which depend on substrate grain sizes.

The spatial distribution of peak shear stresses during a flood, locally over the various zones of the spawning riffle, is extremely difficult to measure or reconstruct. However, the average shear stress over a whole reach can be estimated from hydraulic principles (Chang 1992) using simple measures of the flood flow geometry, particularly the flow hydraulic radius (approximately mean flow depth) and energy slope (approximately water surface slope). Precise peak water surface levels for all three flood events were reconstructed using observations from maximum stage recorders installed at the upstream and downstream limits of each study reach. Flood flow geometry (cross-sectional depths, etc.) was derived by comparing the channel topographic model (excluding floodplain zones) with the elevation of the flood water surface. The average shear stress on the bed at flood peak ($\bar{\tau}_o$) is given by

$$(1) \qquad \bar{\tau}_o = \rho g R S$$

where ρ is water density and g is acceleration due to gravity. The flood hydraulic radius (R) in each reach was averaged over several cross sections. The energy slope (S) was assumed equal to the water surface slope to a good approximation, since peak flow cross sections (and thus mean velocities) were very similar at the entrance and exit sections of each reach.

The nominal critical shear stress (τ_c) required to entrain the surface layer of substrate at riffles was estimated from riffle surface median diameter (D_{50}) using Shield's law (Dingman 1984):

$$(2) \qquad \tau_c / (\rho_S - \rho) g D_{50} = 0.06$$

which corresponds to the rough equivalence τ_c (pascals) = D_{50} (millimetres) for particles with the density of quartz (ρ_S = 2.65 times the density of water). The average riffle zone median grain size (D_{50}) in each reach was estimated from standard Wolman, or grid-by-number, samples (Church et al. 1987) measured on the high-velocity side of each riffle or at the adjacent point bar head (Fig. 3). Where riffle substrate could not be sampled accurately underwater, samples were taken at the head of the adjacent point bar, as close as possible to water's edge and to the submerged riffle (a common practice in fluvial geomorphology). Such bar head samples taken at low stages generally reflect the coarsest mobile alluvium within a pool–riffle reach and have a median size comparable with that found on the adjacent high-velocity side of the submerged riffle. Finally, the reach-average mobility ratio was defined as

© 2000 NRC Canada

Fig. 2. Map and long profile of study reaches A, B, and C located in the upper section of the main branch of the Sainte-Marguerite River approximately 50 km from the mouth of the river in the Saguenay Fjord.

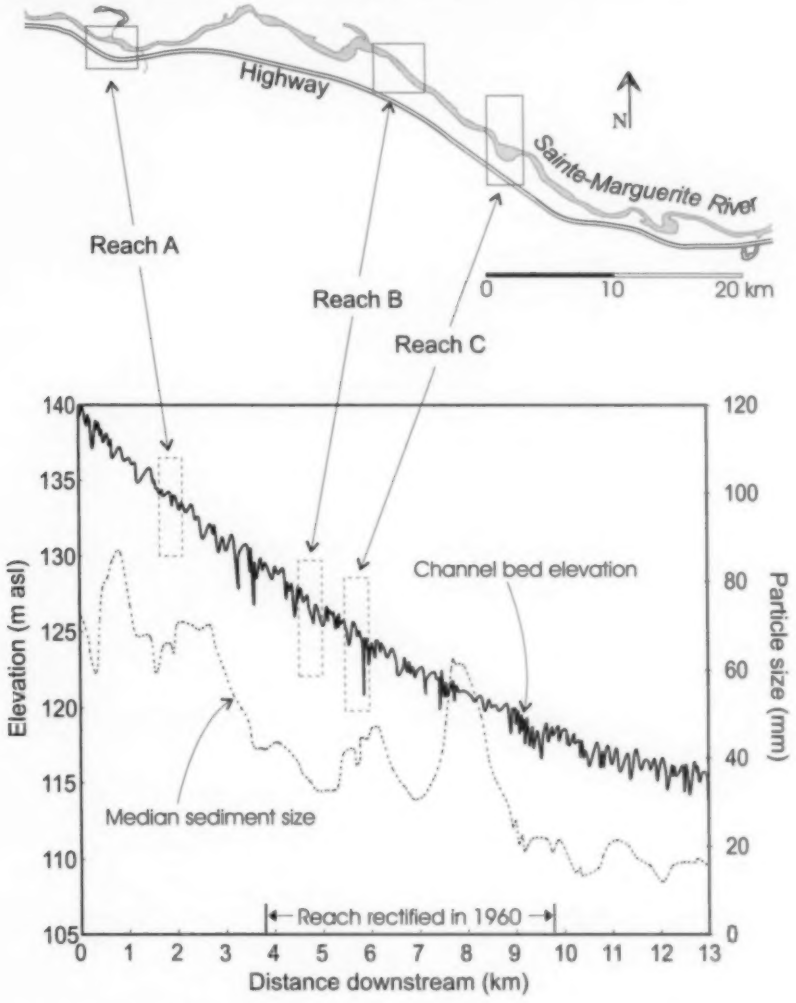

Table 1. Main geomorphological characteristics of the study reaches.

Study reach	Total length (m)	Bankfull width (m)	Bankfull water surface slope	Average D_{50} on bar heads (mm)
A	385	44	0.0033	42.5
B	335	38	0.0028	29
C	392	58	0.0026	45.5

Note: D_{50} refers to the median diameter of surface pavement particles.

$$(3) \quad \text{Mobility ratio} = \bar{\tau}_o/\bar{\tau}_c$$

where $\bar{\tau}_o$ is the estimate of reach-average shear stresses and $\bar{\tau}_c$ applies to the reach-average riffle zone substrate (i.e., applying eq. 2 to the average D_{50} for all riffle zones in the reach).

For ease of estimation and application to other systems, the simple form of mobility index used here is based on reach-average shear stresses (rather than difficult to estimate local stresses) and riffle zone mean substrate size (rather than the much harder to estimate reach-average substrate size). Because of variations in bed pavement structure, there is some uncertainty in the literature concerning the precise value of Shield's constant (0.06 in eq. 2 is the conventional value) that best describes the onset of sediment motion (Dingman 1984). The value selected under any given conditions will affect the computed τ_c and predicted local bed transport rates. However, given the uncertainty in the precise distribution of local shear stresses, and given the variation in substrate size among individual riffles in a reach, the computed reach-average mobility ratio (eq. 3) is not intended, nor is it designed, to produce meaningful estimates of local gravel transport rates. The mobility ratio is used here only as an empirical predictor, useful for explaining observed variations in levels of spawning bed disturbances across a range of reach characteristics and flood levels.

Results

The main hydraulic variables reconstructed for each flood

© 2000 NRC Canada

Fig. 3. Definition diagram illustrating the distinction between high- and low-velocity sides of the thalweg at riffles and potential spawning zones. See text for further explanation.

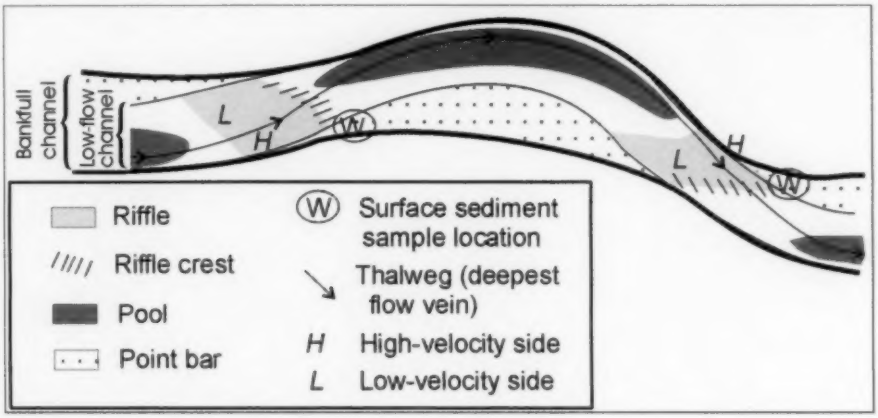

Table 2. Hydraulic and sediment transport characteristics of the study floods in each reach.

Flood event	Reach	Peak discharge ($m^3 \cdot s^{-1}$)	R (m)	$\bar{\omega}$ ($W \cdot m^{-2}$)	$\bar{\tau}_o$ (Pa)	$\bar{\tau}_c$ (Pa)	Mobility ratio
May 16, 1996	B	140	1.5	104	41	29.0	1.4
	C		1.5	61	38	45.5	0.8
July 20, 1996	B	250	2.0	178	54	29.0	1.9
	C		2.1	105	53	45.5	1.2
May 25, 1997	A	90	1.2	71	39	42.5	0.9
	B		1.4	54	38	29.0	1.3
	C		1.3	37	33	45.5	0.7

Note: $\bar{\omega}$ is the reach-average unit flow power (Dingman 1984). Other symbols are as described in Materials and methods.

in the three study reaches are presented for a total seven reach–flood combinations (Table 2). Reach A measurements were made only for the May 1997 flood. Mobility ratios vary by a factor of 2.7, from a minimum of 0.7 (May 1997 flood in reach C) to a maximum of 1.9 (July 1996 flood in reach B). Potential spawning zones and corresponding high-velocity, thalweg, and low-velocity subzones were delimited for each reach and flood event (e.g., Fig. 4). Reach A includes three distinct riffle zones, while reaches B and C each include two.

Important scour and fill disturbances were triggered in the study reaches and the corresponding spawning zones by each of the three study flood events (Fig. 5). Over large areas, vertical changes exceeded 0.4 m in amplitude. In the downstream half of reach B, the extreme July 1996 flood produced over 0.8 m of scour near the eroding left bank, extending to the head of the following point bar. Over 0.8 m of fill accompanied the advance of the right bank point bar in that zone.

The statistics on the distribution of scour and fill in the spawning zones and subzones are summarized for the three reaches and flood events (Table 3). During the extreme flood of July 1996, 43% of the entire potential spawning area of reach B underwent over 20 cm of net scour, with 78% of the high-velocity subzones similarly affected. Net fill greater than 20 cm, for the same event, affected 19% of the total spawning area in reach B and 36% of the low-velocity subzones. The 20- and 30-cm scour thresholds were chosen conservatively, in light of the published egg scour criteria for Atlantic salmon (15 cm depth to top and 30 cm to bottom of egg pockets; DeVries 1997). These two thresholds thus correspond to different intensities of damage to existing egg pockets. Scour exceeding 20 cm would most likely lead to some egg loss at any Atlantic salmon redd site, while essentially complete egg loss would be expected where scour exceeds 30 cm. A symmetrical tabulation to that for scour was also done for fill using the same 20- and 30-cm thresholds (Table 3). However, until studies establish clear criteria for thickness of freshly accreted sediments (i.e., net fill) causing entombment, these results are merely descriptive and cannot be firmly tied to fry mortality. The probable implications of net accretion of more than 30 cm over redd sites will be considered further in the Discussion.

Given the interreach variability in slope, channel geometry, and substrate size, the estimated reach-scale mobility ratios, integrating information on these three types of factors, can be used as empirical predictors of the intensity of scour and fill disturbance for various flood events and reaches (Fig. 6). Regressions are given for the percentages of reach-aggregate spawning areas having undergone more than 20 and 30 cm of scour and fill plotted against mean event mobility ratio in each reach (N = 7, corresponding to each reach–event combination listed in Table 2). The plots display clearly that the higher the mobility ratio achieved by the peak flow, the more spatially extensive are the spawning areas deeply disturbed by either scour or fill (all regression

© 2000 NRC Canada

Fig. 4. Bed topography prior to the first study flood in the three study reaches. Potential spawning zones and corresponding hydraulic subzones for that period are shown.

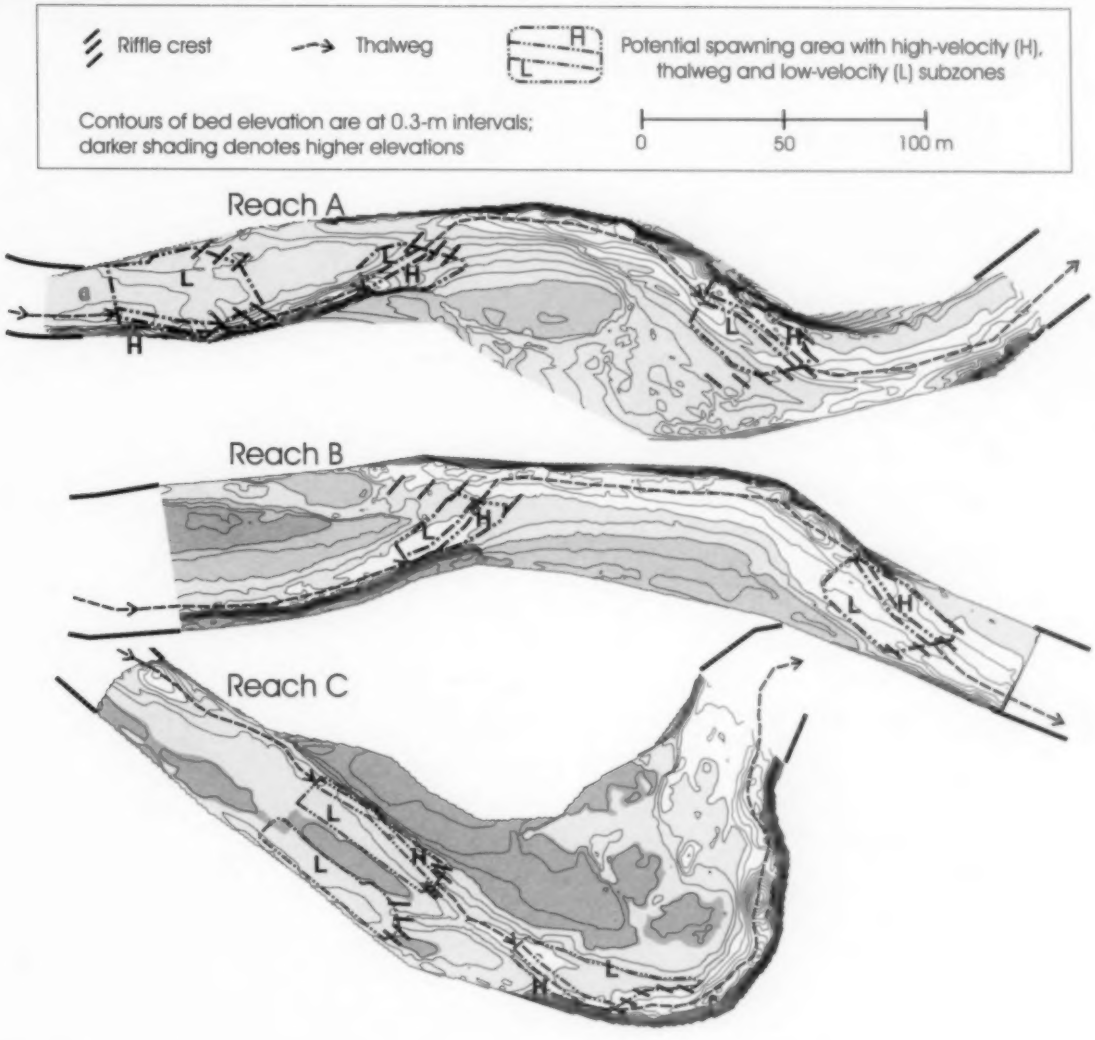

slopes are significantly greater than zero at the $p = 0.05$ level). In the study reaches, the nominal mobility ratio explains between 31 and 58% of the variations in the relative extent of disturbed areas within the potential spawning habitat (i.e., combining all subzones).

Analysis of the disturbance patterns for each hydraulic subzone separately (Fig. 7) discloses spatial differences among subzones (i.e., high velocity, thalweg, and low velocity) in the susceptibility to scour or fill, particularly for stronger flood events. The relationships for scour exceeding 20- and 30-cm thresholds (Fig. 7) reveal that the percentage of spawning areas undergoing significant scour increases with event mobility ratio in the high-velocity and thalweg subzones (although less rapidly in the latter). In the low-velocity subzones, however, the percent scoured areas (approximately 10%) is essentially invariant with flood mobility ratio (Fig. 7*c*). The patterns for the spatial distribution of net fill (Fig. 7) are qualitatively the opposite of those just described for scour. The proportions of areas within the low-velocity subzones undergoing significant fill increase with mobility ratio (Fig. 7*c*), while in the thalweg and high-velocity zones, they are variable and relatively unresponsive to flood strength. The mobility ratio explains around 75% of the variation in areal extent of scour within high-velocity subzones (Fig. 7*a*) and 75–79% of the areal extent of fill within low-velocity subzones (Fig. 7*c*).

Discussion

The residual scatter observed about the regression models is to be expected, given the simplified nature of the reach-average mobility ratio as a predictor of riffle surface distur-

© 2000 NRC Canada

Fig. 5. Maps of net changes to the channel bed (scour or fill) in reach B caused by each of the three flood events. Note that because of the ongoing bed change, the limits of the potential spawning zones were redefined prior to each flood using the criteria described in the text (see Materials and methods).

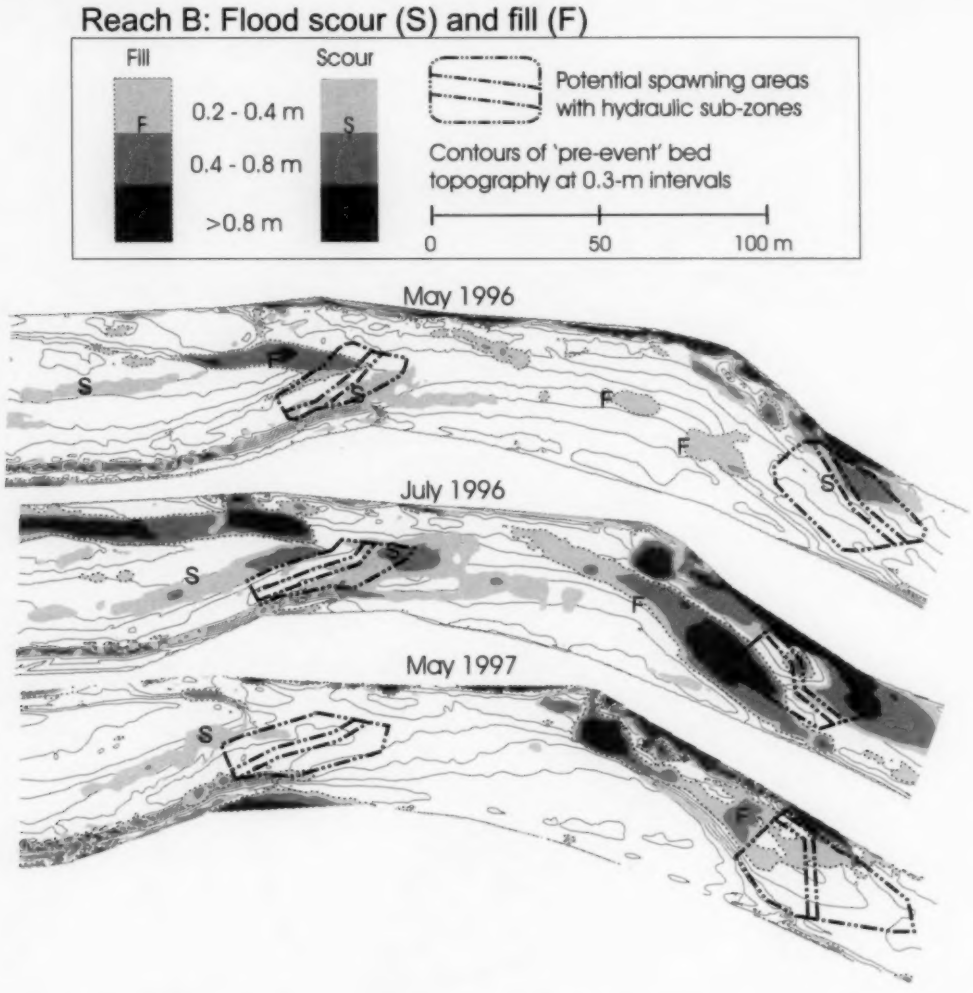

bance. This scatter mostly reflects the considerable variability of local geomorphic conditions over riffles of various shapes within a natural reach. The overall trends are relatively clear, however, linking mobility ratio to average percentage of spawning area undergoing significant scour or fill.

It is important to recall that the mobility ratio calculated here does not represent a ratio of shear stress at one riffle to the threshold for the entrainment of the bed material at the same location. Instead, a much more easily estimated ratio was employed, relating reach-average shear stress to the nominal stress level necessary to mobilize the average material located on riffles (or point bar heads) within the reach. Therefore, scour that was observed in riffle zones at mobility ratios as low as 0.7–0.8 in our data set reflected that, during floods, shear stresses systematically greater than reach-averaged values tend to affect high-velocity sides of riffles and nearby point bar heads (Yen 1970).

Andrews (1984), Ferguson and Ashworth (1991), and Milhous (1998) use reach-averaged mobility indices (or related Shield's stress ratios), conceptually similar to the one used here, to compare average sediment mobilization conditions among river reaches. Such reach-scale mobility ratios, although crude, provide a simple method of scaling flow strength by bed material calibre for interreach and interevent comparison. Development of more precise riffle-specific mobilization ratios based on two- or three-dimensional numerical resolutions of local stress distributions may eventually improve predictions of spawning bed evolution, but at a substantial cost in analytical complexity.

Interpreting scour and fill patterns in terms of egg loss probabilities

Observed scour patterns can further be interpreted in terms of probabilities of erosion of egg pockets for a flood of a given magnitude occurring during the egg incubation period. In light of the egg pocket scour criteria of DeVries

© 2000 NRC Canada

Table 3. Spawning zone disturbance statistics.

Reach	Event	Percentage of high-velocity subzone		Percentage of thalweg subzone		Percentage of low-velocity subzone		Percentage of total spawning area	
		S	F	S	F	S	F	S	F
A	May 1997	7 (5)	16 (14)	2 (0)	25 (12)	0 (0)	7 (4)	2 (1)	11 (7)
B	May 1996	57 (37)	0 (0)	32 (20)	0 (0)	6 (1)	8 (6)	25 (14)	4 (3)
	July 1996	78 (56)	6 (4)	37 (10)	10 (8)	12 (2)	36 (33)	43 (26)	19 (17)
	May 1997	0 (0)	13 (5)	0 (0)	11 (6)	6 (0)	21 (8)	2 (0)	16 (6)
C	May 1996	8 (1)	2 (0)	1 (0)	9 (5)	0 (0)	5 (2)	1 (0)	5 (2)
	July 1996	29 (26)	53 (48)	13 (8)	53 (47)	16 (9)	11 (9)	17 (10)	20 (18)
	May 1997	1 (0)	5 (3)	0 (0)	3 (1)	24 (15)	5 (0)	16 (10)	5 (1)

Note: Given are the percentages of the total area of spawning zones within each reach that underwent scour (S) or fill (F) exceeding significant thresholds during each flood event. Values are for scour or fill beyond the 20-cm threshold followed by values corresponding to the 30-cm threshold in parentheses.

Fig. 6. Regressions of the proportion of the total spawning areas within each reach that was affected (*a*) by over 20 cm or (*b*) by over 30 cm of net scour or net fill against the mobility ratio achieved by the flood in the reach; *p* values for the slope terms are given.

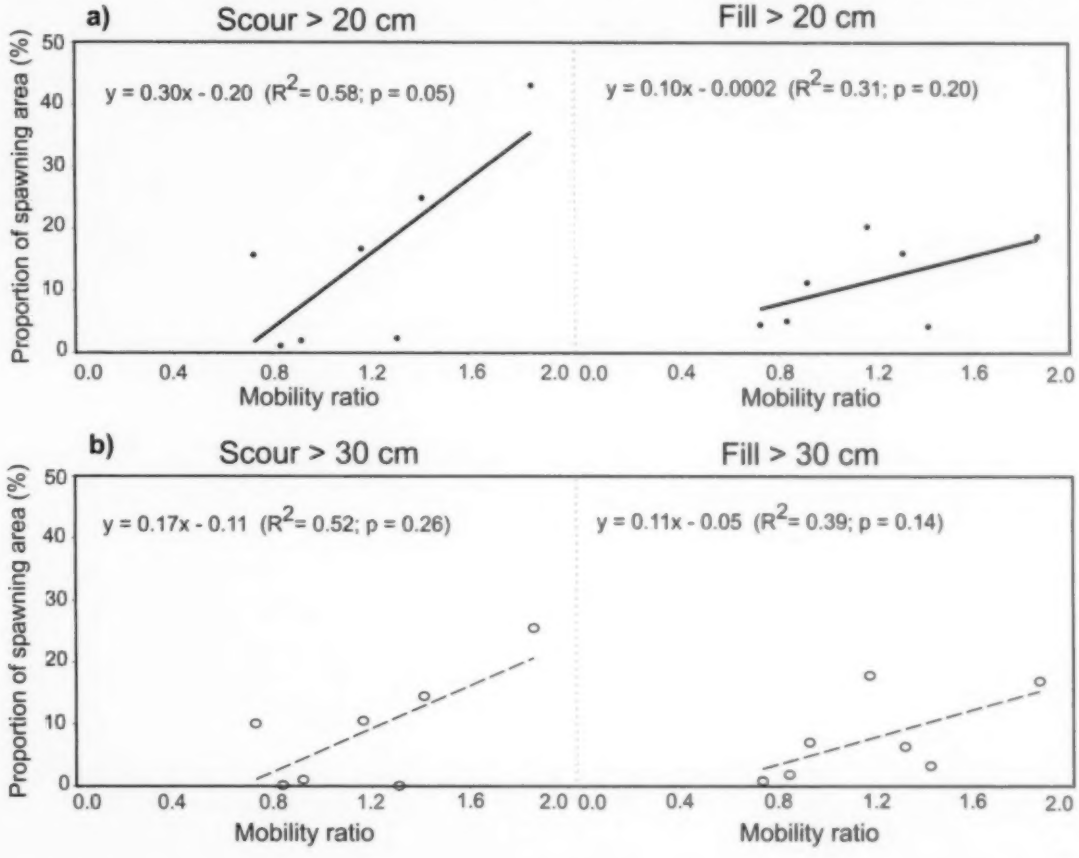
a)
Scour > 20 cm
Fill > 20 cm
y = 0.30x - 0.20 (R2= 0.58; p = 0.05)
y = 0.10x - 0.0002 (R2= 0.31; p = 0.20)
Proportion of spawning area (%)
Mobility ratio
b)
Scour > 30 cm
Fill > 30 cm
y = 0.17x - 0.11 (R2= 0.52; p = 0.26)
y = 0.11x - 0.05 (R2= 0.39; p = 0.14)
Proportion of spawning area (%)
Mobility ratio

(1997), the areal percentages of spawning zones with scour greater than the two thresholds can be interpreted as the probability of partial (scour >20 cm) or total destruction (scour >30 cm) of Atlantic salmon egg pockets, assuming that the pockets are uniformly distributed in the spawning zones of the reach. The trends for scour exceeding 30 cm imply that, during the weakest flood events recorded (mobility ratio = 0.7–0.8), egg pockets randomly distributed in the spawning zones had approximately a 2–3% probability of being totally eroded. For an extreme flood (e.g., mobility ratio = 1.8) occurring while eggs are incubating, the probability of total egg pocket destruction rises to around 20%, although pockets situated in high-velocity subzones would have a better than even (i.e., >50%) chance of being eroded in such strong events. The effects on Atlantic salmon reproduction of flood fill deposits exceeding 20 or 30 cm over

© 2000 NRC Canada

Fig. 7. Regressions of the proportions of (*a*) high-velocity, (*b*) thalweg, and (*c*) low-velocity spawning area subzones that were affected by net scour or net fill over the 20- and 30-cm thresholds against the mobility ratio achieved by the flood in the reach. The solid circles and solid regression lines are for the 20-cm threshold, and the open circles and broken lines are for the 30-cm threshold; *p* values for the slope terms are given.

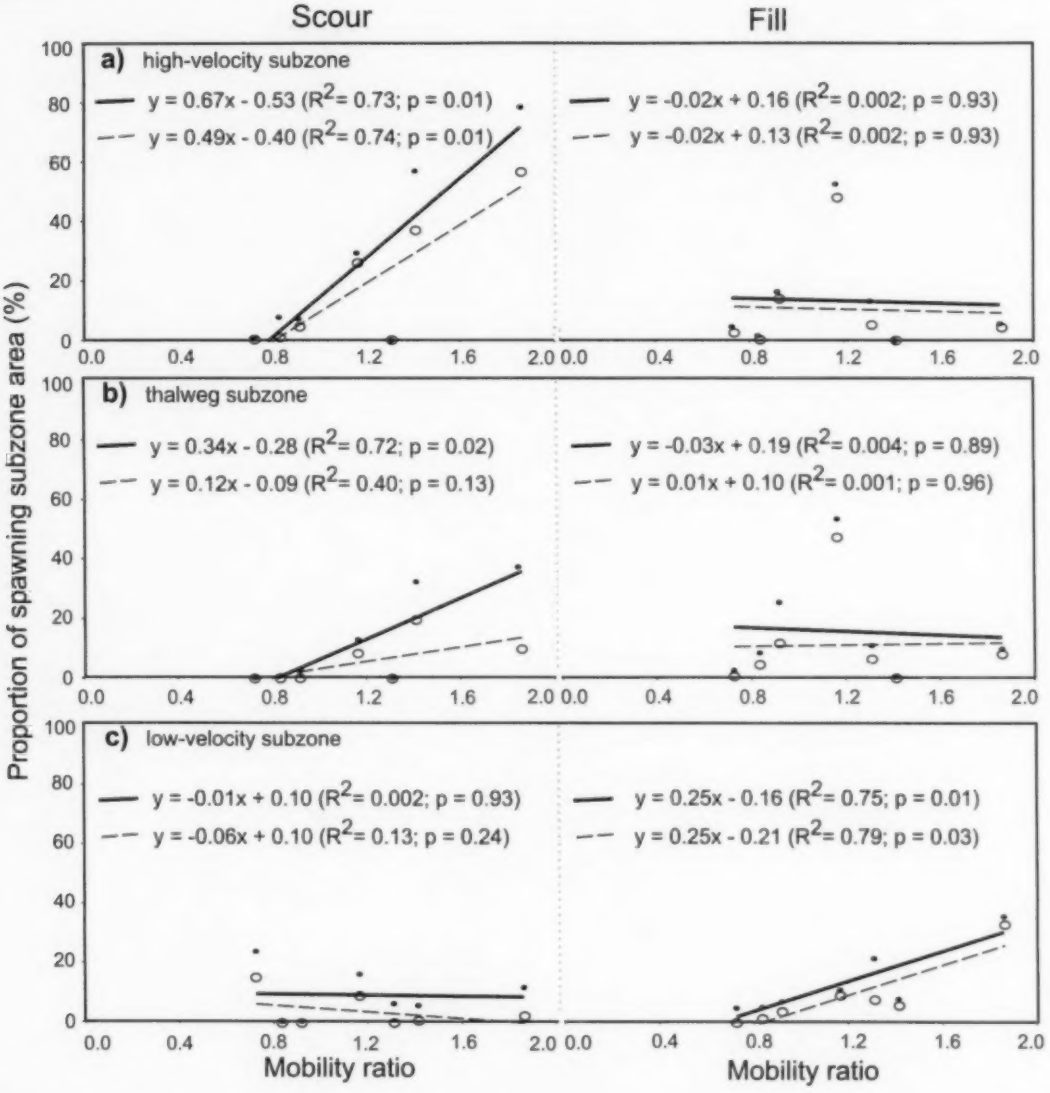
Scour
Fill
a) high-velocity subzone
y = 0.67x - 0.53 (R2= 0.73; p = 0.01)
y = 0.49x - 0.40 (R2= 0.74; p = 0.01)
y = -0.02x + 0.16 (R2= 0.002; p = 0.93)
y = -0.02x + 0.13 (R2= 0.002; p = 0.93)
b) thalweg subzone
y = 0.34x - 0.28 (R2= 0.72; p = 0.02)
y = 0.12x - 0.09 (R2= 0.40; p = 0.13)
y = -0.03x + 0.19 (R2= 0.004; p = 0.89)
y = 0.01x + 0.10 (R2= 0.001; p = 0.96)
c) low-velocity subzone
y = -0.01x + 0.10 (R2= 0.002; p = 0.93)
y = -0.06x + 0.10 (R2= 0.13; p = 0.24)
y = 0.25x - 0.16 (R2= 0.75; p = 0.01)
y = 0.25x - 0.21 (R2= 0.79; p = 0.03)
Proportion of spawning subzone area (%)
Mobility ratio
Mobility ratio

redds are less clear. Precise criteria based on thickness and sediment texture of flood accumulations will need to be developed and tested before our predictions of the extent of spawning zones with over 20 and 30 cm of fill can be interpreted explicitly in terms of probabilities of embryo mortality. However, the common occurrence of a high sand matrix content in flood fills over 30 cm thick, within low-velocity subzones in the study reaches, suggests a real potential for entombment of incubating embryos.

Potential egg scour in the absence of net bed lowering

In certain situations, egg scour might occur during floods in the absence of net bed lowering. During a single flood event, scour greater than 20–30 cm over a given redd could potentially be followed immediately by comparable fill. As well, egg pocket scour could theoretically ensue simply from deep gravel mobilization over a redd site in association with very intense transport, the bed level remaining essentially constant throughout. In theory, both of these processes could lead to the scouring of egg pockets that would not be detected by our field surveys of net change.

Hydraulic principles and published scour chain surveys suggest, however, that alternating sequences of scour and fill during a single flood wave occur mostly at pool cross sections or at constricted cross sections that are narrower than the reach average and are less common at riffle sites. Fur-

© 2000 NRC Canada

thermore, the detailed analysis of all flood change maps in this study (e.g., Fig. 5) indicated that the nature of bed change (either net scour or net fill) at any point on the riffle was generally predictable from the lateral position of the point, the antecedent channel shape, and the volume of gravel produced upstream by an eroding bank. These patterns suggest that, at least in moderate-energy and -sinuosity streams such as the one in this study, flood-induced disturbance over individual egg pockets will consist predominantly of either scour or fill, depending on lateral position. In very high intensity transport systems (e.g., braided rivers) or during protracted flood events, the occurrence of alternating scour/fill at a given point on a riffle during a single flood may, however, be more common.

Diverse lines of evidence also suggest that the thickness of the layer of gravel in motion at any instant during high flow is less than the depth at which egg pockets of many salmonid species are buried. A range of gravel transport studies (Carling 1987; Wilcock et al. 1996) indicate that the mean thickness of the mobilized gravel layer is in the order of the diameter of the coarsest particles common in the surface substrate (approximated by the D_{84} or D_{90} diameters in the mix), with a maximum thickness of mobilized gravels at any given time that may approach twice the local D_{90}. Many large salmonids appear to excavate redds below this one- to two-particle-deep surface layer. After comparing scour chain and egg pocket depth data at chum salmon (*Onchorhynchus keta*) spawning sites in Washington and Alaska, Montgomery et al. (1996) concluded that the top of egg pockets systematically lay below the surface traction layer of flood-entrained gravel. At Atlantic salmon redds, median subarmour particle diameter is often in the range of 1.5–3.0 cm, and the D_{90} at the redd surface rarely exceeds 7–8 cm (Peterson 1978; Kondolf and Wolman 1993). Thus, the maximum thickness of entrained bedload layers at high flow may in general be less than 15 cm, the typical depth corresponding to the top of egg pockets (DeVries 1997), implying that egg pocket scour is unlikely in the absence of bed lowering. This evidence suggests that our surveys of net change captured the dominant mode of egg pocket scour in the study reaches. We believe that the egg scour probability estimates presented above, although they may be conservative, are generally realistic for moderate-energy and -sinuosity streams comparable with the study system.

Redd location and spawner fitness: implications

The evidence presented, showing a systematic contrast in susceptibility to scour between high- and low-velocity sides of spawning zones, raises interesting questions concerning evolutionary pressures towards selection by salmonids of precise redd location at riffle sites. During the strongest floods, probabilities of significant scour are much greater in high-velocity subzones (over 50%), where flood shear stresses are particularly strong, compared with spawning sites on the low-velocity side of the riffles (probabilities under 10%). Our data thus indicate that there is a greater risk of loss of progeny if adults spawn on the high-velocity side of the thalweg, should a strong flood occur during the incubation period. Conversely, spawning on the low-velocity side may lead to higher probabilities of entombment due to fill during large floods. Moreover, gravel substrate on the low-velocity side of riffles often has significantly higher sand content (Payne and Lapointe 1997) due to somewhat weaker flood shear stresses and a helical circulation pattern that accumulates a finer sediment mix on this side of the riffle, closer to the downstream end of the previous point bar. Thus, irrespective of the heightened risk of postflood entombment, sedimentary cues might induce females to avoid spawning in these low-velocity subzones. One can hypothesize that, at least for the kind of simple riffle geometries illustrated in Fig. 3, observed gradients in flood disturbance probabilities across spawning zones and their implications for fitness may entail a selection for spawning behaviour in the deeper thalweg subzone at riffle sites.

In conclusion, fisheries biologists are aware of the possible adverse effects of strong floods on incubating salmonid embryos. The challenge for resource managers, however, is to quantify, even approximately, the effect on subsequent fry emergence of a strong flood in a given spawning reach or to identify stream reaches that are, due to their geomorphic characteristics, more susceptible to geomorphic disturbance and salmonid egg scour. The models presented provide a simple tool for predicting the average degree of riffle substrate disturbance and potential egg loss associated with a flood event in a given reach. The validity of the empirical relationships fitted to the Sainte-Marguerite River should, however, be further tested in gravel bed rivers of very different size and sedimentology. In particular, these empirical models are unlikely to apply to very small boulder-rich streams, where flood shear stresses are largely dissipated on well-anchored boulder structures that shelter pocket-sized gravel–cobble spawning beds from the full force of the flood.

Acknowledgements

This project was funded through the senior author's Natural Sciences and Engineering Research Council of Canada grant and through the support of CIRSA (Centre Interuniversitaire de Recherche sur le Saumon Atlantique) and its main funding partners (Natural Sciences and Engineering Research Council of Canada special collaborative grant (1995–1998), Economic Development Canada, Ministère de l'Environnement et Faune du Québec, and Alcan).

References

Allen, K.R. 1951. The Horokiwi stream: a study of a trout population. N.Z. Mar. Dep. Fish. Bull. No. 10.

Allen, J.D. 1995. Stream ecology. Structure and function of running waters. Chapman and Hall, London, U.K.

Andrews, E.D. 1984. Bed material entrainment and hydraulic geometry of gravel-bed rivers in Colorado. Geol. Soc. Am. Bull. **95**: 371–378.

Beland, K.F., Jordan, R.M., and Meister, A.L. 1982. Water depth and velocity preferences for spawning Atlantic salmon in Maine rivers. N. Am. J. Fish. Manage. **2**: 11–13.

Carling, P.A. 1987. Bed stability in gravel streams, with reference to stream regulation and ecology. *In* River channels: environment and process. *Edited by* K.S. Richards. Basil Blackwell, Oxford, U.K. pp. 321–347.

Chang, H.H. 1992. Fluvial processes in river engineering. Krieger Publishing Co., Malabar, Fla.

© 2000 NRC Canada

Church, M.A., McLean, D.G., and Wolcott, J.F. 1987. River bed gravel, sampling and analysis. *In* Sediment transport in gravel bed rivers. *Edited by* C.R. Thorne, J.C. Bathurst, and R.D. Hey. Wiley, Chichester, U.K. pp. 43–88.

DeVries, P. 1997. Riverine salmonid egg burial depths: review of published data and implications for scour studies. Can. J. Fish. Aquat. Sci. **54**: 1685–1698.

Dingman, S.L. 1984. Fluvial hydrology. W.H. Freeman and Company, New York.

Elwood, J.W., and Waters, T.F. 1969. Effects of floods on food consumption and production rates of a stream brook trout population. Trans. Am. Fish. Soc. **98**: 253–262.

Erman, D.C., Andrews, E.D., and Yoder-Williams, M. 1988. Effects of winter floods on fishes in the Sierra Nevada. Can. J. Fish. Aquat. Sci. **45**: 2195–2200.

Ferguson, R.I., and Ashworth, P. 1991. Slope induced changes in channel character along a gravel bed stream: the Alt-Dubhaig, Scotland. Earth Surf. Processes Landforms, **16**: 65–82.

Gibbons, D.R., and Salo, E.O. 1973. An annotated bibliography of the effects of logging on fish of the western United States and Canada. USDA For. Serv. Gen. Tech. Rep. PNW-10. Fisheries Research Institute, University of Washington, Seattle, Wash.

Gibson, R.J. 1993. The Atlantic salmon in fresh water: spawning, rearing and production. Rev. Fish Biol. Fish. **3**: 39–73.

Holtby, L.B., and Healy, M.C. 1986. Selection for adult size in female coho salmon (*Oncorhynchus kisutch*). Can. J. Fish. Aquat. Sci. **43**: 1946–1959.

Kondolf, G.M., and Wilcock, P.R. 1996. The flushing flow problem: defining and evaluating objectives. Water Resour. Res. **32**: 2589–2599.

Kondolf, G.M., and Wolman, M.G. 1993. The sizes of salmonid spawning gravels. Water Resour. Res. **29**: 2275–2285.

Kondolf, G.M., Cada, G.F., Sale, M.J., and Felando, T. 1991. Distribution and stability of potential salmonid spawning gravels in steep boulder-bed streams of the Eastern Sierra Nevada. Trans. Am. Fish. Soc. **120**: 177–186.

Lapointe, M.F., Secretan, Y., Driscoll, S.N., Bergeron, N., and Leclerc, M. 1998. Response of the Ha! Ha! River to the flood of July 1996 in the Saguenay Region of Quebec: large-scale avulsion in a glaciated valley. Water Resour. Res. **34**: 2383–2392.

Lisle, T.E. 1989. Sediment transport and resulting deposition in spawning gravels, north coastal California. Water Resour. Res. **25**: 1303–1319.

Lisle, T.E., and Lewis, J. 1992. Effects of sediment transport on survival of salmonid embryos in a natural stream: a simulation approach. Can. J. Fish. Aquat. Sci. **49**: 2337–2344.

Milhous, R.T. 1998. Modelling of instream flow needs: the link between sediment and aquatic habitat. Regul. Rivers Res. Manage. **14**: 79–94.

Milner, N.J., Scullion, J., Carling, P.A., and Crisp, T. 1981. The effects of discharge on sediment dynamics and consequent effects on invertebrates and salmonids in upland rivers. Adv. Appl. Biol. **6**: 152–220.

Montgomery, D.R., Buffington, J.M., Peterson, N.P., Schuett-Hames, D., and Quinn, T.P. 1996. Stream-bed scour, egg burial depths, and the influence of salmonid spawning on bed surface mobility and embryo survival. Can. J. Fish. Aquat. Sci. **53**: 1061–1070.

Montgomery, D.R., Beamer, E.M., Pess, G.R., and Quinn, T.P. 1999. Channel type and salmonid spawning distribution and abundance. Can. J. Fish. Aquat. Sci. **56**: 377–387.

Payne, B.A., and Lapointe, M.F. 1997. Channel morphology and lateral stability: effects on distribution of spawning and rearing habitat for Atlantic salmon in a wandering cobble-bed river. Can. J. Fish. Aquat. Sci. **54**: 2627–2636.

Pearsons, T.N., Li, H.W., and Lamberti, G.A. 1992. Influence of habitat complexity on resistance to flooding and resilience of stream fish assemblages. Trans. Am. Fish. Soc. **121**: 427–436.

Peterson, R.H. 1978. Physical characteristics of Atlantic salmon spawning gravel in some New Brunswick streams. Fish. Mar. Serv. Tech. Rep. 785. Fisheries and Oceans Canada, St. Andrews, N.B.

Resh, V.A., et al. 1988. The role of disturbance in stream ecology. J. North Am. Benthol. Soc. **7**: 433–455.

Scrivener, J.C., and Brownlee, M.J. 1989. Effects of forest harvesting on spawning gravel and incubation survival of chum (*Oncorhynchus keta*) and coho salmon (*O. kisutch*) in Carnation Creek, British Columbia. Can. J. Fish. Aquat. Sci. **46**: 681–696.

Seegrist, D.W., and Gard, R. 1972. Effects of floods on trout in Sagehen Creek, California. Trans. Am. Fish. Soc. **101**: 478–482.

Sparks, R.E., and Spink, A. 1998. Disturbance, succession and ecosystem processes in rivers and estuaries: effects of extreme hydrologic events. Regul. Rivers Res. Manage. **14**: 155–159.

Waters, T.F. 1995. Sediment in streams; sources, biological effects and control. American Fisheries Society, Bethesda, Md.

Wilcock, P.R., Kondolf, G.M., Graham Matthews, W.V., and Barta, A.F. 1996. Specification of sediment maintenance flows for a large gravel-bed river. Water Resour. Res. **32**: 2911–2921.

Yen, C.-L. 1970. Bed topography effect on flow in a meander. J. Hydraulics Division, ASCE, **96**(HY1): 57–73.

Ziemer, R.R., Lewis, J., Rice, R.M., and Lisle, T.E. 1991. Modelling the cumulative watershed effects of forest management strategies. J. Environ. Qual. **20**: 36–42.

© 2000 NRC Canada

Determining sampling date interval for precise in situ estimates of cumulative food consumption by fishes

Gregory W. Whitledge and Robert S. Hayward

Abstract: We tested the influence of sampling date interval (SDI) on precision of in situ estimates of cumulative food consumption by fishes. Daily rations of stream-dwelling green sunfish (*Lepomis cyanellus*) and impoundment-dwelling bluegill (*Lepomis macrochirus*) were estimated for 30 consecutive days using a low-effort procedure. Cumulative consumption by each species over the 30-day period (and 95% CIs) was estimated using Monte Carlo simulations. The effect of SDI on cumulative consumption estimates was examined by calculating cumulative consumption for SDIs of 1, 2, 3, 4, 5, 6, 7, 10, 14, and 30 days; the 1-day SDI served as a standard for evaluation of other SDIs. Cumulative consumption estimates began to fall outside the 95% CI for the 1-day SDI at SDIs of 3–4 days and did so with with increasing frequency as SDI increased. Error in estimating cumulative consumption was almost always ≤15% relative to the 1-day SDI standard at SDIs of 5 days or less but was as high as 26 and 39% at SDIs of 6 and 7 days, respectively. Our results suggest that sampling at least every 5 days may be required to obtain precise estimates of cumulative consumption by fishes in lotic systems and small impoundments.

Résumé : Nous avons vérifié l'influence du pas d'échantillonnage sur la précision des estimations *in situ* de la consommation alimentaire cumulative chez les poissons. Les rations quotidiennes administrées au crapet vert (*Lepomis cyanellus*) de milieu lotique et au crapet arlequin (*Lepomis macrochirus*) de milieu lentique ont été évaluées pendant 30 jours consécutifs au moyen d'une méthode simple. La consommation cumulative de chaque espèce pendant la période de 30 jours (intervalle de confiance de 95%) a été estimée à l'aide de simulations Monte Carlo. L'effet du pas d'échantillonnage sur les estimations de la consommation cumulative a été examiné par un calcul de la consommation cumulative pour les pas d'échantillonnage de 1, 2, 3, 4, 5, 6, 7, 10, 14 et 30 jours; le pas d'échantillonnage de 1 jour a servi de norme d'évaluation des autres pas d'échantillonnage. Les estimations de consommation cumulative ont commencé à dépasser l'intervalle de confiance de 95% du pas d'un jour aux pas d'échantillonnage de 3 et 4 jours, et ainsi de suite avec une fréquence croissante à mesure que le pas d'échantillonnage augmentait. L'erreur de l'estimation de la consommation cumulative était presque toujours ≤15% par rapport à la norme d'un jour pour les pas de 5 jours ou moins, mais atteignait respectivement 26% et 39% pour les pas de 6 et 7 jours. D'après nos résultats, il faudrait effectuer un échantillonnage tous les cinq jours au moins pour obtenir une estimation précise de la consommation cumulative des poissons dans des systèmes lotiques et des petites retenues d'eau.

[Traduit par la Rédaction]

Introduction

In situ estimates of food consumption have been used to predict the impact of fishes on prey populations (Ruggerone 1989; Maldeniya 1996; Buckel and Conover 1997), to assess the effects of pollution on fish population energetics (Hayward and Margraf 1987), to test for the existence of competition among fishes (Hanson and Leggett 1986; Persson 1986), to evaluate submaintenance feeding as a possible cause for declines in a trophy trout fishery (Weiland and Hayward 1997), to assess the energetic implications of diel migrations (Gauthier and Boisclair 1997), and to explain natural patterns of fish mortality (McGurk 1984) and growth (Boisclair and Leggett 1989). Field estimates of food consumption by fishes are also frequently used to test bioenergetics model predictions (e.g., Rice and Cochran 1984; Arrhenius and Hansson 1994; Schaeffer et al. 1999) and to test radioisotopic estimates of consumption (J. Gingras and D. Boisclair, unpublished data). Determination of fish daily ration in situ is labor intensive, requiring estimates of food weights in fish stomachs or complete digestive tracts over a 24-h period and estimates of gastric evacuation rates (Eggers 1977; Elliott and Persson 1978; Jobling 1981), although some labor-reducing procedures have been developed (Boisclair and Leggett 1988; Hayward and Hiebert 1993).

Estimates of food consumption by fishes over relatively long time periods, such as a month, season, or year, have been made by integrating time series of daily ration estimates (e.g., Persson 1983; Boisclair and Leggett 1985; Hayward and Margraf 1987). However, because in situ estimation of fish daily ration is so labor intensive, such time series usually involve daily ration estimates made at weekly, monthly, or even longer intervals (e.g., Hayward and

Received July 27, 1999. Accepted December 16, 1999.
J15263

G.W. Whitledge[1] and R.S. Hayward. Department of Fisheries and Wildlife Sciences, School of Natural Resources, 302 Anheuser-Busch Natural Resources Building, University of Missouri, Columbia, MO 65211, U.S.A.

[1]Author to whom all correspondence should be addressed.
e-mail: c615099@showme.missouri.edu

© 2000 NRC Canada

Margraf 1987; Boisclair and Leggett 1989; Weiland and Hayward 1997). The basis for selecting such sampling date intervals (SDIs) is not well established, is rarely justified, and is often based as much or more on availability of funds or human resources than on the need to sample frequently enough to ensure a desired level of precision.

The accuracy of in situ food consumption estimates over long time periods depends on the assumption that fish daily ration does not exhibit large day-to-day variations during intervals between sampling dates (Trudel and Boisclair 1993). Using a simulated 60-day series of daily ration values, Trudel and Boisclair (1993) showed that estimates of cumulative food consumption by hybrids of northern redbelly dace and finescale dace (*Phoxinus eos* × *Phoxinus neogaeus*) in a Canadian lake did not vary by more than 19.3% for 1- to 30-day SDIs and suggested that accurate estimates of long-term consumption rates could be determined by sampling at 3- to 4-week SDIs. However, Trudel and Boisclair (1993) noted that greater levels of environmental variation could result in larger day-to-day variation in food consumption than they observed and that a fuller picture of such variation was warranted across environments and fish species so that appropriate SDIs could be applied in long-term consumption studies. In this paper, we evaluate the influence of SDI on estimates of cumulative food consumption by centrarchids in a stream and a small impoundment, two system types in which relatively high levels of environmental variation might be expected to result in larger day-to-day variation in fish daily ration than in natural lakes.

Methods

Species and study areas

This study was conducted using a lentic population of bluegill (*Lepomis macrochirus*) and a lotic population of green sunfish (*Lepomis cyanellus*). Bluegill (50–100 mm total length) were collected from Ashland Lake, a small impoundment (surface area = 13 ha, mean depth = 2 m) near Columbia, Missouri. Green sunfish (53–105 mm total length) were collected from Hinkson Creek, a third-order stream that flows through the city limits of Columbia. Although the two study sites are in close proximity to one another, they are in separate watersheds.

Field procedures and estimates of daily ration

Daily rations of each population were estimated for 30 consecutive days beginning on 15 July 1996 using a low-effort in situ procedure (Hayward et al. 1991; Hayward and Hiebert 1993; Madon 1998). This approach is based on consistent findings across different fish species that constant proportions (b_t) exist between food weights in the stomachs of fish in a population at particular times of the day (F_t) and average food weights in stomachs over 24-h periods (F) (Hayward and Hiebert 1993; Madon 1998). When b is known for a particular time of day, average daily food weight in stomachs can be estimated for a given day from the mean food weight in stomachs of fish collected in a single sample at time (t) on that day according to

$$F = b_t \times F_t. \quad (1)$$

Once F has been estimated for a given day, daily ration (DR) can be readily estimated according to Eggers' (1977) model as

$$\mathrm{DR} = F \times R \times 24 \quad (2)$$

where R is gastric evacuation rate. Best estimates of F have been found to arise from collections made at times of the day when feeding activity is relatively high, this being indicated by relatively high food weights in stomachs. Values of b_t have been shown to remain remarkably stable over time (weeks to years) such that b values, once estimated, can be used to determine F values on future days from single fish collections (Hayward et al. 1991; Hayward and Hiebert 1993). Low-effort regression models developed for a particular species have also been shown to reliably estimate daily ration for closely related species in geographically and temporally distinct systems when both are diel feeders (Madon 1998).

Diel sampling was conducted for each population 3 days prior to the beginning of the 30-day sampling series in July 1996. This was done to identify times of day when food weights in stomachs were relatively high and to estimate b_t values. Fish were collected every 4 h over 24 h (seven collections per site) by seining (Ashland Lake) or by backpack electrofishing (Hinkson Creek). Specific food weights (grams per gram dry weight) were determined individually for 10 fish from each sampling time at each site. Diel collections revealed that relatively high food weights occurred near 22:00 for both fish populations (Fig. 1). Although fish stomachs were also relatively full at other times, we selected 22:00 as the sampling time so that our work would not coincide with boating and fishing activity.

To estimate $b_{22:00}$ and its standard error and to verify that $b_{22:00}$ values were stable over time, seven additional diel collections of bluegill from Ashland Lake were made weekly during May and June 1998. Values of $b_{22:00}$ and its standard error were estimated by regressing the means of median food weights in fish stomachs from each of these seven diel collections on mean food weights in stomachs at 22:00, where $b_{22:00}$ is the slope of the regression line. There was a significant linear relationship between these variables ($r^2 = 0.78$, $p < 0.02$), indicating that food weights in stomachs at 22:00 were a good predictor of mean daily food weight in stomachs of fish from this population during May and June 1998. Values of $b_{22:00}$ derived solely from the 1996 diel collections from Ashland Lake (0.82) and Hinkson Creek (0.91) were within 1 and 2 standard errors, respectively, of the $b_{22:00}$ value estimated for the seven diel collections made in 1998 (0.79), suggesting that the diel feeding patterns and $b_{22:00}$ values observed during 1996 were not atypical for these populations during summer. Therefore, values for $b_{22:00}$ and its standard error that were ultimately used in calculating daily rations for both populations were estimated by regressing means of median food weights in fish stomachs from all nine diel collections (eight from Ashland Lake, one from Hinkson Creek) on mean food weights in stomachs at 22:00. This relationship was highly significant ($r^2 = 0.93$, $p < 0.0001$) and had an intercept that was not significantly different from zero. Therefore, a second regression was performed in which the intercept was forced through the origin. The slope of the resulting regression line (0.88) and its standard error (0.035) were used as estimates of $b_{22:00}$ and its standard error in all subsequent calculations of daily ration for both populations.

To construct a time series of daily rations for each population, once-daily collections were made at 22:00 at each site for 30 consecutive days beginning on 15 July 1996 and specific food weights (grams per gram dry weight) in fish stomachs were estimated for 7–10 fish from each site on most dates. On one date in Hinkson Creek and on five dates in Ashland Lake, only one or two fish could be collected. Catches of fewer than 10 fish per sample occurred consistently after about 15 days of sampling, which suggests that we began to deplete local fish densities during our sampling period (Fig. 2). However, comparison of fish catches with daily ration estimates indicated that decreasing densities were not influencing consumption rates. Sampling was not conducted on one date (day 6) in Hinkson Creek due to high discharge; daily ration for Hinkson Creek green sunfish on this date was estimated by

© 2000 NRC Canada

Fig. 1. Means (±SE) of specific food weight in stomachs of (*a*) bluegill from Ashland Lake and (*b*) green sunfish from Hinkson Creek at 4-h intervals over a 24-h period on 14 July 1996.

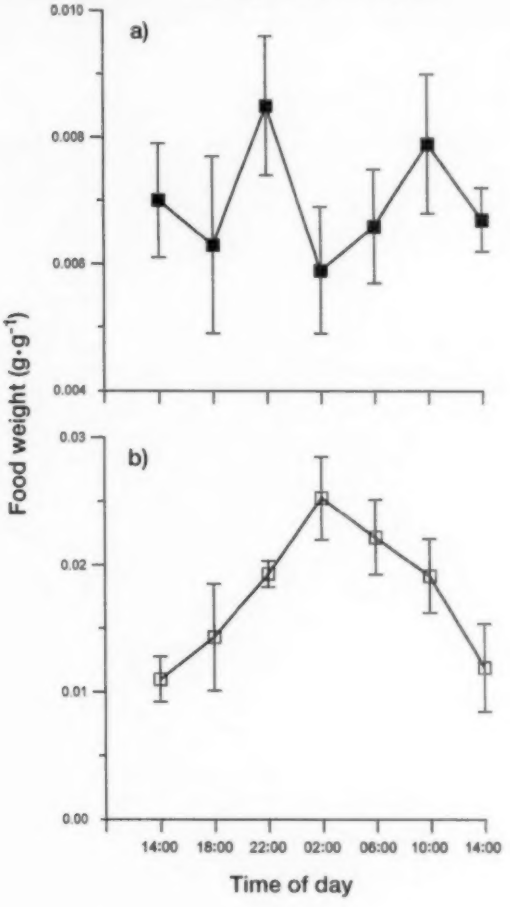

Fig. 2. Estimated mean daily rations and 95% CIs of mean daily rations for (*a*) bluegill from Ashland Lake and (*b*) green sunfish from Hinkson Creek over the 30-day period beginning 15 July 1996. Numbers above or below data points indicate the number of fish collected on each date.

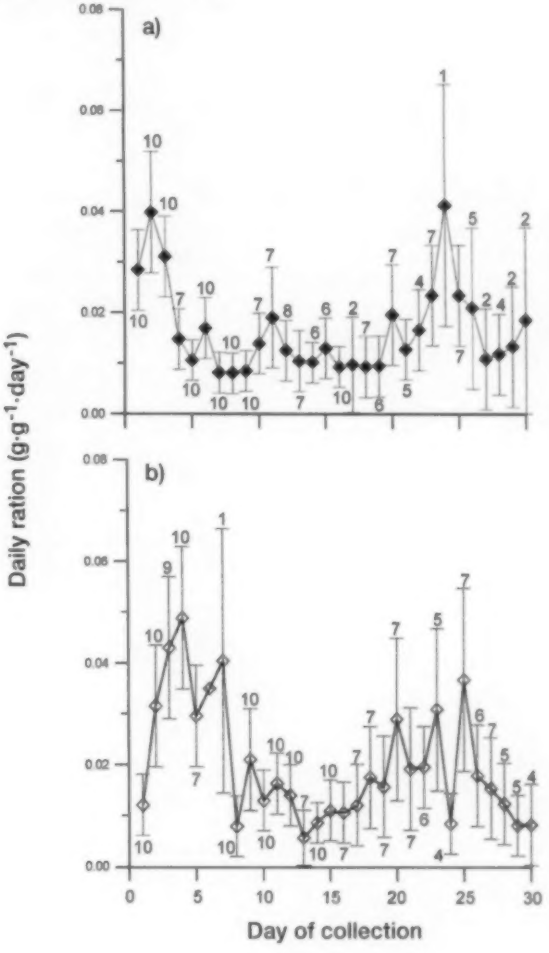

linearly interpolating between daily rations estimated for days 5 and 7. Mean specific food weights for each population on each date and their associated standard errors were log transformed to correct departures from normality. On dates when only one fish was collected (one date for each site), the standard error of mean log-transformed food weights (SELFW) was estimated using multiple linear regressions with mean of log-transformed food weight (MLFW) and sample size (N) as independent variables: SELFW = $-0.0766 \times \text{MLFW} - 0.0259 \times N + 0.0261$ (Hinkson Creek: $r^2 = 0.45$, $p < 0.001$) and SELFW = $-0.0227 \times \text{MLFW} - 0.0229 \times N + 0.2343$ (Ashland Lake: $r^2 = 0.42$, $p < 0.05$). These regressions were derived from values of MLFW, SELFW, and N from the other sampling dates for each population.

Daily ration (grams dry weight of food consumed per gram dry body weight per day) and its standard error were estimated for each population on each date using Monte Carlo simulations. To estimate gastric evacuation rate and account for error associated with gastric evacuation rate in calculations of daily ration, a temperature-dependent gastric evacuation function was constructed using data from Windell (1966), Seaburg and Moyle (1964), and Richardson and Nickol (1998) and was used for both species. A previous study has indicated that energetic responses to temperature and body weight are similar for bluegill and hybrid sunfish (bluegill × green sunfish) (Whitledge et al. 1998). Pseudo-values of gastric evacuation rate (R^*) were generated as

$$(3) \quad R^* = (-0.9089 + (\text{SE}_i \times \text{RN}_1)) + (0.3226 + (\text{SE}_s \times \text{RN}_2)) \times \text{LNTEMP}$$

where LNTEMP is the natural log of water temperature on each date, RN_1 and RN_2 are normally distributed random variables, each with a mean of zero and a standard deviation of 1, and SE_i and SE_s are standard errors of the y-intercept (0.0704) and slope (0.0227) of the gastric evacuation function, respectively. For each population on each date, 100 series of pseudo-values of daily ration were produced. Pseudo-values of daily ration were generated as

$$(4) \quad \text{DR} = (F_d + (\text{SEF}_d \times \text{RN}_3)) \times (b_{22:00} + (\text{SE}b_{22:00} \times \text{RN}_4)) \times R^* \times 24$$

where F_d is mean log-transformed food weight in fish stomachs on date d at 22:00, SEF_d is the SE of mean log-transformed food

© 2000 NRC Canada

weight on date d, $b_{22:00}$ is the proportion (0.88) relating food weight at 22:00 to average 24-h food weight, $SEb_{22:00}$ is the SE of $b_{22:00}$ (0.035), R^* is a pseudo-value for gastric evacuation rate at the water temperature measured on each date, and RN_3 and RN_4 are normally distributed random numbers, each with a mean of zero and a standard deviation of 1. The mean and 95% CI of daily ration on each date were defined by the 50, 2.5, and 97.5 percentiles of the 100 time series of pseudo-values of daily ration, respectively. Standard error of mean daily ration on each date was estimated by dividing the standard deviation of estimated mean daily ration by the square root of the number of fish sampled on that date.

Environmental conditions

Water temperature (degrees Celsius) was measured daily just below the surface at both sites so that gastric evacuation rates could be estimated on each day for each population. For evaluation of environmental correlates of daily consumption, degree of turbidity was generally noted and diet composition of up to five fish was assessed on each sampling date in both Hinkson Creek and Ashland Lake. Daily rainfall data applicable to both sites were secured for the full sampling period from a local weather station. Correlation analysis was used to assess which environmental variables may have influenced the daily ration patterns at the two sites.

Influence of SDI on precision of cumulative consumption estimates

Cumulative consumption by bluegill and green sunfish during the 30-day period and the respective 95% CIs were estimated from our 30-day time series of daily ration values using Monte Carlo simulations. Daily rations and their associated standard errors were log transformed prior to simulations to correct departures from normality. The influence of SDI on precision of cumulative consumption estimates was evaluated by calculating cumulative consumption, defined as the area under the curve delineated by pseudo-values of daily ration, for SDIs of 1, 2, 3, 4, 5, 6, 7, 10, 14, and 30 days. For each SDI, 100 series of pseudo-values of daily ration were produced. Pseudo-values of mean daily ration were generated independently for each sampling date as

$$(5) \qquad DR_d^* = DR_d + (SE_{DR} \times RN)$$

where DR_d^* is a pseudo-value of mean daily ration on day d, DR_d is the estimated mean daily ration, SE_{DR} is the standard error of the estimated mean daily ration, and RN is a normally distributed random number with a mean of zero and a standard deviation of 1 (Trudel and Boisclair 1993). Daily rations for dates not sampled using a particular SDI were linearly interpolated between daily ration values for dates being simulated, as is typically done in field studies to calculate cumulative consumption from a series of in situ food consumption estimates when SDI is >1 day (Boisclair and Leggett 1989). The mean and 95% CI of cumulative consumption for each SDI were defined by the 50, 2.5, and 97.5 percentiles of the 100 time series of pseudo-values of daily ration, respectively. Because not all SDIs included daily rations for days 1 and 30 of the data set, the duration of the time series of daily ration values varied with SDI (ranging from 21 to 30 days). To standardize cumulative feeding rates to a 30-day period for all SDIs, cumulative consumption was multiplied by 30 and divided by the duration of the time series for each SDI. Cumulative consumption calculated for a SDI of 1 day served as the standard for comparison of all other SDIs.

Starting date (the first day of sampling) could have a strong influence on precision of cumulative consumption estimates for a given SDI >1 day if large day-to-day variations in fish daily ration are present. To account for the potentially important influence of starting date on precision of cumulative consumption estimates, cumulative consumption for each population over the 30-day period was also calculated using all possible starting dates for each SDI. This procedure yielded two estimates of cumulative consumption for an SDI of 2 days, three estimates for an SDI of 3 days, etc. Only two starting dates were considered for the 14-day SDI because any of the other 12 possible starting dates would have excluded a relatively large portion of the data set. Cumulative consumption rates were standardized to a 30-day period by multiplying by 30 and dividing by the duration of the time series for each SDI.

Because SDI required for precisely estimating cumulative consumption is influenced by temporal variation in fish daily ration, accuracy of daily ration estimates used in determining appropriate SDIs is important. Since stomach contents are frequently quite variable among fish during a given sampling period, the accuracy of mean food weights in fish stomachs obtained on dates when only one or two fish were sampled is questionable. To account for the possibility that estimates of daily ration on dates when only one or two fish were sampled may have biased our estimates of cumulative consumption, and hence our conclusions of SDI required for both populations, we repeated our analysis without the estimates of daily ration for these dates (one date in Hinkson Creek and four dates in Ashland Lake). Instead, daily ration values for these dates were obtained by linearly interpolating between the previous and subsequent days' estimates of mean daily ration. Daily ration for day 30 in Ashland Lake was not interpolated because it was at the end of the data set. When we performed our analysis using interpolated daily ration values for dates on which only one or two fish were sampled, our conclusions regarding SDI required for obtaining precise cumulative consumption estimates for both populations were not altered. Therefore, our results and discussion will be limited to our analysis using our original estimates of daily ration on these dates for both populations.

Results

Daily ration

Mean daily ration ranged from 0.008 to 0.042 g·g dry weight^{-1} for bluegill in Ashland Lake (Fig. 2*a*) and from 0.006 to 0.049 g·g dry weight^{-1} for green sunfish in Hinkson Creek (Fig. 2*b*). Nonoverlapping 95% CIs of mean daily ration for several pairs of sampling dates within each 30-day series indicated significant differences in mean daily ration among sampling dates for each population.

Environmental conditions

Water temperature ranged from 22 to 33°C in Ashland Lake and from 21 to 32°C in Hinkson Creek. Sharp declines in daily ration for both bluegill in Ashland lake and green sunfish in Hinkson Creek on days 7 and 8 and days 26 and 27 (Fig. 2) coincided with large increases in discharge (Hinkson Creek) and turbidity (Ashland Lake) immediately following heavy rain events.

As expected, daily rations were positively correlated with food weights in fish stomachs at 22:00 at both sites ($p < 0.05$). Pairwise correlations among daily water temperature, rainfall, turbidity, mean weight of fish sampled, diet diversity (number of prey taxa in fish diet), and food weights were evaluated for each site. Food weight was used as a response variable surrogate for daily ration so that possible correlations between consumption level and temperature could be validly assessed (daily ration values were calculated, in part, from temperature whereas food weights were not). At both sites, positive correlation was observed between food weight and temperature and between turbidity

© 2000 NRC Canada

and prior-day rainfall ($p < 0.05$). Negative correlation was found at both sites between temperature and prior-day rainfall and between temperature and turbidity ($p < 0.05$, except that $p = 0.08$ for the temperature versus rainfall relationship for Hinkson Creek). Hints of negative relationships between food weight and turbidity were also observed for both sites ($p = 0.18$ and 0.11 for Ashland Lake and Hinkson Creek, respectively). A marginal negative correlation was observed between food weight and number of prey items in the diet of green sunfish in Hinkson Creek ($p = 0.08$). There was a hint of a positive correlation between prior-day rainfall and number of prey items in the diet of green sunfish from Hinkson Creek, but this relationship was nonsignificant ($p = 0.18$).

Influence of SDI on precision of cumulative consumption estimates

Cumulative consumption estimated over the 30-day period using a 1-day SDI averaged 1133 mg dry for individual bluegill in Ashland Lake (Fig. 3*a*) and 2035 mg dry for individual green sunfish in Hinkson Creek (Fig. 3*b*). Cumulative consumption using SDIs >1 day ranged from 959 (6 days) to 1587 mg dry (30 days) for bluegill in Ashland Lake (Fig. 3*a*) and from 1005 (30 days) to 2228 mg dry (3 days) for green sunfish in Hinkson Creek (Fig. 3*b*). Estimates of cumulative consumption by bluegill in Ashland Lake over the 30-day period fell outside the 95% CI of the mean value for the 1-day SDI at SDIs of 4, 6, 10, and 30 days (Fig. 3*a*). The 95% CIs of the mean values for SDIs of 14 and 30 days overlapped the 95% CI of the mean value for the 1-day SDI; this occurred because 95% CIs of the mean values became much larger as SDI increased (Fig. 3*a*). For green sunfish in Hinkson Creek, cumulative consumption estimates began to differ from the reference value obtained using a 1-day SDI at an SDI of 7 days; consumption estimates obtained at greater SDIs were also significantly different from the reference value (Fig. 3*b*).

When all possible starting dates for each SDI were accounted for, cumulative consumption estimates over the 30-day period began to fall outside the 95% CI of the mean value for the 1-day SDI at SDIs of 3 and 4 days for both bluegill in Ashland Lake and green sunfish in Hinkson Creek (Fig. 4). Error in estimating cumulative consumption was almost always ≤15% relative to the mean value obtained from the 1-day SDI at SDIs of ≤5 days for both populations but rose to as high as 26 and 39% at SDIs of 6 and 7 days, respectively (Fig. 5). For both populations, at least one estimate of cumulative consumption was ≥33% different from the mean value obtained from the 1-day SDI at SDIs ≥7 days (Fig. 5). Maximum errors in estimating cumulative consumption were 44% (SDI = 10 days) for bluegill in Ashland Lake (Fig. 5*a*) and 51% (SDI = 30 days) for green sunfish in Hinkson Creek (Fig. 5*b*).

Discussion

Our results indicate that large day-to-day variations in fish daily ration can occur in lotic systems and small impoundments and that these day-to-day variations may strongly influence precision of cumulative consumption estimates with respect to a 1-day SDI. These results also indicate that sampling at least every 5 days would be required to obtain precise estimates of cumulative consumption for either of these two fish populations given the environmental conditions present at the time of our sampling. Our findings are in contrast with those of Trudel and Boisclair (1993), who found that long-term consumption rates of minnows in a Quebec lake did not vary by more than 19.3% among SDIs ranging from 1 to 30 days. Greater levels of environmental variation associated with lotic systems and impoundments as opposed to natural lakes may have resulted in greater day-to-day variations in daily ration observed in our study, resulting in a smaller SDI required to obtain precise estimates of cumulative consumption. Differences in fish species, fish size, and prey availability, size, and taxonomic composition could also be involved. Correlation analyses indicated two mechanistic pathways, both linked to rainfall, that may have influenced food consumption patterns of bluegill in Ashland Lake and green sunfish in Hinkson Creek during our 30-day study period and caused the patterns to be strikingly similar.

Fig. 3. Mean cumulative food consumption by (*a*) bluegill in Ashland Lake and (*b*) green sunfish in Hinkson Creek during the 30-day period estimated using SDI ranging from 1 to 30 days. Vertical lines represent 95% CIs of the mean values.

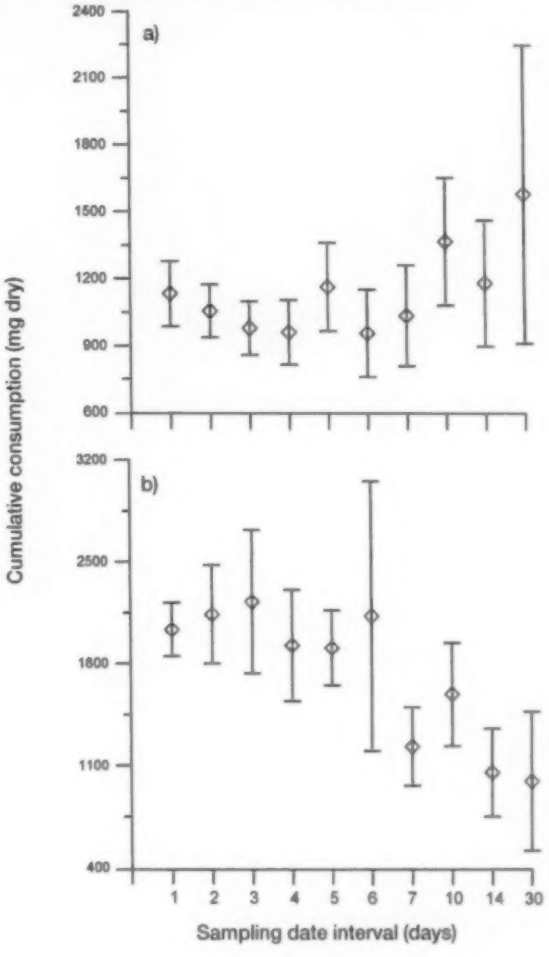

© 2000 NRC Canada

Fig. 4. Mean cumulative food consumption by (*a*) bluegill in Ashland Lake and (*b*) green sunfish in Hinkson Creek during the 30-day period estimated using SDI ranging from 1 to 30 days and all possible starting dates for each SDI. The vertical line around the mean value at SDI = 1 and the horizontal dashed lines indicate the 95% CIs around the mean value for SDI = 1.

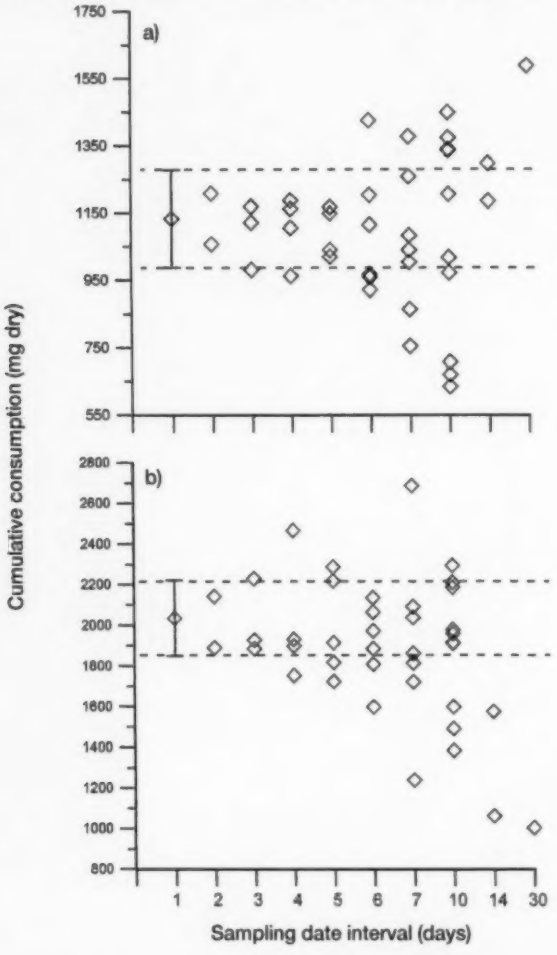

Fig. 5. Percent error in estimating mean cumulative food consumption (relative to sampling daily) during the 30-day period for (*a*) bluegill in Ashland Lake and (*b*) green sunfish in Hinkson Creek using SDI ranging from 2 to 30 days and all possible starting dates for each SDI.

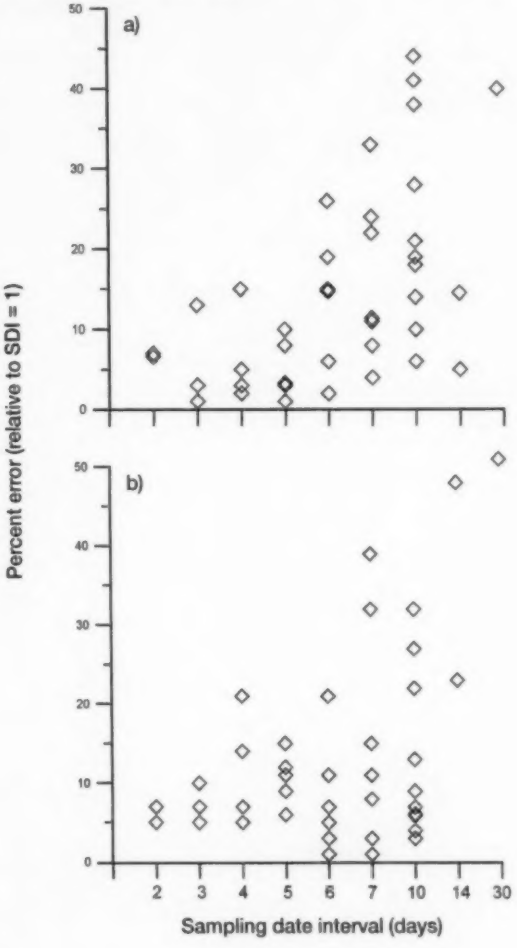

First, strong correlative results suggest that three multiday episodes of rainfall during the study period brought about significant declines in water temperatures that in turn reduced daily rations, probably by lowering fish appetites. A second indicated pathway was based on weaker but consistent correlation across both sites and appeared to involve impeded feeding capacity as a result of significant increases in turbidity at both sites within 24 h of rain events. Both sites showed weak negative responses in fish daily rations to the increased turbidity. These two mechanisms, both apparently triggered by rainfall, may explain the relatively high day-to-day variation in fish daily ration at our two study sites as well as the similarity of the 30-day consumption patterns of these two populations. Rainfall is likely an important source of environmental variation in lotic systems and small impoundments due to the relatively high watershed to surface area ratios of these systems, which result in greater fluctuations in water levels and turbidity compared with natural lakes. The effect of rainfall on environmental variation in streams and small impoundments in central Missouri is likely exacerbated during summer due to a favorable climate for frequent thunderstorms and the availability of sediment for transport into streams as a result of erodable soils and agricultural and other land-use activities. Further studies are needed to advance our understanding of how rainfall and other sources of environmental variation influence day-to-day variations in fish daily ration in aquatic systems in other geographic areas and how these in turn influence SDI required for precise estimates of cumulative food consumption by fishes. In the absence of additional information, we suggest that sampling should be conducted at least every 5 days when generating in situ estimates of cumulative food con-

© 2000 NRC Canada

sumption by fishes when high levels of environmental variation are expected a priori (e.g., in streams and riverine impoundments subject to the effects of fluctuating discharge).

Our findings also have implications for evaluation of bioenergetics model and radioisotopic estimates of food consumption by fishes (Ney 1990, 1993; J. Gingras and D. Boisclair, unpublished data). Tests of such models and procedures typically involve comparison of their predictions of food consumption with those of independent in situ estimates (e.g., Wahl and Stein 1991; Cartwright et al. 1998; Worischka and Mehner 1998). Thus, accuracy of these independent in situ estimates of food consumption is critical to the evaluation of a model's or procedure's ability to make accurate predictions itself. If cumulative consumption estimates are derived from field estimates of fish daily ration obtained using an SDI that is too large, bioenergetics model or radioisotopic predictions and in situ estimates of cumulative consumption may be in agreement but inaccurate, yielding a misleading corroboration. Inaccurate in situ consumption estimates also have the potential to yield false indications of deficiencies in radioisotopic procedures or bioenergetics models when predictions generated by these approaches and in situ estimates are not in agreement.

Our findings also illustrate the utility of low-effort procedures for estimating fish daily ration (Hayward et al. 1991; Hayward and Hiebert 1993; Madon 1998). The low-effort procedure allows estimates of fish daily ration to be made on consecutive days with relatively little sampling effort, reducing the likelihood of problems such as fish population depletion and lack of human resources. Use of this approach may facilitate studies similar to this one in other systems, leading to definition of a more general pattern of the influence of SDI on cumulative consumption estimates for fishes.

Acknowledgements

This study was supported by funds and equipment provided by the Missouri Agricultural Experiment Station and the Missouri Cooperative Fish and Wildlife Research Unit. We thank C.V. Bove for collecting the field and laboratory data.

References

Arrhenius, F., and Hansson, S. 1994. In situ food consumption of young-of-the-year Baltic Sea herring *Clupea harengus*: a test of predictions from a bioenergetics model. Mar. Ecol. Prog. Ser. **110**: 145–149.

Boisclair, D., and Leggett, W.C. 1985. Rates of food exploitation by littoral fishes in a mesotrophic lake. Can. J. Fish. Aquat. Sci. **42**: 556–566.

Boisclair, D., and Leggett, W.C. 1988. An in situ experimental evaluation of the Elliott and Persson and the Eggers models for estimating fish daily rations. Can. J. Fish. Aquat. Sci. **45**: 138–145.

Boisclair, D., and Leggett, W.C. 1989. Among-population variability of fish growth. I. Influence of the quantity of food consumed. Can. J. Fish. Aquat. Sci. **46**: 457–467.

Buckel, J.A., and Conover, D.O. 1997. Movements, feeding periods, and daily ration of piscivorous young-of-the-year bluefish, *Pomatomus saltatrix*, in the Hudson River estuary. Fish. Bull. U.S. **95**: 665–679.

Cartwright, M.A., Beauchamp, D.A., and Bryant, M.D. 1998. Quantifying cutthroat trout (*Oncorhynchus clarki*) predation on sockeye salmon (*Oncorhynchus nerka*) fry using a bioenergetics approach. Can. J. Fish. Aquat. Sci. **55**: 1285–1295.

Eggers, D.M. 1977. Factors in interpreting data obtained by diel sampling of fish stomachs. J. Fish. Res. Board Can. **34**: 290–294.

Elliott, J.M., and Persson, L. 1978. The estimation of daily rates of food consumption for fish. J. Anim. Ecol. **47**: 977–991.

Gauthier, S., and Boisclair, D. 1997. The energetic implications of diel onshore–offshore migration by dace (*Phoxinus eos* × *P. neogaeus*) in a small oligotrophic lake. Can. J. Fish. Aquat. Sci. **54**: 1996–2006.

Hanson, J.M., and Leggett, W.C. 1986. Effect of competition between two freshwater fishes on prey consumption and abundance. Can. J. Fish. Aquat. Sci. **43**: 1363–1372.

Hayward, R.S., and Hiebert, J.F. 1993. Low-effort regression estimation of average daily food weight in fishes: application to larval gizzard shad. Trans. Am. Fish. Soc. **122**: 834–844.

Hayward, R.S., and Margraf, F.J. 1987. Eutrophication effects on prey size and food available to yellow perch in Lake Erie. Trans. Am. Fish. Soc. **116**: 210–223.

Hayward, R.S., Margraf, F.J., Jr., Parrish, D.L., and Vondracek, B. 1991. Low-cost field estimation of yellow perch daily ration. Trans. Am. Fish. Soc. **120**: 589–604.

Jobling, M. 1981. Mathematical models of gastric emptying and the estimation of daily rates of food consumption for fish. J. Fish Biol. **19**: 245–257.

Madon, S.P. 1998. Low-effort regression estimation of daily ration in young walleye, *Stizostedion vitreum*. Can. J. Fish. Aquat. Sci. **55**: 2058–2066.

Maldeniya, R. 1996. Food consumption of yellowfin tuna, *Thunnus albacares*, in Sri Lankan waters. Environ. Biol. Fishes, **47**: 101–107.

McGurk, M.D. 1984. Effects of delayed feeding and temperature on the age of irreversible starvation and on the rates of growth and mortality of Pacific herring larvae. Mar. Biol. **84**: 13–26.

Ney, J.J. 1990. Trophic economics in fisheries: assessment of demand–supply relationships between predators and prey. Rev. Aquat. Sci. **2**: 55–81.

Ney, J.J. 1993. Bioenergetics modeling today: growing pains on the cutting edge. Trans. Am. Fish. Soc. **122**: 736–748.

Persson, L. 1983. Food consumption and competition between age classes in a perch *Perca fluviatilis* population in a shallow eutrophic lake. Oikos, **40**: 197–207.

Persson, L. 1986. Effects of reduced interspecific competition on resource utilisation in perch (*Perca fluviatilis*). Ecology, **67**: 355–364.

Rice, J.A., and Cochran, P.A. 1984. Independent evaluation of a bioenergetics model for largemouth bass. Ecology, **65**: 732–739.

Richardson, D.J., and Nickol, B.B. 1998. Gastric evacuation and movement of materials through the alimentary canal of green sunfish. Trans. Am. Fish. Soc. **127**: 1059–1066.

Ruggerone, G.T. 1989. Gastric evacuation rates and daily ration of piscivorous coho salmon (*Oncorhynchus kisutch* (Walbaum)). J. Fish Biol. **34**: 451–463.

Schaeffer, J.S., Haas, R.C., Diana, J.S., and Breck, J.E. 1999. Field test of two energetic models for yellow perch. Trans. Am. Fish. Soc. **128**: 414–435.

Seaburg, K.G., and Moyle, J.B. 1964. Feeding habits, digestion rates, and growth of some Minnesota warmwater fishes. Trans. Am. Fish. Soc. **93**: 269–285.

Trudel, M., and Boisclair, D. 1993. An in situ evaluation of the day-to-day variation in the quantity of food consumed by fish. Can. J. Fish. Aquat. Sci. **50**: 2157–2165.

Wahl, D.H., and Stein, R.A. 1991. Food consumption and growth of three esocids: field tests of a bioenergetics model. Trans. Am. Fish. Soc. **120**: 230–246.

© 2000 NRC Canada

Weiland, M., and Hayward, R.S. 1997. Cause for the decline of large rainbow trout in a tailwater fishery: too much putting or too much taking? Trans. Am. Fish. Soc. **126**: 758–773.

Whitledge, G.W., Hayward, R.S., Noltie, D.B., and Wang, N. 1998. Testing bioenergetics models under feeding regimes that elicit compensatory growth. Trans. Am. Fish. Soc. **127**: 740–746.

Windell, J.T. 1966. Rate of digestion in bluegill sunfish. Invest. Indiana Lakes Streams, **7**: 185–214.

Worischka, S., and Mehner, T. 1998. Comparison of field-based and indirect estimates of daily food consumption in larval perch and zander. J. Fish Biol. **53**: 1050–1059.

© 2000 NRC Canada

Detritivorous fish contamination in the Río de la Plata estuary: a critical accumulation pathway in the cycle of anthropogenic compounds

Juan C. Colombo, Claudio Bilos, Mauricio Remes Lenicov, Dario Colautti, Patricia Landoni, and Charles Brochu

Abstract: Aliphatic hydrocarbons, chlorinated pesticides, polychlorinated biphenyls (PCBs), dioxins, furans, and trace metals have been quantified in fishes collected at four stations in Río de la Plata to determine contaminant sources, elucidate interstation and interspecies differences, and assess the health risks associated with fish consumption. Río de la Plata fish present low trace metal concentrations and moderate to high levels of organic pollutants, particularly aliphatic hydrocarbons and PCBs. The highest concentrations were recorded in *Prochilodus lineatus*, a dominant and remarkably specialized fatty detritivore that feeds on contaminated organic-rich flocculent matter. Lower levels were registered in *Cyprinus carpio* and especially in *Mugil cephalus*, reflecting different feeding preferences. A geographical pattern of higher contaminant concentrations close to the Buenos Aires urban center and lower levels in distant stations was also observed. The multivariate analysis of contaminant signatures indicated that most contaminated *Prochilodus* had fresh petrogenic and PCB traces, similar to fossil fuels and Aroclor 1254–1260, whereas *Mugil* and fish from distant sites presented a higher proportion of biogenic hydrocarbons and of more chlorinated PCBs. Toxicity equivalents ranged from 11 to 39 pg·g fresh weight^{-1} in *Prochilodus*, exceeding the guideline of 25 pg·g^{-1} for human consumption, with allowable consumption rates as low as 1 g fish·day^{-1}.

Résumé : Nous avons quantifié les hydrocarbures aliphatiques, les pesticides chlorés, les polychlorobiphényles (PCB), les dioxines, les furanes et les métaux-traces chez des poissons prélevés à quatre stations dans le Río de la Plata en vue de déterminer les sources de contaminants, d'éclaircir les différences entre stations et entre espèces et d'évaluer les risques pour la santé associé à la consommation de poissons. Les poissons du Río de la Plata présentent de faibles concentrations de métaux-traces et des teneurs modérées à élevées en polluants organiques, particulièrement les hydrocarbures aliphatiques et les PCB. Les concentrations les plus élevées ont été observées chez *Prochilodus lineatus*, poisson gras détritivore dominant et remarquablement spécialisé, qui se nourrit de matière floculée contaminée riche en substances organiques. Des concentrations plus faibles ont été enregistrées chez *Cyprinus carpio* et particulièrement chez *Mugil cephalus*, ce qui correspond à des différences sur le plan de l'alimentation. Nous avons aussi observé un patron géographique, les concentrations de contaminants étant plus élevées à proximité du centre urbain de Buenos Aires et plus faibles aux stations éloignées. L'analyse multivariée des signatures des contaminants a indiqué que la plupart des *Prochilodus* contaminés présentaient des traces fraîches de matériel pétrogénétique et de PCB, semblables à celles des combustibles fossiles et de l'Aroclor 1254–1260, tandis que les *Mugil* et les poissons des stations éloignées présentaient une plus forte proportion d'hydrocarbures biogéniques et des PCB les plus chlorés. Les valeurs des équivalents toxiques allaient de 11 à 39 pg·g poids frais^{-1} chez *Prochilodus*, dépassant donc la limite de 25 pg·g^{-1} fixée pour la consommation humaine, de sorte que la quantité autorisée à la consommation pouvait descendre à 1 g poisson·jour^{-1}.

[Traduit par la Rédaction]

Received June 22, 1999. Accepted January 5, 2000.
J15205

J.C. Colombo.[1] Laboratorio de Química Ambiental y Biogeoquímica, Facultad de Ciencias Naturales y Museo, Universidad Nacional de La Plata, Paseo del Bosque s/n, 1900 La Plata, Argentina, and Comisión de Investigaciones Científicas de la Provincia de Buenos Aires, Argentina.
C. Bilos and P. Landoni. Laboratorio de Química Ambiental y Biogeoquímica, Facultad de Ciencias Naturales y Museo, Universidad Nacional de La Plata, Paseo del Bosque s/n, 1900 La Plata, Argentina.
M.R. Lenicov and D. Colautti. Instituto de Limnología, Facultad de Ciencias Naturales y Museo, Universidad Nacional de La Plata, Paseo del Bosque s/n, 1900 La Plata, Argentina.
C. Brochu. Centre d'Expertise en Analyse Environnementale du Québec, Ministère de l'Environnement du Québec, 850 boul. Vanier, Laval, QC H7C 2M7, Canada.

[1]Author to whom all correspondence should be sent at the following address: Laboratorio de Química Ambiental y Biogeoquímica, Facultad de Ciencias Naturales y Museo, Universidad Nacional de La Plata, Paseo del Bosque s/n, 1900 La Plata, Argentina.
e-mail: colombo@museo.fcnym.unlp.edu.ar

© 2000 NRC Canada

Fig. 1. Río de la Plata estuary and sampling locations (arrows). TIG, Tigre; QUI, Quilmes; PL, Punta Lara; MG, Magdalena. The main urban centers are indicated.

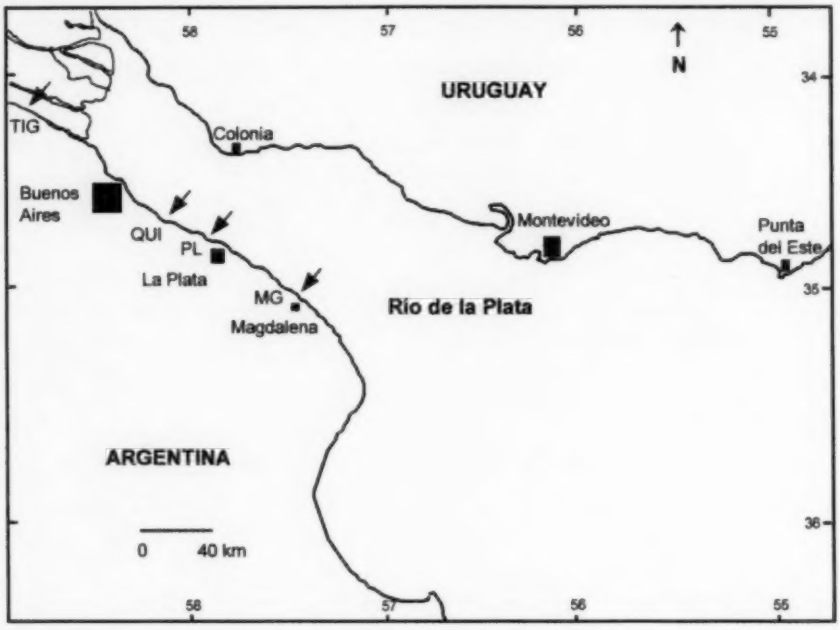

Introduction

Organic pollutants and trace metals are ubiquitous contaminants in the global environment and they are usually concentrated in the waters, sediments, and biota of heavily populated estuaries of the world. The Río de la Plata estuary is, after the Amazon, the second largest river system in South America and conforms well to this generalization. The strong demographic and industrial pressure (about 13 million people and 50% of the country's industrial capacity) around Buenos Aires and La Plata cities (Fig. 1) produces a severe environmental impact. The widespread presence of hydrocarbons and chlorinated compounds in sediments and biota along the coast has been reported (Colombo et al. 1989, 1990). Petrogenic inputs predominate in polluted tributaries and nearby coastal areas whereas pirogenic hydrocarbons dominate in offshore areas. Chlorinated pesticides and polychlorinated biphenyls (PCBs) are abundant in aquatic organisms, with a composition denoting the integration of water column and sediment traces. Chlorinated organics and trace metals show geographical gradients of decreasing concentrations in suspended particles, sediments, and bivalves with increasing distance from the Buenos Aires area (Colombo et al. 1995; Bilos et al. 1998). The study of the long-term accumulation of xenobiotics, including dioxins and furans, in Asiatic clams indicated a doubling of the toxic equivalents over 4 years of clam growth (Colombo et al. 1997). These studies provided a general picture of the contamination status in the urbanized, freshwater area of the estuary. However, a detailed evaluation of the impact of anthropogenic contaminants on the rich local fisheries has not yet been performed.

The contamination of fish stocks by persistent organochlorines such as PCBs and DDTs and degradation products produces economic as well as ecological and health-related effects. High PCB levels have triggered the periodic closures of commercial fisheries affected by the discharge of industrialized rivers and estuaries; the Atlantic coast striped bass (*Morone saxatilis*) and Great Lakes fisheries are perhaps the most illustrative examples (White et al. 1985; Bush et al. 1989; Fabrizio et al. 1991). The importance of fish as a critical pathway in the transfer of organochlorines to higher trophic level wildlife, e.g., birds and mammals, and humans is well established (e.g., Fox et al. 1991; Law and Gudaitis 1994; Tillitt et al. 1996). In this context, the epidemiological studies carried out in the Great Lakes during the last 25 years suggest a relationship between health effects and contaminated fish consumption in sport fishers, even in second-generation infants due to in utero exposure and breast milk residue transfer (Gilbertson 1985; Manno et al. 1995). In order to manage this health risk, fish consumption advisories have been issued, e.g., five consumption categories are recommended based on PCB levels (milligrams per kilogram fresh weight): (*i*) PCBs < 0.05, no restriction; (*ii*) PCBs = 0.05–0.2, 52 meals per year; (*iii*) PCBs = 0.2–1.0, 12 meals per year; (*iv*) PCBs = 1.0–1.9, six meals per year; (*v*) PCBs > 1.9, no consumption is recommended (Stow and Qian 1998).

In this paper, we study the accumulation of persistent organochlorines, hydrocarbons, and trace metals in four dominant fish species of the Río de la Plata estuary, including a highly specialized detritivore, collected at four stations with differing land uses. The objectives of the study are to (*i*) assess the contamination status of the biological resource, (*ii*) examine interspecies differences, (*iii*) investigate possible geographical patterns, (*iv*) examine the relationship be-

© 2000 NRC Canada

Table 1. Total concentrations and major components of organic contaminants and trace metals in Río de la Plata fish.

	Relative abundance (%)											
	Sabalo				Carp				Boga,	Mullet		
	TIG	QUI	PL	MG	TIG	QUI	PL	MG	TIG	QUI	PL	MG
Aliphatic hydrocarbons												
n-C14	6.2	10.2	7.0	—	4.1	34.3	10.2	—	5.8	12.0	46.3	—
Farnesane	5.3	5.7	5.4	—	4.7	4.9	3.6	—	8.9	6.9	—	—
n-C15	11.6	13.6	9.6	—	6.5	15.4	9.5	—	7.0	7.2	—	—
n-C16	7.4	9.2	12.7	—	9.2	17.5	10.9	—	5.3	4.1	—	—
Norpristane	6.6	7.1	9.2	—	3.9	6.1	5.1	—	8.3	8.5	—	—
n-C17	22.6	7.5	12.9	—	21.3	18.4	12.0	—	41.5	42.7	26.2	—
Pristane	8.7	9.7	15.9	—	4.1	3.3	4.2	—	5.8	9.0	27.7	—
n-C18	4.3	5.1	6.6	—	12.8	—	7.4	—	6.1	4.7	—	—
Phytane	5.8	6.3	10.2	—	4.5	—	5.9	—	3.2	5.0	—	—
Total (μg·g dry weight^{-1})	37.6	77.3	85.6	—	5.9	3.1	75.6	—	7.3	3.2	0.7	—
Total (μg·g fresh weight^{-1})	9.5	34.6	27.9	—	1.2	0.7	21.0		2.1	0.9	0.2	—
Total (μg·g lipids^{-1})	135.6	224.9	356.2	—	244.8	284.4	287.6	—	16.9	70.9	20.9	—
Mean ± SD (μg·g lipids^{-1})		238.9	110.95			272.2	23.9			45.9	35.4	
PCBs												
52	2.9	3.2	2.8	—	1.4	2.2	3.1	2.2	—	3.0	2.6	3.3
49	2.0	2.7	2.0	—	0.7	—	2.0	1.2	—	1.9	—	2.2
95-66	4.2	4.3	3.8	8.1	3.7	3.6	4.6	4.7	—	4.4	2.8	5.0
101-90	7.7	7.8	7.6	5.6	8.4	8.7	7.5	9.0	4.8	9.0	7.9	10.1
110-77	3.0	3.0	3.0	3.1	4.4	4.7	4.0	4.3	3.7	4.1	3.2	4.2
149-123	5.4	5.1	5.3	6.2	7.2	7.1	5.3	7.2	2.5	6.6	3.8	4.8
118	4.1	4.2	4.2	3.1	4.3	4.9	4.1	4.2	4.5	4.1	3.4	4.5
153	8.9	8.7	8.7	11.5	14.3	14.8	8.4	12.6	18.4	13.3	9.7	11.5
138-160	5.6	5.2	5.3	8.0	8.4	9.4	5.5	8.3	8.4	7.4	6.6	7.3
180	4.0	3.5	3.4	7.8	4.2	5.1	3.2	4.0	5.6	4.9	3.3	3.6
170-190	3.1	2.9	2.9	10.1	2.9	3.8	2.8	2.7	—	3.3	2.1	4.0
Total (μg·g dry weight^{-1})	3.5	5.9	6.6	0.3	0.9	0.4	7.0	0.8	0.2	0.5	0.2	0.9
Total (μg·g fresh weight^{-1})	0.9	2.6	2.1	0.1	0.2	0.1	2.0	0.2	0.1	0.1	0.1	0.3
Total (μg·g lipids^{-1})	12.7	17.1	27.6	2.2	38.4	39.1	26.8	68.3	0.4	10.2	5.7	14.1
Mean ± SD (μg·g lipids^{-1})		14.9	10.5			43.1	17.7			10.0	4.2	
Chlorinated pesticides												
γ-BHC (lindane)	2.4	4.4	2.9	11.6	7.0	5.9	2.8	4.0	8.2	7.2	21.4	3.9
Heptachlor epoxide	3.5	5.5	3.4	5.2	2.5	6.9	1.6	0.0	7.8	9.8	3.8	4.9
trans-Chlordane	25.0	12.3	29.2	19.3	22.7	25.1	29.7	17.9	4.9	17.5	22.0	16.1
cis-Chlordane	12.2	8.8	11.8	10.5	9.6	9.0	12.2	7.6	3.6	11.3	13.4	11.5
trans-Nonachlor	9.5	7.7	9.5	—	9.8	6.0	9.3	2.7	2.7	7.8	6.7	7.5
DDE	13.1	25.1	19.0	26.8	21.8	19.6	28.4	40.8	52.9	16.6	11.2	28.0
TDE	19.0	14.9	12.3	11.7	21.0	19.6	11.1	11.8	7.2	14.6	10.8	13.2
DDT	12.4	10.0	7.0	2.9	1.5	2.3	0.3	1.1	7.7	9.3	2.0	9.0
Total (μg·g dry weight^{-1})	0.59	0.34	1.15	0.05	0.08	0.04	0.74	0.07	0.06	0.05	0.05	0.14
Total (μg·g fresh weight^{-1})	0.15	0.15	0.37	0.01	0.02	0.01	0.21	0.01	0.02	0.01	0.01	0.04
Total (μg·g lipids^{-1})	2.12	0.98	4.81	0.34	3.17	4.07	2.83	6.14	0.13	1.15	1.44	2.17
Mean ± SD (μg·g lipids^{-1})		2.1	2.0			4.1	1.5			1.6	0.5	
Metals												
Zn	70.2	70.9	64.6	72.0	88.4	92.3	89.8	89.0	72.5	83.6	70.3	82.8
Cu	5.6	11.8	17.0	5.2	4.3	3.4	3.1	2.1	15.5	8.2	9.9	7.5
Mn	15.2	8.0	6.3	10.6	4.2	2.6	2.1	4.9	5.0	3.4	4.1	2.7
Cr	4.2	3.2	7.4	6.1	1.9	0.4	3.5	1.9	4.3	1.6	10.6	3.1
Ni	4.8	6.1	4.7	6.1	1.2	1.2	1.5	2.2	2.8	3.2	5.0	3.9
Total (μg·g dry weight^{-1})	24.6	13.1	16.1	20.0	55.9	57.4	73.8	65.0	20.0	18.6	17.3	21.9
Total (μg·g fresh weight^{-1})	6.3	5.8	5.3	4.2	11.9	12.6	20.5	12.6	5.8	5.3	4.5	5.7

Note: TIG, Tigre; QUI, Quilmes; PL, Punta Lara; MG, Magdalena; —, not detectable.

© 2000 NRC Canada

Table 2. PCDDs and PCDFs in sabalo from the Río de la Plata.

	Relative abundance (%)		
	TIG	QUI	MG
PCDDs			
TCDDs	—	—	—
PCDDs	30.0	14.3	—
Hexa-CDDs	—	67.7	—
Hepta-CDDs	34.9	9.7	—
OCDD	35.0	8.3	100.0
Total PCDDs ($pg \cdot g^{-1}$)	16.6	91.3	76.0
PCDFs			
TCDFs	100.0	51.6	—
PCDFs	—	48.4	—
Hexa-CDFs	—	—	—
Hepta-CDFs	—	—	—
OCDF	—	—	—
Total PCDFs ($pg \cdot g^{-1}$)	21.1	106.5	—

Note: TIG, Tigre; QUI, Quilmes; MG, Magdalena; —, not detectable.

tween feeding habits and bioaccumulation of xenobiotics, and (*v*) evaluate the possible health risks associated with fish consumption in the area.

Materials and methods

Three fish species that collectively make up >80% of the fish biomass in the Río de la Plata estuary, sabalo (*Prochilodus lineatus*), carp (*Cyprinus carpio*), and mullet (*Mugil cephalus*), were collected between October 26 and December 6 1996 at four stations with differing land uses (Fig. 1): Tigre, on the Paraná delta, upstream from the major urban/industrial center of Buenos Aires, Quilmes, in a heavily populated area downstream from Buenos Aires, Punta Lara, a popular beach located downstream from Quilmes and close to the La Plata City petrochemical port, and Magdalena, a less urbanized coastal area 100 km downstream from Buenos Aires. Due to the scarcity of mullet at Tigre, it was substituted by boga (*Leporinus obtusidens*).

At each station, between two and 10 adult individuals of each species were collected using gill nets, measured, weighed, and dissected to extract dorsolateral muscle samples. A total of 92 fishes of homogeneous standard lengths and weights with a higher proportion of females were collected (sabalo: 43 ± 1.9 cm (average ± SD), 2.4 ± 0.6 kg, female to male ratio = 1.2, n = 29; carp: 53 ± 9.0 cm, 4.1 ± 2.1 kg, female to male ratio = 1.3, n = 30; mullet: 41 ± 2.0 cm, 1.2 ± 0.2 kg, female to male ratio = 2.1, n = 25; boga: 45 ± 2.4 cm, 1.9 ± 0.3 kg, female to male ratio = 1, n = 8). Pooled muscle tissue samples from each species at each site were transported to the laboratory in refrigerated glass flasks and frozen at –20°C. Initial sample processing included homogenization of muscle samples with a stainless steel blender and determination of the water content (24 h at 105°C).

For organic analyses, aliquots of 7–10 g of muscle homogenates were mixed with preextracted sodium sulfate (1:2) and Soxhlet extracted with a 1:1 dichloromethane – petroleum ether mixture. The extracts were concentrated at 25–30°C under a nitrogen flow to determine total lipids (gravimetry) and subsequently digested with 1 mL of concentrated sulfuric acid in 10 mL of petroleum ether. The supernatant was then purified on silica gel microcolumns (1 g, 5% hydrated) eluted with petroleum ether (F1: PCBs, aliphatic hydrocarbons) and 1:4 dichloromethane – petroleum ether (F2: chlorinated pesticides). Quantification was performed using a KONIK 3000 gas chromatograph equipped with a split-splitless injector operated at 250°C, a flame ionization and an electron capture detector, both operated at 320°C, and a 30-m DB5 capillary column programmed from 50°C (2-min hold) to 135°C (2-min hold) at $15°C \cdot min^{-1}$ and then to 295°C (10-min hold) at $5°C \cdot min^{-1}$. Aliphatic hydrocarbons were quantified using individual standards (Supelco) and local diesel fuel and crude oil samples. PCB response factors were calculated for each resolved peak using a 1:1:1 Aroclor 1242–1254–1260 mixture, the published complete composition of the formulations, and CLB1 individual congener standards from the Marine Analytical Chemistry Standards Program, CNRC (Colombo et al. 1995). Chlorinated pesticides were quantified using a standard solution containing α-, β-, and γ-benzene hexachloride (BHC), hexachlorobenzene (HCB), heptachlor, heptachlor epoxide, *trans*-chlordane, *cis*-chlordane, DDT and dechlorintation products (DDE and TDE), dieldrin, endrin, and methoxichlor; *trans*-nonachlor was identified using a technical chlordane solution. PCB method accuracy, checked through the analysis of mussel tissue reference material (NIST SRM 2974), averaged 92.5 ± 27.5% for 17 certified congeners. PCB analytic precision calculated from duplicate fish analysis averaged 11% for 41 congeners. Detection limits ranged from 0.5 $ng \cdot g$ dry $weight^{-1}$ for chlorinated pesticides and PCBs to 100 $ng \cdot g^{-1}$ for hydrocarbons.

Selected lipid aliquots were analyzed at the "Ministère de l'Environnement et de la Faune du Québec" to determine coplanar PCBs, dioxins, and furans following previously reported procedures (Colombo et al. 1997). Briefly, extracts spiked with $^{13}C12$-labelled PCBs and polychlorinated dibenzodioxin (PCDD) and dibenzofuran (PCDF) isomers were purified on multilayer silica columns followed by a fractionation of PCBs, planar PCBs, PCDD, and PCDF on alumina columns and additional cleanup on carbon columns for the PCDD/PCDF fractions. Planar PCBs and PCDD/PCDF were spiked with $^{13}C12$-labelled PCDDs and PCDFs and analyzed by HRGC/HRMS (Hewlett-Packard 5890-VG AutospecQ, 34 eV, source at 260°C, static resolution of 10 000) using a 0.25 mm × 60 m DB5 capillary column programmed from 100°C (1-min hold) to 200°C at $40°C \cdot min^{-1}$, from 200 to 235°C (10-min hold) at $3°C \cdot min^{-1}$, and to 310°C (15-min hold) at $8°C \cdot min^{-1}$. Relative response factors over a four-point calibration curve were calculated for each congener of PCDD/PCDF and planar PCBs. Procedural blanks and standard reference material (Carp-1, National Research Council of Canada) were processed along with the samples.

For trace metal analyses, muscle homogenates (1–2 g dry weight) were incinerated (16 h at 450°C) and then sequentially treated with nitric acid, hydrochloric acid, and hydrogen peroxide (5:1:2) at 90°C. After centrifugation, the extracts were diluted to 25 mL with deionized water and analyzed by flame atomic absorption spectrophotometry using a Perkin Elmer 3110 spectrophotometer equipped with deuterium background corrector, an air–acetylene flame, and Perkin Elmer or ISTC hollow cathode lamps. High-purity Johnson Matthey PLC original standards were used to prepare calibration mixtures. The accuracy of the analytical procedure ranged from ±3 to 11% of the values reported for a certified reference sediment (BCSS-1, National Research Council of Canada). The precision of the data ranged from 2 to 11% (RSD). Detection limits ranged from 0.4 to 0.5 $\mu g \cdot g$ dry $weight^{-1}$ for Zn, Cd, Cu, and Mn, from 0.7 to 0.9 $\mu g \cdot g^{-1}$ for Cr and Fe, and from 1.5 to 2.0 $\mu g \cdot g^{-1}$ for Ni and Pb.

Results and discussion

Contamination status of Río de la Plata fish

Tables 1 and 2 present total contaminant concentrations on a dry weight, fresh weight, and lipid basis as well as the major components of hydrocarbons, organochlorines, and trace metals in Río de la Plata fish. Figure 2 shows the total dry weight concentrations and the relative abundance of

© 2000 NRC Canada

Fig. 2. Concentrations of (*a*) aliphatic hydrocarbons, (*b*) chlorinated pesticides, (*c*) PCBs, and (*d*) trace metals in Río de la Plata fish. TIG, Tigre; QUI, Quilmes; PL, Punta Lara; MG, Magdalena. The boga sample collected at TIG is grouped with mullet (see text for explanation).

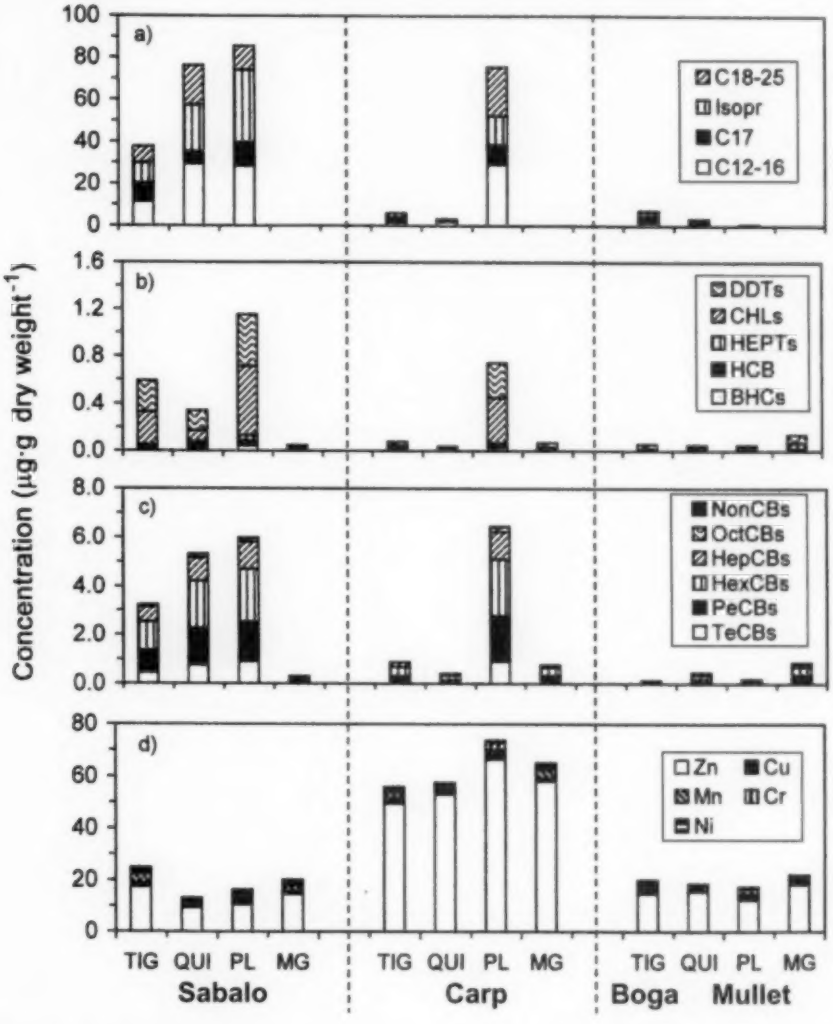

major components. Among the organic pollutants analyzed, aliphatic hydrocarbons exhibit the highest concentrations in fish muscle (0.7–86 µg·g dry weight^{-1}), with a dominant contribution of lower molecular weight *n*-alkanes (*n*-C12–17) and isoprenoids (farnesane, norpristane, pristane, and phytane). In decreasing order, they are followed by PCBs (0.2–7.0 µg·g dry weight^{-1}), with a clear predominance of penta- and hexa-chlorobiphenyls, and chlorinated pesticides (0.04–1.1 µg·g dry weight^{-1}), chiefly as chlordanes (*trans*-chlordane, *cis*-chlordane, and *trans*-nonachlor) and DDTs (DDE, TDE, and DDT). As expected, dioxins and furans are in the lower ppt range (17–91 and 21–106 pg·g dry weight^{-1}, respectively). Total trace metal concentrations oscillate between 13 and 74 µg·g dry weight^{-1} with a clear predominance of Zn, especially in carp (88–92 versus 65–84% total metals in the other species).

Table 3 compares the average contaminant concentrations in Río de la Plata fish with those in species from other environments. Overall, trace metals and organic micropollutants display a different situation; trace metal levels in Río de la Plata fish are in the low range of the reported values, except perhaps Cr, whereas organic contaminants are in the middle to high range, indicating a more critical situation. Among these compounds, hydrocarbon concentrations are quite high, with little data to compare from other environments. Nevertheless, a mean of 18 µg·g^{-1} in sabalo with values as high as 35 µg aliphatic hydrocarbons·g^{-1} with a clear petrogenic signature (see Sources and composition of fish microcontaminant residues section) denote the strong impact of oil discharges into the estuary. This corroborates previous findings (Colombo et al. 1989), indicating that discharges of petrochemical effluents, tanker ballast washings, and furtive spillages are still a major problem in this coastal area. PCBs also display a delicate situation; the concentrations are in the

© 2000 NRC Canada

Table 3. Contaminant concentrations in Río de la Plata fish compared with those in species from other environments.

Environment	Species	Concentration (μg·g fresh weight^{-1})						Concentration (pg·g fresh weight^{-1})			Reference
		Hydrocarbons	Pesticides	PCB	Zn	Cu	Cr	PCDD	PCDF	TEQ	
Río de la Plata	*Prochilodus lineatus*	18.0	0.17	1.44	3.6	0.47	0.27	16.1	11.2	39.3	This study
	Cyprinus carpio	5.7	0.06	0.60	12.5	0.44	0.28				This study
	Mugil cephalus	0.4	0.02	0.14	4.1	0.44	0.25				This study
Buffalo River	*Cyprinus carpio* (middle aged)		0.15	4.3				25.0	42	75.0	Loganathan et al. 1995
Mean U.S. rivers	*Cyprinus chrysops*		0.57	2.94				7.8	10.2	13.1	Kuehl et al. 1994
	Ictalurus punctatus		0.75	1.30				11.6	2.22	14.8	Kuehl et al. 1994
	Castostomus commersoni		0.13	1.70				8.1	22.9	12.8	Kuehl et al. 1994
Polluted U.S. rivers	*Cyprinus chrysops*			30.74							Kuehl et al. 1994
Long Island – Hudson	*Morone saxatilis*			5.50							Bush et al. 1989
Lake Ontario	*Oncorhynchus mykiss* (previously *Salmo gairdneri*)		0.66	2.13							Niimi and Oliver 1989
	Oncorhynchus kisutch		0.72	2.30							Niimi and Oliver 1989
	Salvelinus namaycush		1.14	3.88							Niimi and Oliver 1989
Michigan rivers	*Cyprinus chrysops*		0.45	3.08						36.8	Giesy et al. 1994
	Oncorhynchus tshawytscha		0.39	1.70						38.0	Giesy et al. 1994
	Catostomus commersoni		0.08	0.27						8.6	Giesy et al. 1994
Lake Michigan	*Oncorhynchus tshawytscha*		0.98	3.8							Miller 1994
Lahn River	*Perca fluviatilis* and *Rutilus rutilus*		0.03	0.78							Schüler et al. 1985
Western Mediterranean	*Thunnus thynnus*	1.74		0.02							Porte and Albaigés 1993
Western Mediterranean	*Mullus barbatus*	0.72	0.05	0.20							Albaigés et al. 1987
	Merluccius merluccius	0.20	0.01	0.08							Albaigés et al. 1987
	Engraulis encrasicholus	2.08	0.02	0.07							Albaigés et al. 1987
Israel coast	*Mullus barbatus*		0.04	0.07							Ravid et al. 1985
	Merluccius merluccius		0.04	0.02							Ravid et al. 1985
South and east coastal Asia	Multispecific average		0.03	0.01							Kannan et al. 1995
Tigris River	*Cyprinus macrostomus*				59.0	141					Gümgüm et al. 1994
	Garra rufa				88.5	138					Gümgüm et al. 1994
Jacarepaguá lagoons	*Mugil* sp.				2.20	0.40	0.09				Fernandes et al. 1994
	Tilapia sp.				2.20	0.20	0.08				Fernandes et al. 1994
Lake Balaton	*Carassius auratus*				14.8	1.24					Salánki et al. 1992
	Esox lucius				10.5	1.38					Salánki et al. 1992

© 2000 NRC Canada

Tanganyika Lake	*Stolothrissa tanganyikae*	29.5	1.10		Benemariya et al. 1991
	Oreochromis niloticus	4.4	0.18		Benemariya et al. 1991
African lakes	*Tilapia* sp.	9.12	2.87		Benemariya et al. 1991
Switzerland lakes	*Perca fluviatilis*	5.65	0.19		Benemariya et al. 1991
U.S. freshwater	Multispecific average	24.7	0.77		Benemariya et al. 1991
Six Ontario lakes	*Catostomus commersoni*	5.79	0.95		Miller et al. 1992

middle to high range, with sabalo values comparable with those of moderately polluted Great Lakes and U.S. river fishes. Chlorinated pesticides in Río de la Plata fish are in the middle to low range, lower than Great Lakes and U.S. river mean concentrations, whereas dioxins and furans are in the range of values commonly found.

In summary, the comparison of contaminant levels in Río de la Plata fish with values reported for other environments suggests a low impact of trace metals, corroborating previous results obtained for suspended particles, sediments, and Asiatic clams (Bilos et al. 1998). Organic compounds, on the other hand, evidence a more critical situation with hydrocarbons and PCBs as the most abundant contaminants, reflecting the continued discharge of these highly bioaccumulative compounds.

Interspecies and geographical differences

On a dry or fresh weight basis, all the organic contaminants examined showed a consistent interspecies pattern: the concentrations are higher in sabalo and lowest in mullet and boga. Only carp collected at Punta Lara show high levels, comparable with levels in sabalo from Tigre, Quilmes, and Punta Lara (Fig. 2). Hydrocarbon, PCB, and pesticide concentrations in fish from these four most contaminated sites are 11–22 times higher than the background levels registered in the other fish (e.g., high sabalo and carp versus background: 23 ± 11 versus 1.0 ± 0.7, 1.9 ± 0.7 versus 0.13 ± 0.07, and 0.22 ± 0.11 versus 0.02 ± 0.01 μg·g fresh weight^{-1} for hydrocarbons, PCBs, and pesticides, respectively). The background levels of PCBs and pesticides in fishes are comparable with the values registered in Asiatic clams along the Río de la Plata coast: 0.11 ± 0.05 and 0.05 ± 0.02 μg·g fresh weight^{-1}, respectively (Colombo et al. 1995). The contrasted loads of hydrophobic contaminants in fish are principally related to differences in lipid contents (average 25% in sabalo, 7.7% in carp, except at Punta Lara (26%), and 4.7% in mullet) and in feeding habits of the organisms. Lipid-normalized concentrations are comparable for sabalo and carp, but still clearly discriminate mullet and boga as the least contaminated species (Table 1). The low lipid-normalized values of boga result from the high lipid contents of this species (43%). Conversely, the high lipid-normalized values of carp relative to sabalo reflect the lower and also more variable lipid levels of carp (1.1–26 versus 14–34% in sabalo), suggesting interspecies differences in lipid metabolism. Further studies are needed to evaluate the significance of these sources of variability.

In addition to the differences in lipid content, feeding habits are a crucial factor to interpret the interspecies variations observed. The sabalo is a highly specialized ilyophagous species, which exclusively feeds on fine, organic-rich flocculent detritus. While detritus is certainly important for the other species, these organisms tend to be more selective, avoiding severely polluted muds and feeding primarily on benthic invertebrates, vegetal detritus, zooplankton, and algae (Sibbing 1988; Cardona et al. 1996). Sabalo has several mechanical and physiological adaptations to maximize the assimilation of detrital organic matter, e.g., sucking mouth, secreting pharyngeal diverticles, complex and mucous gill-rakers to separate flocculent detritus from water, cardiac stomach, and a labyrinthine intestine with increased relief of

© 2000 NRC Canada

Fig. 3. PCA of the relative contribution of individual contaminants in Río de la Plata fish. Fish samples are identified by species (solid circles, *Prochilodus* (P); triangles, *Cyprinus* (C); open circles, *Mugil* (M) and *Leporinus* (L)) followed by the initial of the sampling station (T, Tigre; Q, Quilmes; P, Punta Lara; M, Magdalena). (*a*) Aliphatic hydrocarbons; sources: crude oil and oiled sediment (CR and OS, respectively, solid squares) and plankton (PK1 and PK2, open squares). (*b*) PCBs; sources: Aroclor 1242, 1254, and 1260 (A42, A54, and A60, respectively, crosses). (*c*) Chlorinated pesticides. (*d*) Trace metals; source: local macrophyte (SC, square).

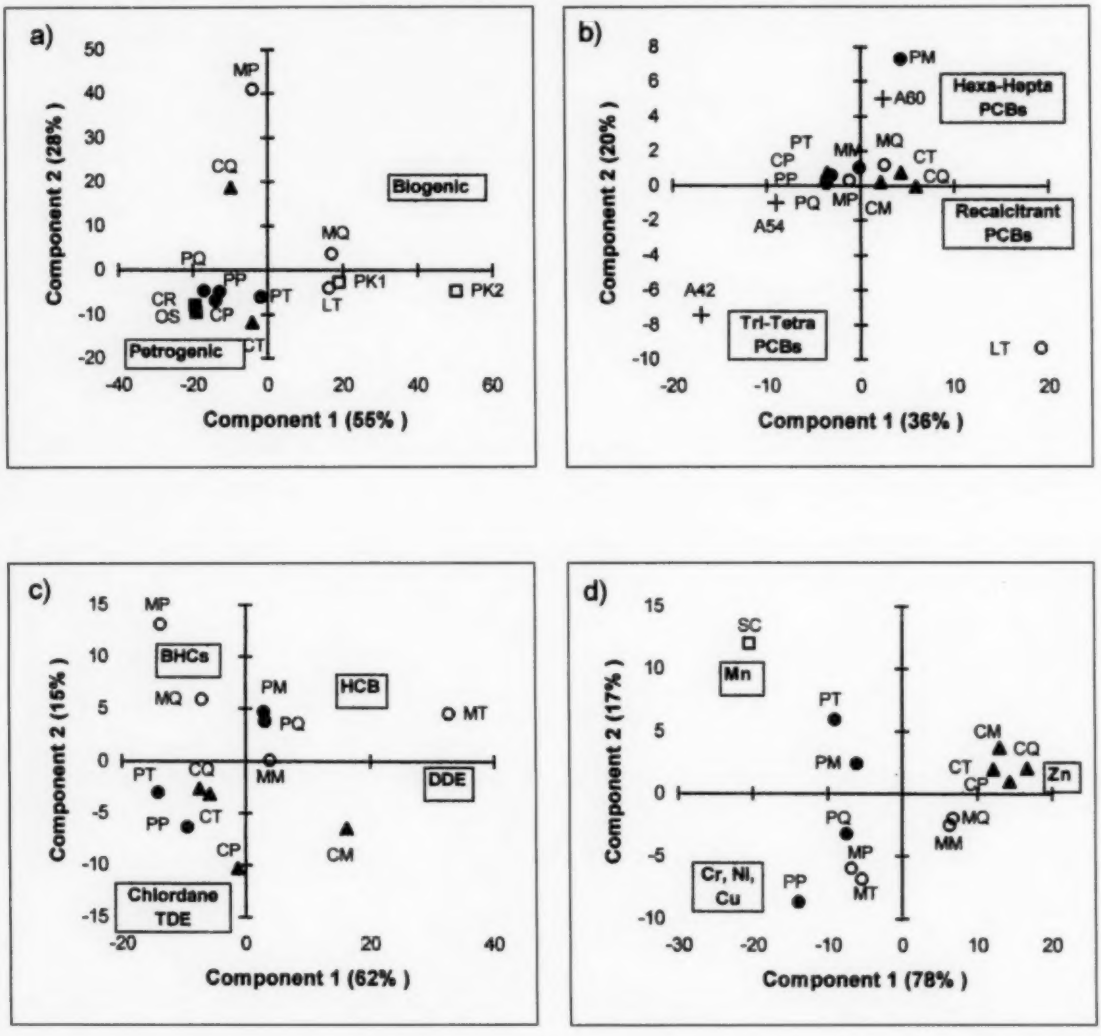

the mucous membrane that produces a fourfold increase in the absorptive surface (Bowen 1983). Assimilation efficiencies of 30–60% of the organic matter ingested have been reported (Bowen et al. 1984). Due to this high specialization, in severely polluted habitats, sabalo acts as an efficient bioaccumulator of persistent, hydrophobic compounds that are concentrated in the organic muds. These characteristics, together with its large distribution area (the entire Río de la Plata basin, $>3 \times 10^6$ km^2), vast abundance (>70% of the total fish biomass), and migrating habits (several hundred kilometres; Sverlij et al. 1993), make the sabalo an efficient carrier of persistent anthropogenic contaminants throughout the region. In addition, the comercial exploitation of the sabalo (87% of total Río de la Plata fishery), which is locally consumed, exported to Asiatic and African countries, e.g., >10 000 tons in 1982 (Sverlij et al. 1993), and used to produce oil and fish flour, converts this organism into a critical contamination pathway for humans.

The pattern of interspecies differences changes in the case of trace metals. Effectively, trace metal concentrations are more homogeneous, reflecting the well-know regulation capabilities of organisms for essential trace metals such as Zn. The most conspicuous trend observed for metals is the consistently higher concentrations in the carp. This pattern almost exclusively reflects the behavior of Zn, which comprised 65–92% of the total metals analyzed.

Superimposed on the interspecies differences, there are clear geographical variations in fish contaminant levels. Fish

© 2000 NRC Canada

from Quilmes and Punta Lara, located downstream from the Buenos Aires major urban/industrial center, present the highest concentrations of organics, whereas those from the more distant Tigre (upstream) and especially Magdalena sites (downstream) show lower levels. Surprisingly, these results suggest some degree of habitat fidelity for these species, some of them well-known migratory species such as sabalo and mullet. The multivariate analyses of the contaminant signatures effectively support these interspecies and spatial trends, suggesting that they could be useful for tracking fish from different locations. As indicated previously, trace metal results are more homogeneous and do not show marked differences between the four sampling stations. However, their relative abundance suggests some subtle trends (see the next section).

Sources and composition of fish microcontaminant residues

The evaluation of total contaminant concentrations in fish revealed the main interspecies and geographical trends. However, this approach does not adequately reflect the grouping of the samples according to their composition. To evaluate this aspect and elucidate the major contaminant sources, principal components analyses (PCA) were performed using the relative contribution of the individual constituents in fish samples and in known sources when available for each contaminant group.

In the case of hydrocarbons, the analyses were performed using the relative abundance of individual aliphatics in fish, a local crude, an oiled sediment from La Plata port, and two phytoplanktonic samples. The first two components explain 83% of the total variability, 55% PC1 and 28% PC2 (Fig. 3*a*). PC1 is defined by the contribution of odd low molecular weight *n*-alkanes (*n*-C15–17) on the positive side (+PC1), a typical signature of microalgae (Blumer et al. 1971), and of the other components on the negative side (–PC1). PC2 is chiefly determined by *n*-C14 and the acyclic isoprenoid pristane (+PC2), abundant in zooplankton (Colombo et al. 1996), and by the rest of the components which are clustered in the negative quadrant. Thus, this virtual space defines basically petrogenic (–PC1, –PC2) versus planktonic (+PC1, +PC2) influences. The crude oil and the oiled sediment sample are clustered together in the negative quadrant, close to sabalo from Quilmes and Punta Lara and carp from Punta Lara, indicating an almost exclusive petrogenic hydrocarbon source for these fish. The hydrocarbon profile of these organisms effectively shows a clear *n*-C12–25 continuous petrogenic pattern. The signal is only partially degraded, as indicated by the small change in the *n*-alkane/isoprenoid ratios relative to fossil fuels, e.g., C17/pristane (0.8–2.8 versus 1.7), and C18/phytane ratios (0.7–1.2 versus 2.5, fish versus crude). This minor degradation is surprising considering the relatively high susceptibility of aliphatics to decay, especially of low molecular weight components. These results suggest that the organisms are feeding on very fresh organic residues arising from petrochemical, industrial, and sewage discharges, e.g., La Plata and Buenos Aires ports, channels, and small polluted tributaries, or the main Buenos Aires sewage that discharges about 2×10^6 m^3 of crude effluent per day upstream from Quilmes.

The contrasting "natural" group in the PCA of hydrocarbons is represented by mullet and boga samples, which are clustered in the planktonic area, reflecting dominant biogenic hydrocarbon sources. Interestingly, carp and sabalo from Tigre show an intermediate position, closer to petrogenic sources but with some biogenic influence. These results on the hydrocarbon composition agree well with the concentration patterns indicating prevalence of fresh petrogenic residues in the most contaminated sabalo and carp, specially at the Quilmes and Punta Lara sites, and dominance of biogenic hydrocarbons in the less polluted mullet and boga.

The PCA of PCBs was performed using the relative abundance of the different congeners in fish and in Aroclor 1242, 1254, and 1260 formulations. The first two components explain 56% of the total variability, 36% PC1 and 20% PC2 (Fig. 3*b*). This PCA is largely determined by the opposition between lower chlorinated PCBs (tri- and tetra-CBs) on the negative quadrant (–PC1, –PC2) and higher chlorinated congeners (hexa- and hepta-CBs) on the positive side, which includes highly recalcitrant and bioacumulative PCBs, e.g., 138, 153, and 180 (+PC1). This PCA again separates sabalo from Punta Lara, Tigre, and Quilmes with carp from Punta Lara, with the strongest contribution of lower chlorinated congeners, midway between the Aroclor 1254 and 1260 composition. The other samples show a progressive shift toward a higher contribution of more recalcitrant congeners, grouping the other carp samples with mullet from Quilmes. Varying Aroclor residue inputs along the coast are unlikely to explain this shift, since fish from the same locations are segregated into different groups, e.g., sabalo from Tigre and Quilmes and carp from the same sites. This trend most probably results from the selective elimination of lower chlorinated PCBs in less contaminated fish, which thus show

Table 4. TEQs of PCBs, PCDDs, and PCDFs in sabalo from the Río de la Plata.

	TEQ (pg·g fresh weight^{-1})		
	TIG	QUI	MG
PCBs			
77	0.0008	0.003	0.00003
126	0.01	0.05	—
118	3.14	9.69	0.06
105	1.33	4.15	0.05
156	2.48	8.46	0.09
180	0.49	1.28	—
170	2.51	7.23	0.11
Total PCBs	9.96	30.86	0.31
PCDDs			
1,2,3,7,8-PCDD	0.63	2.92	—
1,2,3,6,7,8-hexa-CDD	—	1.00	—
1,2,3,4,6,7,8-hepta-CDD	0.01	0.04	—
OCDD	0.001	0.003	—
Total PCDDs	0.641	3.963	—
PCDFs			
2,3,7,8-TCDF	0.53	1.85	—
2,3,4,7,8-PCDF	—	2.62	—
Total PCDFs	0.53	4.47	—
Grand total	11.13	39.30	0.31

Note: TIG, Tigre; QUI, Quilmes; MG, Magdalena; —, not detectable.

© 2000 NRC Canada

degraded PCB patterns dominated by the most recalcitrant hexa- (153, 138) and hepta-CBs (187, 183, 174, 180). Lower residue levels in fish with nondetection of less chlorinated congeners would produce an equivalent pattern. This is certainly the case for boga and also probably for sabalo from Magdalena, which are at the extremes of the trend (Fig. 3*b*), but not for the other samples, which show almost complete PCB detections. Furthermore, a similar decay of the Aroclor composition has been previously observed along the Río de la Plata coast and with increasing age of Asiatic clams (Colombo et al. 1995). These results indicate that most contaminated sabalo, together with carp from Punta Lara, show fresher PCB signatures with a higher proportion of less chlorinated congeners. This is consistent with hydrocarbon results, indicating that these organisms with the highest concentrations and adipose contents feed on fresh residues close to input sources and act as efficient accumulators with minimal degradation of the contaminant signature.

The PCA of chlorinated pesticides groups the samples according to the prevailing residues. The first two components account for 77% of the total variability, 62% PC1 and 15% PC2 (Fig. 3*c*). PC1 is basically determined by the contribution of chlordanes and TDE (–PC1) and DDE and heptachlor (+PC1). PC2 has a dominant contribution of BHCs, heptachlor epoxide, and HCB (+PC2). The most consistent cluster in this PCA is that formed by sabalo from Tigre and Punta Lara and carp from Quilmes, Tigre, and, to a lesser degree, Punta Lara, which are characterized by a higher relative abundance of chlordanes and TDE. Mullet and boga are again discriminated by their different composition but are distributed among BHC- (Punta Lara, Quilmes) and HCB/DDE-dominated (Magdalena, Tigre) patterns. Sabalo from Magdalena and Quilmes are very close, showing a stronger contribution of heptachlor epoxide. The PCA of pesticides groups the samples in a manner different from that of hydrocarbons, reflecting the decoupling of industrial and rural signals (e.g., main hydrocarbon inputs are not primary sources of pesticides) and the variability of agricultural loads along the coast following the distribution of small plantations. This would explain the relatively high pesticide concentrations in mullet from the rural area of Magdalena (Table 1). Nevertheless, the PCA of pesticides supports the pattern of mullet and boga segregation from the other species and also the discrimination of Magdalena from the other sampling sites.

For the final PCA of trace metals, the relative abundances of the elements in fish and a common local aquatic macrophyte (*Scirpus schenoplectum*) were used for the calculations. The first two components explain 95% of the total variance, 78% PC1 and 17% PC2 (Fig. 3*d*). The opposition between Zn (+PC1) and Cr, Ni, and Cu (–PC1) largely determines the first component, whereas that of Mn (+PC2) and the rest (–PC2) defines PC2. In this space, carp samples are clearly discriminated by their high Zn contents, suggesting a specific physiological requirement. The other major trend in the data is the separation of sabalo from Tigre and Magdalena with a higher Mn contribution, closer to the local macrophyte. As Mn is a major natural element, very abundant in suspended particles and sediments (Bilos et al. 1998), this trend interestingly agrees with the hydrocarbon results, suggesting a more "natural" diet in these organisms. The other fish in the negative quadrant have a stronger contribution of predominantly anthropogenic metals such as Cr, Ni, and Cu. Mullet samples from Quilmes and Magdalena occupy an intermediate position between this group and carp.

Health risks associated with fish consumption

The possible health risks associated with consumption of Río de la Plata fish were evaluated considering the tolerances and action levels fixed for human consumption (U.S. Food and Drug Administration 1990), the allowable consumption rates of fish calculated from dose factors (U.S. Environmental Protection Agency 1997), and the total toxicity equivalents (TEQ) for PCBs, dioxins, and furans.

In the case of trace metals, Río de la Plata fish levels are one to two orders of magnitude below the limits acceptable for human consumption, e.g., 1000 and 30 $\mu g \cdot g$ fresh weight^{-1} for Zn and Cu, respectively (Benemariya et al. 1991). The allowable fish consumption rates are estimates of exposure levels (milligrams per kilogram of body weight per day) that are not expected to cause adverse effects over a lifetime period. The allowable consumption of Río de la Plata fish for a 70-kg person based on the dose factors of Zn and Cu (200 and 15 $\mu g \cdot kg^{-1} \cdot day^{-1}$, respectively), and considering only the fish pathway uptake, would be (Zn–Cu) 3700–2000, 1100–2300, and 3400–2400 $g \cdot day^{-1}$ for average sabalo, carp and mullet, respectively. Considering a Cd dose factor (1 $\mu g \cdot kg^{-1} \cdot day^{-1}$) and half of the detection limit in fish (0.1 $\mu g \cdot g^{-1}$), the allowable consumption would be 700 $g \cdot day^{-1}$. These results indicate that for trace metals, there is no risk associated with fish consumption in the Río de la Plata.

The concentrations of chlorinated pesticides in Río de la Plata fish are generally low, below the action levels, e.g., for DDTs, 0.003–0.14 versus a level of 5 $\mu g \cdot g$ fresh weight^{-1}. Chlordane concentrations in fish are more critical, 0.006–0.51 versus an action level of 0.3 $\mu g \cdot g$ fresh weight^{-1}. The allowable fish consumption rates for a 70-kg person based on the reference dose factors of DDTs and chlordane (0.5 and 0.06 $\mu g \cdot kg^{-1} \cdot day^{-1}$, respectively) would be (DDTs–chlordane) 480–20, 1400–43, and 3500–210 g $fish \cdot day^{-1}$ for average sabalo, carp, and mullet, respectively. Heptachlor epoxide (dose factor 0.013 $\mu g \cdot kg^{-1} \cdot day^{-1}$) is the next most critical pesticide, whereas lindane (dose factor 0.3 $\mu g \cdot kg^{-1} \cdot day^{-1}$) is the least conflicting one, e.g., Punta Lara sabalo daily allowable consumption rate would be 8.3, 72, 240, and 2000 g $fish \cdot day^{-1}$ based on chlordane, heptachlor epoxide, DDTs, and lindane, respectively.

The risk related to consumption of Río de la Plata fish is even more critical when PCBs, dioxins, and furans are considered. Effectively, total PCB levels range from a low value of 0.05 $\mu g \cdot g^{-1}$ in mullet to 2.2–2.6 $\mu g \cdot g^{-1}$ in sabalo, which exceeds the action level for human consumption (2 $\mu g \cdot g^{-1}$). The allowable fish consumption rate for a 70-kg person based on the reference dose factor of PCBs (0.02 $\mu g \cdot kg^{-1} \cdot day^{-1}$) would be 1.0, 2.3, and 12 $g \cdot day^{-1}$ for average sabalo, carp, and mullet, respectively. The value decreases to 0.5–0.6 $g \cdot day^{-1}$ for sabalo from Quilmes or Punta Lara.

A more precise estimation of the risk associated with fish consumption is obtained through the calculation of TEQs. These factors take into account the abundance and the individual toxicity of PCBs, dioxins, and furans relative to 2,3,7,8-TCDD (Ahlborg et al. 1994). Table 4 presents the TEQs of sabalo collected at Tigre, Quilmes, and Magdalena.

© 2000 NRC Canada

Total values range from 0.31–11.1 to 39 pg·g fresh weight^{-1} at Quilmes, which exceeds the U.S. Food and Drug Administration advisory of 25 pg·g^{-1}. From these TEQs, PCBs account for about 80%, corroborating that these are the most critical contaminants in the Río de la Plata. This agrees with previous results from Asiatic clams whose TEQs ranged from 7 to13 pg·g^{-1}, with PCBs accounting for 83–88% (Colombo et al. 1997). The allowable consumption rates of Río de la Plata sabalo for a 70-kg person based on TEQ and U.S. Environmental Protection Agency reference doses, potency factors, and risk levels for carcinogenesis (0.6410 pg TEQs·kg^{-1}·day^{-1} = risk level, 10^{-4} per potency factor, 1.56×10^{5}) would be 145, 4.0, and 1.1 g·day^{-1} for Magdalena, Tigre, and Quilmes, respectively. The Quilmes result is comparable with those reported for Buffalo River carp, 0.4–1.0 g·day^{-1} (Loganathan et al. 1995).

Persistent organic contaminants and trace metals have been quantified in four fish species from the Río de la Plata estuary collected at four station with differing land uses. Río de la Plata fish present low levels of trace metal pollution but a more critical situation regarding organic pollutants. The highest concentrations were recorded in the sabalo, a dominant and remarkably specialized fatty detritivore. Other known detritivores such as carp and especially mullet presented a lower degree of contamination, indicating different feeding preferences. Superimposed on these interspecies differences, a geographical pattern of highest concentrations in fish from the major Buenos Aires urban center and lowest levels in fish from distant stations was also observed.

The analysis of contaminant signatures by multivariate techniques revealed subtle compositional differences between species and stations. Most contaminated sabalo showed the presence of fresh petrogenic and PCB signatures in the flesh, with levels exceeding tolerance limits (2.2–2.6 μg PCBs·g^{-1}). Mullet and, in general, fish from distant sites presented higher proportions of biogenic hydrocarbons and of more recalcitrant PCB congeners. Toxicity equivalents calculated for PCBs, dioxins, and furans ranged from 0.3 to >39 pg·g^{-1}, exceeding the recommended guideline. The calculation of allowable consumption rates based on reference dose factors indicated values as low as 0.6 g fish·day^{-1} for contaminated sabalo from the industrial area with a clear residue hazard ranking: PCBs > (3.7 times) PCDD/PCDF > (3.5 times) chlordane > (8.3 times) heptachlor epoxide > (3.3 times) DDTs > (8.3 times) lindane ≈ trace metals. Overall, these results indicate that, as a specialized detritivore, in contaminated areas, the sabalo acts as an effective accumulator of hydrophobic contaminants, feeding on polluted, organic-rich muds close to sewage and major industrial effluents. This feeding strategy probably represents a competitive advantage over other species, which avoid eating these materials. According to the contaminant load, carp appears to exploit a similar resource, most probably indirectly, i.e., not through direct mud ingestion but feeding on invertebrates inhabiting polluted sediments. The limited degradation of the contaminant signatures indicates that sabalo efficiently stores the residues in its rich adipose muscle compartment. Consequently, this fish constitutes a critical contamination pathway with potential health risks for humans. This would comprise foreign countries where the fish is exported and local fishers who include a significant proportion of Río de la Plata fish in their diets. These critical targets would be exposed to a much higher risk than the general Argentinean population, whose freshwater fish consumption is low. Nevertheless, the sabalo is frequently found in large supermarkets and food stores in the region, emphasizing the necessity for further studies to issue responsible management practices for this resource.

Acknowledgments

This research was supported by grants from the National University of La Plata (UNLP), Argentina, the Agencia de Promoción Científica y Tecnológica (PICT98 No. 13-04198), the Fisheries Direction of the Ministerio de Asuntos Agrarios de la Provincia de Buenos Aires, the Comisión de Investigaciones Científicas de la Provincia de Buenos Aires, and the Centre d'Expertise en Analyse Environnementale du Québec, Ministere de l'Environement du Québec, Canada.

References

Ahlborg, U.G., Becking, G.C., Birnbaum, L.S., Brouwer, A., Derks, H.J.G.M., Feeley, M., Golor, G., Hanberg, A., Larsen, J.C., Liem, A.K.D., Safe, S.H., Schlatter, C., Waern, F., Younes, M., and Yrjänheikki, E. 1994. Toxic equivalency factors for dioxin-like PCBs. Chemosphere, **28**: 1049–1067.

Albaigés, J., Farrán, A., Soler, M., and Gallifa, A. 1987. Accumulation and distribution of biogenic and pollutant hydrocarbons, PCBs and DDT in tissues of western Mediterranean fishes. Mar. Environ. Res. **22**: 1–18.

Benemariya, H., Robberecht, H., and Deelstra, H. 1991. Atomic absorption spectrometric determination of zinc, copper, and selenium in fish from Lake Tanganyika, Burundi, Africa. Sci. Total Environ. **105**: 73–85.

Bilos, C., Colombo, J.C., and Rodriguez Presa, M.J. 1998. Trace metals in suspended particles, sediments and Asiatic clams (*Corbicula fluminea*) of the Río de la Plata Estuary, Argentina. Environ. Pollut. **99**: 1–11.

Blumer, M., Guillard, R.R., and Chase, T. 1971. Hydrocarbons of marine phytoplankton. Mar. Biol. **8**: 183–189.

Bowen, S.H. 1983. Detritivory in neotropical fish communities. Environ. Biol. Fishes, **2**: 137–144.

Bowen, S.H., Bonetto, A.A., and Ahlgren, M.O. 1984. Microorganisms and detritus in the diet of a typical neotropical riverine detritivore, *Prochilodus platensis* (Pisces: Prochilodontidae). Limnol. Oceanogr. **29**: 1120–1122.

Bush, B., Streeter, R.W., and Sloan, R.J. 1989. Polychlorobiphenyl (PCB) congeners in striped bass (*Morone saxatilis*) from marine and estuarine waters of New York State determined by capillary gas chromatography. Arch. Environ. Contam. Toxicol. **19**: 49–61.

Cardona, L., Torras, X., Gisbert, E., and Castello, F. 1996. The effect of striped grey mullet (*Mugil cephalus*) on freshwater ecosystems. Isr. J. Aquacult. **48**: 179–185.

Colombo, J.C., Pelletier, E., Brochu, C., Khalil, M., and Catoggio, J.A. 1989. Determination of hydrocarbon sources using *n*-alkane and polyaromatic hydrocarbon distribution indexes. Case study: Río de la Plata Estuary, Argentina. Environ. Sci. Technol. **23**: 888–894.

Colombo, J.C., Khalil, M.F., Arnac, M., Horth, A.C., and Catoggio, J.A. 1990. Distribution of chlorinated pesticides and individual polychlorinated biphenyls in biotic and abiotic compartments of the Río de la Plata, Argentina. Environ. Sci. Technol. **24**: 498–505.

Colombo, J.C., Bilos, C., Campanaro, M., Rodriguez Presa, M.J., and Catoggio, J.A. 1995. Bioaccumulation of polychlorinated

© 2000 NRC Canada

biphenyls and chlorinated pesticides by the Asiatic clam *Corbicula fluminea*: its use as sentinel organism in the Río de la Plata estuary, Argentina. Environ. Sci. Technol. **29**: 914–927.

Colombo, J.C., Silverberg, N., and Gearing, J.N. 1996. Lipid biogeochemistry in the Laurentian Trough: I. Fatty acids, sterols and aliphatic hydrocarbons in rapidly settling particles. Org. Geochem. **25**: 211–225.

Colombo, J.C., Brochu, C., Bilos, C., Landoni, P., and Moore, S. 1997. Long-term accumulation of individual PCBs, dioxins, furans and trace metals in Asiatic clams from the Río de la Plata Estuary, Argentina. Environ. Sci. Technol. **31**: 3551–3557.

Fabrizio, M.C., Sloan, R.J., and O'Brien, J.F. 1991. Striped bass stocks and concentrations of polychlorinated biphenyls. Trans. Am. Fish. Soc. **120**: 541–551.

Fernandes, M.H., Bidone, E.D., Sadler Veiga, L.H., and Patchineelam, R. 1994. Heavy-metal pollution assessment in the coastal lagoons of Jacarepaguá, Río de Janeiro, Brazil. Environ. Pollut. **85**: 259–264.

Fox, G.A., Weseloh, D.V., Kubiak, T.J., and Erdman, T.C. 1991. Reproductive outcomes in colonial fish-eating birds: a biomarker for developmental toxicants in Great Lakes food chains. I. Historical and ecotoxicological perspectives. J. Gt. Lakes Res. **17**: 153–157.

Giesy, J.P., Verbrugge, D.A., Othout, R.A., Bowerman, W.W., Mora, M.A., Jones, P.D., Newsted, J.L., Vandervoort, C., Heaton, S.N., Aulerich, R.J., Bursian, S.J., Ludwig, J.P., Ludwig, M., Dawson, G.A., Kubiak, T.J., Best, D.A., and Tillitt, D.E. 1994. Contaminants in fishes from Great Lakes-influenced sections and above dams of three Michigan rivers. I: concentrations of organochlorine insecticides, polychlorinated biphenyls, dioxin equivalents, and mercury. Arch. Environ. Contam. Toxicol. **27**: 202–212.

Gilbertson, M. 1985. The Niagara labyrinth — the human ecology of producing organochlorine chemicals. Can. J. Fish. Aquat. Sci. **42**: 1681–1692.

Gümgüm, B., Ünlü, E., Tez, Z., and Gülsün, Z. 1994. Heavy metal pollution in water, sediment and fish from the Tigris River in Turkey. Chemosphere, **29**: 111–116.

Kannan, K., Tanabe, S., and Tatsukawa, R. 1995. Geographical distribution and accumulation features of organochlorine residues in fish in tropical Asia and Oceania. Environ. Sci. Technol. **29**: 2673–2683.

Kuehl, D.W., Butterworth, B., and Marquis, P.J. 1994. A national study of chemical residues in fish. III: study results. Chemosphere, **29**: 523–535.

Law, F.C.P., and Gudaitis, J.A. 1994. A preliminary assessment of human health risks due to consumption of fish contaminated by dioxins and furans in the Fraser and Thompson rivers. Chemosphere, **28**: 1079–1086.

Loganathan, B.G., Kannan, K., Watanabe, I., Kawano, M., Irvine, K., Kumar, S., and Sikka, H.C. 1995. Isomer-specific determination and toxic evaluation of polychlorinated biphenyls, polychlorinated/brominated dibenzo-*p*-dioxins and dibenzofurans, polybrominated biphenyl ethers, and extractable organic halogen in carp from the Buffalo River, New York. Environ. Sci. Technol. **29**: 1832–1838.

Manno, J., Myers, S., Riedel, D., and Trembley, N. 1995. Effects of Great Lakes basin environmental contaminants on human health. SOLEC Working Paper. EPA 905-R-95-013. U.S. Environmental Protection Agency, Washington, D.C.

Miller, M.A. 1994. Organochlorine concentration dynamics in Lake Michigan chinook salmon (*Oncorhynchus tshawytscha*). Arch. Environ. Contam. Toxicol. **27**: 367–374.

Miller, P.A., Munkittrick, K.R., and Dixon, D.G. 1992. Relationship between concentrations of copper and zinc in water, sediment, benthic invertebrates, and tissue of white sucker (*Catostomus commersoni*) at metal-contaminated sites. Can. J. Fish. Aquat. Sci. **49**: 978–984.

Niimi, A.J., and Oliver, B.G. 1989. Distribution of polychlorinated biphenyl congeners and other halocarbons in whole fish and muscle among Lake Ontario salmonids. Environ. Sci. Technol. **23**: 83–88.

Porte, C., and Albaigés, J. 1993. Bioaccumulation patterns of hydrocarbons and polychlorinated biphenyls in bivalves, crustaceans, and fishes. Arch. Environ. Contam. Toxicol. **26**: 273–281.

Ravid, R., Ben-Yosef, J., And Hornung, H. 1985. PCBs, DDTs and other chlorinated hydrocarbons in marine organisms from the Mediterranean coast of Israel. Mar. Pollut. Bull. **16**: 35–38.

Salánki, J., Licskó, I., László, F., Balogh, K.V., Varanka, I., and Mastala, Z. 1992. Changes in the concentration of heavy metals in the Zala Minor Balaton – Zala system (water, sediment, aquatic life). Water Sci. Technol. **25**: 173–180.

Schüler, W., Brunn, H., and Manz, D. 1985. Pesticides and polychlorinated biophenyls in fish from the Lahn River. Bull. Environ. Contam. Toxicol. **34**: 608–616.

Sibbing, F.A. 1988. Specializations and limitations in the utilization of food resources by the carp, *Cyprinus carpio*: a study of oral food processing. Environ. Biol. Fishes, **22**: 161–178.

Stow, C.A., and Qian, S.S. 1998. A size-based probabilistic assessment of PCB exposure from Lake Michigan fish consumption. Environ. Sci. Technol. **32**: 2325–2330.

Sverlij, S.B., Espinach Ros, A., and Orti, G. 1993. Sinopsis de los datos biológicos y pesqueros del sabalo *Prochilodus lineatus* (Valenciennes, 1847). FAO Sinopsis sobre la pesca No. 154. FAO, Rome.

Tillitt, D.E., Gale, R.W., Meadows, J.C., Zalicek, J.L., Peterman, P.H., Heaton, S.N., Jones, P.D., Bursian, S.J., Kubiak, T.J., Giesy, J.P., and Aulerich, R.J. 1996. Dietary exposure of mink to carp from Saginaw Bay. 3. Characterization of dietary exposure to planar halogenated hydrocarbons, dioxin, equivalents, and biomagnification. Environ. Sci. Technol. **30**: 283–291.

U.S. Environmental Protection Agency. 1997. Guidance for assessing chemical contaminant data for use in fish advisories. Vol. 2. Risk assessment and fish consumption limits. 2nd ed. Office of Science and Technology, Office of Water, U.S. Environmental Protection Agency, Washington, D.C.

U.S. Food and Drug Administration. 1990. Residues in foods 1990. Food and Drug Administration Pesticide Program. U.S. Food and Drug Administration, Washington, D.C.

White, R.J., Kim, H.T., and Kim, J.S. 1985. PCBs in striped bass collected from the Hudson River, New York, during fall, 1981. Bull. Environ. Contam. Toxicol. **34**: 883–889.

© 2000 NRC Canada

Effect of aluminum and silicic acid on the behaviour of the freshwater snail *Lymnaea stagnalis*

Morag M. Campbell, Keith N. White, Ravin Jugdaohsingh, Jonathan J. Powell, and Catherine R. McCrohan

Abstract: A major factor influencing the toxicity of Al at neutral pH is the presence of complexing ligands. This study compared the effect of exposure to aluminum nitrate, aluminum lactate, and aluminum maltol, in the presence or absence of monomeric silica (Si), on the behaviour of the pond snail *Lymnaea stagnalis*. Concentrations of Al and Si used were similar to those found in the natural environment. Soluble Al concentration in the water fell significantly with time over 48 h following addition as the nitrate or lactate (500 $\mu g \cdot L^{-1}$), presumably owing to polymerisation as the colloidal hydroxide. This loss was enhanced by the presence of snails or Si (Al:Si = 1:15). Aluminum maltol largely remained in solution. Snails exposed to all three Al compounds showed depression of behavioural activity after 7 days; this effect was ameliorated in the presence of higher (Al:Si = 1:15) but not lower (Al:Si = 1:1) concentrations of Si. Depression of feeding behaviour occurred with all three Al compounds, although it was delayed in the presence of aluminum maltol. Expression of conditioned feeding was inhibited in snails exposed to aluminum nitrate during training and testing. The behavioural changes are likely to be mirrored in the field, with adverse consequences for the "fitness" of natural populations.

Résumé : Un facteur important qui influe sur la toxicité de l'aluminium (Al) dans un milieu au pH neutre est la présence de complexes de ligands. La présente étude a comparé l'incidence de l'exposition au nitrate d'aluminium, au lactate d'aluminium et au maltolate d'aluminium, en présence ou non de silice monomère (Si), sur le comportement des lymnées (*Lymnaea stagnalis*). Les concentrations d'Al et de Si utilisées étaient semblables à celles que l'on retrouve dans le milieu naturel. La concentration dans l'eau d'Al soluble, sous forme de nitrate ou de lactate (500 $\mu g \cdot L^{-1}$), a considérablement diminué avec le temps sur une période de 48 h suivant l'ajout, probablement à cause de la polymérisation sous forme d'hydroxyde colloïdal. Cette baisse était davantage marquée par la présence de gastropodes ou de Si (Al:Si 1:15). Le maltolate d'aluminium est resté pour l'essentiel en solution. Les gastropodes exposés aux trois composés d'aluminium ont montré un ralentissement dans leurs activités de comportement après 7 jours. Ce ralentissement était moins marqué quand les concentrations de Si augmentaient (Al:Si 1:15), mais non quand elles diminuaient (Al:Si 1:1). Une baisse du comportement de nourrissage a été observée chez les gastropodes exposés aux trois composés d'aluminium, mais elle s'est manifestée un peu plus tard dans le cas du maltolate d'aluminium. Pendant l'entraînement et les tests, l'expression de la réaction conditionnée au nourrissage était inhibée chez les gastropodes exposés au nitrate d'aluminium. Les changements de comportement observés existent sûrement dans le milieu naturel, ce qui fait craindre des conséquences néfastes pour le succès reproducteur des populations naturelles.

[Traduit par la Rédaction]

Introduction

Aluminum is both harmful to and accumulated by organisms in acid waters (Havas and Likens 1985; Pynnönen 1990). Its aqueous solution chemistry predicts the formation of insoluble colloids at neutral pH. Thus, Al would be expected to be only minimally bioavailable, and therefore less toxic, at neutral pH than at acidic pH (Martin 1986). Our recent work, however, has shown significant accumulation of Al by the freshwater snail *Lymnaea stagnalis* at neutral pH (Elangovan et al. 1997), together with changes in behaviour (Truscott et al. 1995), at concentrations (100–500 $\mu g \cdot L^{-1}$) commonly present in natural waters. Similarly, transformation of Al (50–240 $\mu g \cdot L^{-1}$) into high molecular weight colloidal species as pH increased from acidic to near neutral (6.5) values was shown to markedly increase toxicity of Al to salmon, with an LT_{50} of 7 h (Rosseland et al. 1992). In a study of major U.K. rivers, Dixon and Gardner (1998) reported concentrations of total Al ranging from 8.9 to 458 $\mu g \cdot L^{-1}$ at pHs between 7.3 and 8.7.

The main factor influencing bioavailability of Al at neutral pH is the presence of complexing ligands, which, in natural waters, include organic compounds and silicic acid (soluble silica, $SiOH_4$) (Duan and Gregory 1998). Films of extracellular mucopolysaccharide (EPS) are secreted by the

Received March 30, 1999. Accepted February 2, 2000.
J15090

M.M. Campbell, K.N. White, and C.R. McCrohan.[1] School of Biological Sciences, University of Manchester, 1.124 Stopford Building, Oxford Road, Manchester M13 9PT, U.K.
R. Jugdaohsingh and J.J. Powell. Gastrointestinal Laboratory, The Rayne Institute, St Thomas' Hospital, London SE1 7EH, U.K.

[1]Author to whom all correspondence should be addressed.
e-mail: Cathy.McCrohan@man.ac.uk

© 2000 NRC Canada

snail and other organisms associated with the substrate, including bacteria and algae. The EPS biofilm binds polyhydroxy aluminum, thus removing it from the water column (Jugdaohsingh et al. 1998). Subsequently, snails graze on the EPS film and therefore rapidly accumulate Al (Elangovan et al. 1997). Thus, freshwater grazers such as *L. stagnalis* are exposed to particularly high concentrations of Al as a result of feeding on biofilms that are a "sink" for Al released into the water column. Toxicity is evidenced by behavioural changes (Truscott et al. 1995); however, the influence of Al solubility and the presence of silicic acid have not been examined.

A unique affinity exists between Al and Si both in the environment and in biological systems. Silicon is found in natural waters as silicic acid, due to weathering of otherwise highly stable aluminosilicates, which are abundant as rock and soil minerals. In biological systems, Si has already been shown to reduce availability (Edwardson et al. 1993) and ameliorate toxicity of Al (Birchall et al. 1989), but their interactions are poorly understood.

In this study, we compared the effect on *L. stagnalis* of exposure to Al as the nitrate, lactate, and maltol complexes in the presence and absence of soluble monomeric silica. These represent, respectively, strongly hydrolysing and weakly and strongly bound Al complexes, all of which might be expected to be present in the natural environment. All of these compounds have been used previously in Al-based toxicological studies (Zatta et al. 1991), but their availability and toxicities have not been compared in a single organism. In addition, *L. stagnalis* is of interest because, unlike mammals, it significantly accumulates polyhydroxy (i.e., colloidal) aluminum at neutral pH (Elangovan et al. 1997). Sublethal toxicity was assessed by changes in behavioural parameters, including overall activity level and feeding behaviour, and the ability to acquire and express a learned response.

Materials and methods

Lymnaea stagnalis (shell length 25–35 mm) were obtained from Blades Biological (Kent, U.K.). Prior to all experiments, snails were kept in 20-L tanks of aerated standard snail water (SSW, composition (millimolar): $CaCl_2$, 2.0; $MgSO_4$, 0.08; $KHCO_3$, 0.04; KNO_3, 0.05; $NaHCO_3$, 0.07; pH 6.8–7.2) and fed on lettuce for at least 14 days. SSW has been found to contain up to a maximum of 40 μg total $Al \cdot L^{-1}$ as a contaminant (Elangovan et al. 1997). Exposure experiments were carried out at room temperature (17–21°C) in acid-washed 10-L high-density plastic tanks containing 5 L of aerated SSW. The SSW was changed every 48 h and redosed with Al and, where appropriate, Si. Material on the sides of the tanks was not deliberately removed during this procedure. Where necessary, pH was adjusted daily by addition of 0.1 M NaOH or HCl. All reagents were of analytical grade (BDH Ltd., Poole) unless otherwise indicated. Water was ultrapure (UHP) 18 $M\Omega \cdot cm^{-1}$ (Elga water purifier).

Addition of Al and Si

Aluminum nitrate ($Al(NO_3)_3$ nonahydrate), aluminum lactate ($Al(lac)_3$, lac = 2-hydroxoproprionate), and aluminum maltolate ($Al(malt)_3$, malt = 3-hydroxy-2-methyl-4H-pyran-4-onate) were added to the tanks from stock solutions prepared at 500 mg $Al \cdot L^{-1}$. Stock solutions of aluminum nitrate (Aldrich Chemicals, Dorset, U.K.) and aluminum lactate (Fluka Chemicals, Dorset, U.K.) were prepared by dissolving the appropriate amount directly into acidified (pH 3) water. Aluminum maltol was prepared using $AlCl_3$ (Aldrich Chemicals) and maltol (Sigma, Dorset, U.K.) (Finnegan et al. 1986). Briefly, the $AlCl_3$ was dissolved in acidified water and maltol added in a molar ratio of 1:5 (Al:maltol). This ensures an excess of maltol for formation of aluminum(III) tris-maltolate on neutralisation. Aliquots of the stock solution were added to the SSW to give a final concentration of 500 μg $Al \cdot L^{-1}$ (experiments 1, 2, 4, and 5) and 1000 μg $Al \cdot L^{-1}$ (experiment 3) and pH was adjusted appropriately. When Si was present, the appropriate amount of 7 M basic sodium silicate solution (Aldrich, Gillingham, U.K.) was added directly to 5 L of SSW. The solution was aged for 24 h before addition of Al; this ensures that soluble silica is completely monomeric. Silicon was then added at an Al:Si molar ratio of ≤1:15, giving a final Si concentration of 7.77 $mg \cdot L^{-1}$ at 1:15. At this concentration (below the boundary concentration for polymerisation) and at neutral pH, Si exists only in monomeric form as $Si(OH)_4 \approx Si(OH_3)O^- \approx Si(OH_2)O_2^{2-}$ (Iler 1979), and this was confirmed in all experiments using the molybdate assay as previously reported (Taylor et al. 1997).

Measurement of total Al in water

Water samples (10 mL) were taken from 5 cm below the surface at the centre of the tank, acidified to 0.1 M with 70% HNO_3 (Aristar, BDH), and analysed by ICPOES (Jobin-Yvon JY24, Instruments SA, Longjumeau, France). This measures total Al in the water column, which is here referred to as "soluble" Al, although we recognise that this fraction represents Al with varying degrees of hydroxy polymerisation, including colloids. The instrument was fitted with a V-groove nebuliser and conventional Scott-type spray chamber and Al was analysed at 396.152 nm as previously described (Burden et al. 1995). Standards were 0–600 μg $Al \cdot L^{-1}$ prepared in SSW acidified to 0.1 M HNO_3 from a 1000 mg $Al \cdot L^{-1}$ standard stock solution (Spectrosol, Merck, Poole).

Measurement of behavioural parameters

Snails were placed individually in a large (100-mm-diameter) petri dish containing 40 mL of SSW and left for at least 15 min. The dish was raised on a tripod stand with a mirror beneath for observation of mouth and radula movements.

Behavioural state score (BSS) is an established behavioural score (Tuersley and McCrohan 1987), giving an indication of a snail's overall level of activity. Each snail was observed for a total of 2 min and awarded the highest BSS that it achieved in that time according to the following criteria (for details, see Tuersley and McCrohan 1987): fully retracted into shell, 0 point; withdrawn, 1 point; tentacle movements only, 2 points; head protruding but no movement, 3 points; head and foot extended with orientation movements of head, 4 points; active locomotion from place to place, 5 points. Additional points were awarded for biting (2 points), shell twisting (1 point), and mouth movements (1 point).

Three parameters relating to feeding behaviour were recorded: the total number of spontaneous bites (radula protraction and retraction) made in 2 min and latency to the first bite and the total number of bites made in 2 min following presentation of a phagostimulus (0.67% sucrose). These have been used previously to assess the food arousal status of *L. stagnalis* (Tuersley and McCrohan 1987). Eight millilitres of SSW was first added to the dish to control for disturbance. The snail was then observed for 2 min and the number of bites counted. Eight millilitres of 4% sucrose was then added and latency to bite and number of bites in 2 min recorded. If the snail did not bite within 2 min in response to sucrose, it was awarded an arbitrary latency to bite score of 120 s.

Experimental protocols

Experiment 1. Loss of Al from the water

Four experimental conditions were studied as summarised in Ta-

© 2000 NRC Canada

ble 1. For each of these conditions, four tanks were set up: one tank contained no added Al and acted as control and the remaining three had Al (500 $\mu g \cdot L^{-1}$) added as aluminum nitrate, aluminum lactate, or aluminum maltol. Where appropriate, Si was added at an Al:Si molar ratio of 1:15. This was chosen based on the findings of Birchall et al. (1989) who showed amelioration of Al toxicity to fish using this ratio. The pH was adjusted to 7.0 at 0, 24, and 48 h. Snails were unfed throughout. Two water samples were taken for analysis for total Al at 0, 1, 2, 4, 6, 10, 24, 32, and 48 h.

Experiment 2. Changes in BSS in response to Al and Si exposure

In this experiment, a single measure of overall activity, or arousal, the BSS, was used to monitor the snails' activity. Eight tanks (two groups of four) were set up, each containing 12 snails. In the first group, three of the tanks contained aluminum nitrate, aluminum lactate, or aluminum maltol, added at 500 μg $Al \cdot L^{-1}$, which was renewed every 48 h. The fourth tank had no Al added (control). The second group of tanks were the same, except for 24-h prior addition of 7.77 mg $Si \cdot L^{-1}$ to each. The pH of the water was adjusted to 7.0 every 24 h. BSS was measured on days 0 (before addition of Al), 2, 7, and 14.

Experiment 3. Changes in BSS using reduced Si concentration

Six tanks were set up, each containing 15 snails. Two control tanks contained SSW with no added Al or Si, two tanks contained added Al only (1000 $\mu g \cdot L^{-1}$ as nitrate), and two contained added Al plus either 15.54 or 1.04 mg $Si \cdot L^{-1}$ (i.e., Al:Si molar ratios of 1:15 and 1:1, respectively). Tank water was changed and pH maintained as before. BSS was measured on days 0 (before addition of Al) and 7.

Experiment 4. Changes in feeding behaviour in response to Al exposure

Four tanks were set up, each containing 12 snails. Three of the tanks contained aluminum nitrate, aluminum lactate, or aluminum maltol, added at 500 μg $Al \cdot L^{-1}$. The fourth tank had no Al added (control). Feeding behaviour was measured on days 0 (before addition of Al), 2, 7, and 14. Tank water was changed and pH adjusted as before. An identical experiment was carried out, but using control ligands (3.4 mg nitrate$\cdot L^{-1}$, 4.9 mg lactate$\cdot L^{-1}$ and 11.6 mg maltol$\cdot L^{-1}$) instead of the Al–ligand complexes. The concentrations of the ligands in these controls were equal to those in the experimental tanks.

Experiment 5. Changes in learning ability in response to Al

Four tanks were set up, each containing 12 snails. Two groups were exposed to 500 μg $Al \cdot L^{-1}$ added as aluminum nitrate; the other two were not exposed to Al. A classical conditioning paradigm (modified from Audesirk et al. 1982; Whelan and McCrohan 1996) was used in which a previously neutral stimulus (0.004% amyl acetate, conditioned stimulus (CS)) was paired repeatedly with an unconditioned stimulus (UCS) (0.67% sucrose). One of the groups from each treatment was experimentally conditioned; the other was assigned to be a random presentation control. The two experimental groups received 15 training trials (CS–UCS pairings) over 3 days (five trials per day with an intertrial period of 90 min). For each trial, the snails were transferred on a fine mesh to small tanks containing 200 mL of SSW (no added Al). Amyl acetate was then added (50 mL from a stock solution of 0.024%). After 15 s, 50 mL of a 4% sucrose solution was added and snails were left for 2 min and then rinsed with SSW and placed back into the holding tank. The random control groups received a similar SSW–UCS pairing at the same time. At a random time in the intertrial period, the random control groups received a CS–SSW pairing and experimental groups received an SSW–SSW pairing. In this way, exposure to the two stimuli and handling were equalised between experimental and control groups. Behavioural testing was carried out before training or exposure to Al and then at days 2, 7, and 14 after the end of training (i.e., 5, 10, and 17 days after the onset of Al exposure). Testing was carried out individually in a petri dish containing 40 mL of SSW, as before. First, 8 mL of SSW was added and the number of bites in a 2-min interval counted (R1, baseline number of bites). Then, 8 mL of the CS (amyl acetate stock solution) was added and bites counted for a further 2 min (R2). R2–R1 was calculated for each snail so that both increases and decreases in biting activity would be recorded.

Table 1. Summary of experimental (tank) conditions for experiment 1.

Added Al ($\mu g \cdot L^{-1}$)	Added Si ($mg \cdot L^{-1}$)	No. of snails
500	0	12
500	0	0
500	7.77	12
500	7.77	0

Data analysis

Water Al measurements were analysed using parametric statistical methods (Minitab Inc., Pennsylvania). Behavioural data were analysed by nonparametric analysis of variance of ranks (Kruskal–Wallis test) followed by a nonparametric multiple comparison test (Dunn 1964).

Results

Loss of Al from the water column

In all tanks to which Al was added, soluble Al concentration fell with time regardless of the form in which Al was added or whether snails or Si were present (Fig. 1). However, the fall in soluble Al concentration was much greater in tanks to which Al had been added in the form of aluminum nitrate or aluminum lactate compared with aluminum maltol (Figs. 1*b*–1*d*). As expected from recent studies, soluble Al concentrations appeared to fall more quickly in tanks that contained snails (Jugdaohsingh et al. 1998) or monomeric silica (Duan and Gregory 1998). To quantify this, data in Fig. 1 were log transformed, and linear regression coefficients, representing loss of Al over time, were calculated (Table 2). Aluminum concentration in the water was strongly negatively correlated with time for all Al compounds and experimental conditions, with the exception of aluminum maltol where correlations were weak or absent. Analysis of covariance showed that the Al was lost at a similar rate when added as the nitrate and lactate but loss was significantly greater in the presence of snails ($p < 0.002$). In tanks that contained snails, the presence of Si had no additional effect on loss of Al. However, in tanks that contained no snails, the presence of Si significantly ($p < 0.02$) increased the rate at which Al was removed from the water column. Aluminum maltol was lost more slowly ($p < 0.001$) from the water column than aluminum nitrate or aluminum lactate. Indeed, in the absence of snails, there was no correlation between soluble Al concentration and time. However, the presence of snails increased the loss of Al from the water column, which was further increased with the addition of Si ($p < 0.001$).

© 2000 NRC Canada

Fig. 1. Effect of presence or absence of snails and Si on total Al concentrations in the water column of experimental tanks over 48 h. (*a*) No added Al (control); Al (500 $\mu g \cdot L^{-1}$) added as the (*b*) nitrate, (*c*) lactate, and (*d*) maltol. Circles, no added Si; squares, Si (7.77 $mg \cdot L^{-1}$) added at an Al:Si ratio of 1:15; open symbols, no snails; solid symbols, 12 snails.

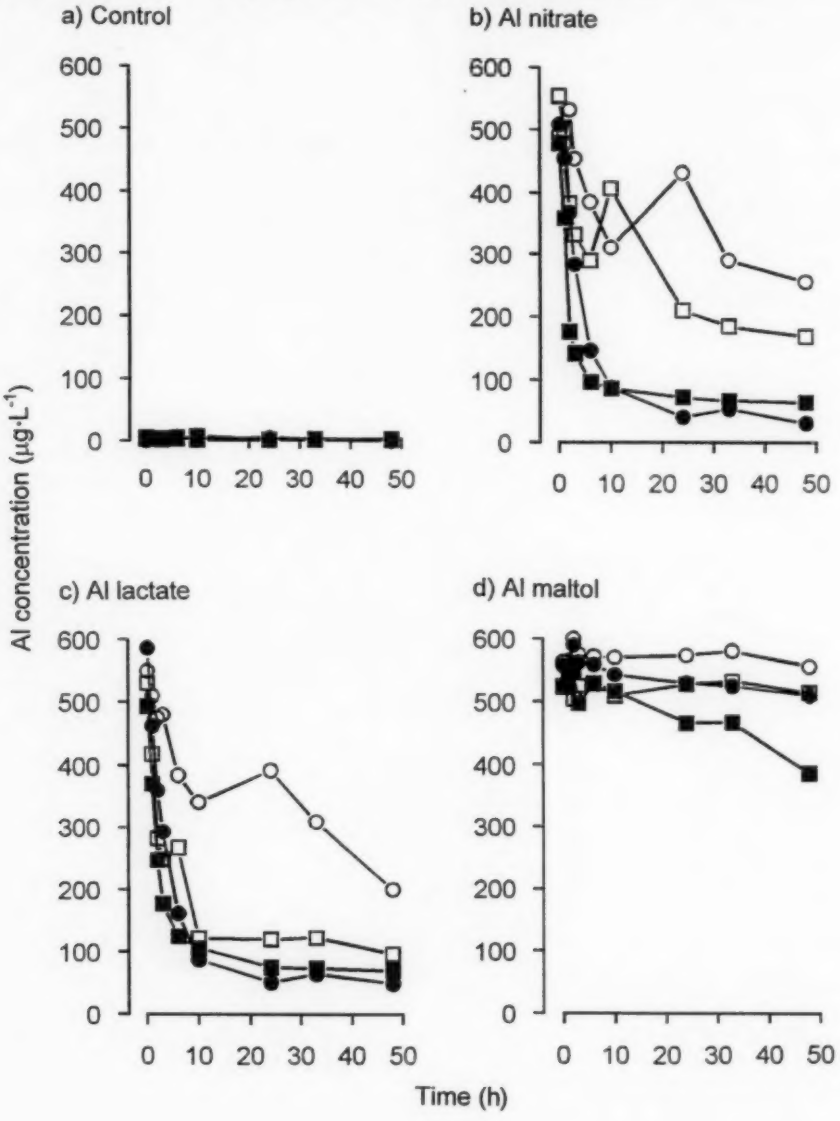

Changes in BSS in response to Al and Si exposure

Prior to exposure (day 0) and after 2 days of exposure, there was no significant difference in BSS between any experimental and control groups (Fig. 2). After 7 days of exposure, BSS was significantly reduced for all groups exposed to Al in the absence of Si ($p < 0.05$–0.005, Kruskal–Wallis test) (Fig. 2). However, in the presence of Si, this effect was blocked so that BSS of Al-exposed snails was not significantly ($p > 0.05$) depressed. BSS was not significantly different between any groups on day 14, suggesting acclimation of snails exposed to Al alone (Fig. 2).

Changes in BSS using reduced Si concentration

After 7 days of exposure, snails exposed to aluminum nitrate alone showed a significantly reduced BSS in the absence of Si ($p < 0.001$, Kruskal–Wallis test) (Fig. 3). This reduction was reversed in the presence of Si at a 1:15 Al:Si molar ratio (Fig. 3*a*) but not with the lower concentration of Si (1:1 molar ratio) (Fig. 3*b*).

Changes in feeding behaviour in response to Al exposure

Prior to Al exposure, no significant differences in spontaneous biting activity were found between experimental

© 2000 NRC Canada

Table 2. Results of linear regression analysis of data from experiment 1.

Conditions	R^2	p
Al added as nitrate		
12 snails, no Si	0.96	<0.001
No snails, no Si	0.67	0.007
12 snails, Si present	0.88	<0.001
No snails, Si present	0.87	<0.001
Al added as lactate		
12 snails, no Si	0.96	<0.001
No snails, no Si	0.78	<0.001
12 snails, Si present	0.95	<0.001
No snails, Si present	0.93	<0.001
Al added as maltol		
12 snails, no Si	0.62	0.011
No snails, no Si	0.01	0.806 (ns)
12 snails, Si present	0.95	0.010
No snails, Si present	0.01	0.748 (ns)

Note: Regression coefficients represent loss of Al over time from tanks under different conditions. ns, not significant ($p > 0.05$).

groups and controls. Addition of Al caused a significant reduction in spontaneous biting compared with controls for all three Al compounds, but the timing of this reduction varied. The reduction was significant after 2 days for groups exposed to aluminum nitrate and aluminum lactate ($p < 0.05$, Kruskal–Wallis test) (Figs. 4*a* and 4*b*). Spontaneous biting in animals exposed to aluminum nitrate returned to control levels by day 7 and for aluminum lactate by day 14 (Fig. 4*b*). However, for animals exposed to aluminum maltol, spontaneous biting activity was not significantly reduced until day 7 ($p < 0.05$) but remained so at day 14 (Fig. 4*c*).

For responses to a phagostimulant, again, there was no difference between control and experimental groups prior to Al exposure (Figs. 5 and 6). On addition of Al, changes in responses generally mirrored those for spontaneous biting activity, although latency to bite was not affected significantly by exposure to aluminum nitrate (Fig. 5*a*). However, it was significantly ($p < 0.05$) increased on days 2 and 7 for animals in the aluminum lactate group and then returned to control levels by day 14 (Fig. 5*b*). Again, with aluminum maltol, the increase in latency to bite was delayed, being significantly elevated on days 7 and 14 ($p < 0.05$) (Fig. 5*c*). The number of bites in response to sucrose was significantly ($p < 0.05$) reduced on day 2 in both the aluminum nitrate and aluminum lactate groups, returning to control levels by day 7 (Figs. 6*a* and 6*b*). This reduction was again delayed in the aluminum maltol group, not appearing until day 7 and continuing to day 14 ($p < 0.05$) (Fig. 6*c*).

No significant differences were seen between ligand-exposed and control groups for any of the parameters on any day, confirming that ligands alone had no effect on behaviour.

Changes in learning ability in response to Al

Figure 7 shows the number of bites (R2–R1) made in response to amyl acetate (CS) prior to training or exposure to Al (naïve) and 2, 7, and 14 days after training (i.e., 5, 10, and 17 days after the onset of exposure to Al). In naïve snails, the CS elicited no feeding response, confirming that

Fig. 2. Effect of presence or absence of Si on BSS during exposure to Al (500 $\mu g \cdot L^{-1}$) added as the (*a*) nitrate, (*b*) lactate, and (*c*) maltol. BSS was measured prior to (day 0) and after 2, 7, and 14 days of exposure. Open bars, control (no Al or Si); cross-hatched bars, Si alone; stippled bars, Al and Si (7.77 $mg \cdot L^{-1}$) added; hatched bars, Al alone. Bars represent median ± interquartile range. $^*p < 0.05$, $^{**}p < 0.01$, and $^{***}p < 0.005$ (Kruskal–Wallis test followed by Dunn's multiple comparison test).

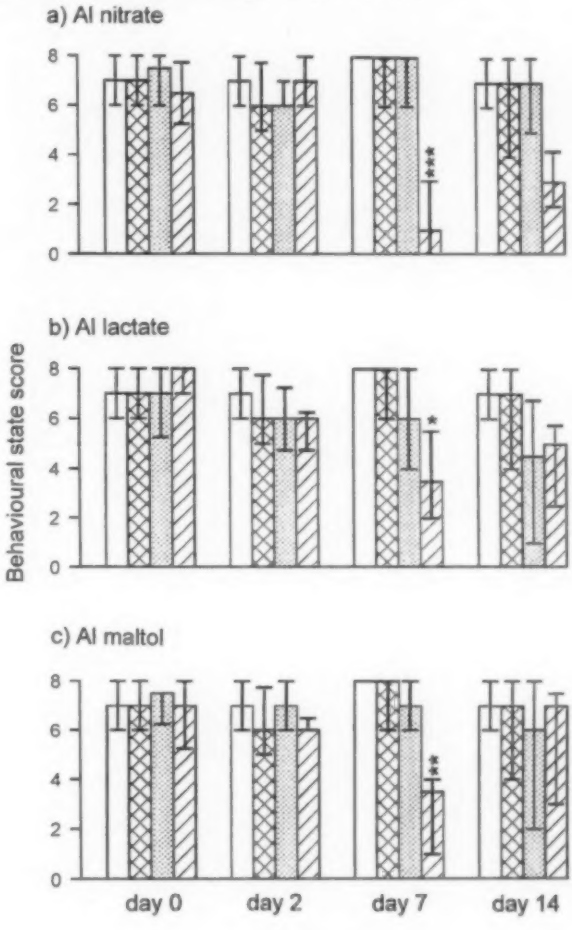

amyl acetate is a neutral stimulus with regard to feeding behaviour (Fig. 7*a*). Two days after training, the experimentally conditioned animals that had not been exposed to Al made significantly more bites in 2 min in response to the CS than the random controls ($p < 0.05$, Kruskal–Wallis followed by Dunn's multiple comparison test), indicating that a conditioned response had been acquired. However, experimentally conditioned animals exposed to Al did not make significantly more bites than controls (Fig. 7*b*). After 7 days, both experimentally conditioned groups showed a significant feeding response to the CS ($p < 0.05$, Fig. 7*c*). This indicates that snails exposed to Al had acquired a conditioned response, but this was not expressed on day 2. At 14 days, there was no significant difference in the biting response of

© 2000 NRC Canada

Fig. 3. Effect of exposure to aluminium nitrate (1000 $\mu g \cdot L^{-1}$) in the presence or absence of different concentrations of Si ((*a*) 15.54 $mg \cdot L^{-1}$; (*b*) 1.04 $mg \cdot L^{-1}$) on BSS measured prior to (day 0) and after 7 days of exposure. Open bars, control (no added Al or Si); stippled bars, Al and Si; hatched bars, Al only. Bars represent median ± interquartile range. $*p < 0.001$ (Kruskal–Wallis test followed by Dunn's multiple comparison test).

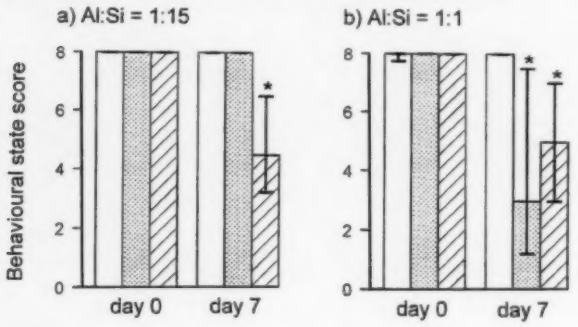

Fig. 4. Effect of Al on spontaneous biting activity measured prior to (day 0) and after 2, 7, and 14 days of exposure to Al (500 $\mu g \cdot L^{-1}$) added as the (*a*) nitrate, (*b*) lactate, and (*c*) maltol. Open bars, control (no added Al); hatched bars, Al added. Bars represent median ± interquartile range. $*p < 0.05$ (Kruskal–Wallis test followed by Dunn's multiple comparison test).

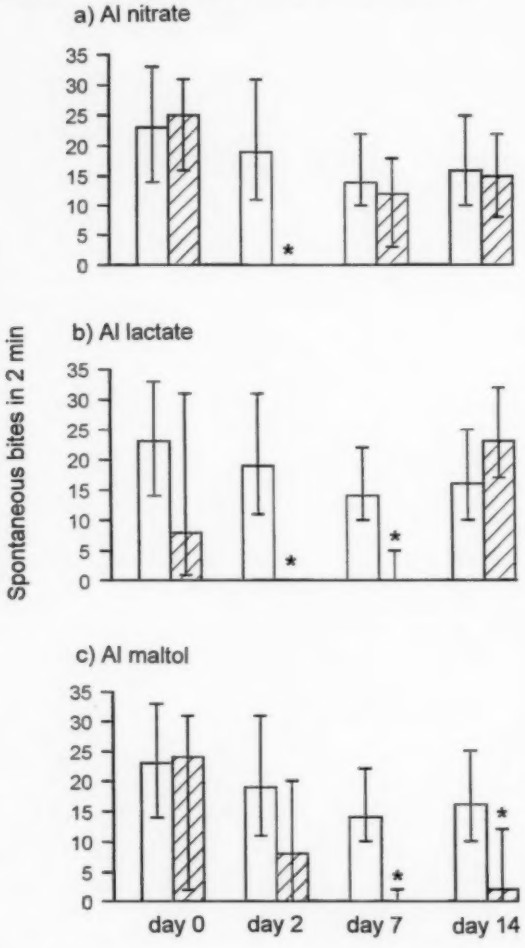

experimental or control groups, suggesting that the conditioned response was no longer retained by either group.

Mortality in all experiments was low (<15%) and did not differ significantly between control groups of snails and those exposed to Al and (or) Si.

Discussion

At neutral pH and in the absence of a strong binding ligand such as maltol, aquated Al rapidly forms polyhydroxy species and precipitates as $AlOH_3 \cdot (H_2O)_3$ (Martin 1986; Corain et al. 1992, 1996). This was confirmed in this study for solutions of aluminum nitrate and, at the concentrations used here, for aluminum lactate. In contrast, but as expected, aluminum maltolate showed little precipitation, since the maltol ligand competes with hydroxy polymerisation. All three Al compounds had significant effects on BSS and feeding behaviour. When feeding behaviour was examined, Al reduced both spontaneous and responsive feeding. However, the time course of these effects differed for different Al compounds. Depression of feeding behaviour occurred by day 2 in snails exposed to aluminum nitrate and aluminum lactate, followed by apparent acclimation by days 7–14. Snails exposed to aluminum maltol did not show reduced feeding until day 7 and had not recovered by day 14. Thus, the sparingly soluble forms of Al (nitrate and lactate) appear to be *more* immediately available to the snails than the soluble form (maltol). This is probably because a mucus film, secreted by the snails, efficiently binds polyhydroxy aluminum and is then ingested by the snails during subsequent grazing (Jugdaohsingh et al. 1998). The slower recovery of behaviour during exposure to aluminum maltol could be due to increased systemic toxicity following entry into the tissues. Aluminum maltol is a hydrophilic and lipophilic complex that is better able to cross cell membranes than polyhydroxy aluminum species (Zatta et al. 1991).

Aluminum is a known neurotoxin (Finnegan et al. 1986; Zatta et al. 1991) and affects electrical activity in the central nervous system of *L. stagnalis* in vitro (Campbell et al. 2000). This, together with direct effects on muscles and peripheral nerves, could account for the depression of feeding behaviour and BSS. However, it is also possible that reduced activity represents an active strategy to minimise uptake and hence toxicity of Al; metal uptake is reduced at lower metabolic rates (Denton and Burdon-Jones 1981). Snails clearly acclimate to the continued presence of polyhydroxy aluminum, and similarly, in a study of the effects of long-term exposure to Al (100–1000 $\mu g \cdot L^{-1}$ added as the nitrate at neutral pH), Truscott et al. (1995) reported depressed locomotory activity of *L. stagnalis* at 19 h followed by hyperactivity at 30 days but normal activity after 1 year. The short-term depression of behaviour seen here (days) could be explained by the recent results of Elangovan et al. (1997) who studied accumulation of polyhydroxy aluminum in *L. stagnalis* at neutral pH over 30 days. By day 20, a shift in the partitioning of the metal occurred, shown as reduced

© 2000 NRC Canada

Fig. 5. Effect of Al on latency to first bite in response to sucrose measured prior to (day 0) and after 2, 7, and 14 days of exposure to Al (500 $\mu g \cdot L^{-1}$) added as the (*a*) nitrate, (*b*) lactate, and (*c*) maltol. Open bars, control (no added Al); hatched bars, Al added. Bars represent median ± interquartile range. $*p < 0.05$ (Kruskal–Wallis test followed by Dunn's multiple comparison test).

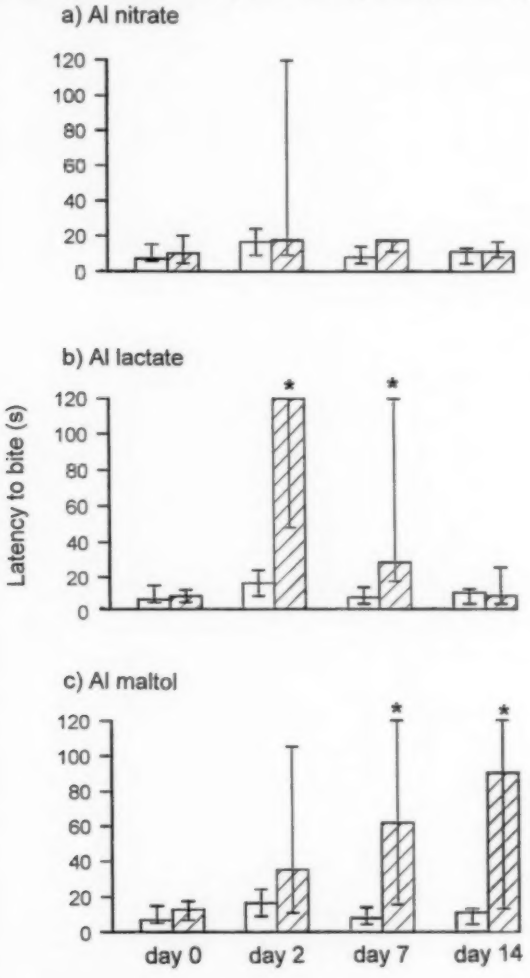

Fig. 6. Effect of Al on number of bites made in 2 min in response to sucrose measured prior to (day 0) and after 2, 7, and 14 days of exposure to Al (500 $\mu g \cdot L^{-1}$) added as the (*a*) nitrate, (*b*) lactate, and (*c*) maltol. Open bars, control (no added Al); hatched bars, Al added. Bars represent median ± interquartile range. $*p < 0.05$ (Kruskal–Wallis test followed by Dunn's multiple comparison test).

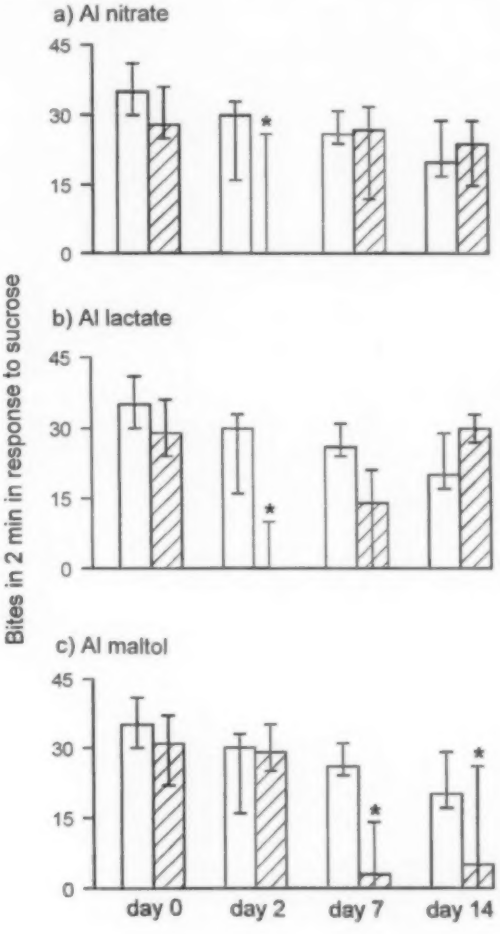

concentrations in the kidney and an increase in the digestive gland; this may have the effect of reducing its toxicity.

The ability of an animal to adapt its behaviour in the light of previous experience is essential to the survival of individuals and populations. Effects of Al on the acquisition of learned response could thus have far-reaching effects. Aluminum has been shown to impair cognitive function and learning ability in higher organisms and humans (Alfrey et al. 1976; Bilkei-Gorzo 1993). Exposure to Al did impair the expression of a learned feeding response on day 2, but the learned response was seen on day 7. This lack of expression of learning may have been due to a more general depression of motivation or an impairment of motor function related to feeding. Audesirk et al. (1982) showed that snails can acquire a conditioned response, but not express it, when their motivational status is low (e.g., after they have eaten), but will express the learned ability when motivation becomes higher.

Soluble silica is ubiquitous in natural waters; Farmer (1986) reported Si concentrations in the range 0.8–15 $mg \cdot L^{-1}$ in natural waters. These compare well with the concentrations used in our laboratory experiments using an Al:Si molar ratio of 1:15, confirming that our experiments are relevant to the natural environment. Silicon has no known toxicity. Indeed, experiments in chicks (Carlisle 1972) and rats (Schwartz and Milne 1972) suggest that it is essential for normal growth and development. Birchall (1995) suggested that soluble silica was utilised by organisms, including in aquatic systems, to bind endogenous Al and thus prevent its toxicity. Although some experiments appeared to confirm this (Carlisle and Curran 1987; Birchall et al. 1989;

© 2000 NRC Canada

Fig. 7. Effect of aluminium nitrate (500 $\mu g \cdot L^{-1}$) on the ability of *L. stagnalis* to express a conditioned response. The number of bites made in response to the conditioned stimulus was measured (*a*) prior to conditioning or exposure to Al (naïve) and (*b*) 2 days, (*c*) 7 days, and (*d*) 14 days after training. RC, random presentation controls; Expt, experimentally conditioned group. Open bars, control (no added Al); hatched bars, Al added. Bars represent median ± interquartile range. *$p < 0.05$ (Kruskal–Wallis test followed by Dunn's multiple comparison test).

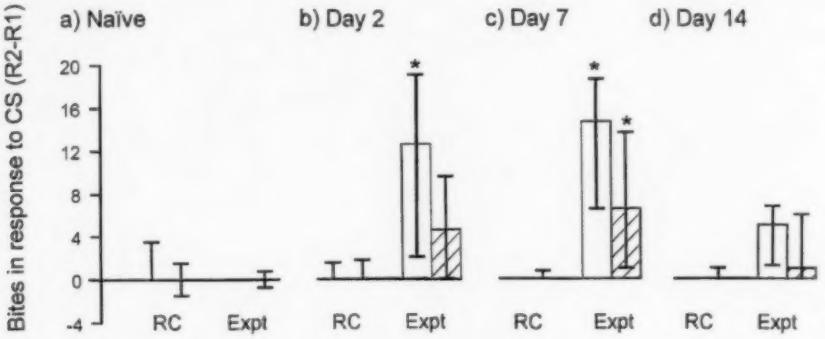

Edwardson et al. 1993), others have failed to do so (Drüeke et al. 1997; Exley et al. 1997; King et al. 1997). These discrepancies are probably due to the fact that the aqueous chemistry of silica and Al is complicated, and, for efficient binding of these species, at least one of them must be polymeric (Taylor et al. 1997; Duan and Gregory 1998). In the present study, using polyhydroxy aluminum, we were careful to maintain silica in its monomeric form.

Under the conditions used here, increased precipitation of polyhydroxy aluminum was expected in the presence of monomeric silica (Duan and Gregory 1998), and this was confirmed in simple solutions. However, in the presence of *L. stagnalis*, loss of Al from solution was not further enhanced by silica, since any effect of silica was masked by the more dominant influence of the snails (and their secreted EPS). In contrast, when the rate of formation of polyhydroxy aluminum was slowed using maltol, silica did show an additive effect with snails in removing Al from solution.

In the behavioural studies, silica (Al:Si = 1:15) reduced the effect of Al. The ameliorative effect of Si appears dependent on the Al:Si ratio (Birchall et al. 1989) and in this model clearly must exceed 1:1. However, the mechanism underlying amelioration is unclear. It is possible that Si reduced Al uptake, or "neutralised" the Al once within the snail. The formation of hydroxy aluminosilicate species could prevent the interaction between Al and its target sites. In studies of Al accumulation in plants, Hodson and Sangster (1993) and Hammond et al. (1995) showed that the roots accumulate Al even in the presence of Si but that Al-induced damage is ameliorated by Si, perhaps due to formation of biologically unavailable Al–Si complexes within the cell wall. By analogy, Al taken up by *L. stagnalis* may be more strongly bound, and thus detoxified, in granules of cells of the digestive gland (R. Elangovan, School of Biological Sciences, University of Manchester, U.K., unpublished data) in the presence of silica than in its absence. Indeed, in snails exposed to Al, these granules show significantly increased content of Si and well as Al compared with controls.

Little is known about the effects of Al and Si on the survival of freshwater communities at neutral pH. The findings presented here, using concentrations of Al relevant to those encountered in the environment, suggest that Al may have significant effects on the fitness of snail populations via changes in behaviour. Furthermore, soluble silica may play a role in moderating these effects. The large amounts of Al accumulated by snails (Elangovan et al. 1997) may have consequences for their consumers and the wider food web, although nothing is known about the degree to which the metal is transferred to predators.

Acknowledgements

We thank the BBSRC, the Special Trustees of St. Thomas' Hospital, and the Wellcome Trust for financial support.

References

Alfrey, A.C., Legendre, G.R., and Kaehny, W.D. 1976. The dialysis encephalopathy syndrome: possible aluminium intoxication. N. Engl. J. Med. **294**: 184.

Audesirk, T.E., Alexander, J.E., Audesirk, G.J., and Moyer, C.M. 1982. Rapid, nonaversive conditioning in a freshwater gastropod. I. Effects of age and motivation. Behav. Neural Biol. **36**: 379–390.

Bilkei-Gorzo, A. 1993. Neurotoxic effect of enteral aluminium. Food Chem. Toxicicol. **31**: 357–361.

Birchall, J.D. 1995. The essentiality of silicon in biology. Chem. Soc. Rev. **24**: 351–357.

Birchall, J.D., Exley, C., Chappell, J.S., and Phillips, M.J. 1989. Acute toxicity to fish eliminated in silicon rich acid waters. Nature (Lond.), **338**: 146–148.

Burden, T.J., Powell, J.J., Thompson, R.P.H., and Taylor, P.D. 1995. Optimal accuracy, precision and sensitivity of inductively coupled plasma optical emission spectrometry: bioanalysis of aluminium. J. Anal. At. Spectrom. **10**: 259–266.

Campbell, M.M., Jugdaohsingh, R., White, K.N., Powell, J.J., and McCrohan, C.R. 2000. Aluminium toxicity in a molluscan neuron: effects of counter ions. J. Toxicol. Environ. Health. **59**: 253–270.

Carlisle, E.M. 1972. Silicon as an essential element for the chick. Science (Washington, D.C.), **178**: 619–621.

Carlisle, E.M., and Curran, M.J. 1987. Effect of dietary silicon and aluminium on silicon and aluminium levels in rat brain. Alzheimer Dis. Assoc. Disord. **1**: 83–89.

© 2000 NRC Canada

Corain, B., Tapparo, A., Sheikh-Osman, A.A., and Bombi, G.G. 1992. The solution state of aluminium(III) as relevant to experimental toxicity: recent data and new perspectives. Coord. Chem. Rev. **122**: 19–32.

Corain, B., Bombi, G.G., Tapparo, A., Perazzolo, M., and Zatta, P. 1996. Aluminium toxicity and metal speciation: established data and open questions. Coord. Chem. Rev. **149**: 11–22.

Denton, G.R.W., and Burdon-Jones, C. 1981. Influence of temperature and salinity on the uptake distribution and depuration of mercury, cadmium and lead by the black lip oyster, *Saccostrea echinata*. Mar. Biol. (Berl.), **64**: 317–326.

Dixon, E., and Gardner, M. 1998. Reactive aluminium in UK surface waters. Chem. Speciation Bioavailability, **10**: 11–17.

Drüeke, T.B., Jouhanneau, P., Banide, H., Lacour, B., Yiou, F., and Raisbeck, G. 1997. Effects of silicon, citrate and the fasting state on the intestinal absorption of aluminium in rats. Clin. Sci. (Lond.), **92**: 63–67.

Duan, J., and Gregory, J. 1998. The influence of silicic acid on aluminium hydroxide precipitation and flocculation by aluminium salts. J. Inorg.Biochem. **69**: 193–201.

Dunn, O.J. 1964. Multiple contrasts using rank sums. Technometrics, **6**: 241–252.

Edwardson, J.A., Moore, P.B., Ferrier, I.N., Lilley, J.S., Newton, G.W.A., Barker, J., Templar, J., and Day, J.P. 1993. Effect of silicon on gastrointestinal absorption of aluminium. Lancet, **342**: 211–212.

Elangovan, R., White, K.N., and McCrohan, C.R. 1997. Bioaccumulation of aluminium in the freshwater snail *Lymnaea stagnalis* at neutral pH. Environ. Pollut. **96**: 29–33.

Exley, C., Pinnegar, J.K., and Taylor, H. 1997. Hydroxyaluminosilicates and acute aluminium toxicity in fish. J. Theor. Biol. **189**: 133–139.

Farmer, V.C. 1986. Sources and speciation of aluminium and silicon in natural waters. *In* Silicon biochemistry. Ciba Foundation Symposium No. 121. *Edited by* D. Evered and M. O'Connor. John Wiley & Sons, Chichester, U.K. pp. 4–23.

Finnegan, M.M., Rettig, S.J., and Orvig, C. 1986. A neutral water-soluble aluminium complex of neurological interest. J. Am. Chem. Soc. **108**: 5033–5035.

Hammond, K.E., Evans, D.E., and Hodson, M.J. 1995. Aluminium/silicon interactions in barley (*Hordeum vulgare* L.) seedlings. Plant Soil, **173**: 89–95.

Havas, M., and Likens, G.E. 1985. Changes in ^{22}Na influx and outflux in *Daphnia magna* (Straus) as a function of elevated aluminium concentrations in soft water at low pH. Proc. Natl. Acad. Sci. U.S.A. **82**: 7345–7349.

Hodson, M.J., and Sangster, A.G. 1993. The interaction between silicon and aluminium in *Sorghum bicolor* (L.) Moench: growth analysis and X-ray microanalysis. Ann. Bot. **72**: 389–400.

Iler, R.K. 1979. The chemistry of silica: solubility, polymerization, colloid and surface properties, and biochemistry. John Wiley & Sons, New York.

Jugdaohsingh, R., Campbell, M.M., Thompson, R.P.H., McCrohan, C.R., White, K.N., and Powell, J.J. 1998. Mucus secretion by the freshwater snail *Lymnaea stagnalis* limits aluminium concentrations of the aqueous environment. Environ. Sci. Technol. **32**: 2591–2595.

King, S.J., Day, J.P., Oldham, C., Popplewell, J.F., Ackrill, P., Moore, P.B., Taylor, J.A., Edwardson, J.A., Fifield, L.K., Lui, K., and Cresswell, R.G. 1997. The influence of dissolved silicate on the physiological chemistry of aluminium, studied in the human using tracer ^{26}Al and accelerator mass spectrometry. Nucl. Instrum. Methods Phys. Res. B, **123**: 254–258.

Martin, R.B. 1986. The chemistry of aluminium as related to biology and medicine. Clin. Chem. **32**: 1797–1806.

Pynnönen, K. 1990. Aluminium accumulation and distribution in the freshwater clams (Unionidae). Comp. Biochem. Physiol. C, Pharmacol. Toxicol. **97**: 111–117.

Rosseland, B.O., Blakar, I.A., Bulger, A., Kroglund, F., Kvellstad, A., Lydersen, E., Oughton, D.H., Salbu, B., Staurnes, M., and Vogt, R. 1992. The mixing zone between limed and acidic river waters: complex aluminium chemistry and extreme toxicity for salmonids. Environ. Pollut. **78**: 3–8.

Schwartz, K., and Milne, D.B. 1972. Growth promoting effects of silicon in rats. Nature (Lond.), **239**: 333–334.

Taylor, P.D., Jugdaohsingh, R., and Powell, J.J. 1997. Soluble silica with high affinity for aluminium under physiological and natural conditions. J. Am. Chem. Soc. **119**: 8852–8856.

Truscott, R., McCrohan, C.R., Bailey, S.E.R., and White, K.N. 1995. Effect of aluminum and lead on activity in the freshwater snail *Lymnaea stagnalis*. Can. J. Fish. Aquat. Sci. **52**: 1623–1629.

Tuersley, M.D., and McCrohan, C.R. 1987. Food arousal in the pond snail *Lymnaea stagnalis*. Behav. Neural Biol. **48**: 222–236.

Whelan, H.A., and McCrohan, C.R. 1996. Food related conditioning and neural correlates in the freshwater snail *Lymnaea stagnalis*. J. Molluscan Stud. **62**: 483–494.

Zatta, P.F., Nicolini, M., and Corain, B. 1991. *In* Aluminium in chemistry biology and medicine. A series of advances. Vol 1. *Edited by* M. Nicolini, P.F. Zatta, and B. Corain. Cortina International, Raven Press, New York. pp. 97–112.

© 2000 NRC Canada

Bioaccumulation and differential partitioning of polychlorinated biphenyls in freshwater, planktonic food webs

Olof Berglund, Per Larsson, Göran Ewald, and Lennart Okla

Abstract: The planktonic food chain phytoplankton – zooplankton – young-of-the-year roach (*Rutilus rutilus*) was studied in 19 lakes in southern Sweden to investigate the bioaccumulation of polychlorinated biphenyls (PCBs). The ΣPCB concentrations did not steadily increase with increasing trophic level. The ΣPCB concentrations in zooplankton (400 ng·g lipid^{-1}) were lower than in both phytoplankton (660 ng·g lipid^{-1}) and fish (890 ng·g lipid^{-1}), which did not differ significantly. Lipid content explained 40% of the total variation in dry weight normalised ΣPCB concentrations in the samples. The PCBs were differentially partitioned between the trophic levels. The log BMFs (biomagnification factors, concentration in predator/concentration in prey) were a function of the $\log K_{ow}$ of the PCB congeners. The $\log \mathrm{BMF}_{zoo/phyto}$ values were < 0 for all PCB congeners on a lipid weight basis, and the $\log \mathrm{BMF}_{fish/zoo}$ values were < 0 for PCB congeners with $\log K_{ow} > 6$. We conclude that no PCBs had higher lipid-normalised concentrations in zooplankton than in phytoplankton and the most lipophilic PCBs had moderately higher concentrations in roach than in zooplankton. PCBs with $\log K_{ow} > 6$ decreased in concentration from phytoplankton to zooplankton to roach. We suggest that the concept of biomagnification did not apply to the planktonic food chain investigated in these lakes.

Résumé : Nous avons étudié la chaîne alimentaire planctonique phytoplancton – zooplancton – jeune gardon (*Rutilus rutilus*) dans 19 lacs du sud de la Suède afin d'analyser la bioaccumulation des polychlorobiphényles (PCB). Les concentrations de ΣPCB n'ont pas augmenté de façon constante avec l'augmentation du niveau trophique. Les concentrations de ΣPCB dans le zooplancton (400 ng·g lipides^{-1}) étaient plus faibles que dans le phytoplancton (660 ng·g lipides^{-1}) et chez les poissons (890 ng·g lipides^{-1}), concentrations qui ne différaient pas de façon significative. La teneur en lipides expliquait 40% de la variation totale des concentrations normalisées de ΣPCB en poids sec dans les échantillons. Les PCB étaient répartis de façon différentielle entre les niveaux trophiques. Le log FBA (facteurs de bioamplification, concentration chez le prédateur/concentration chez les proies) était une fonction du $\log K_{ow}$ des congénères de PCB. Le $\log \mathrm{FBA}_{zoo/phyto}$ était < 0 pour tous les congénères de PCB en fonction du poids en lipides, et le $\log \mathrm{FBA}_{poisson/zoo}$ était < 0 pour les congénères de PCB dont le $\log K_{ow} > 6$. Nous concluons qu'aucun PCB n'avait une concentration normalisée dans les lipides plus élevée chez le zooplancton que chez le phytoplancton, et que les concentrations de PCB les plus lipophiles étaient modérément plus élevées chez le gardon que chez le zooplancton. On observait une diminution de la concentration de PCB dont le $\log K_{ow} > 6$ en passant du phytoplancton au zooplancton puis au gardon. La notion de bioamplification ne semblait donc pas s'appliquer aux organismes de la chaîne alimentaire planctonique étudiés dans ces lacs.

[Traduit par la Rédaction]

Introduction

The concept of biomagnification of persistent organochlorines (OCs) has been investigated since high concentrations of dichlorodiphenyltrichloroethane (DDT) were observed in top predators five decades ago. Aquatic top predators were identified as especially vulnerable for biomagnification of OCs (Rudd 1964). This concentrative process was attributed to the presumed efficient transfer of OCs from one trophic level to the next, in combination with the reduction in biomass associated with each progressive trophic level, due to losses in the biomass conversion between trophic levels (Rudd 1964). This would yield greater concentrations (but not total amounts) of OCs associated with the next trophic level than those present in the previous trophic level. A consequence of the biomagnification process is that an increased number of trophic levels in a food chain will result in higher concentrations in the top predators.

There are indications of an efficient trophic transfer of OCs; 50–80% of polychlorinated biphenyls (PCB) have been estimated to transfer from food to lake trout (*Salvelinus namaycush*) in the Great Lakes (Madenjian et al. 1998). Biomagnification must result in concentrations in the predator that are higher than can be explained by passive diffusion from water. However, higher concentrations in predators than in prey can also be caused by processes other than biomagnification, such as elimination, growth dilution, or differences in age or exposure time. Accumulation of OCs via food rather than via water is necessary for biomagnification.

Received June 24, 1999. Accepted December 9, 1999.
J15210

O. Berglund,[1] P. Larsson, G. Ewald, and L. Okla. Chemical Ecology and Ecotoxicology, Department of Ecology, Lund University, S-22362 Lund, Sweden.

[1]Author to whom all correspondence should be addressed. e-mail: olof.berglund@ecotox.lu.se

© 2000 NRC Canada

When in equilibrium between an organism and water, a chemical's bioconcentration factor (BCF), the ratio of the concentration in the organism to the concentration in water, is assumed to be a function of the octanol–water partitioning coefficient (K_{ow}) with a slope of unity (Mackay 1982). If organism BCFs are above that predicted from K_{ow}, the chemical is considered to have bioaccumulated via food (Oliver and Niimi 1988). However, as accumulation via food can be driven by passive diffusion over a fugacity gradient; food accumulation only is not evidence of biomagnification.

The biomagnification theory has been tested by examining OC concentrations at different trophic levels in aquatic food chains. Oliver and Niimi (1988) observed that PCB concentration increased with trophic level in a four-link food chain in Lake Ontario. Evans et al. (1991) similarly found increasing concentrations of PCB, dichlorodiphenyldichloroethylene (DDE), and toxaphene in a four-link food chain in Lake Michigan. Other, indirect approaches have also led to the conclusion that biomagnification of lipophilic chemicals via the food web is a major contributor to their accumulation in biota at higher trophic levels. Rasmussen et al. (1990) concluded that concentrations of PCB in top predators from different lakes increased with increasing length of the food chains, a result attributed to biomagnification. Russell et al. (1995) showed that concentrations of some PCBs were greater in white bass (*Morone chrysops*) than in their prey, emerald shiner (*Notropis atherinoides*), in Lake Erie, i.e., their biomagnification factors (BMFs) were > 1.

The concept of biomagnification has been questioned (LeBlanc 1995). Increasing concentrations of OCs with trophic level may instead be attributed to differences in lipid content (Bentzen et al. 1996; Kucklick and Baker 1998), depuration rates (LeBlanc 1995; Sijm and Van der Linde 1995), size (Bergner 1985), and exposure duration (Harding et al. 1997). LeBlanc (1995) argued that the apparent increase in lipid content with trophic levels would cause an increase in lipophilic OCs by bioconcentration alone, driven by passive diffusion over a fugacity gradient. Lipid content has been shown to explain a major part of the variation in OC accumulation by aquatic organisms (Larsson et al. 1996; Kucklick and Baker 1998). However, many studies show that even when lipid normalised, food web structure and trophic level may affect OC concentrations (Kiriluk et al. 1995; Bentzen et al. 1996; Kidd et al. 1998).

Most reports on biomagnification have focused on the transfer between planktivorous or benthivorous fish to piscivorous fish. Primary producers (phytoplankton and periphyton) are an important factor in controlling the fate and transport of OCs in natural waters. Settling algae acts as vectors for OCs from the water column to the sediment, and phytoplankton grazed by zooplankton transfer OCs into the pelagic food web (Stange and Swackhamer 1994). Despite the key role of this primary trophic level, to our knowledge, few studies have, in detail, examined the distribution of PCBs in the lower trophic levels of pelagic freshwater ecosystems (cf. Oliver and Niimi 1988; Harding et al. 1997).

Here, we examine the PCB distribution in the lower trophic levels in temperate lakes to determine whether PCBs may be biomagnified, i.e., if the concentration increases with trophic level in the food chain. We examined PCBs in the food chain phytoplankton – zooplankton – young-of-the-year (YOY) roach (*Rutilus rutilus*) in 19 lakes in southern Sweden. YOY roach were chosen for several reasons. Firstly, they are obligate pelagic planktivores (Persson 1997) and occupy the trophic level immediately above zooplankton. Secondly, we chose YOY fish to minimise variation in PCB concentrations due to age or size differences among the fish. Thirdly, we wanted to minimise age and size differences between the trophic levels. By choosing YOY fish, we also avoided differences in PCB concentrations between fish and plankton due to eventual differences in PCB exposure between seasons.

Methods

Study sites and sample collections

The 19 lakes included in this study are located in the southern part of Sweden (56°N, 14°E) within a 19 000-km^2 area and experience a similar climate. Limnological characteristics measured in the investigated lakes are presented in Table 1. For a detailed description of the methods of the limnological variables, see Berglund (1999).

All samples were collected in August 1997. We sampled plankton by towing three nets with 150-, 45-, and 10-μm mesh connected in series. This yielded three size-classes: macrozooplankton (>150 μm), microzooplankton (45–150 μm), and phytoplankton (10–45 μm). The 45–150 μm fraction consisted of ciliates, rotifers, and aggregated phytoplankton. Therefore, the plankton net setup operationally separated phytoplankton and macrozooplankton. As the 45–150 μm fraction contained more than one trophic level, only the 10–45 and >150 μm fractions were included in this study and will hereafter be referred to as phytoplankton and zooplankton, respectively. The compositions of the phytoplankton and zooplankton samples are described in more detail in Berglund (1999). Generally, phytoplankton samples consisted only of phytoplankton, and zooplankton samples only of zooplankton. The zooplankton communities were similar in all lakes. The dominating zooplankton in most lakes were the cladocerans *Daphnia galeata*, *Daphnia cristata*, and *Daphnia cuccullata* and calanoid and cyclopoid copepods. Other common species were the cladocerans *Chydorus*, *Diaphanosoma*, *Bosmina*, *Limnosida*, and *Holopedium*. YOY roach were collected with electrofishing. Fish were pooled into composite samples of 4–21 individuals. In two of the lakes, no YOY fish could be obtained. Plankton and fish were frozen after capture and later freeze-dried before analysis.

PCBs in water were sampled by collecting unfiltered water (50–100 L) just below the water surface and percolating it through two polyurethane columns (PUC) via a stainless steel funnel at a rate of 10–20 L·h^{-1} (Bremle et al. 1995).

PCB analyses

PCBs in plankton, fish, and PUCs were Soxhlet extracted with acetone–hexane according to Bremle et al. (1995) using octachloronaphtalene as an surrogate standard. The solvent was reduced in a vacuum centrifuge and the lipid amounts were determined gravimetrically. The sample was redissolved in hexane followed by an open column step as a cleanup. The column contained two layers of silica gel soaked in concentrated sulphuric acid and 1 M K_2CO_3. The solvent contained in the samples was evaporated in a vacuum centrifuge and was redissolved in isooctane prior to gas chromatographic analysis. For detailed information on preparation of the samples, see Bremle et al. (1995). For every 15 samples processed, a chemical blank was run. The average blank for ΣPCB (for included congeners, see Fig. 2) was 0.7 ng (concentration depends on sample size). PCB adsorption efficiencies on PUCs are given in Agrell et al. (1999). The average PUC

© 2000 NRC Canada

Table 1. Limnological characteristics of the studied lakes.

Lake	Area (km^2)	Maximum depth (m)	Total P ($\mu g \cdot L^{-1}$)	Chl *a* ($\mu g \cdot L^{-1}$)	Secci depth (m)	Biomass ($g \cdot m^{-3}$)	Total organic C ($mg \cdot L^{-1}$)
Krageholmsjön	2.1	10	153	38.7	1.1	1.45	7.2
Sövdesjön	2.8	12	80	105.7	0.5	1.78	11.7
Ringsjön	20	16	80	61.9	0.7	0.78	9.0
Vombsjön	12.8	16	80	15.8	1.1	1.92	6.1
Finjasjön	10	13	70	39.6	1.0	4.79	9.9
Åsnen	150	14	21	12.9	1.3	0.74	8.7
Västersjön	4.6	13	16	5.5	3.2	0.19	5.4
Vidöstern	48	35	15	5.9	2.8	0.18	7.9
Levrasjön	2.6	19	14	1.3	3.5	0.03	5.1
Kösen	11	22	12	4.9	3.5	0.20	8.2
Flåren	34	15	10	3.3	3.4	0.33	7.9
Ivösjön	54	50	10	3.0	2.5	0.23	6.7
Rottnen	33	18	10	4.0	3.2	0.19	9.2
Unnen	17	25	9	2.6	4.3	0.26	6.4
Immeln	24	28	9	3.8	3.0	0.19	6.2
Madkroken	12	21	8	5.9	3.1	0.27	7.2
Änghultasjön	4.4	28	8	6.4	3.4	0.24	8.4
Örken	23	38	7	2.6	5.2	0.24	11.9
Mien	20	39	7	2.6	5.0	0.08	7.5

field blank for ΣPCB was 2.2 ng (concentration depending on sample size). PUC field blank concentrations of domain 8 (IUPAC 16, 32) varied considerably (from below detection limits to 1.9 ng), so sample concentrations of this domain should be interpreted with caution. Sample concentrations were not corrected for blanks.

Gas chromatographic analysis

The samples were analysed for PCB by capillary gas chromatography – electron capture detection on a Varian Star 3400 cx equipped with an on-column injector. The chromatographic conditions and details are described in Bremle et al. (1995). The PCB components were identified and quantified according to Schulz et al. (1989). Thirty PCB domains were included in the analyses (see Fig. 2). PCB domains were identified and quantified on the basis of relative retention times and of response factors obtained for the chromatographic standard pentachlorobenzene. External standards of Clophen and Arochlor mixtures were run regularly to check performance. Extraction efficiencies for octachloronaphtalene were 83 ± 10% for plankton, 71 ± 11% for fish, and 64 ± 7% for PUCs. PCB concentrations in the different matrixes were not corrected for recovery.

Data analyses

Water concentrations of freely dissolved PCBs were calculated using the equations from Burkhard (1998):

$$(1) \qquad f_{fd} = 1/(1 + 0.1 \times DOC \times K_{oc} + POC \times K_{oc})$$

$$(2) \qquad C_w^{fd} = C_w^t f_{fd}$$

where f_{fd} is the fraction of the chemical that is freely dissolved in the water, DOC is the concentration of dissolved organic carbon, POC is the concentration of particulate organic carbon, K_{oc} is the organic carbon – water (freely dissolved basis) partitioning coefficient for the chemical, C_w^t is the total concentration of the chemical in the water, and C_w^{fd} is the freely dissolved concentration of the chemical in the water. Values for K_{oc} were estimated from the chemical's K_{ow} using the relationship from Karickhoff (1981):

$$(3) \qquad K_{oc} = 0.41 K_{ow}.$$

The K_{ow}s for the different PCB congeners were obtained from Hawker and Connell (1988). The K_{ow}s for coeluting congeners were calculated according to the relative composition of the congeners in the commercial Clophen A60 mixture (Schulz et al. 1989). Bioaccumulation factors (BAFs) were calculated by dividing the concentration of PCB in organisms (nanograms per kilogram of lipid or nanograms per kilogram dry weight) by the concentration of freely dissolved PCB in water (nanograms per litre). BMFs were calculated by dividing the concentration of PCB in predators (nanograms per kilogram of lipid or nanograms per kilogram dry weight) by the concentration of PCB in prey (nanograms per kilogram of lipid or nanograms per kilogram dry weight).

Prior to statistical analysis, concentration data were $\log_{10}$ transformed owing to their skewed distributions. *F* tests were performed to investigate homogeneity of variance between the groups (trophic levels). Analysis of variance (ANOVA) was used to investigate the effects of group (trophic level) on BAFs, PCB concentrations, and lipid contents. Sheffe's *F* post hoc test was used after ANOVA to examine which group means were significantly different from each other. Analysis of covariance (ANCOVA) was performed to confirm differences between slopes of regressions by the significant interaction terms. Statistics were carried out using Stat View® (Abacus Concepts, Inc.) and SYSTAT.

Results

Among-lake differences in ΣPCB concentrations in water or in biota on a lipid basis were not correlated with trophic status or any of the lake characteristics measured in this study (Table 1; also see Berglund 1999). The between-lake variance of lipid contents, log BAFs, and ΣPCB concentrations were homogenous in the three trophic levels. The *F* tests for homogeneity of variance showed that the variance ratios were not different from 1 ($p > 0.1$) except in one case, between ΣPCB concentrations (dry weight) in phytoplankton and zooplankton ($p = 0.02$). Therefore, we concluded that lipid and PCB data from all lakes could be compared.

The concentration of ΣPCB freely dissolved in water averaged 13 $pg \cdot L^{-1}$, ranging from 3.1 to 86 $pg \cdot L^{-1}$. We found

© 2000 NRC Canada

Table 2. Mean values (minimum–maximum in parentheses) of lipid content (% of dry weight), ΣPCB_{DW} concentrations (ng·g dry weight^{-1}), and ΣPCB_{LW} concentrations (ng·g extractable lipid^{-1}) in three trophic levels from 19 Swedish lakes.

	Phytoplankton	Zooplankton	Fish	p
Lipids	5.4^b (0.7–13.6)	8.8^a (1.6–14.4)	6.6 (2.9–10.8)	<0.01
ΣPCB_{DW}	28^c (4.8–57)	33 (16–70)	55^a (32–260)	<0.01
ΣPCB_{LW}	660^b (250–1700)	400^{a,c} (190–1000)	890^b (460–2600)	<0.01

Note: Means for PCB concentrations are geometrical. ANOVA p values are given.
^{a}Significantly different from phytoplankton (Sheffe's F, $p < 0.05$).
^{b}Significantly different from zooplankton (Sheffe's F, $p < 0.05$).
^{c}Significantly different from fish (Sheffe's F, $p < 0.05$).

that dry weight normalised ΣPCB concentrations differed significantly between the three trophic levels (Table 2). Concentrations of ΣPCB in the fish (55 ng·g dry weight^{-1}) were higher than in the phytoplankton (28 ng·g dry weight^{-1}) but not significantly different from those in the zooplankton (33 ng·g dry weight^{-1}). The plankton fractions did not differ in dry weight normalised ΣPCB concentration. Lipid content (percentage of dry weight) differed significantly between trophic levels. The zooplankton lipid content (8.8 ± 2.9%) was significantly higher than the phytoplankton lipid content (5.4 ± 3.3%). No difference in lipid content was found between the phytoplankton and the fish (6.6 ± 2.4%) or between the zooplankton and the fish. On a lipid weight basis, the zooplankton ΣPCB concentrations (400 ng·g lipid^{-1}) were lower than both the phytoplankton (660 ng·g lipid^{-1}) and the fish (890 ng·g lipid^{-1}) ΣPCB concentrations. No difference in lipid normalised ΣPCB concentrations was found between the phytoplankton and the fish (Table 2)

BAFs, calculated from concentration in biota/freely dissolved concentration in water, for ΣPCB did not differ between trophic levels when calculated on a dry weight basis (BAF_{DW}) (ANOVA, $p > 0.05$), although the fish log BAFs were higher than the phytoplankton log BAFs (Sheffe's F, significance level 5%). On a lipid weight basis, log BAF_{LW}s differed between trophic levels (ANOVA, $p = 0.026$, Sheffe's F, significance level 5%) in that the fish log BAFs were higher than the zooplankton log BAFs. This pattern was consistent in all lakes but three (Fig. 1).

Lipid content explained 40% of the total variation in ΣPCB concentrations (nanograms per gram dry weight) in all plankton and fish samples (simple regression, $p < 0.01$, $r^2 = 0.40$). We found no trends in degree of explanation or slopes with lipophilicity (K_{ow}) of the individual PCB domains.

The relative compositions of individual PCBs, expressed as a percentage of ΣPCB, are shown in Fig. 2. The log BAF_{LW}s for the individual PCB congeners in the three trophic levels were positively related to log K_{ow} (simple regression, $p < 0.01$, $r^2 = 0.61$, 0.83, and 0.84 for the phytoplankton, zooplankton, and fish, respectively) (Fig. 3). The slopes for the log BAF versus K_{ow} relationships were significantly different between phytoplankton, zooplankton, and roach as determined from the trophic level × log K_{ow} interaction term in ANCOVA ($p < 0.01$). The absolute values of lipid-normalised BAF_{LW}s were 1–1.5 orders of magnitude greater than K_{ow}. On a dry weight basis, BAF_{DW}s were of the same order of magnitude as K_{ow} and the slopes were significantly different (ANCOVA, $p < 0.01$).

The log BMFs for zooplankton/phytoplankton ($BMF_{zoo/phyto}$) and fish/zooplankton ($BMF_{fish/zoo}$) were positively related to log K_{ow}, on both a lipid and a dry weight basis (Figs. 4 and 5) (simple regression, $p < 0.01$, $r^2 = 0.44$, 0.72 and 0.32, 0.69, respectively). The log $BMF_{LWzoo/phyto}$ values were < 0 for all PCBs. The log $BMF_{LWfish/zoo}$ values were < 0 for PCBs with log $K_{ow} < 6$ and > 0 for PCBs with log $K_{ow} > 6$.

Fig. 1. BAFs (nanograms PCB per kilogram lipid in biota/nanograms freely dissolved PCB per litre of water) for the three trophic levels: phytoplankton (10–45 μm), zooplankton (>150 μm), and fish (YOY roach). Solid lines connect the BAFs for each individual lake. Broken lines connect the three lakes in which BAF increased with trophic level.

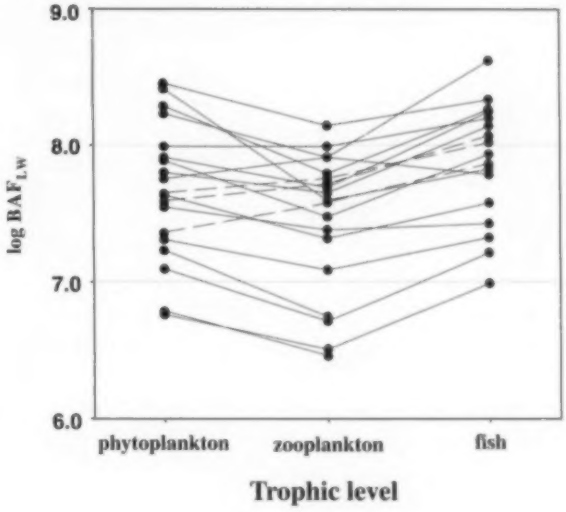

Discussion

The theory of biomagnification predicts that due to more efficient transfer of OCs than energy between trophic levels, OC concentrations will increase in the food chain (Rudd 1964). We could not find an increase in lipid-normalised PCB concentrations from phytoplankton to zooplankton. We found higher concentrations of the most lipophilic PCBs in roach than in zooplankton, but PCBs with log $K_{ow} < 6$ decreased in concentration from phytoplankton to zooplankton to roach. Hence, PCBs were not biomagnified from the primary trophic level to the secondary trophic level. Several studies have failed to find evidence of biomagnification in aquatic ecosystems, especially when investigating planktonic

© 2000 NRC Canada

Fig. 2. Composition of PCB domains in the investigated compartments (*a*) freely dissolved in water, (*b*) phytoplankton (10–45 μm), (*c*) zooplankton (>150 μm), and (*d*) fish. The relative frequencies (% of ΣPCB) are plotted for the 30 different domains (D) (from left to right: D8 (IUPAC Nos. 16, 32), D13 (31, 28), D14 (20, 33, 53), D20 (49), D21 (47, 48, 75), D23 (44), D25 (41, 64), D32 (66, 95), D36 (92), D38 (90, 101), D39 (99), D42 (97), D47 (82, 151), D50 (123, 149, 118), D53 (146), D54 (132, 153, 105), D58 (160, 138, 158), D59 (129, 126, 178), D61 (187), D62 (183), D63 (128), D65 (185), D66 (174), D67 (177), D68 (202, 171, 156), D70 (172), D72 (180), D77 (170, 190), D79 (199), and D84 (194).

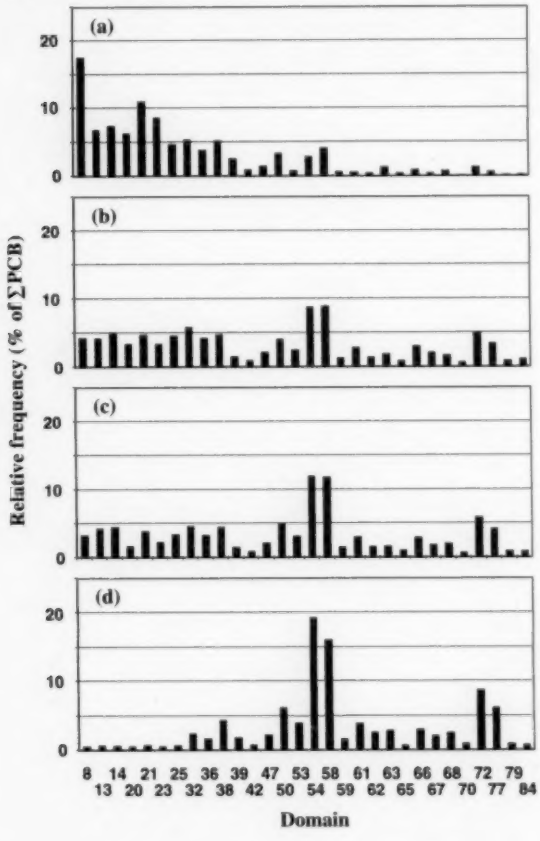

Fig. 3. Relationships between (*a*) BAF_{LW} and (*b*) BAF_{DW} and K_{ow} for the three trophic levels phytoplankton (10–45 μm, circles), zooplankton (>150 μm, squares), and YOY roach (fish, plus signs). Linear regression analysis gave the following relationships. Phytoplankton: $\log BAF_{LW} = 0.62 \log K_{ow} + 3.54$ ($r^2 = 0.61$); zooplankton: $\log BAF_{LW} = 0.78 \log K_{ow} + 2.30$ ($r^2 = 0.83$); fish: $\log BAF_{LW} = 1.02 \log K_{ow} + 0.97$ ($r^2 = 0.84$); phytoplankton: $\log BAF_{DW} = 0.52 \log K_{ow} + 2.87$ ($r^2 = 0.57$); zooplankton: $\log BAF_{DW} = 0.75 \log K_{ow} + 1.36$ ($r^2 = 0.83$); fish: $\log BAF_{DW} = 1.00 \log K_{ow} - 0.10$ ($r^2 = 0.83$).

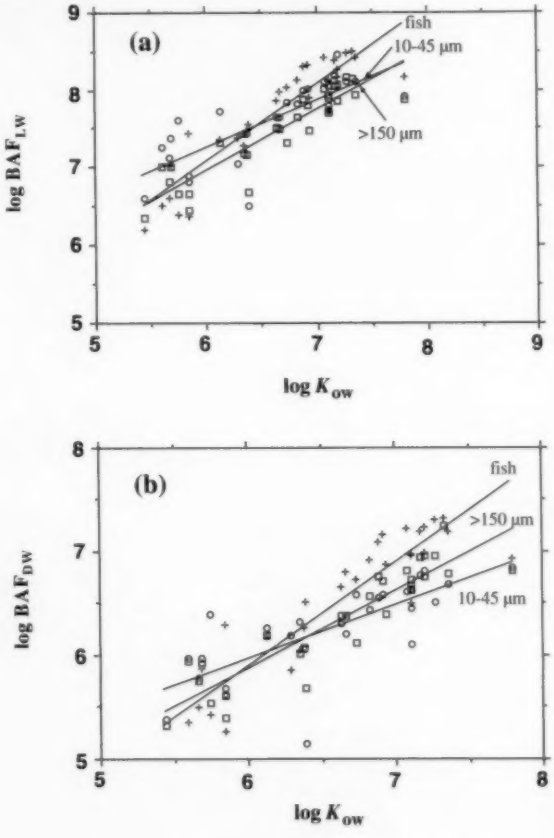

food webs (Harding et al. 1997; Paterson et al. 1998). Kucklick and Baker (1998) concluded that the main influence of trophic position on PCB concentrations in Lake Superior's food web was due to the concurrent increase in lipid content with trophic position.

Daphnia spp. and copepods dominated the zooplankton samples in all lakes. *Daphnia* are generalist herbivorous filter-feeders that feed on a variety of algal taxa. They feed unselectively over a broad range of particle sizes and are unable to handle and reject poor-quality particles individually (DeMott 1995; Repka 1997). Copepods also feed on algae, but cyclopoid copepods are potential omnivores and feed on both algae and invertebrates (Adrian and Frost 1993). However, the *Daphnia* dominated by volume and weight in the zooplankton samples due to the small size of copepods. Therefore, the phytoplankton samples may be representative of the diet of the dominating *Daphnia* in the zooplankton samples. In a gut content analysis, Persson (1997) found that the diet of YOY roach from southern Sweden consisted exclusively of pelagic zooplankton species such as *Daphnia* spp., *Bosmina* spp., *Chydorus sphaericus*, *Leptodora kindtii*, and copepods, species that dominated in the zooplankton samples in this study. Thus, although we did not perform any diet analyses in this study, we feel that the phytoplankton samples and the zooplankton samples may be representative of the diets of the zooplankton samples and roach samples, respectively.

In an expanded analysis of the data used by Rasmussen et al. (1990), Bentzen et al. (1996) found that PCB concentrations in lake trout (*Salvelinus namaycush*) from different lakes were a function of lipid content, but the intercepts of the regressions differed between lakes. This was attributed to

© 2000 NRC Canada

Fig. 4. Relationships between (*a*) lipid-normalised $BMF_{zoo/phyto}$ and (*b*) $BMF_{fish/zoo}$ and K_{ow} for the different PCBs.

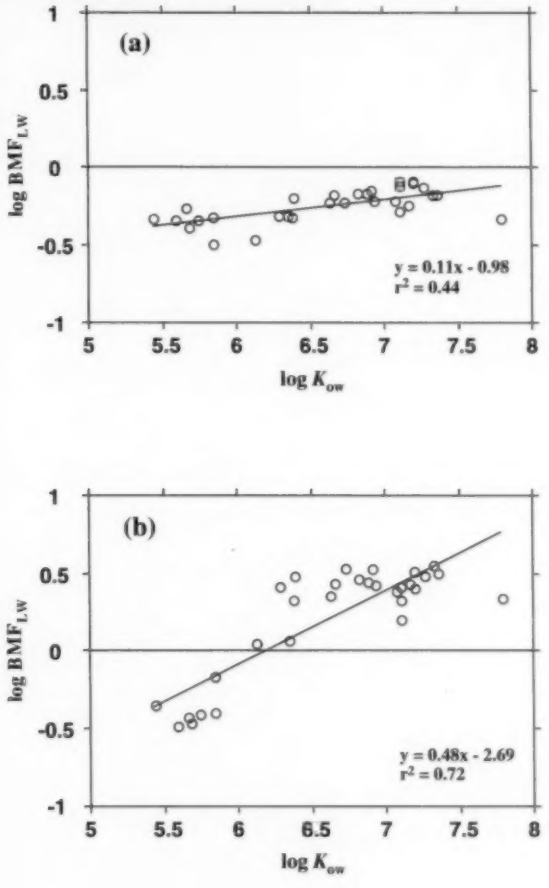

Fig. 5. Relationships between (*a*) dry weight normalised $BMF_{zoo/phyto}$ and (*b*) $BMF_{fish/zoo}$ and K_{ow} for the different PCBs.

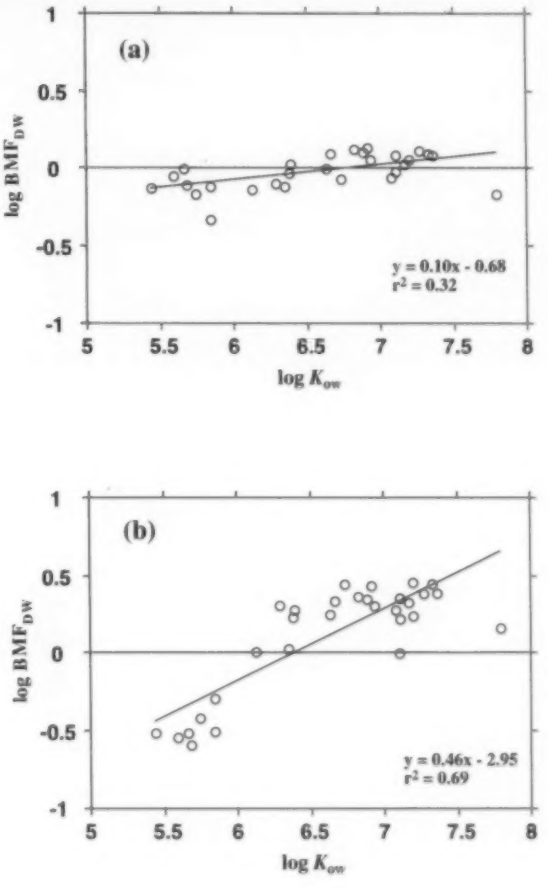

food chain effects and (or) different loading of PCB. In our study, the relationship between BAF and trophic level showed the same behaviour in 14 of 17 investigated lakes. The phytoplankton and the fish BAFs were similar, but the zooplankton BAFs were lower. This pattern was exhibited for the majority of lakes despite a nearly two orders of magnitude difference between lakes in PCB concentration at each trophic level. It is unlikely that there existed any difference in the investigated food chain length between the lakes in our study. In all lakes, our pelagic food chain consisted of primary producers (phytoplankton), herbivore/planktivores (zooplankton), and obligate planktivores (YOY roach) at the very base of the pelagic food chain; therefore, there is no room for additional trophic levels. Hence, food chain differences seem unlikely to be responsible for the among-lake differences in the BAFs of the food chains, i.e., the intercepts for the BAF versus trophic level functions. Differences in loading of PCB to the lakes may affect the results but should be compensated for when comparing BAF rather than concentration in the organisms. The among-lake differences are, therefore, more likely attributable to differences in other processes.

The BAFs for the three trophic levels were positively related to K_{ow}. On a lipid basis, BAFs were 1–1.5 orders of magnitude higher than K_{ow} for all three trophic levels. Swackhamer and Skoglund (1993) found similar results for phytoplankton in natural waters. They suggested that normalisation to POC may be more appropriate than to lipids. When expressed on a dry weight basis, we found that BAFs were of the same magnitude as K_{ow} for all three trophic levels, a result similar to what Swackhamer and Skoglund (1993) obtained for phytoplankton. The slopes of the BAF function of K_{ow} in our study were not affected by normalisation of BAF. The slopes increased with trophic level, i.e., the relative amount of PCBs with low K_{ow} decreased in the organisms, compared with water, with trophic level: phytoplankton > zooplankton > fish. When OCs are in thermodynamic equilibrium between the dissolved phase in water and biota, the BCF should be a linear function of K_{ow} with a slope of 1 (Mackay 1982). We found that the slope for fish was approximately 1, for zooplankton was 0.8, and for phytoplankton was 0.6. Hence, the slopes indicated that the PCBs in fish were in equilibrium or steady state with the dissolved phase in water. The most lipophilic PCBs did not seem to be in steady state between water and zooplankton and even further from steady state between water and phyto-

© 2000 NRC Canada

plankton. The slopes of the BAF function of K_{ow} for the three trophic levels in this study are comparable with those observed by Oliver and Niimi (1988) in Lake Ontario in 1984. The slopes in their food chain were 0.7 for plankton (dominated by phytoplankton), 0.8 for mysids (*Mysis relicta*), and 0.9 for small rainbow smelt (*Osmerus mordax*). Although seldom tested, small planktonic organisms are often considered to be in equilibrium with dissolved water concentrations (Campfens and Mackay 1997). As the BAFs were above the 1:1 line between log BAF and log K_{ow}, the ΣPCB concentrations in phytoplankton, zooplankton, and fish all seemed to exceed equilibrium with water. There may be several explanations as to why the measured BAFs were not identical to the corresponding K_{ow}s for the PCB congeners. Exposure time of organisms to the PCBs may affect the BAFs. The organism PCB concentrations represent integrated measures of contamination over a period of time, and water measures are instantaneous. Therefore, changes in water concentrations may not be reflected in organism concentrations due to a lag period for equilibrium to be reached. Analytical and modelling procedures may also affect the BAF measures. The model used here to estimate freely dissolved water concentrations only provides an approximation, and the influence of POC and DOC on the freely dissolved concentrations may vary considerably. We cannot, therefore, exclude the possibility that we may have underestimated the freely dissolved concentrations and thereby overestimated the BAFs. Also, different methods of lipid extraction can vary in efficiency for different lipid classes (Ewald et al. 1998), which may affect lipid-normalised BAFs. Lipid composition in itself may also affect the relationship between BAF and K_{ow}. Different lipid classes have different affinity for PCBs, and it may not be appropriate to make direct, quantitative comparisons between lipids and octanol as solvents for PCBs.

The phytoplankton concentrations of PCB should only be affected by equilibrium partitioning with the water phase. However, for zooplankton, we found that the PCB pattern was different from that for phytoplankton in that the average lipophilicity increased and the concentrations were lower. Therefore, we believe that some processes other than biomagnification, differing from the phytoplankton–water partitioning, may be responsible for the PCB matrix observed in zooplankton. Thus, although we found strong relationships between log BAF and log K_{ow} for the PCB congeners, care should be taken when assuming equilibrium partitioning with the water phase, based on K_{ow} relationships, when modelling OC concentrations in small aquatic organisms.

If PCBs are biomagnified from prey to predator (Evans et al. 1991), the log BMF (predator/prey) should be > 0. In our study, on a lipid weight basis, no PCB congeners were biomagnified from phytoplankton to zooplankton, as all $BMF_{zoo/phyto}$ values were < 0. The log $BMF_{zoo/phyto}$ values were positively related to log K_{ow}, i.e., PCBs with high log K_{ow} were relatively more abundant in zooplankton than in phytoplankton. Kucklick et al. (1996) suggested that the positive relationship between log BMF (predator/prey) and log K_{ow} found in Lake Baikal could be accounted for by a depuration rate inversely related to log K_{ow}, and lower in the predator than in the prey as suggested by LeBlanc (1995). The log $BMF_{fish/zoo}$ showed the same pattern, but PCB congeners with log K_{ow} > 6 all had log $BMF_{fish/zoo} > 0$, on both a lipid and a dry weight basis, concentrations being two to three times greater in fish than in zooplankton. Here also, PCBs with log $K_{ow} < 6$ had $BMF_{fish/zoo} < 0$, i.e., concentrations were lower in predator than in prey. In our study, the fractionation of the most lipophilic PCBs seemed to cease in the zooplankton to fish step, but the less lipophilic PCBs continued to be fractionated. Oliver and Niimi (1988) concluded that most of the differential PCB fractionation seemed to occur at the lower end of the food chain: in their study, the transfer from water to plankton to mysid. At the higher end of the food chain (mysid to rainbow smelt to adult salmonid), the PCBs seemed to be distributed as a uniform composition mixture. Thus, the concentrations of PCBs with log $K_{ow} < 6$ decreased with increasing trophic level: phytoplankton > zooplankton > fish. Oliver and Niimi (1988) concluded that there was a typical stepwise increase in PCB concentration as they moved up the food chain constituting plankton – mysids – rainbow smelt – salmonids. However, when regarding lipid content at the different trophic levels, it appears as if they also observed decreasing concentrations of trichlorobiphenyls from plankton to mysids to rainbow smelt and decreasing tetrachlorobiphenyl concentrations from plankton to mysids or rainbow smelt. As expected, the PCB pattern in water was skewed towards the low-chlorinated or less lipophilic congeners compared with plankton and fish, reflecting the decreasing water solubility with increasing chlorination of the PCB congeners.

The concentrations of the most lipophilic PCBs were approximately the same in phytoplankton and zooplankton but increased two to three times in fish. It has been shown that factors other than food uptake influence bioaccumulation of OCs and may explain the apparent increase in OC concentrations with trophic level. As mentioned above, lipid content strongly affects OC accumulation. Other factors that influence OC accumulation are elimination and lipid quality and composition. LeBlanc (1995) suggested that because of the sequestration of lipophilic OCs, within the body, in compartments distant from the site of elimination and the reduced ratio of elimination sites to body mass, elimination rates for OCs would be expected to decrease with increasing body mass. Zooplankton eliminate xenobiotics 10–100 times more rapidly than fish, and depuration rates of both fish and zooplankton are inversely related to the lipophilicity of the compound (LeBlanc 1995). The depuration of OCs has also been shown to decrease with increasing size of fish (Sijm and Van der Linde 1995; Fisk et al. 1998). The differences in depuration rates between zooplankton and fish increase with increasing lipophilicity of the xenobiotic (LeBlanc 1995). This would account for the differential partitioning of PCBs between phytoplankton, zooplankton, and phytoplankton in our study. Kucklick et al. (1996) also found positive relationships between BMF (predator/prey) and K_{ow} in the Lake Baikal trophic food chain. Their results indicated that in Lake Baikal, all PCBs were partitioned differentially between trophic levels 3 and 2 (amphipod–netplankton) and between levels 4 and 3 (sculpin–amphipod).

The observed relationship between $BMF_{zoo/phyto}$ and K_{ow} may be caused by increased differences in depuration rate with increased lipophilicity of the compound. Elimination of extremely hydrophobic chemicals is observed in small fish,

© 2000 NRC Canada

but elimination rates decrease with fish size (Sijm and Van der Linde 1995; Fisk et al. 1998). The more lipophilic OCs have longer elimination half-lives in biota than the less lipophilic compounds (Sijm et al. 1992). Therefore, the former accumulate to higher concentrations in an organism's tissues and bioaccumulate to a greater extent through the food chain (Oliver and Niimi 1988).

The lipid composition of aquatic organisms has been shown to affect uptake of lipophilic compounds. Ewald and Larsson (1994) demonstrated that nonpolar triglycerides accumulated more 2,2′,4,4′-tetrachlorobiphenyl than polar phospholipids. Lipid composition differs between phytoplankton, zooplankton, and fish. The polar to nonpolar lipid ratio increases from phytoplankton to zooplankton to fish (Wainman et al. 1993; Ewald and Larsson 1994; Stange and Swackhamer 1994; Napolitano et al. 1996). The higher content of nonpolar lipids, and consequently the higher OC accumulation capacity, in fish compared with zooplankton and phytoplankton may, therefore, be partly responsible for the reported higher concentrations of OCs in fish than in zooplankton and phytoplankton, independent of biomagnification processes.

In conclusion, lipid-normalised ΣPCB concentrations in zooplankton were lower than in both phytoplankton and fish, which did not differ in concentrations. No PCB domains were biomagnified from phytoplankton to zooplankton in the studied lakes. However, the concentrations of the most lipophilic PCBs were higher in fish than in zooplankton. PCB domains were differentially fractionated in all the links of the food chain; the average lipophilicity of the PCBs increased from water to fish. Concentrations of PCBs with $\log K_{ow} < 6$ decreased from phytoplankton to zooplankton to fish. We suggest that this may be an effect of a decreasing depuration rate of the most lipophilic PCBs with increasing size or trophic level.

Acknowledgements

This study was funded by the National Swedish Environmental Protection Agency (the EUCON project area), Swedish Association of Graduate Engineers, and Oscar and Lili Lamm's Memorial Foundation. Thanks to Cecilia Agrell for statistical guidance.

References

Adrian, R., and Frost, T.M. 1993. Omnivory in cyclopoid copepods — comparisons of algae and invertebrates as food for 3 differently sized species. J. Plankton Res. **15**: 643–658.

Agrell, C., Okla, L., Larsson, P., Backe, C., and Wania, F. 1999. Evidence of latitudinal fractionation of polychlorinated biphenyl congeners along the Baltic Sea region. Environ. Sci. Technol. **33**: 1149–1156.

Bentzen, E., Lean, D.R.S., Taylor, W.D., and Mackay, D. 1996. Role of food web structure on lipid and bioaccumulation on organic contaminants by lake trout (*Salvelinus namaycush*). Can. J. Fish. Aquat. Sci. **53**: 2397–2407.

Berglund, O. 1999. The influence of ecological processes on the accumulation of persistent organochlorines in aquatic ecosystems. Ph.D. thesis, Department of Ecology, Lund University, Lund, Sweden.

Bergner, P.-E.E. 1985. On relations between bioaccumulation and weight of organisms. Ecol. Model. **27**: 207–220.

Bremle, G., Okla, L., and Larsson, P. 1995. Uptake of PCB in fish in a contaminated river system: bioconcentration factors measured in the field. Environ. Sci. Technol. **29**: 2010–2015.

Burkhard, L.P. 1998. Comparison of two models for predicting bioaccumulation of hydrophobic organic chemicals in a Great Lakes food web. Environ. Toxicol. Chem. **17**: 383–393.

Campfens, J., and Mackay, D. 1997. Fugacity-based model of PCB bioaccumulation in complex aquatic food webs. Environ. Sci. Technol. **31**: 577–583.

DeMott, W.R. 1995. Effect of prey hardness on size-selective feeding by *Daphnia*. Hydrobiologia, **307**: 127–138.

Evans, M.S., Noguchi, G.E., and Rice, C.P. 1991. The biomagnification of polychlorinated biphenyls, toxaphene, and DDT compounds in a Lake Michigan offshore food web. Arch. Environ. Contam. Toxicol. **20**: 87–93.

Ewald, G., and Larsson, P. 1994. Partitioning of ^{14}C-labelled 2,2′,4,4′- tetrachlorobiphenyl between water and fish lipids. Environ. Toxicol. Chem. **13**: 1577–1580.

Ewald, G., Bremle, G., and Karlsson, A. 1998. Differences between Bligh and Dyer and Soxhlet extractions of PCBs and lipids from fat and lean fish muscle: implications for data evaluation. Mar. Pollut. Bull. **36**: 222–230.

Fisk, A.T., Norstrom, R.J., Cymbalisty, C.D., and Muir, D.C.G. 1998. Dietary accumulation and depuration of hydrophobic organochlorines: bioaccumulation parameters and their relationship with the octanol/water partition coefficient. Environ. Toxicol. Chem. **17**: 951–961.

Harding, G.C., LeBlanc, R.J., Vass, W.P., Addison, R.F., Hargrave, B.T., Pearre, S., Jr., Dupuis, A., and Brodie, P.F. 1997. Bioaccumulation of polychlorinated biphenyls (PCBs) in the marine pelagic food web, based on a seasonal study in the southern Gulf of St. Lawrence, 1976–1977. Mar. Chem. **56**: 145–179.

Hawker, D.W., and Connell, D.W. 1988. Octanol–water partitioning coefficients of polychlorinated biphenyl congeners. Environ. Sci. Technol. **22**: 382–387.

Karickhoff, S.W. 1981. Semi-emperical estimation of sorption of hydrophobic pollutants on natural sediments and soils. Chemosphere, **10**: 833–846.

Kidd, K.A., Schindler, D.W., Hesslein, R.H., and Muir, D.C.G. 1998. Effects of trophic position and lipid on organochlorine concentrations in fishes from subarctic lakes in Yukon Territory. Can. J. Fish. Aquat. Sci. **55**: 869–881.

Kiriluk, R.M., Servos, M.R., Whittle, D.M., Cabana, G., and Rasmussen, J.B. 1995. Using ratios of stable nitrogen and carbon isotopes to characterize the biomagnification of DDE, mirex, and PCB in a Lake Ontario pelagic food web. Can. J. Fish. Aquat. Sci. **52**: 2660–2674.

Kucklick, J.R., and Baker, J.E. 1998. Organochlorines in Lake Superior's food web. Environ. Sci. Technol. **32**: 1192–1198.

Kucklick, J.R., Harvey, H.R., Ostrom, P.H., Ostrom, N.E., and Baker, J.E. 1996. Organochlorine dynamics in the pelagic food web of Lake Baikal. Environ. Toxicol. Chem. **15**: 1388–1400.

Larsson, P., Backe, C., Bremle, G., Eklöv, A., and Okla, L. 1996. Persistent pollutants in a salmon population (*Salmo salar*) of the southern Baltic Sea. Can. J. Fish. Aquat. Sci. **53**: 62–69.

LeBlanc, G.A. 1995. Trophic-level differences in the bioconcentration of chemicals: implications in assessing environmental biomagnification. Environ. Sci. Technol. **29**: 154–160.

Mackay, D. 1982. Correlation of bioconcentration factors. Environ. Sci. Technol. **16**: 274–278.

Madenjian, C.P., Hesselberg, R.J., Desorcie, T.J., Schmidt, L.J., Stedman, R.M., Quintal, R.T., Begnoche, L.J., and Passino-

© 2000 NRC Canada

Reader, D.R. 1998. Estimate of net trophic transfer efficiency of PCBs to Lake Michigan lake trout from their prey. Environ. Sci. Technol. **32**: 886–891.

Napolitano, G.E., Shantha, N.C., Hill, W.R., and Luttrell, A.E. 1996. Lipid and fatty acid compositions of stream periphyton and stoneroller minnows (*Campostoma anomalum*): trophic and environmental implications. Arch. Hydrobiol. **137**: 211–225.

Oliver, B.G., and Niimi, A.J. 1988. Trophodynamic analysis of polychlorinated biphenyl congeners and other chlorinated hydrocarbons in the Lake Ontario ecoystem. Environ. Sci. Technol. **22**: 388–397.

Paterson, M.J., Muir, D.C.G., Rosenberg, B., Fee, E.J., Anema, C., and Franzin, W. 1998. Does lake size affect concentrations of atmospherically derived polychlorinated biphenyls in water, sediment, zooplankton, and fish? Can. J. Fish. Aquat. Sci. **55**: 544–553.

Persson, A. 1997. Fish excretion in relation to internal and external load in a eutrophic lake. Limnol. Oceanogr. **42**: 577–583.

Rasmussen, J.B., Rowan, D.J., Lean, D.R.S., and Carey, J.H. 1990. Food chain structure in Ontario lakes determines PCB levels in lake trout (*Salvelinus namaycush*) and other pelagic fish. Can. J. Fish. Aquat. Sci. **47**: 2030–2038.

Repka, S. 1997. Effects of food type on the life history of *Daphnia* clones from lakes differing in trophic state. I. *Daphnia galeata* feeding on *Scenedesmus* and *Oscillatoria*. Freshwater Biol. **37**: 675–683.

Rudd, R.L. 1964. Biocider och den levande naturen. Wahlström & Widstrand, Stockholm, Sweden.

Russell, R.W., Lazar, R., and Haffner, G.C. 1995. Biomagnification of organochlorines in Lake Eire white bass. Environ. Toxicol. Chem. **14**: 719–724.

Schulz, D.E., Petrick, G., and Duinker, J.C. 1989. Complete characterization of polychlorinated biphenyl congeners in commercial Aroclor and Clophen mixtures by multidimensional gas chromatography – electron capture detection. Environ. Sci. Technol. **23**: 852–859.

Sijm, D.T.H.M., and Van der Linde, A. 1995. Size-dependent bioconcentration kinetics of hydrophobic organic chemicals in fish based on diffusive mass tranfer and allometric relationships. Environ. Sci. Technol. **29**: 2769–2777.

Sijm, D.T.H.M., Seinen, W., and Opperhuizen, A. 1992. Life-cycle biomagnification study in fish. Environ. Sci. Technol. **26**: 2162–2174.

Stange, K., and Swackhamer, D.L. 1994. Factors affecting phytoplankton species-specific differences in accumulation of 40 polychlorinated biphenyls (PCBs). Environ. Toxicol. Chem. **13**: 1849–1860.

Swackhamer, D.L., and Skoglund, R.S. 1993. Bioaccumulation of PCBs by algae: kinetics versus equilibrium. Environ. Toxicol. Chem. **12**: 831–838.

Wainman, B.C., McQueen, D.J., and Lean, D.R.S. 1993. Seasonal trends in zooplankton lipid concentration and class in freshwater lakes. J. Plankton Res. **15**: 1319–1332.

© 2000 NRC Canada

Changes in species composition of the demersal fish community in nearshore waters of Kodiak Island, Alaska

Franz J. Mueter and Brenda L. Norcross

Abstract: We examined the species composition of the demersal fish and shrimp community in seven different areas in the nearshore waters of Kodiak Island based on trawl survey data. A major part of the variability in the data set was attributed to trends over time, indicating a significant change in species composition in the early 1980s. Results agree with work by others and show a shift from a community dominated by shrimp and small forage fishes to one dominated by large piscivorous gadid and flatfish species. The shift occurred rather abruptly in most areas between 1980 and 1982, but the pattern of change differed significantly among areas. Correlations between trends in the two groups of species were weak but were consistent with the hypothesis that the decline in shrimp and forage fishes followed, rather than preceded, the increase in large piscivorous fishes. The results suggest predation as a possible mechanism to explain the observed changes.

Résumé : Nous avons examiné la composition spécifique de la communauté benthique de poissons et de crevettes de sept lieux différents des eaux côtières de l'île Kodiak en nous fondant sur les données obtenues par relevés au chalut. Une grande partie de la variabilité de l'ensemble des données a été attribuée à des tendances temporelles, indiquant un changement appréciable de la composition en espèces au début des années 1980. Les résultats concordent avec ceux d'autres chercheurs et montrent la transformation d'une communauté dominée par les crevettes et les petits poissons proies à une communauté dominée par des gadidés et des poissons plats piscivores de grande taille. Le changement est survenu relativement abruptement dans la plupart des zones entre 1980 et 1982, mais son allure différait de façon appréciable entre les zones. Les corrélations entre les tendances des deux groupes d'espèces étaient faibles et cela est conforme avec l'hypothèse selon laquelle le déclin des crevettes et des poissons proies a suivi, et non précédé, l'accroissement des gros poissons piscivores. Les résultats obtenus montrent que la prédation pourrait être le mécanisme des changements observés.

[Traduit par la Rédaction]

Introduction

In the late 1970s, large-scale climatic and oceanographic changes occurred in the North Pacific, which affected many parts of the marine ecosystem (Brodeur and Ware 1992, 1995; Francis and Hare 1994; Hollowed and Wooster 1995). At the same time, shrimp and crab stocks declined precipitously in the Gulf of Alaska as well as in the eastern Bering Sea, and most of the fisheries they supported have collapsed since 1980 (Orensanz et al. 1998). Declining shrimp populations in Pavlof Bay and in other nearshore areas in the central Gulf of Alaska were accompanied by declines in capelin and other forage fishes (Piatt and Anderson 1996; Anderson et al. 1997). A decrease in the occurrence of capelin in the nearshore environment is also evidenced by their reduced frequency of occurrence in the diet of seabirds in the 1980s and 1990s compared with the 1970s (Piatt and Anderson 1996). At the same time, the abundance of flatfishes and gadids in the nearshore areas increased (Anderson et al. 1997).

Causes of this apparent shift in species composition are not well understood at present and may include environmental effects, overfishing, or multiple causes acting simultaneously. Shrimp catches around Kodiak Island peaked in 1971 and began a steady decline into the early 1980s (Orensanz et al. 1998). Fishing effort remained high through most of this period, although fishery-independent biomass indices for shrimp around Kodiak Island and in Pavlof Bay showed a strong declining trend (Anderson et al. 1997). Although there is evidence that overfishing contributed to the decline in shrimp stocks, the influence of large-scale environmental forcing is hard to dismiss (Piatt and Anderson 1996; Orensanz et al. 1998). A strong increase in water temperature in the northern Gulf of Alaska (Royer 1989) may be in part responsible for the observed changes (Piatt and Anderson 1996; Anderson et al. 1997).

Much of the evidence for a shift in species composition is based on abundance data aggregated at the family level, since trends in individual species may be obscured by high variability (Anderson et al. 1997). While long-term and large-scale trends are evident in the aggregated data, there has not been an analysis at the species level to test whether the change in species composition was significant, which species were affected, and whether the changes followed the

Received January 12, 1999. Accepted August 26, 1999. J14969

F.J. Mueter.[1] School of Resource and Environmental Management, Simon Fraser University, Burnaby, BC V5A 1S6, Canada.
B.L. Norcross. Institute of Marine Science, University of Alaska-Fairbanks, P.O. Box 757220, Fairbanks, AK 99775-7220, U.S.A.

[1]Author to whom all correspondence should be addressed. e-mail: mueter@ims.uaf.edu

© 2000 NRC Canada

same pattern in different areas. The primary goal of our study was to statistically test changes in species composition of the groundfish community in the bays around Kodiak Island. Specifically, we derived multivariate indices that summarize the major patterns of variation in species composition, tested for significant changes in these indices over time, identified species that are primarily responsible for the observed changes, and compared the patterns of change among areas.

Materials and methods

To test for changes in species composition, we analyzed trawl survey data collected between 1976 and 1995 by the Alaska Department of Fish and Game and the National Marine Fisheries Service in nearshore areas of the central Gulf of Alaska. All sampling was conducted during daylight using a 32-mm-mesh, high-opening shrimp trawl with an 18.6-m headrope and footrope (Anderson 1991). Although several different vessels were used in the surveys, gear was fished at approximately the same speed and using similar scope for all vessels; thus, differences over time cannot be attributed to differences in sampling gear or methods. The survey targeted primarily shrimp; however, many groundfish species were caught incidentally. Assuming that there were no underlying trends in catchability or in the size structure of fishes over time, the survey provides indices of abundance that reflect true changes in the sampled populations within the area covered by the survey.

We selected seven bays and nearshore areas on the east and south sides of Kodiak Island for our analysis: Marmot Island, Marmot Bay, Chiniak Bay, Ugak Bay, Kiliuda Bay, Twoheaded Gully, and Alitak Bay (Fig. 1). Within each of the seven areas, between two and five strata were sampled following a stratified random sampling design (J.E. Blackburn, Alaska Department of Fish and Game, 211 Mission Rd., Kodiak, AK 99615, U.S.A., personal communication). We considered only strata that were sampled during at least 4 years of the survey, since our primary interest was to detect trends over time in the data. Within a year, sampling often extended from early May to early November with few or no samples collected in the month of July. To minimize bias due to seasonal differences, we selected only tows collected between August and October. The final data set comprised 1035 hauls from a total of 15 survey years (Table 1). Areas for each sampling stratum were not available for analysis. Therefore, we analyzed trends within strata only or pooled strata by area if strata means did not differ significantly within an area.

Invertebrates and fish were grouped into 32 taxa (Table 2), primarily at the species and genus level. Shrimp were combined because we were primarily interested in the fish community. Fish were grouped at the coarsest level at which specimens were identified. Members of rare families that occurred in less than 1% of the hauls were excluded, as they may distort inferred patterns in species composition (Koch 1987). Catches of all species groups were standardized to catch-per-unit-effort (CPUE, kilograms per kilometre towed) for analysis. CPUE data were transformed using a fourth-root transformation, as recommended by Field et al. (1982). We did not use proportional data because all species CPUEs were measured on the same scale and because standardization to proportions eliminates information on differences in absolute abundances of species among sites. While some authors advocate using proportional data or some other form of standardization to equal site or species totals (Kenkel and Orloci 1986; Faith et al. 1987), Jackson (1997) argued that such standardization may produce artifacts in the patterns that emerge from compositional data.

To detect and relate patterns in the abundance of a large number of species to environmental or other independent variables, community ecologists have developed a variety of techniques that can be classified into two basic approaches: direct gradient analysis and indirect gradient analysis (Whittaker 1967; Ter Braak and Prentice 1988). Direct gradient analysis incorporates information about the environment directly into the analysis. Regression analysis is a form of direct gradient analysis with a single response variable, e.g., a regression of the abundance of one species on one or more independent variables (Ter Braak 1995). In the case of multiple species, multivariate direct gradient analysis techniques are needed to detect the main pattern in the relationship between species abundances and independent variables. Commonly used techniques are canonical correlation analysis, redundancy analysis, and canonical correspondence analysis (CCA). Correlation analysis and redundancy analysis assume that species are linearly related to ecological gradients, but CCA allows a nonlinear response of the species to underlying variables. A disadvantage of direct gradient analysis is that the set of relevant independent variables needs to be determined a priori. If noisy or irrelevant variables are included, patterns in species composition can be greatly distorted (McCune 1997).

By contrast, indirect gradient analysis is a two-stage approach (Whittaker 1967). In the first step, species abundance data from a potentially large number of species and sites are summarized and sites are arranged in ordination space. Resulting patterns in the ordination of sites are subsequently related to independent variables, e.g., by regressing site scores from one or more ordination axes on the variables. Commonly used ordination techniques for indirect gradient analysis are principal components analysis (PCA), correspondence analysis (CA), detrended correspondence analysis (DCA), and nonmetric multidimensional scaling (NMDS). PCA assumes a linear response between each species and underlying ecological gradients, while CA and DCA allow a unimodal response. No particular response model underlies NMDS, but it has been shown to be robust to a wide variety of potential relationships between individual species abundances and environmental gradients (Minchin 1987).

All ordination techniques are based on a measure of between-site dissimilarities. In the case of PCA, the implicit dissimilarity measure is Euclidean distance, while chi square distance is the built-in dissimilarity measure in all forms of CA. In contrast, NMDS allows the choice of any dissimilarity measure; thus, a measure that is appropriate to the data at hand can be chosen. A confusing variety of dissimilarity measures have been proposed in the literature (e.g., Washington 1984), and few authors agree as to which measure is most appropriate. Trawl data are characterized by the joint absence of many species from a large number of sites, resulting in many zero values in the data matrix. Dissimilarity measures that are not affected by such joint absences are clearly preferable. One such measure, the Bray–Curtis index, has been shown to be a robust measure of ecological distance (dissimilarity) in the presence of joint absences (Field et al. 1982). Based on a suitable measure of between-site dissimilarities, NMDS attempts to arrange sites in a low-dimensional space such that distances in the ordination space are close to the underlying between-site dissimilarities (Kruskal 1964).

We used Bray–Curtis dissimilarities between each pair of sites, followed by an NMDS ordination, to summarize patterns in species composition of the groundfish community based on a matrix of transformed abundances consisting of 1035 rows (sites) and 32 columns (taxa). The initial ordination was carried out in two dimensions, and the number of dimensions was increased until a given goodness-of-fit criterion was achieved. Goodness-of-fit was assessed using Kruskal's stress criterion, a measure of discrepancy between the Euclidean distances in ordination space and the underlying Bray–Curtis dissimilarities (Kruskal 1964). We accepted the fit if Kruskal's stress was less than 15%. The final configuration from the ordination was rotated such that the first axis corresponded to the axis of maximum variation. The scores for each site along each rotated ordination axis were used as indices of species

© 2000 NRC Canada

Fig. 1. Kodiak Island showing the seven sampling areas where shrimp trawl surveys were conducted.

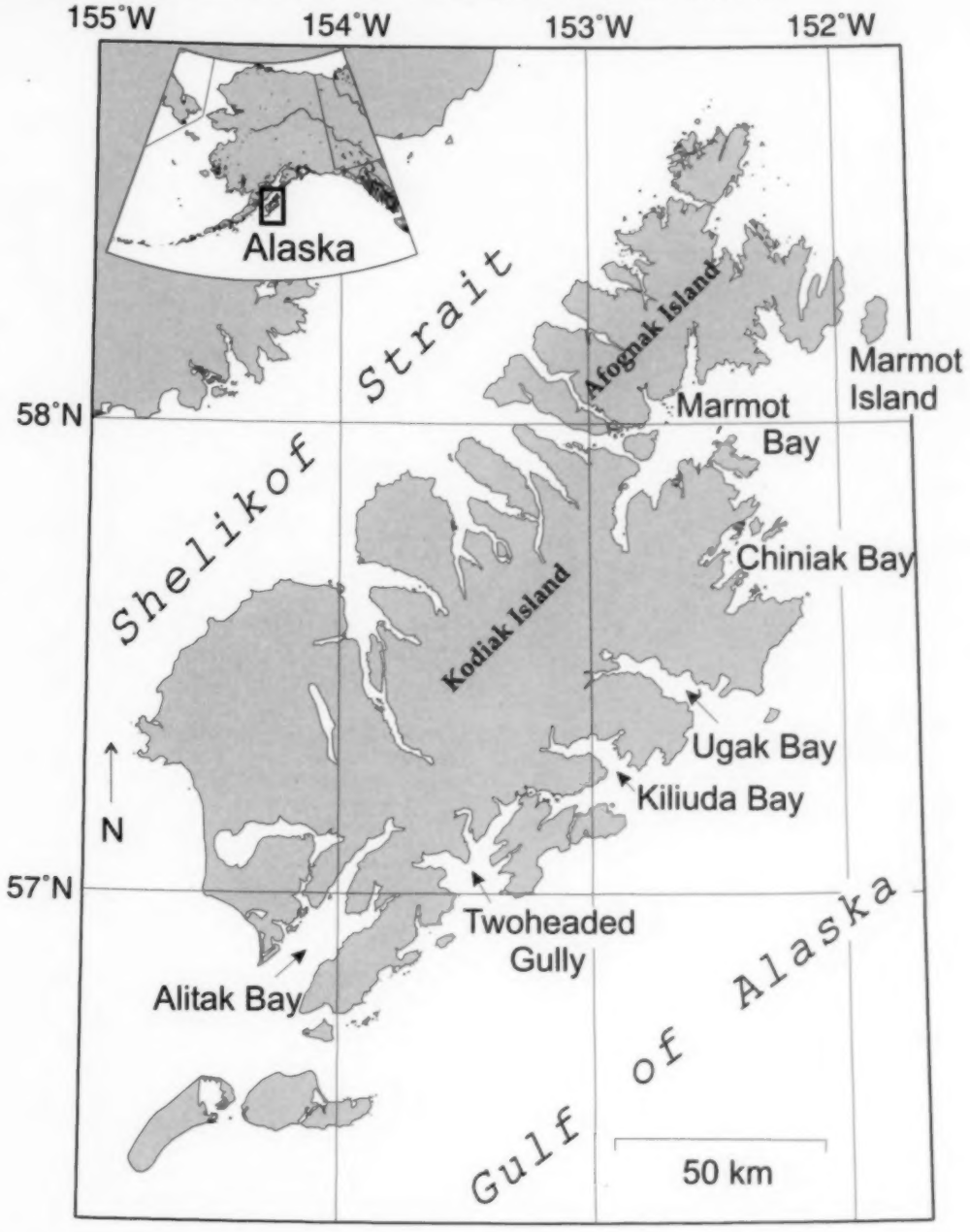

composition. Each axis can be interpreted as representing a different, independent aspect of species composition, with axis 1 scores representing the major mode of variation in species composition. The axis scores have no units, as they reflect relative dissimilarities only.

We estimated and tested trends in species composition over time for significance within each sample stratum using an analysis of covariance of axis scores with depth and date of sampling (Julian day) as covariates:

$$\text{(A)}\quad (\text{Axis scores})_{ijk} = \alpha + (\text{stratum})_i + (\text{year})_{j(i)} + \beta_1 \times \text{depth} + \beta_2 \times \text{Julian} + \varepsilon_{ijk}$$

where the subscripts denote strata (i), years within strata (j), and observations within each stratum–year combination (k). Depth was included because species composition is typically strongly related to depth (Mueter and Norcross 1999). Initially, we assumed that the depth response does not differ among strata. To test this as-

© 2000 NRC Canada

Table 1. Number of stations sampled by the Alaska Department of Fish and Game in the August–October sampling period between 1976 and 1995 by area and year.

	1976	1977	1978	1979	1980	1981	1982	1983	1984	1985	1986	1987	1989	1992	1995
Marmot Bay	6	12	12		7	8	8		10	8		9	10	14	16
Marmot Island	22	52	46		4	40	8		6	6		7	6		
Chiniak Bay			4	4	7	10	7	9	5			6	7	3	6
Ugak Bay	19	7	6		11	12	10		5	9	10		10		
Kiliuda Bay	24	10	35	27	18	10	9		10	9	10		10	10	6
Twoheaded Gully		21	16	32	13	13	16		12	10	13		13	8	8
Alitak Bay		10	9	12	16	28	21	9	12	22	12	12	9	7	9

Table 2. Species and species groups used in analysis and proportion of total catch averaged over all hauls.

Scientific name	Common name	Proportion (%)
Pandalidae and Crangonidae	Shrimp	39.1
Theragra chalcogramma	Walleye pollock	24.3
Hippoglossoides elassodon	Flathead sole	14.6
Atheresthes stomias	Arrowtooth flounder	6.3
Gadus macrocephalus	Pacific cod	3.8
Pleuronectes asper	Yellowfin sole	1.6
Cottidae	Sculpins	1.5
Mallotus villosus	Capelin	1.3
Hippoglossus stenolepis	Pacific halibut	0.8
Chionoecetes bairdi	Tanner crab	0.8
Paralithodes camtschatica	Red king crab	0.7
Microgadus proximus	Pacific tomcod	0.6
Trichodon trichodon	Pacific sandfish	0.6
Anoplopoma fimbria	Sablefish	0.6
Pleuronectes bilineatus	Rock sole	0.6
Zoarcidae	Eelpouts	0.5
Clupea pallasi	Pacific herring	0.5
Thaleichthys pacificus	Eulachon	0.4
Lumpenella longirostris	Longsnout prickleback	0.3
Rajidae	Skates	0.3
Platichthys stellatus	Starry flounder	0.2
Osmeridae	Smelts	0.1
Sebastes spp.	Rockfishes	0.1
Errex zachirus	Rex sole	0.1
Bathymaster signatus	Searcher	0.1
Squalus acanthias	Spiny dogfish	0.1
Microstomus pacificus	Dover sole	0.1
Stichaeidae	Pricklebacks	0.1
Cyclopteridae (Cyclopterinae)	Snailfishes	0.03
Podothecus acipenserinus	Sturgeon poacher	0.02
Cancer magister	Dungeness crab	0.02
Zaprora silenus	Prowfish	0.01

sumption, we compared the above model with a model allowing a separate depth response within each stratum. Date of sampling was included as a covariate because species composition may vary over time within the 3-month sampling period. Model A was further compared with a model pooling observations over all strata within an area to test whether the trend in axis scores over time differed significantly among strata. To test whether the time trend could be approximated by a polynomial fit, we fitted models including second- and third-degree polynomials of year instead of estimating separate means for each year. Models were compared using F tests.

Scatterplots and rank correlations between axes scores and individual species abundances were used to identify which species were associated with each ordination axis. Plotting the abundance of a species against axis scores helps to identify individual species that are strongly related to an axis and to assess the nature of the relationship. The use of rank correlations is only appropriate if the relationship between the abundance of a species and the axis scores is at least monotone. While it is not clear what the nature of the relationship should be on theoretical grounds, we found that species were almost always monotonically related to the ordination axes. Based on visual inspection of scatterplots, we chose a cutoff point for the magnitude of rank correlations of 0.35 to identify species that were clearly associated with an ordination axis. Correlations between species abundances and axes scores cannot formally be tested for significance at a given significance level because the scores are based on an ordination of species abundances; thus, they are inherently related.

Results

The NMDS ordination of species abundance data in five dimensions achieved a stress of 12.1% and there was a tight relationship between Bray–Curtis dissimilarities and Euclidean distances in the final configuration of the ordination (Spearman's rank correlation = 0.93). Therefore, we considered the fit in five dimensions satisfactory. The ordination was repeated with several different starting configurations to minimize the chances of obtaining a solution corresponding to a local minimum in the stress criterion. The first ordination axis accounted for 30% of the overall variation, while axes 2–5 accounted for 22, 20, 16, and 13% of the variance, respectively.

The first NMDS axis (model A fit: $F = 19.81$, $p < 0.001$, $r^2 = 0.77$) primarily reflected interannual variation, i.e., there were much stronger differences in axis 1 scores with time than with strata or depth, as indicated by a high coefficient of partial determination for the year effect ($r^2_{year} = 0.69$). The trend in axis 1 scores over time differed significantly among strata within areas ($F = 5.15$, $p < 0.001$). When examining each area individually, we found that most areas had significant differences among strata ($p < 0.005$),

© 2000 NRC Canada

Fig. 2. Estimated means for the first index of species composition (axis 1 scores) by year and area with 95% pointwise confidence intervals based on model A (see text). Observations in Chiniak Bay and Alitak Bay were pooled across strata.

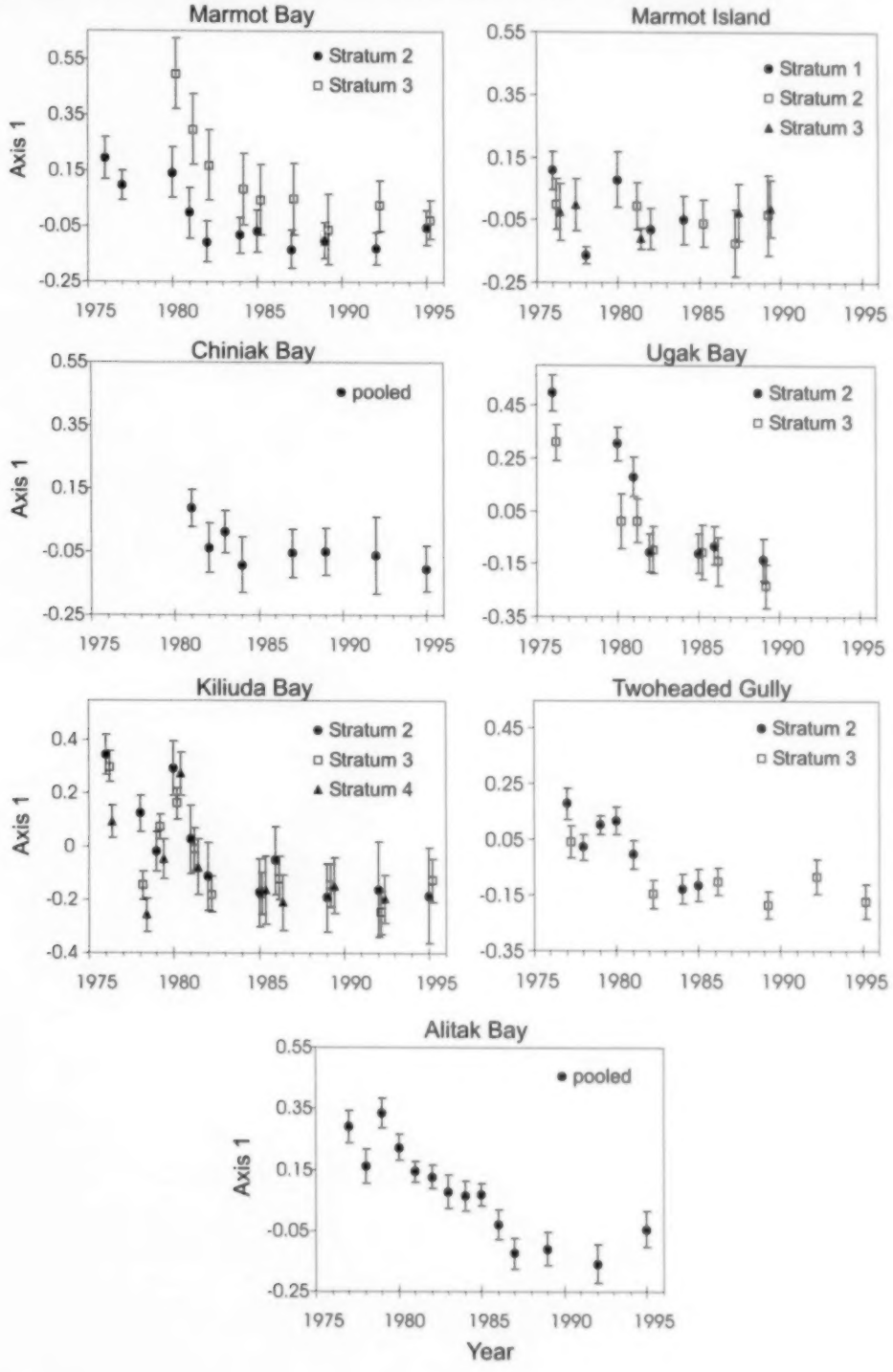

© 2000 NRC Canada

Fig. 3. Scatterplot of log(CPUE + 1) against the first index of species composition (axis 1 scores) for five species that were positively correlated with the index (group A, left panels) and four species that were negatively correlated with the index (group B, right panels). Group A consists of (*a*) shrimp, (*b*) Pacific herring, (*c*) capelin, (*d*) Pacific sandfish, and (*e*) Pacific tomcod. Group B consists of (*f*) arrowtooth flounder, (*g*) flathead sole, (*h*) Pacific cod, and (*i*) walleye pollock. Zero CPUE values were jittered along the *y*-axis by adding a small random component to indicate the number of observations. Nonparametric smooth trend (LOWESS, line) was fitted to positive CPUEs (excluding zeros).

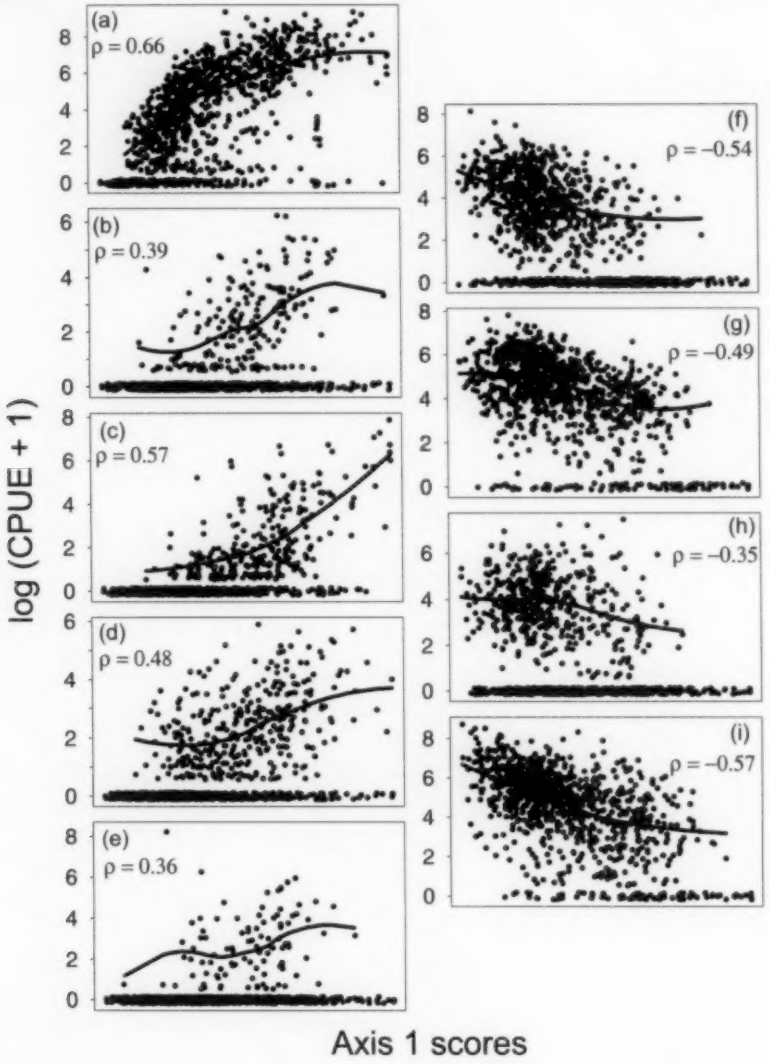

except Chiniak Bay ($F = 0.42$, $p = 0.531$) and Alitak Bay ($F = 1.92$, $p = 0.110$). Thus, we pooled observations over strata within these two areas but estimated separate time trends for each stratum in all other areas (Fig. 2). Approximating the time trend by a polynomial fit was inadequate because residuals were highly autocorrelated and model A fit significantly better ($F = 6.51$, $p < 0.001$). Therefore, separate means for the axis 1 scores were estimated for each year. The depth effect appeared to differ among areas ($F = 4.93$, $p < 0.001$) but not among strata within individual areas ($p > 0.15$ in all cases). Including Julian date as a covariate in model A did not significantly improve the fit ($F = 1.414$, $p = 0.235$); thus, there was no indication that axis 1 scores varied over time within years.

Axes 2 and 3 were primarily related to variations in species composition along the depth gradient and among areas (model A fits: $F = 10.80$, $p < 0.001$, $r^2 = 0.64$ and $F = 8.10$, $p < 0.001$, $r^2 = 0.58$). Only a small proportion of the variance in axis 4 and axis 5 scores was explained by model A ($r^2 = 0.37$ and 0.30, respectively). Most of the variation in these axis scores was related to other, unknown gradients. Because the focus of our paper is on differences in species composition over time, only results for axis 1 are presented.

The estimated means for axis 1 scores declined signifi-

© 2000 NRC Canada

Fig. 4. Estimated means and 95% confidence intervals for trends over time of the combined CPUE of group A, shrimp, Pacific herring, capelin, Pacific sandfish, and Pacific tomcod (hatched), and the combined CPUE of group B, arrowtooth flounder, flathead sole, Pacific cod, and walleye pollock (stippled), in (*a*) Marmot Bay, (*b*) Marmot Island, (*c*) Chiniak Bay, (*d*) Ugak Bay, (*e*) Kiliuda Bay, (*f*) Twoheaded Gully, and (*g*) Alitak Bay.

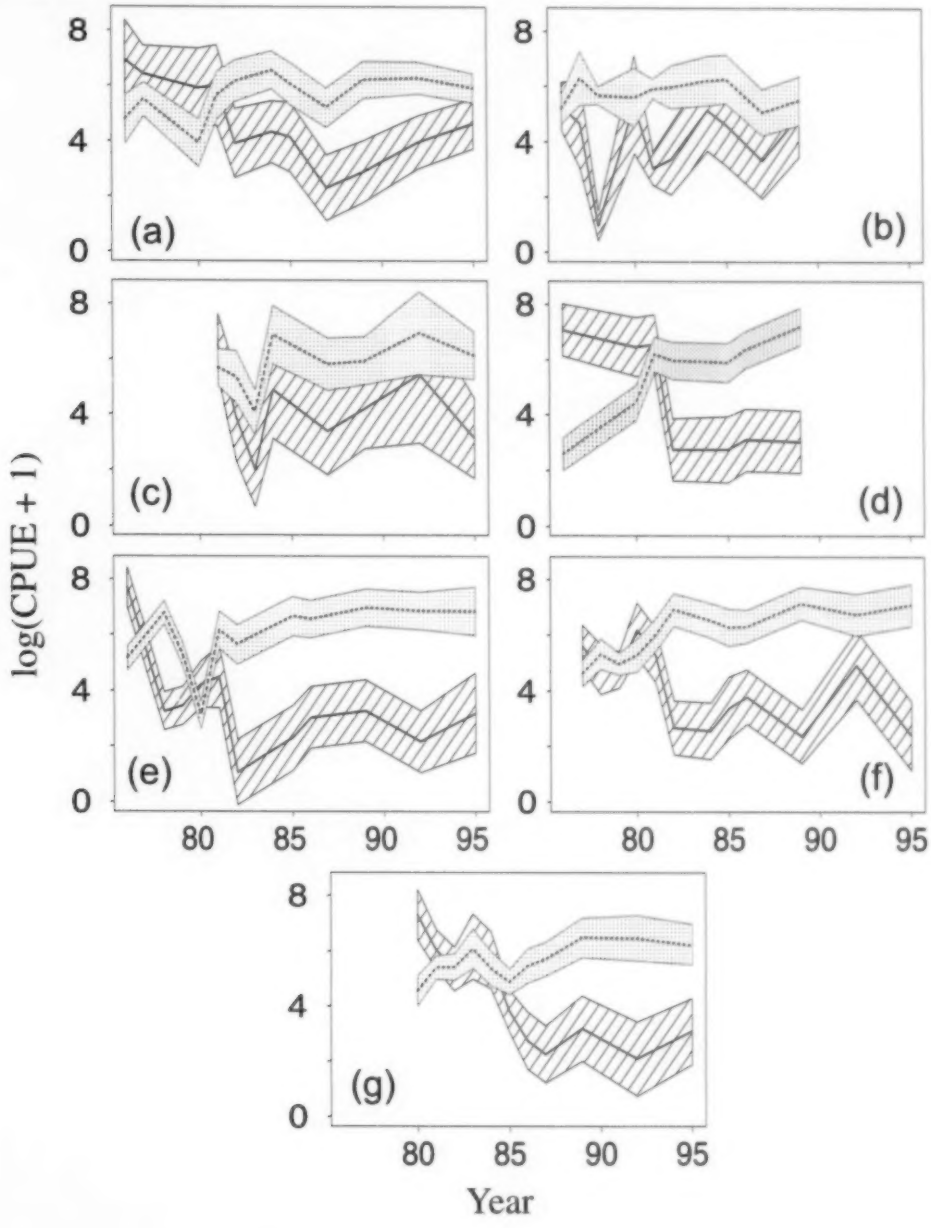

cantly in most areas between 1980 and 1982 (Fig. 2). Although the mean scores differed among strata within most areas, the same sharp drop was evident in all strata. The decline was least evident at Marmot Island and in Chiniak Bay. Alitak Bay was unique in that the decline was much more gradual and the most significant change occurred after 1985 (Fig. 2).

Examination of the underlying species abundances revealed that the decline in axis 1 scores was related to a strong decrease in the CPUE of shrimp, as well as small schooling forage fishes, and a near simultaneous increase of several piscivorous flatfish and gadid species. A group of five taxa (shrimp, Pacific herring, capelin, Pacific sandfish, and Pacific tomcod) had a positive association with the axis 1 scores (group A, Fig. 3). A second group consisting of arrowtooth flounder, flathead sole, Pacific cod, and walleye

© 2000 NRC Canada

Fig. 5. Trajectories of the means of the first index of species composition (axis 1) from the seven areas sampled. Means for Alitak Bay include error bars indicating 95% confidence intervals.

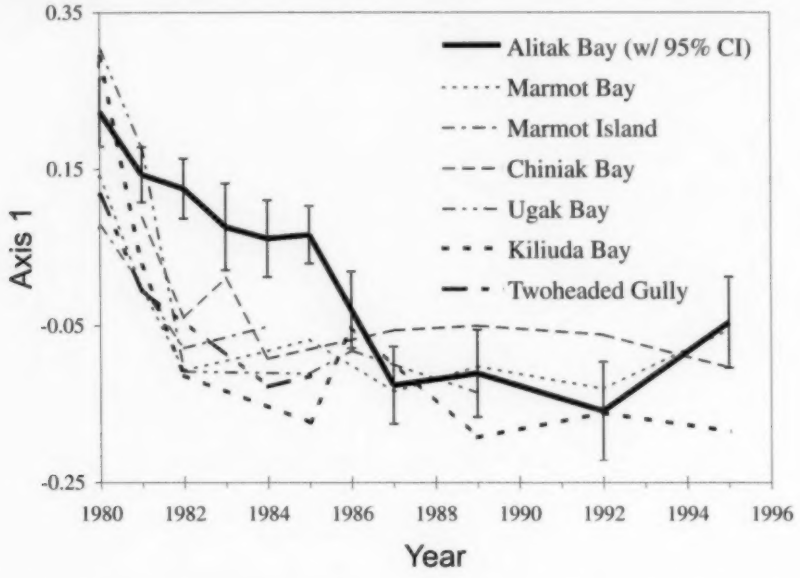

Table 3. Summary of cross-correlations between differenced trends in two species groups at three different lags by area.

Area	Lag –1	Lag 0	Lag 1
Marmot Bay	–0.26	0.21	–0.27
Marmot Island	0.16	0.29	–0.73*
Chiniak Bay	–0.29	0.89*	–0.55
Ugak Bay	0.24	0.41	–0.55
Kiliuda Bay	0.14	–0.12	–0.48
Twoheaded Gully	0.40	–0.73*	0.05
Alitak Bay	–0.39	0.30	0.004

Note: Trends were estimated for the combined CPUE of shrimp, Pacific herring, capelin, Pacific sandfish, and Pacific tomcod (group A) and the combined CPUE of arrowtooth flounder, flathead sole, Pacific cod, and walleye pollock (group B). Each time series was differenced by taking the difference in estimated CPUE between consecutive sampling periods. Cross-correlations are shown for lag –1 (group A leading group B), lag 0, and lag 1 (group B leading group A).

*Significant at $\alpha = 0.05$.

pollock (group B) was negatively rank correlated with axis 1 scores (group B, Fig. 3). Axis 1 can thus be interpreted as contrasting these two species groups.

Estimates of the combined CPUE of group A and the combined CPUE of group B over time for each of the seven areas suggest a clear shift in community composition in at least four of the seven areas between 1980 and 1982 (Fig. 4). CPUE estimates were obtained by modeling log(CPUE + 1) as a function of area and year, after pooling strata within each area to examine overall trends by area. Model fits were poor because there were significant differences among strata in most cases and residuals were skewed due to the presence of zero values. While the fitted means indicated the main trends in the two species groups, confidence intervals are unlikely to be accurate at the stated significance level due to the poor model fits. The CPUE of group A, consisting of shrimp and small forage fishes, decreased in all areas from 1980 to 1982, but the sharpest decline in Alitak Bay did not occur until after 1984. Catches of group B, consisting of large piscivorous species, tended to increase during the same time period, although the increase was generally less pronounced (Fig. 4). Marmot Bay, Ugak Bay, and Twoheaded Gully most clearly showed a shift in community composition between 1980 and 1982.

To examine possible cause and effect relationships between changes in the two groups, we examined correlations between the abundances of group A and group B species at different lags. Because of the time series nature of the data and strong autocorrelation, we used differences in abundance between consecutive sampling years rather than the abundances themselves. Differencing is commonly used to remove autocorrelation in time series data (Diggle 1990). Cross-correlations between the differenced trends in groups A and B showed few significant correlations (Table 3). Correlations at lag –1 were weak and inconsistent. At lag 0, most correlations were positive, suggesting that in most bays, a trend in group A was accompanied by a parallel trend in the piscivorous group (group B) between consecutive sampling years. However, only one of the positive correlations (Chiniak Bay) was significant. Two correlations at lag 0 were negative, but only one (Twoheaded Gully) was significant. For lag 1, in five out of seven bays, an increase in the piscivorous group between two sampling events was followed by a decrease in group A; however, the correlation was significant only at Marmot Island. Positive correlations at lag 0 and negative correlations at lag 1 in four of the bays suggest that the increase in gadids and flatfish species preceded the decline in shrimp and small forage fishes in these bays.

We examined changes in Alitak Bay more closely because of differences in the observed time trends between Alitak Bay and the other bays (Fig. 5). The CPUE of Pacific cod

© 2000 NRC Canada

Fig. 6. Observed abundances (log(CPUE + 1)) of (*a*) Pacific cod, (*b*) walleye pollock, (*c*) flathead sole, and (*d*) arrowtooth flounder in Alitak Bay by sampling year. Boxplots indicate, for each species and year, the median (heavy horizontal bar), lower and upper quartiles (stippled box), and range (dotted "whiskers"). Outliers that are more than 1.5 times the interquartile range above the upper quartile or below the lower quartile are shown as individual light horizontal bars.

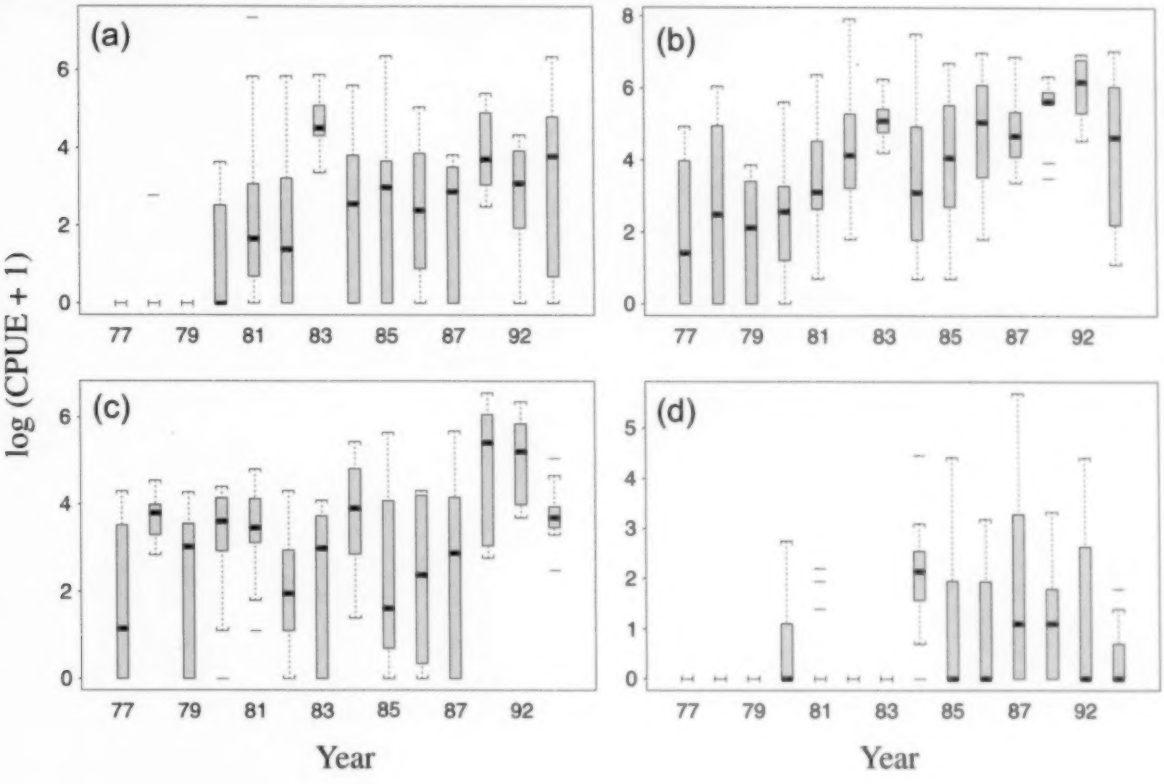

and walleye pollock increased in Alitak Bay from 1980 to 1983, while flathead sole did not increase over the same time period (Fig. 6). Arrowtooth flounder was found in very low abundances in Alitak Bay prior to 1984 and increased strongly between 1984 and 1985. Pacific cod showed a pattern of increasing CPUEs from 1980 to 1985 that was very similar in all areas, including Alitak Bay (Fig. 7). Arrowtooth flounder CPUEs, while increasing in all other areas between 1980 and 1981, did not increase in Alitak Bay until 1984, suggesting that the delayed decline in shrimp and forage fishes in Alitak Bay (Fig. 4) may have been related to the absence of arrowtooth flounder prior to 1984.

Discussion

Nearshore groundfish community around Kodiak Island

Although the patterns of change in our index of species composition (axis 1 scores) differed between Alitak Bay and the other areas, there is likely to be a single underlying cause of the observed shift in species composition because of the wide geographic extent of the changes (Orensanz et al. 1998). Because the observed changes around Kodiak Island were related to the dynamics of two species groups, changes in the relative abundance of these groups within each area provide a means to examine possible cause and effect relationships. Environmental changes may influence both groups simultaneously or lead to changes in one group, which in turn results in changes in the other group. There was little statistical support for a relationship between the trends in species groups A and B at the level of individual bays. There was some evidence that increases in the gadid and flatfish group were followed by decreases in the shrimp and forage fish group (Table 3).

One obvious mechanism that is consistent with this pattern is predation of large piscivorous fish on shrimp and small fish. All species in group B are known predators of shrimp (Yang 1993), and there is anecdotal evidence that Pacific cod in the bays around Kodiak preyed heavily on shrimp during the early 1980s (J.E. Blackburn, Alaska Department of Fish and Game, 211 Mission Rd., Kodiak, AK 99615, U.S.A., personal communication). In other areas in southcentral Alaska, the crash in pink shrimp populations in the 1980s has been attributed to an increase in natural mortality, presumably resulting from predation (Fu et al. 1999). Thus, there is some support for the hypothesis that the decrease in the abundance of shrimp and small forage fishes in the early 1980s was related to and followed an increase in the abundance of large piscivorous flatfish and gadid spe-

© 2000 NRC Canada

Fig. 7. Estimated time trends of CPUE for (*a*) arrowtooth flounder and (*b*) Pacific cod in seven areas sampled around Kodiak Island between 1976 and 1995.

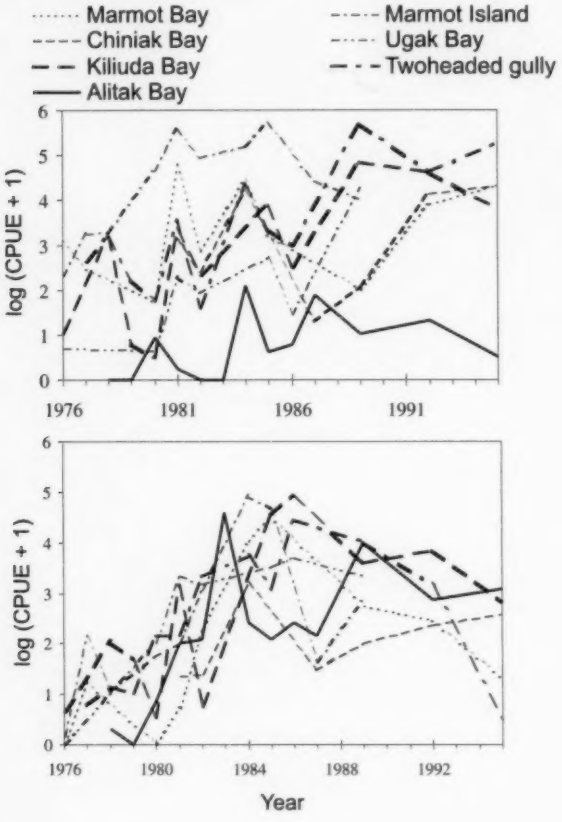

cies. The hypothesis does not address the ultimate factor responsible for the increase in predatory fishes in the nearshore environment during the early 1980s.

If the ultimate cause of the observed changes was overfishing of shrimp, an increase in the piscivorous group would be expected to follow the decline in shrimp. We found no support for this hypothesis (Table 3, lag –1), and overfishing of shrimp cannot explain the fact that small forage fishes declined simultaneously with the shrimp resource. Furthermore, it would be difficult to explain why large piscivorous fishes would replace shrimp and small forage fishes because the two groups occupy very different trophic niches.

Alternatively, overfishing and environmental changes could have acted in concert to cause the observed shift in species composition. The most likely scenario is that heavy fishing contributed to the initial decline in shrimp abundance after the fishery peaked in the early 1970s (Orensanz et al. 1998). Possibly as a result of changes in the physical environment, the abundance of large predatory fishes in nearshore areas increased in the early 1980s, which may have led to the rapid demise of already depressed shrimp populations and to a simultaneous decline in abundance of small forage fish species.

Whatever the ultimate cause of the observed shift in species composition, the patterns of change clearly differed among areas spanning a relatively restricted geographical range (Fig. 2). Therefore, statistical linkages between changes in species composition and large-scale environmental factors will be difficult to establish, as they require the use of aggregate measures of species composition or species abundances. Such measures may be misleading if they average over responses from a number of areas with different trends. When trying to elucidate mechanisms that led to the observed changes, differences among areas may be more important than the average response over a large area. Understanding the marked difference in the timing of the observed shift in community composition between Alitak Bay and the other areas sampled (Fig. 5) may be more helpful in understanding possible causes of the shift than correlations at larger scales.

One obvious physical difference between Alitak Bay and the other areas is the presence of a relatively shallow sill (~40 m) in Alitak Bay, which may affect water mass characteristics and the distribution of demersal fishes. Bottom temperatures in Alitak Bay indicate that low temperatures (<4°C) can persist inside Alitak Bay below 70 m, in contrast with comparable depths in other bays and on the shelf outside Alitak Bay (B.L. Norcross, unpublished data). If warm temperatures contributed to the decline in shrimp and small forage fishes (Piatt and Anderson 1996; Anderson et al. 1997), cold temperatures in the deep waters of inner Alitak Bay may have provided a "cold refuge" for these species for several years.

A different hypothesis, relating to predation, is that the shallow sill isolated shrimp in Alitak Bay from shelf species, reducing predation by cod and other piscivores common on the shelf (J.E. Blackburn, Alaska Department of Fish and Game, 211 Mission Rd., Kodiak, AK 99615, U.S.A., personal communication). However, Pacific cod catches increased in Alitak Bay after 1980, at the same time as in all other areas (Fig. 7). Thus, while the increase in Pacific cod in all areas may have contributed to the decline in shrimp and forage fishes, it cannot explain the delayed decline in Alitak Bay. Unlike Pacific cod, arrowtooth flounder did not show a strong increase in Alitak Bay from 1980 to 1981, although such an increase was observed in all other areas (Fig. 7). The CPUE of group A species remained high in Alitak Bay until 1984, in spite of high abundances of Pacific cod, but collapsed after 1984, simultaneously with a strong increase in arrowtooth flounder CPUE. The biomass of arrowtooth flounder in the Gulf of Alaska greatly increased from the 1970s to the 1990s (North Pacific Fisheries Management Council 1997), particularly in areas of less than 100 m depth (Mueter 1999). In the Gulf of Alaska, shrimp, capelin, and herring, three of the taxa that declined sharply around Kodiak Island in the early 1980s, are important components of arrowtooth flounder diets (Yang 1993). Thus, increases in the abundance of arrowtooth flounder may have contributed to the decline in shrimp and small forage fishes in the nearshore areas around Kodiak Island.

Modeling changes in species composition

The multivariate approach used here allowed us to directly test for differences in species composition over time while taking the effects of other covariates and of the sampling de-

© 2000 NRC Canada

sign into account. The ordination axes provide indicators of species composition and can be used to identify the most important species that contribute to observed changes. Axes scores were suitable for statistical modeling, as they were close to normally distributed after conditioning on relevant independent variables. Therefore, statistical tests based on the normal distribution could be used to test specific hypotheses regarding species composition. Multivariate indices generally are more sensitive to variations in species composition; therefore, trends that may not be obvious otherwise can be detected (Austen and Warwick 1989).

A major concern when using any measure of species composition is whether the measure is sensitive to the level of aggregation in the species abundance data or to the inclusion or elimination of certain species or taxa. Of particular concern is whether the observed differences in species composition are primarily due to one or a few abundant species. When shrimp, the dominant species group in our example, was eliminated from the species abundance matrix, the resulting patterns in the first axis over time were virtually identical to the patterns observed with shrimp included (F.J. Mueter, unpublished data). The same was true when rare species were included in the analysis, suggesting that the index is highly robust to the subjective choices required in selecting species to include.

Another concern with the approach is the subjectivity required in choosing the number of dimensions in which to conduct the ordination. It is doubtful that the true dimensionality of the data can ever be known, i.e., what proportion of the variance in species composition can be attributed to noise. Kruskal's stress (Kruskal 1964) provides an objective criterion for choosing the number of axes; however, the choice of an acceptable level of stress is arbitrary. We have some evidence that the approach is robust to the number of axes. Whether the ordination was conducted in five, six, or seven dimensions had virtually no effect on the first two axes (F.J. Mueter, unpublished data), which might be expected because the first axes typically account for most of the overall variation.

Unlike other ordination techniques, the orientation of axes in NMDS ordination is arbitrary. Therefore, we inserted an additional step in the analysis by rotating the final configuration of the NMDS ordination such that the major axis of variation was chosen as the first axis of species composition. Each further axis was perpendicular to the previous axis and was oriented along the major axis of the remaining variation. As in other indirect ordination techniques, there is no guarantee that the axes are aligned with any of the environmental gradients included in the analysis.

As an alternative to selecting the axis of major variation, the ordination axes may be rotated to maximize the correlation between the first axis and a specific gradient in order to examine species composition along the chosen gradient. Patterns in species composition along this gradient can thus be examined. However, hypothesis tests involving this gradient would be no longer valid, as the index was chosen a priori to maximize variation along the gradient.

Acknowledgments

We thank the field crews that spent countless hours collecting the survey data, Jim Blackburn for making the data available to us, and Ron Barry, Sue Hills, Mark Johnson, Terry Quinn, and Jim Blackburn for thoroughly reviewing the manuscript. Funding for this research was provided by NOAA Saltonstall–Kennedy grant No. 50ABNF700086.

References

Anderson, P.J. 1991. Age, growth, and mortality of the northern shrimp, *Pandalus borealis* Kröyer in Pavlof Bay, Alaska. Fish. Bull. U.S. **89**: 541–553.

Anderson, P.J., Blackburn, J.E., and Johnson, B.A. 1997. Declines of forage species in the Gulf of Alaska, 1972–1995, as an indicator of regime shift. *In* Forage fishes in marine ecosystems. Proceedings of the International Symposium on the Role of Forage Fishes in Marine Ecosystems. Alaska Sea Grant College Program Rep. No. 97-01. University of Alaska Fairbanks, Fairbanks, Alaska. pp. 531–543.

Austen, M.C., and Warwick, R.M. 1989. Comparison of univariate and multivariate aspects of estuarine meiobenthic community structure. Estuarine Coastal Shelf Sci. **29**: 23–32.

Brodeur, R.D., and Ware, D.M. 1992. Long-term variability in zooplankton biomass in the Subarctic Pacific Ocean. Fish. Oceanogr. **1**: 32–38.

Brodeur, R.D., and Ware, D.M. 1995. Interdecadal variability in distribution and catch rates of epipelagic nekton in the Northeast Pacific Ocean. *In* Climate change and northern fish populations *Edited by* R.J. Beamish. Can. Spec. Publ. Fish. Aquat. Sci. No. 121. pp. 329–356.

Diggle, P.J. 1990. Time series: a biostatistical introduction. Oxford University Press, Oxford, U.K.

Faith, D.P., Minchin, P.R., and Belbin, L. 1987. Compositional dissimilarity as a robust measure of ecological distance. Vegetatio, **69**: 57–68.

Field, J.G., Clarke, K.R., and Warwick, R.M. 1982. A practical strategy for analyzing multispecies distribution patterns. Mar. Ecol. Prog. Ser. **8**: 37–52.

Francis, R.C., and Hare, S.R. 1994. Decadal-scale regime shifts in the large marine ecosystem of the Northeast Pacific: a case for historical science. Fish. Oceanogr. **3**: 279–291.

Fu, C., Quinn, T.J., II, and Adkison, M.D. 1999. Retrospective projection using Monte Carlo simulation: an application of a length-based model to Kachemak Bay pink shrimp. *In* Ecosytem approaches for fisheries management. University of Alaska Sea Grant, AK-SG-99-01, Fairbanks, Alaska. pp. 59–77.

Hollowed, A.B., and Wooster, W.S. 1995. Decadal-scale variations in the eastern subarctic Pacific: II. Response of Northeast Pacific fish stocks. *In* Climate change and northern fish populations *Edited by* R.J. Beamish. Can. Spec. Publ. Fish. Aquat. Sci. No. 121. pp. 373–385.

Jackson, D.A. 1997. Compositional data in community ecology: the paradigm or peril of proportions? Ecology, **78**: 929–940.

Kenkel, N.C., and Orloci, L. 1986. Applying metric and nonmetric multidimensional scaling to ecological studies: some new results. Ecology, **67**: 919–928.

Koch, C.F. 1987. Prediction of sample size effects on the measured temporal and geographic distribution patterns of species. Paleobiology, **13**: 100–107.

Kruskal, J.B. 1964. Multidimensional scaling by optimizing goodness of fit to a nonmetric hypothesis. Psychometrika, **29**: 1–27.

McCune, B. 1997. Influence of noisy environmental data on canonical correspondence analysis. Ecology, **78**: 2617–2623.

Minchin, P.R. 1987. An evaluation of the robustness of techniques for ecological ordination. Vegetatio, **69**: 89–107.

© 2000 NRC Canada

Mueter, F.J. 1999. Spatial and temporal patterns in the Gulf of Alaska groundfish community in relation to the environment. Ph.D. Thesis, University of Alaska, Fairbanks, Alaska.

Mueter, F.J., and Norcross, B.L. 1999. Linking community structure of small demersal fishes around Kodiak Island, Alaska, to environmental variables. Mar. Ecol. Prog. Ser. **190**: 37–51.

North Pacific Fisheries Management Council. 1997. Stock assessment and fishery evaluation report for the groundfish resources of the Gulf of Alaska. North Pacific Fisheries Management Council, 605 West 4th Ave., Suite 306, Anchorage, AK 99501, U.S.A.

Orensanz, J.M., Armstrong, J., Armstrong, D., and Hilborn, R. 1998. Crustacean resources are vulnerable to serial depletion — the multifaceted decline of crab and shrimp fisheries in the greater Gulf of Alaska. Rev. Fish Biol. Fish. **8**: 117–176.

Piatt, J.F., and Anderson, P. 1996. Response of common murres to *Exxon Valdez* oil spill and long-term changes in the Gulf of Alaska marine ecosystem. Am. Fish. Soc. Symp. **18**: 720–737.

Royer, T.C. 1989. Upper ocean temperature variability in the northeastern Pacific Ocean: is it an indicator of global warming? J. Geophys. Res. **98**: 4639–4644.

Ter Braak, C.J.F. 1995. Ordination. *In* Data analysis in community and landscape ecology. *Edited by* R.H.G. Jongman, C.J.F. Ter Braak,, and O.F.R. Van Tongeren. Cambridge University Press, Cambridge, U.K. pp. 91–173.

Ter Braak, C.J.F., and Prentice, I.C. 1988. A theory of gradient analysis. Adv. Ecol. Res. **18**: 271–317.

Washington, H.G. 1984. Diversity, biotic and similarity indices. Water Res. **18**: 653–694.

Whittaker, R.H. 1967. Gradient analysis of vegetation. Biol. Rev. **42**: 207–264.

Yang, M. 1993. Food habits of the commercially important groundfishes in the Gulf of Alaska in 1990. NOAA Tech. Memo. NMFS-AFSC-22.

© 2000 NRC Canada

Growth patterns of Labrador Sea Atlantic salmon postsmolts and the temporal scale of recruitment synchrony for North American salmon stocks

Kevin D. Friedland and David G. Reddin

Abstract: We measured postsmolt growth patterns from scales of Atlantic salmon postsmolts captured in the Labrador Sea and adult returns from stocks at the southern end of the range of salmon in North America. Because Labrador Sea postsmolts are believed to represent the juvenile nursery for the entire stock complex, the growth variation for southern stocks may yield insights on the time scale of stock mixing during the postsmolt year. Circuli spacing patterns were extracted from the scales of 1525 salmon for 3 smolt years. For 2 of the 3 years, growth trajectories for fish from the southern stocks intersected the trajectories for Labrador Sea postsmolts after 4–5 circuli pairs. The time that it takes to deposit a circulus during the spring and summer seasons suggests that distribution patterns for regional groups begin to overlap or stocks begin to experience similar environmental conditions by June or July of the postsmolt year, or 1 to 2 months after their migration to sea. In some years, however, it would appear that this mixing does not occur until fall. These data provide the first indication of the time scale of events during the postsmolt year that regional influences may be acting on stocks to produce synchronous recruitment.

Résumé : Nous avons mesuré les profils de croissance après la smoltification à partir d'écailles de post-smolts de saumon atlantique capturés en mer du Labrador et d'adultes en remonte provenant de stocks de l'extrémité méridionale de l'aire de répartition du saumon en Amérique du Nord. Comme les post-smolts de la mer du Labrador semblent représenter le groupe de juvéniles pour l'ensemble du complexe de stocks, la variation de la croissance des stocks méridionaux permettrait de comprendre l'échelle chronologique du mélange des stocks pendant l'année post-smoltification. Les profils d'espacement des anneaux de croissance ont été établis à partir des écailles de 1 525 saumons prélevés sur une période de trois ans. Dans le cas de deux des trois années, les trajectoires de croissance des poissons des stocks méridionaux coupaient les trajectoires des post-smolts de la mer du Labrador après 4–5 paires d'anneaux. D'après le temps nécessaire à la formation d'un anneau de croissance au printemps et en été, il semble que les profils de distribution des groupes régionaux commencent à se chevaucher ou que les stocks commencent à connaître des conditions environnementales similaires dès le mois de juin ou de juillet de l'année post-smoltification, ou un à deux mois après leur migration en mer. Certaines années, cependant, il semblerait que ce mélange ne se produise pas avant l'automne. Ces données sont la première indication de l'échelle temporelle des phénomènes pendant l'année post-smoltification et du fait que les influences régionales peuvent agir sur les stocks pour donner un recrutement synchrone.

[Traduit par la Rédaction]

Introduction

Recruitment synchrony is being described on both regional and continental scales for Atlantic salmon. Regional synchrony has been described with data for both wild and hatchery stocks (Crozier and Kennedy 1993; Friedland et al. 1998*a*, 1993). In these examples, tagged stocks show similar patterns of survival rate by cohort suggesting that survival during the postsmolt year defines recruitment to spawning. Continental and subcontinental synchrony can be seen in long-term catch data for both North American and European stocks (Friedland et al. 1993). Furthermore, synchrony between the continental stock complexes is evident in these catch time series (Friedland 1998). The linkage between recruitment synchrony of Pacific salmon and regime shifts of North Pacific climate and primary production provides a framework to describe and predict recruitment processes for these populations (Mantua et al. 1997; Hare et al. 1999). However, the relationship between Atlantic salmon populations and climate is not completely understood and there are few analyses of the relationship between primary production and the recruitment process (Friedland 1998).

When synchrony is observed for populations, it is logical to examine the biological and physical factors that act on populations as they overlap in time and space or, if their distributions do not overlap, those factors of sufficient spatial scale, such as climate variability, that can simultaneously affect them in various locations. Which of these two possibilities exists for Atlantic salmon is an important question that may be addressed in part by determining the time, during the postsmolt year, that stocks aggregate or begin to experience similar growth conditions. Recruitment variability is attrib-

Received September 28, 1999. Accepted March 21, 2000. J15378

K. Friedland.[1] UMass/NOAA CMER Program, Blaisdell House, University of Massachusetts, Amherst, MA 01003, U.S.A.
D. Reddin. Science Branch, Department of Fisheries and Oceans, P.O. Box 5667, St. John's, NF A1C 5X1, Canada.

[1]Author to whom all correspondence should be addressed. e-mail: friedlandk@forwild.umass.edu

© 2000 NRC Canada

Fig. 1. Map of the Northwest Atlantic showing the area of research fishing for postsmolts (solid line), sub-area where postsmolts were encountered (broken line), and location of stocks used in postsmolt growth comparisons.

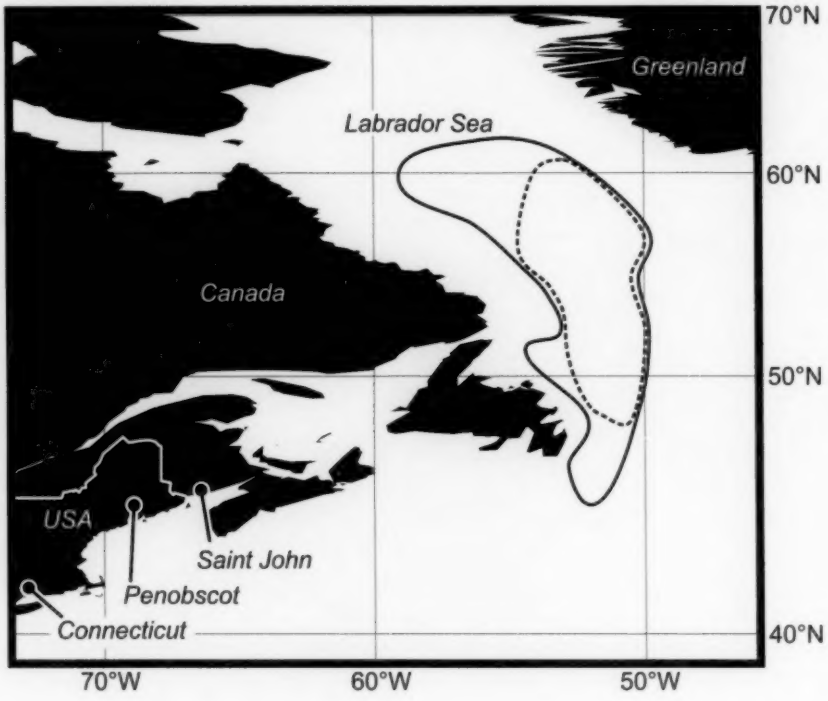

uted to mortality that stocks experience during their first year at sea. Most of this mortality is thought to occur a short time after smolts enter the ocean. This hypothesis is supported by mortality rate estimates with tagging experiments in the Baltic region (Eriksson 1994) and indirectly by relationships between regional spring climate conditions and survival (Salminen et al. 1995; Friedland et al. 1998*a*). However, if survival is defined during this early segment of the postsmolt year, it occurs when stocks are not likely to overlap spatially because of the wide geographic range of smolt production. Therefore, synchrony in recruitment related to mortality would most likely result from regional scale phenomena that occur while the fish are not aggregated. On the other hand, life history events such as maturation, which act on stocks later in the postsmolt year, may affect recruitment patterns independently of mortality (Martin and Mitchell 1985; Friedland et al. 1998*b*). Because these phenomena will be evaluated by patterns of returns, it is important to keep both of these life history events in mind during hypothesis evaluation.

Tagging studies from many North American salmon stocks (Ruggles and Ritter 1980; Caron 1983; Meister 1984; Ritter 1989) as well as directed research fishing for salmon in the Gulf of St. Lawrence (Dutil and Coutu 1988), near and on the Grand Banks of Newfoundland (Lear 1976; Reddin 1985), and in the Labrador Sea (Reddin and Short 1991) indicate that most of the North American salmon stock complex moves northward into the Labrador Sea to overwinter. The only exception is salmon stocks from inner Bay of Fundy rivers (Ritter 1989). Although the generalized movement into the Labrador Sea is well known and accepted, the timing of arrival is not, although it seems to occur any time from late summer into the fall.

In this study, we applied scale circuli spacing and aging analyses to attempt to differentiate the temporal scales of regional versus continental recruitment synchrony. We compared scale growth patterns from a mixed stock group of postsmolt salmon captured in the Labrador Sea to the patterns from a group of hatchery stocks from the southern end of the range of salmon in North America. Our objective was to interpret the growth patterns as to what they suggest about the temporal and spatial overlap of the stocks and then consider how they might relate to the stock complex as a whole.

Materials and methods

We collected scale circuli spacing patterns, representative of postsmolt growth, for postsmolt salmon captured in the Labrador Sea and for adult returns to three rivers from the southern end of the range of salmon in North America. The postsmolts were collected in a directed research survey in the Labrador Sea during 1988, 1989, and 1991 (Reddin and Short 1991). These fish were captured using gill nets over a series of stations distributed over much of the Labrador Sea during the fall of the year, with most of the captures occurring during the month of October (Fig. 1). Data from the returning adults of hatchery origin stocks in the Connecticut, Penobscot, and Saint John rivers, all located south of the Gulf of St. Lawrence, were collected to compare with the postsmolt data (Fig. 1). Sample sizes sorted by smolt year of migration to sea and age of maturity are reported in Table 1. There were insufficient numbers of one sea winter (1SW) Connecticut River samples to analyze.

© 2000 NRC Canada

Table 1. Sample sizes for scale analysis organized by stock, age, and smolt year.

Stock	Age	Smolt year		
		1988	1989	1991
Connecticut	2SW	170	121	178
Penobscot	1SW	70	105	89
	2SW	64	83	79
Saint John	1SW	73	95	90
	2SW	52	78	78
Labrador Sea	Postsmolt	32	35	33

Postsmolt growth intensity and timing was interpreted from circuli spacing patterns. Scales were cleaned and mounted between glass slides and the spacing of scale circuli was measured with an Optimas® image-processing system (reference to tradename does not suggest endorsement). The first spacing was measured between the first circulus of the postsmolt growth zone and the next circulus and continued with successive pairs. Measurements were made on a single scale from each specimen at a pixel resolution of 0.004 mm along the 360° axis of the scale. For fish captured as postsmolts, measurements were taken to the edge of the scale (Fig. 2A). For maturing fish returning to the southern rivers, the measurements were made through the first sea winter annulus of the scale and thus captured the entire postsmolt growth zone (Fig. 2B). Only the measurements from the postsmolt portion of the scale were used in the analysis. Additionally, the river age distributions for Labrador Sea postsmolt specimens were determined using conventional aging techniques (Shearer 1992).

Return rates by sea age and fraction of the smolt cohort that matured after one sea winter were computed for the three southern stocks. Return rates are simple percentages of the number of returns-at-age to the number of smolts released either 1 or 2 years prior. Return rates for the Connecticut and Penobscot stocks, originally reported in Friedland et al. (1996), are updated here. Return rates for the Saint John stock are newly reported here.

The fraction of the smolt cohort that matured after one sea winter, the 1SW fraction, was computed using the methods of Friedland et al. (1996). The fraction of a cohort or smolt year class that matured after only a single winter at sea was derived using counts of adult returns by sea age and the fishing mortality that impacted the cohort. Fish from the Penobscot, Connecticut, and Saint John rivers were exploited in marine fisheries in Canada and Greenland during the study period. To account for this, we applied annual instantaneous fishing mortality rates (Friedland et al. 1996) for North American stock components maturing as 2SW salmon (Table 2). The observed return of 1SW salmon to freshwater (R_1) is the product of the 1SW fraction (ψ) and the size of the cohort immediately before the 1SW fish return to homewaters and 1SW fisheries commenced (N_0). Because we are modeling the cohort split immediately before the 1SW runs occur, natural mortality for this fraction of the cohort (M_1) is zero.

$$(1) \qquad R_1 = N_0 \cdot \psi \cdot \exp^{-M_1}$$

The observed return of 2SW salmon (R_2) is assumed to be the remainder of the cohort that did not mature as 1SW fish and survived for an additional 10 months at sea plus the mortality associated with fishing ($M_2 = 0.1$, Friedland et al. 1996). The additional time that 2SW salmon stay at sea is assumed to be 10 months, compared with 1 year, because 2SW salmon usually return to the river earlier in the year than 1SW fish.

$$(2) \qquad R_2 = N_0 \cdot (1 - \psi) \cdot \exp^{-(M_2 + F)}$$

Both equations contain N_0 and thus can be simplified to the expression

Fig. 2. Atlantic salmon scales from (A) postsmolt salmon and (B) 1SW salmon, illustrating the locations of the postsmolt growth zones characterized with image processing. The figures are not in scale with each other.

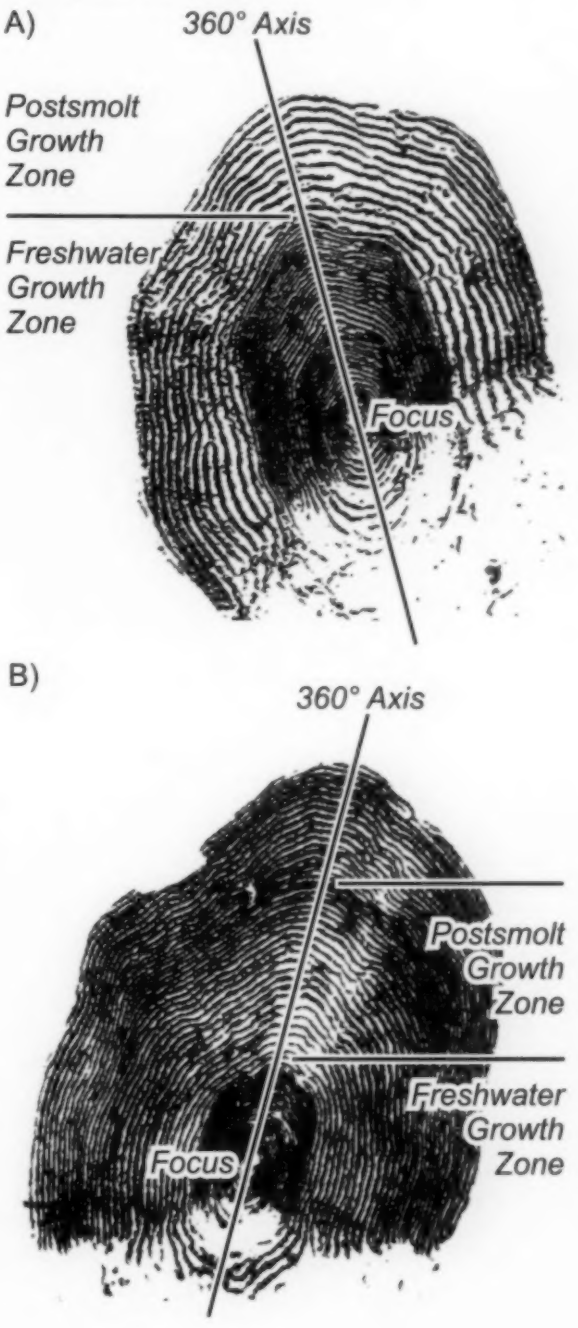

$$(3) \qquad \psi = \frac{\Phi}{(\Phi + 1)}$$

where

© 2000 NRC Canada

Table 2. Return rate data and 1SW fraction (ψ) analysis for Connecticut (Conn), Penobscot (Pen), and Saint John (SJ) stocks.

	Smolt release			1SW return rate			2SW return rate				ISW fraction (ψ)		
Smolt year	Conn	Pen	SJ	Conn	Pen	SJ	Conn	Pen	SJ	Fishing Mortality	Conn	Pen	SJ
1974		100 200	337 281		0.045	1.890		0.562	0.683	0.55		0.04	0.59
1975		110 600	324 186		0.068	2.799		0.525	0.841	0.34		0.08	0.68
1976		234 800	297 350		0.019	2.351		0.659	0.852	0.54		0.01	0.59
1977	96 400	338 500	293 132	0.003	0.036	1.038	0.052	0.198	0.405	0.59	0.03	0.08	0.56
1978	32 100	202 500	196 196	0.012	0.100	1.951	0.511	1.269	1.525	0.41	0.01	0.05	0.44
1979	124 900	296 300	244 012	0.003	0.220	4.423	0.411	0.828	1.118	0.50	0.00	0.13	0.68
1980	51 800	584 600	232 258	0.012	0.152	2.423	0.110	0.665	0.762	0.65	0.05	0.10	0.60
1981	78 600	199 500	189 090	0.004	0.078	1.607	0.050	0.353	0.584	0.66	0.03	0.09	0.56
1982	209 900	329 700	172 231	0.000	0.054	0.908	0.031	0.421	0.647	0.26	0.00	0.08	0.49
1983	98 000	436 700	144 549	0.007	0.055	1.004	0.299	0.657	0.605	0.24	0.02	0.06	0.54
1984	312 300	617 100	206 462	0.000	0.040	0.977	0.088	0.587	0.386	0.47	0.00	0.04	0.59
1985	255 000	580 900	89 051	0.000	0.092	0.968	0.135	0.254	0.539	0.56	0.00	0.16	0.48
1986	276 100	589 200	191 495	0.000	0.127	1.738	0.034	0.338	0.363	0.69	0.00	0.15	0.69
1987	205 800	539 200	113 439	0.000	0.133	0.700	0.028	0.372	0.352	0.55	0.01	0.16	0.51
1988	395 300	687 000	142 195	0.000	0.126	0.807	0.057	0.367	0.355	0.39	0.00	0.17	0.58
1989	217 700	416 600	238 204	0.000	0.103	0.411	0.077	0.260	0.196	0.47	0.00	0.18	0.54
1990	475 900	429 100	241 078	0.000	0.041	0.714	0.074	0.274	0.264	0.58	0.00	0.07	0.58
1991	351 000	672 800	178 127	0.001	0.139	0.735	0.039	0.190	0.125	0.32	0.01	0.32	0.79
1992	313 300	824 700	204 836	0.000	0.042	0.406	0.084	0.076	0.228	0.02	0.00	0.33	0.61
Mean				0.003	0.088	1.466	0.130	0.466	0.570		0.01	0.12	0.59

Note: Return rates are in percent where 1SW fraction is the proportion of a cohort maturing after one sea winter. Fishing mortality is instantaneous annual F for ocean fisheries harvesting the subject stocks.

Table 3. Results of age analysis for postsmolts collected in the Labrador Sea showing number aged and the percent contribution to the sample by smolt year.

	River age											
	1		2		3		4		5+			
Smolt year	Number	%	Number	%	Number	%	Number	%	Number	%	Total Number	
1988	11	6.0	36	19.8	83	45.6	40	22.0	12	6.6	182	
1989	18	8.7	72	34.6	69	33.2	30	14.4	19	9.1	208	
1991	8	9.0	37	41.6	26	29.2	15	16.9	3	3.4	89	

$$(4) \qquad \Phi = \frac{R_1 \cdot \exp^{-(M_2+F)}}{R_2 \cdot \exp^{-M_1}}$$

This formulation assumes that all individuals mature as either 1SW or 2SW fish. This is reasonable in that returns of 3SW and older fish were insignificant during the study period (typically less than 1% of the total runs). Like the return rate data, this information is updated for the Connecticut and Penobscot stocks and newly reported for the Saint John stock.

The circuli spacing data for the postsmolts were compared among years and with the data for the three southern stocks. The comparisons were done with analysis of variance (ANOVA) and were limited to the data for the first 15 circuli pairs. This restriction was put in place because most scales from the postsmolts did not have data for the higher number circuli pairs. The first comparisons were three group ANOVAs that compared the yearly differences in the postsmolt data only. For the second set of statistics, postsmolt circuli spacing patterns were compared with the data for the three comparison stocks. The tests were simplified to two group ANOVAs comparing circuli spacing of the postsmolts to each smolt year–age combination of the comparison stocks. Results of the ANOVA analyses are presented graphically in the circuli spacing figures, where significant tests ($p = 0.05$) are indicated with bold error bars.

Results

Circuli spacing patterns for the postsmolt growth zones of Labrador Sea postsmolts were similar for the 3 year-classes we examined. These fish ranged in river ages from 1 to 7 years, with over 80% of the fish falling into ages 2 to 4 years (Table 3). Most of these fish were of wild origin because only the river age-1 fish would be expected to come from hatcheries in either Canada or the United States. The mode river age was either 2 or 3 years. Circuli spacing for the first few pairs, associated with the first few weeks in the marine environment, were similar in all 3 years, measuring approximately 0.029 to 0.048 mm (Fig. 3). Beyond these initial pairs, the spacings were nearly the same except for some minor differences around circuli pair 9. Spacings during the summer growth period ranged from approximately 0.055 to 0.077 mm. ANOVA results indicated that the yearly spacing means were not significantly different for any of the first 15 spacing pairs.

Circuli spacing patterns for Labrador Sea postsmolts were markedly different from the patterns observed for the three comparison stocks. We found that the postsmolt specimens had narrower circuli spacings for the early marine period,

© 2000 NRC Canada

Fig. 3. Circuli spacing versus circuli pair for Labrador Sea postsmolts from 3 smolt years: 1988(□), 1989(○), and 1991(◇). Error bars show 95% confidence intervals.

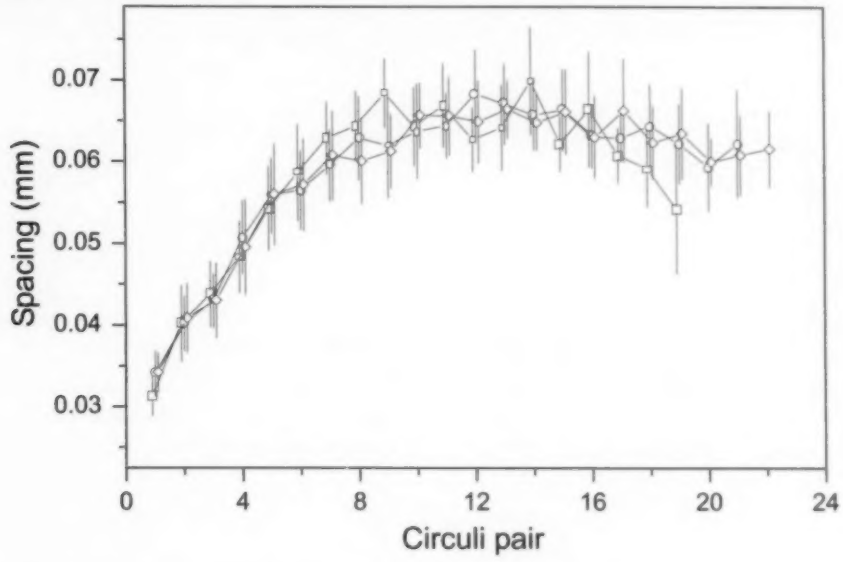

represented by the first 6 or so circuli pairs. However, circuli spacings for the balance of the postsmolt period, limited to first 15 circuli pairs, were similar. For Connecticut River 2SW returns, postsmolt growth trajectories do not intersect the trajectories for the Labrador Sea postsmolts until 5 to 7 circuli are laid down (Fig. 4). The results of ANOVA show that there are significant differences between these pairs and an inconsistent pattern of differences between the stocks on comparison of the higher circuli pairs from year to year. In particular, the higher circuli spacings from Connecticut River salmon appear to be narrower than those from the postsmolts in the years 1988 and 1991 (Figs. 4A and 4C).

Circuli spacings for Penobscot fish were also wider in the beginning of the postsmolt year, but fewer of the early spacing pairs were significantly different for this stock (Fig. 5). The statistical comparison shows that for 1988 and 1989, 1SW and 2SW Penobscot spacings are different from the postsmolt spacings for either the first 4 or 5 spacing pairs. In 1991, differences exist for the first 10 and 8 pairs for 1SW and 2SW fish, respectively. Only pairs 13 to 15 for Penobscot 2SW fish are significantly narrower than postsmolt spacings.

Overall growth patterns for the Saint John returns related to the postsmolt patterns in much the same way as the Penobscot data with only a few exceptions (Fig. 6). One of the more interesting contrasts was the number of early season circuli pairs at variance to the postsmolt data. For the Saint John 2SW returns, the spacings for the first 3 and 4 pairs were significantly different from postsmolt spacings during 1988 and 1989, respectively, which is slightly less than for the Penobscot fish (Fig. 6). In 1991, growth patterns for the Saint John fish did not intersect the postsmolt data until about the 12th pair for both 1SW and 2SW salmon.

The three stocks provided for comparison to Labrador Sea postsmolts displayed a range of return rates and 1SW fractions reflecting differences in stock characteristics. For the Connecticut stock, return rate of 2SW fish and 1SW fraction averaged 0.13% and 0.01%, respectively (Table 2). Penobscot River smolts returned at higher rates, 0.09% and 0.47% for 1SW and 2SW fish, respectively. Typically, 12% of the Penobscot cohort matures at one sea winter. The Saint John stock had the highest return rates with the largest proportion of the cohort maturing after one sea winter. The return rate for 1SW fish averaged 1.47% and the 1SW fraction averaged 0.59. The 2SW return rate for the Saint John stock was slightly higher than that observed for the Penobscot stock. In summary, the Connecticut stock had the lowest survival and produced few early-maturing fish, the Saint John had the highest survival and produced many early-maturing fish, and the Penobscot stock was intermediate between the other two.

Discussion

Our principal finding from the circuli spacing data was that continental-scale recruitment synchrony most likely occurs after the period of time smolts are in the ocean associated with the deposition of four to eight circuli pairs. The samples of postsmolts from the Labrador Sea had an age composition typical of a cross section of North American salmon stocks (Power 1981; Saunders 1981). Additionally, this mixed-stock group of fish was destined to spawn the following year as 2SW salmon, as indicated by the time and location of capture (Reddin and Short 1991). The 2SW returns to the Penobscot and Saint John stocks intersect and generally overlap the composite trajectory for the mixed-stock group after approximately four circuli pair. The more southerly stock, the 2SW Connecticut fish, appeared to have a greater delay before mixing with other stocks, as suggested by the higher number of circuli pairs deposited before the growth trajectories overlap.

The period of time that it takes to deposit a circulus changes with season. Recaptures of postsmolts used in this

© 2000 NRC Canada

Fig. 4. Circuli spacing versus circuli pair for Connecticut River 2SW returns (▽) and Labrador Sea postsmolts (●) from 3 smolt years: (A) 1988, (B) 1989, and (C) 1991. Error bars show 95% confidence intervals, bold error bars indicate significant ANOVAs (p = 0.05) between Connecticut fish and postsmolts.

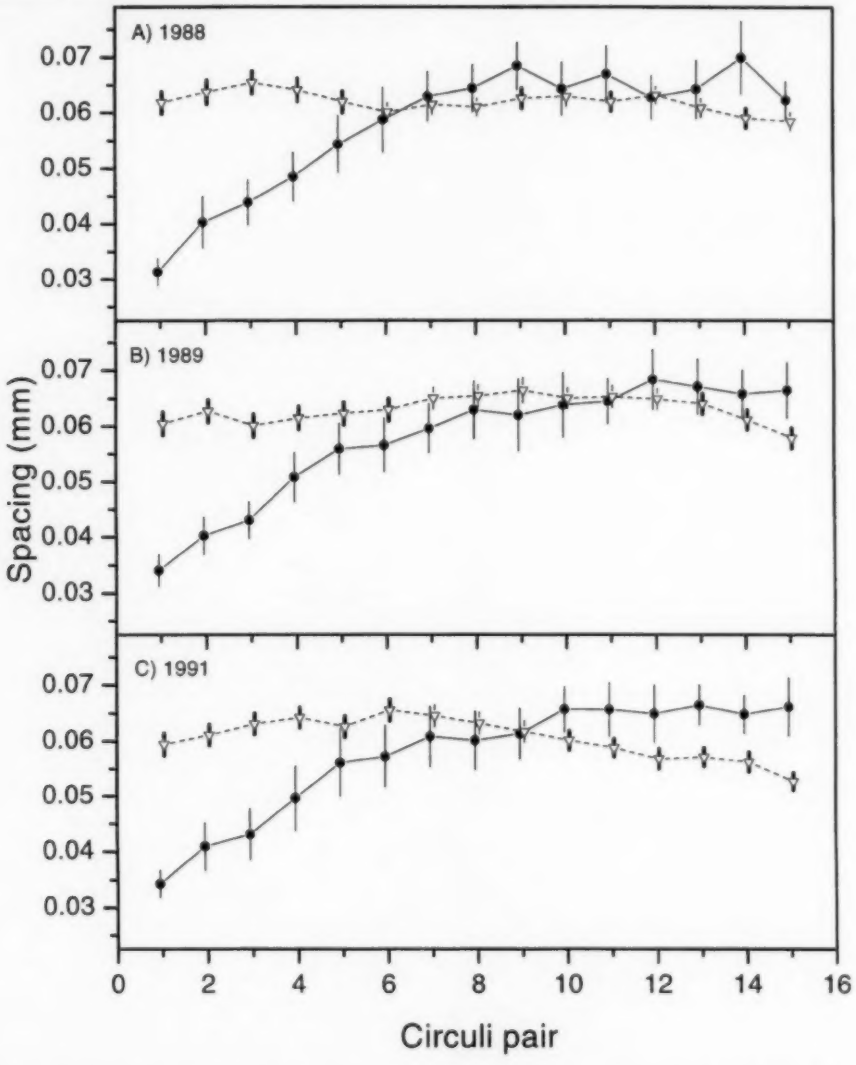

study were analyzed to estimate the average date of deposition for specific circuli (Friedland et al. 1993). These data suggest that circuli deposition is spaced by nearly a week during the spring and summer growth seasons and progressively slows to nearly 2 weeks by winter. This would suggest that Penobscot and Saint John fish do not overlap with other stocks in the North American stock complex for at least as 1 month after their seaward migration in some years; however, this period of regional isolation may last longer.

The higher growth rate of southern stocks during the critical early period of marine residency may confer a survival advantage that counteracts the survival disadvantages with which they must contend, stating their migrations at the end of the range. Size-mediated predation interactions are likely to be a critical factor for Atlantic salmon postsmolts during the first months at sea (Holtby et al. 1990; L'Abée-Lund et al. 1993). Although these fish may be growing faster than their counterparts from more northern locations, they are also potentially overlapping more diverse fields of predator species entering the Gulf of Maine and the Scotian Shelf during the spring season (Murawski 1993). Additionally, these fish must migrate greater distances to reach the common feeding and overwintering areas associated with the Labrador Sea and Grand Banks.

These data allow us to suggest a frame of reference for the temporal and spatial scales of regional synchrony of North American salmon stocks. Regional effects would be expected to dominate an individual salmon stock for at least the first month at sea. The temporal scale of regional synchrony also implies limits for the spatial scale of regional synchrony. Postsmolt salmon are, in part, passively transported during their first months at sea (Jonsson et al. 1993);

© 2000 NRC Canada

Fig. 5. Circuli spacing versus circuli pair for Penobscot River 1SW (△) and 2SW (▽) returns and Labrador Sea postsmolts (●) from 3 smolt years: (A) 1988, (B) 1989, and (C) 1991. Error bars show 95% confidence intervals, bold error bars indicate significant ANOVAs ($p = 0.05$) between Penobscot fish and postsmolts.

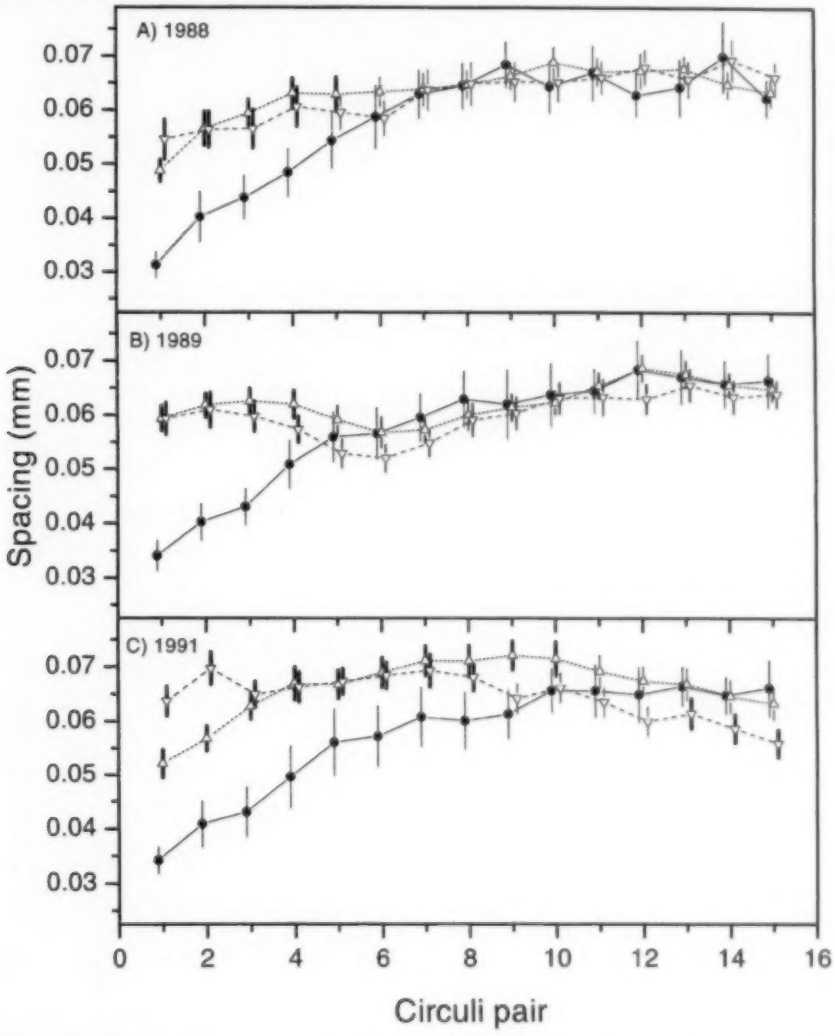

thus, a combination of swimming potential and current transport vectors will circumscribe an area relevant to a specific stock. After a few months at sea, postsmolts attain sufficient size to out-swim currents and will distribute according to other behaviors such as foraging and open-ocean migration. Thus, regional scale synchrony is likely limited to hundreds of kilometres in Atlantic salmon.

This prediction is consistent with preliminary observations for North American Atlantic salmon stocks and analyses of Pacific salmon species. A preliminary analysis of regional return data for salmon throughout Atlantic Canada shows that at least three major groups of stocks can be identified (DFO 1998). This analysis is consistent with the suggestion of a spatial scale of regional synchrony on the order of hundreds of kilometres. Regional synchrony for Pacific salmonids in the Northeast Pacific has been divided into three regional groups and is believed to be the result of ocean climate forcing (Coronado and Hilborn 1998; Peterman et al. 1998). These analyses would also suggest a scale of regional recruitment synchrony on the order of hundreds of kilometres. Taking a different approach, Myers et al. (1997) considered the problem across functional groups of fishes and produced a statistical fit suggesting that the spatial scales for freshwater and marine species are 50 and 500 km, respectively, which brackets the spatial scale for anadromous species. However, there is a final point to consider. Stock groups of Pacific salmon, showing regional synchrony, are in negative phase to neighboring groups and appear to respond to the same climate signals. Thus, the overall system distance for synchronous behavior is more on the order of thousands of kilometres for these species.

It would appear that climate dependencies described for Pacific salmon are consistent with spatial scales of hundreds to thousands of kilometres, whereas empirical observations

© 2000 NRC Canada

Fig. 6. Circuli spacing versus circuli pair for Saint John River 1SW (△) and 2SW (▽) returns and Labrador Sea postsmolts (●) from 3 smolt years: (A) 1988, (B) 1989, and (C) 1991. Error bars show 95% confidence intervals, bold error bars indicate significant ANOVAs ($p = 0.05$) between Saint John fish and postsmolts.

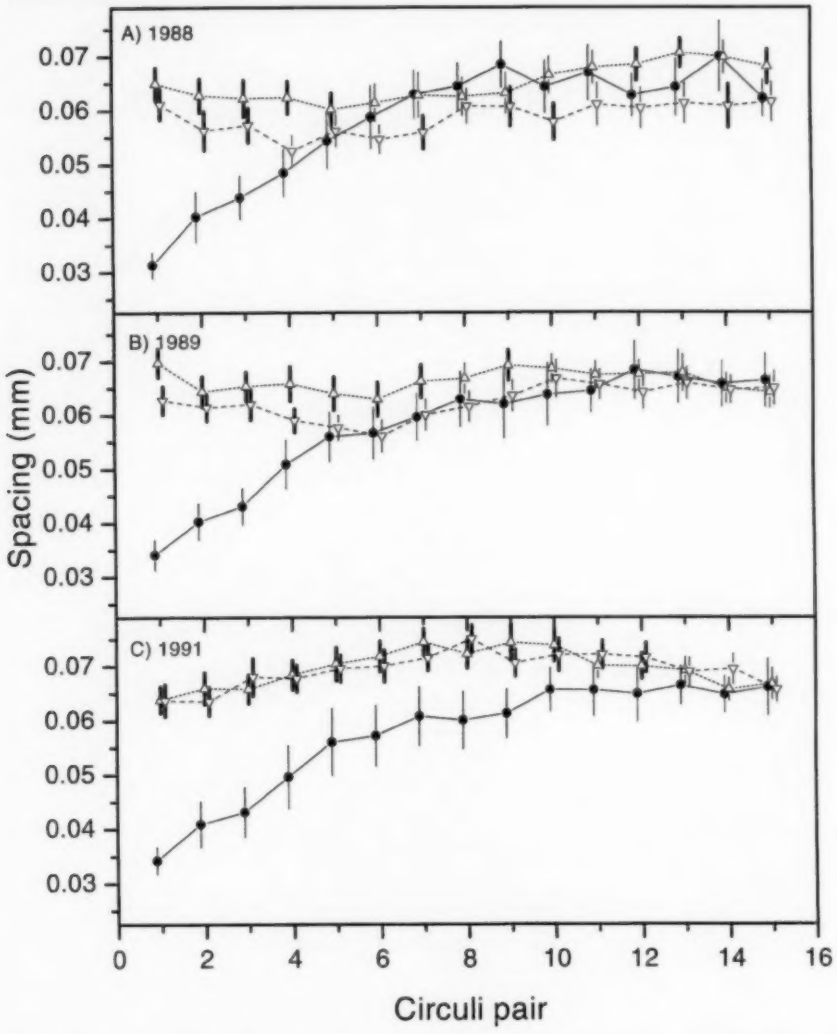

for Atlantic salmon in North America suggest slightly lesser distances. No single hypothesis has emerged concerning postsmolt survival of Atlantic salmon over its entire range. Relationships between climate forcing and recruitment have been described for European stocks (Friedland 1998), thus suggesting the potential for spatial scales of synchrony on the same order as those observed for Pacific salmon. However, the same climate relationships have not been observed for North American fish. Instead, it has been suggested that the postsmolt nursery for North American salmon varies annually and is often inshore, which supports the notion of smaller scale regional synchrony affecting these stock groups (Friedland et al. 1999). Interestingly, these same ideas on postsmolt nurseries are also being applied to Pacific salmon populations (Macdonald and Change 1993; Fukuwaka and Suzuki 1998).

Regional scale synchrony patterns should be taken into account when considering models and analyses that attempt to explain survival mechanisms mediated by climate factors. The spatial scale of any survival forcing function should be designed to match the likely spatial scale of the stock group being analyzed and take into account emerging ideas on postsmolt nursery complexity. Thus, broad-scale ocean climate indicators may be insufficient to characterize the physical–biological factors affecting a year-class of salmon postsmolts in some cases.

These and other questions concerning regional stock dynamics could be more effectively addressed with the analysis of circuli spacing patterns for other stocks, especially wild-origin fish, which may have different growth responses than those represented by the hatchery strains used in this study. We hope our study provides the impetus for additional work of this type and that it may lead to the development of a database of growth data, which could be of interest to the

© 2000 NRC Canada

community of scientists working on recruitment problems with salmon and other species.

Acknowledgments

We thank Dr. L. Marshall, Department of Fisheries and Oceans, Halifax, for providing scale samples from the Mactaquac Hatchery and return rate data. We also thank Dr. J. Carscadden for reviewing an earlier draft of the manuscript.

References

Caron, F. 1983. Migration toward the Atlantic of post-smolt (*Salmo salar*) from the Gulf of St. Lawrence. Nat. Can. **110**: 223–227. (In French.)

Coronado, C., and Hilborn, R. 1998. Spatial and temporal factors affecting survival in coho salmon (*Oncorhynchus kisutch*) in the Pacific Northwest. Can. J. Fish. Aquat. Sci. **55**: 2067–2077.

Crozier, W.W., and Kennedy, G.J.A. 1993. Marine survival of wild and hatchery-reared Atlantic salmon (*Salmo salar* L.) from the River Bush, Northern Ireland. *In* Salmon in the sea. *Edited by* D. Mills. Fishing News Books, London. pp. 139–162.

DFO (Department of Fisheries and Oceans). 1998. DFO Science Stock Status Report Atlantic Salmon Abundance Overview for 1997. Department of Fisheries and Oceans Report DO-02, Ottawa, Canada.

Dutil, J.-D., and Coutu, J.-M. 1988. Early marine life of Atlantic salmon, *Salmo salar*, postsmolts in the northern Gulf of St. Lawrence. Fish. Bull. **86**: 197–212.

Eriksson, T. 1994. Mortality risks of Baltic salmon during downstream migration and early sea-phase: effects of body size and season. Nord. J. Freshw. Res. **69**: 100.

Friedland, K.D. 1998. Ocean climate influences on critical Atlantic salmon (*Salmo salar*) life history events. Can. J. Fish. Aquat. Sci. **55**(Suppl. 1): 119–130.

Friedland, K.D., Reddin, D.G., and Kocik, J.F. 1993. Marine survival of North American and European Atlantic salmon: effects of growth and environment. ICES J. Mar. Sci. **50**: 481–492.

Friedland, K.D., Haas, R.E., and Sheehan, T.F. 1996. Post-smolt growth, maturation, and survival of two stocks of Atlantic salmon. Fish. Bull. **94**: 654–663.

Friedland, K.D., Hansen, L.P., and Dunkley, D.A. 1998*a*. Marine temperatures experienced by post-smolts and the survival of Atlantic Salmon (*Salmo salar* L.) in the North Sea area. Fish. Oceanogr. **7**: 22–34.

Friedland, K.D., Reddin, D.G., Shimizu, N., Haas, R.E., and Youngson, A.F. 1998*b*. Strontium:calcium ratios in Atlantic salmon (*Salmo salar*) otoliths and observations on growth and maturation. Can. J. Fish. Aquat. Sci. **55**: 1158–1168.

Friedland, K.D., Dutil, J.-D., and Sadusky, T. 1999. Growth patterns in postsmolts and the nature of the marine juvenile nursery for Atlantic salmon, *Salmo salar*. Fish. Bull. **97**: 472–481.

Fukuwaka, M., and Suzuki, T. 1998. Role of a riverine plume as a nursery area for chum salmon *Oncorhynchus keta*. Mar. Ecol. Prog. Ser. **173**: 289–297.

Hare, S.R., Mantua, N.J., and Francis, R.C. 1999. Inverse production regimes: Alaska and west coast Pacific salmon. Fisheries, **24**: 6–14.

Holtby, L.B., Andersen, B.C., and Kadowaki, R.K. 1990. Importance of smolt size and early ocean growth to interannual variability in marine survival of coho salmon (*Oncorhynchus kisutch*). Can. J. Fish. Aquat. Sci. **47**: 2181–2194.

Jonsson, N., Hansen, L.P., and Jonsson, B. 1993. Migratory behavior and growth of hatchery-reared post-smolt Atlantic salmon *Salmo salar*. J. Fish Biol. **42**: 435–443.

L'Abée-Lund, J.H., Langeland, A., Jonsson, B., and Ugedal, O. 1993. Spatial segregation by age and size in Arctic charr: a trade-off between feeding possibility and risk of predation. J. Anim. Ecol. **62**: 160–168.

Lear, W.H. 1976. Migrating Atlantic salmon (*Salmo salar*) caught by otter trawl on the Newfoundland continental shelf. J. Fish. Res. Board Can. **33**: 1202–1205.

Macdonald, J.S., and Change, B.D. 1993. Seasonal use by fish of nearshore areas in an urbanized coastal inlet in southern British Columbia. Northwest Sci. **67**: 63–77.

Mantua, N.J., Hare, S.R., Zhang, Y., Wallace, J.M., and Francis, R.C. 1997. A Pacific interdecdal climate oscillation with impacts on salmon production. Bull. Am. Meteor. Soc. **78**: 1069–1079.

Martin, J.H.A., and Mitchell, K.A. 1985. Influence of sea temperature upon the numbers of grilse and multi-sea winter Atlantic salmon (*Salmo salar*) caught in the vicinity of the River Dee (Aberdeenshire). Can. J. Fish. Aquat. Sci. **42**: 1513–1521.

Meister, A.L. 1984. The marine migrations of tagged Atlantic salmon (*Salmo salar* L.) of U.S.A. origin. ICES CM 1984/M: 27.

Murawski, S.A. 1993. Climate-change and marine fish distributions — forecasting from historical analogy. Trans. Am. Fish. Soc. **122**: 647–658

Myers, R.A., Mertz, G., and Bridson, J. 1997. Spatial scales of interannual recruitment variations of marine, anadromous, and freshwater fish. Can. J. Fish. Aquat. Sci. **54**: 1400–1407.

Peterman, R.M., Pyper, B.J., Lapointe, M.F., Adkison, M.D., and Walters, C.J. 1998. Patterns of covariation in survival rates of British Columbian and Alaskan sockeye salmon (*Oncorhynchus nerka*) stocks. Can. J. Fish. Aquat. Sci. **55**: 2503–2517.

Power, G. 1981. Stock characteristics and catches of Atlantic salmon, *Salmo salar*, in Quebec and Newfoundland and Labrador in relation to environmental variables. Can. J. Fish. Aquat. Sci. **38**: 1601–1611.

Reddin, D.G. 1985. Atlantic salmon (*Salmo salar*) on and east of the Grand Bank. J. Northwest Atl. Fish. Sci. **6**: 157–164.

Reddin, D.G., and Short, P.B. 1991. Postsmolt Atlantic salmon (*Salmo salar*) in the Labrador Sea. Can. J. Fish. Aquat. Sci. **48**: 2–6.

Ritter, J.A. 1989. Marine migration and natural mortality of North American Atlantic salmon (*Salmo salar* L.). Can. Manuscr. Rep. Fish. Aquat. Sci. No. 2041.

Ruggles, C.P., and Ritter, J.A. 1980. Review of North American smolt tagging to assess the Atlantic salmon fishery off West Greenland. *In* ICES/ICNAF Joint Investigation on North Atlantic Salmon. *Edited by* B.B. Parrish and Horsted Sv Aa. Rapp. P.-v. Reun. Cons. Int. Explor. Mer, **176**: 82–92.

Salminen, M., Kuikka, S., and Erkamo, E. 1995. Annual variability in survival of sea ranched Baltic salmon, *Salmo salar* L.: significance of smolt size and marine conditions. Fish. Manag. Ecol. **2**: 171–184.

Saunders, R. 1981. Atlantic salmon (*Salmo salar*) stocks and management implications in the Canadian Atlantic provinces and New England, U.S.A. Can. J. Fish. Aquat. Sci. **38**: 1612–1625.

Shearer, W.M. 1992. Atlantic salmon scale reading guidelines. ICES Coop. Res. Rep. 188.

© 2000 NRC Canada

Assessing density-dependent establishment and dispersal: an example using caddisfly larvae

B.L. Kerans, Peter L. Chesson, and Roy A. Stein

Abstract: Density dependence in colonization is poorly understood. We studied colonization by a benthic, stream-dwelling caddisfly, *Hydropsyche slossonae*, through experiments varying conspecific densities and environmental conditions. A model of larval acceptance or rejection of a locality (dispersal from the locality) was developed and fitted to the data to estimate the relative strengths of density-dependent and density-independent processes underlying dispersal. In spring and fall, we varied density, substrate size, and current velocity in laboratory experiments and varied density in field experiments. In the laboratory, dispersal of fifth instars was always density dependent, but the strength of density dependence was highest in spring when the proportion dispersing was lowest. Dispersal in field experiments was density dependent only in spring. Proportion dispersing was highest under low flow. The model fit to laboratory data suggested that stronger density dependence in spring occurred because of a reduction in density-independent dispersal stimuli with no change in density-dependent stimuli. In contrast, a change in density-dependent stimuli did appear to cause differences between the proportions dispersing under the two flow regimes. The model reveals the potential for density-independent dispersal stimuli to modify the strength of density dependence detectable at the population level.

Résumé : La dépendance à l'égard de la densité dans la colonisation est un phénomène mal connu. Nous avons étudié la colonisation par une phrygane, *Hydropsyche slossonae*, insecte benthique des milieux lotiques, grâce à des expériences faisant varier les densités conspécifiques et les conditions environnementales. Nous avons élaboré un modèle de l'acceptation ou du rejet par la larve d'une localité (dispersion à partir de la localité), et nous l'avons ajusté aux données pour estimer les forces relatives des processus dépendants et indépendants de la densité qui régissent la dispersion. Au printemps et à l'automne, nous avons fait varier en laboratoire la densité, la taille du substrat et la vitesse du courant, et nous avons fait varier la densité dans les expériences de terrain. En laboratoire, la dispersion des cinquièmes instars était toujours dépendante de la densité, mais la force de la dépendance à l'égard de la densité était au plus fort au printemps, quand la proportion qui se dispersait était la plus faible. Dans les expériences de terrain, c'est seulement au printemps que la dispersion était dépendante de la densité. La proportion qui se dispersait était la plus forte par faible écoulement. Le modèle ajusté aux données de laboratoire semble montrer que la plus forte dépendance à l'égard de la densité observée au printemps était liée à une réduction des stimuli de dispersion indépendants de la densité, sans changement dans les stimuli dépendants de la densité. Par contre, un changement dans les stimuli dépendants de la densité semblait bien causer des différences entre les proportions qui se dispersaient dans les deux régimes d'écoulement. Le modèle fait ressortir que les stimuli de la dispersion indépendante de la densité ont le potentiel de modifier la force de la dépendance à l'égard de la densité qui est détectable au niveau de la population.

[Traduit par la Rédaction]

Introduction

Processes involved in colonization by organisms as diverse as insects, fish, and small mammals may have major influences on local population densities (e.g., Kareiva 1987) and ultimately on the distribution and abundance of organisms on larger spatial scales. A key question in this regard is the extent to which establishment and dispersal of individuals among habitat patches are influenced by local population density. Density-dependent establishment can restrict the range of local population densities (e.g., set ceilings for patch densities), and density-dependent dispersal may influence regional population regulation and persistence (Anholt 1995). In the common situation where dispersal is risky (e.g., Wilzbach et al. 1986), density-dependent dispersal can lead to density-dependent mortality or density-dependent loss from the system when dispersal processes are unidirectional, as is often the case in streams (Anholt 1995). In such cases, density-dependent dispersal can act as a density-dependent regulatory mechanism on a regional scale. Thus, colonization processes may play an important role in the regulation of population density on both small and large spatial scales.

Density-dependent colonization processes are not well understood. This is particularly true in streams despite the fact that invertebrate dispersal is a conspicuous process (e.g., Waters 1972). While there have been many attempts to ex-

Received December 3, 1999. Accepted February 14, 2000. J15463

B.L. Kerans,[1] P.L. Chesson,[2] and R.A. Stein. Department of Zoology, Ohio State University, Columbus, OH 43210, U.S.A.

[1]Author to whom all correspondence should be sent at the following address: Department of Biology, Montana State University, Bozeman, MT 59717, U.S.A.

[2]Present address: Section of Evolution and Ecology, Storer Hall, University of California, Davis, CA 95616, U.S.A.

© 2000 NRC Canada

amine dispersal in stream insects, the relative importance of density-dependent versus density-independent dispersal remains ambiguous. Part of the ambiguity revolves around the lack of quantitative tools to directly compare the strength of density-dependent and density-independent processes underlying establishment and dispersal. We studied this question using larvae of the caddisfly *Hydropsyche slossonae*, a common inhabitant of stream riffles in the United States. Although hydropsychids have a sedentary lifestyle, constructing fixed retreats and filtering nets on rocks, they are often found drifting in the water column, reflecting dispersal activities (Walton 1980). Moreover, behavioral observations show that hydropyschids compete for retreat placement sites and defend their retreats from intrusion by conspecifics (Jansson and Vuoristo 1979; Matczak and Mackay 1990). Larvae also build retreats with more regular spacing patterns than expected by chance (Glass and Bovbjerg 1969; Kerans 1989). These results suggest that density dependence and interference are important for hydropyschid establishment and dispersal.

Colonization processes in hydropsychids and many other sedentary stream insect larvae can be usefully divided into the following four stages: (1) dispersal from a substrate by resident larvae (e.g., hydropsychids that have built retreats and capture nets), (2) drift in the water column (or less frequently crawling on substrate), (3) settling out of the water column onto a new substrate, and (4) acceptance of the new substrate and establishment and retreat construction, or rejection of the substrate and further dispersal. This model is a modification of one proposed by Minshall and Petersen (1985). One modification is the addition of the fourth stage, which is the focus of our empirical research. For hydropsychids, stages 1 and 4 are biologically distinct. Conditions promoting dispersal may differ between stages 1 and 4 because stage 1 larvae have already invested energy in retreat construction. Moreover, stage 4 commonly involves an active process of movement over the new substrate and provides a larva with the opportunity to assess the suitability of the microhabitat prior to retreat construction. Thus, this stage provides a strong opportunity for the abiotic and biotic conditions of the microhabitat to affect the organism's decision to stay or disperse. Abiotic conditions like current velocity and substrate size are often correlated with hydropsychid population densities (e.g., Statzner et. al 1988; Schlosser and Ebel 1989; Georgian and Thorp 1992); thus, they have the potential to influence colonization processes during stage 4. Moreover, Matczak and Mackay (1990) showed that aggressive interactions that influence hydropsychid establishment and dispersal are confined to stage 4.

We studied the establishment and dispersal of *H. slossonae* through (*i*) development of a model and related statistical tests that allowed for straightforward tests of density-dependent and density-independent establishment and dispersal, (*ii*) empirical studies of how establishment and dispersal of *H. slossonae* changed temporally and were influenced by conspecific density and varying environmental conditions (current velocity and substrate size), and (*iii*) fitting the model to the data generated by the empirical studies to assess how the strengths of the underlying density-dependent and density-independent processes changed when establishment and dispersal varied.

Density dependence and the establishment and dispersal model

If the probability that an individual expresses a particular behavior is not related to the density of other individuals in the population, then that behavior can be considered density independent. In practice, probabilities are estimated as proportions of individuals in test groups that express a particular behavior, such as dispersal. Density independence is assumed to occur when the proportion exhibiting the behavior does not vary with the density of individuals. If the proportion varies with density, then density dependence occurs.

Typically, in studies of colonization of stream insects, density-dependent dispersal is empirically tested using one of two statistical methods. The first, and most direct, test uses the general linear model (analysis of variance (ANOVA)) to determine whether the proportion dispersing varies among densities (Walton et al. 1977; Wiley 1981). If significant variation is found, then density dependence is concluded. Patterns in the proportion dispersing are elucidated using pairwise comparisons among treatment means; typically, the proportion dispersing increases with increasing density. The second method regresses the number of individuals dispersing against density (Hildebrand 1974). This method relies on the relationships among proportion dispersing, numbers of individuals dispersing, and density. Theoretically, this method can detect density dependence and can provide more information than ANOVA. If the proportion dispersing increases with density (is density dependent), then the number of individuals dispersing plotted against density will exhibit a curvilinear relationship. If the proportion dispersing is constant across densities (is density independent), then the number of individuals dispersing will exhibit a linear relationship when plotted against density with the intercept through the origin. Thus, this technique relies on fitting curves of different shapes to graphs of number dispersing against density to determine if a density-dependent curve provides a better fit than a straight line through the origin. Often, this technique does not provide a clear test of density dependence because it is difficult to statistically distinguish between curvilinear and linear regressions.

We develop a model that is based on biological features underlying the phenomena of establishment and dispersal. In this case, we use the model in concert with ANOVAs to examine the strengths of density-independent and density-dependent processes underlying density dependence in the proportion dispersing. We envision these processes as density-dependent and density-independent stimuli experienced by individuals. Our model provides several benefits over traditional approaches used to assess density-dependent dispersal in stream insects. First, the model is a general one allowing for both density-dependent and density-independent stimuli, with density dependence occurring as a special case. Second, our model allows for direct comparisons of the strengths of density-dependent and density-independent processes underlying establishment and dispersal. Third, the model has additional benefits to the interpretation of the results. In particular, it shows that density dependence at the population level can be much reduced without any change in the underlying density-dependent behavior of the organisms because other factors have overriding effects.

© 2000 NRC Canada

Following the definition of density dependence, our model of establishment and dispersal (stage 4) is expressed in terms of the proportion of a population dispersing. The proportion remaining (1 minus the proportion dispersing) includes those larvae settling and establishing on the substrate. Consider an individual insect larva present on a particular substrate subject to particular biotic and abiotic conditions. We assume that it disperses from that substrate as the result of either a sufficient density-independent stimulus (di) or a sufficient density-dependent stimulus (dd) or both. Using standard probability formulas, this means

$$(1)\quad \begin{aligned} P[\text{disperse}] &= P[\text{di or dd}] \\ &= P[\text{di}] + P[\text{dd and no di}] \\ &= P[\text{di}] + P[\text{dd}|\text{no di}](1 - P[\text{di}]). \end{aligned}$$

The term $P[\text{dd}|\text{no di}]$, a conditional probability, is the probability of receiving a sufficient density-dependent stimulus and dispersing, given that the individual did not receive a density-independent stimulus sufficient to cause dispersal. Note that this expression involves no assumptions beyond the existence of the two different types of stimuli. We use the conditional probability because we do not assume independence of the density-dependent and density-independent stimuli. There are two alternatives to eq. 1, viz $P[\text{disperse}] = P[\text{dd}] + P[\text{di}|\text{no dd}](1 - P[\text{dd}])$ and $P[\text{disperse}] = P[\text{dd}] + P[\text{di}] - P[\text{dd and di}]$. All three equations are alternative, mathematically correct ways of relating dispersal to the underlying stimuli. If the stimuli are independent, then $P[\text{dd}|\text{no di}] = P[\text{dd}]$, $P[\text{di}|\text{no dd}] = P[\text{di}]$, and $P[\text{dd and di}] = P[\text{dd}]P[\text{di}]$, and all three equations reduce to the common form $P[\text{disperse}] = P[\text{dd}] + P[\text{di}] - P[\text{dd}]P[\text{di}]$, and there is no reason for choosing one over another. However, when independence of density-dependent and density-independent stimuli is not assumed, eq. 1 has the advantage that density-dependent stimuli occur in just one term, and under the reasonable assumption that the strength of density-independent stimuli does not vary as a function of density, only one of the three terms in eq. 1 has to be expressed as a function of density, greatly simplifying model fitting and interpretation.

Equation 1 immediately reveals some important information. If the probability of a sufficient density-independent stimulus is high, then the additional effects that a density-dependent stimulus may have on dispersal are weak. There are two reasons for this. First, in eq. 1, $P[\text{dd}|\text{no di}]$ accounts for density-dependent stimuli, but it is multiplied by $(1 - P[\text{di}])$, which will be small if the probability of a density-independent stimulus is high. The effects on the dispersal probability of $P[\text{dd}|\text{no di}]$ are therefore reduced if the probability of a sufficient density-independent stimulus is high. Second, as the dispersal probability must lie between $P[\text{di}]$ and 1, if $P[\text{di}]$ is high, the effect that density dependence can have on dispersal is restricted to a narrow range, regardless of how strong those density-dependent stimuli are.

Equation 1 represents the proportion dispersing in terms of specific behavioral components. To estimate these components from experimental data, some assumptions are necessary. Let the probability of receiving a sufficient density-independent stimulus be a constant, b_0. The probability of a sufficient density-dependent stimulus (given no di) is presumably a monotonically increasing function of density taking the value 0 at 0 density of conspecifics and leveling off at 1 as the density becomes very high (i.e., it is nonlinear). One such function is the following:

$$(2)\quad P[\text{dd}|\text{no di}] = 1 - \exp(-b_1X)$$

where b_1 is a constant and X is the initial density. The parameter b_1 gives the per unit effect of density on the probability of dispersing by a density-dependent stimulus, given no sufficient density-independent stimulus. We refer to it as the interference coefficient. A function with properties similar to those of eq. 2 is the rectangular hyperbola

$$(3)\quad P[\text{dd}|\text{no di}] = b_1X/(1 + b_1X).$$

With the precision of the data commonly available in the study of stream insects, there is little reason to choose between these different functions or between these and some other function with properties required to represent the density-dependent response. However, eq. 2 has the benefit of being interpreted in terms of a random encounter process, as follows. Suppose that (*i*) encounters with other larvae are random, (*ii*) density-dependent dispersal occurs solely as a result of an encounter above some threshold level, which may be specific to the individual, and (*iii*) such above-threshold encounters occur with a frequency proportional to initial density. Then the probability of not receiving a sufficient density-dependent stimulus is the zero term of the Poisson probability distribution (Hassell 1978) and can be written in the form $\exp(-b_1X)$. Equation 2 now follows directly. We emphasize, however, that there are many other ways in which a formula indistinguishable in practice from eq. 2 might arise, and its use to separate density-dependent and density-independent processes is in no way dependent on special conditions.

We can now put together the components of the model to get the proportion of larvae dispersing under experimental conditions. Recognizing that the theoretical mean of the proportion of larvae dispersing in an experiment is the probability of dispersing, we obtain the equation

$$(4)\quad \text{Proportion dispersing} = b_0 + (1 - b_0)(1 - \exp(-b_1X)) + \text{random error}.$$

This equation provides a nonlinear regression equation that can be fitted to data, with the parameters b_0 and b_1 being measures, respectively, of the density-dependent and density-independent processes underlying dispersal. The interference coefficient, b_1, measures directly the per capita rate at which individuals receive density-dependent dispersal stimuli, and therefore, b_1X is the total rate that an individual experiences. The model highlights an important distinction between the intensity of the underlying interactions between individuals, as measured by the interference coefficient, b_1, and the strength of the relationship between the proportion dispersing and density. Figure 1 shows that holding b_1 constant (maintaining the level of interactions between individuals) and increasing b_0 weakens the relationship between the proportion dispersing and density, making density-dependent dispersal more difficult to detect. The parameter b_0 may be affected by abiotic conditions of the microhabitat on the substrate and can be expected to vary as such conditions change. The parameter b_1 could also vary with changes in

© 2000 NRC Canada

Fig. 1. Mean proportion of hydropyschids dispersing as a function of density for different values of density-independent stimuli, b_0, but with a fixed value of the interference coefficient, b_1 (0.003). Relative change in the proportion dispersing across densities expresses the intensity of density-dependent dispersal. Note that as b_0 becomes large, the slope of the curve approaches zero and the strength of density dependence decreases.

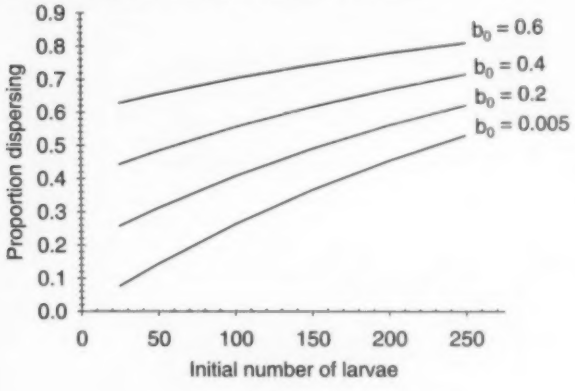

abiotic factors. In such cases, it measures the interaction between abiotic and biotic conditions.

We fitted the nonlinear regression to data generated in laboratory experiments examining establishment and dispersal of fourth- and fifth-instar *H. slossonae* larvae across various densities, environmental conditions (substrate sizes and flow regimes), and seasons. The model allowed us to evaluate how the density-dependent and density-independent establishment and dispersal processes changed under these varying conditions.

Methods

Study site and organism

Hydropsyche slossonae larvae were collected and field experiments were conducted in Macochee Creek, a third-order tributary of the Mad River flowing through primarily agricultural land in southern Logan County, Ohio. The creek is 15.5 km long and 6–15 m wide and is composed of a series of runs and pools interspersed with shallow (<10 cm) riffles. *Hydropsyche slossonae* is the most abundant hydropsychid within Macochee Creek, which is dominated by caddisfly and dipteran larvae (B.L. Kerans, unpublished data). *Hydropsyche slossonae* densities can be high (maximum of 57.1 larvae per 100 cm^2 of rock surface area, $\bar{x} = 6.1 \pm 0.9$, $n = 135$, Kerans 1989; these and all other means are presented ±1 SE). Populations of *H. slossonae* are usually univoltine (Mackay 1986). Larvae in Macochee Creek overwinter as third, fourth, and fifth instars with pupation occurring in late spring.

Laboratory experiments

In laboratory experiments, we investigated how larval density, substrate size, and current velocity affected dispersal of fourth and fifth instars during two seasons (spring, fall–winter). In May, the experimental design was two-way factorial manipulating three densities (25, 100, and 200 larvae, which are equivalent to 5, 20, and 40 larvae·100 cm^{-2}, respectively) and three substrate sizes (gravel, 1.25 cm in diameter; pebble, 5.00 cm in diameter; cobble, 8.00 cm in diameter). Only low-velocity conditions (≈30 $cm \cdot s^{-1}$) and fifth instars were tested (Table 1) (fourth instars were uncommon in spring). Fuller and Mackay (1980) showed that velocities of 30 $cm \cdot s^{-1}$ are adequate for net construction.

Fall–winter trials were conducted mostly between November and February, with some additional trials (seven of 64 total) conducted in early April. Fourth and fifth instars were tested in separate experiments. Experimental design was a three-way factorial manipulating three densities (as in spring), two substrate sizes (gravel, pebble), and two current velocities (≈30 and ≈60 $cm \cdot s^{-1}$; Table 1). Three replicates were run for all treatment combinations except the fall–winter high-density trials using fourth instars, where only one replicate could be completed. Larval densities were within the range of those found in Macochee Creek (see Study site and organism section).

Experiments were conducted in four identical artificial stream tanks (length 117.7 cm, width 15 cm, depth 15.7 cm). Water entered tanks through an approximately 7.6-cm PVC pipe and passed through two mesh baffles to reduce turbulence. At the downstream end, water flowed through a 200-μm-mesh drift net and was collected in a large holding tank. Electric pumps recirculated the water, and temperature was regulated by a chilling unit in the holding tank. An experimental section (15 × 15 cm) was positioned about 20 cm from the upstream end of each tank. Gravel (<4 mm in diameter, the material used for larval retreat construction) and one size of test substrate were added to each upstream section. All substrates were periphyton-covered stones collected from Macochee Creek. Because hydropsychids inhabit and defend retreats attached to stone surfaces, the surface area available for establishment could influence dispersal (Reice 1980), and total surface area of stones was held constant (≈500 cm^2). Surface area was estimated by individually wrapping all stones in aluminum foil and using standard regressions relating foil weight to surface area (Reice 1980).

Larvae were fed finely ground trout chow ad libitum and held at 12–15°C in well-aerated tanks for ≤3 days before experiments. Larvae were added to the experimental section in still water. During the first hour, larvae were prevented from leaving the experimental section by plastic dividers placed slightly upstream and downstream of the section, and larvae that swam off stones were returned to the stones. After 1 h, we removed the dividers and gradually increased flow over 5 min. Drifting larvae were captured in the downstream net. No suspended food material was provided during a trial.

Trials began between 14:00 and 16:00 EST and ended the following morning between 9:00 and 10:00 EST, encompassing the peak drift period (Kerans 1996). We counted the number of larvae that had left the experimental section at the end of the trial. In addition, to check for the possibility of artifacts arising from the initial setup, we counted the number that had left 0.5 h after flow had been increased. Thus, we calculated two different dispersal proportions: P_I, the total number of larvae that dispersed divided by initial number, and P_R, the number of larvae dispersing after the first 0.5 h divided by those remaining in the upstream section after the first 0.5 h.

Field experiments

The laboratory experiments allowed us to maintain controlled situations; however, we conducted field experiments to test for density-dependent establishment and dispersal under more natural conditions. In particular, these experiments tested for density dependence with natural levels of suspended organic particulates. Such particulates are difficult to maintain in laboratory trials but can influence hydropsychid dispersal, spacing of retreats, and distribution and abundance (Matczak and Mackay 1990; Richardson and Mackay 1991; Georgian and Thorp 1992).

We conducted two field experiments (spring, 4–7 June; fall, 3–17 December). Both current velocity (≈30 and 60 $cm \cdot s^{-1}$) and density (0, 12, and 100 larvae·$tile^{-1}$, which are equivalent to 0, 5.5, and 45.5 larvae·100 cm^{-2}, respectively) were investigated in a fac-

© 2000 NRC Canada

Table 1. Physical conditions ($\bar{x}$ ± 1 SE) in laboratory and field experiments.

	Flow ($cm \cdot s^{-1}$)			
	Low	High	Depth (cm)	Water temperature (°C)
Laboratory experiments				
Spring				
Instar V	33.0±0.3 (n = 27)		8.3±0.2 (n = 27)	14.1±0.1 (n = 27)
Fall				
Instar V	32.3±0.5 (n = 18)	59.2±0.4 (n = 18)	8.2±0.2 (n = 36)	13.0±0.1 (n = 36)
Instar IV	31.6±0.5 (n = 14)	58.9±0.4 (n = 14)	8.5±0.2 (n = 28)	13.1±0.2 (n = 28)
Field experiments				
Spring	31.0±3.0 (n = 5)	67.5±7.6 (n = 6)		17.8±1.8 (n = 11)
Fall	36.8±4.1 (n = 12)			5.0±1.0 (n = 12)

torial design in spring, but in fall, only the effects of density were studied. Densities were similar to those used in laboratory experiments. Larvae were marked by attaching metallic glitter to the thorax with Zapagap® superglue, which has little or no effect on mortality or behavior (Kerans 1989).

Artificial substrates were made from plastic containers (15 × 15 × 6 cm) and slate tiles (10 × 10 × 0.5 cm, surface area 220 cm^2). Tiles were attached to the inner surface (15 × 15 × 1 cm) of container tops. Gravel for retreat construction was placed between each tile and container top, producing a "sandwich." Bottoms of containers (15 × 15 × 5 cm) had 500-μm mesh on two sides to allow water flow and formed covers to confine larvae initially.

Sandwiches were conditioned in stream riffles for 1 month. They were then cleaned of any colonizing organisms and debris and positioned in riffles such that tiles were flush with the stream bottom. A Marsh-McBirney current meter was used to choose appropriate flows. In a preliminary study, *H. slossonae* larvae readily colonized these sandwiches and built retreats.

At the beginning of an experiment, sandwiches were covered and marked larvae were added. After 1 h, lids were removed and a downstream Surber sampler caught drifting larvae. Sandwiches remained in the riffle for 3 days in spring, whereas in fall, they were in place for 2 weeks (duration of the fall experiment was longer to increase colonization). To quantify mark loss during spring, 12 larvae were placed in two replicates in which covers were left in place. No marking control was done in the fall experiment because covers restricted flow and we expected survival to be low if larvae were confined by covers for 2 weeks. Mark retention was 100% in spring. At experiment's end, we determined the number of marked larvae that left and the number of unmarked *H. slossonae* and other hydropsychids that had colonized the sandwiches.

Statistical analyses

We assessed establishment and dispersal of hydropsychids using two sequential procedures. First, for both laboratory and field experiments, we used ANOVAs on the proportion dispersing. We then fit the model discussed above to portions of the laboratory data, specifically to main effects significant in ANOVAs, to gain the additional information available from this more quantitative approach. Thus, we assess the gains made from a model tailored to the system compared with a more traditional statistical approach.

Standard statistical analyses included separate, initial ANOVAs on P_I and P_R, including all interaction effects, except in the case of the fourth-instar experiment where the three-way interaction was omitted from the model because in some cells, only one trial was completed. Proportions were not transformed because examination of the residuals suggested that variances were homogeneous. Residuals from ANOVAs were plotted against other potential influencing variables (e.g., water depth, date of experiment). If a plot suggested a relationship, variables were included in an analysis of covariance (ANCOVA) and retained if significant ($p < 0.05$). We did not test for heterogeneity of regression slopes because significant covariates were balanced across all treatment combinations. Thus, any regression heterogeneity would not influence the outcome of treatments, and accounting for it would add unnecessary complexity to models (Smith 1957).

Where needed, comparisons of means, adjusted for any covariates, were done using population marginal means (i.e., SAS least squares means, Searle et al. 1980; SAS Institute Inc. 1985), with significance levels adjusted for the number of comparisons using the Bonferroni inequality. We also used one-way ANOVA, combining observations collected under similar laboratory conditions (all initial densities, gravel and pebble, and low flow), to compare dispersal between seasons.

In the field experiments, statistical analyses included separate ANOVAs on both P_I and P_R, as defined in the laboratory experiments, and on number of unmarked colonists. We also examined residuals as above. Proportions of marked larvae dispersing from the sandwiches did not require transformation; however, (ln + 1) transformations were used on the number of unmarked colonists to stabilize variances.

In the second method of analyses of laboratory data, we fit the model to P_I from the laboratory experiments (for main effects that were significant in ANOVAs) using SAS procedure NLIN and the Gauss–Newton iteration method (SAS Institute Inc. 1985). During the procedure, b_0 was constrained to be between 0 and 1, whereas b_1 was >0. A multiple regression technique, using X and indicator variables for each treatment in a pair of comparisons (e.g., spring versus fall–winter), allowed simultaneous fitting of separate regressions for each treatment and comparison of the coefficients between regressions (Neter et al. 1983). Asymptotic maximum likelihood ratio tests were used to test whether coefficients differed signficantly from zero and differed between individual regressions. If b_0 differs from zero, then dispersal has a constant, density-independent component. If b_1 differs from zero, then dispersal is density dependent. Significant differences between regressions in b_0 and b_1 values indicate that the treatments affect density-independent and density-dependent processes, respectively. Both density-dependent and density-independent effects may be influenced by treatments; thus, comparisons of two regressions (e.g., between low and high flows) may yield significant differences between both b_0 values and b_1 values.

Results

Laboratory experiments

Few larvae left during the first 0.5 h; consequently, P_I and P_R were similar in magnitude (always ±0.10). In most cases, treatments influenced P_I and P_R similarly; therefore, we report results for P_R only when different from P_I.

© 2000 NRC Canada

During spring, dispersal of fifth instars was density dependent; P_I increased with increasing initial density (Table 2; Fig. 2). We detected no difference in dispersal rates among substrate sizes, but P_I declined 1%·day^{-1} with trial date (Table 2). During fall and winter, P_I increased with initial density and declined with increasing current velocity (Table 3; Fig. 3*a*). A significant three-way interaction (density, substrate, flow) probably occurred for two reasons. First, P_I was similar across treatments at low density, but at high density, dispersal rates segregated by both current velocity and substrate size (Fig. 3*a*). Second, P_I in the pebble/high current velocity treatment did not match the pattern in other treatments (Fig. 3*a*). The P_I declined 3%·day^{-1} for each day that larvae were held in the laboratory before a trial (Table 3). When the ANCOVA was run on P_R, only initial density ($F_{2,23} = 26.19$, $p < 0.0001$) and the covariate ($F_{1,23} = 4.31$, $p = 0.0492$) affected dispersal.

Dispersal of fourth instars was also density dependent (Table 3; Fig. 3*b*). Overall, fewer larvae dispersed from gravel than pebble; however, the proportion dispersing exhibited considerable variation between flows and substrate sizes. As with fifth instars, P_I declined with increasing current velocity (Fig. 3*b*), although the response was marginally nonsignificant ($p = 0.0565$; Table 3). The P_I declined 7%·day^{-1} for each day that larvae were held in the laboratory before a trial (Table 3). When ANCOVA was run on P_R, only substrate size ($F_{1,17} = 1.75$, $p < 0.0449$) and the covariate ($F_{1,17} = 8.64$, $p < 0.0092$) influenced dispersal.

Under similar conditions (gravel and pebble substrates and low current velocity), P_I differed between instars and seasons (one-way ANOVA, $F_{2,47} = 15.05$, $p < 0.0001$). In spring, fifth instars had lower dispersal rates than either fourth or fifth instars in fall–winter ($p < 0.0002$ and 0.0001, respectively), whereas in fall–winter, dispersal rates of fourth and fifth instars did not differ ($p > 0.46$; compare solid and open bars in Figs. 2 and 3).

In both spring and fall–winter experiments, most larvae remaining in the upstream subsection had constructed retreats. Mean proportion constructing retreats was high for fifth instars (spring, 0.83 ± 0.02, $n = 27$; fall–winter, 0.88 ± 0.02, $n = 36$) and slightly lower for fourth instars (0.69 ± 0.03, $n = 28$).

Field experiments

The spring field experiment supported laboratory results. The P_I was larger when initial density was high than when it was low (0.425 ± 0.073 and 0.125 ± 0.06, respectively; two-way ANOVA, $F_{1,3} = 10.12$, $p = 0.05$). We detected no difference in dispersal under different current velocities ($F_{1,3} = 1.28$, $p = 0.3403$), nor was the interaction between current velocity and density significant ($F_{1,3} = 0.06$, $p = 0.8205$). The P_I was higher in fall than in spring but density independent (low density, 0.670 ± 0.076; high density, 0.650 ± 0.055; one-way ANOVA, $F_{1,6} = 0.04$, $p = 0.8447$). In both experiments, results for P_I and P_R were similar.

Number of unmarked *H. slossonae* and total number of hydropsychids colonizing tiles were low in both spring (*H. slossonae*, $\bar{x} = 0.73 \pm 0.30$; hydropsychids, $\bar{x} = 2.0 \pm 0.54$; $n = 11$) and fall (*H. slossonae*, $\bar{x} = 1.25 \pm 0.40$; hydropsychids, $\bar{x} = 3.67 \pm 0.80$; $n = 12$). We detected no difference in the number of unmarked *H. slossonae* colonists or hydropsychid colonists between densities, current velocities, and their interaction in spring or among densities in fall (all p values in ANOVAs >0.05).

Table 2. ANCOVA for P_I, number of larvae dispersing divided by initital number of fifth-instar *H. slossonae* in spring laboratory experiments.

Source of variation	df	MS	F	p
Initial number	2	0.2783	71.42	0.0001
Substrate size	2	0.0002	0.05	0.9511
Substrate size × initial number	4	0.0009	0.23	0.9195
Date of trial (slope –0.0107)[a]	1	0.0330	8.47	0.0097
Error	17	0.0039		

[a]Date of each trial.

Fig. 2. Means, adjusted for the covariate (date), from the ANCOVA on P_I, the number of fifth-instar *H. slossonae* dispersing divided by initial number, for each substrate size at each initial number in the spring laboratory experiment. Open bars, gravel; solid bars, pebble; hatched bars, cobble. Least-squares pairwise comparisons of mean P_Is indicated differences among all initial densities (all p values <0.0001). Error bars represent ±1 SE.

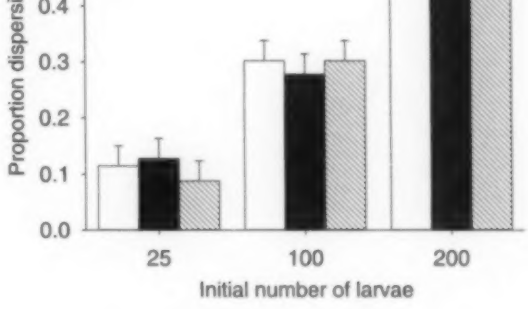

Model application

The nonlinear regressions provided a good fit in both the fifth instar/season ($R^2 = 0.983$, $F_{4,32} = 457.98$, $p < 0.001$) and fifth instar/current velocity comparisons ($R^2 = 0.989$, $F_{4,32} = 696.53$, $p < 0.001$). In all regressions, b_0 and $b_1 > 0$; therefore, both density-dependent and density-independent processes contributed to dispersal (Table 4). However, reduction in dispersal of fifth instars from fall–winter to spring was related to a low b_0 (probability of sufficient density-independent stimulus) in spring rather than to differences in intraspecific interactions (about 80% reduction in b_0; Table 4). Conversely, reduced dispersal under high-flow conditions resulted from a lowered interference coefficient, b_1 (38% decrease in b_1; Table 4), which is interpreted in the model as a lower per capita rate of density-dependent stimuli, given no sufficient density-independent stimuli, thus suggesting a change in the underlying intensity of interactions between individuals at any given larval density. Although the nonlinear regressions provided a good fit to the data on fourth instars ($R^2 = 0.924$, $F_{4,28} = 72.47$, $p < 0.001$),

© 2000 NRC Canada

Table 3. ANCOVAs for P_I, number of larvae dispersing divided by initial number of fourth- and fifth-instar *H. slossonae* in fall–winter laboratory experiments.

	Fifth instars				Fourth instars			
Source of variation	df	MS	*F*	*p*	df	MS	*F*	*p*
Initial number	2	0.1474	57.61	0.0001	2	0.0500	3.99	0.0380
Current velocity	1	0.0256	10.01	0.0043	1	0.0525	4.19	0.0565
Substrate size	1	0.0006	0.24	0.6258	1	0.0877	6.99	0.0171
Substrate size × current velocity	1	0.0075	2.94	0.1000	1	0.0158	1.26	0.2772
Current velocity × initial number	2	0.0052	2.03	0.1538	2	0.0060	0.47	0.6312
Substrate size × initial number	2	0.0032	1.24	0.3077	2	0.0268	2.13	0.1490
Substrate size × current velocity × initial number	2	0.0104	4.04	0.0313				
Days in laboratory (slope –0.0254 fifth instars, –0.0715 fourth instars)[a]	1	0.0155	6.06	0.0217	1	0.0861	6.87	0.0179
Error	23	0.0026			17	0.0125		

[a]Number of days that larvae were held in the laboratory before a trial.

Fig. 3. Means, adjusted for the covariate (days in the laboratory), from the ANCOVA on P_I, the number of larvae dispersing divided by initial number of (*a*) fifth- and (*b*) fourth-instar *H. slossonae* in fall–winter laboratory experiments. Open bars, low flow/gravel; solid bars, low flow/pebble; hatched bars, high flow/gravel; cross-hatched bars, high flow/pebble. For fifth instars, least-squares pairwise comparisons of mean P_Is revealed significant differences among the three densities ($p < 0.017$, chosen by the Bonferroni inequality). Although there was an overall effect of density for fourth instars, pairwise comparisons by least-squares means did not detect specific differences ($p > 0.017$, chosen by the Bonferroni inequality). Error bars represent ± 1 SE.

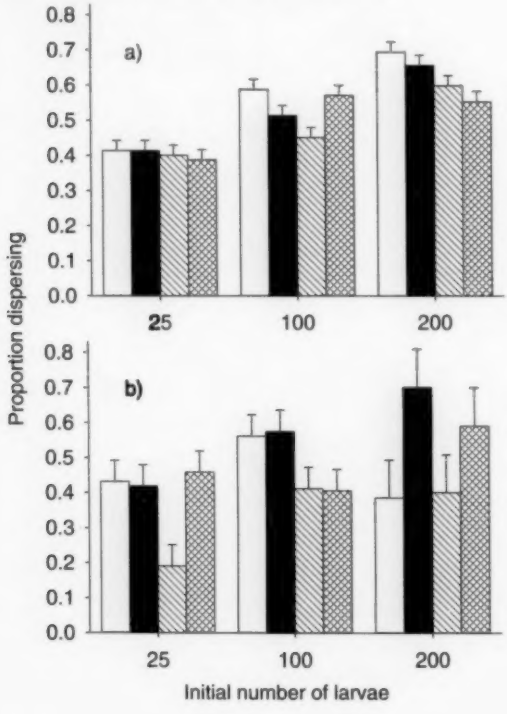

we were unable to determine whether the differences in dispersal across substrate sizes detected in the ANCOVA were due to density-dependent or density-independent stimuli (Table 4).

Discussion

Across season and microhabitat, establishment and dispersal of fifth-instar *H. slossonae* larvae were shown to be density dependent in the laboratory using ANOVAs. Field experiments yielded results similar to those in spring when dispersal rates were low but strongly density dependent (in laboratory and field experiments, dispersal tripled from low to high density). Conversely, in fall, dispersal rates were high and density independent in Macochee Creek and weakly density dependent in the laboratory (dispersal rate increased only 50% from low to high density). Fourth-instar dispersal was density dependent during the initial 0.5 h of trials but subsequently became density independent.

Using the model revealed more quantitative information about the relationship between individual dispersal behavior and density-dependent dispersal. In particular, density dependence in the probability of dispersal may not be proportional to the level of intraspecific interference occurring among individuals. Indeed, expressing the probability of dispersal as the joint outcome of density-dependent and density-independent stimuli (eq. 1) shows that such proportionality would not ordinarily be expected unless no density-independent stimuli were present. Equation 1, which involves no assumptions beyond the existence of the two types of stimuli, shows that the effects of density-dependent and density-independent stimuli are necessarily interactive. The quantity $P[\mathrm{dd}|\mathrm{di}]$ in eq. 1 can be regarded as measuring the strength of density-dependent stimuli and therefore quantifies the strength of interactions between larvae. However, the effect of $P[\mathrm{dd}|\mathrm{di}]$ on the probability of dispersal is equal to the product of $P[\mathrm{dd}|\mathrm{di}]$ and the probability of no sufficient density-independent stimulus. Thus, the effects that density-dependent stimuli have on dispersal are reduced by density-independent stimuli. Put another way, if a high proportion of larvae would leave anyway as a result of density-independent stimuli, there is little additional effect that density-dependent stimuli can have.

These interactive effects of density-dependent and density-independent stimuli on dispersal clarify the results of the ex-

© 2000 NRC Canada

Table 4. Nonlinear regression coefficients (± asympotic SEs) for comparing hypothesized behavioral bases of differences among P_1s, number dispersing divided by initial number of *H. slossonae* larvae.

	Coefficient	
	b_0	b_1
Fifth instar, season		
Spring	0.0621 (0.0314)***	0.0029 (0.0003)***
Fall[a]	0.3634 (0.0323)***	0.0034 (0.0005)***
Fifth instar, current velocity		
Low[a]	0.3634 (0.0323)***	0.0034 (0.0005)***
High	0.3717 (0.0282)***	0.0021 (0.0004)***
Fourth instar, substrate size		
Gravel	0.2969 (0.0714)***	0.0021 (0.0012)**
Pebble	0.3902 (0.0716)***	0.0022 (0.0014)*

Note: Regressions were for season, current velocity, and substrate size effects shown to be significantly different in ANOVA (ANCOVA). Asterisks indicate asymptotic t test H_0: b_0, $b_1 > 0$; ***$p < 0.0005$, **$p < 0.05$, *$p < 0.1$. Vertical lines connect coefficients that did not differ ($p > 0.05$) as determined by nonlinear regressions with indicator variables.

[a]Fall fifth instar and low current velocity are the same regressions.

periments. For instance, the fact that density dependence is weaker in fall than in spring experiments does not necessarily mean that individual larvae have fewer encounters in fall than in spring at the same larval densities; the similar interference coefficients (b_1) in the spring and fall suggest that negative interactions between individuals are similar in these two seasons. Here, the reduction in the strength of density dependence simply reflects much greater density-independent dispersal in fall than in spring, which weakens the relationship between the proportion dispersing and density (Fig. 1).

The reduction in the propensity of an individual to disperse in spring may be related to features of the life cycle or the environment. For example, fifth instars may become less apt to disperse, reducing density-independent movement as they approach pupation in spring. In spring, fifth instars are heaviest and drift infrequently (Kerans 1992). In the laboratory, temperatures and flows were kept the same in the different seasons, and so, those factors cannot explain the differences in dispersal behavior. Morever, the similarities of results of our laboratory experiments (where no food was provided) and field experiments suggest that variation in food quality or quantity between seasons does not explain differences in dispersal.

The ANOVAs showed that both fourth and fifth instars dispersed less frequently when flows were high. Results of the model suggest that these differences in dispersal between flow regimes resulted from an alteration in the interference coefficient (significant differences between b_1 but not b_0 between regressions) rather than any direct affect of the abiotic condition on the density-independent stimulus to leave. Because interactions between organisms are often based on direct encounters, any environmental factor that influences the frequency, intensity, or outcome of an encounter has the potential to influence the outcome of the interaction and thus the interference coefficient. Such effects are common. For example, Fletcher and Underwood (1987) have shown that physical features of the substrate influence competition between two limpet species. Moreover, microhabitat factors, such as the presence of refuges, influence interactions between many types of predators and their prey (e.g., Stein 1977; Sih 1987). Trichopteran fighting success, locomotory activity, and net building are influenced by flow (for a review, see Statzner et al. 1988). Reduction in encounters with other larvae under high flows could result because larvae are less active under high flows. Alternatively, Fuller and Mackay (1980) have shown that *H. slossonae* constructs more capture nets under high flows. In this case, larvae would spend less time actively searching for suitable sites and construct retreats sooner than under low-flow conditions. Involvement in retreat and net construction may reduce the number of encounters with other larvae. Moreover, under high flows, more larvae will invest energy in constructing retreats and nets than under low flow and may be less likely to leave after an aggressive encounter.

The behavior of larvae predicted by fitting the model to data from experiments conducted under low and high flow is also consistent with the theory that larvae exhibit density-dependent habitat rejection (i.e., habitat selection). Theories of density-dependent habitat selection assume that individuals select those habitats that convey the greatness fitness (e.g., Fretwell and Lucas 1970). In the simplest models, fitness is expected to be inversely related to population densities, and the distribution and abundance of individuals across habitats will reflect a trade-off between physical habitat quality and intraspecific density. Our high-flow regime may support higher densities than our low-flow regime because it provides a better quality habitat for hydropsychids. Hydropsychid densities often increase with increasing flow (Schlosser and Ebel 1989). Using simulations, Loudon and Alstad (1990) showed that particle capture rates for hydropsychid nets increase with flow, and Georgian and Thorp (1992) found that hydropsychids select high-flow regimes that deliver food at higher rates than low-flow regimes. Although little is known directly about habitat-related fitness of hydropsychids, Englund (1991) has shown that hydropsychids in the rear of larval aggregations experience lower flow and are smaller than those in the front of aggregations. The results from our model suggest that dispersal differences between flow regimes are related to an interaction between the quality of the habitat and interference.

Our results also have implications for field studies of drift of hydropsychids. The density-dependent establishment and dispersal found in our studies suggest that drift should be

© 2000 NRC Canada

density dependent; however, most studies suggest that hydropsychid drift is density independent (Reisen and Prins 1972; Hildebrand 1974; Statzner et al. 1985). These studies were conducted on larger spatial scales than our experiments. The detection of density dependence on large spatial scales depends on the strength of density dependence on local scales, the variability of the response, and the strength of other factors influencing hydropsychid movement. Our results show that on local scales, strong, density-dependent dispersal is an intermittent process. For *H. slossonae*, density-dependent dispersal is probably most easily detected on large spatial scales in spring when the local density-dependent dispersal response is strong. In fall, weak density dependence combined with high variability on local scales (i.e., the patchy nature of stream benthos) may preclude detection of density dependence on larger spatial scales. When density dependence is weak on local scales, the influence of other environmental factors may make detection of density dependence difficult even on local scales, as shown by our fall field experiments and implied by our model analysis. If strong density dependence is intermittent for other hydropsychids, then the lack of detection of density-dependent dispersal on large spatial scales could result because studies were conducted when density dependence was weak. Lack of detection of density dependence during a single time period does not mean that interference could not be strong at other times and important in population regulation. Intermittent density-dependent dispersal could, as discussed by Wiens (1977) for resource competition, cause "ecological crunch" periods that may influence populations long after competition can be detected.

For *H. slossonae* larvae, establishment and dispersal are influenced by microhabitat characteristics and local population density. Density-dependent dispersal probably plays a key role in local populations through density-dependent habitat selection. However, the effect of density dependence on dispersal varies across space and time. Because variability in density dependence at the population level may be caused by changes in individual behavior unrelated to density, density-dependent interactions among larvae, or both, there is no simple, direct relationship between strength of density dependence at the population level and the level of interference an individual experiences, unless other factors are controlled. Quantitative expression of the results in a nonlinear regression model was essential to understand such interactions in this study. By estimating the interference coefficient, b_1, we measured the strength of the underlying interference among larvae because the model factors out the effect of a density-independent stimulus, even when strong, to reveal the full potential of density-dependent stimuli. The model cannot compensate for reduced information on density dependence that exists naturally when there is a strong density-independent effect, but it does correct for the bias in estimation of the density-dependent effects that would occur in a standard linear analysis of the problem.

Acknowledgements

Comments by J. Brawn, M. Butler, D. Culver, R. Fuller, J. Jannot, M. Mather, T. McMahon, and anonymous reviewers greatly improved earlier versions of this manuscript. We also would like to thank K. Gross, E. Marschall, G. Mittelbach, J. Reeve, A. Taylor, the Ohio State ECOLUNCH and EDIT groups, and individuals associated with the Aquatic Ecology Laboratory for many helpful discussions. We are especially grateful to D. Armstrong, P. Cunningham, C. Habicht, J. Kerans, S. Klosiewski, C. Knight, C. Mallison, J. Miner, D. Parrish, C. Price, S. Savage, J. Wahl, and F. Weng for help in the field and laboratory. C. Cowan helped with some figures. Special thanks go to B. Peckarsky and J. Karr, as the manuscript was revised while B.L.K. was a postdoctoral associate in their laboratories. Funds for this research were provided by National Science Foundation Dissertation Improvement Grant BSR 8701166, a Grant-in-Aid from Sigma Xi, an Alumni Research Award (Graduate School, Ohio State University), and the Department of Zoology and Aquatic Ecology Laboratory (Ohio State University).

References

Anholt, B.R. 1995. Density dependence resolves the stream drift paradox. Ecology, **76**: 2235–2239.

Englund, G. 1991. Asymmetric resource competition in a filter-feeding stream insect (*Hydropsyche siltalai*: Trichoptera). Freshwater Biol. **26**: 425–432.

Fletcher, W.J., and Underwood, A.J. 1987. Interspecific competition among subtidal limpets: effect of substratum heterogeneity. Ecology, **68**: 387–400.

Fretwell, S.D., and Lucas, H.L., Jr. 1970. On territorial behavior and other factors influencing habitat distribution in birds. I. Theoretical development. Acta Biotheor. **19**: 16–36.

Fuller, R.L., and Mackay, R.J. 1980. Field and laboratory studies of net-spinning activity by *Hydropsyche* larvae (Trichoptera: Hydropsychidae). Can. J. Zool. **58**: 2006–2014.

Georgian, T., and Thorp, J.H. 1992. Effects of microhabitat selection on feeding rates of net-spinning caddisfly larvae. Ecology, **73**: 229–240.

Glass, L.W., and Bovbjerg, R.V. 1969. Density and dispersion in laboratory populations of caddisfly larvae (*Cheumatopsyche*, Hydropsychidae). Ecology, **50**: 1082–1084.

Hassell, M.P. 1978. The dynamics of arthropod predator–prey systems. Princeton University Press, Princeton, N.J.

Hildebrand, S.G. 1974. The relation of drift to benthos density and food level in an artificial stream. Limnol. Oceanogr. **19**: 951–957.

Jansson, A., and Vuoristo, T. 1979. Significance of stridulation in larval Hydropsychidae (Trichoptera). Behaviour, **71**: 167–185.

Kareiva, P.1987. Habitat fragmentation and the stability of predator–prey interactions. Nature (Lond.), **326**: 388–390.

Kerans, B.L. 1989. Causes and consequences of density-dependent dispersal of the caddisfly *Hydropsyche slossonae*. Ph.D. dissertation, Ohio State University, Columbus, Ohio.

Kerans, B.L. 1992. Season and body size influence movement of hydropsychid caddisfly larvae. Can. J. Fish. Aquat. Sci. **49**: 259–265.

Kerans, B.L. 1996. The influence of periphyton and rock texture on the diel drift periodicity of a hydropsychid caddisfly. J. Freshwater Ecol. **11**: 163–169.

Loudon, C., and Alstad, D.N. 1990. Theoretical mechanics of particle capture: predictions for hydropsychid caddisfly distributional ecology. Am. Nat. **135**: 360–381.

Mackay, R.J. 1986. Life cycles of *Hydropsyche riola*, *H. slossonae* and *Cheumatopsyche pettiti* (Trichoptera: Hydropsychidae) in a spring-fed stream in Minnesota. Am. Midl. Nat. **115**: 19–24.

© 2000 NRC Canada

Matczak, T.Z., and Mackay, R.J. 1990. Territoriality in filter-feeding caddisfly larvae: laboratory experiments. J. North Am. Benthol. Soc. **9**: 26–34.

Minshall, G.E., and Petersen, R.C., Jr. 1985. Towards a theory of macroinvertebrate community structure in stream ecosystems. Arch. Hydrobiol. **104**: 49–76.

Neter, J., Wasserman, W., and Kutner, M.H. 1983. Applied linear regression models. R.D. Irwin, Inc., Homewood, Ill.

Reice, S.R. 1980. The role of substratum in benthic macroinvertebrate microdistribution and litter decomposition in a woodland stream. Ecology, **61**: 580–590.

Reisen, W.K., and Prins, R. 1972. Some ecological relationships of the invertebrate drift in Praters Creek, Pickens County, South Carolina. Ecology, **53**: 876–884.

Richardson, J.S., and Mackay, R.J. 1991. Lake outlets and the distribution of filter feeders: an assessment of hypotheses. Oikos, **62**: 370–380.

SAS Institute Inc. 1985. SAS user's guide: statistics, version 5 edition. SAS Institute Inc., Cary, N.C.

Schlosser, I.J., and Ebel, K.K. 1989. Effects of flow regime and cyprinid predation on a headwater stream. Ecol. Monogr. **59**: 41–57.

Searle, S.R., Speed, F.M., and Milliken, G.A. 1980. Population marginal means in the linear model: an alternative to least squares means. Am. Stat. **34**: 216–221.

Sih, A. 1987. Predators and prey life-styles: an evolutionary and ecological overview. *In* Predation direct and indirect impacts on aquatic communities. *Edited by* W.C. Kerfoot and A. Sih. University Press of New England, Hanover, N.H. pp. 203–224.

Smith, H.F. 1957. Interpretation of adjusted treatment means and regressions in analysis of covariance. Biometrics, **13**: 282–308.

Statzner, B., Elouard, J.-M., and Dejoux, C. 1985. Field experiments on the relationship between drift and benthic densities of aquatic insects in tropical streams (Ivory Coast). II. *Cheumatopsyche falcifera* (Trichoptera: Hydropsychidae). J. Anim. Ecol. **55**: 93–110.

Statzner, B., Gore, J.A., and Resh, V.H. 1988. Hydraulic stream ecology: observed patterns and potential applications. J. North Am. Benthol. Soc. **7**: 307–360.

Stein, R.A. 1977. Selective predation, optimal foraging, and the predator–prey interaction between fish and crayfish. Ecology, **58**: 1237–1253.

Walton, O.E., Jr. 1980. Active entry of stream benthic macroinvertebrates into the water column. Hydrobiologia, **74**: 129–139.

Walton, O.E., Jr., Reice, S.R., and Andrews, R.W. 1977. The effects of density, sediment particle size and velocity on drift of *Acroneuria abnormis* (Plecoptera). Oikos, **28**: 291–298.

Waters, T.F. 1972. The drift of stream insects. Annu. Rev. Entomol. **17**: 253–272.

Wiens, J.A. 1977. On competition and variable environments. Am. Sci. **65**: 590–597.

Wiley, M.J. 1981. Interacting influences of density and preference on the emigration rates of some lotic chironomid larvae (Diptera: Chironomidae). Ecology, **62**: 426–438.

Wilzbach, M., Cummins, K.W., and Hall, J.D. 1986. Influence of habitat manipulations on interactions between cutthroat trout and invertebrate drift. Ecology, **67**: 898–911.

© 2000 NRC Canada

Factors affecting the swimming endurance and catchability of Atlantic cod (*Gadus morhua*)

Paul D. Winger, Pingguo He, and Stephen J. Walsh

Abstract: The swimming endurance of Atlantic cod (*Gadus morhua*), native to the cold waters off the east coast of Newfoundland and Labrador, was investigated under laboratory conditions. Using a swimming flume, endurance was tested at swimming speeds ranging from 0.6 to 1.3 $m \cdot s^{-1}$ using water temperatures from 0.0 to 9.8°C ($\bar{x}$ = 3.2°C, SD = 2.8) and fish lengths from 41.0 to 86.0 cm ($\bar{x}$ = 57.8 cm, SD = 10.5). The results revealed that swimming speed was the only significant factor affecting the endurance of cod. The maximum sustained swimming speed (U_{ms}) was predicted to be 0.66 $m \cdot s^{-1}$. Statistical analysis of the data was conducted using failure time analysis. The hazard, or risk of exhaustion, was found to increase rapidly with increasing swimming speed, i.e., there was a decrease in the probability of cod achieving a given swimming endurance. Probability curves for the endurance of cod were calculated for different swimming speeds. The findings suggest that the catching efficiency of commercially targeted cod (>41.0 cm) by otter trawls may be highly sensitive to changes in towing speed while being independent of both fish length and water temperature.

Résumé : L'endurance à la nage de morues franches (*Gadus morhua*), provenant des eaux froides de la côte est de Terre-Neuve et du Labrador, a été étudiée en laboratoire. Dans un bassin de nage, nous avons testé l'endurance des poissons à des vitesses de nage allant de 0,6 à 1,3 $m \cdot s^{-1}$ à des températures de l'eau allant de 0,0 à 9,8°C ($\bar{x}$ = 3,2°C, ET = 2,8), la longueur des poissons allant de 41,0 à 86,0 cm ($\bar{x}$ = 57,8 cm; ET = 10,5). Les résultats ont révélé que la vitesse de nage était le seul facteur significatif agissant sur l'endurance des morues. La vitesse de nage soutenue maximale (U_{ms}) prédite était de 0,66 $m \cdot s^{-1}$. L'analyse statistique des données a été effectuée par analyse de la durée jusqu'à défaillance. Le danger potentiel, ou risque d'épuisement, augmentait rapidement avec la hausse de la vitesse de nage, c'est-à-dire qu'il y avait une diminution de la probabilité d'atteinte par les morues d'une endurance de nage donnée. Nous avons calculé les courbes de probabilité de l'endurance des morues pour différentes vitesses de nage. Nos résultats permettent de penser que l'efficacité de capture des morues visées par la pêche commerciale (>41,0 cm) utilisant des chaluts à panneaux peut être fortement sensible à des changements dans la vitesse de remorquage mais être indépendante à la fois de la longueur des poissons et de la température de l'eau.

[Traduit par la Rédaction]

Introduction

The study of fish behaviour reactions to mobile fishing gears has grown substantially since the 1960s. Since that time, direct observations of fish behaviour near otter trawls have been collected for a number of marine groundfish species (e.g., Beamish 1969; Glass and Wardle 1989; Walsh and Hickey 1993). Video and photographic observations have revealed that many species, once they are herded into the mouth of a trawl, tend to orient in the direction of tow and keep station with the advancing trawl. The period of time that fish are capable of swimming in the trawl mouth and hence their vulnerability to capture is dependent on their swimming endurance. Factors known to affect endurance include the towing speed of the trawl and fish size (Main and Sangster 1981; Wardle 1993). Although empirical evidence has not been shown, other factors such as bottom temperature (e.g., Foster et al. 1981; He 1993; Smith and Page 1996), bottom type (Engås 1994), and fish density (Godø et al. 1999) are also suspected to affect swimming endurance and hence capture vulnerability.

Several laboratory studies have investigated the swimming endurance of marine groundfish species (e.g., Beamish 1966; He 1991; Winger et al. 1999). Because of its commercial importance, Atlantic cod (*Gadus morhua*) has received much of this attention. Previous studies by Beamish (1966) and He (1991) have measured the effects of swimming speed (0.42–1.36 $m \cdot s^{-1}$) and water temperature (–0.3 to 8.0°C) on the endurance of cod (35.0–52.0 cm). A comparative analysis by He (1991) of the available literature indicated the likelihood of a temperature effect on the endurance of cod at speeds less than or equal to 1.0 $m \cdot s^{-1}$. The author suggested that the catchability of cod by otter trawls might be greatly enhanced at low temperatures due to a reduction in swimming performance. However, the influence of experimental design and

Received June 2, 1999. Accepted February 4, 2000.
J15165

P.D. Winger.[1] Biopsychology Program, Memorial University of Newfoundland, St. John's, NF A1B 3X9, Canada.
P. He. Fisheries and Marine Institute, Memorial University of Newfoundland, P.O. Box 4920, St. John's, NF A1C 5R3, Canada.
S.J. Walsh. Department of Fisheries and Oceans, Science Branch, Northwest Atlantic Fisheries Centre, P.O. Box 5667, St. John's, NF A1C 5X1, Canada.

[1]Author to whom all correspondence should be sent at the following address: Fisheries and Marine Institute, Memorial University of Newfoundland, P.O. Box 4920, St. John's, NF A1C 5R3, Canada. e-mail: wingerp@athena.nwafc.nf.ca

© 2000 NRC Canada

apparatus on the performance of fish has raised concern over the validity of comparing experimental data (Videler 1993). This has justified the need for a complete examination of the endurance of cod within a single study.

This paper describes the results of a laboratory investigation into the factors affecting the swimming endurance of cod native to the cold waters off the east coast of Newfoundland and Labrador. In this part of the Northwest Atlantic, cod are known to occupy temperatures as low as –1.5°C (Wroblewski et al. 1994) and as high as 12.0°C (Clark and Green 1990) depending on the region and season. We test the hypotheses that swimming endurance is independent of water temperature, fish size, and swimming speed. We specifically examine temperatures commonly inhabited by cod, fish sizes selective to commercial otter trawls, and swimming speeds comparable with commercial towing speeds that are typical of this region. The results are discussed in relation to the implications for catchability of cod by otter trawls.

Materials and methods

Specimens

Atlantic cod were captured by handline, cod trap, and otter trawl off the east and southeast coasts of Newfoundland throughout 1996–1997. The fish were transported to the Ocean Sciences Centre of the Memorial University of Newfoundland where they were held for a minimum period of 3 weeks for tank adaptation prior to endurance testing. The fish were kept in a 2.5 × 2.5 × 1.0 m holding area with a continuous supply of ambient temperature coastal seawater. Photoperiod was synchronized with seasonal changes in day length using an outdoor photocell switch. The fish were fed a diet of chopped Atlantic herring (*Clupea harengus*) once a week to satiation. All fish were starved for a minimum of 48 h prior to endurance testing, and only fish that appeared in good physical condition were used. Fish size was recorded as total fish length measured to the nearest centimetre. Endurance trials were carried out using cod ranging in length from 41.0 to 86.0 cm ($\bar{x}$ = 57.8 cm, SD = 10.5).

Apparatus

The swimming flume and many aspects of the experimental design followed He (1991) and Winger et al. (1999). The dimensions of the swimming chamber were 1.80 × 0.50 × 0.46 m (length × width × water depth). Electrical stimulation from pairs of electrodes located in the downstream end of the swimming chamber encouraged cod to swim against the water flow until exhausted. A pulsing stimulus (2 Hz) was applied across the electrodes with peak voltage of approximately 15 V. An area of bright light projected near the downstream end created a gradient of light along the length of the swimming chamber that encouraged cod to swim against the water flow (Brett 1982; He 1991; Nelson et al. 1994). Light levels were 1.44×10^4, 12.80, and 6.35 lx for the downstream, midstream, and upstream sections of the swimming chamber, respectively.

The floor of the swimming chamber was equipped with a continuously moving belt that moved at the same speed and in the same direction as the water flow (for details, see Winger et al. 1999). The moving floor served several purposes: (*i*) it prevented the fish from settling on the floor of the chamber, (*ii*) it simulated ground passing under a swimming fish as it would appear in the ocean, and (*iii*) it maintained uniformity of flow near the floor of the chamber, thus preventing fish from taking advantage of reduced flow in that area.

The swimming flume was operated on a flow-through basis with a continuous supply of ambient-temperature coastal seawater. Measures of water temperature, dissolved oxygen content, and oxygen saturation were recorded using a portable digital meter (model UK-2000, Central Kagaku Corp.). Calibration of flow speeds was conducted using a Seba minicurrent meter (model 486, Geneq Inc.).

Endurance trials

Endurance trials were carried out over a period of 32 weeks from November 1996 to July 1997. Seasonal changes in the ambient temperature of the incoming seawater allowed us to test for temperature effects on swimming endurance. Trials were conducted at temperatures ranging from 0.0 to 9.8°C ($\bar{x}$ = 3.2°C, SD = 2.8).

Endurance was evaluated using the "fixed-velocity" method (Brett 1967). This technique involves measuring the time to fatigue (endurance) for fish swimming at a constant speed. Swimming speeds ranged from 0.6 to 1.3 $m \cdot s^{-1}$. Flow speeds were not corrected for the volume of the swimming chamber that was displaced by the fish, referred to as "solid-blocking" (Bell and Terhune 1970), since the maximum cross-sectional area of our largest fish (86 cm) did not exceed 5% of the chamber section area.

A standardized routine was developed for testing the endurance of cod. Twenty-four hours prior to each trial, individual cod were randomly chosen and transferred to an auxiliary tank (1.3 × 1.3 × 1.3 m) located next to the swimming flume. This eliminated the need for lengthy or cumbersome transfers at the beginning of each swimming trial and reduced the stress associated with handling. He (1991) found that cod responded well to an initial conditioning period at low swimming speeds before beginning endurance testing. The conditioning routine used here was two-tiered, lasting 25–30 min depending on the intended target swimming speed (V_t). This routine began with a 10-min period of habituation at a reduced flow speed of 0.1 $m \cdot s^{-1}$. This was followed by a 10-min period at 0.5 body length $(BL) \cdot s^{-1}$ (V_1), coinciding with the activation of the floor belt, downstream lighting, and electrodes. At this point, if the intended V_t was less than 1.0 $BL \cdot s^{-1}$, the flow speed was gradually increased from V_1 to V_t over a period of 5 min. If, however, V_t was greater than 1.0 $BL \cdot s^{-1}$, then an additional 5-min period at 1.0 $BL \cdot s^{-1}$ (V_2) was required. This was followed by a gradual increase from V_2 to V_t over a period of 5 min. This two-tiered routine was adapted from He (1991) and has been found to be an effective means for conditioning cod to swim at speeds greater than 1.0 $BL \cdot s^{-1}$.

Endurance was defined as the period of time that a fish was able to swim at V_t before becoming exhausted. A fish was considered exhausted when it was unable to lift off the downstream electrodes after a duration of 10 s. Prodding techniques used in other studies were not used here to avoid the possibility of subjectively biasing the results. In cases where endurance exceeded 200 min, the trials were terminated and the data were treated as "censored" observations (see Analysis section). At the end of each trial, the fish were transferred to a second auxiliary tank (1.3 × 1.3 × 1.3 m) located near the flume for short-term recovery before being transferred back to the main holding area.

Given the limited numbers of fish available, endurance testing of the same fish occurred a number of times over the period of study. The experimental fish were not individually identifiable, and hence, within-individual differences in swimming endurance could not be assessed. The minimum recovery period was generally 1 week and it was estimated that the maximum number of trials for any given fish did not exceed three.

Analysis

Statistical analysis of the data was conducted using failure time analysis. A detailed description of this technique and its application to swimming endurance data is given in Winger et al. (1999).

© 2000 NRC Canada

Fig. 1. Logarithm of endurance plotted against swimming speed for different size ranges of Atlantic cod: <50 cm (□), 50–59 cm (○), 60–69 cm (△), and >69 cm (+). Swimming trials exceeding 200 min were terminated and the values in parentheses represent the number of occurrences (>1) observed.

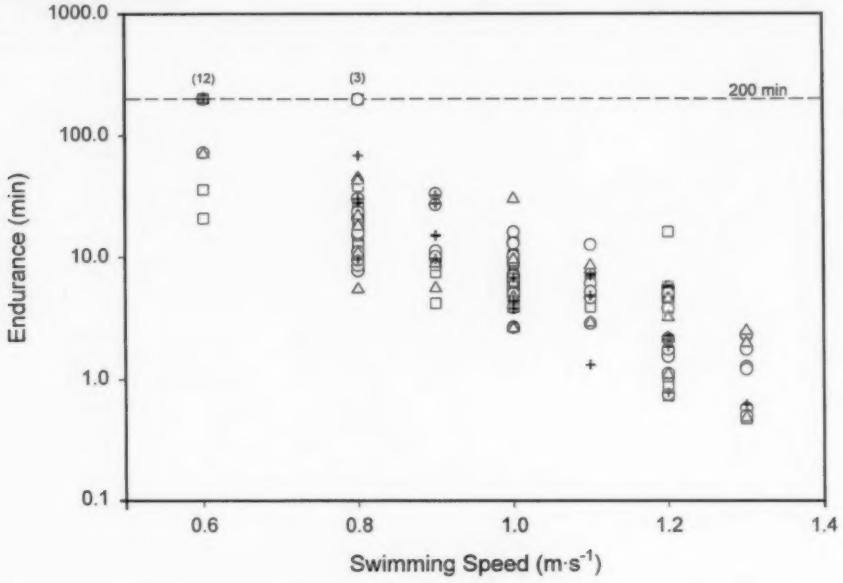

The primary advantage of this technique over commonly used regression models (for reviews, see Beamish 1978; Videler 1993) is its ability to accommodate censored observations. In swimming endurance studies, these refer to trials in which the fish fail to exhaust within an appreciable period of time and the experimenter must eventually terminate the trial. The 200-min time limit used in this study was chosen a priori and is consistent with the methodology of recent swimming endurance studies (e.g., Xu et al. 1994; DeAlteris and La Valley 1999; Winger et al. 1999). Because exhaustion is not observed in censored trials, the total time to fatigue is not known. While data of this type are common in swimming endurance studies, they are frequently excluded from the analyses to satisfy the requirements of conventional regression models (e.g., He and Wardle 1988; Xu et al. 1994; Peake et al. 1995). We feel that the exclusion of censored observations is a loss of valuable information and hence, we have pursued a statistical technique that permits their inclusion.

Endurance times for cod were analyzed using the Cox proportional hazards model (Cox and Oakes 1984), which assessed the effect of different variables on swimming endurance in the manner similar to that in Winger et al. (1999). Variables in the analysis included swimming speed, fish length, and water temperature. The model uses swimming endurance times to estimate a baseline hazard function and coefficients of the individual variables using forward stepwise variable selection analogous to multiple regression analysis. The order of entry of the variables into the model was based on their level of significance of the score statistic (Norušis 1994). The criterion for removal of a variable from the model was based on its level of contribution to the reduction of the log-likelihood value for the model (likelihood ratio test, Lee 1992). All independent variables were treated as continuous variables. Diagnostic methods for the examination of potential outliers consisted of DfBeta plots and partial residual plots. The assumption of proportional hazards was checked by plotting the log of the negative of the log of the cumulative survival function against swimming endurance, i.e., log-minus-log plots (Norušis 1994). All analyses were carried out using SPSS version 6.1 (SPSS Inc.).

The maximum sustained swimming speed (U_{ms}) is defined as the upper limit of the sustained swimming speed range (Brett 1967). At speeds exceeding U_{ms}, endurance becomes limited due to increasing lactate concentrations and declining glycogen reserves (for reviews, see He 1993; Hammer 1995). Estimates of U_{ms} are most commonly determined either by direct measurement (He and Wardle 1988; He 1991; Xu et al. 1994) or by prediction using regression analysis (Peake et al. 1995) or probit analysis (Brett 1967, 1982; Bernatchez and Dodson 1985). In this study, U_{ms} for cod was considered equivalent to the median critical (maximum) swimming speed, similar to probit analysis. This corresponds to the speed at which 50% of the fish have fatigued after the maximum time period. Using the hazards model, the median endurance for cod can only be predicted up to a period for which exhaustion is actually observed, i.e., it cannot be extended beyond the longest endurance time. Thus, we consider the maximum endurance for which exhaustion was observed to mark the transition from sustained to prolonged swimming speeds and use it to predict the U_{ms} for cod.

Table 1. Fish length, number of fish, temperature range, and mean temperature for 154 swimming endurance trials of Atlantic cod.

Fish length (cm)	No. of fish	Temperature range (°C)	Mean temperature (SD) (°C)
<50	35	0.0–9.7	4.5 (3.1)
50–59	66	0.0–9.7	3.0 (2.7)
60–69	32	0.0–9.6	2.6 (2.5)
≥70	21	0.1–9.8	2.6 (2.5)

Results

A total of 229 swimming trials were completed during the 32-week experiment. Of these, 154 trials were classified as successful (Table 1), in which 139 Atlantic cod swam to exhaustion and 15 cod were censored after exceeding an endurance of 200 min. The remaining trials (n = 75) comprised

© 2000 NRC Canada

Fig. 2. Logarithm of endurance plotted against swimming speed for Atlantic cod at different temperature ranges: 0.0–2.9°C (△), 3.0–5.9°C (□), and >6.0°C (○). Swimming trials exceeding 200 min were terminated and the values in parentheses represent the number of occurrences (>1) observed.

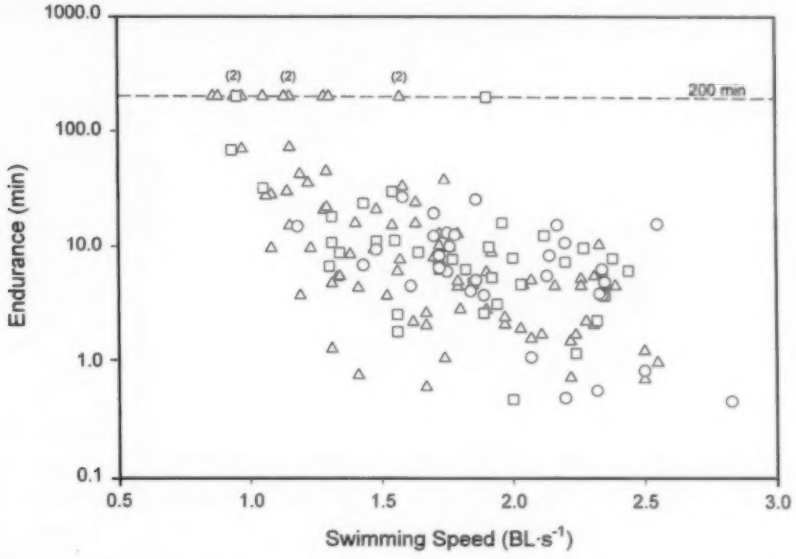

Table 2. Failure time analysis of the swimming endurance of Atlantic cod using the Cox proportional hazards model.

Variables in the model						
Step No.	Variable	Coefficient (SE)	Log likelihood of model	χ^2	df	p
0	—	—	–597.332	—	—	—
1	Speed (cm·s^{-1})	0.082 (0.007)	–504.605	185.455	1	<0.0001
		Global χ^2	df	p		
		170.390	1	<0.0001		
Variables not in the model						
Variable	Score	df	p			
Fish length (cm)	1.024	1	0.312			
Temperature (°C)	2.343	1	0.126			
Speed × fish length	2.316	1	0.128			
Speed × temperature	3.552	1	0.060			
Temperature × fish length	2.030	1	0.154			
Speed × temperature × fish length	2.723	1	0.099			

Note: Variables were entered into the model using forward stepwise selection. The significance of the variables was tested on the basis of their reduction of the log likelihood value for the model. The likelihood ratio test statistic (χ^2) is defined as –2(log likelihood before variable added – log likelihood after variable added).

fish that failed to reach their V_t for suitable endurance testing. These trials were considered unsuccessful and were excluded from the analysis.

Swimming speed was the only factor found to affect the swimming endurance of cod. A decreasing trend in the logarithm of endurance was observed with increasing swimming speed (Fig. 1). The mean endurance was 50.1 min at 0.6 m·s^{-1}, dropping to 8.0 min at 1.0 m·s^{-1} and 1.3 min at 1.3 m·s^{-1}. A similar trend is found when endurance is plotted nondimensionally against the relative swimming speed (body lengths per second) of the fish (Fig. 2). Censored trials were only observed at the slower swimming speeds. At 0.6 m·s^{-1}, a total of 75% of the trials were censored (n = 12), consisting of cod 46–70 cm in length at temperatures from 0.1 to 2.6°C. At 0.8 m·s^{-1}, only 10% of the trials were censored (n = 3), consisting of cod 42–51 cm in length at temperatures from 2.1 to 2.7°C. Variability in endurance was consistent across the range of swimming speeds tested, and no noticeable relationships were evident between endurance and the independent variables fish length and water temperature (Figs. 1 and 2).

The results of the failure time analysis (Table 2) indicate that swimming speed had a highly significant effect (p < 0.0001) on the endurance hazard rate. The remaining vari-

© 2000 NRC Canada

Fig. 3. Estimated probability curves for the swimming endurance of Atlantic cod at swimming speeds of (*a*) 0.6–1.0 m·s^{-1} and (*b*) 1.1–1.5 m·s^{-1}. Solid curves represent swimming speeds tested in the current study and broken curves represent probability curves extrapolated using the hazards model developed.

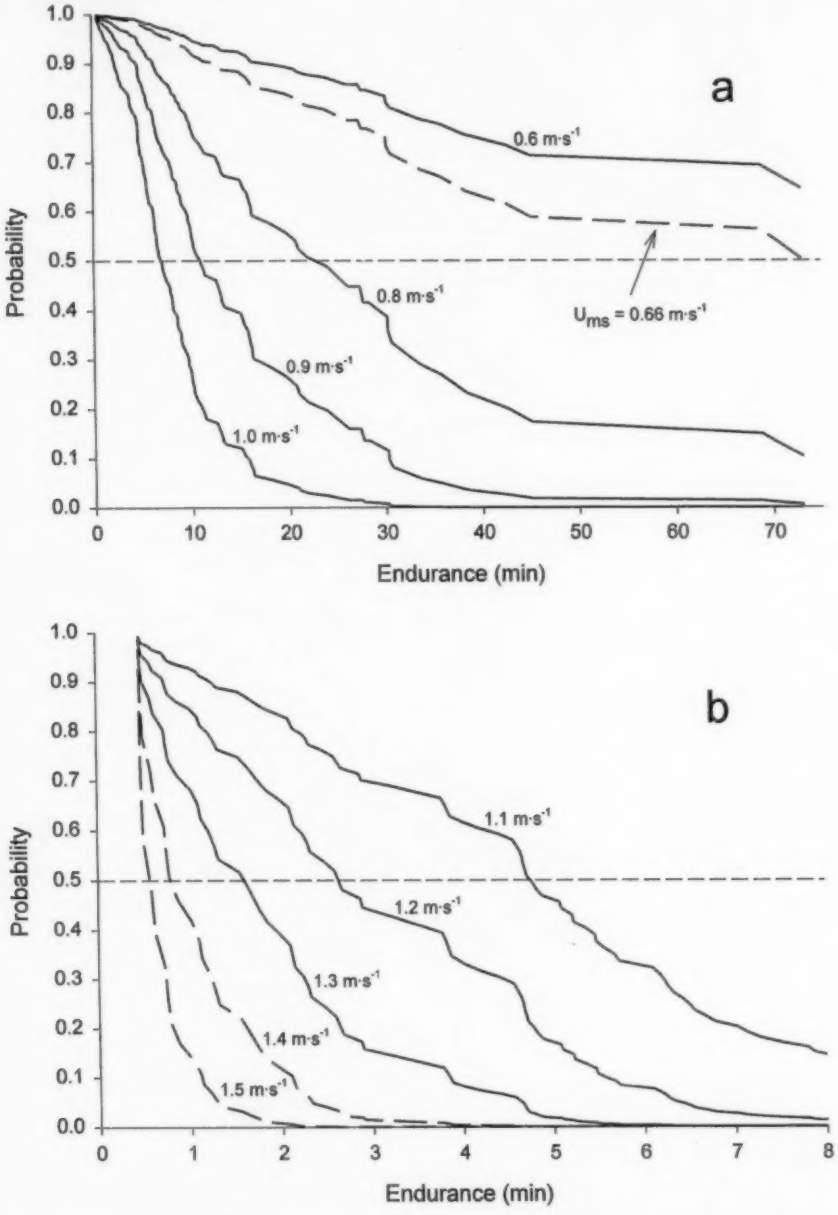

ables for fish length, water temperature, and the four interaction terms were not statistically significant ($p > 0.05$) and were not entered into the model. The positive coefficient for swimming speed indicates that the risk of exhaustion increased with increasing swimming speed. This increase is equivalent to a decrease in the probability of cod achieving a given endurance. Using the hazards model, estimates of endurance probability can be calculated from the predicted endurance hazard rates. Some examples of probability curves for different swimming speeds are illustrated in Fig. 3. These curves show that the probability of cod achieving a given endurance decreases rapidly with increasing swimming speed. For example, the probability that cod has endurance greater than 10 min is 95% at 0.6 m·s^{-1}, dropping to 27% at 1.0 m·s^{-1} and 0% at speeds equal to or greater than 1.2 m·s^{-1}. The median endurance, i.e., where probability equals 0.5, is also shown to decline rapidly with increasing swimming speed. At a speed of 0.8 m·s^{-1}, cod had a median

© 2000 NRC Canada

endurance of 23.0 min, falling to 7.0 min at 1.0 $m \cdot s^{-1}$ and 1.6 min at 1.3 $m \cdot s^{-1}$.

The maximum swimming endurance for which exhaustion was observed was 73 min. Beyond this period, cod were swimming within sustainable limits and were capable of swimming a minimum of 200 min. The U_{ms} was predicted to be 0.66 $m \cdot s^{-1}$. This corresponds to the speed at which 50% of cod would fatigue after a period of 73 min (Fig. 3*a*).

The global χ^2 for the model was highly significant ($p < 0.0001$), indicating that the endurance times for cod resulted in a good fit of the Cox proportional hazards model. Diagnostic investigation of the data revealed no obvious trends in the partial residual plot or DfBeta plot for swimming speed. Only one potential outlier was observed. This was a cod that demonstrated an endurance time of greater than 16 min at a swimming speed of 1.2 $m \cdot s^{-1}$ (length = 47 cm, temperature = 6.9°C). While this endurance time was exceptionally high when compared with the other fish tested at the same speed, there was no biological or technical reason for eliminating the trial from the analysis.

Dissolved oxygen content within the flume remained high throughout the experiment. The mean concentration was 13.2 mg $O_2 \cdot L^{-1}$ (SD = 1.8), with the percentage of dissolved oxygen saturation never falling below 85.9%.

Discussion

Swimming endurance

The results revealed that the swimming endurance of Atlantic cod was highly dependent on swimming speed. The logarithmic relationship shown in Fig. 1 is consistent with the previously published data for cod (Beamish 1966; He 1991) and other marine/freshwater species (e.g., Bainbridge 1960; Brett 1982; He and Wardle 1988). The U_{ms} found in this study (0.66 $m \cdot s^{-1}$) is comparable with previous estimates for cod. Using the same flume as in this study with some differences in experimental design, He (1991) determined the U_{ms} of cod (36–43 cm) native to Newfoundland waters to be 0.42 $m \cdot s^{-1}$ at temperatures ranging from –0.3 to 1.4°C. He (1991), using Beamish's (1966) data, which were derived from a small Blažka-type respirometer, estimated the U_{ms} for cod (35–36 cm) native to the Bay of Fundy to be 0.75 $m \cdot s^{-1}$ at 5°C and 0.90 $m \cdot s^{-1}$ at 8°C. Differences in the experimental design and swimming apparatus used in these studies may account for some of the variation in U_{ms} observed. In addition, this study incorporated a larger size range of fish and a larger temperature regime than the other studies.

Length-dependent swimming endurance among fish has been well documented (e.g., Bainbridge 1960; He and Wardle 1988; Winger et al. 1999). This study presents the first empirical analysis of the effect of body size on the swimming endurance of cod. Using fish in the size range of 41–86 cm, no significant length effect was found.[2] Our inability to detect this effect may have been related to the absence of smaller cod in our experiment.

The effect of water temperature on the swimming endurance of cod may be more subtle than previously thought. Our results do not support the hypothesis of temperature-dependent swimming endurance for the temperature range examined.[2] Similar temperature-independent swimming performance has been reported in other marine groundfish species, including winter flounder (*Pleuronectes americanus*) across temperatures of 5, 8, and 11°C (Beamish 1966) and common dab (*Limanda limanda*) and lemon sole (*Microstomus kitt*) across temperatures of 5, 10, and 15°C (Duthie 1982). However, our finding is inconsistent with earlier studies on the endurance of cod. Beamish (1966) tested cod (35–36 cm) collected from the Bay of Fundy region and found that at 1.05 $m \cdot s^{-1}$, cod could swim for about 16 min at 8.0°C, decreasing to 6 min at 5.0°C. He (1991) found that cod (36–52 cm), native to the waters off the east coast of Newfoundland, could only swim for about 2 min at 1.0 $m \cdot s^{-1}$ at temperatures ranging from –0.3 to 1.4°C. In comparing his findings with Beamish's (1966) results, He (1991) concluded that there was a noticeable temperature effect on the endurance of cod at speeds less than or equal to 1.0 $m \cdot s^{-1}$. In the current study, our endurance times are intermediate to those published, approximately 8 min at 0.0°C, 6 min at 5.0°C, and 6 min at 8.0°C for trials similarly at 1.0 $m \cdot s^{-1}$. Differences in the experimental approach, apparatus, temperature range, and size range of the fish tested may account for the variations observed among these studies. Caution should always be used when comparing estimates of swimming performance between studies, given the potential for population effects (Nelson et al. 1994) and differences in experimental design (Beamish 1978; Videler 1993).

Cold acclimation may account in part for the undetected effect of temperature on the swimming endurance of cod in this study. Thermal compensation at the lower temperatures may have reduced the apparent effect of temperature on endurance. Guderley and Blier (1988) argued that thermal compensation in certain species can result in an increase in the capacity for sustained swimming at low temperatures. The authors outlined several types of positive thermal compensation, including changes in muscle contractile properties, myosin ATPase activity, the proportion of red muscle fibers, and the levels of aerobic enzymes in the musculature. Under laboratory conditions, Foster et al. (1993) found that cold acclimation of cod resulted in higher cytochrome *c* oxidase activity in the white muscle tissues compared with cod with warm-acclimated tissues. Given that increased cytochrome *c* oxidase activity has been shown to be associated with increased aerobic metabolic rates of tissues (Smith and Chong 1982), this supports the hypothesis of increased aerobic swimming capacity of cod at low temperatures. Whether such thermal responses do in fact improve the swimming performance of cod at low temperatures has not yet been established. However, given that the fish used in this study were maintained under conditions of ambient temperature and photoperiod, the natural physiological cues associated with a change in seasons should have occurred. Therefore, our experimental cod should have had sufficient time to acclimate to the seasonal changes in water temperature and, if capable, the potential to develop thermal compensatory responses.

Otter trawl catchability

It is well established that the towing speed of a trawl is a

[2] This finding is consistent with our previous examination of the data using multiple regression analysis (P.D. Winger et al., unpublished data).

© 2000 NRC Canada

critical factor affecting the efficiency of fish capture. Off the east coast of Canada, groundfish species such as cod are typically harvested using towing speeds in the range of 2.0–3.5 kn (1.0–1.8 $m \cdot s^{-1}$) depending on the fishing operation. While in many cases the speed of a trawl relative to the ground may remain constant, its speed relative to the water and to the fish may be highly variable, depending on ocean currents near the seafloor (Carrothers 1981). If the results from the current study are representative of field conditions, then the endurance of cod swimming in the trawl mouth is expected to be highly sensitive to changes in the speed of a trawl relative to the water. Figure 3*b* shows the estimated probability curves for the endurance of cod at swimming speeds comparable with towing speeds used by commercial trawlers. Extrapolated curves for 1.4 and 1.5 $m \cdot s^{-1}$ (broken curves) predict a median endurance of only 47 and 35 s, respectively. These endurance times are similar to those estimated for North Sea cod based on underwater video observations of fish swimming in the trawl mouth (Main and Sangster 1981).

The length range of cod examined in this study is comparable with the length range that is targeted by commercial groundfish otter trawls in Atlantic Canada. Our smallest cod tested (41 cm) corresponds to the minimum regulated landing size of 41–45 cm (varies regionally) that is currently enforced (Department of Fisheries and Oceans 1998; North Atlantic Fisheries Organization 1998). Given that the current study found no effect of fish length on endurance, this suggests that commercially targeted cod (i.e., >41 cm) swimming in the trawl mouth are not expected to suffer differential catchability as a result of length-dependent endurance. However, Main and Sangster (1981) observed in video recordings of North Sea cod (27–45 cm) that larger fish were capable of swimming in the trawl mouth for 50–70 s, while smaller cod tended to exhaust within 20–40 s. Quantitative data on the endurance of individual cod remain otherwise limited but are necessary in order to adequately test the hypothesis of length-dependent endurance while swimming in the trawl mouth.

Although empirical data have never been presented, it is generally assumed that the catchability of groundfish species is greatly enhanced at low temperatures due to a reduction in swimming performance (e.g., Foster et al. 1981; He 1993; Smith and Page 1996). Laboratory studies investigating the endurance of cod at different temperatures have lent support to this hypothesis (Beamish 1966; He 1991). However, direct video observations have indicated that large cod (>80 cm) are in fact capable of swimming in the trawl mouth for a considerable time and distance at temperatures well below 0.0°C (S.J. Walsh and W. Hickey, Department of Fisheries and Oceans, Northwest Atlantic Fisheries Centre, St. John's, NF A1C 5X1, Canada, personal communication). Our results suggest that water temperature may not impact the swimming endurance of cod in the trawl mouth. We suggest that a seasonal thermal compensation in the swimming performance of cod may be responsible for the maintenance of endurance at low temperatures.

In summary, our findings indicate that the swimming endurance of cod native to Newfoundland waters is highly dependent on swimming speed while being independent of both fish size and water temperature, given the size and temperature ranges tested. The findings suggest that the catching efficiency of cod by otter trawls may be highly sensitive to changes in towing speed due to differential vulnerability to capture.

Acknowledgements

This project was funded through Department of Fisheries and Oceans ADM Strategic Science Project No. 9040 and by the Fisheries and Marine Institute of the Memorial University of Newfoundland. The manuscript benefitted greatly from reviews by David Cote and Helga Guderley. Thanks are given to G. Legge at the Fisheries and Marine Institute for his assistance with the swimming flume and to P. Higdon, D. Orr, and M. Veitch for the collection and care of live fish. Special thanks go to N. Cadigan and S. Smith at the Department of Fisheries and Oceans for statistical consultation.

References

Bainbridge, R. 1960. Swimming and stamina in three fish. J. Exp. Biol. **37**: 129–153.

Beamish, F.W.H. 1966. Swimming endurance of some Northwest Atlantic fishes. J. Fish. Res. Board Can. **23**: 341–347.

Beamish, F.W.H. 1969. Photographic observations on reactions of fish ahead of otter trawls. Proceedings of the FAO Conference on Fish Behaviour in Relation to Fishing Techniques and Tactics, Bergen, 19–27 October 1967. FAO Fish. Rep. **3**(62): 511–521.

Beamish, F.W.H. 1978. Swimming capacity. *In* Fish physiology. Vol. 7. *Edited by* W.S. Hoar and D.J. Randall. Academic Press, New York. pp. 101–187.

Bell, W.H., and Terhune, L.D.B. 1970. Water tunnel design for fisheries research. Fish. Res. Board Can. Tech. Rep. No. 195.

Bernatchez, L., and Dodson, J.J. 1985. Influence of temperature and current speed on the swimming capacity of lake whitefish (*Coregonus clupeaformis*) and cisco (*C. artedi*). Can. J. Fish. Aquat. Sci. **42**: 1522–1529.

Brett, J.R. 1967. Swimming performance of sockeye salmon (*Oncorhynchus nerka*) in relation to fatigue time and temperature. J. Fish. Res. Board Can. **24**: 1731–1741.

Brett, J.R. 1982. The swimming speed of adult pink salmon, *Oncorhynchus gorbuscha*, at 20°C and a comparison with sockeye salmon, *O. nerka*. Can. Tech. Rep. Fish. Aquat. Sci. No. 1143.

Carrothers, P.J.G. 1981. Catch variability due to variations in groundfish otter trawl behaviour and possibilities to reduce it through instrumented fishing gear studies and improved fishing procedures. Can. Spec. Publ. Fish. Aquat. Sci. No. 58. pp. 247–257.

Clark, D.S., and Green, J.M. 1990. Activity and movement patterns of juvenile Atlantic cod, *Gadus morhua*, in Conception Bay, Newfoundland, as determined by sonic telemetry. Can. J. Zool. **68**: 1434–1442.

Cox, D.R., and Oakes, D. 1984. Analysis of survival data. Chapman and Hall, London, U.K.

DeAlteris, J.T., and La Valley, K.J. 1999. Physiological response of scup, *Stenotomus chrysops*, to a simulated trawl capture and escape event. Mar. Technol. Soc. J. **33**(2): 25–34.

Department of Fisheries and Oceans. 1998. Integrated fisheries management plan: Atlantic groundfish 1998. Department of Fisheries and Oceans, Ottawa, Ont.

Duthie, G.G. 1982. The respiratory metabolism of temperature-adapted flatfish at rest and during swimming activity and the use

© 2000 NRC Canada

of anaerobic metabolism at moderate swimming speeds. J. Exp. Biol. **97**: 359–373.

Engås, A. 1994. The effects of trawl performance and fish behaviour on the catching efficiency of demersal sampling trawls. *In* Marine fish behaviour in capture and abundance estimation. *Edited by* A. Fernö and S. Olsen. Fishing News Books, Oxford, U.K. pp. 45–68.

Foster, J.J., Campbell, C.M., and Sabin, G.C.W. 1981. The fish catching process relevant to trawls. Can. Spec. Publ. Fish. Aquat. Sci. No. 58. pp. 229–246.

Foster, A.R., Hall, S.J., and Houlihan, D.F. 1993. The effects of temperature acclimation on organ/tissue mass and cytochrome *c* oxidase activity in juvenile cod (*Gadus morhua*). J. Fish Biol. **42**: 947–957.

Glass, C.W., and Wardle, C.S. 1989. Comparison of the reactions of fish to a trawl gear, at high and low light intensities. Fish. Res. **7**: 249–266.

Godø, O.R., Walsh, S.J., and Engås, A. 1999. Investigating density-dependent catchability in bottom trawl surveys. ICES J. Mar. Sci. **56**: 292–298.

Guderley, H., and Blier, P. 1988. Thermal acclimation in fish: conservative and labile properties of swimming muscle. Can. J. Zool. **66**: 1105–1115.

Hammer, C. 1995. Fatigue and exercise tests with fish. Comp. Biochem. Physiol. A, Comp. Physiol. **112**: 1–20.

He, P. 1991. Swimming endurance of Atlantic cod, *Gadus morhua* L., at low temperatures. Fish. Res. **12**: 65–73.

He, P. 1993. Swimming speeds of marine fish in relation to fishing gears. ICES Mar. Sci. Symp. **196**: 183–189.

He, P., and Wardle, C.S. 1988. Endurance at intermediate swimming speeds of Atlantic mackerel, *Scomber scombrus* L., herring, *Clupea harengus* L., and saithe, *Pollachius virens* L. J. Fish Biol. **35**: 255–266.

Lee, E.T. 1992. Statistical methods for survival data analysis. 2nd ed. John Wiley & Sons, Inc., New York.

Main, J., and Sangster, G.I. 1981. A study of the fish capture process in a bottom trawl by direct observations from a towed underwater vehicle. Scott. Fish. Res. Rep. No. 23.

Nelson, J.A., Tang,Y., and Boutilier, R.G. 1994. Differences in exercise physiology between two Atlantic cod (*Gadus morhua*) populations from different environments. Physiol. Zool. **67**: 330–354.

North Atlantic Fisheries Organization. 1998. Conservation and enforcement measures. NAFO/FC Doc. 98/1 Ser. No. N2976.

Norušis, M.J. 1994. SPSS advanced statistics 6.1. SPSS Inc., Chicago, Ill.

Peake, S., Beamish, F.W.H., McKinley, R.S., Katopodis, C., and Scuton, D.A. 1995. Swimming performance of lake sturgeon, *Acipenser fulvescens*. Can. Tech. Rep. Fish. Aquat. Sci. No. 2063.

Smith, J.C., and Chong, C.K. 1982. Body weight, activities of cytochrome oxidase and electron transport system in the liver of the American plaice *Hippoglossoides platessoides*. Can these activities serve as indicators of metabolism? Mar. Ecol. Prog. Ser. **9**: 171–179.

Smith, S.J., and Page, F.H. 1996. Associations between Atlantic cod (*Gadus morhua*) and hydrographic variables: implications for the management of the 4VsW cod stock. ICES J. Mar. Sci. **53**: 597–614.

Videler, J.J. 1993. Fish swimming. Chapman and Hall, London, U.K.

Walsh, S.J., and Hickey, W.M. 1993. Behavioural reactions of demersal fish to bottom trawls at various light conditions. ICES Mar. Sci. Symp. **196**: 68–76.

Wardle, C.S. 1993. Fish behaviour and fishing gear. *In* Behaviour of teleost fishes. 2nd ed. *Edited by* T.J. Pitcher. Chapman and Hall, London, U.K. pp. 609–643.

Winger, P.D., He, P., and Walsh, S.J. 1999. Swimming endurance of American plaice (*Hippoglossoides platessoides*) and its role in fish capture. ICES J. Mar. Sci. **56**: 252–265.

Wroblewski, J.S., Wade, L.B., and Howse, K.A. 1994. Observations of adult Atlantic cod (*Gadus morhua*) overwintering in nearshore waters of Trinity Bay, Newfoundland. Can. J. Fish. Aquat. Sci. **51**: 142–150.

Xu, G., Shirai, T., and Arimoto, T. 1994. Endurance and muscle lactic acid of swimming jack mackerel. Fish. Sci. **60**: 657–659.

© 2000 NRC Canada

Effects of fish on plankton dynamics: a theoretical analysis

Marten Scheffer, Sergio Rinaldi, and Yuri A. Kuznetsov

Abstract: We present an expansion of a classical minimal *Daphnia*–algae model to account for effects of fish as a top predator. Our analyses suggest that in most situations, the plankton should show hysteresis in response to predation pressure by fish. Thus, there exist two distinct regimes, one in which *Daphnia* is controlled (overexploited) by fish and phytoplankton biomass is high and another in which *Daphnia* is relatively unaffected (underexploited) by planktivores and algae are controlled by *Daphnia*. Switches from one regime to the other occur abruptly at a critical fish density. This is in line with field observations and experimental results. Our model predicts that the critical fish density for *Daphnia* collapse is higher in systems with higher ambient nutrient concentrations. The model also shows how intrinsic predator–prey oscillations in the planktonic system can facilitate the switch to the algal-dominated regime where *Daphnia* is controlled by fish. In terms of dynamical systems theory, this switch happens through a homoclinic bifurcation. In biological terms, *Daphnia* collapses due to food limitation and is subsequently overexploited by fish. This is indeed the sequence of mechanisms observed at the end of the spring clearwater phase in lakes where *Daphnia* is absent during the summer when the biomass of young-of-the-year planktivorous fish becomes high.

Résumé : Nous présentons une expansion d'un modèle classique minimal *Daphnia*–algues pour rendre compte des effets des poissons comme prédateurs supérieurs. Nos analyses permettent de penser que, dans la plupart des situations, le plancton devrait manifester une hystérésis en réponse à la pression de prédation des poissons. Il existe donc deux régimes distincts, l'un dans lequel *Daphnia* est contrôlée (surexploitée) par les poissons et où la biomasse phytoplanctonique est élevée, et un autre régime dans lequel *Daphnia* est relativement peu affectée (sous-exploitée) par les planctonophages, et où les algues sont contrôlées par *Daphnia*. Les passages d'un régime à l'autre se produisent de façon brutale à une densité critique de poissons, ce qui concorde avec les observations de terrain et les résultats expérimentaux. Notre modèle prédit que la densité critique de poissons pour l'effondrement de *Daphnia* est plus élevé dans les systèmes où les concentrations ambiantes de nutriants sont plus élevées. Le modèle montre aussi que les oscillations intrinsèques de la relation prédateur–proie dans le système planctonique peuvent faciliter le passage au régime dominé par les algues dans lequel *Daphnia* est contrôlée par les poissons. En termes de théorie des systèmes dynamiques, ce passage se produit par le biais d'une bifurcation homocline. En termes biologiques, l'effondrement de *Daphnia* est dû à une limitation de la nourriture, et le crustacé est ensuite surexploité par les poissons. Il s'agit là exactement de la séquence de mécanismes observée à la fin de la phase printanière d'eau claire dans les lacs où *Daphnia* est absente pendant l'été au moment où s'élève la biomasse des jeunes de l'année des poissons planctonophages.

[Traduit par la Rédaction]

Introduction

There is a long tradition of using simple predator–prey models to describe the dynamics of *Daphnia* and algae (e.g., Rosenzweig 1971; Caughley and Lawton 1981). Although such models more or less mimic the oscillations observed in the laboratory and in the field, there are conspicuous differences between the predicted patterns and observed dynamics. Real oscillations, for instance, are typically faster and smaller than the ones produced by models (McCauley and Murdoch 1987; McCauley et al. 1990). Also, enrichment tends to lead to an increase in both *Daphnia* and algae and not to an increase in *Daphnia* alone, as predicted by the classical models (Sarnelle 1992). Several factors may explain these discrepancies, but the unrealistic predictions may largely be accounted for by the fact that lakes are not homogeneously mixed systems, as implicitly assumed in the classical models (Scheffer and DeBoer 1995).

Although the interaction of *Daphnia* and algae explains the occurrence of oscillations, many of the interesting patterns in plankton dynamics in the field are known to be driven at least in part by predation by planktivorous fish.

Received October 21, 1998. Accepted January 12, 2000.
J14848

M. Scheffer.[1] Aquatic Ecology and Water Quality Management Group, Department of Environmental Sciences, Wageningen Agricultural University, P.O. Box 8080, NL-6700 DD Wageningen, The Netherlands.
S. Rinaldi. CIRITA, Politecnico di Milano, Via Ponzio 34/5, 20133 Milano, Italy.
Y.A. Kuznetsov. Mathematical Institute, Utrecht University, Postbus 80.010, 3508 TA Utrecht, The Netherlands, and Institute of Mathematical Problems to Biology, Russian Academy of Sciences, Pushchino, Moscow Region, 142292 Russia.

[1]Author to whom all correspondence should be addressed. e-mail: marten.scheffer@aqec.wkao.wau.nl

© 2000 NRC Canada

The discussion about effects of fish on plankton was triggered by Hrbácek et al. (1961), who drew attention to the large differences between the plankton of different ponds depending on the presence of fish. In ponds with fish, zooplankton consisted mainly of small-bodied species and algal biomass was high. In ponds without fish, phytoplankton biomass was low and larger herbivores like *Daphnia* dominated the zooplankton. Soon after, Brooks and Dodson (1965) observed similar relationships in New England lakes and developed the so-called "size-efficiency hypothesis" to explain such shifts.

Later work confirmed Brooks and Dodson's (1965) suggestion that high densities of planktivorous fish lead to zooplankton communities dominated by small, relatively inefficient grazers (Shapiro and Wright 1984; Hambright 1994; Seda and Duncan 1994), although fish effects on zooplankton community are less predictable than originally thought. Selective predation by fish not only removes larger zooplankters, but behavior and life history strategy of some *Daphnia* clones also change in response to chemicals released by fish (Dodson 1988; De Meester et al. 1995; Stirling 1995), leading to a smaller average size of individuals (Weider and Pijanowska 1993; Engelmayer 1995). Lakes with a high fish stock are frequently dominated by large filamentous blue-green algae, which have been shown to inhibit the growth of large-bodied *Daphnia* species under some conditions (Gliwicz 1990; Gliwicz and Lampert 1990), suggesting an additional explanation for their absence in such lakes. Obviously, a complex interplay of mechanisms leads to shifts in size distributions of zooplankton and algae in the field. The problem becomes much simpler when considering strong top-down control of algal biomass, as observed during the often-studied spring clearwater phase (e.g., Lampert et al. 1986; Luecke et al. 1990) or after elimination of fish by natural winterkills (Schindler and Comita 1972; Sarnelle 1993) or human interference (e.g., Shapiro and Wright 1984; Van Donk et al. 1990). In virtually all of these cases, large-bodied *Daphnia* were responsible for grazing down algal biomass to very low levels, and repression of large *Daphnia* is typically explained by fish predation, as illustrated by the winterkill and biomanipulation cases. Although the "trophic cascade" of fish, large *Daphnia*, and algae is clearly important, details of the resulting patterns are not always straightforward. Field studies (Mills et al. 1987) and enclosure experiments (McQueen and Post 1988) indicate that *Daphnia* populations collapse at a critical fish density rather than becoming gradually less abundant with increasing predation pressure. Also, although fish predation seems to be a main mechanism in keeping *Daphnia* numbers low, actual collapse of *Daphnia* most often seems due to food shortage (Mills and Forney 1981; Luecke et al. 1990).

In this paper, we show that an extension of a traditional "minimal" model of *Daphnia* and algae helps to explain many of the patterns observed in the field. In the first section, we present the model and explain the rationale behind the formulation. The subsequent Results section gives a systematic analysis of the effects variation in fish predation pressure on the model using isocline analysis, plots of equilibria and cycles, and bifurcation analysis. We discuss how the model predictions relate to field patterns and conclude with three testable hypotheses about the effect of planktivory on plankton dynamics.

Methods

Model

We used a model of plankton dynamics consisting of two differential equations, one for edible algae (A) and one for large herbivorous zooplankton (Z):

$$(1)\qquad \frac{dA}{dt} = rA\left(1-\frac{A}{K}\right) - Zg\left(\frac{A}{A+h_A}\right) + i(K-A)$$

$$(2)\qquad \frac{dZ}{dt} = egZ\left(\frac{A}{A+h_A}\right) - mZ - F\left(\frac{Z^2}{Z^2+h_Z^2}\right).$$

Algal growth is basically logistic with a maximum growth rate of r and a carrying capacity of K. Losses are due to grazing by zooplankton following a simple saturating (type II) functional response formulated as a Monod function of algal density with a half-saturation value of h_A and a maximum per capita grazing rate of g. A small diffusive inflow, i, proportional to the concentration difference between the algae in the studied part and those in an ungrazed refugium where algae are at carrying capacity is also added. Food intake by zooplankton is converted into growth with an efficiency of e. In addition to a fixed mortality, m, zooplankton suffers losses from predation depending on the planktivorous capacity, F, of the fish community, and the value of the sigmoidal (type III) functional response of fish with a half-saturation value of h_Z. Reference values and dimensions of all parameters are summarized in Table 1.

This or comparable formulations have often been used to describe the interaction of *Daphnia* and algae (e.g., Rosenzweig 1971; Caughley and Lawton 1981; Scheffer 1991). Incorporation of the stabilizing inflow term ($i(K - A)$) and the formulation of planktivory are probably the least "classical" parts of the model and deserve some further explanation.

The rationale behind the use of the stabilizing inflow term is given extensively elsewhere (Scheffer and DeBoer 1995). In fact, this term could be left out of the model without affecting any of the qualitative results that we present. However, use of this stabilizing term makes the quantitative patterns generated by simple plankton models far more realistic. As a rule, field oscillations in plankton are much smaller than those produced by a wide range of minimal models. This is because stabilizing mechanisms are missing from such models. Scheffer and DeBoer (1995) summarized such mechanisms and argued that patchiness has strong stabilizing effects and that, in fact, there are virtually no spatially homogeneous plankton communities. The formulation used here corresponds to a first-order Taylor expansion approximation of the more elaborate model of spatial heterogeneity presented in the cited paper. We further simplified the compound term ($dl/(1 - f)$) used by Scheffer and DeBoer (1995) to one parameter (i).

With respect to the formulation of planktivory, it should be noted that we do not model fish dynamically. We analyze seasonal effects of varying fish predation pressure, but we do not model fish growth as a function of zooplankton consumption (see Doveri et al. (1993) for an example where a fish is modeled dynamically). Although fish benefit from consumption of *Daphnia*, this food is usually just a portion of their diet. Therefore, overall fish density depends on the lake productivity but does not react as directly to *Daphnia* density as *Daphnia* dynamics respond to phytoplankton. Therefore, it is reasonable to study the impact of fish on *Daphnia* dynamics without directly considering the effects of *Daphnia* on the population dynamics of fish. Also, it should be noted that the

© 2000 NRC Canada

Table 1. Reference parameter values and their dimensions.

Symbol	Value	Units	Definition
r	0.5	day^{-1}	Maximum growth rate algae
K	10	mg dry weight·L^{-1}	Carrying capacity algae
g	0.4	day^{-1}	Maximum grazing rate zooplankton
h_A	0.6	mg dry weight·L^{-1}	Half-saturation functional response zooplankton
i	0.01	—	Diffusive inflow of algae
e	0.6	—	Food transfer efficiency zooplankton
m	0.15	day^{-1}	Loss term zooplankton
h_Z	0.5	mg dry weight·L^{-1}	Half-saturation functional response fish

predation loss term, $F(Z^2/(Z^2 + h_Z^2)$, in the zooplankton equation represents the impact of the fish community as a whole. In reality, different groups of fish forage on *Daphnia* with different functional responses. Therefore, this term is really just a pragmatic solution to mimic the effect of many different animals switching to foraging on *Daphnia* at different moments with different efficiencies. Because most of the larger individuals usually switch to *Daphnia* only when the latter are quite abundant (Mills and Forney 1983; Lammens 1985), predation pressure is likely to increase more than linearly with *Daphnia* density over this initial range. Because of this prey-switching behavior of fish, the overall functional response is likely to be sigmoidal. The maximum consumption rate (F) is set directly rather than as the product of the fish biomass and their weight-specific maximum intake. The latter is not easily defined for a whole community because large animals consume less per gram of body weight than small ones.

Analysis

The aim of our analysis is to check which patterns in plankton dynamics may be explained from the mechanisms included in the model. To do this, we first need to produce a complete overview of the behavioral repertoire of the model. The simplest approach to produce such an overview is to run the model for all reasonable combinations of parameter values and starting from all different initial states. However, one of the merits of minimal models such as the one presented here is that they can be analyzed thoroughly by means of more sophisticated techniques. The most classical of those techniques is to plot the zero-growth isoclines of the two species for different parameter values and use these to understand which types of equilibria can arise under different conditions. We start our analysis with such an isocline approach, supplemented by simulations showing the nature of cycles that occur under soime conditions.

A powerful and more recent approach is to focus on the "bifurcations" of the model (e.g., Kuznetsov 1995). Contrary to simulation, bifurcation analysis does not provide information about the transient dynamics of the system starting from a certain initial state. Instead, it focuses on the asymptotic behavior (attractors) to which the model settles if it is allowed to run for a sufficiently long period of time (and on repellors, which are the opposite). Attractors can be equilibria, but also cycles, or more complex types of structures such as strange attractors. If one changes the value of a parameter in a model slightly, the usual effect is that the attractors change only slightly too. For instance, an equilibrium concentration of algae may increase a little if the nutrient concentration in the model is increased somewhat. However, it can also be that if a certain crucial threshold value of a parameter is reached, the nature of the attractor really changes in an important way. This is called a bifurcation. For instance, a stable equilibrium may change into a cyclic attractor on which the system oscillates (a "Hopf bifurcation"), or an equilibrium may disappear, implying a "catastrophic transition" of the system to another state (e.g., a "fold bifurcation"). It can also be that an intrinsic oscillation in the system becomes large enough to bring it within the basin of attraction of another attractor, inducing a catastrophic transition ("homoclinic bifurcation"). Obviously, bifurcations are of particular interest, as they mark crucial changes in the model behavior. Therefore, finding bifurcations is an efficient way to produce maps of the parameter space showing areas that are essentially different with respect to the types of attractors that occur.

In the first part of the Results section, we use isocline analysis and simulations to show how an increase in fish predation may affect plankton dynamics in the model and to explain which types of bifurcations may arise. In the next part, we expand the analysis by looking at the combined effects of fish and nutrients, using graphs that show the effects of fish under different conditions, and also a full bifurcation analysis. The final part focuses on the fact that fish predation varies over the season and shows how the model may be used to explain some aspects of seasonal patterns of plankton dynamics from this.

Results

Effects of fish on equilibria and cycles

We start our study of the impact of fish on the zooplankton–algae interaction by looking at its effect on the zero-growth isoclines. In the absence of fish, the isoclines of zooplankton and algae are the classical ones, except that the algal isocline bends up asymptotically at the left (Fig. 1). The latter is due to the small diffusive inflow, used to mimic the stabilizing effect of spatial heterogeneity (Scheffer and DeBoer 1995). The intersection of the zero-growth isoclines is a point in which (by definition) growth of both populations is zero, implying that the system is in equilibrium. However, in this case, it is an unstable equilibrium. The asymptotic behavior to which the system tends irrespective of the initial mix of Z and A is a stable limit cycle (indicated by the dashed line with arrowheads). The effect of increasing fish density is mimicked by means of the parameter F. Because fish occurs only in the zooplankton equation, the algal isocline remains unaffected. The zooplankton isocline, however, starts bending out with increasing fish (Fig. 2). This causes the existing intersection to move to the right but also causes new intersections when the bend in the Z isocline hits the algal isocline.

A more complete overview is obtained by adding fish as an extra dimension to the isocline picture (Fig. 3). This representation shows how the intersections change smoothly with fish predation to form one continuous equilibrium curve. Projected in the fish–algae plane or the fish–zooplankton plane, this curve shows an S shape, indicating a hysteresis of the planktonic system with respect to changes in fish (Fig. 4). Alternative equilibria exist over a range of

© 2000 NRC Canada

Fig. 1. Zero growth isoclines of zooplankton ($dZ/dt = 0$) and algae ($dA/dt = 0$) and the limit cycle (dashed line) of the model in the absence of fish predation. The intersection of the isoclines is an unstable point. The asymptotic increase in the algal isocline at low algal densities is caused by the diffusive inflow term in the algal growth equation. Due to this inflow, the predator–prey oscillations are not extremely large as in the classical minimal models.

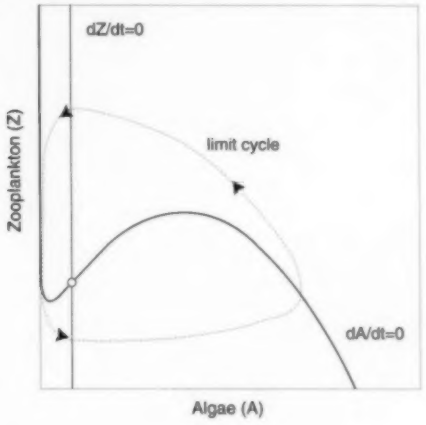

Fig. 2. Effect of fish predation (G_f) on the isoclines. The zooplankton isocline bends out with increasing fish density, while the algal isocline remains unaffected. Solid circles denote stable equilibria, and open circles denote unstable ones. The half-open circles and corresponding isoclines are associated with fold bifurcations.

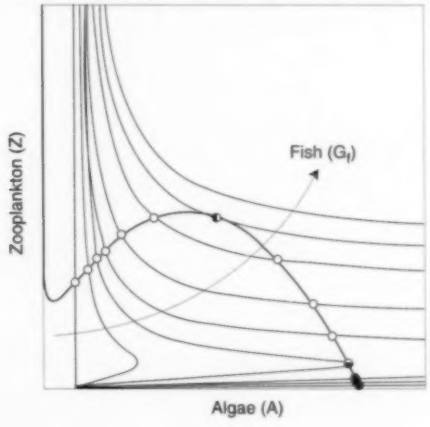

intermediate fish densities ($F_1 < F < F_2$). The behavior of this system, however, is very different from that of most classical hysteresis models, because in this case, one of the branches is the unstable focus of a limit cycle (except for a small part where it is stable, $H < F < F_2$).

To understand the implications of the limit cycles, it is informative to look directly at the effects of fish on the equilibria and cycles (Fig. 5). Snapshots at fixed fish densities (Fig. 6) clarify the link to the change in isoclines. For zero fish, we have a limit cycle where zooplankton and algae oscillate (grey cylinder in Fig. 5). Increasing fish in Fig. 5, we

Fig. 3. Zero-growth surfaces of zooplankton and algae (the manifolds $dZ/dt = 0$ and $dA/dt = 0$) obtained by adding fish (G_f) as an extra dimension to the isocline picture. The intersection of these surfaces represents the system's stable and unstable equilibria (corresponding to the intersection points in Fig. 2).

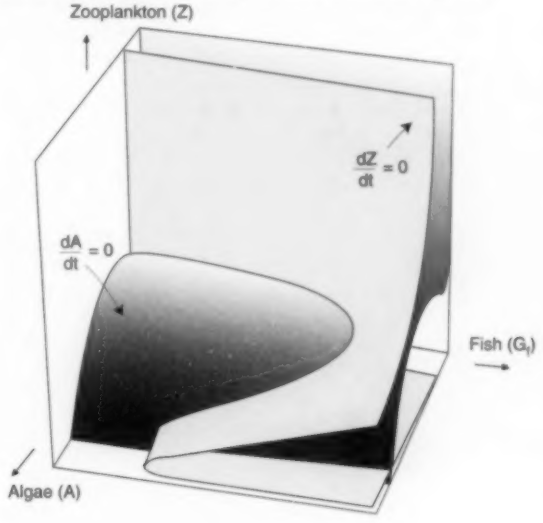

first arrive at a bend in the equilibrium curve called a fold bifurcation (F_1) (Guckenheimer and Holmes 1983; Kuznetsov 1995). At fish densities beyond this point, two new equilibria are found in addition to the cycle that already existed. One of these equilibria is stable (solid line). The other one (dashed line) is unstable and is called a "saddle." The stable equilibrium (the solid line rooted in F_1) has almost no zooplankton and a high algal density. In view of the corresponding state of the lake water, we refer to it hereafter as the "green state" for short.

The unstable equilibrium (dashed line between F_1 and F_2) marks the border between the basins of attraction of the limit cycle and the green state. This can be understood better from the isocline representation (Fig. 6). In terms of isoclines, the fold bifurcation (F_1) occurs when the zooplankton isocline hits the algal isocline, giving rise to two new intersections, the saddle and the node (Fig. 6*a*). Increasing fish predation further, the saddle and the node move apart until the saddle collides with the limit cycle (Fig. 6*b*). This is a so-called homoclinic bifurcation (O_1). It implies the disappearance of the limit cycle, as beyond this bifurcation, all trajectories end up in the green state (Fig. 6*c*).

Increasing fish more, one can see in Fig. 5 that a limit cycle reappears through a second homoclinic bifurcation (O_2). Then, for higher fish predation, the limit cycle shrinks and becomes a stable point (at the Hopf bifurcation (H)). The last qualitative change with increasing fish density is a fold bifurcation (F_2) again (also see Fig. 6*d*). The stable point (the line between H and F_2) now collides with the saddle. The whole right-hand part (Fig. 5), from O_2 to F_2, is mainly of theoretical interest, as the system will normally not arrive at those attractors. This can be seen if we imagine the response of the system to changes in fish predation. A simulation with slowly increasing F, starting from zero fish, will

© 2000 NRC Canada

Fig. 4. Two-dimensional projections of the intersection of the surfaces in Fig. 3. The resulting hysteresis graphs show how the density of (*a*) zooplankton and (*b*) algae in equilibrium depends on the fish predation pressure. For intermediate fish densities ($F_1 < F < F_2$), the system has alternative equilibria in which either zooplankton or algae dominate. The dashed parts of the curves represent unstable equilibria. The segment between fold bifurcations F_1 and F_2 consists of "saddle points" that mark the border between the basins of attraction of the two alternative attractors (also see Fig. 6). The algal-dominated branch consists of stable equilibria. The zooplankton-dominated branch of the equilibrium curve, however, is the unstable focus of a limit cycle except for a small part where it has gone through a Hopf bifurcation (*H*).

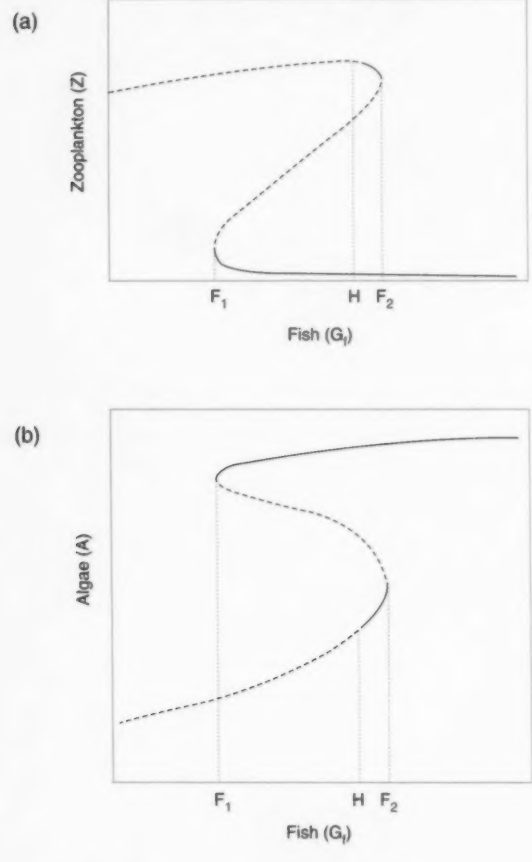

show oscillations until the homoclinic (O_1) is reached. At this threshold, the system jumps to the only remaining stable equilibrium, namely the algal-dominated lower branch of the hysteresis that we termed the green state. Here it will stay, no matter how much the fish predation is increased. Lowering the amount of fish from this point, the system will remain in the green state until F_1 is reached. At this point, it will jump back to the oscillatory mode. Only a disturbance could potentially move the system toward the attractors around *H*. However, since their basins of attraction are rather small, this is unlikely to happen. For all practical purposes, we can therefore ignore this part of the diagram.

Fig. 5. Schematic representation of the effect of fish predation pressure on the equilibria and cycles of the system. Points F_1 and F_2 are fold bifurcations. At the Hopf bifurcation (*H*), the limit cycle changes into a stable point. Furthermore, the limit cycle does not exist between the two homoclinic bifurcations (O_1 and O_2) where it collides with the saddle that marks the border of the basin of attraction of the stable algal-dominated equilibrium. Note that the plankton oscillations along the limit cycle cause the system to settle in the algal-dominated stable state (solid line from F_1) if fish increases beyond O_1.

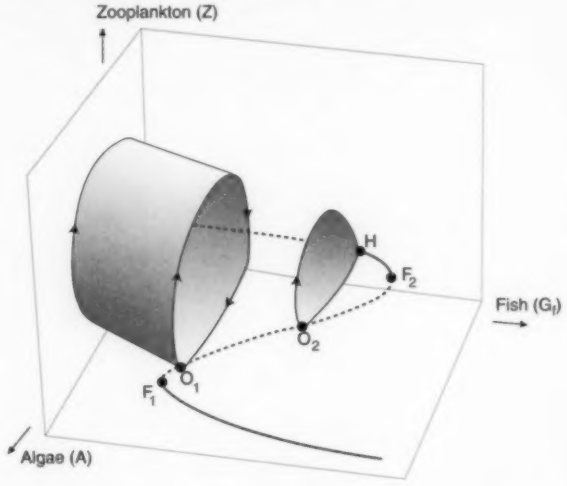

Combined effects of nutrients and fish

Importantly, if the nutrient concentration or other parameter values are different, the response of the model to fish may be quite different from the one presented in Fig. 5. In fact, the above scenario with five bifurcations is one of the most complex ones that can arise, although there may also be an extra Hopf bifurcation (*H*) for low fish densities (Fig. 7*a*). Most changes in parameters will let the complex scenario degenerate into more simple cases. The *H* and the homoclinic O_2 on the right part of the figure, for instance, can be absent (Fig. 7*b*). Another simplification occurs when F_1 and O_1 coincide (Fig. 7*c*). The limit cycle can also remain sufficiently small to avoid touching the saddle. In that case, homoclinic bifurcations do not occur (Fig. 7*d*). The simplest situations arise if there are no oscillations (Fig. 7*e*) and eventually no folds (Fig. 7*f*). In the latter case, there are no bifurcations at all, and the system responds smoothly to an increase in fish, shifting from a stationary regime with predominantly *Daphnia* to a regime with mainly algae.

Figure 7 shows the response of the model to fish for only six different combinations of nutrient concentrations and inflow rates (*i*) of algae. A more systematic image of the combined effects of nutrients and fish can be obtained by plotting the lines at which the bifurcations occur in the fish–nutrients plane (Fig. 8). Since the bifurcations mark all qualitative changes in equilibria and cycles, such bifurcation diagrams can be interpreted as maps of behavior. We produced the diagrams in Fig. 8 by means of the software packages LOCBIF (Khibnik et al. 1992) and HOMCONT (Champneys and Kuznetsov 1994; Champneys et al. 1996). First, consider

© 2000 NRC Canada

Fig. 6. Trajectories and isocline configurations corresponding to the (*a*) first (F_1) and (*d*) second (F_2) fold bifurcations, the (*b*) first homoclinic (O_1), and (*c*) a fish density in the range between the two homoclinics. Symbols as defined in Fig. 2.

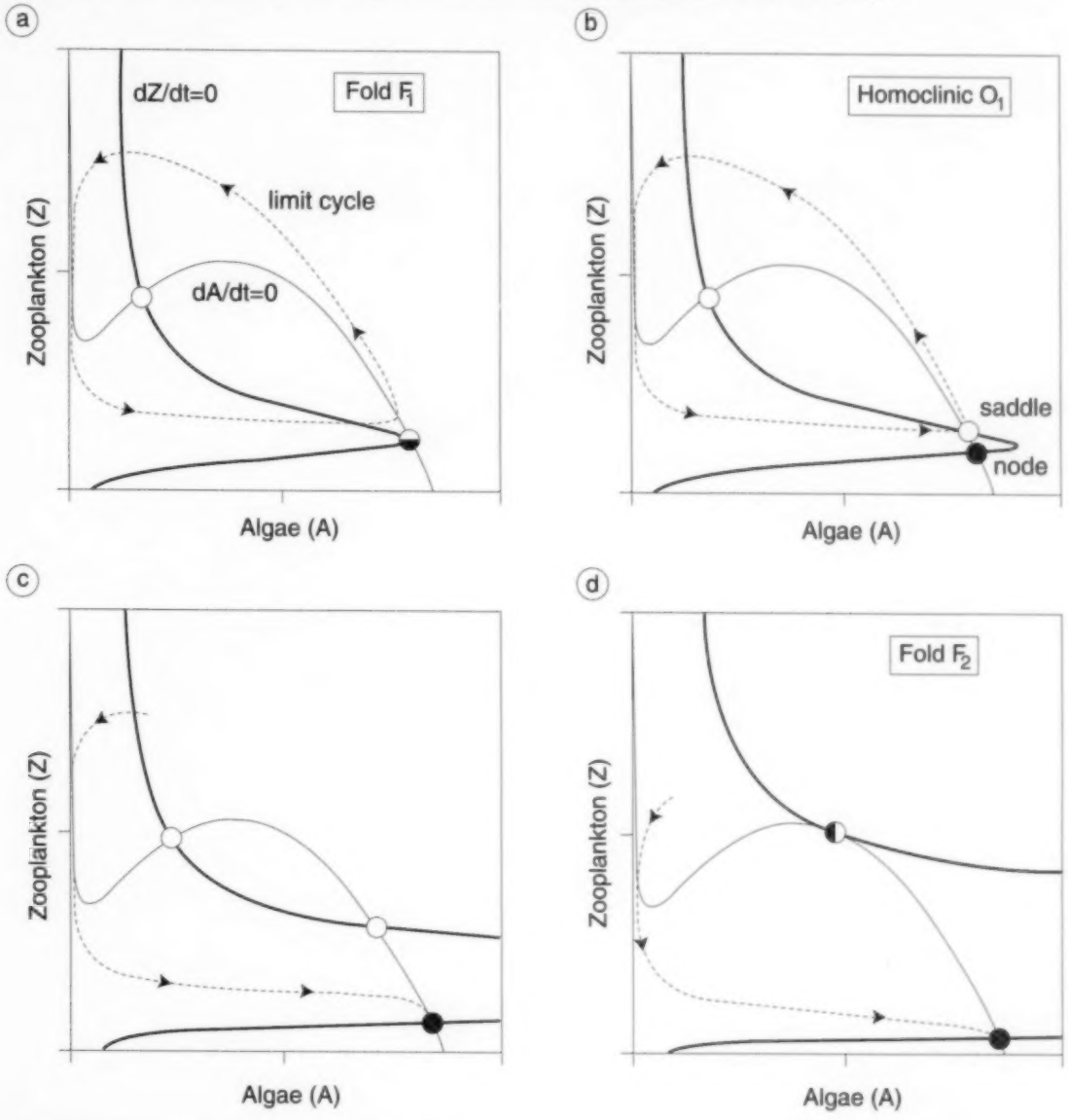

Fig. 8*a*. In the absence of fish ($G_f = 0$), the system reduces to the classical *Daphnia*–phytoplankton model, which has only a Hopf bifurcation (*H*). This bifurcation stays present if fish is increased until it merges with the second fold (F_2) and homoclinic (*O*) bifurcations in a so-called Bogdanov–Takens point (BT). Such points in parameter space where different bifurcations meet are called codimension-two points. Our model has three other codimension-two points: one at which the hysteresis is born and two fold bifurcations emerge (F^*) and two points at which the fold and homoclinic curves merge (F_{O_1} and F_{O_2}). As indicated in the figure, the scenarios of change in equilibria and cycles with fish density (Fig. 7) represent horizontal sections through this bifurcation graph. Obviously, the bifurcation map depends on the values of the other parameters as well. Figure 8*b* shows the effect of an increase in parameter *i* used to mimic the stabilizing effect of a nonhomogeneous spatial distribution of *Daphnia*. If *i* is increased sufficiently, the system does not oscillate in the absence of fish. Increasing fish can be destabilizing in this case, as it can bring the system through the Hopf.

Roughly speaking, all lines in the bifurcation graphs have a positive slope, indicating that in systems that are richer in nutrients (higher algal carrying capacity (*K*)), all bifurcations appear at higher fish levels. The model thus predicts that higher fish densities are associated with a collapse of

© 2000 NRC Canada

Fig. 7. Six qualitatively different diagrams showing the equilibria and cycles of the system that can be obtained by manipulating the carrying capacity for algae (K) and the stabilizing diffusive inflow of algae (i).

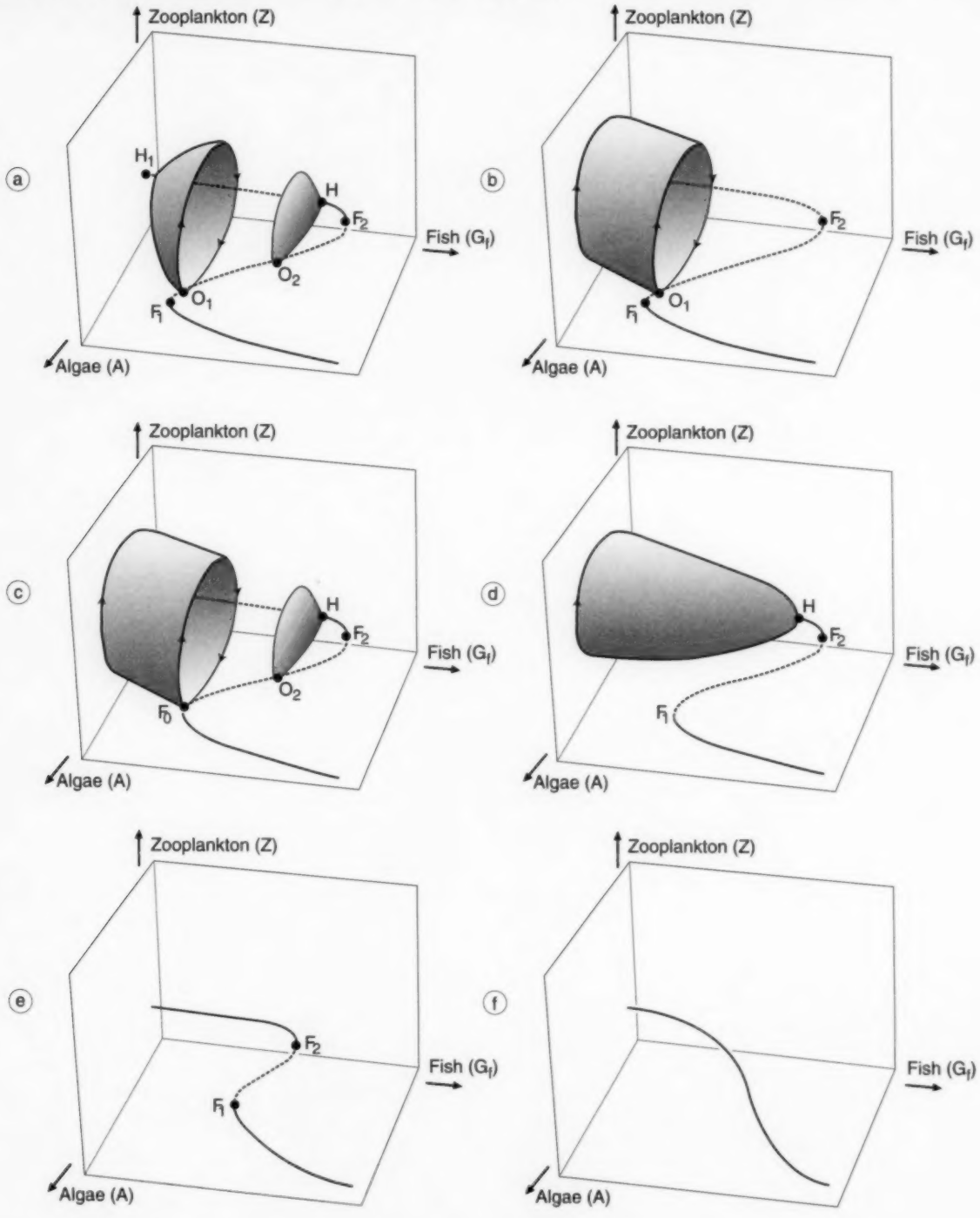

Daphnia as lakes become more eutrophic. There is, however, an important complication on top of this. If K is low enough, the system does not go through homoclinic bifurcations with increasing fish predation, and *Daphnia* does not collapse until the second fold is reached (F_2), whereas if K is larger, *Daphnia* collapses much earlier due to the

© 2000 NRC Canada

Fig. 8. (*a*) Bifurcation diagram showing when the Hopf (*H*), fold (*F*), and homoclinic (*O*) bifurcations occur depending on the fish predation and the carrying capacity for algae (*K*). The horizontal sections that are indicated correspond to the diagrams in Figs. 5 and 7 as indicated. The Hopf, homoclinic, and fold are very close together before merging in the Bogdanov-Takens point (BT), indicating that the part between O_2 and F_2 in Figs. 5 and 7 is very small in reality. Circles denote codimension-two bifurcation points. (*b*) For a higher value of the stabilizing diffusive inflow parameter *i*, the Hopf bifurcation is no longer rooted in the vertical axis, implying that in the absence of fish, there are no plankton oscillations.

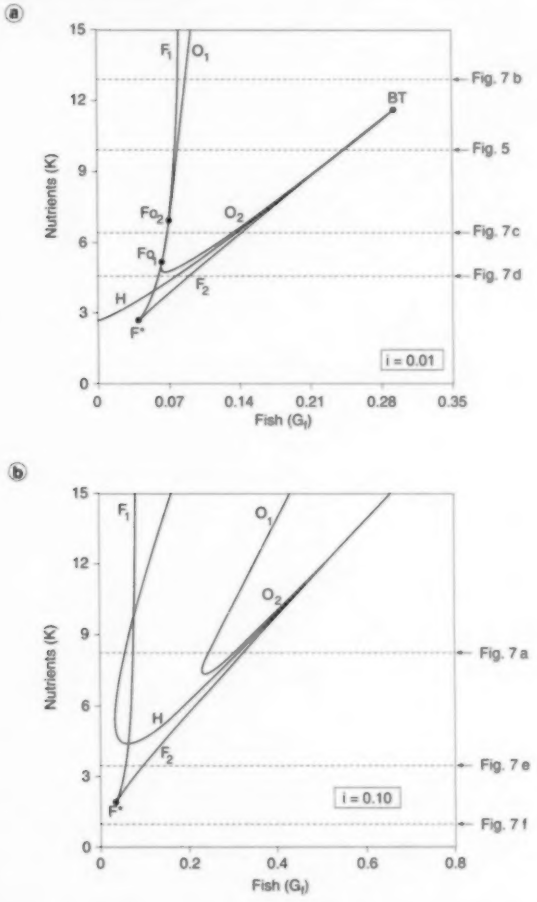

homoclinic bifurcation (O_1). In biological terms, the oscillation in *Daphnia* makes them vulnerable to fish. This is because it periodically brings the density down to a level that is low enough to let a relatively small amount of fish prevent recovery of the population. If there is no such oscillation, a much higher fish predation is needed to let the *Daphnia* population collapse into the overexploited state. Note that in general, any factor that stabilizes *Daphnia* oscillations will help to prevent the homoclinic bifurcation that triggers the collapse of *Daphnia*.

Implications of seasonal variation in fish

Fish predation on *Daphnia* shows a pronounced seasonal cycle. Fish reproduction in spring sets off the development of an often massive cohort of young animals that feed preferentially on zooplankton. The biomass development of the new cohort is a function of individual growth and mortality. Initial growth is very fast, but only a small fraction of the individuals survive to recruit into the second year-class next spring. Effects of consumption by the young-of-the-year fish are cumulative with the rest of the community to produce a peak in planktivory somewhere during summer (Mills and Forney 1983).

To evaluate effects of the annual cycle in planktivory, we focus on the two bifurcations in the model that mark the transitions from the oscillatory regime to the stationary one (O_1) and vice versa (F_1) (Fig. 5). As argued, those are the most important bifurcations in systems where *Daphnia* are not strongly stabilized by factors such as spatial aggregation of zooplankton. Tilting the resulting figure of generalized behavior, we can see how the bifurcations correspond to the seasonal variation in the planktivorous capacity of the fish community (Fig. 9). The exact development of planktivory over the season is obviously difficult to estimate, but if we assume that it can be mimicked in the model by a cycle in the consumptive capacity for plankton (*F*) with a maximum in summer, three qualitatively different scenarios can be distinguished: (I) planktivory remains above the threshold below which *Daphnia* can recover from overexploitation (the fold bifurcation F_1), (II) annual minimum in planktivory is below this threshold, but the maximum is above the threshold at which the oscillating *Daphnia* state collapses due to the homoclinic bifurcation (O_1), and (III) planktivory stays entirely below the homoclinic threshold (O_1).

The first scenario corresponds to lakes where large zooplankters are absent throughout the season and phytoplankton shows no dips due to *Daphnia* grazing. The second situation corresponds to the classical clearwater phase scenario, with a *Daphnia* peak in spring but low *Daphnia* numbers and high algal biomass in summer. The third scenario represents a situation where *Daphnia* keeps oscillating throughout the season.

Fish predation is not the only thing changing over the season. Light and temperature are probably the most important driving forces behind the seasonal cycle in ecosystems, and both factors affect the phytoplankton–zooplankton system directly. Therefore, the current approach of studying the effect of changing fish predation pressure in spring and summer is really too simple to describe the complete annual pattern of plankton dynamics. The consequences of seasonality for the dynamics of the plankton can be analyzed in more detail by periodically varying all parameters of the model that should depend on light or temperature. One way to look at the consequences of such a seasonal variation is to compute the attractors of the system for each day of the year with the appropriate seasonal values of the parameters. Figure 10 is an example produced in this way using a sinusoidal variation of the parameters *r*, *K*, *g*, *m*, and *F* over the season (from high in summer to low in winter). It shows that plankton has the tendency to oscillate in spring and autumn (grey cones) and to be stationary with high algal biomass in summer and stationary with low algal biomass in winter (solid lines). In the middle of summer, the cycles do not exist, and a solid line represents the green state. The discontinuous

© 2000 NRC Canada

Fig. 9. Seasonal variation in biomass of planktivorous fish (right-hand panel) can cause the system to switch between a cycle with periodic *Daphnia* peaks and a stable algal-dominated state, depending on whether the two main bifurcations in the system are crossed. If planktivory is high (I), no *Daphnia* peaks will occur at all. When planktivorous fish stays low (III), *Daphnia* can remain abundant throughout the summer. However, intermediate scenarios cause *Daphnia* to collapse through a homoclinic bifurcation in spring, leaving algae to dominate throughout the summer.

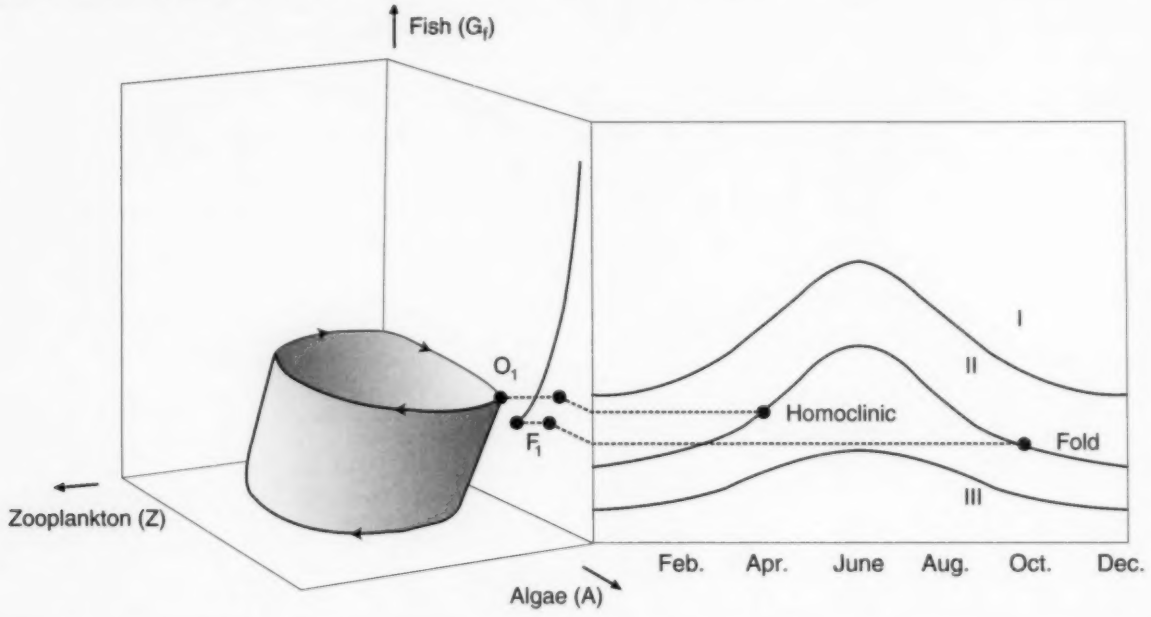

Fig. 10. Equilibria (solid lines) and cycles (grey hemispheres) of the model (eqs. 1 and 2) for any day t of the year using parameter values $r(t)$, $K(t)$, $g(t)$, $m(t)$, and $F(t)$ that are a sinusoidal function of the day number (high in summer and low in winter). The dashed line represents the true dynamics of the seasonally forced model. Note that this trajectory does not follow the sequence of "frozen attractors" for separate days of the year.

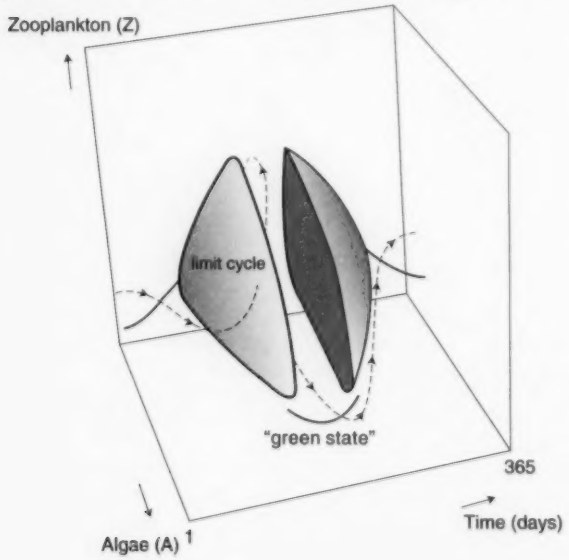

interruption of the cycles in summer corresponds to the homoclinic and fold bifurcations, as discussed above. The dynamic behavior of a periodically forced system cannot really be inferred from such an assemblage of frozen asymptotic behaviors. This becomes apparent if we simulate the dynamics (dashed line in Fig. 10). The values of algae and zooplankton follow the attractor manifolds only approximately. A thorough analysis of the periodically perturbed model requires complex techniques and is presented elsewhere (Scheffer et al. 1997).

Discussion

One of the most robust results of our model is that effects of fish on *Daphnia* are discontinuous. For almost all examined parameter settings, increasing fish predation does not lead to a gradual decline in *Daphnia* but rather to a collapse when a critical fish density is exceeded. Indeed, in limnocorrals where fish biomass increased slowly over the season due to individual growth, zooplankton biomass was shown to respond discontinuously (McQueen and Post 1988), and above a critical fish biomass of around 50 kg·ha^{-1}, zooplankton was severely reduced. Long-term studies of the community dynamics in Lake Oneida also indicate that there is a threshold in predation pressure above which zooplankton collapses (Mills et al. 1987). Here, the most important planktivorous fish is yellow perch (*Perca flavescens*) during the first year of life. The density of age-0 yellow perch differs significantly from year to year. In years in which the density of age-0 yellow perch on August 1 exceeds a threshold of 14 000 individuals·ha^{-1}, the late-summer *Daphnia*

© 2000 NRC Canada

pulex population of the lake appears to collapse completely. In those years, the abundance of phytoplankton is elevated.

In addition to the discontinuous effect of planktivores, our model suggests that *Daphnia* collapse with increasing fish predation normally occurs through what is known in dynamical systems theory as a homoclinic bifurcation. In biological terms, the homoclinic scenario implies that *Daphnia* collapses primarily due to food shortage, whereas recovery of the remaining sparse population is prevented by predation by fish. The traditional explanation for the failure of *Daphnia* to recover from the spring collapse has been that the quality of the algal food in summer is poor due to a dominance of the phytoplankton by inedible algal colonies (Threlkeld 1985; Lampert et al. 1986). However, other evidence suggests that early-summer increase in predation pressure due to the young-of-the-year fish development could be the main mechanism responsible for concurrent suppression of *Daphnia*. In Oneida Lake, New York, for instance, *Daphnia* recovers after the spring collapse only in years when the density of planktivorous young yellow perch is low (Mills and Forney 1981, 1983). Obviously, the effects of predation and of shortage of suitable food are usually strongly intertwined. For example, Luecke et al. (1990) demonstrated that in Lake Mendota, Wisconsin, the number of eggs per adult female *Daphnia* decreased dramatically during the spring peak, indicating food shortage. However, although fertility recovered in summer, *Daphnia* density remained very low after the collapse. Using the egg numbers, the potential reproductive rate of the population was estimated over spring and summer. Comparing this with the realized rate of increase gives an estimate of *Daphnia* mortality. Subsequently, using fish censuses, fish stomach analysis, and bioenergetics models, the *Daphnia* consumption by the fish community was reconstructed over the same period. The results showed that fish consumption accounted completely for *Daphnia* mortality in summer while contributing only 2% to the mortality at the collapse of the spring peak. Obviously, these results fit very well with the homoclinic scenario predicted by our model.

An important assumption that allows the relative simple analysis of our three-level food chain is that the dynamics of the top predator, fish, are relatively slow and independent of those of *Daphnia*. If this assumption cannot be made, things rapidly become more complex. If the top predator is still slow relative to the rest of the system, the singular perturbation approach (Hoppensteadt 1974) can be used as an alternative to fixing top predator density (e.g., Muratori and Rinaldi 1992; Rinaldi and Muratori 1992).

Obviously, there can be factors other than fish affecting the abundance of *Daphnia* in lakes. Peaks of large-bodied *Daphnia* and clearwater phases are often entirely absent, especially in very eutrophic lakes (e.g., Gulati 1983; Meijer et al. 1994; Jeppesen et al. 1996). Here, fish biomass is typically very high, and this may well explain the lack of clearwater phases characteristic of the lakes (Jeppesen et al. 1996). Importantly, however, hypertrophic lakes are also frequently dominated by filamentous blue-greens (e.g., Berger 1975; Sas 1989). Since those algae are not very edible (e.g., Arnold 1971; Schindler 1971), and *Daphnia* growth has been shown to be severely reduced in their presence (Gliwicz 1990; Gliwicz and Lampert 1990), this may contribute to the absence of clearwater phases in hypertrophic lakes. Recent analysis of data from Danish lakes indicates that fish predation tends to be of overriding importance in repressing zooplankton, especially in shallow eutrophic lakes (E. Jeppesen, NERI, Denmark, personal communication). This view is supported by many examples of natural fishkills and biomanipulation experiments where a strong reduction of fish has led to an outbreak of large-bodied *Daphnia*, leading to clear water even in very eutrophic situations (e.g., Shapiro and Wright 1984; Van Donk et al. 1990; Meijer et al. 1994).

Our seasonal analysis (Fig. 9) suggests that complete absence of *Daphnia* peaks is typical for lakes where fish predation is high year-round, whereas the classical spring clearwater phase scenario with subsequent absence of *Daphnia* during the summer is typical of lakes with a moderate fish stock. In lakes with few fish, a longer sequence of zooplankton peaks is predicted to occur within a year. Indeed, many case studies demonstrate that recurrent *Daphnia* peaks can cause several clearwater phases during the summer. Examples are the French Lake Aydat where three *Daphnia* peaks and corresponding clearwater phases were found in one year (Lair and Ayadi 1989) and the German Lake Grosser Binnensee where four *Daphnia* peaks occurred in one season, three of which led to conspicuous clearwater phases (Lampert and Rothhaupt 1991). Also, sequences of *Daphnia* peaks are often observed in the first years after drastic removal of fish from a lake (Munro and Bailey 1980; Van Donk et al. 1990), suggesting that such repeated outbreaks are indeed typical of situations with very few planktivorous fish.

The simple techniques used here are sufficient to show how several important features of plankton dynamics can be understood from a slightly extended classical predator–prey model. However, the approach is not really suitable for addressing dynamics in a seasonally changing environment. A thorough analysis of a periodically perturbed version of the model requires much more complex techniques and is presented elsewhere (Scheffer et al. 1997). The interested reader is also referred to Doveri et al. (1993) for the analysis of an elaborate seasonally forced plankton model.

As do all minimal models, the one analyzed in this paper focuses on a small subset of the mechanisms that operate in the field. Indeed, in any field situation, patterns are obviously affected by a multitude of simultaneously operating mechanisms. Consequently, it would be an illusion to think that one would ever be able to come up with the "right" model (Quinn and Dunham 1983; Roughgarden 1983). Our analysis, however, demonstrates that the simple trophic cascade mechanism in this minimal model is sufficient to potentially account for a wide range of patterns observed in the field. In particular, three major hypothesis are generated by the model. (*i*) The effect of planktivory on plankton dynamics is predicted to be discontinuous. Beyond a critical density of planktivorous fish, *Daphnia* populations collapse. (*ii*) The critical fish density for *Daphnia* is predicted to be higher when the nutrient level of the system is higher. (*iii*) When *Daphnia* dynamics are oscillatory, as during the spring clearwater phase, the collapse with increasing fish predation is predicted to occur through a homoclinic scenario: an initial crash of *Daphnia* density due to food shortage followed by prolonged absence due to fish predation.

© 2000 NRC Canada

Acknowledgements

We highly appreciate the detailed comments by M.G. Butler and two anonymous reviewers. This work was carried out in part at the International Institute of Applied Systems Analysis, Laxenburg, Austria, and has been partially supported by the Italian Ministry of Scientific Research and Technology, contract MURST 40% Teoria dei sistemi e del controllo.

References

Arnold, D.E. 1971. Ingestion, assimilation, survival, and reproduction of *Daphnia pulex* fed seven species of blue-green algae. Limnol. Oceanogr. **16**: 906–920.

Berger, C. 1975. Occurrence of *Oscillatoriacea agardhii* Gom. in some shallow eutrophic lakes. Verh. Int. Ver. Theor. Angew. Limnol. **19**: 2689–2697.

Brooks, J.L., and Dodson, S.I. 1965. Predation, body size, and composition of plankton. Science (Washington, D.C.), **150**: 28–35.

Caughley, G., and Lawton, J.H. 1981. Plant–herbivore systems. *In* Theoretical ecology, principles and applications. *Edited by* R.M. May. Blackwell Scientific Publications, Oxford, U.K. pp. 132–166.

Champneys, A.R., and Kuznetsov, Y.A. 1994. Numerical detection and continuation of codimension-two homoclinic bifurcations. Int. J. Bifurcation Chaos, **4**: 795–822.

Champneys, A.R., Kuznetsov, Y.A., and Sandstede, B. 1996. A numerical toolbox for homoclinic bifurcation analysis. Int. J. Bifurcation Chaos Appl. Sci. Eng. **6**: 867–887.

De Meester, L., Weider, L.J., and Tollrian, R. 1995. Alternative antipredator defences and genetic polymorphism in a pelagic predator–prey system. Nature (Lond.), **378**: 483–485.

Dodson, S. 1988. The ecological role of chemical stimuli for the zooplankton predator-avoidance behavior in *Daphnia*. Limnol. Oceanogr. **33**: 1431–1439.

Doveri, F., Scheffer, M., Rinaldi, S., Muratori, S., and Kuznetsov, Y.A. 1993. Seasonality and chaos in a plankton–fish model. Theor. Popul. Biol. **43**: 159–183.

Engelmayer, A. 1995. Effects of predator-released chemicals on some life history parameters of *Daphnia pulex*. Hydrobiologia, **307**: 203–206.

Gliwicz, Z.M. 1990. Why do cladocerans fail to control algal blooms? Hydrobiologia, **200/201**: 83–98.

Gliwicz, Z.M., and Lampert, W. 1990. Food thresholds in *Daphnia* species in the absence and presence of blue-green filaments. Ecology, **71**: 691–702.

Guckenheimer, J., and Holmes, P. 1983. Nonlinear oscillations, dynamical systems and bifurcations of vector fields. Springer-Verlag, New York.

Gulati, R.D. 1983. Zooplankton and its grazing as indicators of trophic status in Dutch lakes. Environ. Monit. Assess. **3**: 343–354.

Hambright, K.D. 1994. Can zooplanktivorous fish really affect lake thermal dynamics? Arch. Hydrobiol. **130**: 429–438.

Hoppensteadt, F. 1974. Asymptotic stability in singular perturbation problems. J. Differential Eqs. **15**: 510–521.

Hrbácek, J., Dvorakova, M., Korinek, V., and Prochazkova, L. 1961. Demonstration of the effect of the fish stock on the species composition of zooplankton and the intensity of metabolism of the whole plankton association. Verh. Int. Ver. Theor. Angew. Limnol. **14**: 192–195.

Jeppesen, E., Sondergaard, M., Jensen, J.P., Mortensen, E., and Sortkjaer, O. 1996. Fish-induced changes in zooplankton grazing on phytoplankton and bacterioplankton: a long-term study in shallow hypertrophic Lake Sobygaard. J. Plankton Res. **18**: 1605–1625.

Khibnik, A.I., Kuznetsov, Y.A., Levitin, V.V., and Nikolaev, E.V. 1992. Continuation techniques and interactive software for bifurcation analysis of ODE's and iterative maps. Physica D, **62**: 360–370.

Kuznetsov, Y.A. 1995. Elements of applied bifurcation theory. Springer-Verlag, New York.

Lair, N., and Ayadi, H. 1989. The seasonal succession of planktonic events in Lake Aydat, France: a comparison with the PEG model. Arch. Hydrobiol. **115**: 589–602.

Lammens, E.H.R.R. 1985. A test of a model for planktivorous filter feeding by bream *Abramis brama*. Environ. Biol. Fishes, **13**: 289–296.

Lampert, W., and Rothhaupt, K.O. 1991. Alternating dynamics of rotifers and *Daphnia magna* in a shallow lake. Arch. Hydrobiol. **120**: 447–456.

Lampert, W., Fleckner, W., Rai, H., and Taylor, B.E. 1986. Phytoplankton control by grazing zooplankton: a study on the spring clear-water phase. Limnol. Oceanogr. **31**: 478–490.

Luecke, C., Vanni, M.J., Magnuson, J.J., and Kitchell, J.F. 1990. Seasonal regulation of *Daphnia* populations by planktivorous fish: implications for the spring clear-water phase. Limnol. Oceanogr. **35**: 1718–1733.

McCauley, E., and Murdoch, W.W. 1987. Cyclic and stable populations: plankton as paradigm. Am. Nat. **129**: 97–121.

McCauley, E., Murdoch, W.E., and Nisbet, R.M. 1990. Growth, reproduction and mortality of *Daphnia pulex* Leydig: life at low food. Funct. Ecol. **4**: 505–514.

McQueen, D.J., and Post, J.R. 1988. Cascading trophic interactions uncoupling at the zooplankton–phytoplankton link. Hydrobiologia, **159**: 277–296.

Meijer, M.L., Jeppesen, E., Van Donk, E., and Moss, B. 1994. Long-term responses to fish-stock reduction in small shallow lakes — interpretation of five-year results of four biomanipulation cases in The Netherlands and Denmark. Hydrobiologia, **276**: 457–466.

Mills, E.L., and Forney, J.L. 1981. Energetics food consumption and growth of young yellow perch *Perca flavescens* in Oneida Lake, New York. Trans. Am. Fish. Soc. **110**: 479–488.

Mills, E.L., and Forney, J.L. 1983. Impact on *Daphnia pulex* of predation by young yellow perch *Perca flavescens* in Oneida Lake, New York. Trans. Am. Fish. Soc. **112**: 154–161.

Mills, E.L., Forney, J.L., and Wagner, K.J. 1987. Fish predation and its cascading effect on the Oneida Lake food chain. *In* Predation: direct and indirect impacts on aquatic communities. *Edited by* W.C. Kerfoot and A. Sih. University Press of New England, Hanover, N.H. pp. 118–131.

Munro, I.G., and Bailey, R.G. 1980. Early composition and biomass of the crustacean zooplankton in Bough Beech Reservoir, southeast England, U.K. Freshwater Biol. **10**: 85–96.

Muratori, S., and Rinaldi, S. 1992. Low- and high-frequency oscillations in three-dimensional food chain systems. SIAM Soc. Ind. Appl. Math. **52**: 1688–1706.

Quinn, J.F., and Dunham, A.E. 1983. On hypothesis testing in ecology and evolution. Am. Nat. **122**: 602–617.

Rinaldi, S., and Muratori, S. 1992. Slow–fast limit cycles in predator–prey models. Ecol. Model. **61**: 287–308.

Rosenzweig, M.L. 1971. Paradox of enrichement: destabilization of exploitation ecosystems in ecological time. Science (Washington, D.C.), **171**: 385–387.

Roughgarden, J. 1983. Competition and theory in community ecology. Am. Nat. **122**: 583–601.

Sarnelle, O. 1992. Nutrient enrichment and grazer effects on phytoplankton in lakes. Ecology, **73**: 551–560.

Sarnelle, O. 1993. Herbivore effects on phytoplankton succession in a eutrophic lake. Ecol. Monogr. **63**: 129–149.

© 2000 NRC Canada

Sas, H. 1989. Lake restoration by reduction of nutrient loading: expectations, experiences, extrapolations. Academia Verlag Richarz, St. Augustin.

Scheffer, M. 1991. Fish and nutrients interplay determines algal biomass: a minimal model. Oikos, **62**: 271–282.

Scheffer, M., and DeBoer, R.J. 1995. Implications of spatial heterogeneity for the paradox of enrichment. Ecology, **76**: 2270–2277.

Scheffer, M., Rinaldi, S., Kuznetsov, Y.A., and Van Nes, E.H. 1997. Seasonal dynamics of *Daphnia* and algae explained as a periodically forced predator–prey system. Oikos, **80**: 519–532.

Schindler, D.E. 1971. Food quality and zooplankton nutrition. J. Anim. Ecol. **40**: 589–595.

Schindler, D.W., and Comita, G.W. 1972. The dependence of primary production upon physical and chemical factors in a small, scenescing lake, including the effects of complete winter oxygen depletion. Arch. Hydrobiol. **69**: 413–451.

Seda, J., and Duncan, A. 1994. Low fish predation pressure in London reservoirs: 2. Consequences to zooplankton community structure. Hydrobiologia, **291**: 179–191.

Shapiro, J., and Wright, D.I. 1984. Lake restoration by biomanipulation Round Lake, Minnesota, the first two years. Freshwater Biol. **14**: 371–384.

Stirling, G. 1995. *Daphnia* behaviour as a bioassay of fish presence or predation. Funct. Ecol. **9**: 778–784.

Threlkeld, S.T. 1985. Resource variation and the initiation of midsummer declines of cladoceran populations. Ergeb. Limnol. **21**: 333–340.

Van Donk, E., Grimm, M.P., Gulati, R.D., and Klein, B. 1990. Whole-lake food-web manipulation as a means to study community interactions in a small ecosystem. Hydrobiologia, **200–201**: 275–290.

Weider, L.J., and Pijanowska, J. 1993. Plasticity of *Daphnia* life histories in response to chemical cues from predators. Oikos, **67**: 385–392.

© 2000 NRC Canada

Density-dependent intercohort interactions and recruitment dynamics: models and a bull trout (*Salvelinus confluentus*) time series

Andrew J. Paul, John R. Post, George L. Sterling, and Carl Hunt

Abstract: A simple theoretical model shows that mechanisms of density-dependent survival that result in stable dynamics for populations with only intracohort interactions during the juvenile phase can produce cyclic behaviour when cohorts interact together. We compared these theoretical results with a time series (1971–1985) on juvenile bull trout (*Salvelinus confluentus*) from Eunice Creek, Alberta. Abundance of bull trout in Eunice Creek ranged over two orders of magnitude over the 15 years. By assigning age-classes to the abundance data (using a probabilistic length–frequency analysis), we assessed yearly survival rates for age-classes 1–3. Survival rates for age-classes 1 and 2 were negatively correlated ($P < 0.05$) with the effective density (an index of total consumption) of all juvenile bull trout in Eunice Creek. These observations support the hypothesis that different age cohorts of juvenile bull trout do interact. Using a stochastic version of the model and parameter values estimated from Eunice Creek, we hypothesize that even moderate levels of adult mortality (an average adult spawns during two seasons) coupled with random variation in the density-independent co.nponent of juvenile mortality can result in an apparent cyclic pattern for bull trout. Finally, stock–recruitment relationships for these populations are not represented by a single average curve.

Résumé : Un modèle théorique simple montre que les mécanismes de survie dépendante de la densité qui se traduisent par une dynamique stable des populations connaissant seulement des interactions intra-cohortes pendant la phase juvénile peuvent produire un comportement cyclique quand les cohortes interagissent. Nous avons comparé ces résultats théoriques à une série chronologique (1971–1985) concernant l'omble à tête plate (*Salvelinus confluentus*) du ruisseau Eunice (Alberta). L'abondance de l'omble à tête plate dans ce ruisseau a joué sur deux ordres de grandeur pendant les 15 ans de l'étude. En assignant des classes d'âge aux données sur l'abondance (à l'aide d'une analyse probabiliste de la fréquence des longueurs), nous avons évalué les taux annuels de survie pour les classes annuelles 1 à 3. Les taux de survie des classes 1 et 2 étaient négativement corrélés ($P < 0,05$) à la densité effective (indice de la consommation totale) de tous les ombles à tête plate du ruisseau Eunice. Ces observations confirment l'hypothèse d'une interaction entre les différentes cohortes d'âge des ombles juvéniles. À l'aide d'une version stochastique du modèle et des valeurs des paramètres estimées pour le ruisseau Eunice, nous posons que des niveaux même moyens de mortalité adulte (un adulte moyen se reproduit pendant deux saisons) couplés à des variations aléatoires de la composante indépendante de la densité de la mortalité des juvéniles peuvent se traduire par un patron apparemment cyclique chez l'omble à tête plate. Enfin, la relation stock–recrutement de ces populations n'est pas représentée par une simple courbe des moyennes.

[Traduit par la Rédaction]

Introduction

Understanding the production, or rate of change, for reproducing individuals in a population is a key component to fisheries management (Roughgarden 1998). A manager is faced with the fundamental problem of, "given a certain adult stock now, how many adults will I expect in x years?" Stock–recruitment (SR) relationships have a long history in fisheries management (Ricker 1954; Beverton and Holt 1957) and can provide an answer to this question (Hilborn and Walters 1992). The SR relationship describes the number of new individuals recruited into some stage from a given stock (e.g., number of adults or number of eggs). The relationship is often developed statistically as an average curve from a set of stock and recruitment data collected through time; however, reliance on these SR relationships can be problematic. First, for highly fecund species such as fishes, moderate variability in natural mortality during the prerecruitment phase can obscure any deterministic relationship between stock and recruits (Koslow 1992). Second, when using an average curve, we may neglect to account for the processes that give rise to such relationships. In other words, we do not consider whether the set of assumptions necessary to produce a proposed SR curve are reasonable. Thus, it has been proposed that fishery science take a more

Received August 18, 1999. Accepted February 10, 2000. J15324

A.J. Paul[1] **and J.R. Post.** Department of Biological Sciences, University of Calgary, Calgary, AB T2N 1N4, Canada.
G.L. Sterling. Alberta Environment, Natural Resource Service, Suite 203, Provincial Building, 111-54 St., Edson, AB T7E 1T2, Canada.
C. Hunt. 4312-8th Ave., Edson, AB T7E 1A8, Canada.

[1]Author to whom all correspondence should be addressed.
e-mail: ajpaul@ucalgary.ca

© 2000 NRC Canada

process-oriented approach when determining SR relationships (Koslow 1992; Roughgarden 1998).

Salmonids that rear as juveniles in streams present an interesting case to examine SR relationships because of our knowledge of behaviourial and physiological processes that give rise to their growth and survival (Chapman 1966; Grant and Kramer 1990). If we make the assumption that a year-class of juvenile salmonids (hereafter referred to as a cohort) compete only among themselves for a limited amount of space or food (i.e., intracohort interactions), then we would expect an SR relationship to be asymptotic (Beverton and Holt 1957; Ricker 1975). For example, if an individual requires a minimum amount of habitat to survive (say x m^2·fish^{-1}), then the maximum cohort density that the habitat can support will be x^{-1} fish·m^{-2} (Grant and Kramer 1990). Or, if survival in a cohort increases after reaching some critical stage and the time required to reach that stage is dependent on the initial cohort density, then we would expect an SR relationship to be dome shaped (Beverton and Holt 1957; Elliott 1989). However, what happens to survival and the SR relationship when interactions occur among juvenile cohorts (i.e., intercohort interactions)? To our knowledge, this question has remained unaddressed for stream-dwelling salmonids or fishes in general.

Bull trout (*Salvelinus confluentus*) populations are a concern to many fisheries managers due to the observed decline or extirpation of populations throughout their native range in western North America (Williams et al. 1989; Rieman and McIntyre 1996; references in Mackay et al. 1997). Much of the research on the juvenile life stages of bull trout has focused on habitat use (e.g., see references in Mackay et al. 1997). While these studies are necessary to preserving habitat (Bovee 1982), they do not directly address questions of age-specific survival. Because bull trout juveniles of several age-classes can coexist in rearing streams (Fraley and Shepard 1989), they may be exposed to intercohort interactions that influence the form of their SR relationship.

This brings us to the three objectives of this study: (*i*) to assess a general form of the SR relationship for situations where there are relatively simple intercohort interactions, (*ii*) to develop an empirical SR relationship for a bull trout time series and to assess its qualitative agreement with predictions from the intercohort SR model, and (*iii*) to examine the empirical data for evidence of intercohort interactions.

Materials and methods

Model development

We developed a simple population model to evaluate the consequences of intercohort interactions to SR relationships. The model is merely an extension of the SR models originally put forth by Beverton and Holt (1957), but we extend to this model intercohort interactions during the juvenile phase. Our model is similar to those formulated by Rodríguez (1998) and relies on the work of Gurney et al. (1983) to make this extension mathematically rigorous yet accessible.

The model assumes a closed population (no migration) and is formulated in continuous time. The model is structured by two states: juveniles (j) and adults (N), $j(t)$ or $N(t)$ representing the number of juveniles or adults at time t, respectively. Juveniles are recruited into the adult state after a developmental time period τ (years). Therefore, the number of adults that produced juveniles that recruit at time t will be $N(t - \tau)$. As we are interested in processes that affect survival of juveniles, instantaneous rates of adult mortality and fecundity are held constant at δ (deaths per adult per year) and f (fry per adult per year), respectively. We assume that half of the adults are female (i.e., fry per female per year is twice the fry per adult per year) and that reproduction occurs continuously, which allows us to maintain the model's simplicity.

The change in the adult population size can now be viewed as the difference between the number of new recruits to the adult population (R) and those adults that die and is described by

$$(1) \qquad \frac{dN(t)}{dt} = R - \delta N(t).$$

When new recruits (R) equals mortalities, then the population remains stable and eq. 1 equates to zero. We must now determine R. Assuming that juvenile mortality is density dependent and is described as a linear function of current juvenile density gives

$$(2) \qquad \nu(j(t)) = \nu_0 + \nu_1 j(t)$$

where $\nu(j(t))$ is the instantaneous mortality rate (deaths per juvenile per year) at a juvenile density of $j(t)$, ν_0 is the density-independent mortality rate (deaths per juvenile per year), and ν_1 the density-dependent coefficient (deaths per juvenile per year per unit density). This assumption is identical to that made for the Beverton–Holt SR relationship (Beverton and Holt 1957; Harris 1975) except that we have introduced intercohort interactions by summing juvenile density over all prerecruit ages. In the case of intracohort interactions, eq. 2 will always produce the asymptotic Beverton–Holt SR curve and the population will approach its equilibrium monotonically, without oscillations or cycles (Rodríguez 1998).

Because we must now incorporate age structure (at least implicitly) into our models, we use the methods of Gurney et al. (1983) for stage-structured populations. We define $P(t)$ as the proportion of juveniles born at time $t - \tau$ that survive to become adults at time t:

$$(3) \qquad P(t) = \exp\left(- \int_{t-\tau}^{t} \nu(j(x))\, dx \right)$$

where $j(x)$ is juvenile abundance at a given time x. Using the definition $P(t)$, the rate of change in juvenile abundance is

$$(4) \qquad \frac{dj(t)}{dt} = fN(t) - fN(t-\tau)P(t) - \nu(j(t))j(t).$$

Equation 4 states that the change in juvenile abundance depends on the addition of new fry ($fN(t)$) minus juveniles that die ($\nu(j(t))j(t)$) minus juveniles that survived and are maturing into the adult stock ($fN(t - \tau)P(t)$). The recruitment of juveniles into the adult population is

$$(5) \qquad R = fN(t - \tau)P(t).$$

We can determine the rate of change in $P(t)$ by differentiating eq. 3 (realizing that $dx = dt$) to get

$$(6) \qquad \frac{dP(t)}{dt} = P(t)(\nu(j(t-\tau)) - \nu(j(t)))$$

which leaves us with the set of delay-differential equations (eqs. 1, 4, and 6). Rodríguez (1998) showed that the nonzero equilibria for these equations are

$$(7) \qquad j^* = \frac{\dfrac{\ln\left(\dfrac{f}{\delta}\right)}{\tau} - \nu_0}{\nu_1}$$

© 2000 NRC Canada

$$(8)\qquad N^* = \frac{\left(\frac{\ln\left(\frac{f}{\delta}\right)}{\tau(f-\delta)}\right)\left(\frac{\ln\left(\frac{f}{\delta}\right)}{\tau} - \nu_0\right)}{\nu_1}$$

provided $f > \delta \exp(\nu_0 \tau)$. Furthermore, from eqs. 1 and 5, it can be easily shown that at equilibrium, P^* is

$$(9)\qquad P^* = \frac{\delta}{f}.$$

We studied the dynamics of eqs. 1, 4, and 6 by numerical simulations using the program SOLVER (Gurney et al. 1996). Specifically, we wished to explore (*i*) the stability of the above equilibria (eqs. 7–9) and (*ii*) the shape of the SR relationship given density-dependent mortality in interacting juvenile cohorts. To achieve these objectives, the numerical simulations were started from equilibrium using biologically reasonable parameter values and allowed to progress until a perturbation was introduced that pushed the population away from its steady-state conditions. The perturbation consisted of a 75% reduction in the juvenile population at one instant in time. We then noted whether the population returned to its original equilibrium (i.e., a stable equilibrium) or approached a new state (i.e., original equilibrium was unstable). During these simulated perturbation experiments, we kept track of the adults that gave rise to a specific number of recruits. These data were used to plot the SR relationship.

Study area

We have a 15-year time series of bull trout abundance and size structure from Eunice Creek, Alberta. Eunice Creek is a tributary to the McLeod River and then the Athabasca River, which form part of the MacKenzie River drainage basin (Fig. 1). Spawning adults move into Eunice Creek from the McLeod River in August and then return to the McLeod River following spawning (Sterling 1978). Eggs hatch and juveniles spend several years rearing in Eunice Creek (Sterling 1978) before migrating back into the McLeod River. This type of behaviour is consistent with migratory populations of bull trout (Northcote 1997) where the amount of time spent by juveniles in their rearing streams ranges from 1 to 4 years (Fraley and Shepard 1989).

Population estimates

The abundance of fish was estimated in lower Eunice Creek from 1971 to 1985 over an approximately 1000-m reach (range 950–1 620 m) (Fig. 1) with a mean wetted width of 3.3 m. Abundance was estimated using a mark–recapture study design assuming population closure within the sampled reach. Fish were collected by electrofishing over the reach for each of the marking and recapture phases. During the marking phase, fish were always released within at least 50 m of their original capture location. There was an average of 5 days (minimum 1 day, maximum 18 days) separating each electrofishing run. All electrofishing was conducted during low-flow conditions in late summer.

All fish sampled were measured to the nearest millimetre in fork length (FL), and those fish caught during the marking run were identified by a fin clip. Water discharge was measured from a recording station located within the sampling reach; the station operated from April to October (Anonymous 1987). We utilized the mean discharge (cubic metres per second) over the April–October period and daily maximum discharge (cubic metres per second) over the same period (Anonymous 1987).

Abundance within the sampling reach was estimated for each species using Chapman's modification of the Petersen–Lincoln estimator:

$$(10)\qquad N = \frac{(M+1)(C+1)}{(R+1)} - 1$$

where M is the number of fish for a given species that are marked and released, C is the total number for that species that are captured during a second sampling event, and R is the number of C that were previously marked (White et al. 1982). Confidence intervals for our estimates of abundance were computed from the log-likelihood profile assuming that R follows a binomial distribution. The probability density function of observing R given C captures is

$$(11)\qquad \Pr\{R|C,p\} = \left(\frac{C!}{R!(C-R)!}\right)p^R(1-p)^{(C-R)}$$

where p is the probability of capture (M/N ; Hilborn and Walters 1992). The most likely value of N, given the data, is the value that maximizes eq. 11 and can be solved analytically as $N_{\mathrm{MLE}} = MC/R$ (i.e., the classic Petersen–Lincoln estimator). Based on the likelihood ratio test (Hilborn and Mangel 1997), the 95% confidence interval in N is the range of values for which the natural logarithm of eq. 11 does not exceed the natural logarithm of $\Pr\{R|C,M/N_{\mathrm{MLE}}\} - 1.92$. The value 1.92 comes from the critical value for a chi square distribution (df = 1, $\alpha = 0.05$) divided by 2 to account for a confidence interval that lies to either side of N_{MLE} (Hilborn and Mangel 1997).

Age composition and survival

We partitioned the overall abundance data into age-classes to determine age-specific abundance and yearly rates of local survival (losses to a cohort occur through both mortality and net outward migration). Furthermore, the age-specific abundance data were used to develop an SR curve for Eunice Creek. Stock was represented by the density of the youngest cohort effectively captured by electrofishing and recruits by the density of the same cohort several years later.

Because the only information that we had to assign ages to individual fish was their FLs, we used length–frequency analysis as a means of age determination for deriving estimates of age-class abundance. We structured this length–frequency analysis into a conditional probability function (Bayesian framework) for an individual being age a_i if it had an FL l_j:

$$(12)\qquad \Pr\{a_i|l_j\} = \frac{\mathcal{L}\{l_j|a_i\}\Pr\{a_i\}}{\sum_{i=0}^{i=a_{\max}}\mathcal{L}\{l_j|a_i\}\Pr\{a_i\}}$$

where $\mathcal{L}\{l_j|a_i\}$ is the likelihood of an individual being FL l_j given that they are age a_i, $\Pr\{a_i\}$ is the probability of a captured individual being age a_i regardless of its FL, the denominator is the sum of the likelihood and probability over all age-classes, and $a_{\max}$ is the maximum number of age-classes. The probability $\Pr\{a_i\}$ accounts for differences in cohort survival and year-class strength among years that if not accounted for can bias an ageing key (Westrheim and Ricker 1978). Both the likelihood $\mathcal{L}\{l_j|a_i\}$ and probability $\Pr\{a_i\}$ were determined by the simultaneous analysis of length–frequency samples for each of the 15 years using the computer program MULTIFAN (Fournier et al. 1990). The technique assumes that growth follows a von Bertalanffy model and the distribution in FLs for age-class a_i are normally distributed. The mean (m_i) and standard deviation (s_i) estimated for the distribution in FLs for age-class a_i give rise to the likelihood

$$(13)\qquad \mathcal{L}\{l_j|a_i\} = \frac{1}{\sqrt{2\pi s_i^2}}\exp\left(\frac{-(l_j-m_i)^2}{2s_i^2}\right)$$

© 2000 NRC Canada

Fig. 1. Location of Eunice Creek and the study area within the province of Alberta. The major drainage basins of Alberta are shown with Eunice Creek lying within the Athabasca River and MacKenzie River drainage basins.

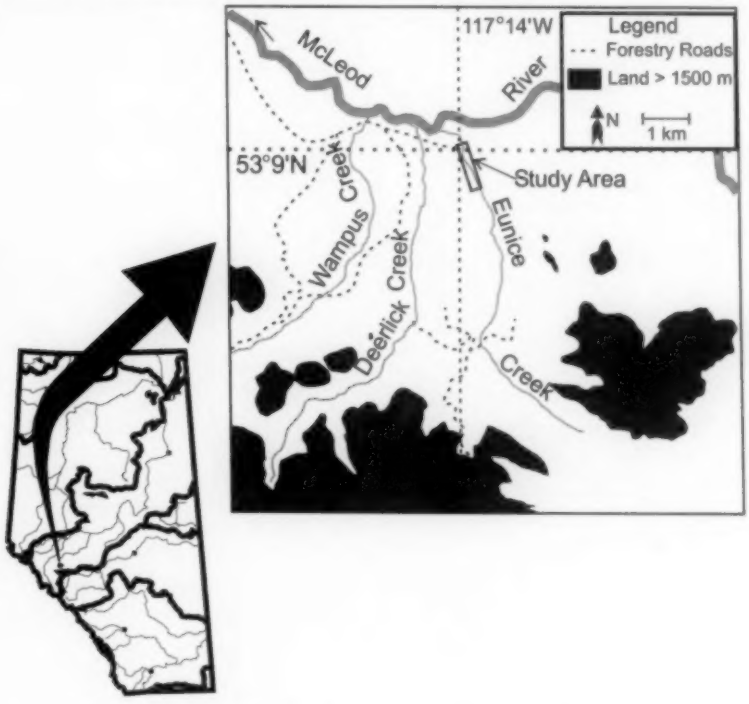

for an individual of FL l_j assuming a normal distribution. The means and standard deviations estimated by MULTIFAN were compared with otolith-aged bull trout previously collected from Eunice Creek and the McLeod River (Dietz 1971; Sterling 1978). The $\Pr\{a_i\}$ for a given year is also an estimated parameter in the length–frequency analysis of MULTIFAN (Fournier et al. 1990). Therefore, we can now calculate $\Pr\{a_i|l_j\}$ for bull trout of FL l_j assuming that size-at-age is constant among years.

To assign ages given the conditional probability $\Pr\{a_i|l_j\}$, we used a stochastic process where we choose a uniform random variable (between 0 and 1) for each individual and then based on the cumulative distribution for $\Pr\{a|l_j\}$ assign an age. Once ages were assigned to individual fish, we used eq. 10 to estimate age-class abundance. The finite local survival rate for each age-class over 1 year was then estimated from the abundance of that age-class in year t and the abundance of the same cohort (i.e., next age-class) in year $t + 1$. This entire process was repeated 1000 times. The mean and variance for age-specific abundance and survival were calculated over the 1000 iterations. We constructed 95% confidence intervals on our estimates of mean abundance and mean survival assuming a normal distribution. It is important to realize that these confidence intervals only represent the uncertainty in our mean estimate due to the stochastic age-assignment process.

Predicting patterns in survival

We looked for patterns in age-specific survival of bull trout with age-specific density, density of all juvenile bull trout, effective density (sensu Post et al. 1999) of all juvenile bull trout, biomass of all juvenile bull trout, and mean and daily maximum discharge between April and October using linear regression. We arbitrarily assigned bull trout as juveniles if they were age 4 or younger. Variables that had a coefficient (slope) significantly different from zero ($\alpha < 0.05$) were included in the model. Statistical significance was determined for each variable and the overall model using analysis of variance with $\alpha < 0.05$.

Effective density is an expression of the intensity of exploitative competition and incorporates the allometry of consumption for differences in size of juvenile bull trout (Walters and Post 1993; Post et al. 1999). The energy requirements, per gram of individual, will decrease as the size of the individual increases. Therefore, we use the sum of squared FL as a measure of effective density (Walters and Post 1993; Post et al. 1999). Quite simply, the consumption rate of an individual fish (U) will be proportional to its weight raised to an exponent <1. If we say that this exponent is 2/3 and accept that weight is proportional to length cubed, then U will be directly proportional to length squared (Walters and Post 1993; Post et al. 1999). The units we use for effective density are FL^2 per square metre (where FL is measured in millimetres).

We used principal components analysis (PCA) to explore the relationships among variables before developing predictive relationships using regression analysis. The PCA was conducted using the correlation matrix with component loadings determined using the varimax rotation (Wilkinson et al. 1992). We then plotted the individual variable loadings, from the PCA, against the three dominant components (or axes). We used this plot to select variables for the regression analysis based on both component loadings and biological considerations.

Results

Model

For given values of ν_0 and ν_1, the stability of the model's equilibria depends on τ, f, and δ. Following a perturbation, the population returns to its stable equilibrium for lower values of τ, f, or δ (Fig. 2). However, as τ, f, or δ increases, the region for which the equilibrium is unstable increases

© 2000 NRC Canada

Fig. 2. Qualitative behaviour of the model determined numerically as a function of fecundity (f, hatching eggs·adult^{-1}), instantaneous rate of adult mortality (δ, deaths·adult^{-1}·year^{-1}), and juvenile development period (τ, years). The parameter ν_1 (deaths·juvenile^{-1}·year^{-1}·unit density^{-1}) was set at 0.0005. The solid lines are for ν_0 = 0.007 deaths·juvenile^{-1}·year^{-1} and the dotted lines are for ν_0 = 0.07 deaths·juvenile^{-1}·year^{-1}. Model behaviour is divided into only two regions, stable or locally unstable with limit cycles. The arrow indicates that the region to the right of the lines is locally unstable. The model will always return to its equilibrium following a perturbation either monotonically or through damped oscillations in the region of stability.

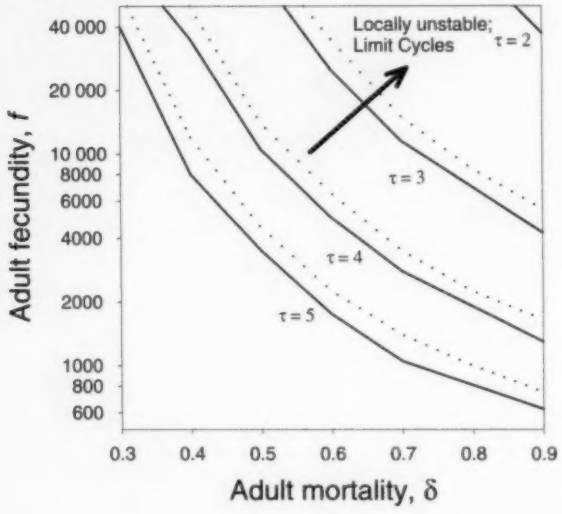

(Fig. 2). When parameter values are located in the region of instability, the modelled population does not return to its original equilibria following the perturbation. Instead, the population moves to a new state of persistent cycles (i.e., deterministic limit cycles). The SR relationship (Fig. 3) illustrates this behaviour. After perturbing the system, the SR relationship spirals outward in a counterclockwise rotation from the centre until reaching its outer orbit, which is maintained indefinitely (Fig. 3). For this example, the adult population cycled from a low of two to a high of seven individuals when at its outer orbit (Fig. 3); the period of these cycles was approximately 8 years.

What happens to the stability of the equilibria when the juvenile mortality parameters (ν_0 and ν_1) are changed? The coefficient of juvenile density-dependent mortality (ν_1) has no affect on the stability of the model equilibria (Rodríguez 1998) and serves only to scale the equilibria (see eqs. 7 and 8). The density-independent parameter (ν_0) does affect the stability of the equilibria (Rodríguez 1998). Increasing the parameter ν_0 has a stabilizing affect on the population model; that is to say, as ν_0 increases, the regions of local instability (Fig. 2) decrease.

Population abundance and age structure

The densities of bull trout and rainbow trout (*Oncorhynchus mykiss*) in Eunice Creek fluctuated over the 15 years of study (Fig. 4). Bull trout densities ranged over two orders of magnitude from a low of 0.06 fish·100 m^{-2} in 1983 to a high of 19.57 fish·100 m^{-2} in 1985 (Fig. 4). In contrast, rainbow trout densities varied less than an order of magnitude from a low of 0.45 fish·100 m^{-2} in 1972 to a high of 3.29 fish·100 m^{-2} in 1985 (Fig. 4). On average, the rainbow trout population showed an increasing trend over the 15 years, whereas the bull trout population showed a more cyclic pattern with population lows occurring in 1973 and 1983.

Fig. 3. SR relationship from the model. The original equilibrium (centre) spirals outward, following a perturbation, until the outer stable orbit is reached. The parameter values for the model were f = 1000, δ = 0.9, τ = 5, ν_0 = 0.007, and ν_1 = 0.0005.

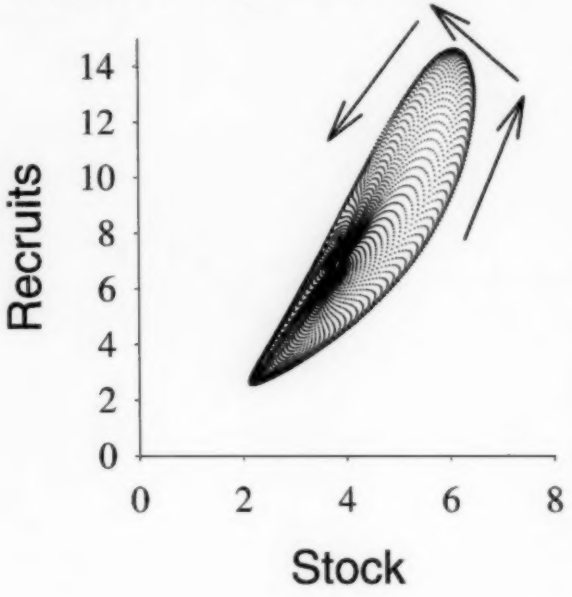

The size structure of the bull trout population over the 15 years indicated that the majority of bull trout captured in Eunice Creek were under 250 mm FL. Several modes in the combined length–frequency diagram were apparent and likely represented age-classes 0–5; this was supported by the length–frequency analysis of MULTIFAN (Table 1). Lengths-at-age based on MULTIFAN were similar to otolith-aged bull trout from the McLeod River drainage for ages 0–5 (Table 1). The discrepancy in length-at-age between length–frequency-aged and otolith-aged fish diverged strongly after age 5, with length–frequency-aged fish being substantially smaller (Table 1).

The age-structured density estimates based on the stochastic age-assignment method had a high degree of precision for bull trout aged 0–4. After 1000 stochastic age-assignment steps, the 95% confidence intervals for age-specific densities were always less than 1% of the mean value and therefore were not shown on the age-structured density plots (Fig. 5). Aged 0 bull trout were not fully vulnerable to electrofishing and are excluded from the plots and from any further analysis. Bull trout aged 5 and older were aggregated, as they likely represent mature adults (Fraley and Shepard 1989) and, more importantly, would have likely been assigned biased ages due to the increasing discrepancy

© 2000 NRC Canada

Table 1. Mean and standard deviation in FL-at-age (mm) (during late August) for bull trout in Eunice Creek as derived from the analysis of length–frequency data.

Age group	Ages based on length–frequency mean (SD)	Ages derived from otoliths: Sterling (1978) mean (SD)	Ages derived from otoliths: Dietz (1971) mean (range)
0	54 (7)	—	38
1	87 (8)	80 (7)	73 (61–81)
2	121 (8)	118 (15)	111 (92–126)
3	154 (8)	155 (13)	148 (120–191)
4	187 (9)	194 (28)	189 (159–236)
5	220 (9)	250 (55)	229 (218–247)
6	252 (10)	324	249 (246–252)
7	284 (10)	—	373 (331–403)
8	315 (11)	—	450 (391–505)
9	347 (11)	485	480 (450–495)

Note: For comparison, length-at-age information for otolith-aged bull trout collected in Eunice Creek (Sterling 1978) and in the McLeod River plus tributaries (Dietz 1971) has been included. Length-at-age information for otolith-aged bull trout has not been standardized to a specific time.

between length–frequency-aged and otolith-aged fish for these age-classes (Table 1). Densities of age-5 and older bull trout were not calculated, as they were both caught infrequently and consisted of migratory adults. Instead, we only present the total catch of bull trout age 5 and older for each year (Fig. 5).

The catch was dominated in most years by age-1 bull trout (Fig. 5). The greatest densities of age-1 bull trout occurred in 1971 and 1985. Extremely low densities of age-1 bull trout occurred from 1972 to 1973 (0.02 and 0.01 fish·100 m^{-2}, respectively), and age-1 bull trout were completely absent in our samples from 1981 to 1983 (Fig. 5). The absence of age-1 bull trout from 1981 to 1983 carries through to an absence of age-2 bull trout from 1982 to 1984 and corresponds to an absence of any spawning-sized fish during the years (1979–1981) that eggs would have been deposited for these juvenile cohorts (Fig. 5). This 3-year absence of juvenile cohorts carries through to age-3 fish but only for the first year (1983) (Fig. 5); in the following 2 years (1984 and 1985), age-3 fish were captured in our samples (Fig. 5).

An SR relationship was developed between age-1 and age-4 bull trout, as these were the youngest and oldest ages for which we had quantitative data (Fig. 6). Following the time series from 1971 to 1980, the SR relationship shows a circular pattern that progresses in a counterclockwise direction. For 1981 and 1982, age-1 cohorts were absent in Eunice Creek, and after 1982, we no longer have information on abundance for the recruitment cohorts.

Patterns in juvenile survival

The relationship among the variables that we used to predict survival rates in juvenile bull trout was evident from the PCA (Fig. 7). Effective density, juvenile biomass, juvenile density, and age-1 density all loaded strongly on axis 1 of the PCA, indicating that they contain essentially the same information but scaled differently. The second axis from the PCA consisted almost exclusively of two variables: mean

Fig. 4. Density of bull trout and rainbow trout, as estimated using electrofishing and mark–recapture techniques, in Eunice Creek from 1971 to 1985. The 95% likelihood profiles are shown for bull trout; 95% likelihood profiles are omitted for rainbow trout to improve clarity.

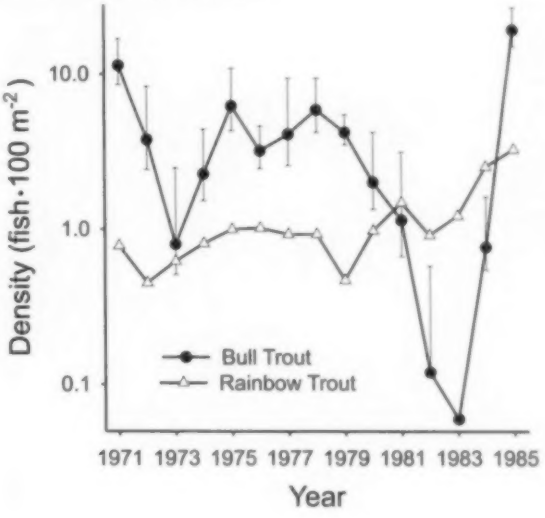

and maximum daily discharge. As with the first axis, both maximum daily discharge and mean discharge had component loadings close to 1, implying that both are effectively similar measures. The third axis was a combination of our remaining variables, age-2 density and age-3 density.

The predictor variables that we chose to regress against our juvenile survival rates were effective density (FL^2 per square metre), mean discharge over the April–October period (cubic metres per second), age-2 density (fish per 100 m^2), and age-3 density (fish per 100 m^2). First, we used effective density, as it was a measure from the first axis of the PCA. We chose this measure over juvenile biomass, juvenile density, and density of age-1 bull trout (all which would have explained this axis equally well), as we felt that effective density had the most reasonable biological justification based on size-specific consumption rates (for complete arguments, see Walters and Post 1993; Post et al. 1999). Second, we used mean discharge instead of maximum daily discharge as our measure from the second PCA axis, as this measure likely provided a contrast between wet and dry years rather than extreme flood events. Finally, we included both age-2 density and age-3 density, as they had very little relationship to the first two axes of the PCA (Fig. 7) and could contain information that has not yet been accounted for (e.g., cannabalism, aggressive interactions).

Effective density was significant in predicting finite yearly survival for age-1 and age-2 bull trout (Table 2; Figs. 8*a* and 8*b*). Effective density alone was marginally nonsignificant ($P = 0.084$) (Table 2; Fig. 8*c*) in predicting survival of age-3 bull trout. The model for survival of age-2 bull trout was significantly improved by including mean discharge into the model, with survival being positively related to discharge (Table 2). Also, the inclusion of age-3 density into the regression for survival of age-3 bull trout significantly im-

© 2000 NRC Canada

Fig. 5. Estimated density of age-1 to age-3 bull trout and total catch of bull trout aged 5 and older from Eunice Creek: (*a*) age 5 and older; (*b*) age 1; (*c*) age 2; (*d*) age 3. Age-class densities are the mean of 1000 simulations of the stochastic age assignment process (see Materials and methods). The 95% confidence intervals based on the stochastic age assignments (see Materials and methods) were always less than 1% of the mean value and are not shown in the figure.

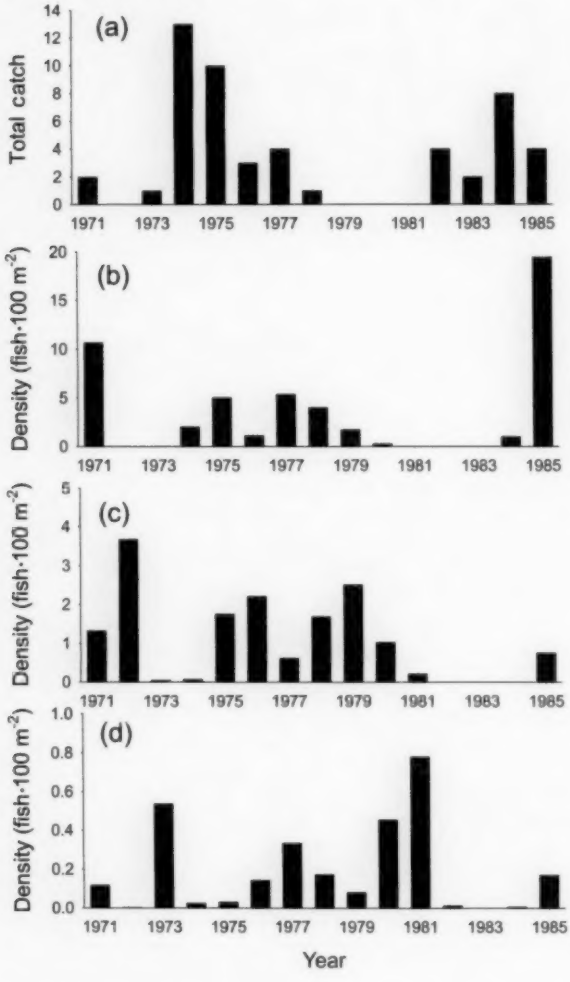

proved the model fit (Table 2). This latter model should be treated with skepticism, as the two predictor variables are not independent. However, the PCA (Fig. 7) indicated there was little information in age-3 density that explained effective density, and vice versa.

The slopes of the regressions for effective density were not significantly different among age-classes 1–3 (analysis of variance, $P = 0.975$) (Fig. 8). There was, however, a significant difference in survival among age-classes at a given effective density (analysis of covariance, $P = 0.0003$) (Fig. 8). A post hoc test among mean differences (Tukey test) indicated that survival of age-1 bull trout was significantly greater than that of age-2 fish ($P = 0.001$) but not significantly greater than that of age-3 fish ($P = 0.077$), although only marginally. The difference in survival between age-2 and age-3 fish was not significant ($P = 0.179$).

Discussion

Using a simple deterministic model, we present a mechanism by which fish populations may not follow single-curve SR relationships and can exhibit cyclic behaviour. The key component to our model and population cycles is intercohort interactions among juveniles. Models in which juveniles show only intracohort interactions (Beverton and Holt 1957; Harris 1975) produce dynamics in which the population approach equilibria monotonically leading to a single asymptotic SR curve. With the onset of intercohort interactions, cyclic behaviour becomes possible and SR relationships occupy a region in phase space rather than only a single curve. However, from our simulations, this behaviour is unlikely unless the developmental period (over which these intercohort interactions occur) is sufficiently long. In fact, the juvenile development period need likely be on the order of 3 or more years for true deterministic cycles to occur. We hypothesize that this is possible in freshwater salmonid populations, such as bull trout, that inhabit small unproductive systems for several years during their juvenile life stages.

Local survival of juvenile bull trout in Eunice Creek indicate that intercohort interactions do occur. While it is hard to come to this conclusion based only on the age-1 fish (since our measure of effective density was largely weighted by age-1 density), the negative relationship between age-2 and age-3 survival as a function of effective density indicates that there are interactions occurring among juvenile cohorts. However, it is unlikely that the relationship between finite survival and effective density is linear as we have plotted. Assuming that instantaneous mortality of juveniles is given by eq. 2, we would expect the finite mortality rate for a juvenile age-class to be an exponentially decaying relationship with effective density. Using this form did not improve the fit of our models and tended to put large leverage on points measured at the maximum effective density. This does not suggest that the finite survival rate is either linear or an exponentially decaying function with effective density, only that our data were unable to distinguish between these functions.

An assumption in our analysis is that growth remains constant and density-dependent interactions are expressed through local survival. We know this to likely be false, as density-dependent growth can occur in stream-dwelling salmonids (see Grant and Kramer 1990). However, the occurrence of density-dependent growth does not alter the main findings of this study. First, the Monte Carlo age-assignment process indicated good precision in our ageing method. Therefore, over the entire time series, there was good separation among the average size distributions for each juvenile age-class. Second, density-dependent growth coupled with our size-dependent ageing method would likley obscure any relationship between survival and effective density. This was not the case. However, the variability in age-3 survival as a function of effective density may have resulted

© 2000 NRC Canada

Fig. 6. Observed SR relationship in age-1 bull trout in year t (stock) and age-4 bull trout in year $t + 3$ (recruits) for Eunice Creek. The time series is divided into separate periods: 1971–1975 (circles), 1976–1980 (squares), and 1981–1982 (triangles). Solid symbols represent data points used in the series indicated by the years shown.

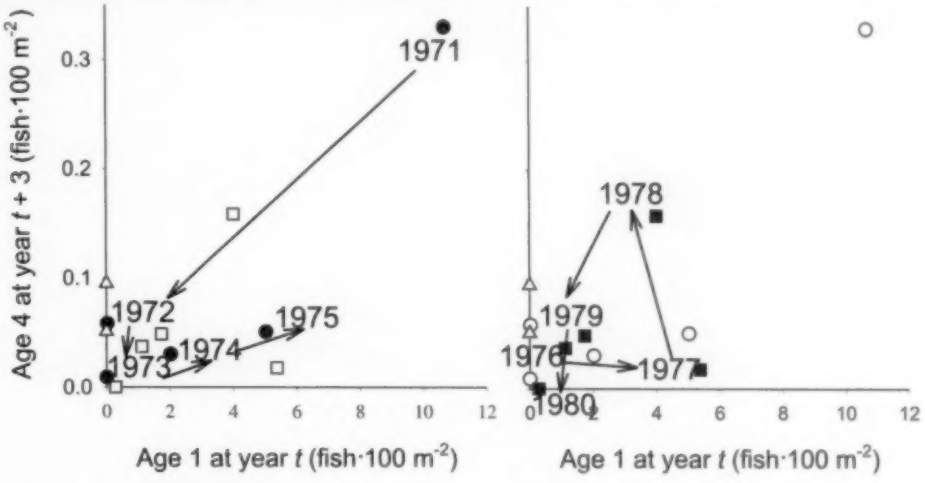

Fig. 7. PCA plots for the first three component axes given a set of eight variables collected from Eunice Creek from 1971 to 1985. The variables are age-1 density (Age 1, fish·100 m^{-2}), age-2 density (Age 2, fish·100 m^{-2}), age-3 density (Age 3, fish·100 m^{-2}), density of bull trout 4 years of age or younger (Density, fish·100 m^{-2}), effective density of bull trout 4 years of age or younger (Effective Density, FL^2·100 m^{-2}), biomass of bull trout 4 years of age or younger (Biomass, g·100 m^{-2}), daily maximum discharge from April to October (Max Q, $m^3 \cdot s^{-1}$), and mean discharge from April to October (Mean Q, $m^3 \cdot s^{-1}$).

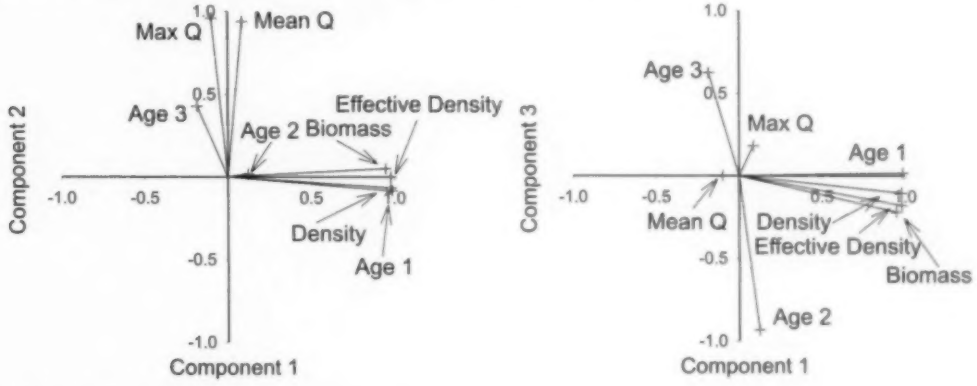

from the combined affects of density-dependent growth and age misclassification. Third, we are not dismissing the importance of density-dependent growth. Rather, food availability and growth may very well be the mechanism that produces the observed pattern in density-dependent local survival.

Density-dependent survival in stream-dwelling salmonids likely arises through limitations in food or space (Chapman 1966; Grant and Kramer 1990). Although we did not directly test for mechanisms that would give rise to density-dependent survival of bull trout in Eunice Creek, the similar slopes regressing finite survival as a function of effective density support the hypothesis that density-dependent survival arises through exploitative competition on a limited food resource. If bull trout were competing for space through territoriality, we would expect an inequitable partitioning of resources (including food) among large and small fish, resulting in larger dominant individuals having greater growth or survival (Post et al. 1999).

We found that at a given effective density, local survival of juvenile bull trout was greatest for the youngest age-class (age 1) than for older age-classes (anout 50% less in the older age-classes). This produces an interesting contrast to the study of Post et al. (1999) who found survival in age-0 and age-1 rainbow trout from lentic systems to be related to the effective density of the age-1 juveniles. However, survival at a given effective density was lower for the age-0 fish than for the age-1 fish (Post et al. 1999). We hypothesize that for lotic bull trout, the density-independent mortality rate represented a constant emigration rate that occurred regardless of effective density. Age-1 bull trout showed almost no emigration at low effective densities, but age-2 and age-3

© 2000 NRC Canada

Table 2. Linear regression models for estimated finite yearly survival for age-1, age-2, and age-3 bull trout in Eunice Creek as a function of effective density ($FL^2 \cdot m^{-2}$), mean discharge over the April–October period (Mean Q, $m^3 \cdot s^{-1}$), or age-3 density (Age 3, fish·100 m^{-2}).

Age-class	Model	r^2	P
1	Survival = $0.9410 - 6.157 \times 10^{-4}$(Effective Density)	0.58	0.006
2	Survival = $0.5391 - 5.936 \times 10^{-4}$(Effective Density)	0.41	0.034
2	Survival = $0.2531 - 5.906 \times 10^{-4}$(Effective Density) + 1.405(Mean Q)	0.7	0.014
3	Survival = $0.7523 - 6.759 \times 10^{-4}$(Effective Density)	0.27	0.084
3	Survival = $1.073 - 9.252 \times 10^{-4}$(Effective Density) − 0.9309(Age 3)	0.66	0.008

Note: Models for each of the age-classes are presented showing the forward selection of variables ending with the best-fit model. The squared correlation coefficient and probability that the given model arose from chance alone are shown for each model.

Fig. 8. Relationship between finite yearly survival for (*a*) age-1, (*b*) age-2, or (*c*) age-3 bull trout and effective density of bull trout 4 years of age or younger in Eunice Creek from 1971 to 1985. The best-fit line using least squares regression is shown for each plot (95% confidence intervals in the regressions are shown by the dotted lines); only the regression lines for age 1 and age 2 are significant ($P < 0.05$).

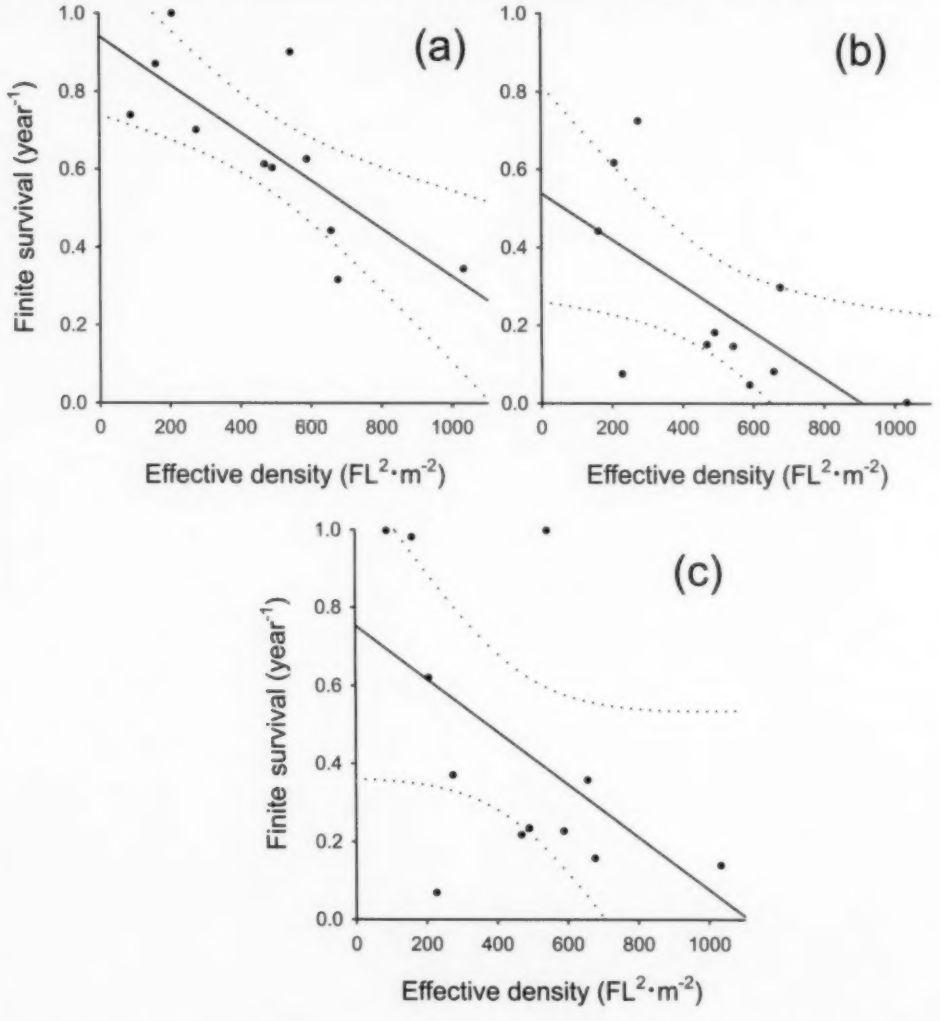

bull trout had emigration rates of between 25 and 50%·year^{-1}, even at low effective densities. Survival in the lentic systems of Post et al. (1999) was a true measure of survival in the sense that losses occurred only through mortality rather than through a combination of mortality and emigration. Furthermore, they showed that growth was related to effec-

© 2000 NRC Canada

Fig. 9. Total juvenile population numbers from our model for the simulated years 200–250 given that the density-independent juvenile mortality rate (ν_0) is constant ($\nu_0 = 0.07$, broken line) or stochastic among years (lognormal distribution, geometric mean = 0.07, SD = 1.0, solid line). The SR relationship is shown for the stochastic model in the bottom panel. Values for the other parameters in either simulation were $\nu_1 = 0.0005$, $\tau = 4$, $\delta = 0.7$, and $f = 750$.

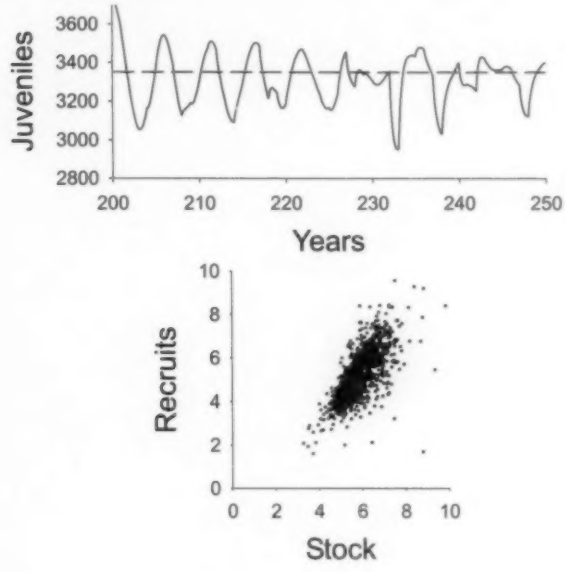

tive density and survival was mediated through size-dependent predation. Therefore, as rainbow trout grew larger, their predation risk decreased, and hence, survival increased.

Based on our simple model and field results, deterministic population cycles can arise in bull trout populations due to exploitative competition among juvenile cohorts coupled with their relatively long developmental period. The question that arises is do Eunice Creek bull trout show deterministic population cycles? Because the period for a complete cycle is on the order of 6–7 years, it is difficult to conclusively determine a cyclic pattern in our 15 years of data. However, there does appear to be a cyclic pattern to our abundance with a period of between 7 and 10 years. Furthermore, the predicted pattern of counterclockwise orbits in the SR relationship is supported by the observed data.

An alternative approach to assessing whether bull trout in Eunice Creek show a cyclic pattern is to determine whether estimated parameter values are in a region of parameter space that would result in deterministic limit cycles. We will assume that female bull trout deposit 3000 eggs when spawning (Goetz 1989), 50% of these eggs survive to emergence (Fraley and Shepard 1989), and juveniles spend 4 years in their rearing streams (Fraley and Shepard 1989). The rate of density-independent juvenile mortality used in previous model simulations ($\nu_0 = 0.007$) is very low. Estimated finite rates of density-independent survival from Eunice Creek (i.e., the intercepts from Table 2) suggest that the value $\nu_0 = 0.007$ is likely an order of magnitude too low. If we increase this rate to $\nu_0 = 0.07$, then the finite yearly rate of adult mortality need be on the order of 70% or greater (i.e., $\delta \geq 1.2$) for deterministic population cycles to occur. This level of mortality implies that on average, an adult survives for less than one spawning season. High levels of adult mortality (approaching 70%) are possible in exploited bull trout populations (Stelfox 1997). Bull trout in the McLeod River (i.e., adult population from Eunice Creek) were likely subjected to at least moderate angler exploitation through the 1970s and 1980s (Nelson and Paetz 1992), but whether mortality rates were 70% or greater is unknown. However, the possibility for moderately exploited bull trout populations to still show cyclic patterns is not ruled out.

A variable environment can drive cycles in a population through either of two means (Nisbet and Gurney 1976*a*, 1976*b*). First, a cycling environmental variable can directly drive observed cycles in a population (Nisbet and Gurney 1976*a*). Although this has been hypothesized as a mechanism behind the roughly 10-year cycles in snowshoe hare (*Lepus americanus*) populations (Sinclair et al. 1993), we can think of no regular cyclic environmental conditions that bull trout may be subjected to at the decadal scale. Second, and perhaps less obvious, random environmental variability can drive cyclic patterns in a population through the internal dampening of the system (Nisbet and Gurney 1976*b*). Theory shows that a population that returns to an equilibrium following a perturbation via oscillations of decreasing amplitude can, in the presence of random environmental variability, show a persistent cyclic pattern referred to as quasi-cycles (Nisbet and Gurney 1976*b*).

Our data show that the density-independent mortality rates for juvenile bull trout may be related to environmental variability. More specifically, the survival of age-2 bull trout was significantly related to mean summer flows in Eunice Creek. If we assume that mean summer flows vary in some random fashion, then density-independent mortality rates (at least for age-2 bull trout) will also vary randomly. The introduction of random variability onto our revised estimate of juvenile density-independent mortality ($\nu_0 = 0.07$) indicates that quasi-cycles are possible at lower levels of adult mortality ($\delta = 0.7$) (Fig. 9). Therefore, we conclude that the bull trout population in Eunice Creek was likely to show a cyclic pattern, but these were true deterministic limit cycles only if adult mortality rates were high ($\delta \geq 1.2$).

Our hypothesized mechanism of intercohort density-dependent survival that results in cyclic or quasi-cyclic population dynamics is not new. Gurney and Nisbet (1980) concluded that density dependence in age-structured single-species populations will only result in resonant behaviour should the population have a long immature phase followed by a relatively short period of intense reproduction. The concept that fish populations show cyclic dynamics is also not new (Townsend 1989). However, it is probably generally accepted that many fish populations (especially freshwater salmonids) do not show cyclic behaviour but rather erratic dynamics that reflect the uncertainty of many factors (Platts and Nelson 1988; Townsend 1989). The idea that we present here is that freshwater salmonid populations living in an uncertain environment can show cyclic, or quasi-cyclic, popu-

© 2000 NRC Canada

lation dynamics, provided juveniles mature over several years in unproductive habitats and adults, on average, spawn for 2 years or less. Unfortunately, given our predicted cycle period (about 6–7 years), sufficiently long-term data sets to detect these cycles in freshwater salmonids are relatively few (but see Platts and Nelson 1988; Rieman and Myers 1997).

The concept of intercohort interactions in juvenile bull trout leading to SR regions rather than curves and cyclic behaviour requires further study. First, direct experimental studies need be conducted to confirm whether competition occurs among juvenile bull trout and if it is symmetrical or asymmetrical among different-sized individuals. Second, our field data provided no information on survival of age-0 bull trout. Interactions (e.g., cannibalism) occurring during the first year of life for bull trout may play a role in structuring the SR relationship. However, this does not detract from the significant results of this study that show that finite survival in older juveniles can decrease by 60% within observed ranges of effective density. Finally, bull trout are a migratory fish showing all forms of potamodromy, including fluvial, fluvial–adfluvial, lacustrine–adfluvial, and allacustrine life history types (Carl et al. 1989; Northcote 1997). The dynamics of bull trout populations with stages separated among habitats will depend on processes occurring within habitats and by the movement of individuals among habitats. However, this study focused only on the local survival of juveniles in one habitat type. A full understanding of the recruitment dynamics of bull trout will depend on the survival of juveniles in rearing habitats and during their migratory movements among habitats.

Acknowledgements

We thank the project and seasonal staff of Alberta Environment, Natural Resources Service and Lands and Forest Service, who assisted in the collection of data from 1971 to 1985 as part of the Tri-Creeks Experimental Watershed Study. Funding for the collection of fisheries data was provided by Natural Resources Service, Fisheries Management Branch, as part of their annual budgetary commitment to the Tri-Creeks Experimental Watershed Study. Funding to A.J.P. and J.R.P. was provided by hunters and anglers of Alberta through the Fisheries Management and Enhancement Program of Alberta Environment and the Alberta Conservation Association. We thank two anonymous reviewers for their comments which improved this manuscript.

References

Anonymous. 1987. Historical streamflow summary: Alberta to 1986. Inland Waters/Land Directorate, Ottawa, Ont.

Beverton, R.J.H., and Holt, S.J. 1957. On the dynamics of exploited fish of exploited fish populations. Fish. Invest. Ser. 2. Vol. 19. U.K. Ministry of Agriculture and Fisheries, London, U.K.

Bovee, K.D. 1982. A guide to stream habitat analysis using the instream flow incremental methodology. Instream Flow Inf. Pap. 12. U.S. Fish Wildl. Serv. FWS/OBS-82/26.

Carl, L.M., Kraft, M., and Rhude, L. 1989. Growth and taxonomy ob bull charr, *Salvelinus confluentus*, in Pinto Lake, Alberta. Environ. Biol. Fishes, **26**: 239–246.

Chapman, D.W. 1966. Food and space as regulators of salmonid populations in streams. Am. Nat. **100**: 345–357.

Dietz, K. 1971. The fish populations of three streams in the foothills of Alberta. M.Sc. thesis, University of Alberta, Edmonton, Alta.

Elliott, J.M. 1989. Mechanisms responsible for population regulation in young migratory trout, *Salmo trutta*. I. The critical time for survival. J. Anim. Ecol. **58**: 987–1001.

Fournier, D.A., Sibert, J.R., Majkowski, J., and Hampton, J. 1990. MULTIFAN a likelihood-based method for estimating growth parameters and age composition from multiple length frequency data sets illustrated using data for southern bluefin tuna (*Thunnus maccoyii*). Can. J. Fish. Aquat. Sci. **47**: 301–317.

Fraley, J.J., and Shepard, B.B. 1989. Life history, ecology and population status of migratory bull trout (*Salvelinus confluentus*) in the Flathead Lake and River system, Montana. Northwest Sci. **63**: 133–143.

Goetz, F. 1989. Biology of the bull trout, *Salvelinus confluentus*: a literature review. U.S. Department of Agriculture, Forest Service, Willamette National Forest, Oregon.

Grant, J.W.A., and Kramer, D.L. 1990. Territory size as a predictor of the upper limit to population density of juvenile salmonids in streams. Can. J. Fish. Aquat. Sci. **47**: 1724–1737.

Gurney, W.S.C., and Nisbet, R.M. 1980. Age- and density-dependent population dynamics in static and variable environments. Theor. Popul. Biol. **17**: 321–344.

Gurney, W.S.C., Nisbet, R.M., and Lawton, J.H. 1983. The systematic formulation of tractable single-species population models incorporating age structure. J. Anim. Ecol. **52**: 479–495.

Gurney, W.S.C., Tobia, S., Watt, G., and Dobby, H. 1996. SOLVER Rev. 5.05, a program template for initial value problems expressible as sets of coupled ordinary or delay differential equations. STAMS, University of Strathclyde, Glasgow, U.K.

Harris, J.G.K. 1975. The effect of density-dependent mortality on the shape of the stock and recruitment curve. J. Cons. Cons. Int. Explor. Mer, **36**: 144–149.

Hilborn, R., and Mangel, M. 1997. The ecological detective confronting models with data. Monogr. Popul. Biol. No. 28. Princeton University Press, Princeton, N.J.

Hilborn, R., and Walters, C.J. 1992. Quantitative fisheries stock assessment: choice, dynamics and uncertainty. Chapman and Hall, New York.

Koslow, J.A. 1992. Fecundity and the stock–recruitment relation. Can. J. Fish. Aquat. Sci. **49**: 210–217.

Mackay, W.C., Brewin, M.K., and Monita, M. 1997. Friends of the bull trout conference proceedings. Bull Trout Task Force (Alberta), c/o Trout Unlimited Canada, Calgary, Alta.

Nelson, J.S., and Paetz, M.J. 1992. The fishes of Alberta. 2nd ed. University of Alberta Press, Edmonton, Alta., and University of Calgary Press, Calgary, Alta.

Nisbet, R.M., and Gurney, W.S.C. 1976*a*. Population dynamics in a periodically varying environment. J. Theor. Biol. **56**: 459–475.

Nisbet, R.M., and Gurney, W.S.C. 1976*b*. A simple mechanism for population cycles. Nature (Lond.), **263**: 319–320.

Northcote, T.G. 1997. Potamodromy in Salmonidae — living and moving in the fast lane. N. Am. J. Fish. Manage. **17**: 1029–1045.

Platts, W.S., and Nelson, R.L. 1988. Fluctuations in trout populations and their implications for land-use evaluation. N. Am. J. Fish. Manage. **8**: 333–345.

Post, J.R., Parkinson, E.A., and Johnston, N.T. 1999. Density-dependent processes in structured fish populations: interaction strengths in whole-lake experiments. Ecol. Monogr. **69**: 155–175.

Ricker, W.E. 1954. Stock and recruitment. J. Fish. Res. Board Can. **11**: 559–623.

Ricker, W.E. 1975. Computation and interpretation of biological statistics of fish populations. Bull. Fish. Res. Board Can. No. 191.

© 2000 NRC Canada

Rieman, B.E., and McIntyre, J.D. 1996. Spatial and temporal variability in bull trout redd counts. N. Am. J. Fish. Manage. **16**: 132–141.

Rieman, B.E., and Myers, D.L. 1997. Use of redd counts to detect trends in bull trout (*Salvelinus confluentus*) populations. Conserv. Biol. **11**: 1015–1018.

Rodríguez, D.J. 1998. Time delays in density dependence are often not destabilizing. J. Theor. Biol. **191**: 95–101.

Roughgarden, J. 1998. How to manage fisheries. Ecol. Appl. **8**(Suppl.): 160–164.

Sinclair, A.R.E., Gosline, J.M., Holdsworth, G., Krebs, C.J., Boutin, S., Smith, J.N.M., Boonstra, R., and Dale, M. 1993. Can the solar cycle and climate synchronize the snowshoe hare cycle in Canada? Evidence from tree rings and ice cores. Am. Nat. **141**: 173–198.

Stelfox, J.D. 1997. Seasonal movements, growth, survival and population status of the adfluvial bull trout population in Lower Kananaskis Lake, Alberta. *In* Friends of the Bull Trout Conference Proceedings. *Edited by* W.C. Mackay, M.K. Brewin, and M. Monita. Bull Trout Task Force (Alberta), c/o Trout Unlimited Canada, Calgary, Alta. pp. 309–316.

Sterling, G.L. 1978. Population dynamics, age and growth of rainbow trout (*Salmo gairdneri*) and Dolly Varden (*Salvelinus malma*) in the Tri-Creeks watershed, 1971 to 1977. Rep. No. 2. Alberta Energy and Natural Resources, Alberta Forest Service and Alberta Recreation, Parks and Wildlife, Fish and Wildlife Division, Edmonton, Alta.

Townsend, C.R. 1989. Population cycles in freshwater fish. J. Fish Biol. **35**(Suppl. A): 125–131.

Walters, C.J., and Post, J.R. 1993. Density-dependent growth and competitive asymmetries in size-structured fish populations: a theoretical model and recommendations for field experiments. Trans. Am. Fish. Soc. **122**: 34–45.

Westrheim, S.J., and Ricker, W.E. 1978. Bias in using an age–length key to estimate age–freqency distributions. J. Fish. Res. Board Can. **35**: 184–189.

White, G.C., Anderson, D.R., Burnham, K.P., and Otis, D.L. 1982. Capture–recapture and removal methods for sampling closed populations. LA-8787-NERP. Los Alamos National Laboratory, Los Alamos, Los Alamos, N.M.

Wilkinson, L., Hill, M., Welna, J.P., and Birkenbeuel, G.K. 1992. Systat for windows: statistics, version 5 edition. Systat, Inc., Evanston, Ill.

Williams, J.E., Johnson, J.E., Hendrickson, D.A., Contreras-Balderas, S., Williams, J.D., Navarro-Mendoza, M., McAllister, D.E., and Deacon, J.E. 1989. Fishes of North America endangered, threatened, or of special concern: 1989. Fisheries (Bethesda), **14**: 2–20.

© 2000 NRC Canada

In situ analysis of trace elements and isotope ratios in fish otoliths using laser ablation sector field inductively coupled plasma mass spectrometry

Simon R. Thorrold and Stephen Shuttleworth

Abstract: We applied laser ablation sector field inductively coupled plasma mass spectrometry (SF-ICP-MS) to the analysis of trace element and isotopic signatures in fish otoliths. Manganese, Sr, and Ba profiles across juvenile Atlantic croaker (*Micropogonias undulatus*) otoliths, expressed as ratios to Ca, showed considerable spatial and temporal variations that were presumably reflective of variations in water chemistry over the same scales. Differences in otolith Mn:Ca ratios between adjacent rivers in Pamlico Sound, North Carolina, may be related to dissolved oxygen levels in the rivers through reductive release of Mn^{2+} from sediments. Strontium and Ba profiles appeared to accurately reflect differences in dissolved Sr and Ba in freshwater end-members, both between Pamlico Sound and Chesapeake Bay and between seasons within Chesapeake Bay. High-precision analyses of Sr:Ca ratios in a black drum (*Pogonias cromis*) otolith showed distinctive quasi-sinusoidal cycles that were correlated with validated annual bands. Analyses of Sr and Pb isotopes, in otoliths and standard reference material, respectively, found that SF-ICP-MS produced accurate and precise estimates of isotope ratios in both solution-based and laser ablation assays.

Résumé : Nous avons appliqué la spectrométrie de masse couplée à un plasma inductif à champ sectoriel avec prélèvement par ablation laser (SF-ICP-MS) à l'analyse des éléments traces et des signatures isotopiques dans les otolithes de poissons. Les profils du Mn, du Sr et du Ba dans les otolithes de juvéniles de tambour brésilien (*Micropogonias undulatus*), exprimés en termes de rapports au Ca, présentaient des variations spatiales et temporelles considérables qui correspondaient vraisemblablement à des variations de la chimie de l'eau sur les mêmes échelles. Les différences dans le rapport Mn:Ca dans les otolithes entre des cours d'eau adjacents de la baie Pamlico (Caroline du Nord) peuvent être en rapport avec la teneur en oxygène dissous des cours d'eau par le biais d'une libération réductrice du Mn^{2+} des sédiments. Les profils du Sr et du Ba semblaient représenter avec exactitude les différences du Sr et du Ba dissous dans les termes extrêmes d'eau douce, tant entre la baie Pamlico et la baie Chesapeake qu'entre les saisons au sein de la baie Chesapeake. Les analyses à haute précision des rapports Sr:Ca dans un otolithe de grand tambour (*Pogonias cromis*) ont montré des cycles caractéristiques quasi-sinusoïdaux qui étaient corrélés aux bandes annuelles validées. L'analyse des isotopes de Sr et de Pb dans les otolithes et dans du matériel de référence standard, respectivement, ont fait ressortir que la méthode SF-ICP-MS donnait des estimations exactes et précises des rapports des isotopes tant dans les essais sur solution qu'avec l'ablation laser.

[Traduit par la Rédaction]

Introduction

The geochemistry of carbonate skeletons, shells, and bones represents a valuable record of environmental conditions experienced by a diverse array of marine organisms including foraminifera (Boyle 1988), hematypic corals (Guilderson et al. 1994), bivalve mollusks (Hart and Blusztajn 1998), and teleost fishes (Patterson et al. 1993). In coral skeletons, mollusk shells, and fish otoliths, the presence of temporal markers in the aragonite structure allows for the collection of time-resolved data, providing sampling can be conducted on a sufficiently small spatial scale. High-resolution sampling of increments in biogenic aragonite has traditionally been achieved through the use of micromilling equipment and subsequent analysis of the resulting powder using solution-based assays (e.g., Guilderson et al. 1994). More recently, in situ sampling of these structures using the ion microprobe and laser ablation inductively coupled plasma mass spectrometry (LA-ICP-MS) has demonstrated the advantages of probe-based methodologies (Hart and Cohen 1996; Sinclair et al. 1998). Although these instruments generally suffer from decreased sensitivity and precision compared with solution-based techniques (Campana et al. 1997), they offer less opportunity for sample contamination

Received July 27, 1999. Accepted January 11, 2000.
J15259

S.R. Thorrold.[1] Department of Biological Sciences, Old Dominion University, Norfolk, VA 23529, U.S.A.
S. Shuttleworth.[2] Department of Earth and Planetary Sciences, Washington University, St. Louis, MO 63130, U.S.A.

[1]Author to whom all correspondence should be addressed. e-mail: sthorrol@odu.edu
[2]Present address: Merchantek EO, P.O. Box 2277, Del Mar, CA 92014, U.S.A.

© 2000 NRC Canada

and are substantially faster on a per-sample basis. Probe-based techniques are particularly useful for life history scans of otolith microchemistry, as daily increments are rarely wider than 20 μm and annual increments typically are less than 200 μm in width.

All otolith studies that have used ICP-MS to quantify otolith chemistry to date have been conducted on instruments with quadrupole-based mass analyzers (Q-ICP-MS). Recently, new-generation ICP-MS instruments have become commercially available that utilize sector field mass analyzers. Sector field instruments have several advantages over quadrupole instruments, including the ability to operate at high mass resolution (e.g., Moens et al. 1995). This allows potential mass interferences on isotopes of interest to be identified and eliminated. For instance, molecular interferences from argon and calcium oxides make quantification of Mn, Ni, Cu, and Zn in otoliths difficult on quadrupole instruments (Turner et al. 1998). These interferences are largely intractable in solid-sample analyses with Q-ICP-MS because it is difficult to remove the interfering ions or molecules with a separation technique, as can be done with solution-based assays. Laser ablation in conjunction with sector field ICP-MS (SF-ICP-MS) may, then, significantly improve data quality when quantifying a number of trace elements found in otoliths.

Stable isotope studies of otoliths, other than C and O, are still rare. However, isotope ratios of elements such as Sr and Pb may also contain significant information on environmental conditions experienced by individual fish (Kennedy et al. 1997). Measurement of isotopic ratios places a premium on precision and repeatability of the analytical instrument, as isotopic differences are often subtle. The precision of isotope ratio measurements using Q-ICP-MS is limited by instabilities in the plasma and the peak shape characteristics of the quadrupole mass analyzer. The result is that isotopic ratios cannot be routinely determined with a precision of less than 0.5% in solution ICP-MS applications and 1% when coupled with a laser ablation device (Beary and Paulson 1993; Machado and Gauthier 1996). Recently, several studies have reported excellent precision in isotopic ratio measurements using SF-ICP-MS (Vanhaecke et al. 1996; Latkoczy et al. 1998). Although instability in the plasma remains, the flat top peaks and increased stability of the magnetic sector mass analyzer has given precision estimates on the order of 0.05%. These data suggest that the sector field instrument, when coupled with a laser probe, may be capable of in situ analyses of isotope ratios in otoliths with significantly better precision than can be achieved with Q-ICP-MS.

In this study, we applied laser ablation SF-ICP-MS to the analysis of trace elements and isotopic ratios in biogenic aragonite. We used fish otoliths as our aragonite source, although this is in some ways a more demanding test for the technique than other biogenic carbonates such as coral skeletons and mollusk shells. The specific objectives of this work were firstly to develop a methodology for in situ, semi-quantitative trace metal analyses, both with and without the presence of significant molecular interferences, using laser ablation SF-ICP-MS. We were particularly interested in the potential for high-precision in situ measurements of Sr:Ca ratios in otoliths, given the current uncertainty in the interpretation of Sr:Ca ratios in fish otoliths. Our second objective was to examine the potential for determining Sr and Pb isotope ratios, both solution based and with laser ablation, in fish otoliths on the sector field instrument. Data on isotope ratios, if determined with sufficient precision, could significantly increase the amount of environmental information obtained from the otoliths of individual fish.

Materials and methods

Fish otoliths used in this study came from several sources. Juvenile Atlantic croaker (*Micropogonias undulatus*) were taken from collections made as part of a larger study on the early life history of the species in the Mid- and South Atlantic Bights (Thorrold et al. 1997). Fish were collected from the lower Chesapeake Bay and two tributaries (the James and York rivers) and from the Pamlico and Neuse rivers in Pamlico Sound, North Carolina, in October 1996 and March 1997 (Fig. 1). All collections were made with a semiballoon otter trawl. Fish were stored on ice immediately after capture and then frozen upon return to the laboratory. Three juvenile Atlantic croaker, between the sizes of 50 and 60 mm standard length (SL), were randomly chosen from each location in November (Chesapeake Bay samples only) and May (Chesapeake Bay and Pamlico Sound). Otoliths were removed from the juvenile Atlantic croaker using acid-washed, nonmetallic instruments, sonified for 5 min in Milli-Q water, rinsed in ultrapure H_2O_2 for 1 min to remove any remaining tissue, triple rinsed again in Milli-Q water, and placed under a class 100 laminar flow hood to dry. The otoliths were then mounted on acid-washed microscope slides and ground to the midplane using 30- and 3-μm Al_2O_3 lapping paper. Finally, the otoliths were sonified again for 5 min in Milli-Q water, dried under the clean hood, and then placed in acid-washed, high-density polyethylene vials for transportation to the ICP-MS facility.

To investigate spatial variability in Sr:Ca ratios, we used an otolith section taken from a 48-year-old black drum (*Pogonias cromis*) collected in 1991 on the Eastern Shore of Virginia, just north of the Chesapeake Bay mouth. The deposition rate of growth increments in black drum otoliths has been validated using marginal increment analysis and bomb-carbon chronologies (Campana and Jones 1998). The otolith was sectioned using an isomet high-speed saw equipped with a diamond blade. The section was mounted on an acid-washed slide, rinsed with dilute HNO_3, and sonified in Milli-Q water for 5 min. The section was then air-dried under the clean hood and placed in an acid-washed polyethylene vial until analysis at the ICP-MS laboratory.

To get otoliths with a range of Sr and Pb isotope ratios and absolute concentrations, we analyzed a number of fish from both freshwater and estuarine systems. Juvenile steelhead (*Oncorhynchus mykiss*) were collected by electrofishing in the Black, St. Joseph's, and Manistee rivers, all tributaries of Lake Michigan, in the fall of 1996. Juvenile weakfish (*Cynoscion regalis*) were collected in trawl nets from Doboy Sound, Georgia, Pamlico Sound, North Carolina, and Chesapeake Bay, Virginia, in July 1996. In both cases, fish were stored on ice immediately after capture and then frozen upon return to the laboratory. Dissection protocols for the otoliths followed those outlined above for juvenile Atlantic croaker.

Instrumentation

All measurements were carried out on a Finnigan MAT Element ICP-MS located in the Department of Earth and Planetary Sciences at Washington University in St Louis, Mo. The Finnigan MAT Element is a double-focussing SF-ICP-MS in reverse Nier–Johnson geometry. The ionization source consists of a grounded argon ICP operated at atmospheric pressure. Ions produced in the central channel of the ICP enter the mass spectrometer through a mechanical slit of varying width. Three slit widths are available for the Ele-

© 2000 NRC Canada

Fig. 1. Map of the sampling locations for juvenile Atlantic croaker and weakfish in Doboy Sound, Georgia, Pamlico Sound, North Carolina, and Chesapeake Bay, Virginia.

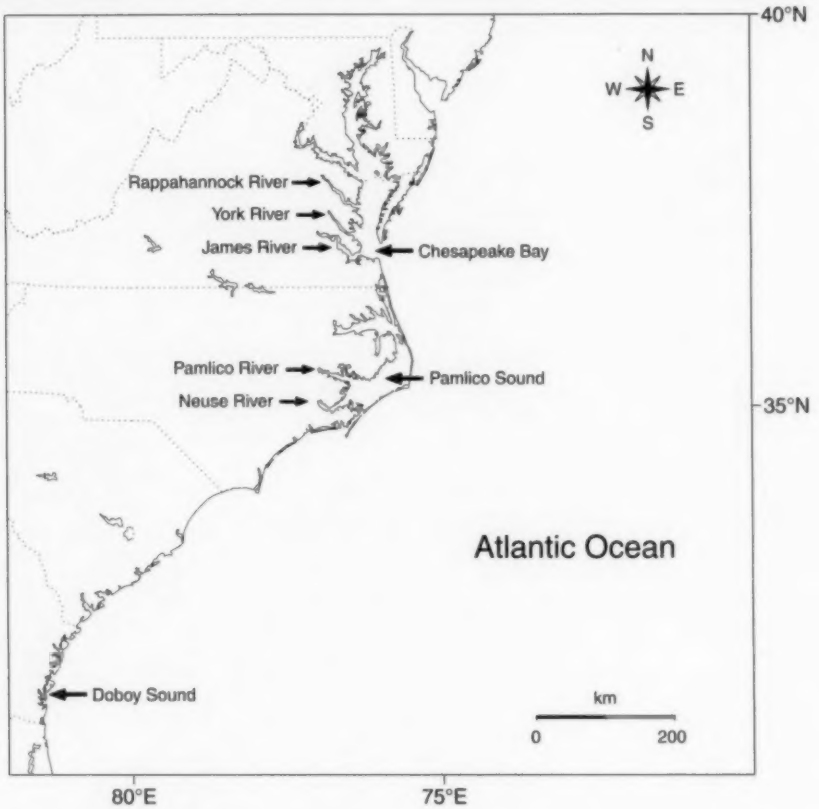

ment corresponding to low (R = 300), medium (R = 3000), and high (R = 9000) resolutions. Several methods of scanning across the mass range are available with the Element: magnet field strength scanning (B-scanning), acceleration voltage scanning (E-scanning), or a combination of the two in which the magnetic field is constantly cycled while the accelerating voltage is used to scan the peak tops (synchroscanning). We used a combination of scanning approaches, depending on the mass range that was required for each of the applications.

Sample introduction to the ICP-MS was achieved with a microconcentric nebulizer for solution-based assays and laser ablation for solid samples. The laser ablation system consisted of a 4-mJ Q-switched Nd:YAG laser, frequency-quadrupled to 266 nm and with a beam diameter of approximately 5 μm. The laser is mounted to a computer-controlled XYZ translation stage with 0.25-μm resolution, and the sample is viewed live through a video microscope on the computer screen. The energy profile of the laser is similar across the width of the beam ("top hat"), unlike earlier systems in which the energy profile of the laser beam had a Gaussian distribution (e.g., Thorrold et al. 1997). An even spread of energy across the beam allows for better depth control of individual craters, which is important for otolith applications where a three-dimensional structure is reduced to two dimensions during sectioning. Coupling of the laser with the sample otoliths and effective crater size of a laser beam with a diameter of 5 μm were evaluated by imaging the crater from a single laser blast using scanning electron microscopy (Fig. 2A). The image showed that the laser coupled well with otolith aragonite, as evidenced by both the symmetry and the sharp edge of the crater. This suggested that the interaction between the laser and the otolith was dominated by nonthermal processes, which minimized the amount of mass fractionation during ablation. The laser can be operated in single-pulse mode or can be programmed to raster a rectangle of user-specified dimensions. Due to the relatively long acquisition times (90 s) required for high-precision isotope ratios, we rastered an area of approximately 200 × 100 μm during the trace element and Sr isotope analyses (Fig. 2B). However, to maximize spatial resolution of the Sr:Ca ratio measurements in the adult black drum otolith, we programmed the laser to trace out a series of lines parallel to the annual growth increments. Data acquisition was made while the laser traced out each individual line. This, in turn, provided monthly estimates of Sr:Ca ratios throughout the 4 years of life represented by the four annual increments that we sampled across.

Quantification of trace elements in laser ablation ICP-MS remains difficult due to a lack of matrix-matched solid standards. In our earlier work (Thorrold et al. 1997), we achieved instrument calibration through the use of glass reference material supplied by the National Institute of Standards and Technology (NIST). However, the performance of SF-ICP-MS in NIST glasses has already been assessed (Shuttleworth and Kremser 1998). We have, therefore, taken a semiquantitative approach in the present study and simply ratioed all elemental data to Ca to account for differences in the amount of otolith material removed during laser ablation. To determine the accuracy of Sr isotope analyses, matching otoliths from the same fish as those used in the SF-ICP-MS analyses were also measured using thermal ionization mass spectrometry (TIMS).

© 2000 NRC Canada

Fig. 2. Scanning electron microscope micrographs of craters in juvenile Atlantic croaker otoliths from (A) a single pulse from the laser with a nominal beam diameter of 5 μm (scale bar = 10 μm) and (B) a 200 × 100 μm area rastered with the laser ablation system using a nominal beam diameter of 5 μm (scale bar = 50 μm).

A

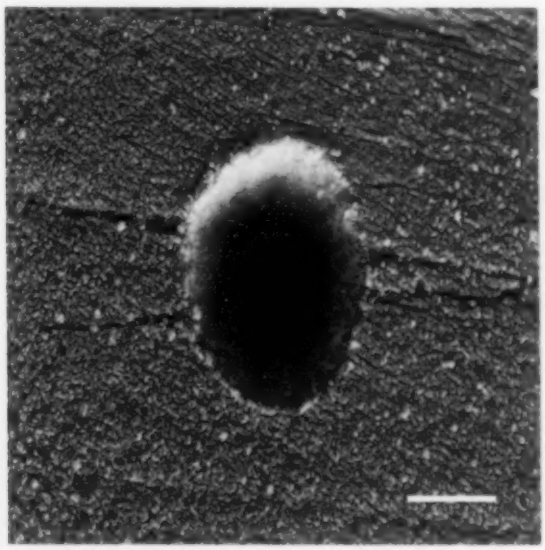

B

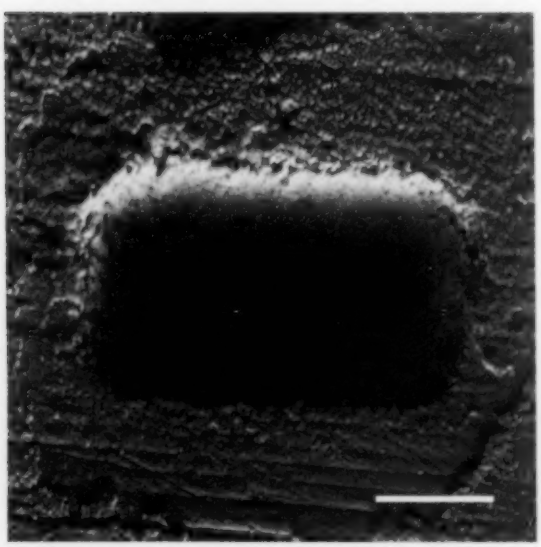

Three otoliths from each of the rivers or estuaries were pooled before analysis to provide an average ^{87}Sr:^{86}Sr ratio for each of the locations. Lead isotope analyses proved difficult due to extremely low Pb concentrations in both the steelhead and weakfish otoliths. Indeed, concentrations were so low (low nanograms per gram) that we could not extract meaningful ratios from any of the samples that we examined. Instead, we assayed Pb isotopes in NIST standard reference material (SRM) 981, a natural Pb reference material with certified values for ^{207}Pb:^{206}Pb and ^{208}Pb:^{206}Pb ratios. The SRM was digested and then diluted until Pb concentrations in solution were similar (10 $ng \cdot g^{-1}$) to those reported in otoliths by other studies (Campana et al. 1997). The data presented here should, therefore, be relevant to otolith chemistry applications in systems and species other than the ones that we examined.

Data analysis

Data analyses beyond descriptive statistics were restricted to trace element profiles from juvenile Atlantic croaker otoliths. Otolith profiles are examples of longitudinal data, in which measurements from an individual otolith are assumed to be dependent. Therefore, we used a repeated measures multivariate analysis of variance (RM-MANOVA) approach to examine differences in trace element profiles between collection dates and locations (e.g., Chambers and Miller 1995). A number of hypotheses can be tested using the RM-MANOVA approaches. We were primarily interested in testing the following null hypotheses: (*i*) there is no variation in trace element profiles across individual otoliths (i.e., from the center to the edge), (*ii*) there are no differences in mean element concentrations among locations, determined by averaging data across individual otolith profiles, and (*iii*) there are no differences in the pattern of element profiles across otoliths among locations. A priori contrasts were used to test specific null hypotheses concerning differences between November and May collections from Chesapeake Bay and differences between May collections from Chesapeake Bay and Pamlico Sound.

Results

Trace elements

Routine analysis of five elements (Mg, Ca, Mn, Sr, and Ba) was possible in the otoliths from juvenile Atlantic croaker using laser ablation SF-ICP-MS. Scans of each isotope (^{24}Mg, ^{43}Ca, ^{55}Mn, ^{88}Sr, and ^{138}Ba) in medium-resolution mode (R = 3000) revealed significant isobaric interferences on ^{24}Mg and ^{55}Mn (Fig. 3). The interference on ^{24}Mg appeared to be from a single ion source ($^{48}Ca^{2+}$). More importantly, the observation that this interference came from the sample matrix rather than the Ar blank meant ^{24}Mg intensities did not adequately blank-correct in low-resolution mode. The interference on ^{55}Mn was more complex and appears to have been attributable to at least two molecular species. Closer examination of the data suggested that the larger of the two interfering peaks was an argon hydride, while the secondary peak was potassium oxide. In this instance, the argon hydride interference would blank-correct to some degree, while the potassium oxide interference would not. Therefore, all subsequent data for Mg and Mn were collected in medium-resolution mode, while Sr and Ba were collected in low-resolution mode (R = 300). Data on ^{43}Ca were collected in both medium- and low-resolution modes, as this isotope was used as an internal standard.

Life history scans across the otoliths of juvenile Atlantic croaker revealed variation in Mn:Ca, Sr:Ca, and Ba:Ca ratios across individual otoliths and among otoliths from different locations and times (Fig. 4). No patterns were discernable in the Mg:Ca scans, and hence these data were not considered further. RM-MANOVA detected significant differences in

© 2000 NRC Canada

Fig. 3. Medium-resolution (R = 3000) scans of a juvenile Atlantic croaker otolith over mass/charge (m/z) values centered on the atomic weights of ^{24}Mg and ^{55}Mn and with sample input by laser ablation.

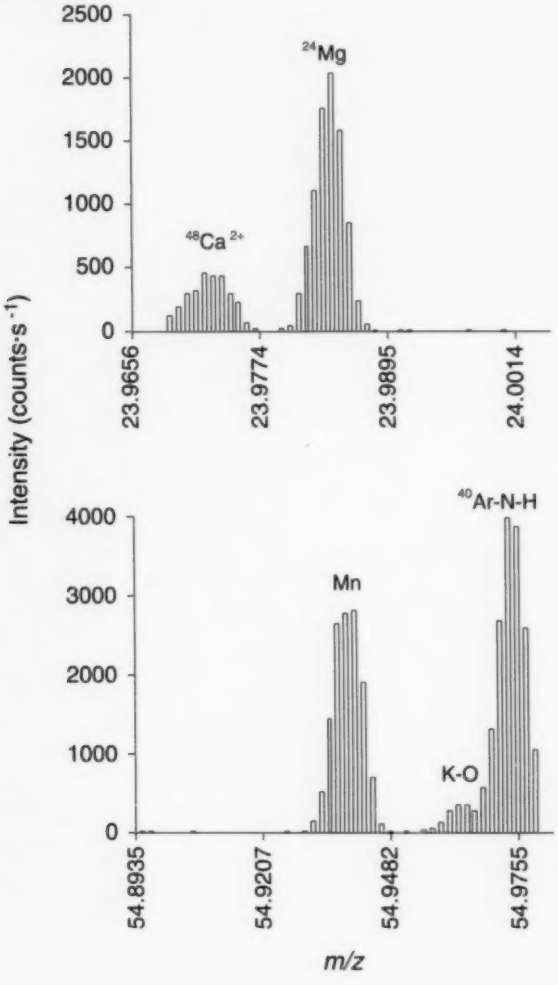

Mn:Ca ratios across the otoliths from the center to the edge and among locations (Table 1). Profiles across otoliths also varied significantly between May collections in Chesapeake Bay and Pamlico Sound (Table 1). Differences between Pamlico Sound and Chesapeake Bay were generated by extremely high Mn:Ca ratio values towards the outer edge of otoliths from fish collected in the Neuse River in May. Differences between rivers within both Chesapeake Bay and Pamlico Sound were noticeable, largely due to low variability among replicate fish within each location.

The Sr:Ca ratios showed a general, and statistically significant, trend of decreasing values from the center to the edge of the otoliths at all locations (Table 1). Otolith Sr:Ca profiles from both the Neuse River and Pamlico River samples declined sharply from the center of the otoliths to the middle position and remained constant thereafter out to the edge (Fig. 4). Life history scans from Chesapeake Bay otoliths were more variable but still retained the general trend of highest Sr:Ca ratio values at the center and lowest values at the edge. The RM-MANOVA found a significant difference in otolith Sr:Ca profiles between Pamlico Sound and Chesapeake Bay in May but not between November and May collections in Chesapeake Bay. Small, but consistent, differences in Sr:Ca ratios were also found between sites in both Chesapeake Bay and Pamlico Sound at the otolith edge. This resulted in a significant difference in Sr:Ca ratios, averaged across all positions on individual otoliths, between May collections from the two locations.

Analysis of Ba:Ca profiles found significant variability from the center to the edge of individual otoliths and averaged across positions among locations (Fig. 4). Significant differences in these average values were found both between November and May samples from Chesapeake Bay and between May samples from Chesapeake Bay and Pamlico Sound (Table 1). Within-otolith Ba:Ca profiles followed an overall pattern similar to that of Mn:Ca ratios, with lowest values consistently found at the otolith center and higher, but variable, ratios found towards the otolith edge. Otolith profiles were significantly different between November and May in the Chesapeake Bay samples and between Chesapeake Bay and Pamlico Sound. There were also obvious differences between the Mn:Ca and Ba:Ca profiles. For instance, Ba:Ca profiles from the Neuse River did not show large increases towards the edge of the otolith, unlike the corresponding Mn:Ca profiles from the same otoliths. Indeed, Ba:Ca ratios from Pamlico Sound fish were surprisingly constant among replicate fish from the same river and within otoliths from individual fish.

High-precision Sr:Ca ratios

A total of 33 Sr:Ca ratios, encompassing two annuli deposited in 1974–1976 and 1964–1966, were asssayed from the otolith of a 48-year-old adult black drum. Individual samples therefore incorporated material deposited over an approximately 1-month period. There was comparatively little spatial variation across each of the two annual increments: minimum and maximum values differed by 18% during 1964–1966 and by 25% during 1974–1976 (Fig. 5). Despite the relatively low variation, there were distinctive quasi-sinusoidal patterns in both of the sets of measurements with a period of approximately 1 year. The amplitude of the Sr:Ca measurements was increased slightly in 1974–1976 and positively shifted by approximately 12%. The precision of these analyses was difficult to quantify, as there are no solid carbonate standards homogeneous to the 1% level. However, precision can be calculated by treating adjacent samples as replicates. In this case, such a value will be an overestimate, as adjacent samples are not independent. Using this conservative measure, the mean relative standard deviation (RSD) from a total of 17 sets of three adjacent samples was 3.5%.

Strontium and Pb isotope ratios

Strontium isotope analyses were conducted on otoliths from both steelhead and weakfish, with sample introduction done using a microconcentric nebulizer and a laser ablation system. Isotopic values (^{87}Sr:^{86}Sr) of individual dissolved steelhead otoliths ranged from 0.7090 to 0.7119, with a

© 2000 NRC Canada

Fig. 4. Trace element profiles from the center (C) to the edge (E) of otoliths from juvenile Atlantic croaker collected from the James River (open diamonds) and the York River (solid squares) in November 1996 and the York River (solid squares), lower Chesapeake Bay (open circles), the Neuse River (open squares), and the Pamlico River (solid circles) in May 1997.

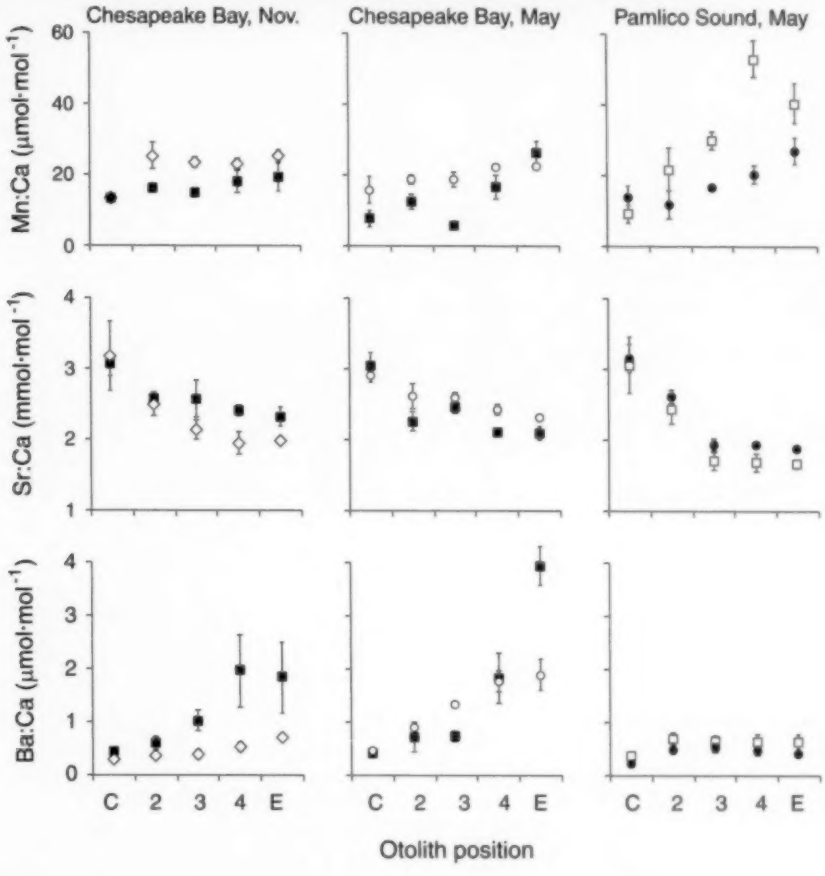

mean RSD of 0.29 from three replicate measurements of 18 otoliths (Fig. 6). TIMS analysis of a pooled sample consisting of three otoliths from each of the three rivers provided ^{87}Sr:^{86}Sr values of 0.70971 for the Black River, 0.70921 for the St. Joseph's River, and 0.70962 for the Manistee River. Mean ^{87}Sr:^{86}Sr values from ICP-MS analyses of individual otoliths from the three rivers were within 1 SD of those obtained from TIMS analyses. Highest values were seen in the Black River (0.7103 ± 0.00015) followed by St. Joseph's River (0.7010 ± 0.0008) and the Manistee River (0.7094 ± 0.0003). Not surprisingly, laser data from otoliths were less precise than those of the solution-based analyses (Fig. 6). Strontium isotope values using laser ablation varied from 0.7093 to 0.7128, with a mean RSD of 0.56. Values for the St. Joseph's River (0.7102 ± 0.0004) and the Manistee River (0.7118 ± 0.0014) were slightly outside 1 SD of the TIMS values for these rivers, while data from the Black River (0.7105 ± 0.00017) were within 1 SD of the TIMS number.

Weakfish otoliths have higher Sr concentrations than freshwater fishes such as steelhead, and this in turn influenced the precision of Sr isotope ratios. Strontium isotope values from solution-based analyses of weakfish otoliths ranged from 0.70866 to 0.70923, with a mean RSD of 0.07% (Fig. 6). Mean ^{87}Sr:^{86}Sr values from Pamlico Sound (0.70899 ± 0.00013) and the Rappahannock River (0.70914 ± 0.00009) were within 1 SD of the TIMS data (0.70906 and 0.70913, respectively), while the Doboy Sound value (0.70873 ± 0.00007) was slightly below the corresponding TIMS number (0.70906). Results from analyses of weakfish otoliths using laser ablation were, like the steelhead data, less precise than the solution-based values (Fig. 6), ranging from 0.7086 to 0.7096 (RSD = 0.097). Mean values from Pamlico Sound (0.70896 ± 0.00014) and the Rappahannock River (0.70919 ± 0.00038) were within 1 SD of the TIMS numbers, while the Doboy Sound data were, again, slightly lower than the value from the TIMS analysis.

We quantified ^{207}Pb:^{206}Pb and ^{208}Pb:^{206}Pb ratios in NIST SRM 981 at a total Pb concentration of 0.01 $\mu g \cdot g^{-1}$. Short-term analyses ($n = 4$ within a single day) of ^{207}Pb:^{206}Pb ratios (0.9148 ± 0.0004) and ^{208}Pb:^{206}Pb ratios (2.1674 ± 0.0009) showed excellent agreement with the certified values for the SRM (0.9146 and 2.1681, respectively). Precision (RSD) of both ratios was 0.08%. Long-term analyses ($n = 40$

© 2000 NRC Canada

Table 1. Results of RM-MANOVA of Mn:Ca, Sr:Ca, and Ba:Ca profiles across otoliths from juvenile Atlantic croaker collected from locations (Loc) in Chesapeake Bay (CB) in November and May and Pamlico Sound (PS) in May.

	SS	*F*	Num df	Den df	Pr > *F*
Mn:Ca					
Pos	0.981	114	4	9	0.0001
Pos × Loc contrasts					
CB vs. PS	0.939	34.7	4	9	0.0001
Nov. vs. May	0.873	15.4	4	9	0.0005
Loc contrasts					
CB vs. PS	1.5×10^{-7}	45.74	1	12	0.0001
Nov. vs. May	0.8×10^{-7}	22.52	1	12	0.0005
Sr:Ca					
Pos	0.896	19.5	4	9	0.0002
Pos × Loc contrasts					
CB vs. PS	0.621	3.69	4	9	0.0481
Nov. vs. May	0.170	0.46	4	9	0.7631
Loc contrasts					
CB vs. PS	9.5×10^{-6}	8.47	1	12	0.0131
Nov. vs. May	2×10^{-8}	0.02	1	12	0.8991
Ba:Ca					
Pos	0.845	12.3	4	9	0.0011
Pos × Loc contrasts					
CB vs. PS	0.799	8.96	4	9	0.0033
Nov. vs. May	0.463	1.94	4	9	0.1878
Loc contrasts					
CB vs. PS		26.05	1	12	0.0003
Nov. vs. May		2.82	1	12	0.1188

Note: Values across individual otoliths are designated as positions (Pos) in the repeated measures analysis. Pillai's trace was used for all multivariate tests.

over several months) of both ratios in the SRM (^{207}Pb:$^{206}Pb = 0.9149 \pm 0.0009$, ^{208}Pb:$^{206}Pb = 2.175 \pm 0.006$) were also within 1 SD of the certified values. Precision (RSD) was not as good as the short-term estimates (^{207}Pb:^{206}Pb = 0.19%, ^{208}Pb:^{206}Pb = 0.55%) but was still better than 1% for both ratios.

Discussion

A number of probe-based instruments are available for chemical analyses of biogenic carbonates such as otoliths (Campana et al. 1997). SF-ICP-MS is a relatively new technique that is particularly well suited to otolith chemistry assays. The instruments are characterized by extremely low levels of detection, largely due to background counts of less than 0.1 ion·s^{-1}. For instance, Turner et al. (1998) were able to detect ^{238}U at a total U concentration of 24 fg·L^{-1} using SF-ICP-MS. If the element of interest cannot be reliably detected by the instrument, we can conclude that it must be present in otoliths at extremely low concentrations. The high-resolution capabilities of the instrument are useful for detection of isobaric interferences. The ability to resolve complex interferences on ^{55}Mn improved both precision and accuracy of Mn measurements in juvenile Atlantic croaker otoliths. Other transition-row metals, including Fe, Ni, and Cu, also have molecular interferences from argon and calcium oxides that, while making quantification problematic using Q-ICP-MS, are easily resolved using high-resolution ICP-MS (Turner et al. 1998).

Trace element profiles across Atlantic croaker otoliths revealed several trends that were not evident in a recent study of juvenile Atlantic croaker from similar locations using laser ablation Q-ICP-MS (Thorrold et al. 1997). Manganese was not measured in the earlier paper but in the present study showed considerable variation, both within and between Chesapeake Bay and Pamlico Sound. The most obvious feature in the Mn:Ca profiles was the extremely high ratios seen towards the edge of otoliths collected from the Neuse River. The pattern was not, however, present in Pamlico River otoliths. If Mn:Ca ratios in otoliths are reflecting Mn:Ca ratios in the water column, then dissolved Mn in the Neuse River must have been comparatively high in March and April of 1997. The observation that Ba:Ca ratios did not show concomitant increases argues against a solely terrestrial source for the Mn ions, as we would expect significant freshwater input to raise ambient Mn and Ba levels. It is possible that the Mn increase may have been due to enhanced reductive redissolution of particulate MnO_x, either from the water column or from sediments (Sunda and Huntsman 1987). Given the propensity for hypoxia to develop during spring and summer in the Neuse River (Paerl et al. 1998), reducing conditions in hypoxic bottom waters may have led to enhanced dissolved Mn concentrations in the river and ultimately to the increased Mn:Ca levels that we saw in the Atlantic croaker otoliths. If this hypothesis can be validated, Mn:Ca levels in otoliths may be a useful proxy for hypoxia in aquatic environments

We found that, as in a previous study, Sr:Ca and Ba:Ca ra-

© 2000 NRC Canada

Fig. 5. Profile of Sr:Ca ratios across a black drum otolith from material deposited in 1965–1966 and 1974–1976. Arrows indicate the end of annulus (opaque zone) formation, assumed to be in April of each year. The error bar is calculated as the mean SD of each of three adjacent values across the otolith and is a conservative estimate (see text).

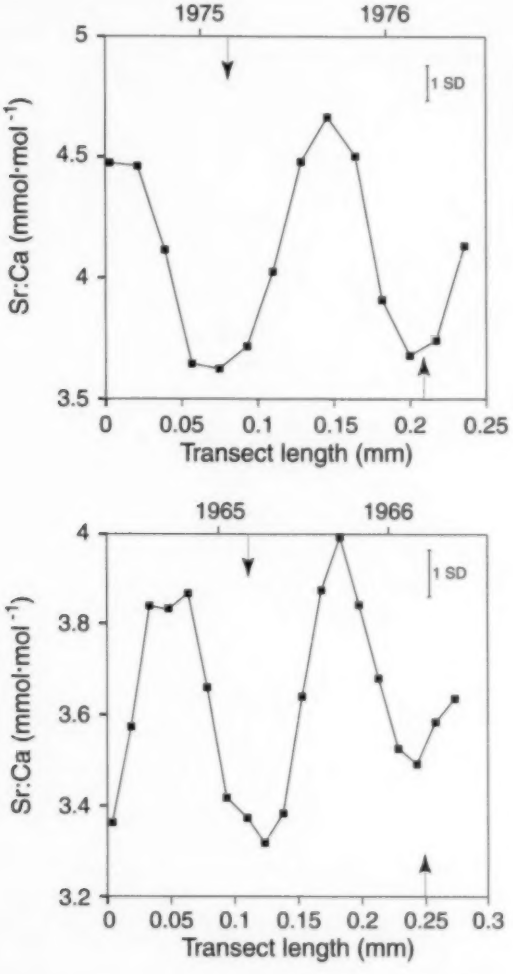

tios in Atlantic croaker otoliths from Chesapeake Bay are generally negatively correlated (Thorrold et al. 1997). This is to be expected if the juvenile Atlantic croaker are migrating from high-Sr, low-Ba oceanic spawning locations to low-Sr, high-Ba estuarine nursery areas. There was also significant temporal variation in the relationship between the two elements. For instance, high Ba:Ca ratios in May were not reflected in low Sr:Ca ratios in the same month, indicating that the discharge of high-Ba freshwater into Chesapeake Bay in the spring is having relatively little impact on the concentrations of the Sr freshwater end-member during this time. Both Sr:Ca and Ba:Ca profiles from Pamlico Sound Atlantic croaker were remarkably consistent across sites, suggesting little spatial variation in dissolved Sr and Ba levels between the Neuse and Pamlico rivers. These data

Fig. 6. Solution-based and laser ablation Sr isotope (^{87}Sr:^{86}Sr) values from individual steelhead and weakfish otoliths (open squares), mean values for each of the locations (solid squares) using solution-based SF-ICP-MS (±SD), and TIMS values for each of the locations (open circles) based on a pooled sample of three otoliths (±SD). Steelhead samples are from the Black River, the St. Joseph's (St. Jos.) River, and the Manistee (Manis.) River, and weakfish samples are from Doboy Sound, Pamlico Sound, and the Rappahannock (Rapp.) River. The inset on both graphs magnifies the scale on the *y*-axis for weakfish samples.

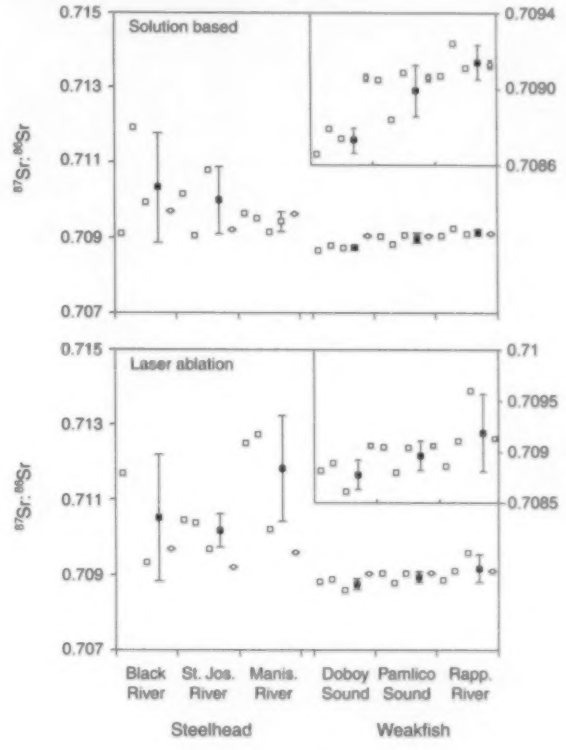

also suggest that there are large differences in water chemistry between Chesapeake Bay and Pamlico Sound during peak recruitment (fall through early spring) of Atlantic croaker. Juvenile weakfish otoliths collected from the same locations in July indicate that these differences are also present through the summer (Thorrold et al. 1998). The limited data available on dissolved Ba concentrations suggest that indeed the freshwater end-member in Chesapeake Bay is approximately twice that of rivers in the South Atlantic Bight (Coffey et al. 1997; Shaw et al. 1998).

High-resolution sampling of an adult black drum otolith revealed distinctive quasi-periodic patterns in Sr:Ca ratios that were in phase with predicted seasonal temperature histories based on an April formation of the annulus (Beckman et al. 1990). Although temperature-driven seasonal patterns in $\delta^{18}O$ have been retrieved from otoliths (Patterson et al. 1993), this appears to be one of the few convincing examples of annual cycles in Sr:Ca ratios from fish otoliths. Negative relationships between Sr:Ca ratios and temperature have been documented in coral skeletons (e.g., Shen et al.

© 2000 NRC Canada

1996) and fish otoliths (Townsend et al. 1995). However, recent data from laboratory-reared Atlantic croaker (Fowler et al. 1995) and spot (*Leiostomus xanthurus*) (Bath et al. 2000) showed that Sr:Ca ratios and temperature in otoliths were positively correlated, with similar estimates of temperature dependence (0.08 $mmol \cdot mol^{-1} \cdot °C^{-1}$ for Atlantic croaker and 0.09 $mmol \cdot mol^{-1} \cdot °C^{-1}$ for spot). The Sr:Ca temperature dependency for corals of the genus *Porites* is, for comparison, –0.051 $mmol \cdot mol^{-1} \cdot °C^{-1}$ (Shen et al. 1996). Applying the temperature dependence estimated by Bath et al. (2000), the seasonal temperature range experienced by the black drum was approximately 16°C in 1965–1966 and 28°C in 1974–1976. The seasonal temperature range at the mouth of the Chesapeake Bay is approximately 20°C, suggesting that factors other than temperature may also be exerting an influence on Sr:Ca ratios in otoliths. Temperature effects in the otoliths of adult fish may be aliased by seasonal changes in reproductive physiology, which can also influence otolith Sr:Ca ratios (Kalish 1991; Friedland et al. 1998). Seasonal migrations into estuarine waters with lower Sr:Ca ratios than adjacent coastal water masses could also generate annual patterns in otolith Sr:Ca ratios (e.g., Secor and Piccoli 1996), although such an explanation would suggest lower, not higher, values in spring–summer as the fish moved into estuarine habitats. These data do, however, serve to emphasize the analytical precision necessary for accurate Sr:Ca thermometry in otoliths if temperature fluctuations are determining Sr:Ca ratios in otoliths. A 25% difference in otolith Sr:Ca values in the present study corresponded to a 28°C difference in minimum and maximum temperatures. Detecting more subtle differences in temperature from Sr:Ca ratios in otoliths will clearly be beyond the analytical capabilities of instruments such as the electron microprobe (Campana et al. 1997).

High-precision measurements of isotope ratios of elements in otoliths are still comparatively new but have great potential as natural tracers of water mass residency (Campana 1999). The power of an approach utilizing isotope ratios relies on the observation that although fish may discriminate against an element, such as Sr, the isotope ratios of the element within the otolith remain identical to that of the ambient environment (Kennedy et al. 1997). Typically, measurements of isotope ratios for geochemical applications have been performed using TIMS or, more recently, multicollector ICP-MS (Christensen et al. 1995; Kennedy et al. 1997). Both techniques are capable of high-precision (<0.005%) measurements, but analyses are time-consuming and expensive. Our data confirmed earlier work that suggested that Sr isotope ratios could be measured with SF-ICP-MS quickly and inexpensively at a precision approaching 0.03% (Latkoczy et al. 1998). The ability to correct for Rb isotope interferences on ^{87}Sr by monitoring ^{85}Rb allowed for in situ analyses via laser ablation with an external precision better than 0.1% in otoliths from marine fish. Accurate Pb isotope ratios were also recovered from the Pb SRM. Natural Pb and anthrogenic Pb in the environment are often characterized by unique isotopic signatures (Ritson et al. 1994) and as such are excellent tracers of pollution that should be accurately reflected in fish otoliths. Precision of the ratio estimates compared favorably with that obtained for ^{87}Sr:^{86}Sr ratios using secondary ionization mass spectrometry (0.2%, Exley and Jones 1983) and Pb isotopes using Q-ICP-MS (1–10%, Machado and Gauthier 1996). Multicollector ICP-MS instruments offer much greater precision than that that can be achieved by the sequential, single-collector ICP-MS used in the present study (Christensen et al. 1995). However, detection efficiency is typically less than 1% in commercial multicollector instruments, and therefore, isotopic analyses of trace elements in solid samples are challenging using multicollector ICP-MS. Thus, in situ isotope analyses of trace elements in otoliths such as Cu and Pb, and even Sr in freshwater otoliths, may require the sensitivity of SF-ICP-MS instrumentation, albeit with reduced precision compared with multicollector ICP-MS.

In conclusion, analyses from freshwater and marine fishes highlighted the potential of SF-ICP-MS instruments for quantifying trace elements and isotope ratios in otoliths. Excellent sensitivity, the ability to resolve molecular interferences, precise isotope ratio measurements, and spatial resolution of approximately 5 μm make laser ablation SF-ICP-MS a powerful tool for profiling otolith geochemistry. Ultimately, the choice of instrumentation should be governed by the questions being asked, as no one technique is currently suitable for all applications (Campana et al. 1997). For instance, determining the natal tributary of salmonids in a single river system from Sr isotope ratios in otoliths will in all likelihood require the precision of TIMS (Kennedy et al. 1997). However, Sr isotope ratios can be measured with sufficient precision using SF-ICP-MS to track migrations from marine waters to rivers in most cases. Lead isotopes in otoliths have yet to be used as a pollution indicator, but the combination of high sensitivity and high precision will likely make SF-ICP-MS the instrument of choice for such measurements in the future. Pollution indicators that rely on isotopic signatures are particularly useful, as it seems unlikely that there will be significant biological fractionation of metal isotopes between ambient waters and otoliths. In contrast, trace elements in otoliths appear to be only weakly correlated with pollution exposure (Hanson and Zdanowicz 1999). The overall stability of SF-ICP-MS instruments and flat-topped ion peaks also allow for accurate measurements of elemental concentrations in otoliths, which will be critical if Mn:Ca, Sr:Ca, and Ba:Ca ratios prove to be useful proxies for dissolved oxygen, temperature, or salinity. These instrument characteristics are important for both solution-based applications for whole otoliths, including isotope dilution approaches, and trace element and isotope profiles of sectioned otoliths using laser ablation.

Acknowledgements

We are grateful to several people in the Department of Earth and Planetary Sciences at Washington University. Everett Shock provided access to the SF-ICP-MS laboratory, Joyce Brannon generously ran the TIMS Sr isotope samples, and Dan Kremser provided the scanning electron microscope micrographs. We thank Merchantek EO for the loan of the laser system used in this study. Luiz Barbieri (University of Georgia), Pat Geer (VIMS), Mike Greene (NOS, Beaufort Laboratory), and Ed Rutherford (University of Michigan) provided specimens used in the analyses. This research was supported by the National Science Foundation under grant

© 2000 NRC Canada

No. OCE-9416579 to Cynthia M. Jones and Steven E. Campana and grant No. OCE-9876565 to Cynthia M. Jones and S.R.T.

References

Bath, G.E., Thorrold, S.R., Jones, C.M., and Campana, S.E. 2000. Strontium and barium uptake in aragonitic otoliths of marine fish. Geochim. Cosmochim. Acta, **64**: 1705–1714.

Beary, E.S., and Paulson, P.J. 1993. Selective application of chemical separations to isotope dilution inductively coupled plasma mass spectrometric analyses of standard reference materials. Anal. Chem. **65**: 1602–1608.

Beckman, D.W., Wilson, C.A., and Stanley, A.L. 1990. Age and growth of black drum in Louisiana waters of the Gulf of Mexico. Trans. Am. Fish. Soc. **19**: 537–544.

Boyle, E.A. 1988. Cadmium: chemical tracer of deepwater paleoceanography. Paleoceanography, **3**: 471–489.

Campana, S.E. 1999. Chemistry and composition of fish otoliths: pathways, mechanisms and applications. Mar. Ecol. Prog. Ser. **188**: 263–297.

Campana, S.E., and Jones, C.M. 1998. Radiocarbon from nuclear testing applied to age validation of black drum, *Pogonias cromis*. Fish. Bull. U.S. **96**: 185–192.

Campana, S.E., Thorrold, S.R., Jones, C.M., Günther, D., Tubrett, M., Longerich, H., Jackson, S., Halden, N.M., Kalish, J.M., Piccoli, P., de Pontual, H., Troadec, H., Panfili, J., Secor, D.H., Severin, K.P., Sie, S.H., Thresher, R., Teesdale, W.J., and Campbell, J.L. 1997. Comparison of accuracy, precision, and sensitivity in elemental assays of fish otoliths using the electron microprobe, proton-induced X-ray emission, and laser ablation inductively coupled plasma mass spectrometry. Can. J. Fish. Aquat. Sci. **54**: 2068–2079.

Chambers, R.C., and Miller, T.J. 1995. Evaluating fish growth by means of otolith increment analysis: special properties of individual-level longitudinal data. *In* Recent developments in fish otolith research. *Edited by* D.H. Secor, J.M. Dean, and S.E. Campana. University of South Carolina Press, Columbia, S.C. pp. 155–175.

Christensen, J.N., Halliday, A.N., Lee, D.-C., and Hall, C.M. 1995. In situ Sr isotopic analysis by laser ablation. Earth Planet. Sci. Lett. **136**: 79–85.

Coffey, M., Dehairs, F., Collette, O., Luther, G., Church, T., and Jickells, T. 1997. The behaviour of dissolved barium in estuaries. Estuarine Coastal Shelf Sci. **45**: 113–121.

Exley, R.A., and Jones, A.P. 1983. $^{87}Sr/^{86}Sr$ in kimberlite carbonates by ion microprobe: hydrothermal alteration, crustal contamination and relation to carbonatite. Contrib. Mineral. Petrol. **83**: 288–292.

Fowler, A.J., Campana, S.E., Jones, C.M., and Thorrold, S.R. 1995. Experimental assessment of the effect of temperature and salinity on elemental composition of otoliths using solution-based ICPMS. Can. J. Fish. Aquat. Sci. **52**: 1421–1430.

Friedland, K.D., Reddin, D.G., Shimizu, N., Haas, R.E., and Youngson, A.F. 1998. Strontium: calcium ratios in Atlantic salmon (*Salmo salar*) otoliths and observations on growth and maturity. Can. J. Fish. Aquat. Sci. **55**: 1158–1168.

Guilderson, T.P., Fairbanks, R.G., and Rubenstone, J.L. 1994. Tropical temperature variations since 20,000 years ago: modulating interhemispheric climate change. Science (Washington, D.C.), **263**: 663–665.

Hanson, P.J., and Zdanowicz, V.S. 1999. Elemental composition of otoliths from Atlantic croaker along an estuarine pollution gradient. J. Fish Biol. **54**: 656–668.

Hart, S.R., and Blusztajn, J. 1998. Clams as recorders of ocean ridge volcanism and hydrothermal vent field activity. Science (Washington, D.C.), **280**: 883–886.

Hart, S.R., and Cohen, A.L. 1996. An ion probe study of annual cycles of Sr/Ca and other trace elements in corals. Geochim. Cosmochim. Acta, **60**: 3075–3084.

Kalish, J.M. 1991. Determinants of otolith chemistry: seasonal variation in composition of blood plasma, endolymph and otoliths of bearded rock cod *Pseudophycis barbatus*. Mar. Ecol. Prog. Ser. **74**: 137–159.

Kennedy, B.D., Folt, C.L., Blum, J.D., and Chamberlain, C.P. 1997. Natural isotope markers in salmon. Nature (Lond.), **387**: 766–767.

Latkoczy, C., Prohaska, T., Stingeder, G., and Teschler-Nicola, M. 1998. Strontium isotope ratio measurements in prehistoric human bone samples by means of high-resolution inductively coupled plasma mass spectrometry (HR-ICP-MS). J. Anal. At. Spectrom. **13**: 561–566.

Machado, N., and Gauthier, G. 1996. Determination of $^{207}Pb/^{206}Pb$ ages on zircon and monazite by laser-ablation ICPMS and application to a study of sedimentary provenance and metamorphism in southeastern Brazil. Geochim. Cosmochim. Acta, **60**: 5063–5073.

Moens, L., Vanhaecke, F., Riondato, J., and Dams, R. 1995. Some figures of merit of a new double focusing inductively coupled plasma mass spectrometer. J. Anal. At. Spectrom. **10**: 569–574.

Paerl, H.W., Pinckney, J.L., Fear, J.M., and Peierls, B.L. 1998. Ecosystem responses to internal and watershed organic matter loading: consequences for hypoxia in the eutrophying Neuse River Estuary, North Carolina, USA. Mar. Ecol. Prog. Ser. **166**: 17–25.

Patterson, W.P., Smith, G.R., and Lohmann, K.C. 1993. Continental paleothermometry and seasonality using the isotopic composition of aragonitic otoliths of freshwater fishes. Geophys. Monogr. **78**: 191–202.

Ritson, P.I., Esser, B.K., Niemeyer, S., and Flegal, A.R. 1994. Lead isotopic determination of historical sources of lead to Lake Erie, North America. Geochim. Cosmochim. Acta, **58**: 3297–3305.

Secor, D.H., and Piccoli, P.M. 1996. Age- and sex-dependent migrations of striped bass in the Hudson River as determined by chemical microanalysis of otoliths. Estuaries, **19**: 778–793.

Shaw, T.J., Moore, W.S., Kloepfer, J., and Sochaski, M.A. 1998. The flux of barium to the coastal waters of the southeastern USA: the importance of submarine groundwater discharge. Geochim. Cosmochim. Acta, **62**: 3047–3054.

Shen, C.C., Lee, T., Chen, C.Y., Wang, C.H., Dai, C.F., and Li, L.A. 1996. The calibration of D[Sr/Ca] versus sea surface temperature relationship for *Porites* corals. Geochim. Cosmochim. Acta, **60**: 3849–3858.

Shuttleworth, S., and Kremser, D.T. 1998. Assessment of laser ablation and sector field inductively coupled plasma mass spectrometry for elemental analysis of solid samples. J. Anal. At. Spectrom. **13**: 697–699.

Sinclair, D.J., Kinsley, L.P.J., and McCulloch, M.T. 1998. High resolution analysis of trace elements in corals by laser ablation ICP-MS. Geochim. Cosmochim. Acta, **62**: 1889–1901.

Sunda, W.G., and Huntsman, S.A. 1987. Microbial oxidation of manganese in a North Carolina estuary. Limnol. Oceanogr. **32**: 552–564.

Thorrold, S.R., Jones, C.M., and Campana, S.E. 1997. Response of otolith microchemistry to environmental variations experienced by larval and juvenile Atlantic croaker (*Micropogonias undulatus*). Limnol. Oceanogr. **42**: 102–111.

Thorrold, S.R., Jones, C.M., Swart, P.K., and Targett, T.E. 1998. Accurate classification of juvenile weakfish *Cynoscion regalis* to

© 2000 NRC Canada

estuarine nursery habitats based on chemical signatures in otoliths. Mar. Ecol. Prog. Ser. **173**: 253–265.

Townsend, D.W., Radtke, R.L., Malone, D.P., and Wallinga, J.P. 1995. Use of otolith strontium: calcium ratios for hindcasting larval cod distributions relative to water masses on Georges Bank. Mar. Ecol. Prog. Ser. **119**: 37–44.

Turner, P.J., Mills, D.J., Schröder, E., Lapitajs, G., Jung, G., Iacone, L.A., Haydar, D.A., and Montaser, A. 1998. Instrumentation for low- and high-resolution ICPMS. *In* Inductively coupled plasma mass spectrometry. *Edited by* A. Montaser. Wiley-VCH, New York. pp. 421–501.

Vanhaecke, F., Moens, L., Dams, R., and Taylor, P. 1996. Precise measurement of isotopic ratios with a double-focusing magnetic sector ICP mass spectrometer. Anal. Chem. **68**: 567–569.

© 2000 NRC Canada

Factors influencing carbon, nitrogen, and phosphorus content of fish from a Lake Superior coastal wetland

Danny K. Tanner, John C. Brazner, and Valerie J. Brady

Abstract: The narrow fish nutrient ranges (C, 42.8–48.4%; N, 9.6–12.7%; P, 1.91–2.74%) in this study suggest that overall mean values are adequate for quantifying movement of C, N, or P as part of fish-mediated nutrient transport. We measured C, N, and P in 20 species of Lake Superior coastal wetland fish to better understand variability in fish elemental content caused by differences in species, habitat, season, life stage, or size. Fish were sampled within Bark Bay slough and at its inlet/outlet to Bark Bay, Lake Superior, from May to November 1995. Elemental content averaged across all fish (n = 192) was 45.1% for C, 11.3% for N, and 2.45% for P. We did find significant differences ($p \leq 0.05$) among nine tested species. However, less than one third of the analyses were significant for effects of location or date of capture or fish length on fish nutrient content and nutrient ratios. Regressions of N:P ratios against growth rate indices and, separately, fineness ratios were significant, suggesting that growth rate and body shape are important factors driving N:P ratios in fish.

Résumé : Les fourchettes étroites des teneurs en nutriants des poissons (C, 42,8–48,4%; N, 9,6–12,7%; P, 1,91–2,74%) notées dans notre étude permettent de penser que les valeurs globales moyennes conviennent pour quantifier le mouvement du carbone (C), d'azote (N) et du phosphore (P) dans le cadre du transport de ces nutriants par l'intermédiaire des poissons. Nous avons mesuré C, N ou P chez 20 espèces de poissons d'un marécage littoral du lac Supérieur pour mieux comprendre la variabilité des teneurs en éléments des poissons dans son lien avec des différences dans l'espèce, l'habitat, la saison, le stade biologique ou la taille. Les poissons ont été échantillonnés dans le marécage de la baie Bark et au point où il communique avec la baie Bark, dans le lac Supérieur, de mai à novembre 1995. La moyenne de la teneur en éléments pour l'ensemble des poissons (n = 192) était de 45,1% pour C, 11,3% pour N et 2,45% pour P. Nous avons cependant observé des différences significatives ($p \leq 0,05$) entre les neuf espèces étudiées. Toutefois, moins d'un tiers des analyses étaient significatives en ce qui concerne les effets du lieu ou de la date de capture ou de la longueur du poisson sur la teneur en nutriants et sur les rapports des nutriants. Les régressions sur les rapports N:P en fonction des indices du taux de croissance et, d'autre part, sur les rapports de finesse étaient significatives, ce qui permet de penser que le taux de croissance et la forme du corps sont des facteurs importants qui régissent les rapports N:P chez les poissons.

[Traduit par la Rédaction]

Introduction

Carbon, N, and P are essential elements that are found in relatively consistent proportions in biological organisms. Because these essential elements can limit phytoplankton production in aquatic ecosystems, the manner in which fish store or move nutrients between habitats and ecosystems can have implications for many levels of the food web. Fish store much of their C as lipids, N is stored as protein in muscle, and nearly half of the P in fish is located in bone and scales (DaCosta and Stern 1956). Fish are often long-lived and thus can serve as reservoirs of nutrients, maintaining them through more than one annual cycle (Kitchell et al. 1975). For example, Kitchell et. al. (1975) found that 74% of total epilimnetic P in a Wisconsin lake was contained within fish biomass. Fish may also transport nutrients between compartments within an ecosystem or transfer nutrients to other ecosystems. Fish transport nutrients within lakes through ingestion of food in one habitat and excretion in another (Vanni 1995), and migrating salmon transport nutrients between saltwater and freshwater ecosystems (Richey et al. 1975). Deegan (1993) examined fish-mediated transport of nutrients between estuarine and marine ecosystems and reported that gulf menhaden export 5–10% of the total primary production of estuaries through their migration out to coastal marine environments. Fish-mediated transport of nutrients between Great Lakes coastal wetlands and adjacent bays may be similar in magnitude to that in marine ecosystems, but currently, there is little direct evidence from either ecosystem type.

Nutrient ratios are used to interpret important ecological food web interactions and are often more informative than analyses utilizing only individual nutrients. Food web inter-

Received July 2, 1999. Accepted March 10, 2000.
J15231

D.K. Tanner[1], J.C. Brazner, and V.J. Brady.[2]
U.S. Environmental Protection Agency, National Health and Environmental Effects Research Laboratory, Mid-Continent Ecology Division, 6201 Congdon Blvd., Duluth, MN 55804, U.S.A.

[1]Author to whom all correspondence should be addressed.
e-mail: tanner.danny@epa.gov
[2]National Research Council postdoctoral fellow.

© 2000 NRC Canada

actions have been examined using a stoichiometric framework explicitly described by Reiners (1986) and further developed by Elser et al. (1996) and Sterner (1996). Using this framework, lake water N:P ratios have been correlated with different zooplankton assemblages (Stemberger and Miller 1998), and zooplankton N:P ratios have been linked to N- or P-limited phytoplankton (Sterner 1990). Phytoplankton, in turn, can be resupplied with nutrients by zooplankton, since copepods, because of their higher N:P ratios, utilize more N than P and excrete P, and cladocerans, with lower N:P ratios, retain more P and excrete N. Elser et al. (1996) predicted that fish could have lower body N:P ratios than most of their prey, and therefore, fish should retain P relative to N, i.e., having high N:P excretion ratios. However, Schindler and Eby (1997) maintained that fish excretion N:P ratios are low with relatively little variation.

A thorough understanding of fish–nutrient–ecosystem interactions requires an accurate determination of fish nutrient content and nutrient ratios. Although some information has been published on the nutrient content of whole-body samples of freshwater fish (e.g., Lawrence 1968; Davis and Boyd 1978; Penczak 1985), data on N and P for most wetland fish species are scant and for C are nearly nonexistent. Additionally, there have been conflicting reports on the influence of habitat, season, and age or size on fish nutrient composition and nutrient ratios.

This research was undertaken in support of an effort to characterize the significance of fish-mediated nutrient exchange between Great Lakes coastal wetlands and their adjacent lake waters, which will be published separately. Therefore the primary goal of this study was to obtain a better understanding of nutrient content (C, N, and P) and nutrient ratios (N:P and C:N) typical of Great Lakes coastal wetland and nearshore fishes. More specifically, the main objectives were to determine whether fish nutrient content and nutrient ratios were affected by (*i*) species, (*ii*) location (lake or wetland), (*iii*) life stage, (*iv*) season, or (*v*) length. Additionally, we examined whether fish N:P ratios were correlated with the life history traits of growth rate and trophic level in a manner similar to relationships proposed for zooplankton. Finally, we tested whether body shape was predictive of fish N:P ratios.

Materials and methods

Study site

Bark Bay is located 7 km east of Herbster, Wisconsin, on the southwest shore of Lake Superior (Fig. 1). Bark Bay slough is a barrier-beach lagoon that is surrounded by coastal bog and fen. This slough is located south of Bark Bay proper and is separated from the bay by a sand spit 3.5 km in length and 50 m wide. The total area of Bark Bay wetland is 335 ha, of which 26 ha is open water (maximum depth 3 m). A small stream flows into the western end of the wetland, while the eastern end of the wetland drains into a narrow outlet channel that joins the Bark River just before it empties into Bark Bay (Fig. 1). Wetland vegetation in the lagoon is dominated by *Sparganium eurycarpum* and *Potamogeton amplifolius*, while in the inlet/outlet channel the predominant species are *Potamogeton richardsoni*, *Ceratophyllum demersum*, and *Elodea canadensis*.

Sampling

Fish were sampled with fyke nets the first week of each month (except for the July sampling, which was done the last week of June) from May to November 1995. All fyke nets (4-mm bar mesh, 5 m in length, 1.1 × 1.4 m front opening, 8-m leads, 3-m wings) were set on Monday, removed on Friday, and tended daily. The nets were set to catch fish from three locations: (*i*) within the slough (slough), (*ii*) entering the slough (inlet), and (*iii*) leaving the slough (outlet). Slough fish were captured by setting two fyke nets lead-to-lead and parallel to shore. At the junction of the slough with the Bark River, two fyke nets were set adjacent to each other facing opposite directions such that one caught fish entering the slough (inlet fish) and the other caught fish leaving the slough (outlet fish). The nets had wings that completely blocked the inlet/outlet and funneled fish into the openings of the fyke nets.

Captured fish were identified (Becker 1983), enumerated, measured (±0.1 cm), and weighed (±0.1 g). Life stage (young-of-the-year (YOY), yearling, adult) was estimated using observed length–frequency distributions, information reported by Becker (1983), and field observations of ontogeny. A subset of the most common species was kept for elemental analysis; these fish were placed on ice and frozen until analyzed. Remaining captured fish were released in the direction that they were going when captured.

Sample processing and analysis

Large fish (>200 g) were ground whole in a commercial food grinder (Hobart model 4532, Troy, Ohio), and smaller fish (10–200 g) were ground whole with a smaller grinder (Waring model 315610, Hartford, Conn.). To insure homogenization, all tissue was passed through the grinders three times. Following processing, tissue was dried in a convection oven for 24 h at 60°C and ground with a mortar and pestle. Small fish (<10 g) were not processed in a food grinder; instead, they were dried whole at 60°C and ground with a mortar and pestle. Samples were stored in a freezer until analysis. Samples (2 mg) were analyzed in triplicate for C and N with a Perkin Elmer (Norwalk, Conn.) 2400 CHN analyzer; acetanilide was used as the reference standard.

For total P analysis, duplicate 100-mg samples were digested with 10 mL of 70% HNO_3 in a CEM MDS 81 D microwave oven (Tanner et al. 1999), neutralized with 10 N NaOH, and analyzed spectrophotometrically using the vanadomolybdophosphoric acid method (Analytical Methods Committee 1979). Dried oyster tissue obtained from the National Institute of Standards and Technology (Gaithersburg, Md.) was used as the P reference standard. Precision and accuracy in the measurement of fish P content using the modified microwave method were excellent, with a mean relative percent difference of only 5% for 192 fish samples in duplicate and a 90% recovery of P in the oyster tissue reference material (Tanner et al. 1999).

Data analysis

Initially, differences in C, N, P, and nutrient ratios (N:P and C:N) for each species were analyzed using a three-way analysis of covariance (ANCOVA) with location, life stage, and season as main effects and length as a covariate. To increase statistical power and because of the limited size of our data set, we combined parts of the data from location, life stage, and season. The outlet and slough locations were combined because fish that were caught at the outlet were assumed to be emigrating from the slough; this combination allowed seven species to be tested for differences relating to location (inlet versus slough/outlet). Yearling and adult fish (2 years or older) were combined into one life stage group, with the other being YOY; six species were tested for age-related differences. Monthly data were combined into two seasons, early (May–July) and late (August–November); seven species were tested for seasonal differences.

© 2000 NRC Canada

Fig. 1. Location of Bark Bay slough, Wisconsin, in western Lake Superior. The stippled area adjacent to the slough indicates coastal fen/bog habitat.

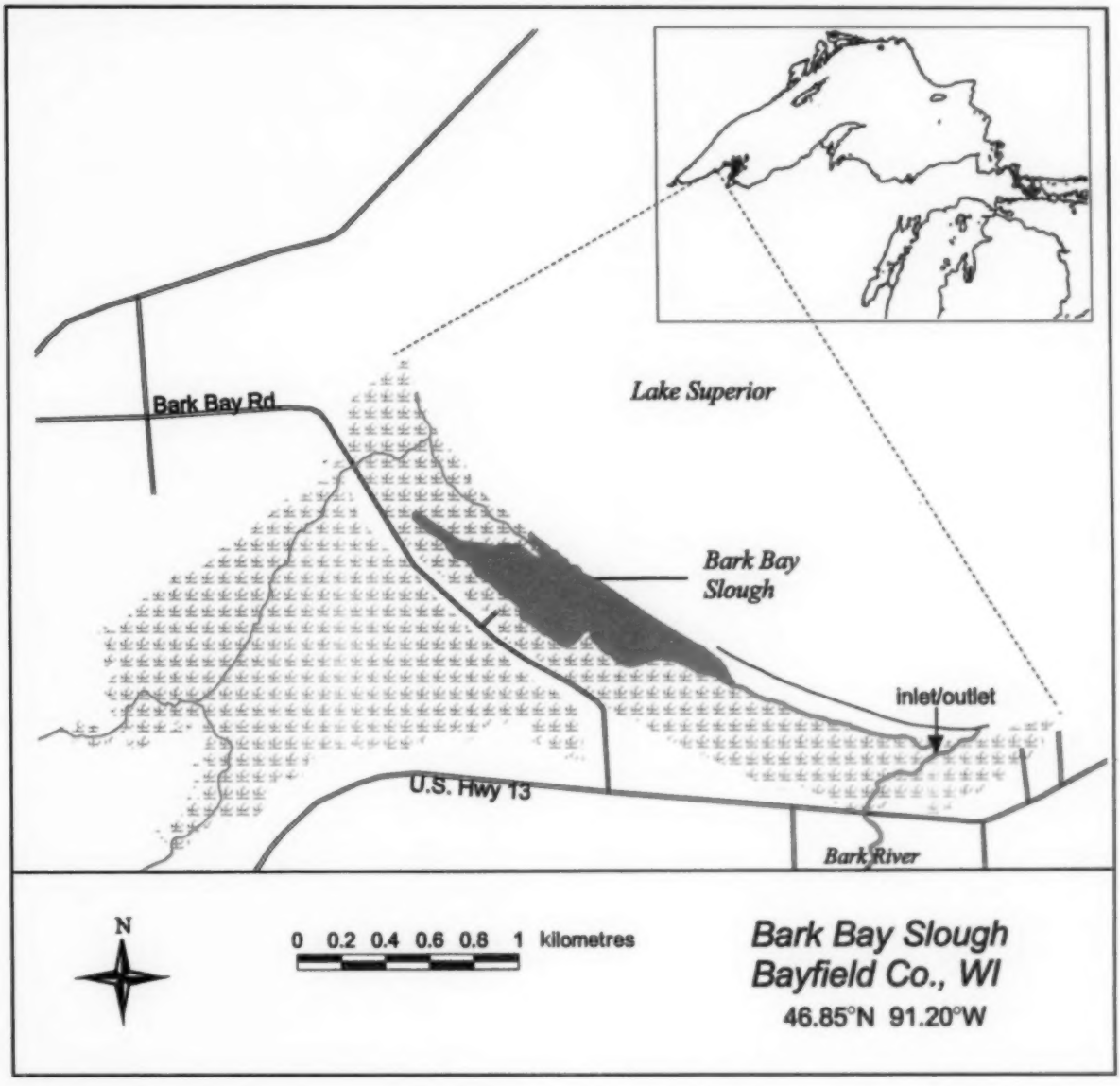

For all analyses where significant differences were apparent ($p \leq 0.05$), main factors were sorted into statistically homogeneous subsets for each species prior to use of regression analyses to examine relationships between nutrients or nutrient ratios and fish length. This allowed 10 species to be tested for a relationship between nutrients and length. To test for differences in nutrient content among species, only fish from the inlet were used because location was a significant factor for many species. Differences in nutrient content among nine species were analyzed using one-way analysis of variance with Tukey's honestly significant difference test for pairwise comparisons among means.

Our study design did not allow accurate measurement of fish growth rates. Thus, indices of growth rates were calculated from published data on fish from lakes in northern Wisconsin (Becker 1983). To standardize growth rates across species, growth rates were calculated as indices by dividing total length (millimetres) of the oldest adults by their age (years) using the data in Becker (1983). The correlation between N:P ratio and growth rate index was examined by regression.

Most of the fish fineness ratios (Scarnecchia 1988) used to examine N:P relationships among fish species were obtained from Poff and Allan (1995). Fineness ratio is a measure of body shape and is calculated as follows: fineness ratio = total body length/maximum body depth. Fineness ratios for the longnose sucker, blacknose shiner, and ruffe were calculated based on morphological measurements of graphic representations or pictures (Hubbs and Lagler 1967). In addition, N:P ratios calculated from nutrient data in Davis and Boyd (1978) for six fish species were included in regressions of N:P ratios versus fineness ratios to provide a better representation of the lower range of fineness ratio values (i.e., fish

© 2000 NRC Canada

Table 1. Fineness ratio (total body length/maximum body depth), growth rate index (mm·day^{-1}), mean N:P and C:N atomic ratios, and C, N, and P % dry weight (mean ± SD) in 20 species of fish from Bark Bay, Wisconsin.

Species	Common name	Fineness ratio	Growth rate index	N:P (atoms)	C:N (atoms)	% C	% N	% P	*n*
Esox lucius	Northern pike	7.12	0.229	12.76	4.29	45.07±1.59	12.27±0.42	2.13±0.34	25
Lota lota	Burbot	7.57	0.162	12.24	5.28	47.83±4.66	10.56±0.99	1.91±0.24	2
Catostomus catostomus	Longnose sucker	5.92	0.115	11.44	4.58	46.23	11.78	2.28	1
Moxostoma anisurum	Silver redhorse	4.22	0.156	11.43	5.00	48.25±1.80	11.25±0.20	2.18±0.62	3
Percopsis omiscomaycus	Trout-perch	5.61	0.092	11.39	4.56	44.87±0.65	11.47±0.03	2.23±0.29	2
Notropis atherinoides	Emerald shiner	5.97	0.084	10.88	4.73	45.83±2.69	11.30±0.70	2.30±0.20	19
Gymnocephalus cernuus	Ruffe	4.32	0.106	10.54	4.77	44.96	11.00	2.31	1
Stizostedion vitreum	Walleye	5.85	0.119	10.45	4.06	44.03	12.65	2.68	1
Etheostoma nigrum	Johnny darter	6.55	0.062	10.36	4.95	46.59	10.99	2.35	1
Catostomus commersoni	White sucker	5.55	0.106	10.34	4.11	44.09	12.51	2.68	1
Umbra limi	Central mudminnow	5.29	0.054	10.03	4.26	43.12±1.32	11.82±0.35	2.61±0.22	8
Notropis hudsonius	Spottail shiner	5.06	0.068	9.85	4.64	44.43±2.71	11.16±0.63	2.51±0.30	13
Pungitius pungitius	Ninespine stickleback	6.00	0.044	9.72	5.90	48.39±0.77	9.57±0.69	2.18±0.13	8
Ameiurus nebulosus	Brown bullhead	5.26	0.148	9.45	4.69	44.13±3.14	10.97±0.68	2.57±0.62	14
Notemigonus crysoleucas	Golden shiner	4.02	0.072	9.44	4.48	44.09±2.08	11.47±0.65	2.69±0.31	30
Perca flavescens	Yellow perch	4.00	0.084	9.28	4.38	43.14±1.86	11.48±0.50	2.74±0.33	23
Notropis heterolepis	Blacknose shiner	5.73	0.098	9.22	5.04	45.73±2.66	10.58±0.61	2.54±0.24	21
Ambloplites rupestris	Rock bass	2.87	0.081	9.16	4.81	45.71±2.27	11.09±0.70	2.68±0.36	12
Cottus bairdi	Mottled sculpin	5.11	0.065	9.13	4.51	42.75±2.59	11.05±0.53	2.68±0.24	3
Culaea inconstans	Brook stickleback	4.84	0.062	8.41	4.95	43.55±4.91	10.26±1.64	2.70±0.27	4
Pimphales promelas	Fathead minnow	3.69		10.9[a]					
Micropterus salmoides	Largemouth bass	3.82		8.44[a]					
Dorosoma cepedianum	Gizzard shad	3.08		8.30[a]					
Lepomis macrochirus	Bluegill	2.33		7.23[a]					
Lepomis cyanellus	Green sunfish	2.98		6.98[a]					
Pomoxis nigromaculatus	Black crappie	2.84		6.43[a]					
Total *n*									192
Mean ± SD of all species						45.14±1.68	11.26±0.74	2.45±0.25	
Range (all species)						42.75–48.39	9.57–12.65	1.91–2.74	

Note: All percent nutrient values can be converted to μg·g^{-1} by mutiplying by 10 000.
[a]N:P values (multiplied by 1.25) calculated from % dry weight N and P data reported by Davis and Boyd (1978).

with flat shapes). Comparisons of N:P ratios based on Davis and Boyd (1978) versus our data for the only two fish species collected in both studies indicated that the ratios based on their data were approximately 25% lower than the ratios that we measured. Because analytical techniques have improved considerably since Davis and Boyd (1978) did their study, and to maximize consistency among ratio comparisons, we increased the N:P ratios from Davis and Boyd (1978) by 25% before including these values in the regression analyses. Although results were not markedly different using untransformed Davis and Boyd (1978) data, this still seemed to be the most prudent approach.

Results

Twenty species of fish were analyzed for C, N, and P. Percent C in whole-body tissues was highest in ninespine stickleback at 48.39% and lowest in mottled sculpin at 42.75%, with a mean for all species of 45.14% (Table 1). Percent N in whole-body tissues was highest in northern pike at 12.27% and lowest in ninespine stickleback at 9.57% and had a mean for all species of 11.26%. Percent P whole-body tissue values were highest in yellow perch at 2.74% and lowest in burbot at 1.91% and had a mean for all species of 2.45%. Because location of capture made a significant difference for many species, differences in nutrient content among species were only analyzed for fish captured at the inlet. Significant differences in nutrient proportions among species were not uncommon among these nine species (Fig. 2).

Location was not a significant factor in C content or C:N

© 2000 NRC Canada

Fig. 2. Mean and standard error of (*a*) C, (*b*) N, and (*c*) P as % dry weight in nine fish species captured entering Bark Bay slough through the inlet. NS, ninespine stickleback; ES, emerald shiner; SS, spottail shiner; NP, northern pike; GS, golden shiner; MM, mudminnow; BS, blacknose shiner; YP, yellow perch; BB, brown bullhead. Data points with dissimilar letters are significantly different ($p \leq 0.05$).

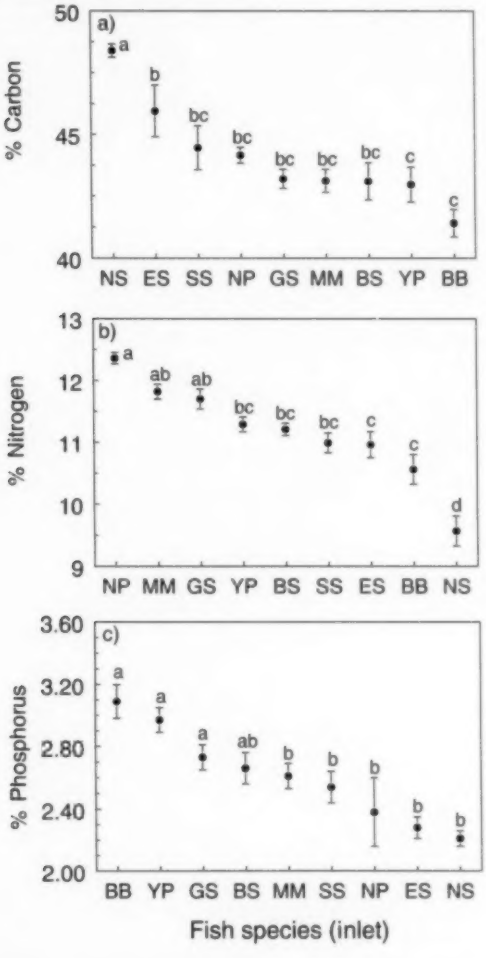

ratios of fish, and only 29% of analyses were significant for proportions of N and P and N:P ratios for the seven tested species. Emerald shiner and spottail shiner from the inlet had significantly lower N proportions than those in the slough and outlet (Table 2). Percent P was significantly higher in northern pike and yellow perch from the inlet than from the slough/outlet (Table 2). Thus, the pattern for these four species was toward lower N:P ratios for fish captured at the inlet (i.e., from Bark Bay), although this ratio was only significantly lower for northern pike and yellow perch (Table 3). Life stage was not an important determinant of nutrient content or nutrient ratios in the six species tested. The only life stage difference that was even marginally significant was for yellow perch: YOY had lower percent N than adults and yearlings ($p = 0.06$) (Table 2).

Date of capture had a significant influence on nutrient content and nutrient ratios in 31% of the analyses of seven fish species. Northern pike that were caught in August–November (late) had significantly lower percent P than those that were caught in May–July (early) (Table 2), causing late-caught northern pike to have higher N:P ratios than those caught early (Table 3). Both golden shiner and blacknose shiner that were caught early had significantly higher percent N than those that were caught late. As a result, early-caught fish of these two species and brown bullhead had significantly lower C:N ratios than those that were caught late.

Only 23% of the regressions between the nutrient proportions or the nutrient ratios and fish length were significant, and there were no apparent patterns among these for the 10 tested species (Tables 4 and 5). Percent C increased with increasing length in emerald shiner that were captured early and yellow perch captured late (Table 4). Percent N decreased with increasing length in blacknose shiner, northern pike, and yellow perch that were captured late and emerald shiner captured early. Percent P increased with increasing length in early-captured northern pike and late-captured rock bass but decreased with length in early-captured ninespine stickleback. These decreases in N and (or) increases in P led to decreasing N:P ratios as length increased in northern pike that were captured early and blacknose shiner and rock bass that were captured late (Table 5). Similarly, the increases in C and (or) decreases in N caused C:N ratios to increase with increasing length in early-captured emerald shiner and late-captured yellow perch and blacknose shiner. In contrast, C:N ratios decreased with increasing length in early-captured golden shiner.

There was a significant relationship between N:P ratios and species' growth rate indices ($r^2 = 0.51$, $p < 0.001$), with faster growing fish having higher N:P ratios (Fig. 3*a*). The relationship between N:P ratios and species' fineness ratios was also significant ($r^2 = 0.57$, $p < 0.001$) (Fig. 3*b*). Fineness ratios were highest in streamlined and elongate fish such as northern pike (7.12) and burbot (7.57) and lowest in deep-bodied and laterally compressed fish such as black crappie (2.84) and bluegill (2.33) (Table 1).

Discussion

Overall, we found whole-fish nutrient values to be fairly similar to those reported by other researchers. However, N means in these earlier studies were slightly lower (10–16%) than our mean, while P means from two studies prior to 1980 were 35–50% higher than our mean (Table 6). Unfortunately, these other studies did not report whether they used standard reference material for P, so it is not possible to verify the accuracy of their methods (coefficients of variation only measure precision). Ranges in fish nutrient proportions across species were fairly narrow in our study. We agree with Davis and Boyd (1978) that fish nutrient proportions appear to be similar enough to use overall means for making predictions for many ecological applications such as nutrient budget modeling, but this will depend on study objectives. Because there were significant differences in nutrient proportions among species in our study, individual species' nutrient values may give more accurate estimates in systems where only a few species contribute most of the biomass or

© 2000 NRC Canada

Table 2. Probability values for three-way ANCOVA of C, N, and P (% dry weight) values with locale, age, and date as main factors and length as a covariate.

	C				N				P			
Species (*n*)	Length	Locale	Age	Date	Length	Locale	Age	Date	Length	Locale	Age	Date
Northern pike (25)	0.910	0.899	0.453	0.123	0.166	0.880	0.365	0.440	0.257	**0.006**	0.959	**0.019**
Yellow perch (23)	0.712	0.263	0.327	0.567	**0.016**	0.374	0.060	0.457	0.885	**0.021**	0.583	0.981
Brown bullhead (14), no outlet, YOY	0.532	id	id	**0.012**	0.201	id	id	0.763	**0.038**	id	id	0.191
Rock bass (12), no YOY	0.274	0.524	id	0.770	0.655	0.890	id	0.507	**0.021**	0.137	id	0.200
Blacknose shiner (21)	0.567	0.126	0.407	**0.001**	0.081	0.355	0.298	**0.010**	0.933	0.147	0.091	**0.047**
Golden shiner (30)	0.436	0.445	0.964	**0.015**	0.310	0.956	0.995	**0.009**	0.368	0.293	0.420	0.096
Emerald shiner (19)	**0.013**	0.733	0.967	0.674	0.177	**0.008**	0.600	0.363	0.313	0.880	0.881	0.598
Spottail shiner (13), no late dates	0.487	0.968	0.906	id	0.153	**0.003**	**0.033**	id	0.540	0.606	0.353	id

Note: Insufficient data for analysis (id) is explained to the right of the number of samples where applicable. Bolded p values are significant ($p \leq 0.05$).

Table 3. Probability values for three-way ANCOVA of N:P and C:N (% dry weight) values with locale, age, and date as main factors and length as a covariate.

	N:P				C:N			
Species (*n*)	Length	Locale	Age	Date	Length	Locale	Age	Date
Northern pike (25)	0.252	**0.019**	0.777	**0.037**	0.228	0.987	0.819	0.561
Yellow perch (23)	0.405	**0.008**	0.141	0.551	0.121	0.823	0.089	0.421
Brown bullhead (14), no outlet, YOY	**0.012**	id	id	0.807	0.153	id	id	**0.013**
Rock bass (12), no YOY	**0.041**	0.233	id	0.210	0.643	0.581	id	0.698
Blacknose shiner (21)	0.751	0.160	0.172	0.533	0.117	0.617	0.256	**0.001**
Golden shiner (30)	0.126	0.222	0.360	0.657	0.937	0.635	0.999	**0.003**
Emerald shiner (19)	0.630	0.084	0.616	0.173	**0.033**	0.084	0.773	0.851
Spottail shiner (13), no late dates	0.257	0.132	0.871	id	0.909	0.127	0.265	id

Note: Insufficient data for analysis (id) is explained to the right of the number of species where applicable. Bolded p values are significant ($p \leq 0.05$).

when calculating elemental stoichiometric mass balance relationships among species and trophic levels.

The few studies addressing the effect of location or habitat on fish elemental composition have not found these factors to be significant. Penczak (1985) found that percent C, N, or P in whole bream were not significantly different between two lake basins, one mesotrophic and one eutrophic, and only slight differences in nutrients were noted in largemouth bass from six different ponds (Goodyear and Boyd 1972). In contrast, we found significant differences in percent N or percent P or N:P ratios between locations for four of the seven species tested. It may be that the low coefficient of variation associated with our nutrient values, particularly P, enabled us to discern smaller differences than could be detected in other studies (Table 6). Our data show lower N:P ratios (two species) or lower percent N (two species) for fish from Bark Bay (inlet fish) relative to fish from the slough. Additional research that includes analyses of fish condition, fish diet, and prey nutrient content from both locations should help discern the origin of these spatial fish nutrient differences.

Although we found life stage to have little influence on nutrient composition in fish, this has not been the case in several other studies. Deegan (1986) observed percent P to increase and then decrease as gulf menhaden grew from larvae to subadults, while percent N decreased and percent lipid increased during this same period. Shearer (1984) found percent P to decline initially and then increase from early to later stages of growth in rainbow trout. Differences in nutrient content in different life stages may be caused by changes in allocation of energy for growth within the body. Elliot (1976) observed an increase in percent protein and lipid as brown trout grew in size, and Shul'man (1974) found that percent lipid tended to increase with age and size, with the largest differences between young fish and adults. Among adult fish, however, age may have less effect on nutrient content. For example, Penczak and Tatrai (1985) found similar elemental content (C, N, P) among 3- to 7-year-old bream. Restricting age-class separation to just two life stage categories may have reduced the likelihood of detecting age-related differences in our study.

The influence of capture date on C content and C:N ratios is likely related to lipid storage. Lipids, not carbohydrates, are the preferred source of energy storage in fishes (Cowey and Sargent 1979), and lipid reserves increase from spring to fall, are highest at the end of the main yearly feeding period, and then decline in winter (Shul'man 1974; Strange and Pelton 1987). Since lipids are a rich source of C, we would expect percent C to increase from spring to fall, as it did in brown bullhead, blacknose shiner, and golden shiner in this study. Similarly, Penczak and Tatrai (1985) and Penczak et al. (1982) found percent C in bream and rainbow trout to be highest in the fall, while percent N decreased in either summer or early fall. We also observed that percent N was sig-

© 2000 NRC Canada

Table 4. Slope, r^2, and probability value for regressions of C, N, and P (% dry weight) versus length (cm) of fish species.

		C			N			P		
Species capture date	*n*	Slope	r^2	*p*	Slope	r^2	*p*	Slope	r^2	*p*
May–June (early)										
Northern pike	5	–0.02	0.22	ns	–0.01	0.36	ns	+0.03	0.82	**0.03**
Golden shiner	13	+0.04	0.00	ns	+0.06	0.04	ns	+0.02	0.02	ns
Emerald shiner	11	+1.33	0.68	**0.002**	–0.22	0.46	**0.02**	–0.05	0.18	ns
Blacknose shiner	8	–1.44	0.19	ns	–0.14	0.11	ns	+0.09	0.04	ns
Brown bullhead	7	+0.11	0.01	ns	–0.03	0.00	ns	–0.16	0.47	0.09
Ninespine stickleback	8	–0.36	0.06	ns	–0.83	0.38	ns	–0.19	0.51	**0.05**
Central mudminnow	8	+0.27	0.18	ns	+0.07	0.19	ns	+0.01	0.01	ns
Spottail shiner	11	+0.28	0.07	ns	+0.04	0.04	ns	–0.04	0.10	ns
August–November (late)										
Northern pike	6	+0.01	0.00	ns	–0.10	0.80	**0.02**	+0.03	0.17	ns
Yellow perch	7	+0.79	0.64	**0.03**	–0.12	0.63	**0.03**	–0.05	0.32	ns
Golden shiner	12	+0.20	0.05	ns	+0.01	0.00	ns	–0.04	0.09	ns
Blacknose shiner	9	+2.23	0.23	ns	–1.03	0.47	**0.04**	+0.26	0.21	ns
Brown bullhead	7	+0.09	0.07	ns	+0.08	0.49	0.08	–0.05	0.37	ns
Rock bass	8	–2.31	0.22	ns	–0.42	0.15	ns	+0.63	0.82	**0.002**

Note: ns, not significant. Bolded *p* values are significant ($p \leq 0.05$).

Table 5. Slope, r^2, and probability value for regressions of N:P and C:N (% dry weight) versus length (cm) of fish species.

		N:P			C:N		
Species capture date	*n*	Slope	r^2	*p*	Slope	r^2	*p*
May–June (early)							
Northern pike	5	–0.06	0.87	**0.02**	+0.01	0.32	ns
Golden shiner	13	+0.04	0.02	ns	–0.04	0.39	**0.02**
Emerald shiner	11	+0.01	0.01	ns	+0.21	0.62	**0.004**
Blacknose shiner	8	–0.19	0.05	ns	–0.08	0.09	ns
Brown bullhead	7	+0.16	0.22	ns	+0.02	0.06	ns
Ninespine stickleback	8	–0.02	0.00	ns	+0.42	0.30	ns
Central mudminnow	8	+0.01	0.00	ns	+0.01	0.00	ns
Spottail shiner	11	+0.09	0.18	ns	–0.01	0.01	ns
August–November (late)							
Northern pike	6	–0.13	0.29	ns	+0.03	0.47	ns
Yellow perch	7	+0.02	0.07	ns	+0.12	0.89	**0.001**
Golden shiner	12	+0.07	0.17	ns	+0.03	0.024	ns
Blacknose shiner	9	–0.88	0.62	**0.01**	+0.68	0.64	**0.01**
Brown bullhead	7	+0.22	0.48	0.09	+0.02	0.55	0.06
Rock bass	8	–0.96	0.85	**0.001**	–0.05	0.01	ns

Note: ns, not significant. Bolded *p* values are significant ($p \leq 0.05$).

Table 6. Comparison of means (coefficient of variation in parentheses) for C, N, and P (% dry weight) in whole-fish tissue from several studies.

	Present study	Penczak 1985	Davis and Boyd 1978	Lawrence 1968
Location	Wisconsin	Poland	Georgia	Alabama
No. of species	20	5	17	11
C	45.14 (3.7)	42.98 (4.7)		
N	11.26 (6.6)	10.20 (7.4)	9.70 (10.2)	10.04 (7.3)
P	2.45 (10.2)	2.21 (18.1)	3.31 (26.6)	3.75 (23.4)

nificantly less for later-caught blacknose shiner and golden shiner. With increases in percent C and decreases in percent N, it follows that C:N ratios would increase in the fall, as we observed for three species. However, four other tested species had no significant seasonal differences. Although Penczak and Tatrai (1985) noted that the proportion of P increased in the summer and declined in the fall in bream, only a single species (northern pike) followed this trend in

© 2000 NRC Canada

Fig. 3. Linear regression of relationship between mean N:P ratio for each fish species and (*a*) growth rate index and (*b*) fineness ratio (total body length/maximum body depth) for that species. N:P ratios were measured in fish captured at Bark Bay slough (20 species). Figure 3*b* contains N:P ratios calculated from percent P and N data in Davis and Boyd (1978) (six species).

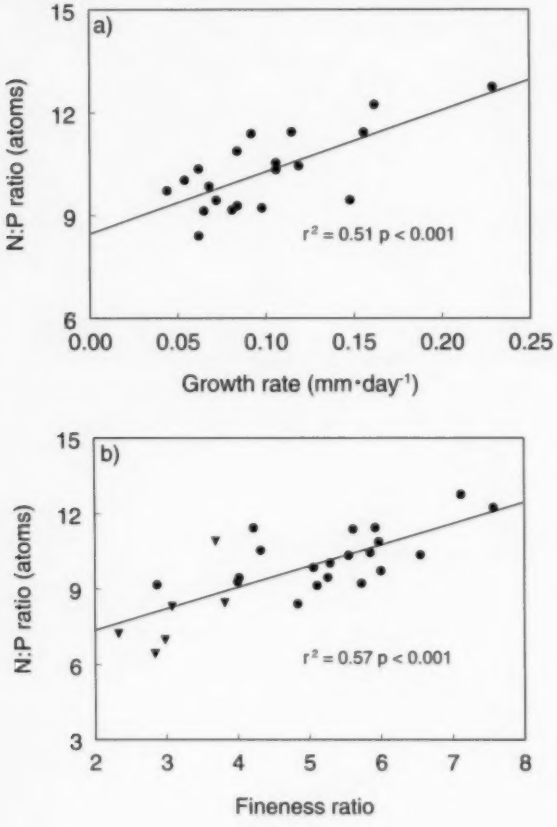

our study. Combining early summer with spring sampling dates and late summer with fall sampling dates may have reduced our ability to discern seasonal differences.

We expected that nutrient proportions and nutrient ratios would be correlated with fish length. Although the C:N ratio increased with increasing length for six species in our study, only three of these regressions were significant; the other four tested species showed either no relationship or had a negative slope. These results suggest that the proportion of lipid to protein remains relatively constant with increased size in at least some species. N:P ratios are predicted to decline with increased size in vertebrates larger than 10 g because of increased amounts of skeletal material necessary for structural support (Elser et al. 1996). Davis and Boyd (1978) observed decreases in percent N and increases in percent P as bluegill increased in size. They attributed these changes to a larger proportion of bone to flesh with increased size, which follows from Elser et al.'s (1996) prediction. However, the majority of species (seven of 10) in our study exhibited either no relationship or the opposite trend. This suggests that the relationship between N:P ratio and size may not be consistent for fish. The hypothesized requirement for increased structural support with increased size may not be true for fish because their weight is primarily supported by water.

Studies of N:P ratios in zooplankton species have indicated a link with life history characteristics such as growth rate. For example, faster growing species of crustacean zooplankton have lower N:P ratios, apparently due to elevated amounts of P-rich RNA in fast-growing taxa (Elser et al. 1996; Main et al. 1997). While we would not expect to see this particular relationship in bony fish due to the much smaller proportion of whole-body P in fish RNA, there may still be a relationship between fish growth rate and N:P ratios. In fact, we found that faster growing fish species had higher N:P ratios. This may be caused by faster growing fish adding proportionately more flesh than bone and scales during growth than do slower growing species.

Trophic level has also been correlated with N:P ratios. Among cladocerans, predatory species have higher N:P ratios than herbivorous species (Sterner and Hessen 1994), and some carnivorous fishes have higher N assimilation efficiencies than those that consume N-poor food (Pandian and Marian 1985). However, trophic level did not seem to be correlated with N:P ratios in our study, with predatory species having both the highest (northern pike and burbot) and lowest (largemouth bass and black crappie) N:P ratios.

Another factor that we considered in our attempt to explain differences in fish N:P ratios was body shape. George (1994) postulated that the lower proportions of N in finescale dace and pearl dace versus fathead minnow was due to the daces' more slender shape, which would result in dace having less muscle mass than the wider, blunter fathead minnow. When comparing nutrient content of different fish species from Davis and Boyd (1978) and our study, we observed that centrarchids had much higher percent P values than other species. Centrarchids (particularly sunfishes and crappies) are much flatter in shape than burbot, suckers, northern pike, or trout-perch and therefore should have a higher proportion of bone and scales to flesh and a correspondingly lower N:P ratio. The significant relationship between fineness and N:P ratios suggests that differences in N:P ratios between species are related to the ratio of bone and scales to flesh. This latter ratio seems to be determined by both growth rate and by the skeletal framework necessary for the different shapes and forms that have evolved in fish to meet the varied swimming functions demanded by their different life history strategies.

In conclusion, the narrow range of fish nutrient values found in our study, and the similarity in fish N:P excretion ratios (Schindler and Eby 1997), suggest that fish N:P ratios may not be as useful as zooplankton N:P ratios in elucidating food web interactions. Therefore, elemental means across species are probably sufficient as inputs for most nutrient budget models. Despite the narrow range in fish nutrient content, we found significant differences among nine species. We also found a few differences in fish nutrient content due to capture date, location, and length. Differences in N:P ratios among fish species were not correlated with trophic level but could be fairly well predicted by both growth rate indices and fineness ratios. We suggest that lower N:P ratios are driven by higher proportions of bone

© 2000 NRC Canada

and scales to flesh in bony fishes, with greater proportions of structural material in species with wider, flatter shapes or with slower growth rates.

Acknowledgments

We thank Armond Lemke for his tireless efforts in sample preparation and Stacey Stark and Leslie Jagger for geographic analysis and mapping assistance. This manuscript was improved by comments and reviews by John Morrice, Anett Trebitz, and three anonymous reviewers.

References

Analytical Methods Committee. 1979. Methods for the examination of fish and fish products. Analyst, **104**: 449–450.

Becker, G.C. 1983. Fishes of Wisconsin. University of Wisconsin Press, Madison, Wis.

Cowey, C.B., and Sargent, J.R. 1979. Nutrition. *In* Fish physiology. Vol. VIII. Bioenergetics and growth. *Edited by* W.S. Hoar, D.J. Randall, and J.R. Brett. Academic Press, New York. pp. 1–69.

DaCosta, A., and Stern, J.A. 1956. The calcium and phosphorus contents of some foreign and domestic canned sardines. Food Res. **21**: 242–249.

Davis, J.A., and Boyd, C.E. 1978. Concentrations of selected elements and ash in bluegill (*Lepomis macrochirus*) and certain other freshwater fish. Trans. Am. Fish. Soc. **107**: 862–867.

Deegan, L.A. 1986. Changes in body composition and morphology of young-of-the-year gulf menhaden, *Brevoortia patronus* Goode, in Fourleague Bay, Louisiana. J. Fish Biol. **29**: 403–415.

Deegan, L.A. 1993. Nutrient and energy transport between estuaries and coastal marine ecosystems by fish migration. Can. J. Fish. Aquat. Sci. **50**: 74–79.

Elliot, J.M. 1976. Body composition of brown trout (*Salmo trutta*) in relation to temperature and ration size. J. Anim. Ecol. **45**: 273–289.

Elser, J.J., Dobberfuhl, N.R., MacKay, N.A., and Schampel, J.H. 1996. Organism size, life history, and N:P stoichiometry. BioScience, **46**: 674–684.

George, N.B. 1994. Nutrient stoichiometry of piscivore–plantivore interactions in two whole-lake experiments. M.S. thesis, University of Texas, Arlington, Tex.

Goodyear, C.P., and Boyd, C.E. 1972. Elemental composition of largemouth bass. Trans. Am. Fish. Soc. **101**: 545–547.

Hubbs, C.L., and Lagler, K.F. 1967. Fishes of the Great Lakes region. University of Michigan Press, Ann Arbor, Mich.

Kitchell, J.F., Koonce, J.F., and Tennis, P.S. 1975. Phosphorous flux through fishes. Verh. Int. Ver. Limnol. **19**: 2478–2484.

Lawrence, J.M. 1968. Dynamics of chemical and physical characteristics of water, bottom muds, and aquatic life in a large impoundment on a river. Auburn Univ. Exp. Stn. Zool. Entomol. Dep. Ser. Fish. No. 6.

Main, T.M., Dobberfuhl, D.R., and Elser, J.J. 1997. N:P stoichiometry and ontogeny of crustacean zooplankton: a test of the growth rate hypothesis. Limnol. Oceanogr. **42**: 1474–1478.

Pandian, T.J., and Marian, M.P. 1985. Nitrogen content of food as an index of absorption efficiency in fishes. Mar. Biol. **85**: 301–311.

Penczak, T. 1985. Phosphorus, nitrogen, and carbon cycling by fish populations in two small lowland rivers in Poland. Hydrobiologia, **120**: 159–165.

Penczak, T., and Tatrai, I. 1985. Contribution of bream, *Abramis brama* (L.), to the nutrient dynamics of Lake Balaton. Hydrobiologia, **126**: 59–64.

Penczak, T., Galicka, W., Molinski, M., Kusto, E., and Zalewski, M. 1982. The enrichment of a mesotrophic lake by carbon, phosphorus, and nitrogen from the cage aquaculture of rainbow trout, *Salmo gairdneri*. J. Appl. Ecol. **19**: 371–393.

Poff, N.L., and Allan, J.D. 1995. Functional organization of stream fish assemblages in relation to hydrological variability. Ecology, **76**: 606–627.

Reiners, W.A. 1986. Complementary models for ecosystems. Am. Nat. **127**: 59–73.

Richey, J.E., Perkins, M.A., and Goldman, C.R. 1975. Effects of kokanee salmon (*Oncorhynchus nerka*) decomposition on the ecology of a subalpine stream. J. Fish. Res. Board Can. **32**: 817–820.

Scarnecchia, D.L. 1988. The importance of streamlining in influencing fish community structure in channelized and unchannelized reaches of a prairie stream. Regul. Rivers, **2**: 155–166.

Schindler, D.E., and Eby, L.A. 1997. Stoichiometry of fishes and their prey: implications for nutrient recycling. Ecology, **78**: 1816–1831.

Shearer, K.D. 1984. Changes in elemental composition of hatchery-reared rainbow trout, *Salmo gairdneri*, associated with growth and reproduction. Can J. Fish. Aquat. Sci. **41**: 1592–1600.

Shul'man, G.E. 1974. Life cycles of fish. Wiley, New York.

Stemberger, R.S., and Miller, E.K. 1998. A zooplankton-N:P ratio indicator for lakes. Environ. Monit. Assess. **51**: 29–51.

Sterner, R.W. 1990. The ratio of nitrogen to phosphorus resupplied by herbivores: zooplankton and the algal competitive arena. Am. Nat. **136**: 209–229.

Sterner, R.W. 1996. Biogeochemistry and trophic ecology: a new food web diagram. *In* Food webs: integration of patterns and dynamics. *Edited by* G. Polis and K. Winemiller. Chapman and Hall, New York. pp. 72–80.

Sterner, R.W, and Hessen, D.O. 1994. Algal nutrient limitation and the nutrition of aquatic herbivores. Annu. Rev. Ecol. Syst. **25**: 1–29.

Strange, R.J., and Pelton, J.C. 1987. Nutrient content of clupeid forage fishes. Trans. Am. Fish. Soc. **116**: 60–66.

Tanner, D.K., Leonard, E.N., and Brazner, J.C. 1999. Microwave digestion method for phosphorous determination of fish tissue. Limnol. Oceanogr. **44**: 926–933.

Vanni, M.J. 1995. Nutrient transport and recycling by consumers in lake food webs: implications for algal communities. *In* Food webs: integration of patterns and dynamics. *Edited by* G. Polis and K. Winemiller. Chapman and Hall, New York. pp. 81–95.

© 2000 NRC Canada

Protandry in Pacific salmon

Yolanda Morbey

Abstract: Protandry, the earlier arrival of males to the spawning grounds than females, has been reported in several studies of Pacific salmon (*Oncorhynchus* spp.). However, the reasons for protandry in salmon are poorly understood and little is known about how protandry varies among and within populations. In this study, protandry was quantified in a total of 105 years using gender-specific timing data from seven populations (one for pink salmon (*O. gorbuscha*), three for coho salmon (*O. kisutch*), two for sockeye salmon (*O. nerka*), and one for chinook salmon (*O. tshawytscha*)). Using a novel statistical procedure, protandry was found to be significant in 90% of the years and in all populations. Protandry may be part of the males' strategy to maximize mating opportunities and may facilitate mate choice by females.

Résumé : La protandrie, c'est-à-dire l'arrivée des mâles sur les frayères avant les femelles, a été signalée dans plusieurs études sur les saumons du Pacifique (*Oncorhynchus* spp.). Toutefois, on connaît mal les raisons de la protandrie chez les saumons, et on sait peu de choses sur les variations de ce phénomène au sein des populations et d'une population à l'autre. Dans notre étude, nous avons quantifié la protandrie sur un total de 105 ans à partir de données d'arrivée en fonction du sexe pour sept populations (une de saumon rose, *O. gorbuscha*; trois de coho, *O. kisutch*; deux de saumon rouge, *O. nerka*; une de quinnat, *O. tshawytscha*). La nouvelle procédure statistique employée a révélé que la protandrie était significative pour 90% des années et dans toutes les populations. Il peut s'agir là d'un élément de la stratégie des mâles pour maximiser les possibilités d'accouplement, ce qui peut faciliter le choix d'un partenaire pour les femelles.

[Traduit par la Rédaction]

Introduction

In the literature on Pacific salmon (*Oncorhynchus* spp.), there are frequent accounts of males migrating or arriving at the spawning grounds earlier on average than females (e.g., Pritchard 1937; Groot and Margolis 1991 and references therein; Quinn and Unwin 1993). The phenomenon of males entering a reproductive life history stage earlier than females is called protandrous reproduction, or more simply, protandry (*proto-*: first, *andr-*: males). The relative timing of males and females is an important component of any mating system, and the occurrence of protandry can provide insight into the selection pressures faced by males and females during the breeding season.

The empirical and theoretical study of protandry began with and has remained focussed on insects (e.g., Wiklund and Fagerström 1977; Botterweg 1982; Iwasa et al. 1983). These authors, among others, formalized the hypothesis that protandry allows males to maximize their opportunities for mating. The first protandry models made the following simplifying assumptions about the insect mating system: (*i*) emergence into the reproductive phase is irreversible, (*ii*) males search for and mate with females during the entire emergence period, (*iii*) males mate several times, (*iv*) females mate immediately after emergence and mate only once, and (*v*) all females mate. The prediction of protandry is robust, even when some of these conditions are relaxed (e.g., Wiklund and Fagerström 1977; Botterweg 1982; Zonneveld and Metz 1991). In a scramble competition situation where males reproduce for a longer period of time than females, initiating breeding early can guarantee males access to a greater number of mates over their lifetime than by breeding late.

Pacific salmon share many features of their mating system with the above conditions (cf. Quinn et al. 1996). First, salmon are semelparous and so entry into the reproductive phase is irreversible. As a probable outcome of their semelparous life history strategy, males engage in intense intraspecific competition for access to spawning females (e.g., Foote 1990; Fleming and Gross 1994; Quinn et al. 1996). Males may spawn with several females during their breeding life span, whereas females may complete spawning over a few days followed by a longer period of nest defence (e.g., Schroder 1981; McPhee and Quinn 1998). Finally, owing to the polygynous breeding system and localized spawning areas, all females likely participate in spawning.

Given that the requirements for protandry seem to be met in salmon, protandrous arrival to the spawning grounds (and initiation of spawning activities) was expected to be a general feature of salmon life histories. Although protandry is known to exist in salmon, the magnitude and frequency of protandry have not been documented. The primary objective of this study was to report on the frequency and magnitude of protandry among and within salmon populations, using a novel analytical approach. A second objective was to evaluate several competing hypotheses for protandry that have been proposed in the literature.

Received March 16, 1999. Accepted March 10, 2000.
J15064

Y. Morbey. Behavioural Ecology Research Group, Department of Biological Sciences, Simon Fraser University, 8888 University Drive, Burnaby, BC V5A 1S6, Canada.
e-mail: ymorbey@sfu.ca

© 2000 NRC Canada

Materials and methods

Data on gender-specific arrival timing to the spawning grounds were sought. Recording gender-specific arrival timing is not a management priority and usually is a byproduct of the spawner enumeration procedure used by managers. Both absolute counts (through fences or by dipnetting) and the marking component of mark–recapture studies (e.g. by dipnetting or seine netting) provided gender-specific timing information. Data were excluded where samples or counts were done on the spawning grounds because these data do not bear on arrival timing per se. To examine within-population variability in protandry, multiple years of data collected in a consistent manner were required. Arrival timing data were obtained for seven populations (Table 1) that met these criteria. Details about the populations and data collection methodology can be found in Schubert and Fanos (1997) and Schubert and Tadey (1997) for the two sockeye salmon (*Oncorhynchus nerka*) populations, in Seiler et al. (1981) for the three coho salmon (*Oncorhynchus kisutch*) populations, in Fukushima and Smoker (1997) for the Auke Creek pink salmon (*Oncorhynchus gorbuscha*) population, and in Unwin (1986) and Unwin and Glova (1997) for the Glenariffe Stream chinook salmon (*Oncorhynchus tshawytscha*) population. For all but the Auke Creek data, males were classified into two age-classes (younger jacks and older adults).

In addition to the timing data, annual estimates of population size, gender ratio (proportion of the population that were males), jack ratio (proportion of males that were jacks), season length, and freshwater migration distance were acquired or calculated from the available data. For the sockeye populations, the annual population sizes, gender ratios, and jack ratios were based on Schubert and Fanos' (1997) and Schubert and Tadey's (1997) estimates. The cumulative counts of males and females were used to calculate annual population sizes, gender ratios, and jack ratios in the other populations. For each year in each population, season length is the last arrival date minus the first arrival date plus 1. Freshwater migration distance for each population was estimated from maps.

For each year, a measure of protandry was generated. The difference in mean arrival dates of males and females was not used as a measure of protandry because the arrival distributions were not normally distributed, but rather were typically episodic. Another potential measure of protandry is the slope of the relationship between the daily gender ratio of arriving salmon and arrival date, but this measure is also inadequate. Protandry is underestimated when a few fish (with an equal gender ratio) arrive over a prolonged period late in the year and overestimated when a few fish (with excess males) arrive over a prolonged period early in the year. Instead, protandry is measured as the area (in units of days) between the cumulative percent distribution of male arrival dates ($M(t)$) and female arrival dates ($F(t)$):

$$\text{Protandry} = \frac{\sum (M(t) - F(t))\mathrm{d}t}{100\%}$$

where $\mathrm{d}t = 1$ day. Protandry represents the number of days lag between the arrival of an equal proportion of males and females, with positive values representing the earlier arrival of males. On days when sampling did not occur, the fish counted on the next sampling day were assumed to have arrived during the previous non-sampling days according to a uniform distribution. Protandry is not standardized for season length because protandry should be a measure that is relative to the longevity of salmon on the spawning grounds and there is no evidence that longevity depends on season length.

The statistical significance of the observed amount of protandry was determined using a statistical procedure based on randomization (Manly 1997). A null distribution of protandry was generated based on the empirical distribution of arrival dates. In each of 200 iterations, each fish's gender was randomized (making sure to maintain the original population gender ratio) and protandry was calculated. The observed protandry was deemed significant if it lay within the upper fifth quantile of the null distribution (i.e., a one-tailed test was used).

In an attempt to explain the observed variation in protandry, analysis of covariance (ANCOVA) was used to determine the effects of population size, gender ratio, season length, and population on protandry. Model selection began with a fully saturated statistical model that included each main effect and all interactions with population. Nonsignificant interaction terms were sequentially dropped from the model. If a significant interaction effect remained, the effects of population size, gender ratio, and season length on protandry were analysed separately for each population using stepwise linear regression. Jack ratio was not included in this analysis because no jacks were present in the Auke Creek pink salmon population. ANCOVA was used to test if jack ratio affected protandry differently among all populations but Auke Creek. Protandry also was compared among the seven populations using analysis of variance (ANOVA), and a post hoc means comparison test determined how the populations differed (Ryan–Einot–Gabriel–Welsch multiple F test; SAS Institute, Inc. 1990). Using the same technique for comparing male and female timing, analyses were undertaken to determine if jacks generally arrived earlier or later than adults.

SAS statistical software was used for all analyses (SAS Institute, Inc. 1990). The significance levels used for the stepwise regression models were $\alpha = 0.5$ for entry and $\alpha = 0.05$ for removal (Myers 1990). The significance level used for main effects was $\alpha = 0.05$ and for interaction effects was $\alpha = 0.15$. The F statistics based on partial (type III) sum of squares for ANOVAs and t statistics (two-tailed) for the linear regression models are presented.

Results

Protandry was significant in most years at Auke Creek (96%, 25 of 26 years), Big Beef Creek (91%, 10 of 11 years), Birkenhead River (64%, nine of 14 years), Chilko Lake (100%, eight of eight years), Deschutes River (95%, 20 of 21 years), Sunset Falls (89%, eight of nine years), and Glenariffe Stream (88%, 14 of 16 years). In all, 90% of the years showed significant protandry (94 of 105 years). By chance alone, protandry should be significant in only five years (5% of 105 years). Protogyny was significant in one year at Sunset Falls and one year at Deschutes River.

Season length affected protandry differently depending on the population ($p = 0.10$), so separate regression analyses were required for each population. Despite this interaction, none of the within-population analyses showed a significant effect of season length on protandry ($ps > 0.14$). Instead, the within-population analyses revealed a significant effect of gender ratio on protandry in Auke Creek ($t_{1,24} = 2.56$, $p = 0.02$, $R^2 = 0.22$) (Fig. 1) but in no other population ($ps > 0.23$). Population size did not affect protandry in any of the seven populations ($ps > 0.28$). Jack ratio did not affect protandry ($p > 0.5$), nor did the effect of jack ratio on protandry differ among populations ($p > 0.5$). The magnitude of protandry differed among populations ($F_{6,98} = 7.90$, $p = 0.0001$), but each population was not distinct from every other population (Fig. 2).

There was no consistent pattern in the arrival schedules of jacks and adult males. Jacks arrived significantly earlier in nine of 11 years at Big Beef Creek, four of 14 years at Birkenhead River, two of eight years at Chilko River, one of 21

© 2000 NRC Canada

Table 1. Sources of data for the analysis of protandry and average population characteristics (±SD).

Population	Species	Sample or absolute count	Years	Total years	Source[a]	Approximate distance from ocean (km)[b]	Arrival period (days)	Average annual gender ratio (male:female)	Average annual jack ratio	Average annual population size
Auke Creek, Alaska	Pink	Absolute	1971–1982, 1984–1997	26	NMFS[c]	0	64±10	0.51±0.02	0	10 349±8020
Birkenhead River, B.C.	Sockeye	Sample	1984–1997	14	DFO	240	25±8	0.51±0.12	0.20±0.23	141 018±110 234
Chilko Lake, B.C.	Sockeye	Sample	1990–1997	8	DFO	550	40±8	0.41±0.03	0.02±0.01	735 933±243 012
Big Beef Creek, Wash.	Coho	Absolute	1978–1980, 1989–1996	11	WDFW	0	94±18	0.65±0.05	0.33±0.13	1 644±761
Deschutes River, Wash.	Coho	Absolute	1976–1996	21	WDFW	2	99±14	0.58±0.04	0.10±0.08	4 147±3045
Sunset Falls, Wash.	Coho	Absolute	1979–1987	9	WDFW	64	105±8	0.54±0.05	0.01±0.01	15 738±7845
Glenariffe Stream, New Zealand	Chinook	Absolute	1965–1980	16	NIWA	100[d]	156±30	0.53±0.08	0.25±0.13	1 893±893

[a]DFO, Department of Fisheries and Oceans, Canada; NIWA, National Institute of Water and Atmospheric Research, New Zealand; NMFS, National Marine Fisheries Service, Alaska; WDFW, Washington Department of Fisheries and Wildlife, Washington.
[b]Distances were estimated from maps.
[c]S.G. Taylor, NMFS, Auke Bay Laboratory, 11305 Glacier Highway, Juneau, Alaska 99801-8626, U.S.A., unpublished data on Auke Creek pink salmon, 1967–1997.
[d]Unwin (1986).

years at Deschutes River, three of nine years at Sunset Falls, and seven of 16 years at Glenariffe Stream. Adult males arrived significantly later than jacks in one of 11 years at Big Beef Creek, six of 14 years at Birkenhead River, four of eight years at Chilko River, 13 of 21 years at Deschutes River, two of nine years at Sunset Falls, and three of 16 years at Glenariffe Stream.

Discussion

Protandrous arrival to the spawning grounds appears to be a general phenomenon in salmon. In the seven salmon populations considered, males almost always arrived at the spawning grounds earlier on average than females. Protandry occurred regardless of population attributes such as population size, jack ratio, season length, and migration distance. However, there was a tendency for protandry to increase when the gender ratio was more male biased in Auke Creek pink salmon. The magnitude of protandry may seem small (population averages range from 1 to 5 days), but nonetheless, the ubiquity of protandry requires an explanation.

Our results are consistent with the mate-opportunity hypothesis, but only because the mating system of salmon is similar to the type of mating system that theoretically selects for protandry. One critical assumption must be made about the data to support the mate-opportunity hypothesis. The mate-opportunity hypothesis strictly relates to the initiation of reproductive activity, so arrival timing must correspond to spawning timing. However, breeding timing may be decoupled from arrival timing through an intervening waiting stage, and gender-specific timing adjustments may occur during this stage. For example, early-arriving chinook entering Glenariffe Stream took longer to mature (produced releasable gametes) than late-arriving chinook, and females matured more slowly than males (T.P. Quinn et al., University of Washington, unpublished data). The consequences of these processes are unclear: protandry (as measured in this study) would underestimate true protandry if female commenced spawning more slowly than males but would overestimate true protandry if both males and females matured more quickly later in the season. Unfortunately, the extent and patterns of postarrival waiting are poorly understood and could not be assessed for the other populations considered here.

Under the mate-opportunity hypothesis, population density or gender ratio could influence the fitness-maximizing degree of protandry in salmon. Conditions that promote greater energy expenditure may accelerate reproductive senescence and, consequently, favour less protandry. This prediction follows logically from models that predict less protandry when mortality rates during reproduction are higher (Botterweg 1982; Iwasa et al. 1983; Parker and Courtney 1983). When gender ratios on the spawning grounds are male biased, males compete more aggressively (Schroder 1981; Fleming and Gross 1989, 1994) and presumably use energy reserves at a higher rate. Males may also compete more when the population density is greater because of closer proximity to neighbouring spawning associations (Hendry et al. 1995). Males do live for slightly fewer days when breeding densities are high (van den Berghe and Gross 1986; Hendry 1998). Estimates of population density were not available to test this prediction, but a

© 2000 NRC Canada

Fig. 1. Effect of gender ratio on protandry for Auke Creek pink salmon (*a*) shown alone and (*b*) in relation to all populations (solid circles, Auke Creek data; open circles, other data). For Auke Creek pink salmon, the linear equation relating protandry and gender ratio is $y = -9.32 + 22.9x$. The effect of gender ratio on protandry was not significant in the other six populations.

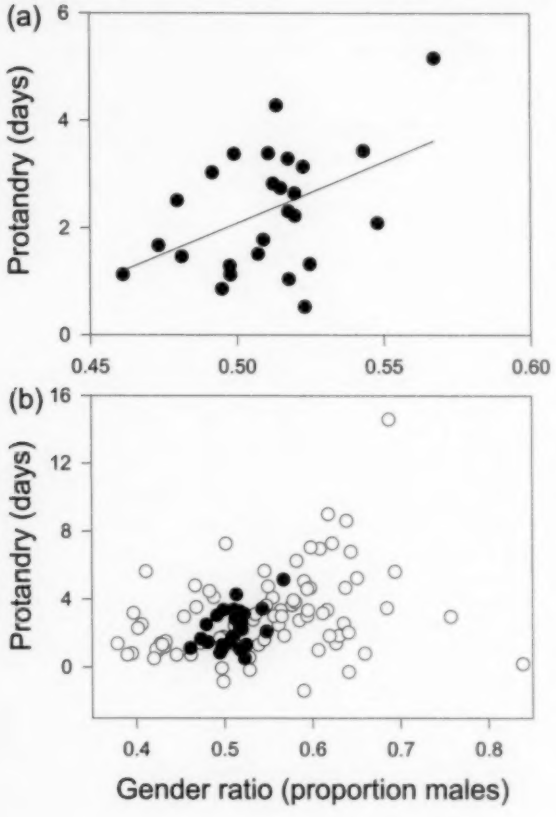

surrogate measure, population size, did not affect protandry. There was also no indication of less protandry with a more male-biased gender ratio.

An opposite result was obtained for Auke Creek pink salmon: greater protandry was observed when the gender ratio was more male biased. The mate-opportunity hypothesis could explain this pattern if a prior-resident advantage is assumed. Males that are familiar with a particular spawning locale have an advantage over an intruder when competing for a female (Foote 1990; Chebanov 1997). If females are not limiting, prior residency would not confer any advantage. If gender ratios are male biased, however, prior residency may confer an advantage during competition for limited females. The generality of this explanation must remain speculative, however, because gender ratio affected protandry in only one of the seven populations. A link between prior residency and protandry was first noted by Foote (1990), who suggested that the prior-residency advantage may explain the occurrence of protandry. However, this hypothesis is unlikely a strict alternative to the mate-opportunity hypothesis. The advantage of prior residency

Fig. 2. Observed interannual variation in protandry among the seven populations. Means are shown with standard deviations and sample sizes. The vertical lines at the right indicate populations with statistically similar protandry based on the post hoc means comparison test.

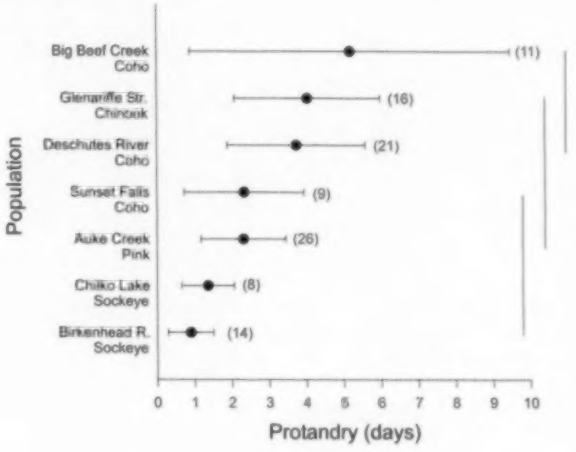

presumably is an increase in a male's mating opportunities through competitive exclusion, but his mating opportunities also must depend on the availability of females.

A different explanation for protandry is that arrival timing is constrained in some way. Perhaps males migrate upstream faster than females so that they arrive at the spawning grounds first. This would assume a gender difference in upstream migration rate, for which there is no evidence. Also, populations with a longer, and possibly more arduous, migration did not show more protandry in this study (compare Table 1 and Fig. 2). A second constraint is differential fishing pressure (i.e., more females are caught early in the run than late), but no evidence could be found to support this explanation.

If factors influence the arrival timing of males independently of females (i.e., there is differential selection among the genders), protandry may be an "incidental" byproduct (Wiklund and Solbreck 1982). Under this hypothesis, different scenarios have been proposed for other taxa showing protandry, but none for salmon. In insects, selection for large size may be greater in females than in males, and therefore, females should terminate growth and emerge later than males (Wiklund and Solbreck 1982). Analagously, female salmon may increase their fecundity by delaying migration and continuing to feed at sea, and male salmon, if they delay migration, may suffer increased predation risk at sea that is not offset by the benefits of continued growth. However, it is questionable whether a few days of extra growth could contribute signficantly to fecundity in the much longer-lived salmon.

In birds that migrate to their breeding grounds, male–male competition for territories may select for the earlier arrival of males (Myers 1981). Environmental conditions would determine the arrival timing of females, independently of males. This hypothesis cannot explain protandry in salmon because males do not establish territories. Another idea, also developed for birds, is that the larger gender (usually male)

© 2000 NRC Canada

can tolerate harsh enviromental conditions that prevail earlier in the year, whereas the smaller gender cannot (Ketterson and Nolan 1983). However, in the current study, size did not appear to influence arrival timing because smaller jack males did not consistently arrive later than larger adult males.

A different set of hypotheses assume direct selection on protandry, as does the mate-opportunity hypothesis, but from the female perspective. In insects, protandry may minimize prereproductive mortality of females while they wait to be encountered by males (Fagerström and Wiklund 1982). This is an unlikely explanation for protandry in salmon because males and females rarely would have difficulty encountering one another. Males and females migrate and arrive on the spawning grounds together, and the linear structure of the spawning grounds probably facilitates encounters. Protandry also may be a female strategy to avoid waiting costs while males prepare to breed (cf. Michener 1984). For example, dominance hierarchies may have to form before breeding is possible. In salmon, the time required to establish dominance hierarchies is probably insufficient to account for the observed degree of protandry. Rankings can be established quickly, and spawning can occur within hours (personal observation). However, protandry also may benefit females by facilitating mate choice while minimizing waiting costs (cf. Wang et al. 1990). If females delay arrival, increased male–male competition during the formation of dominance hierarchies may single out the higher-quality males. This hypothesis may have merit because female salmon do exhibit preference for males based on quality measures such as size (Foote 1989).

Based on the natural history of salmon, sexual selection likely acts directly on protandry. From the male's perspective, protandry is consistent with a strategy to maximize opportunities for mating. From the female's perspective, protandry may facilitate mate choice. However, further study is required to conclusively reject the competing hypotheses and to understand why protandry varies among and within populations. For example, it is unclear why some populations, such as Big Beef Creek coho salmon and Birkenhead River sockeye salmon, differ in protandry. Perhaps population differences in species, breeding longevity, arrival-timing constraints, or postarrival waiting are responsible. Another unexplained pattern is the effect of gender ratio on protandry in Auke Creek pink salmon. In addition to understanding the adaptive significance of protandry, the mechanisms producing protandry need to be understood. The hypotheses explain why protandry exists but not how it comes about (i.e., the proximate mechanisms). If timing cannot be adjusted to the ecological and social factors that define optimal protandry, reproductive output could be compromised.

Acknowledgments

I am especially grateful to Jerry Taylor of the National Marine Fisheries Service, Alaska (NMFS), Neil Schubert and Tracy Cone of Canada's Department of Fisheries and Oceans (DFO), Dave Seiler and Steve Neuhauser of the Washington State Department of Fisheries and Wildlife (WDFW), and Martin Unwin of the National Institute of Water and Atmospheric Research, New Zealand (NIWA), for providing the data that I used in the analyses. This project would have been impossible without their help and the cooperation of NMFS, DFO, WDFW, and NIWA. Bernie Crespi, Larry Dill, Andrew Hendry, Martin Unwin, Ron Ydenberg, and two anonymous reviewers all provided excellent advice on how to improve the manuscript. Ian Hamilton, Stephanie Hazlitt, Andrew Hendry, Don Hugie, and Sharilynn Wardrop contributed helpful advice about measuring protandry, and Martin Unwin suggested the measure that I present here. This research forms part of the Ph.D. dissertation of Y.M. Funding to Y.M. was provided by Natural Sciences and Engineering Research Council of Canada and Simon Fraser University graduate fellowships.

References

Botterweg, P.F. 1982. Protandry in the pine looper, *Bupalus piniarius* (Lep., Geometridae); an explanatory model. Neth. J. Zool. **32**: 169–193.

Chebanov, N.A. 1997. Role of the "prior resident" effect in formation of the dominance–subordination relations and determination of the reproductive success values in Pacific salmons. J. Ichthyol. **37**: 110–115.

Fagerström, T., and Wiklund, C. 1982. Why do males emerge before females? Protandry as a mating strategy in male and female butterflies. Oecologia, **52**: 164–166.

Fleming, I.A., and Gross, M.R. 1989. Evolution of adult female life history and morphology in a Pacific salmon (coho: *Oncorhynchus kisutch*). Evolution, **43**: 141–157.

Fleming, I.A., and Gross, M.R. 1994. Breeding competition in a Pacific salmon (coho: *Oncorhynchus kisutch*): measures of natural and sexual selection. Evolution, **48**: 637–657.

Foote, C.J. 1989. Female mate preference in Pacific salmon. Anim. Behav. **38**: 721–723.

Foote, C.J. 1990. An experimental comparison of male and female spawning territoriality in a Pacific salmon. Behaviour, **115**: 283–314.

Fukushima, M., and Smoker, W.W. 1997. Determinants of stream life, spawning efficiency, and spawning habitat in pink salmon in the Auke Lake system, Alaska. Can. J. Fish. Aquat. Sci. **54**: 96–104.

Groot, C., and Margolis, L. (*Editors*). 1991. Pacific salmon life histories. University of British Columbia Press, Vancouver, B.C.

Hendry, A.P. 1998. Reproductive energetics of Pacific salmon: strategies, tactics, and trade-offs. Ph.D. thesis, University of Washington, Seattle, Wash.

Hendry, A.P., Leonetti, F.E., and Quinn, T.P. 1995. Spatial and temporal isolating mechanisms: the formation of discrete breeding aggregations of sockeye salmon (*Oncorhynchus nerka*). Can. J. Zool. **73**: 339–352.

Iwasa, Y., Odendaal, F.J., Murphy, D.D., Ehrlich, P.R., and Launer, A.E. 1983. Emergence patterns in male butterflies: a hypothesis and a test. Theor. Popul. Biol. **23**: 363–379.

Ketterson, E.D., and Nolan, V., Jr. 1983. The evolution of differential bird migration. *In* Current ornithology. Vol. 1. *Edited by* R.F. Johnston. Plenum Press, New York. pp. 357–402.

Manly, B.F.J. 1997. Randomization, bootstrap and Monte Carlo methods in biology. 2nd ed. Chapman and Hall, New York.

McPhee, M.V., and Quinn, T.P. 1998. Factors affecting the duration of nest defense and reproductive lifespan of female sockeye salmon, *Oncorhynchus nerka*. Environ. Biol. Fishes, **51**: 369–375.

Michener, G.R. 1984. Spring emergence schedules and vernal behavior of Richardson's ground squirrels: why do males emerge from hibernation before females? Behav. Ecol. Sociobiol. **14**: 29–38.

© 2000 NRC Canada

Myers, J.P. 1981. A test of three hypotheses for latitudinal segregation of the sexes in wintering birds. Can. J. Zool. **59**: 1527–1534.

Myers, R.H. 1990. Classical and modern regression with applications. 2nd ed. PWS-KENT, Boston, Mass.

Parker, G.A., and Courtney, S.P. 1983. Seasonal incidence: adaptive variation in the timing of life history stages. J. Theor. Biol. **105**: 147–155.

Pritchard, A.L. 1937. Variation in the time of run, sex proportions, size and egg content of adult pink salmon (*Oncorhynchus gorbuscha*) at McClinton Creek, Masset Inlet, B.C. J. Biol. Board Can. **3**: 403–416.

Quinn, T.P., and Unwin, M.J. 1993. Variation in life history patterns among New Zealand chinook salmon (*Oncorhynchus tshawytscha*) populations. Can. J. Fish. Aquat. Sci. **50**: 1414–1421.

Quinn, T.P., Adkison, M.D., and Ward, M.B. 1996. Behavioral tactics of male sockeye salmon (*Oncorhynchus nerka*) under varying operational sex ratios. Ethology, **102**: 304–322.

SAS Institute, Inc. 1990. SAS/STAT user's guide. SAS Institute, Inc., Cary, N.C.

Schroder, S.L. 1981. The role of sexual selection in determining overall mating patterns and mate choice in chum salmon. Ph.D. thesis, University of Washington, Seattle, Wash.

Schubert, N.D., and Fanos, B.P. 1997. Estimation of the 1994 Chilko River and Chilko Lake system sockeye salmon (*Oncorhynchus nerka*) escapement. Can. Manuscr. Rep. Fish. Aquat. Sci. No. 2428.

Schubert, N.D., and Tadey, J.A. 1997. Estimation of the 1994 Birkenhead River sockeye salmon (*Oncorhynchus nerka*) escapement. Can. Manuscr. Rep. Fish. Aquat. Sci. No. 2399.

Seiler, D., Neuhauser, S., and Ackley, M. 1981. Upstream/downstream salmonid trapping project, 1977–1980. State Wash. Dep. Fish. Prog. Rep. No. 144.

Unwin, M.J. 1986. Stream residence time, size characteristics, and migration patterns of juvenile chinook salmon (*Oncorhynchus tshawytscha*) from a tributary of the Rakaia River, New Zealand. N.Z. J. Mar. Freshwater Res. **20**: 231–252.

Unwin, M.J., and Glova, G.J. 1997. Changes in life history parameters in a naturally spawning population of chinook salmon (*Oncorhynchus tshawytscha*) associated with releases of hatchery-reared fish. Can. J. Fish. Aquat. Sci. **54**: 1235–1245.

van den Berghe, E.P., and Gross, M.R. 1986. Length of breeding life of coho salmon (*Oncorhynchus kisutch*). Can. J. Zool. **64**: 1482–1486.

Wang, G-Y., Greenfield, M.D., and Shelly, T.E. 1990. Inter-male competition for high-quality host-plants: the evolution of protandry in a territorial grasshopper. Behav. Ecol. Sociobiol. **27**: 191–198.

Wiklund, C., and Fagerström, T. 1977. Why do males emerge before females? Oecologia, **31**: 153–158.

Wiklund, C., and Solbreck, C. 1982. Adaptive versus incidental explanations for the occurrence of protandry in a butterfly, *Leptidea sinapis* L. Evolution, **36**: 56–62.

Zonneveld, C., and J.A.J. Metz. 1991. Models on butterfly protandry: virgin females are at risk to die. Theor. Popul. Biol. **40**: 308–321.

© 2000 NRC Canada

Organochlorine transfer in the food web of subalpine Bow Lake, Banff National Park

Linda M. Campbell, David W. Schindler, Derek C.G. Muir, David B. Donald, and Karen A. Kidd

Abstract: Lake trout (*Salvelinus namaycush*) from subalpine Bow Lake, near the Continental Divide in Banff National Park, have been reported to have higher concentrations of toxaphene than other lake trout populations of the Rocky Mountains. Our original hypothesis was that unusually high biomagnification via a long food chain was responsible for elevated levels of toxaphene and other persistent organochlorines in the lake trout. This hypothesis was refuted by the analyses of stable carbon ($\delta^{13}C$) and nitrogen ($\delta^{15}N$) isotope ratios in lake biota. Stable nitrogen isotope analyses demonstrated that the food chain length in Bow Lake was short. The sources of carbon (pelagic or benthic), as indicated by stable carbon isotope values, were highly correlated with organochlorine concentrations in the food web. Lake trout with more pelagic carbon signatures had higher organochlorine concentrations than littoral-feeding mountain whitefish (*Prosopium williamsoni*) and lake trout. The pelagic copepod *Hesperodiaptomus arcticus* had higher organochlorine concentrations (wet weight basis) than any other organism, including the fish. This was attributed to the high lipid content of copepods and possibly their ingestion of suspended solids, including glacial silt or direct absorption from solution in glacial inflows.

Résumé : Les touladis du lac Bow, lac subalpin du parc national Banff situé près de la ligne de partage des eaux, semblent présenter des concentrations de toxaphène plus élevées que d'autres populations de touladis des montagnes Rocheuses. Nous sommes partis de l'hypothèse qu'une bioamplification anormalement forte le long d'une chaîne trophique très longue était responsable des teneurs élevées en toxaphène et en d'autres organochlorés persistants chez les touladis. Cette hypothèse a été réfutée après l'analyse des rapports des isotopes stables du carbone ($\delta^{13}C$) et de l'azote ($\delta^{15}N$) dans le biote du lac. D'après les analyses des isotopes stables de l'azote, nous avons établi que le réseau trophique du lac Bow est raccourci. Les sources de carbone (pélagiques ou benthiques), d'après les valeurs des isotopes stables du carbone, étaient fortement corrélées aux concentrations d'organochlorés dans le réseau trophique. Les touladis présentant de plus fortes signatures de carbone pélagique avaient des concentrations plus élevées d'organochlorés que les ménominis de montagnes et les touladis qui se nourrissaient sur le littoral. Le copépode pélagique *Hesperodiaptomus arcticus* présentait des concentrations d'organochlorés plus élevées (poids humide) que tout autre organisme, poissons y compris. Ce phénomène est attribuable à la forte teneur en lipides des copépodes, et peut-être au fait qu'ils ingèrent des solides en suspension, notamment du silt glaciaire, ou qu'ils absorbent directement des composés en solution dans l'eau d'origine glaciaire.

[Traduit par la Rédaction]

Introduction

In a survey conducted in 1991–1992, persistent organochlorine compounds (toxaphene, total dichlorodiphenyltrichloroethane (ΣDDT), total polychlorinated biphenyls (ΣPCB), and other compounds) were detected in lake trout (*Salvelinus namaycush*) from 14 lakes in the Canadian Rocky Mountains (Donald et al. 1993). Lake trout from subalpine Bow Lake in Banff National Park contained some of the highest toxaphene (chlorobornanes) concentrations in the study, leading to concern about the presence of persistent organochlorine (OC) contaminants in the Rocky Mountain area. Concentrations of toxaphene in lake trout from Bow Lake were up to 10–20 times higher than in fish populations from other nearby lakes (Donald et al. 1998). There was no record of any direct addition of toxaphene or other OCs to

Received July 5, 1999. Accepted March 21, 2000.
J15236

L.M. Campbell[1] **and D.W. Schindler.**[2] Department of Biological Sciences, University of Alberta, Edmonton, AB T6G 2E9, Canada.
D.C.G. Muir. Environment Canada, National Water Research Institute, 867 Lakeshore Road, P.O. Box 5050, Burlington, ON L7R 4A6, Canada.
D.B. Donald. Environment Canada, Room 300 Park Plaza, 2365 Albert Street, Regina, SK S4P 4K1, Canada.
K.A. Kidd. Department of Fisheries and Oceans, Freshwater Institute, 501 University Crescent, Winnipeg, MB R3T 2N6, Canada.

[1]Present address: Department of Biology, University of Waterloo, Waterloo, ON N2L 3GT, Canada.
[2]Author to whom all correspondence should be addressed. e-mail: d.schindler@ualberta.ca

© 2000 NRC Canada

Bow Lake or surrounding areas (Donald et al. 1993), which suggested an atmospheric source. A recent mass-balance study of persistent OCs suggests that Bow Lake may be receiving much of its OCs from glacial water flowing into the lake and from precipitation at high altitudes (Dr. J. Blais, Department of Biology, University of Ottawa, Ottawa, ON K1N 6N5, Canada, personal communication).

In contaminated aquatic ecosystems, there is usually an increase in OC concentrations with each trophic level in a food web (Evans et al. 1991). In an earlier study of Lake Laberge, Yukon Territory, unusually high concentrations of toxaphene and other contaminants in predatory fish were explained by the presence of longer food chains than found in other nearby lakes (Kidd et al. 1998*b*). We hypothesised that Bow Lake might also have a longer food chain than other Rocky Mountain lakes, contributing to the high concentrations in fish.

Stable nitrogen ($\delta^{15}N$) and carbon ($\delta^{13}C$) isotope ratios of biota can be invaluable in characterising food web structure and trophic interactions (Peterson and Fry 1987). Stable carbon and nitrogen isotope ratios integrate long-term dietary patterns, especially in cold-water fish that have slow tissue turnover rates (Hesslein et al. 1993). Stable isotope analyses complement taxonomic data obtained from stomach contents because both long-term and short-term trophic behaviour can be evaluated for individual animals.

^{14}N is selectively eliminated by organisms and ^{15}N incorporated in body tissues, so that with each successive trophic level, $\delta^{15}N$ (^{15}N:^{14}N) values in the tissue of biota increase. Freshwater studies indicate that the average $\delta^{15}N$ difference between trophic levels is between 3.2 and 3.4‰ (Peterson and Fry 1987). Kidd et al. (1995) demonstrated that contaminant uptake by fish and other organisms in Yukon aquatic food chains could be reliably predicted by using stable isotopes of nitrogen to measure trophic positioning. Similar positive significant relationships between OCs and stable nitrogen isotope ratios were observed in Lake Ontario in southern Ontario (Kiriluk et al. 1995), Lake Baikal in Russia (Kucklick et al. 1996), and Peter Lake in Northwest Territories (Kidd et al. 1998*a*).

In contrast, stable carbon isotopes fractionate very little during transfer between trophic levels, with less than 1‰ enrichment in $\delta^{13}C$ (^{13}C:^{12}C) per trophic level (Peterson and Fry 1987). Because of low fractionation rates, the stable carbon isotope values of organisms reflect the average $\delta^{13}C$ of their diets. Differences in $\delta^{13}C$ between pelagic, benthic, and terrestrial sources are transferred up the food chain, revealing the importance of different sources of primary production to organisms (Rau and Anderson 1981; Hecky and Hesslein 1995). The differences in $\delta^{13}C$ between pelagic and benthic consumers can be used in conjunction with OC measurements to determine the relative contribution of these carbon sources to the biomass of any consumer within the food web as well as to contaminant burdens.

This study had two objectives. The first was to determine the food web structure in Bow Lake by using $\delta^{15}N$ and $\delta^{13}C$ to characterise trophic level and carbon sources, respectively. The second was to test the hypothesis that the food web structure and (or) lipid content determine persistent OC concentrations in biota.

Methods

Study area

Bow Lake is an ultraoligotrophic subalpine lake located in northern Banff National Park (51°45′N, 116°30′W) (Table 1). The Icefields Parkway, a major tourist thoroughfare, runs along the eastern side of Bow Lake. The majority of the inflow to Bow Lake comes from the Bow Glacier, a tongue of the Wapta Icefields that straddles the Continental Divide. The lake discharges to the Bow River, which flows southeast through the park, becoming part of the Saskatchewan River system. The current fish community consists of lake trout (*Salvelinus namaycush*) and mountain whitefish (*Prosopium williamsoni*). The large calanoid copepod *Hesperodiaptomus arcticus* is the most abundant zooplankton species, followed by *Daphnia middendorffiana*. Campbell (1997) provides a detailed review of the limnology, fish stocking history, and the environment of Bow Lake.

Field methods and analyses of fish stomach contents

Lake trout and mountain whitefish were captured using gill nets (June 1994) or fish traps (August 1994) set in the littoral zone. Fish stomachs were removed upon capture and were either frozen for stable isotope analyses or preserved in sugar formalin for taxonomic analyses. Sixteen lake trout (1019 ± 411 g, 9.6 ± 2.1 years old) and 12 mountain whitefish (250 ± 238 g, 7.3 ± 4.6 years old) were submitted for OC and stable isotope analyses. All fish and fish stomachs were wrapped in solvent-cleaned aluminium foil, stored on dry ice in the field, and then stored at –60°C in the laboratory. Otoliths were removed from fish in the field and stored in glycerin–alcohol solution. The ages of fish were later determined by counting annuli on otoliths using Calcified Structure Analysis software at the Glenora Fisheries Station (Ontario).

The contents of fish stomachs were examined under a dissecting microscope. Many stomachs contained highly digested material, which precluded accurate weight estimates of the individual taxa. The percent frequency of occurrence of each prey was calculated for lake trout and mountain whitefish (excluding empty stomachs). Mountain whitefish fry, adult Ephemeroptera, and Plecoptera found in lake trout stomachs were included in stable isotope analyses. Additional data for Bow Lake fish dietary habits were obtained from an Environment Canada database for the years of 1984, 1991, and 1993 and from published mountain whitefish studies from the 1930s (Rawson 1939; McHugh 1940). The presence of plerocercoid larval cysts of *Diphyllobothrium ditremum* on the surface of fish stomachs was noted, as it provides an indirect measure of zooplanktivory. *Diphyllobothrium ditremum* is transmitted to fish by feeding upon copepods or infected fish (Anthony 1967). We did not determine the frequency and duration of the plerocercoid infection in fish from Bow Lake.

Zooplankton were collected throughout the summers of 1994 and 1995 by towing a 64-μm-mesh Wisconsin-style net of 1-m diameter through the entire water column and then along the surface for about 5 m to maximise the amount collected. Zooplankton were sorted into adult *H. arcticus*, larval *H. arcticus*, and *D. middendorffiana* using 243- and 947-μm screens and hand sorting. In addition, unsorted zooplankton samples (which were taken directly from the net haul without any separation into species or size-classes) and *H. arcticus* samples were processed for OC and stable isotope analyses. However, large *D. middendorffiana* were analysed for stable isotope ratios only. Phytoplankton could not be collected in sufficient amounts for stable isotope or OC analyses. Benthic algae were obtained for stable isotope analyses by scraping rocks from the littoral zone. Benthic invertebrates were collected by sweeping the shoreline with long-handled collecting nets. In addition, burlap sacks (filled with rocks and marked with a float) were set underwater near the shoreline to provide artificial

© 2000 NRC Canada

Table 1. Physical and chemical parameters for Bow Lake, Banff National Park.

Variable	Value
Area	2.8 km^2
Volume	0.64 km^3
Maximum depth	51 m
Average depth	22.9 m
Elevation	1940 m
Midsummer surface temperature (measured in July 1994 and 1995)	10–12°C
Dissolved organic carbon	0.46±0.12 $mg \cdot L^{-1}$
Total phosphorus	4.6±1.3 $\mu g \cdot L^{-1}$
Total dissolved phosphorus	2.2±1.2 $\mu g \cdot L^{-1}$
Total dissolved nitrogen	83.9±5.2 $\mu g \cdot L^{-1}$
$NO_3 + NO_2$	46.4±2.6 $\mu g \cdot L^{-1}$
Ammonia	3.2±0.9 $\mu g \cdot L^{-1}$
Chlorophyll *a*	0.31±0.2 $\mu g \cdot L^{-1}$
Conductivity	161.8±3.2 $\mu S \cdot cm^{-1}$
pH	8.1±0.06
Turbidity	2.6 NTU
Dissolved inorganic carbon $\delta^{13}C$	–5.86‰
Particulate organic matter + particulate inorganic matter $\delta^{13}C$	–16.44‰ (average)
Particulate organic matter $\delta^{15}N$	0.51‰
Sediment organochlorine content	3.1%

habitat for benthic invertebrates and were found to be a particularly successful tool for collecting the amphipod *Gammarus lacustris*. All invertebrate species were pooled by major taxa for OC and stable isotope analyses except for *H. arcticus*, *G. lacustris*, and *D. middendorffiana*. Samples were stored at –60°C in solvent-cleaned glass jars until analysis.

Laboratory methods

Stable isotope analyses

For stable isotope analyses, skinless dorsal muscle samples were removed from individual fish. All invertebrates were pretreated with 1 N hydrochloric acid to remove carbonates prior to $\delta^{13}C$ analyses. Prepared non-lipid-extracted samples were combusted in a Carlo Erba NA 1500 elemental analyser using the automated methods detailed in Kidd et al. (1998*a*). The precision over several years is 0.4 part per mil (2 SD). The ratios of the stable isotopes were measured against the reference standards PeeDee dolomite for $\delta^{13}C$ and air for $\delta^{15}N$ using the formula below. The delta notation (δ) is used to indicate the parts per mil (‰, or parts per thousand) difference in the isotopic ratio of the sample from the standard. A working standard of Pharmamedium of known isotopic composition was run with every 10 samples. The formula is

$$\delta^{13}C \text{ or } \delta^{15}N = (R_{sample} \times R_{standard}^{-1}) \times 1000$$

where $R = {}^{13}CO_2/{}^{12}CO_2$ for $\delta^{13}C$ and $R = {}^{15}N_2/{}^{14}N_2$ for $\delta^{15}N$.

OC extractions and analysis

Six major OC groups were quantified for this study: toxaphene (chlorobornanes), ΣDDT, ΣPCB, total chlordane (ΣCHL), dieldrin, and total hexachlorocyclohexane (ΣHCH). Extraction and processing of samples for OCs follow the same methods outlined in Kidd et al. (1998*b*). For fish, dorsal muscle samples with skin attached (dissected from the same side of all fish using solvent-cleaned tools) were analysed. Analysis of skin-on fillets may underestimate total OC burdens by as much as 20% but was done to facilitate efficient processing for both stable isotopes and OC analyses in the laboratory. Fish muscle and invertebrate samples were extracted in 1:1 hexane–dichloromethane for 4 h using a Soxhlet apparatus. One-tenth of the Soxhlet extract was set aside to gravimetrically determine the percent extractable lipids. Invertebrate samples were prefiltered to remove fine particles before determining the percent extractable lipids. Lipids were removed using gel permeation chromatography by eluting though SX-3 Bio-bead columns with 1:1 hexane–dichloromethane.

The Soxhlet extracts were separated on 1.2% deactivated Florisil (8 g) columns into three fractions (F1, F2, and F3). F1 contained all PCB congeners, some DDT and DDT metabolites, some toxaphene congeners, and the PCB 30 internal standard in 100% hexane. F2 contained most of HCH, toxaphene, and CHL congeners, the remaining DDT congeners, and the octachloronapthalene internal standard in 85:15 hexane–dichloromethane. F3 contained the remaining OC congeners from the column including dieldrin in 1:1 hexane–dichloromethane. Each fraction was analysed on a Varian 3600 gas chromatograph with a ^{63}Ni electron capture detector. Internal standards (PCB 30 and octachloronapthalene) were used to monitor extraction efficiency, and samples were not corrected for recoveries. Recoveries of internal standards in all fish samples were 78 ± 10% for F1 and 77 ± 11% for F2. Zooplankton samples had 100% recovery rates for both F1 and F2, while benthic invertebrate sample recoveries were 99.1 ± 1.9% for F1 and 99.4 ± 1.2% for F2. Toxaphene in samples was quantified by analysing combined F1 and F2 with high resolution gas chromatography electron capture negative high-resolution mass spectrometry (Miskimmin et al. 1995). All concentrations are reported as wet weight values.

Data analyses

Calculations were made with SAS software (version 6.10, SAS Institute Inc., Cary, N.C.). For fish, weight was chosen as the size variable. Nonpaired Student's *t* tests were used to compare the means of stable nitrogen and carbon isotope values between lake trout and mountain whitefish and between zooplankton and benthic invertebrates. Nonparametric statistics were used for OC data analyses because of the small sample sizes (Zar 1984). Nonparametric Spearman rank correlation coefficients (r_s) were used to measure correlations between OC concentrations and percent lipids, $\delta^{15}N$, and $\delta^{13}C$ in biota. The significance of the Spearman coefficients was based on the sample size at a significance level of $\alpha = 0.05$ and was based on the statistical tables listed in Zar (1984). For fish, weight was chosen as the size variable to examine relationships with OC data.

Results

Fish and copepod gut contents and dietary habits

Lake trout in Bow Lake appeared to preferentially feed upon chironomids (44–94%) and *G. lacustris* (43–79%) (Table 2). Fish (9–46%) were often found in trout stomachs, but the frequency varied greatly between years. Trichoptera, Plecoptera, and Ephemeroptera (4–75%) were occasionally found in these stomachs. Among the least common dietary items found in lake trout stomachs were zooplankton (1–15% of lake trout stomachs in 1993–1994 and 1984). However, in 1994, more than 60% of the lake trout captured had plerocercoid larval cysts of *D. ditremum* on their stomachs, indicating some zooplanktivory.

In Bow Lake, mountain whitefish diets were primarily benthic (Table 2). In 1994, Trichoptera were the dominant prey item (50% of mountain whitefish stomachs), along with

© 2000 NRC Canada

Lymnaeidae (33%). No chironomids were found in 1994 mountain whitefish stomachs, but McHugh (1940) and Rawson (1939) found mostly chironomids (≥20%) in mountain whitefish collected from Bow Lake earlier this century (Table 2). Ephemeroptera nymphs were found in a significant number of mountain whitefish from the 1930s, although not in the mountain whitefish from 1994. *Gammarus lacustris* and Plecoptera were found in low numbers for mountain whitefish in all years. Mountain whitefish also have been found with *D. ditremum* plerocercoid larval cysts (Rawson 1939).

The guts of individual *H. arcticus* collected in 1995 were full of glacial silt, which appeared to be ingested along with diatoms, algae, or other small zooplankton. Diatom shell fragments were observed in some individual gut contents. Glacial silt is very fine suspended sediment (grain size 2–4 μm) derived from rocks and sediment beneath glaciers.

Stable nitrogen isotopes

According to the $\delta^{15}N$ data, all adult fish of both species fed at a similar trophic level (Table 2; Fig. 1). Lake trout values ($\delta^{15}N$ of 5.8–7.6‰) and adult mountain whitefish values ($\delta^{15}N$ of 6.1–7.8‰) were not significantly different, varying within 2‰ of each other (Student's t test, $t = 1.43$, $p = 0.175$) (Fig. 1). Mountain whitefish fry had a $\delta^{15}N$ value (4.3‰) intermediate between $\delta^{15}N$ values for adult mountain whitefish and invertebrates. The average difference between the $\delta^{15}N$ values of Bow Lake invertebrates (excluding the exceptions outlined below) and fish was about 4‰ (Fig. 2), indicating that both lake trout and mountain whitefish were located only one trophic level above invertebrates, with no intermediate fish prey.

$\delta^{15}N$ values for zooplankton and benthic invertebrates (1.3–2.9‰) were not significantly different (Student's t test, $t = 0.853$, $p = 0.216$), indicating that most invertebrates occupied a similar trophic level (Table 2; Fig 1). In Bow Lake, *H. arcticus* and Plecoptera had $\delta^{15}N$ values similar to those of lake trout in 1994 (5.6‰), but *H. arcticus* and Plecoptera had lower $\delta^{15}N$ values in 1995 (2.5 ± 0.3 and 3.6–4.2‰, respectively). Another shift in stable nitrogen isotopes was found with the 1994 Ephemeroptera samples: the adult mayfly sample had a higher $\delta^{15}N$ ratio (4.9‰) than mayfly nymphs (1.7 ± 0.3‰). Nitrogen signatures of benthic algae were variable, with one sample having a very low $\delta^{15}N$ (–1.34‰) and another sample having a $\delta^{15}N$ value (1.27‰) comparable with that of some benthic invertebrates (Fig. 2; Table 1). The range of $\delta^{15}N$ values between algae, invertebrates, and fish suggests that there were only three isotopically distinct trophic levels in Bow Lake.

Stable carbon isotopes

The pelagic and benthic carbon signals at the base of the food web were isotopically distinct, with benthic invertebrates such as *G. lacustris* having significantly heavier $\delta^{13}C$ values (–25.8 to –24.2‰) than pelagic zooplankton (–33.9 to –31.1‰) (Student's t test, $t = 11.2$, $p < 0.001$) (Fig. 2; Table 2). One Ephemeroptera nymph had a $\delta^{13}C$ value similar to that of zooplankton (–30.5‰). The two benthic algae samples had different $\delta^{13}C$ values (–24.05 and –17.98‰). Mountain whitefish adults and fry had carbon signatures similar to those of benthic invertebrates (–25.6 to –20.3‰). Lake trout $\delta^{13}C$ values (–30.7 to –24.8‰) fell between pelagic and benthic invertebrate $\delta^{13}C$ values, indicating a broad dietary range with more pelagic carbon being assimilated than benthic carbon. Mountain whitefish values (–25.6 to –20.3‰) were significantly less negative than those of lake trout (Student's t test, $t = 5.61$, $p < 0.001$), indicating that they fed exclusively on benthic invertebrates.

Lipid content

Hesperodiaptomus arcticus had the highest lipid content (14.9 ± 8.6%) of all Bow Lake biota, including lake trout (6.7 ± 3.1%). *Gammarus lacustris* had higher proportions (7.5 ± 3.4%) than mountain whitefish (4.3 ± 2.2%) (Table 2). The lipid content in biota did not increase with trophic level, as indicated by a lack of a significant correlation with $\delta^{15}N$ ($r_s = -0.357$). However, lipid content in biota significantly increased with more depleted $\delta^{13}C$ values ($r_s = 0.547$) (Fig. 2), indicating that pelagic organisms had higher lipid content.

OCs in the food web

Toxaphene was the major contaminant group detected in all biota. The average concentrations ranged from 181.5 ± ng·g wet weight^{-1} in *H. arcticus* to 2.2 ng·g^{-1} in Lymnaeidae. ΣDDT concentrations were generally less than half those of toxaphene, ranging from 22.5 ± 9.1 ng·g^{-1} in *H. arcticus* to 0.6 ng·g^{-1} in Lymnaeidae. ΣPCB and ΣCHL were found at much lower concentrations than toxaphene, ranging from about 12 ng·g^{-1} in *H. arcticus* to about 0.5 ng·g^{-1} in Lymnaeidae. ΣHCH and dieldrin concentrations were low in all biota, except for zooplankton, which had concentrations comparable with their ΣPCB and ΣCHL concentrations.

The highest OC concentrations were found in *H. arcticus*, an omnivore, and in lake trout, the top predator. Toxaphene tended to be highest in *H. arcticus*, while ΣCHL and ΣHCH concentration values for the two species overlapped (Table 3; Figs. 3–5). ΣDDT, ΣPCB, and ΣCHL were higher in lake trout (Table 3; Figs. 3–5). Mixed zooplankton and other invertebrates had lower OC concentrations. *Gammarus lacustris* had OC concentrations comparable with those for mountain whitefish.

Lipid concentrations (Fig. 3) and carbon sources (Fig. 4) were better correlated with OC bioaccumulation patterns in Bow Lake biota than trophic position as indicated by $\delta^{15}N$ (Fig. 5). Biota with higher lipid content (percent lipids) had significantly higher concentrations of all OC compounds ($r_s = 0.577$ to 0.872) (Fig. 3). The consistent and significant negative correlations of $\delta^{13}C$ with all OC concentrations in the biota of Bow Lake food web ($r_s = -0.477$ to –0.664) (Fig. 4) indicated that OC bioaccumulation was greater in pelagic organisms, which had more depleted carbon signatures and higher lipid. Correlations between contaminants and $\delta^{15}N$ through the food web were nonsignificant ($r_s = -0.216$ to 0.486) (Fig. 5). Similarly, in lake trout, toxaphene and ΣHCH were significantly correlated with lipids ($r_s = 0.880$ and 0.726, respectively) and with $\delta^{13}C$ ($r_s = -0.698$ and –0.726, respectively). However, in lake trout, ΣCHL was

© 2000 NRC Canada

Table 2. Stomach content data for mountain whitefish and lake trout from Bow Lake and stable nitrogen and carbon isotope ratios and percent lipid (mean ± SD) of biota collected in 1994 and 1995.

	Fish (see codes)												
	M	M (<2 years old)[a]	M (≥2 years old)[a]	M[b]	L	L	L	L	Code	Year	*n*	$\delta^{15}N$ (‰)	$\delta^{13}C$ (‰)	% lipid
Year fish captured	Aug. 1994	1936–1938	1936–1938	1938	June–Aug. 1994	July 1993	June 1991	June 1984						
Total no. of stomachs (no. empty)	12 (7)	12	35	81	16 (2)	23 (1)	26 (0)	38 (0)						
Lake trout						2			L	1994	19	6.4±0. 5	–27.3±1.8	6.7±3.1
Mountain whitefish					4		12	6	M	1994	12	6.7±0. 6	–23.0±1.5	4.3±2.2
Mountain whitefish fry									MF	1994	3	4.3	–22.8	
Unidentified fish						5								
Chironomidae		***[3]	***	***	7	16	18	36	C	1995	1	2.8	–24.5	
Tipulidae									T	1995	2	1.3–1.5	–24.2 to –22.8	2.0–5.5
Other Diptera		*	*											
Hemiptera			*											
Trichoptera	6	*	*	*		3	2	15			2		–26.2	
Plecoptera	1	*	*	*	7	1	2	6	P	1994	1	5.6	–23.8	
									P	1995	2	3.6–4.2	–24.6 to –26.9	
Ephemeroptera (adults)		*			12	7		3	EA	1994	1	4.9	–20.6	
Ephemeroptera (nymphs)	1		**	**		2		2	EN	1994	3	1.7±0.3	–27.0±3.0	
G. lacustris	1			*	10	10	13	30	G	1994	1	3.77	–23.9	
									G	1995	2	2.7–2.7	–23.9 to –24.1	5.2–9.9
Unidentified Copepoda			*											
H. arcticus					2	1			H	1994	1	5.6	–31.0	
									H	1995	3	2.5±0.3	–31.2±4.2	14.9±8.6
Unidentified Cladocera								6						
Alona sp.		**	*											
D. middendorffiana					1	4			D	1994	1	0.68	–32.3	
Unsorted zooplankton									Z	1995	2	1.8	–31.1	6.5–11.3
Araneae			×					1						
Hydroachnidia		×	×								1		–33.1	
Sphaeriidae (Mollusca)			*	**										
Lymnaeidae (Gastropoda)	4		×		1		1		S	1995	1	1.4	–25.8	0.4
Oligochaeta			*			2			O	1995	1	1.2	–25.2	
Benthic algae									B1	1994	1	–1.34	–17.98	
									B2	1995	1	1.27	–24.05	

Note: For each taxon listed, the number of fish stomachs containing that taxon is listed. Occurrence by volume: more than 20% (***), 10–20% (**), 1–10% (*), and less than 1% (×). The mountain whitefish stomach data from the 1930s are given on a volumetric basis. Only the samples analysed for OCs were also analysed for lipid content due to laboratory procedures.

[a]Data from McHugh 1940. The author separated the mountain whitefish into "less than 2 years old" and "2 years and older."

[b]Data from Rawson (1939).

© 2000 NRC Canada

Fig. 1. Stable isotope "map" of the Bow Lake food web. $\delta^{13}C$ represents the carbon source of the food web, while $\delta^{15}N$ represents the trophic level. The carbon sources ranging from pelagic to benthic are indicated, along with approximate trophic levels. Codes are defined in Table 2.

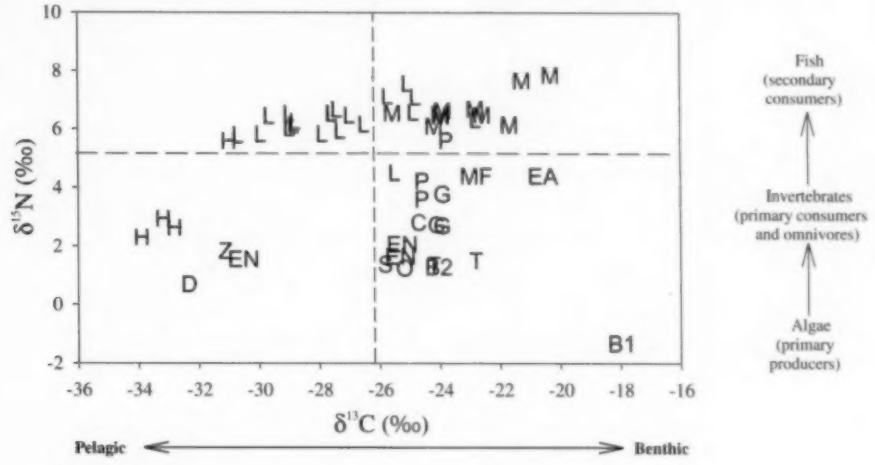

Fig. 2. $\delta^{13}C$ versus lipid content of Bow Lake biota. The Spearman correlation coefficient (r_s) is significant, with significance determined at $\alpha = 0.05$ (Zar 1984). Codes are defined in Table 2.

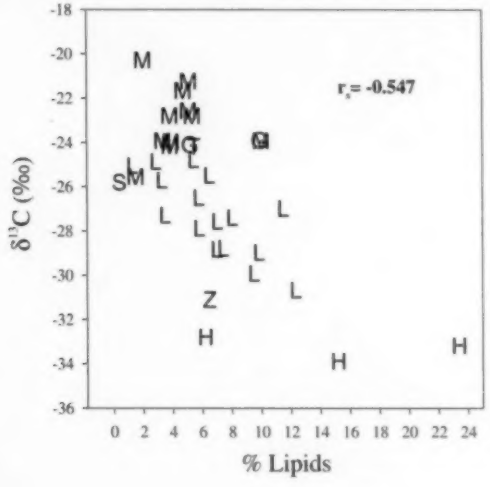

not significantly correlated with $\delta^{13}C$ ($r_s = -0.329$), even though it was correlated with lipids ($r_s = 0.591$).

The ages and weights of lake trout were correlated with toxaphene ($r_s = 0.532$ and 0.565, respectively), ΣPCB ($r_s = 0.549$ and 0.656, respectively), and ΣCHL ($r_s = 0.456$ and 0.570, respectively). No other OC group was significantly correlated with age or weight in lake trout. The ages of mountain whitefish did not correlate with their OC concentrations. Within species, the age and weight of lake trout ($r_s = 0.540$) and mountain whitefish ($r_s = 0.975$) were correlated. In addition, the lipid content of lake trout was correlated with weight ($r_s = 0.630$) but not with age ($r_s = 0.267$). Mountain whitefish lipid content did not show any strong correlation with either age ($r_s = 0.364$) or weight ($r_s = 0.405$).

Discussion

Food web structure

The small range of stable nitrogen isotope data suggests that there are only three trophic levels in Bow Lake: lake trout and mountain whitefish, invertebrates, and algae. The low productivity and biodiversity in Bow Lake may limit the number of potential trophic interactions.

While stable nitrogen isotope results indicated that lake trout and mountain whitefish fed at a similar trophic level, carbon isotope results showed that mountain whitefish had a more enriched carbon signature consistent with a diet of benthic organisms. Carbon isotopes indicated a wide range of feeding for lake trout, from pelagic to benthic. Similar observations were made for a subtropical blue tilapia (*Oreochromis aureus*) population ($\delta^{13}C = -25.9$ to $-9.5‰$) that existed on multiple food sources ranging from detritus to plankton (Gu et al. 1996). The range of $\delta^{13}C$ values within a species, along with its average value, must be considered when examining feeding diversity and dietary carbon sources.

Stomach content analyses confirmed that the food chain in Bow Lake is fairly short and that the mountain whitefish diet is benthic. Inconsistencies were observed between the stomach content and stable isotope data for lake trout; gut contents indicated that this species fed mainly upon benthic invertebrates and small fish whereas $\delta^{13}C$ values indicated that their diet consists mainly of pelagic carbon. This discrepancy may be attributed to the fact that these stomachs were from fish that were sampled during the summer, when benthic production is highest. Stable isotopes integrate dietary habits over a longer period than gut contents and indicate that lake trout have a greater long-term reliance on pelagic, and not benthic, production. Despite evidence that lake trout were responsible for the extirpation of two other trout species in Bow Lake (Donald 1987), $\delta^{15}N$ values indicate that these fish are currently mainly insectivorous and not piscivorous. Lake trout may feed upon zooplankton and

© 2000 NRC Canada

Table 3. Summary data for OC concentrations (ng·g wet weight^{-1}) in Bow Lake biota.

Type	*n*	Toxaphene	ΣDDT[a]	ΣPCB[b]	ΣCHL[c]	Dieldrin	ΣHCH[d]
Lake trout	16	58.4±44.3	22.2±19.1	7.4±5.7	8.1±5.8	2.3±1.8	1.4±0.9
Mountain whitefish	12	13.5±8.4	8.1±6.1	2.8±2.8	2.5±1.8	0.7±0.5	0.6±0.4
H. arcticus	3	181.5±77.1	22.5±9.1	12.9±13.4	12.2±1.9	10.5±12.8	2.0±0.9
Mixed zooplankton	2	21.7–77.0	8.1–20.5	1.9–3.7	7.3–15.5	4.9–19.2	1.9–4.6
G. lacustris	2	44.7–45.3	8.9–9.1	3.7–3.7	4.0–5.5	3.2–4.5	1.1–2.1
Lymnaeidae	1	2.2	0.6	0.5	0.6	0.0	0.03
Tipulidae	2	3.2–9.9	1.8–2.4	2.4–3.5	1.8–2.6	0.0–0.2	0.3–0.5

Note: Average values and standard deviations are indicated for all taxa represented by three or more samples. Ranges indicate OC concentrations for taxa represented by two samples.

[a]ΣDDT is the sum of *p,p'*- and *o,p'*-DDT, *p,p'*- and *o,p'*-DDE, and *p,p'*- and *o,p'*-DDD.

[b]ΣPCB is the sum of 4/10, 7, 6, 8/5, 19, 18, 17, 24/27, 16/32, 26, 25, 31, 28, 33, 22, 45, 46, 52, 49, 47, 48, 44, 42, 41/71, 64, 40, 74, 70/76, 66, 95, 56/60, 91, 84/89, 101, 99, 83, 97, 87, 85, 136, 110, 82, 151, 144/135, 149, 118, 134, 114, 131, 146, 153, 132, 105, 141, 130/176, 179, 137, 138, 158, 178/129, 175, 187, 183, 128, 185, 174, 177, 171, 156, 201/157, 172/197, 180, 193, 191, 200, 170, 190, 198, 199, 196/203, 189, 208, 195, 207, 194, 205, 206, and 209.

[c]ΣCHL is the sum of chlordane-related congeners: heptachlor, heptachlor epoxide, *cis*-chlordane, *trans*-chlordane, *cis*-nonachlor, *trans*-nonachlor, nonachlor III, dihydroheptachlor compounds (C, C1, C2, C3), and octachlordane compounds (C4 and C5).

[d]ΣHCH is the sum of α-HCH, β-HCH, and γ-HCH (lindane).

other invertebrates during the winter, which is up to 8 months long, whereas all fish sampled for stomach analyses were sampled during 2 months of the summer, when high silt concentrations make sight-dependent planktivory ineffective. The presence of copepod-transmitted parasitic cysts on many fish stomachs is further evidence that fish in Bow Lake feed on zooplankton.

In this study the isotopic composition of invertebrates varied over time due to changes in nutrient cycling and also with changes in life stage. For instance, *H. arcticus* apparently occupied different trophic levels in 1994 and 1995, as indicated by very different stable nitrogen isotope ratios (5.6‰ in 1994 and 2.5 ± 0.3‰ in 1995). *Hesperodiaptomus arcticus* are known to have a varied diet ranging from zooplankton to diatoms, depending on the abundance of prey (Paul and Schindler 1994). In addition, in subarctic lakes, the variation in zooplankton isotopic signals has been linked with seasonal variation in the isotopic signatures of sediment detritus and particulate organic matter (Gu et al. 1994). Another example included the 1994 adult mayfly (Ephemeroptera) sample that had a higher $\delta^{15}N$ ratio than the mayfly nymphs. Mihuc and Toetz (1994) reported a similar shift in emerging subalpine chironomids: most species demonstrated heavier $\delta^{15}N$ ratios as adults than as pupae or larvae, which was attributed to changing body composition. More stable isotope studies examining variation in aquatic pelagic and benthic invertebrates are needed to determine the extent of and the reasons for seasonal and developmental variations in isotopic signals.

Lighter $\delta^{13}C$ values in biota were positively correlated with higher lipid content. Studies have shown that lipid is isotopically lighter in $\delta^{13}C$ than protein or carbohydrate, and organisms with higher lipids have lighter $\delta^{13}C$ values (DeNiro and Epstein 1977). However, Kling et al. (1992) found little difference between $\delta^{13}C$ values of whole and lipid-extracted samples of zooplankton (1.2‰) and salmonids (0.1–0.2‰) collected in an Arctic lake. Similarly, a study in Canadian Shield lakes has shown that $\delta^{13}C$ values indicate feeding diversity in aquatic food webs but did not correlate with lipid content (estimated from C:N ratios) within organisms (France 1995). In Bow Lake, lipid content did not alter $\delta^{13}C$ values enough to render stable carbon isotope ratios unusable for determining food sources. Even after adjusting $\delta^{13}C$ data for lipid effects (the lipid content of *H. arcticus* is 14.9 ± 8.6%), based on values (3% for zooplankton and 2% for other biota and fish) given in Kling et al. (1992), similar food chain relationships remained in Bow Lake. Furthermore, it is notable that while lipid content of *H. arcticus* varied, the $\delta^{13}C$ values remained similar, indicating that the present variation in lipid content did not significantly influence the $\delta^{13}C$ values of this zooplankter in Bow Lake.

OCs in the food web

Stable isotope analyses, stomach contents, and the known community structure did not support the hypothesis that a long food chain was responsible for the high OC concentrations in the lake trout in Bow Lake. In addition, OC concentrations in biota were not related to their $\delta^{15}N$ values. This finding is unusual because in other aquatic studies, $\delta^{15}N$ measurements have been excellent predictors of biomagnification of OCs in food webs (Kidd et al. 1995, 1998*b*; Kiriluk et al. 1995; Kucklick et al. 1996). However, the aquatic food chains in other bioaccumulation studies were longer than in Bow Lake. Frequently, several species of forage fish and invertebrates provide intermediate steps between primary producers and predatory fish, leading to a wide range of $\delta^{15}N$ values within the food web. For example, in the food web of Lake Laberge, Yukon Territory, the top predators, burbot (*Lota lota*) and lake trout, had $\delta^{15}N$ values about 8–9‰ above benthic invertebrate values and 6–7‰ above zooplankton values, and there were four forage fish species with intermediate $\delta^{15}N$ values (Kidd et al. 1995). In the pelagic food web of Lake Ontario, the $\delta^{15}N$ values of lake trout were 6–8‰ higher than zooplankton values or amphipod values, while sculpin and alewife (*Alosa pseudoharengus*) values were 3–5‰ above the invertebrate values (Kiriluk et al. 1995). The pelagic-dominated food web of Lake Baikal (Kucklick et al. 1996) had three sculpin species with values 6‰ higher than zooplankton values, 4‰ higher than pelagic amphipod values, and 2‰ higher than benthic amphipod values. In the abbreviated food web of Bow Lake, $\delta^{15}N$ values of fish were only an average of 4‰ higher than invertebrate values. In Bow Lake, other factors

© 2000 NRC Canada

Fig. 3. OC concentrations versus lipid content in Bow Lake. (*a*) Toxaphene; (*b*) ΣDDT; (*c*) ΣPCB; (*d*) ΣCHL; (*e*) dieldrin; (*f*) ΣHCH. The Spearman correlation coefficients (r_s) are significant, with significance determined at $\alpha = 0.05$ (Zar 1984). Codes are defined in Table 2.

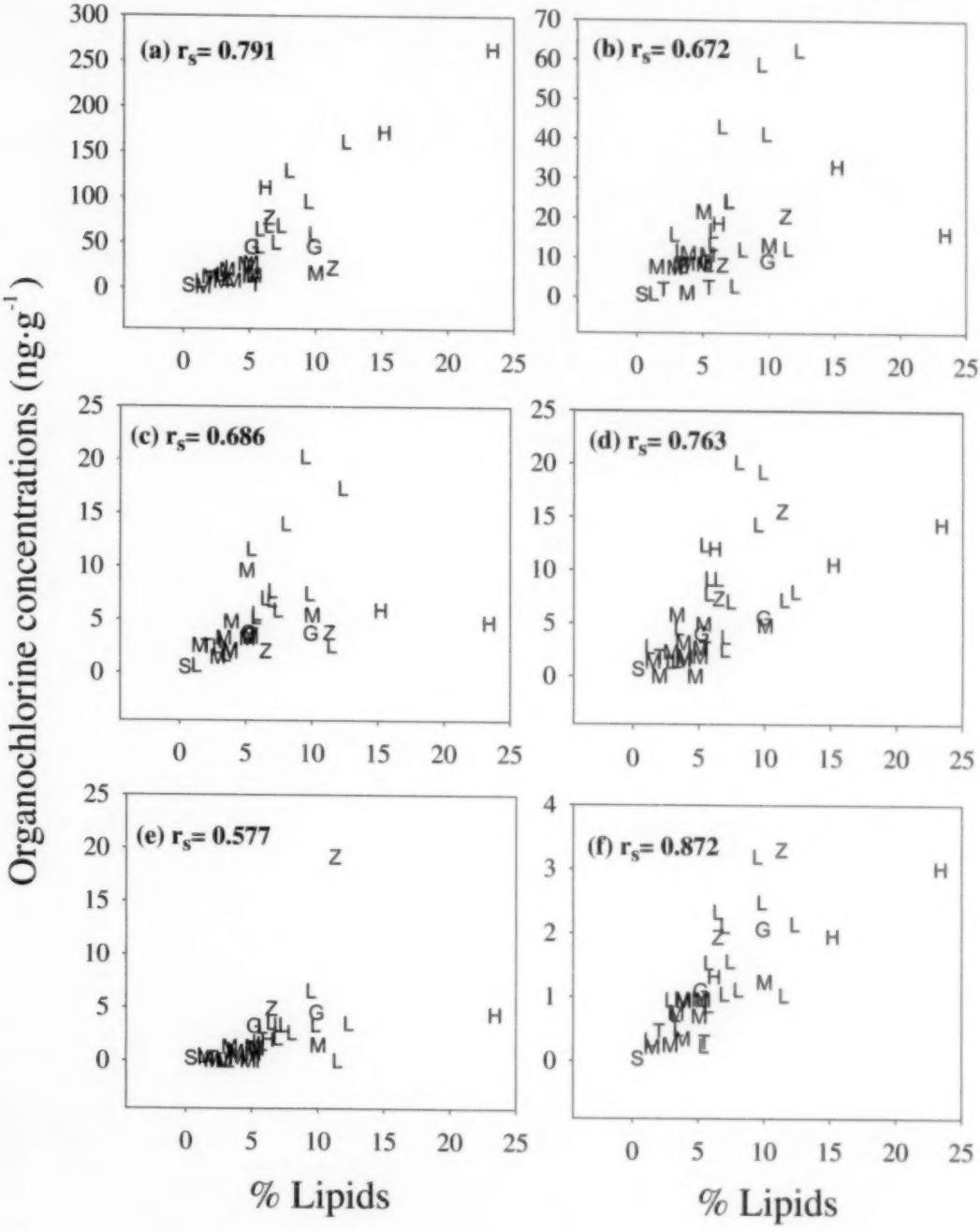

have influenced OC biomagnification to a greater extent because fish at a similar isotopic trophic level have considerably different OC concentrations.

In the Bow Lake food web, $\delta^{13}C$ values correlated significantly with OC concentrations. Lake trout and other organisms that had lighter $\delta^{13}C$ signatures also had higher OC concentrations. No other published study has reported a significant correlation between $\delta^{13}C$ and OC concentrations for a freshwater food web. Despite a 7‰ range in the $\delta^{13}C$ values of lake trout from an arctic lake, no relationship between

© 2000 NRC Canada

Fig. 4. OC concentrations versus $\delta^{13}C$ values in Bow Lake biota. (*a*) Toxaphene; (*b*) ΣDDT; (*c*) ΣPCB; (*d*) ΣCHL; (*e*) dieldrin; (*f*) ΣHCH. The Spearman correlation coefficients (r_s) are significant, with significance determined at $\alpha = 0.05$ (Zar 1984). Codes are defined in Table 2.

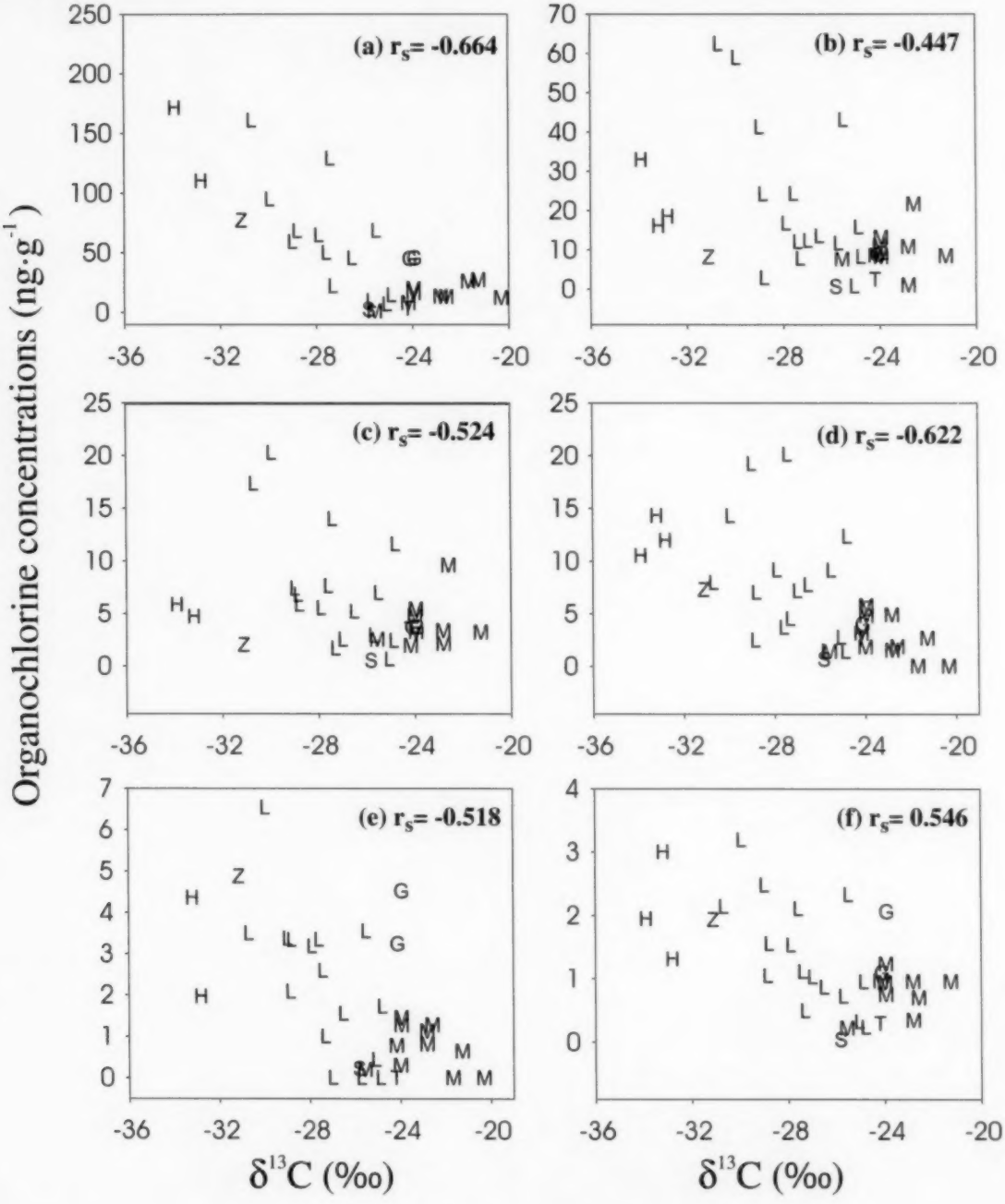

OC concentrations and carbon source was observed (Kidd et al. 1998*a*). Spies et al. (1989), however, reported a positive correlation between average ΣDDT and $\delta^{13}C$ in two offshore marine food webs (southern California) with grouped invertebrates (invertebrate predators and detritivores) and three species of fish. The changes in $\delta^{13}C$ values (approximately 2.5‰ difference between the two sampling sites) resulted from more depleted isotopic values in feeding areas contam-

© 2000 NRC Canada

Fig. 5. OC concentrations versus $\delta^{15}N$ values in Bow Lake biota. (*a*) Toxaphene; (*b*) ΣDDT; (*c*) ΣPCB; (*d*) ΣCHL; (*e*) dieldrin; (*f*) ΣHCH. The Spearman correlation coefficients (r_s) are not significant, with significance determined at $\alpha = 0.05$ (Zar 1984). Codes are defined in Table 2.

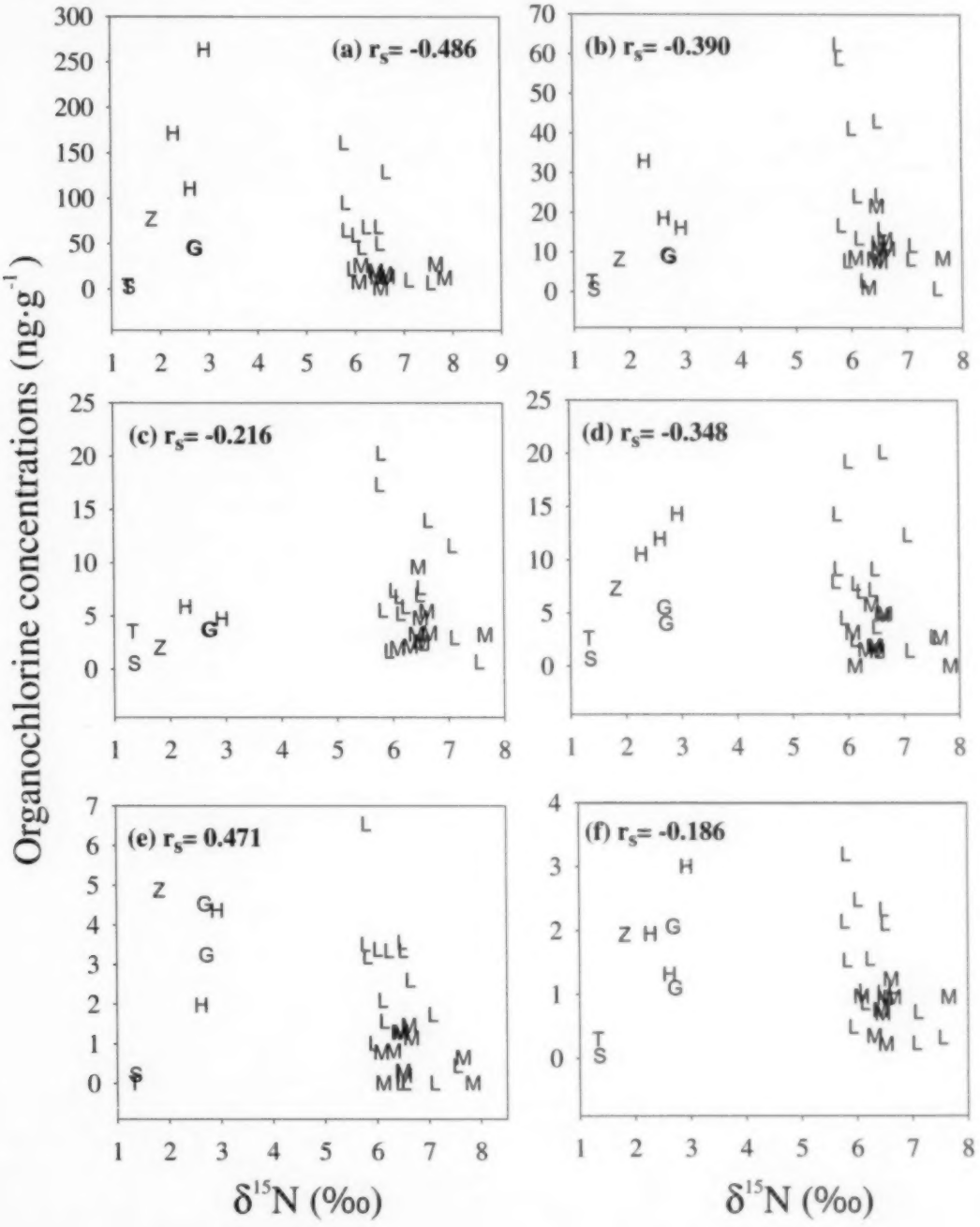

inated by high sewage input. Similarly, the correlation between $\delta^{13}C$ values and OC concentrations in the Bow Lake food web is due to resource partitioning, with the lighter carbon isotope signatures indicative of a more pelagic diet for lake trout when compared with mountain whitefish. As a result, fish in Bow Lake relying on pelagic carbon were more at risk of accumulating OCs than those relying on benthic carbon.

© 2000 NRC Canada

There were some correlations between toxaphene, ΣPCB, and ΣCHL and lake trout age and weight, which suggests that the duration of exposure to these compounds may be important and could contribute towards the increased concentrations in adult lake trout. Similar relationships have been seen in salmonids in other ecosystems (Borgmann and Whittle 1992; Larsson et al. 1996; Kidd et al. 1998*a*). Significant correlations were also observed between lipids and OC concentrations within lake trout, indicating that both weight and lipid were important in predicting concentrations of these contaminants. Higher lipid content has been linked to pelagic diet (as indicated by $\delta^{13}C$), so the OC concentrations in lake trout were probably due to the combination of dietary habits and duration of exposure. While age and weight of mountain whitefish were more significantly correlated than in lake trout, concentrations of OCs were not significantly correlated with lipid, size, or age of this species.

In Bow Lake, which receives most of its water from glaciers and is at a relatively high elevation, organisms must contend with an unproductive environment, low nutrients, and cold temperatures year-round (Campbell 1997). Phytoplankton and zooplankton, especially diatoms (Shifrin and Chisholm 1981) and copepods (Schindler et al. 1971), often become more lipid rich in cold surroundings or nutrient-poor environments. This may lead to increased OC burdens at lower trophic levels, particularly in lipid-rich copepods and phytoplankton. In a laboratory experiment, silicon-limited diatoms (*Nitzchia* sp.) exposed to ^{3}H-labelled tetrachlorodibenzofurans (TCDF) were shown to have higher lipids and correspondingly higher concentrations of OCs than diatoms grown in nutrient-rich cultures (Kilham 1998). When the TCDF-exposed silicon-limited diatoms were fed to *Daphnia magna*, the zooplankton exhibited higher TCDF concentrations than zooplankton fed non-nutrient-limited diatoms (Kilham 1998), indicating that nutrient limitation at the base of the food web can affect the uptake of contaminants at higher trophic levels. In another recent study, the plankton in an oligotrophic Swedish lake had higher lipid content and higher PCB concentrations than the plankton in a eutrophic lake (Larsson et al. 1998). They also discovered that the highest seasonal PCB concentrations in the plankton from the oligotrophic lake coincided with peak dominance of lipid-rich calanoid copepods in the zooplankton community. The lipid content in biota cannot be ignored when studying the fate of OCs in whole food webs, especially in oligotrophic ecosystems.

The high OC concentrations (especially toxaphene) in the zooplankter *H. arcticus* may be the result of either direct absorption or ingestion. The small body size (<2 mm in length) and high lipid content of *H. arcticus* may increase adsorption of OCs from the surrounding water column. Deposition of OCs increases with higher elevations in the mountains (Blais et al. 1998), and glaciers in the Rocky Mountains have high concentrations of OCs that were deposited in the past when OC compounds were in more widespread use (Donald et al. 1999). Despite their hydrophobic nature, a considerable proportion of OCs in the glacial inflow to Bow Lake are in dissolved form, probably because glacial silt has little affinity for OCs (Dr. J. Blais, Department of Biology, University of Ottawa, Ottawa, ON K1N 6N5, Canada, personal communication). Marine copepods exposed to ^{14}C-labelled DDT in water had a significant portion (28–80%) of total body burden DDT in their extractable lipids (Harding and Vass 1977). This matter is currently being investigated by our research group.

Alternatively, a more speculative hypothesis is that the copepods are ingesting glacial silt that has sorbed OCs from glacial sources. In Bow Lake, high proportions of glacial silt are found in copepod fecal pellets in bottom sediments (Smith and Syvitiski 1982), and *H. arcticus* have been found to be important in the sedimentation processes (Smith and Syvitski 1982). If glacial silt from Bow Glacier is a source of contaminants, then *H. arcticus* may be bioaccumulating OCs to higher than expected concentrations due to their high lipid content and consumption of these particulates.

In the simple aquatic community of Bow Lake, bioaccumulation patterns for OCs in the food web did not follow the patterns of stable isotope/OC studies of more complex food webs. Food chain length alone was insufficient to explain why lake trout had higher toxaphene concentrations than the same species from other nearby lakes. Results suggest that OCs were more efficiently transferred in pelagic than in benthic food chains due to the higher lipid content of pelagic organisms. The highest concentrations of OCs were found in lipid-rich pelagic copepods rather than in fish. Dietary patterns (as indicated by stable carbon isotope ratios) and lipid content were more important than trophic-related biomagnification for explaining OC concentrations in lake trout in the short food web of Bow Lake.

Acknowledgements

This research was supported by a Natural Sciences and Engineering Research Council of Canada strategic grant to D.W. Schindler, a Canadian Circumpolar/Boreal Research grant to L.M. Campbell and D.W. Schindler, a Friends of Banff National Park grant, and a Natural Sciences and Engineering Research Council of Canada PG-A scholarship to L.M. Campbell. Dr. G. Stern provided the HRECNIMS toxaphene analyses for this project. We thank B. Rosenberg, B. Ross, and D. Savoie for their technical expertise at the Freshwater Institute (Winnipeg, Man.). R. Crosley and J. Syrgiannis (Environment Canada, Regina, Sask.) assisted with field work in 1994, while M. Campbell, J. Clare, J. Hiebert, S. McNaught, R. Thacker, and F. Wilhelm (University of Alberta, Edmonton, Alta.) provided field assistance in 1995. M. Agbeti (University of Alberta) assisted with the phytoplankton identification and P. Aku (Glenora Fisheries Station, Picton, Ont.) did the fish otolith ageing. A. Shostak (University of Alberta) identified the parasite cysts on lake trout stomachs. R.E. Hecky (Environment Canada, Burlington, Ont.) provided an early review of the manuscript.

References

Anthony, D.D. 1967. Taxonomy and ecology of *Diphyllobothrium* in Alberta and British Columbia. Ph.D. thesis, University of Alberta, Edmonton, Alta.

Blais, J.M., Schindler, D.W., Muir, D.C.G., Kimpe, L.E., Donald, D.B., and Rosenberg, B. 1998. Accumulation of persistent organochlorines in mountains of western Canada. Nature (Lond.), **395**: 585–588.

© 2000 NRC Canada

Borgmann, U., and Whittle, D.M. 1992. Bioenergetics and PCB, DDE, and mercury dynamics in Lake Ontario lake trout (*Salvelinus namaycush*): a model based on surveillance data. Can. J. Fish. Aquat. Sci. **49**: 1086–1096.

Campbell, L.M. 1997. The use of stable isotope ratios to discern organochlorine bioaccumulation patterns in a sub-alpine Rocky Mountain food web. M.Sc. thesis, University of Alberta, Edmonton, Alta. ISBN 0–612–22581-X.

DeNiro, M.J., and Epstein, S. 1977. Mechanism of carbon isotope fractionation associated with lipid synthesis. Science (Washington, D.C.), **197**: 261–263.

Donald, D.B. 1987. Assessment of the outcome of eight decades of trout stocking in the mountain national parks, Canada. N. Am. J. Fish. Manage. **7**: 545–553.

Donald, D.B., Bailey, R.C., Crosley, R., Muir, D., Shaw, P., and Syrgiannis, J. 1993. Polychlorinated biphenyls and organochlorine pesticides in the aquatic environments along the Continental Divide region of Alberta and British Columbia. Inland Waters Directorate (Environment Canada) report to Parks Canada, Regina, Sask.

Donald, D.B., Stern, G.A., Muir, D.C.G., Fowler, B.R., Miskimmin, B.M., and Bailey, R. 1998. Chloroboranes in water, sediment, and fish from toxaphene treated and untreated lakes in western Canada. Environ. Sci. Technol. **32**: 1391–1397.

Donald, D.B., Syrgiannis, J., Crosley, R.W., Holdsworth, G., Muir, D.C.G., Rosenberg, B., Sole, A., and Schindler, D.W. 1999. Delayed deposition of organochlorine pesticides at a temperate glacier. Environ. Sci. Technol. **33**: 1794–1798.

Evans, M.S., Noguchi, G.E., and Rice, C.P. 1991. The biomagnification of polychlorinated biphenyls, toxaphene and DDT compounds in a Lake Michigan offshore food web. Arch. Environ. Contam. Toxicol. **20**: 87–93.

France, R.L. 1995. Carbon isotopic variability in the composite pelagic foodweb of four oligotrophic lakes: feeding diversity or metabolic fractionations? J. Plankton Res. **17**: 1993–1997.

Gu, B., Schell, D.M., and Alexander, V. 1994. Stable carbon and nitrogen isotopic analysis of the plankton food web in a subarctic lake. Can. J. Fish. Aquat. Sci. **51**: 1338–1344.

Gu, B., Schell, D.M., Huang, X., and Yie, F. 1996. Stable isotope evidence for dietary overlap between two planktivorous fishes in aquaculture ponds. Can. J. Fish. Aquat. Sci. **53**: 2814–2818.

Harding, G.C.H., and Vass, W.P. 1977. Uptake from sea water and clearance of ^{14}C-*p,p'*-DDT by the marine copepod *Calanus finmarchicus*. J. Fish. Res. Board Can. **34**: 177–182.

Hecky, R.E., and Hesslein, R.H. 1995. Contributions of benthic algae to lake food webs as revealed by stable isotope analyses. J. North Am. Benthol. Soc. **14**: 631–653.

Hesslein, R.H., Hallard, K.A., and Ramlal, P. 1993. Replacement of sulfur, carbon and nitrogen in tissues of growing broad whitefish (*Coregonus nasus*) in response to a change in diet traced by δ^{34}S, δ^{13}C, and δ^{15}N. Can. J. Fish. Aquat. Sci. **50**: 2071–2076.

Kidd, K.A., Schindler, D.W., Hesslein, R.H., and Muir, D.C.G. 1995. Correlation between stable nitrogen isotope ratios and concentrations of organochlorines in biota from a freshwater food web. Sci. Total Environ. **160/161**: 381–390.

Kidd, K.A., Hesslein, R.H., Ross, B.J., Koczanski, K., Stephens, G.R., and Muir, D.C.G. 1998*a*. Bioaccumulation of organochlorines through a remote freshwater food web in the Canadian Arctic. Environ. Pollut. **102**: 91–103.

Kidd, K.A., Schindler, D.W., Hesslein, R.H., and Muir, D.C.G. 1998*b*. Effects of trophic position and lipid on organochlorine concentrations in fishes from subarctic lakes in Yukon Territory. Can. J. Fish. Aquat. Sci. **55**: 869–881.

Kilham, S.S. 1998. Effects of physiological state on the bioaccumulation of toxic chemicals in algae and their transfer to zooplankton. Verh. Int. Ver. Limnol. **26**: 1734–1736.

Kiriluk, R.M., Servos, M.R., Whittle, D.M., Cabana, G., and Rasmussen, J.B. 1995. Using ratios of stable nitrogen and carbon isotopes to characterize the biomagnification of DDE, mirex, and PCB in a Lake Ontario pelagic food web. Can. J. Fish. Aquat. Sci. **52**: 2660–2674.

Kling, G.W., Fry, B., and O'Brien, W.J. 1992. Stable isotopes and planktonic trophic structure in Arctic lakes. Ecology, **73**: 561–566.

Kucklick, J.R., Harvey, H.R., Ostrom, P.H., Ostrom, N.E., and Baker, J.E. 1996. Organochlorine dynamics in the pelagic food web of Lake Baikal. Environ. Toxicol. Chem. **15**: 1388–1400.

Larsson, P., Backe, C., Bremle, G., Eklöv, A, and Okla, L. 1996. Persistent pollutants in a salmon population (*Salmo salar*) of the southern Baltic Sea. Can. J. Fish. Aquat. Sci. **53**: 62–69.

Larsson, P., Okla, L., and Cronberg, G. 1998. Turnover of polychlorinated biphenyls in an oligotrophic and an eutrophic lake in relation to internal lake processes and atmospheric fallout. Can. J. Fish. Aquat. Sci. **55**: 1926–1937.

McHugh, J.L. 1940. Food of the Rocky Mountain whitefish *Prosopium williamsoni* (Girard). J. Fish. Res. Board Can. **5**: 131–137.

Mihuc, T., and Toetz, D. 1994. Determination of diets of alpine aquatic insects using stable isotopes and gut analysis. Am. Midl. Nat. **131**: 146–155.

Miskimmin, B.M., Muir, D.C.G., Schindler, D.W., Stern, G.A., and Grift, N.P. 1995. Chlorobornanes in sediments and fish thirty years after toxaphene treatment of lakes. Environ. Sci. Technol. **29**: 2490–2495.

Paul, A.J., and Schindler, D.W. 1994. Regulation of rotifers by predatory calanoid copepods (subgenus *Hesperodiaptomus*) in lakes of the Canadian Rocky Mountains. Can. J. Fish. Aquat. Sci. **51**: 2520–2528.

Peterson, B.J., and Fry, B. 1987. Stable isotopes in ecosystem studies. Annu. Rev. Ecol. Syst. **18**: 293–320.

Rau, G.H., and Anderson, N.H. 1981. Use of ^{13}C/^{12}C to trace dissolved and particulate organic matter utilization by populations of an aquatic invertebrate. Oecologia, **48**: 19–21.

Rawson, D.S. 1939. A biological survey and recommendations for fisheries management in waters of the Banff National Park. Department of Mines and Resources, National Parks Bureau, Ottawa, Ont.

Schindler, D.W., Clark, A.S., and Gray, J.R. 1971. Seasonal calorific values of freshwater zooplankton, as determined with a Phillipson bomb calorimeter modified for small samples. J. Fish. Res. Board Can. **28**: 559–564.

Shifrin, N.S., and Chisholm, S.W. 1981. Phytoplankton lipids: interspecific differences and effects of nitrate, silicate and light–dark cycles. J. Phycol. **17**: 374–384.

Smith, N.D., and Syvitiski, J.P.M. 1982. Sedimentation in a glacier-fed lake: the role of pelletization of deposition of fine-grained suspensates. J. Sediment. Petrol. **52**: 503–513.

Spies, R.B., Kruger, H., Ireland, R., and Rice, D.W., Jr. 1989. Stable isotope ratios and contaminant concentrations in a sewage-distorted food web. Mar. Ecol. Prog. Ser. **54**: 157–170.

Zar, J.H. 1984. Biostatistical analysis. Simon & Schuster Co., Englewoods Cliffs, N.J.

© 2000 NRC Canada

Abundance estimation and capture of sablefish (*Anoplopoma fimbria*) by longline gear

Michael F. Sigler

Abstract: Longline surveys in Alaska measure sablefish (*Anoplopoma fimbria*) relative abundance and are the primary information source used for abundance and quota estimation. Hook timer, on-bottom (soak) time, hook density, hook pattern, bait type, and bait condition experiments and mathematical models were used to evaluate the performance of the longline surveys for estimating sablefish relative abundance. The rate that sablefish encountered the longline gear decreased with on-bottom time independently of sablefish density in the sampled area. Sablefish were adept at locating available baits, even when few remained. The decrease in encounter rate appears related to odor concentration at the leading edge of the odor plume. The ability to locate baits, even when few remain, differs from previous models of fish capture by longline in which the probability that a fish located a bait was proportional to the number of available baits. Decreased encounter rate and the ability to locate baits efficiently imply that longline catch rates likely provide an accurate index of fish abundance if the on-bottom time is long enough to cover the period when most fish encounter the gear and the initial bait density is high enough that baits remain available throughout the soak; the weak link between catch rate and abundance is the unknown extent that factors such as temperature and food availability affect the proportion of fish caught.

Résumé : Les relevés à la palangre menés en Alaska pour mesurer l'abondance relative de la morue charbonnière, *Anoplopoma fimbria*, constituent la première source d'information pour l'estimation de l'abondance et l'établissement des quotas. Nous nous sommes servis d'expériences sur le temps nécessaire à la capture, la durée de séjour sur le fond (mouillage), la densité d'hameçons, le mode d'accrochage des hameçons, le type d'appât et l'état des appâts, ainsi que de modèles mathématiques, pour évaluer l'intérêt des relevés à la palangre pour l'estimation de l'abondance relative de la morue charbonnière. Le taux de rencontre de la morue charbonnière et de la palangre baissait en fonction de la durée de mouillage, indépendamment de la densité de ce poisson dans la zone d'étude. Les morues charbonnières étaient promptes à localiser les appâts disponibles, même quand ils étaient peu nombreux sur la ligne. La baisse du taux de rencontre semble liée à la concentration de l'odeur au bord avant du panache d'odeur. La capacité de localiser les appâts, même quand il en reste peu sur la ligne, introduit un nouvel élément par rapport aux modèles antérieurs de capture des poissons à la palangre, dans lesquels la probabilité qu'un poisson trouve un appât était proportionnelle au nombre d'appâts disponibles. La baisse du taux de rencontre et la capacité de localiser efficacement les appâts indiquent que les taux de capture à la palangre peuvent vraisemblablement fournir un indice précis de l'abondance des poissons si la durée de mouillage sur le fond est assez longue pour couvrir la période où la plupart des poissons rencontrent l'engin, et si la densité initiale d'appâts est assez élevée pour qu'il reste des appâts tout au long de la durée de mouillage; il reste un maillon faible entre le taux de capture et l'abondance, du fait qu'on ne sait pas dans quelle mesure des facteurs comme la température et la disponibilité de la nourriture affectent la proportion de poissons capturés.

[Traduit par la Rédaction]

Introduction

Abundance indices generally are determined from catch and effort data of a fishery or research surveys. Understanding the catch rate – abundance relationship and, more generally, the interaction of the target species with the gear is essential for resource assessment (Gunderson 1993). Although nonlinear relationships have been proposed (Bannerot and Austin 1983; Richards and Schnute 1986), the most common hypothesis has catch rate, U, proportional to abundance, $U = qN$, where q is the catchability coefficient and N is abundance. If true, a 10% increase in U is expected to represent a 10% change in abundance. Sablefish (*Anoplopoma fimbria*) relative abundance has been estimated by annual longline surveys in Alaska since 1978 (Sasaki 1985; Sigler and Fujioka 1988; Sigler and Zenger 1989). A better understanding of sablefish capture by longline gear was necessary to determine whether these surveys accurately index sablefish abundance.

Two parameters affecting fish capture by longline gear are the rate that fish encounter the gear (number of fish per unit on-bottom time) and, after encountering the gear, the probability that fish successfully locate an available bait. I conducted a series of field experiments to measure sablefish encounter rate and their ability to locate bait. Capture times were observed during hook timer experiments and used to estimate encounter rate and bait location probability. Soak time experiments were conducted to examine how catch rate,

Received July 16, 1999. Accepted March 21, 2000.
J15252

M.F. Sigler. National Oceanic and Atmospheric Administration, National Marine Fisheries Service, Alaska Fisheries Science Center, Auke Bay Laboratory, 11305 Glacier Highway, Juneau, AK 99801-8626, U.S.A.
e-mail: mike.sigler@noaa.gov

© 2000 NRC Canada

a measure of encounter rate, changed with on-bottom time. Hook density and hook pattern experiments were conducted to examine how bait density affected catch rate, a measure of the ability to locate bait. Bait type and bait condition experiments were conducted to examine how odor concentration affected catch rate, a measure of the relationship of odor concentration and encounter rate.

In this paper, I develop a mathematical model to analyze the hook timer experiments. The model also provides a conceptual framework to discuss the results of all the experiments. The model describes three events in fish capture: encountering gear, locating a bait, and hooking. In the model, encounter rate may vary as a function of time, bait location probability may vary as a function of the number of available baits, and hooking fraction is assumed constant. Mathematical models previously developed to describe gear saturation (Murphy 1960; Rothschild 1967) are a special case of my model and also were tested. In fisheries literature, "gear saturation" (Beverton and Holt 1957) describes bait location probability as "the effect of fish density to reduce the fishing power of a unit of fishing gear as the catch in it increases."

Methods

Hook timer experiments

Capture times were collected to determine how gear saturation and encounter rate affect sablefish capture rates. Capture times were collected in two hook timer experiments conducted from 26 June to 2 July 1992 and from 24 May to 3 June 1993. A hook timer is an electromechanical device that records the capture time of a fish (Somerton and Kikkiwa 1995). An area of historically high sablefish catch rates, Chatham Strait, southeastern Alaska, was selected for the hook timer experiments because the motivation for these experiments was estimation of the effect of gear saturation, which is more likely to occur in an area of high catch rates like Chatham Strait. Two sites were sampled, one near Tenakee Inlet and one near Point Couverden.

A standard skate consisted of 100 m of line with 45 hooks spaced 2 m apart and baited with *Illex* squid, similar to the annual longline surveys. Hook timers were attached to every hook on the standard skates. Skates with 90 hooks spaced 1 m apart also were tested to determine the effect of hook density on capture times. On these skates, timers were attached to every other hook to reduce the number of timers that could be lost in a single set. A set at the Tenakee Inlet site consisted of two standard skates, with and without timers. A set at the Point Couverden site consisted of two skates, standard and 1-m spacing. Timers were attached to only one skate in a set to reduce the number of timers that could be lost in a single set. The hook density of the skate with timers alternated between sets.

A hook timer clock starts running when the timer attached to a baited hook is tripped. At retrieval, the following information was recorded electronically (Sigler 1994): timer status (tripped or untripped), hook status (fish species, baited, or bare), time elapsed since tripping, and time of day. Capture times were computed from this information and the time that the gear reached bottom, which was recorded with a time–depth recorder.

Some captures are not recorded by the hook timers. Observed captures signal their capture by tripping the timer. Observed captures include timers tripped on bottom and retrieved with hooks occupied by fish or bare. Considering bare hooks as captures presumes that a fish or invertebrate stole the bait and that, effectively, the hook is occupied because no bait remains to lure fish. Unobserved captures do not trip the timer when they steal the bait or are caught. The capture time and order are known for the observed, but not the unobserved, captures. Unobserved captures include untripped timers, timers tripped at the rail, and defective timers retrieved occupied with fish or bare. These bare hooks are considered unobserved captures because the bait was removed, yet the timer was not tripped while on bottom to record the removal.

All hooks retrieved with bait were classified as baited hooks, regardless of timer status, because the bait remained available, even if attacked. Ineffective hooks (broken, bent, or tangled) were omitted from the calculations. Skates with more than five ineffective hooks for the 2-m spacing or 10 ineffective hooks for the 1-m spacing also were omitted.

The number of baits available when observed captures occurred is unknown because the capture time and order of the unobserved captures are unknown. The effect of the unobserved captures is approximated by assuming that the distributions of capture times and capture order are the same for observed and unobserved captures. Given N_b, the initial number of baits, N_o, the number of observed captures, and N_u, the number of unobserved captures, an estimate of the number of available baits when the ith observed capture occurred, x_i, is

$$x_i = N_b - (i-1)\frac{N_o + N_u}{N_o}$$

which inflates the number of observed captures before the ith capture $(i - 1)$ according to the ratio of total to observed captures.

Other longline gear experiments

Nine experiments on hook density, hook pattern, soak time, and bait type and condition also were conducted. All experiments including the hook timer experiments were conducted at depths of at least 250 m. In the hook density experiment, three densities of 1-, 2-, and 4-m spacing between hooks were tested. A set consisted of nine skates, three of each hook density. Bait was Pacific herring (*Clupea harengus pallasi*) instead of squid used in annual surveys. The hook density experiment was conducted from 4 to 13 July 1986 in Chatham Strait near Tenakee Inlet.

Hook density was found to affect sablefish catch rates, so two later experiments varied hook pattern while holding hook density constant. Distance between baits was tested by leaving various-sized gaps between sections with baited hooks; hook density was approximately 0.25 hook per metre of line for all patterns. One example of a hook pattern is three hooks spaced 2 m apart, 8 m of bare line, three hooks spaced 2 m apart, etc., denoted 8-m gap. Sections of line without hooks are equivalent to sections without baits, so these experiments also test for gear saturation. Two hook pattern experiments were conducted, one from 27 April to 5 May 1990 in Clarence Strait, Alaska, and the other from 22 to 26 July 1998 in the Gulf of Alaska near Yakutat Bay. In the first experiment, three hook patterns were tested, 4-m gap, 8-m gap, and 24-m gap. A set included six experimental skates. The experimental skates were located in two blocks, with one skate of each pattern in a block. The patterns were blocked to account for variation due to location, time, etc. In the second experiment, four hook patterns were tested, 12-m gap, 22-m gap, 32-m gap, and 42-m gap. A set included 64 experimental skates located in eight blocks with two skates of each hook pattern in a block. Wider gaps were tested in the second experiment after the first experiment failed to detect differences in catch rates among the first experiment's gap sizes. The order of pattern within a block was varied systematically in both experiments.

Four soak-time experiments were conducted in areas differing in sablefish abundance to determine whether catch rate increased with soak time and, if so, whether the relationship varied with abundance. The soak time experiments were conducted from 20 to 26

© 2000 NRC Canada

May 1986 in Chatham Strait near Tenakee Inlet, from 28 June to 3 July 1986 in Icy Strait, Alaska, near Home Shore, from 11 May to 1 June 1987 in Stikine Strait, Alaska, and from 5 to 26 March 1988 in Chatham Strait near Funter Bay. Two soak times, 3 and 7 h, were tested to approximate the shortest and longer soak times of the longline surveys (soak times commonly range to 10 h). Soak time is defined as the time between last buoy deployment and first buoy retrieval. A set consisted of 12 skates. Bait was herring instead of squid used in annual surveys, except for the last experiment, which tested both herring and squid. Several sites within an area were sampled during each experiment. When only herring was tested, each site was sampled twice, once per soak time, with the order of soak times varied systematically among sites to control for the effect of sampling order on catch rate. When both herring and squid were tested, four combinations resulted: herring, 3 h; herring, 7 h; squid, 3 h; squid, 7 h. Eight sites were sampled within the experimental area using a randomized block design. Each combination was tested at each site to account for the effect of site on the resultant catch rates. The order that the four combinations was tested at a site was varied systematically to control for the effect of sampling order on catch rate.

Two experiments with presoaked bait tested the importance of bait odor for attracting sablefish to the gear. The two experiments were conducted simultaneously during 9 August – 1 September 1991 in the Central Gulf of Alaska off Kodiak Island. In the first, baits were presoaked by placing tubs of baited and coiled longline gear into a tank supplied with fresh, flowing seawater. The hooks were baited before presoaking because baiting with squid is difficult when the bait is thawed rather than semifrozen. The duration of presoaking averaged 12 h. In the second, rather than presoaking artificially, reused baits were tested that had been soaked 3–10 h during a previous set. In both experiments, a set consisted of four experimental skates (either presoaked or reused bait) and 80 control skates with bait not soaked previously. Catch rates of the four experimental skates were compared with those of the adjacent four control skates.

Mathematical model

A mathematical model was fit to the capture time data. The model describes three events in fish capture: encounter the gear, locate an available bait, and become hooked. The encounter rate depends on odor plume drift and fish response. The downstream propagation of the odor plume depends essentially on advection; thus, the length of the odor plume at any time is computed as the product of current and time (Sainte-Marie and Hargrave 1987). Odor concentration at the plume's leading edge decreases quickly (Fig. 1). Løkkeborg et al. (1995) measured sablefish response intensity to different odor concentrations in a laboratory and found that response intensity decreased more slowly than odor dispersal (Fig. 1) and was most sensitive to feeding regimen (food ration and duration of food deprivation), more so than to current or fish speed.

Two encounter rate functions were tested, a power function and the exponential function. For the power encounter rate function, the encounter rate (λ) is assumed to be a function of the odor concentration at the leading edge of the odor plume with the response intensity described by Løkkeborg et al. (1995):

$$\lambda_t = \beta_3 10^{\beta_1 \log_{10} \frac{1}{t^2}}$$

See the Appendix for the derivation of this equation. The parameter β_1 is a measure of feeding regimen, the parameter β_3 is proportional to initial encounter rate, and t represents capture time.

For the exponential encounter rate function, the encounter rate (λ) is assumed to decrease exponentially with time at rate r:

$$\lambda_t = \lambda_0 e^{-rt}$$

Fig. 1. Odor concentration (broken line) (Sainte-Marie and Hargrave 1987; Løkkeborg et al. 1995) and sablefish response intensity (×) (Løkkeborg et al. 1995) at the leading edge of the odor plume scaled to the maximum values versus time. The calculation equations for odor concentration and response intensity are shown in the Appendix. Response intensity is assumed to be proportional to the leading edge concentration. The assumed current was 0.08 m·s^{-1}. The assumed sablefish feeding regimen was 1 day of food deprivation.

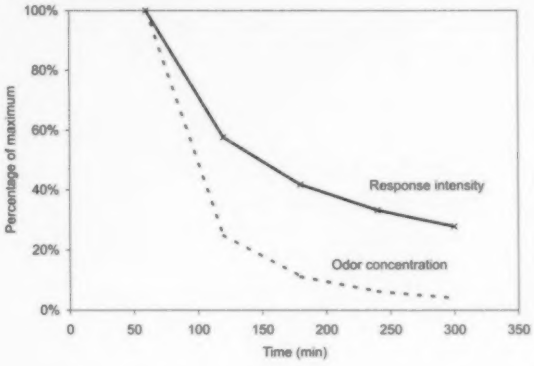

The parameter λ_0 is the initial encounter rate. The exponential function was tested because it well represents encounter rate data reported for whiting (*Gadus merlangus*) (Fernö et al. 1986, their fig. 3). The exponential encounter rate function is similar to the power encounter rate function, except that the power encounter rate function initially decreases more quickly.

After locating the gear, the fish may find an available bait. The bait location probability, p, is assumed to vary with the fraction of baits remaining, x. Initially, p is constant until the fraction of baits remaining has decreased to s, and thereafter, p decreases linearly to zero, i.e., $p_x = 1$ if $x \geq s$, $p_x = x/s$ if $x < s$. The value s is a measure of the fish's willingness to search for an available bait when one is not available at the point where the fish encounters the line. The value of s is estimated.

After locating an available bait, the fish may be hooked. The hooking fraction, h, is not measurable using capture times. I assumed that the hooking fraction was constant, implying that the behavioral or physiological states affecting the decision to attack an available bait and the rate of attack and escape are constant.

The capture rate, θ_{tx}, is the product of encounter rate, bait location probability, and hooking fraction: $\theta_{tx} = \lambda_t p_x h$. Thus, the fitted forms of the model are

$$\theta_{tx} = \beta_3 10^{\beta_1 \log_{10} \frac{1}{t^2}} p_x \text{ (power form)}$$

$$\theta_{tx} = \lambda_0 e^{-rt} p_x \text{ (exponential form)}$$

where $p_x = 1$ if $x \geq s$, $p_x = x/s$ if $x < s$. An encounter rate was estimated for each longline set, reflecting differences in local abundance. Bait location probability was estimated as one parameter for all sets assuming that bait location probability does not vary between sets.

A special case of the model was tested also:

$$\theta_{tx} = \lambda p_x \text{ (historic form)}$$

where $p_x = x$. This special case includes the longline models of Murphy (1960) and Rothschild (1967) for which encounter rate is constant and bait location probability is proportional to the fraction of baits remaining. For example, Murphy (1960) expressed the rate

© 2000 NRC Canada

of change of the number of hooked fish as a linear function of the number of available baits. For the historic form of the model, an encounter rate was estimated for each longline set, reflecting differences in local abundance. The bait location probability is fixed in the historic form but estimated in the exponential and power forms, i.e., the value of s is estimated in the exponential and power forms.

Expected total catch was computed by numerically integrating capture rate over time in 1-min intervals

$$\sum_t \theta_{tx_t}$$

where the fraction of baits remaining, x_t, evolves with time t. The parameters describing encounter rate and bait location probability were estimated by minimizing the negative log-likelihood, assuming that differences between the observed and corresponding expected catches were distributed normally. The log parameters rather than parameters on the original scale were estimated to improve reliability in the estimation process. This places all the parameters on a common scale and probably reduces parameter effects nonlinearity (Ratkowsky 1983).

The encounter rate estimates provide a measure of how much encounter rate affects survey results. Let b represent on-bottom time and b^* represent the maximum on-bottom time. A formula for the expected total number of encounters at b is found by integrating the exponential encounter rate function over on-bottom time and is

$$\frac{\lambda_0}{r}(1 - e^{-rb})$$

The proportion of encounters predicted to occur by b is

$$\frac{1 - e^{-rb}}{1 - e^{-rb^*}}$$

Results

Hook timer experiments

The timers were set successfully 19 times. Of the 845 successfully deployed timers, 136 tripped before or during setting of the longline gear or were defective, 472 tripped while the longline gear was on bottom, and 237 were retrieved untripped. Four hundred and sixty-five fish were caught and 180 timers were retrieved with bait. Most fish caught were sablefish (93%), which generally tripped the timer (85%). Sablefish size did not affect the chance of tripping the timer except for fish shorter than 50 cm fork length; however, these small fish composed only 8% of the sablefish catch. Two thirds of timers that tripped on bottom held a fish, demonstrating that more attacks strong enough to trip the timer result in capture than in escape. The escapes demonstrate that fish can attack a bait without becoming hooked, i.e., hooking fraction less than 1.0. Most (76%) untripped timers held no fish. For empty timers, hook status (baited, bare, or ineffective) was similar for timers tripped on bottom and untripped (contingency table analysis, χ^2 test, $p = 0.47$). The timers did not affect catch rate (19.3 ± 1.14 (SE) fish per skate without timers and 20.9 ± 1.38 with timers, paired t test, $p = 0.25$).

Capture rate decreases, slowly during early soak time, and substantially later (Fig. 2). Capture rate slowed substantially when 20–30% of the baits remained and after 20–100 min on bottom. The substantial slowing sometimes occurred smoothly (e.g., set 10) and sometimes abruptly (e.g., set 6).

The historic longline model (constant encounter rate and bait location probability proportional to the number of baits remaining) represents the capture times fairly well (Fig. 2). Relaxing assumptions of the historic longline model by estimating time-varying encounter rate and by estimating bait location probability improved the fit substantially (Table 1) and represented the capture times better (Fig. 2). The better representation also markedly reduced the range of the residuals (Fig. 3). The representation is similar for the power and exponential models; only estimates for the exponential model are shown. The large negative residuals present early during on-bottom time for all three models (Fig. 3) are due mainly to data of two sets (e.g., set 12, Fig. 2) and imply that the observed encounter rate did not decrease so quickly as that estimated for these two sets.

For both the power and exponential models, the estimated bait location probability was constant until about half the available baits remained, contrary to the bait location probability assumed for the historic model (Fig. 4). The estimated encounter rate decreased with time for the power and exponential models (Fig. 5). The estimated encounter rates for these two models generally were similar for the first 75 min. Later, the encounter rate for the power function decreased slower than that for the exponential function. The exponential model better represented the capture time data based on a test comparing the alternative models (Table 1), the Akaike information criterion (Hilborn and Mangel 1997), so results are presented for the exponential model only. The estimated initial encounter rate, λ_0, ranged from 0.07 to 1.23 encounters·min^{-1}; the estimated instantaneous rate of decrease of the encounter rate, r, ranged from 0.000 to 0.047·min^{-1} and averaged 0.011·min^{-1} (Table 1). The average implies that after 1, 3, and 7 h, the encounter rate was 51, 13, and 1% of the initial rate. This also implies that at 1 and 3 h on bottom, 49 and 87% of fish were caught compared with the expected number caught by 10 h on bottom.

The log-likelihood surface for fitting the capture times does not curve smoothly to the global minimum for the exponential and power models; local minima were present in the surface where the minimization routine sometimes was trapped. Different starting values were used to locate and verify the global minimum. Choice of starting values was based on the observed capture times. For example, if initial captures occurred every 2 min, decreasing to every 10 min after 1 h, then reasonable starting values for λ_0 and r were 0.5 and $-\ln[(1/2)/(1/10)]/60 = 0.027$. The starting value for r was computed by solving the exponential encounter rate function for r, where 1/2 and 1/10 are the capture rates based on the observed capture times and 60 min is the time interval. The observed capture times also were a good check of the reasonableness of the resultant parameter estimates before declaring that a global minimum was found.

The capture rate can be estimated reliably, but because it is the product of λ_t and p_x, reliable estimation of the dependencies of λ_t and p_x on time and available baits is problematic. Both remaining baits and on-bottom time covary: the number of available baits decreases as fish take baits, which occurs through time as the gear is on bottom. For some sets, capture rate did not change as an obvious function of either time or available baits, limiting what can be inferred from these sets. This uninformative behavior happened for some

© 2000 NRC Canada

Fig. 2. Observed (○), expected exponential model (solid line), and expected historic model (broken line) catch for a 45-hook skate versus soak time. The models are described in the Mathematical model section. A constant capture rate is seen as a straight line. Slowing in capture rate is seen as a rightward drift. Off-bottom times are displayed in Fig. 6. The hook spacing of sets 1–13 was 2 m and of sets 14–19 was 1 m. Only a subset of the hook timer data is displayed for brevity.

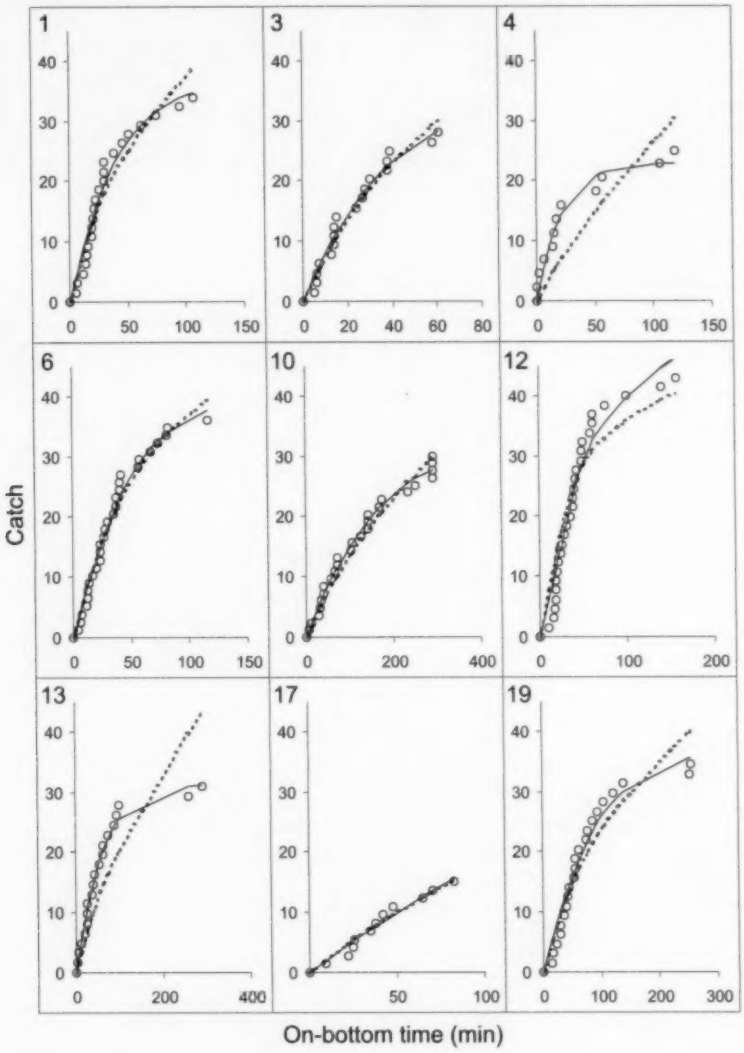

sets where the gear was on bottom for only 1–2 h. Four sets were on bottom about 80 min each, and the capture rate was nearly constant during this interval for three of these sets (e.g., set 17, Fig. 2). The capture rate also was nearly constant at two sets with longer on-bottom times and then fell to zero for the remainder of the on-bottom time. These five sets (5, 15–18) had encounter rate and bait location probability that were nearly constant over the observed interval of available baits and time, so they provided little or no information about when or why the capture rate eventually slows because no substantial slowing was observed.

The general pattern of captures is similar regardless of hook density; initially, capture rate was nearly constant and then slowed substantially for both hook densities (e.g., compare sets 1 and 19, Fig. 2). The initial encounter rate (0.61 for sets 14–19 versus 0.47 for sets 10–13, t test, one-tailed, $p = 0.23$, Point Couverden site) (Table 1) and the encounter rate's decline (0.0082 for sets 14–19 versus 0.0078 for sets 10–13, t test, one-tailed, $p = 0.47$) were similar.

Time to first capture was longer than time to subsequent captures for three sets (e.g., set 12, Fig. 2). This delay may be from (*i*) chance, where these timers reached bottom later than the time–depth recorder, which recorded on-bottom time, or (*ii*) gear encounter, bait location, and hooking sometimes taking a few minutes.

Captures most frequently were not related in both time and space, indicating that most were captured independently (Fig. 6). There were some exceptions: for example, a pair of

© 2000 NRC Canada

Table 1. Parameter estimates from the capture times.

		Exponential model			Power model		
Set	Historic model λ	λ_0	r	s	β_3	β_1	s
1	0.74	0.83	0.017	0.51	1.17	0.132	0.60
2	0.93	0.90	0.009	0.51	1.14	0.077	0.60
3	0.79	0.90	0.023	0.51	1.21	0.137	0.60
4	0.41	1.10	0.047	0.51	2.67	0.382	0.60
5	0.83	0.65	0.001	0.51	0.65	0.000	0.60
6	0.75	0.71	0.011	0.51	0.86	0.075	0.60
7	1.33	1.23	0.017	0.51	1.37	0.068	0.60
8	0.60	0.56	0.007	0.51	0.63	0.051	0.60
9	0.26	0.22	0.002	0.51	0.31	0.064	0.60
10	0.16	0.20	0.006	0.51	0.43	0.156	0.60
11	0.55	0.60	0.011	0.51	1.07	0.151	0.60
12	0.79	0.61	0.000	0.51	0.63	0.000	0.60
13	0.31	0.50	0.015	0.51	1.41	0.264	0.60
14	0.28	0.51	0.034	0.51	1.06	0.282	0.60
15	0.07	0.07	0.000	0.51	0.07	0.000	0.60
16	0.33	0.32	0.004	0.51	0.30	0.001	0.60
17	0.22	0.22	0.004	0.51	0.23	0.027	0.60
18	0.44	0.33	0.000	0.51	0.34	0.000	0.60
19	0.34	0.37	0.008	0.51	0.64	0.131	0.60
Average	0.53	0.57	0.011		0.85	0.105	
Minimum	0.07	0.07	0.000		0.07	0.000	
Maximum	1.33	1.23	0.047		2.67	0.382	
–log-likelihood	950	781			844		
Akaike information criterion	988	859			922		

Note: Sets 1–9 were located in Chatham Strait near Tenakee Inlet and sets 10–19 near Point Couverden. The hook spacing of sets 1–13 was 2 m and for sets 14–19 was 1 m. Parameter estimates are for hooks with hook timers only, which were located on every hook for 2-m-spacing skates and every other hook for 1-m-spacing skates. As a result, the estimated encounter rates for all hooks for 1-m-spacing skates is twice the listed values. λ, encounter rate; λ_0, initial encounter rate; r, rate of decline of encounter rate; s, fraction of baits left when bait location probability began to decrease. β_3 is proportional to initial encounter rate and β_1 is a measure of feeding regimen. The Akaike information criterion measures how well the model represents the data; a lower Akaike information criterion value implies a better fit.

fish were captured nearly simultaneously at positions 37 and 38 of set 7 and may represent fish traveling together or the first capture may have cued the second capture. The spatial distribution of captures was examined to determine whether such simultaneous captures were evidence that sablefish captures were clustered. If captures were clustered, runs of adjacent captures would be longer than if they were randomly distributed. The maximum number of adjacent captures observed was six. A Monte Carlo simulation was used to test whether this maximum was unusual. The test consisted of randomly assigning capture position of the total catch, recording the maximum number of adjacent captures, and then repeating these steps 10 000 times. A maximum of six adjacent captures occurred 16% of the time, and the most frequent maximum was seven, which occurred 28% of the time. In fact, maximum runs of six or more occurred over 95% of the time. Clearly, this evidence does not support clustering of individuals along the longline. Some captures were related in time, but not in space; for example, sablefish were captured in groups at set 3 (Fig. 2), but within each group usually were separated in space (Fig. 6). Such a pattern might occur if sablefish organize spatially into successive pulses or waves of moving, feeding fish or if detection of the gear by an individual leads others to the gear and they begin searching along the line and discovering the remaining baits. Fieldwork on sablefish group feeding behavior is necessary to determine whether something other than chance caused these groupings.

Other longline gear experiments

Hook density, but not hook pattern, affected sablefish catch. Greater hook density led to greater sablefish catch per metre of line and lower catch per hook (ANOVA, $p < 0.001$) (Table 2). In contrast, catch per metre of line was similar regardless of hook pattern in the first hook pattern experiment (regression: sablefish, $p = 0.42$; spiny dogfish (*Squalus acanthias*), $p = 0.82$) (Table 2). Unlike the other experiments, spiny dogfish, not sablefish, was the primary species caught. More hook patterns were tested in the second hook pattern experiment, and catch per metre of line was found to decrease as the gap between hook clusters increased (regression: sablefish, $p = 0.01$), but the estimated decrease was small, only 8% over the tested range of 12- to 42-m gaps.

Most sablefish were caught during the first 3 h of soak time; soaking the gear an additional 4 h resulted in only slightly greater catch per hook (0.28 versus 0.24 for 3 h soak, paired t test, one-tailed, $p < 0.001$) (Table 2). Only 15% more sablefish were caught by soaking an additional 4 h (regression: 7- versus 3-h catch rates, $p < 0.001$); equivalently, the proportion caught during the first 3 h averaged

© 2000 NRC Canada

Fig. 3. Residuals (observed less expected catch) by model. (A) Residuals versus available baits for the historic model; (B) residuals versus time for the historic model; (C) residuals versus available baits for the exponential model; (D) residuals versus time for the exponential model; (E) residuals versus available baits for the power model; (F) residuals versus time for the power model. The models are described in the Mathematical model section.

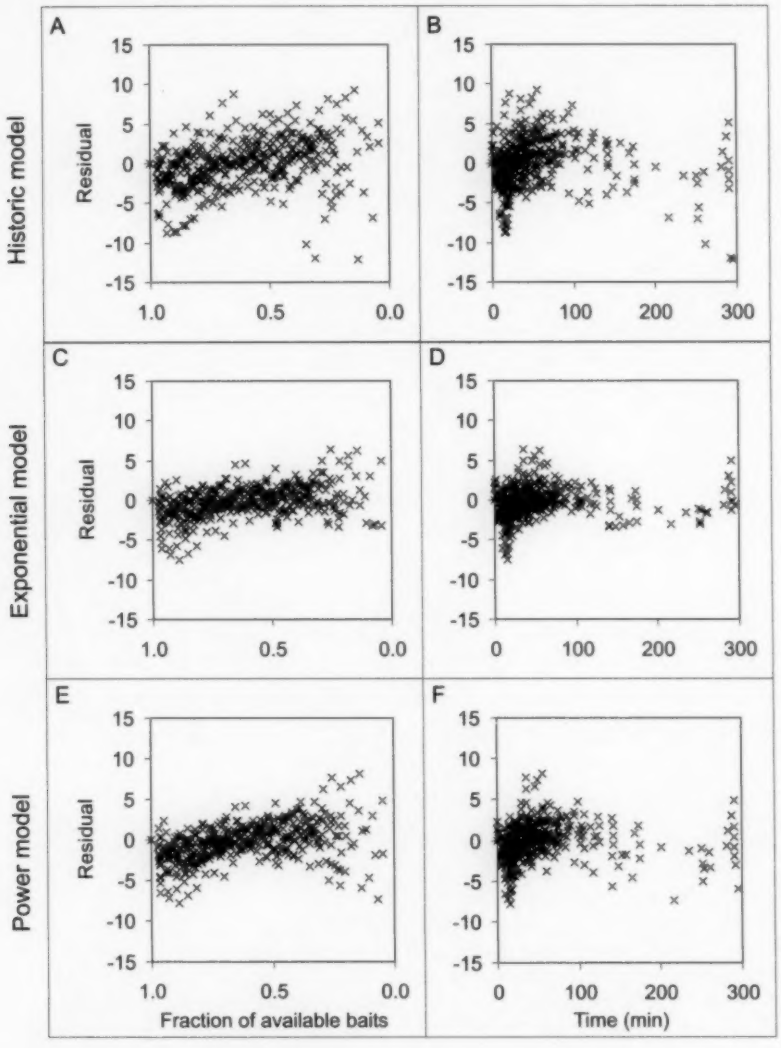

0.87 of the total after 7 h. The proportion was not affected by sablefish density and was similar regardless of catch per hook after 3 h (Fig. 7). Only 3–9% of herring baits, but 28% of squid baits, remained after 7 h of soak time, probably because squid is a tougher bait. Sablefish catch per hook was about 10% greater for squid bait compared with herring bait (1988 experiment, ANOVA, $p < 0.01$).

Sablefish catch per hook for reused bait was 70% of fresh bait (0.20 versus 0.14 for reused bait, paired t test, $p = 0.01$, $n = 8$ sets). The catch rate decreased less than odor production; estimated odor production for reused squid, previously soaked 3–10 h, was no more than 34% of that for fresh bait (Fig. 8). Sablefish catch per hook was unaffected by presoaking (0.31 versus 0.33 for presoaked bait, paired t test, $p = 0.37$, $n = 17$ sets), probably because presoaking is difficult to replicate. Bait loses attractants sinking to 500-m water depth in about 0.5 h because sinking washes the bait of some odor and water pressure squeezes odor from the bait.

Discussion

Encounter rate

Sablefish encounter the longline gear at a decreasing rate. The hook timer estimate of encounter rate after 3 h was only 13% of the initial rate, assuming an exponential encounter rate model. In the soak time experiments, sablefish catch was only 15% higher for 7 versus 3 h. Encounter rate and bait location probability were not directly observed; only the product of encounter rate and bait location probability, the capture rate, was directly observed, so the evidence for what

© 2000 NRC Canada

Fig. 4. Bait location probability versus baits remaining for the historic (line), exponential (○), and power (×) models. The models are described in the Mathematical model section.

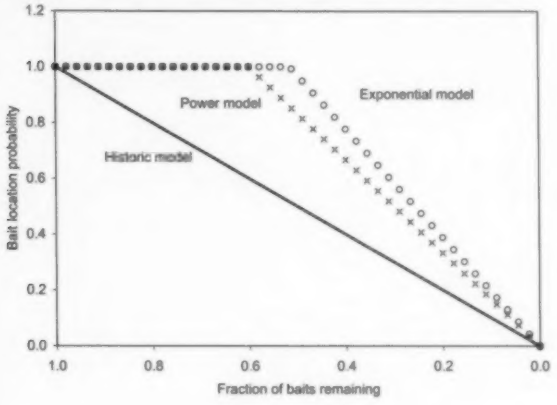

Fig. 5. Estimated encounter rate versus time for set 11. Encounter rate was estimated for the historic (line), exponential (○), and power (×) models. The models are described in the Mathematical model section.

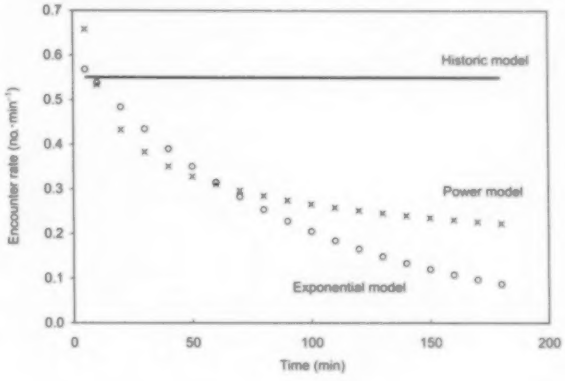

caused the soak time effect is indirect. The soak time effect was insensitive to sablefish density: the 3-h catch was a similar fraction of the 7-h catch, even though fewer baits remained in high-density areas. If the soak time effect was due to decreased bait location probability, then one would expect that the effect would be greater in areas of high sablefish density. Instead, the effect was similar, implying that decreased bait location probability did not cause the soak time effect, leaving decreased encounter rate as the most likely cause of the soak time effect.

At least two sablefish feeding behaviors, response intensity and catch rate, do not change as much as odor concentration. Sablefish response intensity decreased less than odor concentration in a bait odor experiment (Løkkeborg et al. 1995). Sablefish catch rate decreased less than estimated odor production in the reused bait experiment. The catch rate of torsk (*Brosme brosme*) also decreased less than estimated odor production in a presoaked bait experiment (Løkkeborg and Johannessen 1992).

Sablefish response to bait odor may reach a limit at high odor concentrations, which would account for the more limited range of sablefish feeding behaviors compared with odor concentration. A fish has an upper limit for turning rate, response time, swimming speed, etc., and these physical constraints may limit the range of response at higher odor concentrations. The proportion of the fish responding to the bait odor also may be limited, reaching an asymptote when the odor concentration in the plume is above a certain level, far beyond the response threshold, as occurs in the downstream area closest to the gear.

Sablefish also may balance the energy costs of feeding behavior against the likelihood of locating food once scented, limiting energy expenditure when swimming upstream to locate food. The odor concentration is low after the bait has been on bottom for a few hours; from the fish's perspective, the bait will appear as less food or as food that is distant. Sablefish, like Atlantic cod (*Gadus morhua*) and haddock (*Melanogrammus aeglefinus*), may make energy-based choices. Løkkeborg et al. (1989) found that response of both Atlantic cod and haddock to baited hooks decreased in periods of high current and hypothesized that energy optimization was achieved by restricting activity to periods with moderate or low current and staying in shelter when the current was strong.

Sablefish encounter rate appears to track odor concentration at the odor plume edge more closely than odor concentration at the bait. After 6 h, encounter rate and plume edge concentration are about 10% of the 1-h value, whereas at-bait concentration is about 40% (Fig. 9). The odor concentration at the leading edge of the plume is the odor concentration first scented by the fish. The close relationship between plume edge concentration and encounter rate indicates that this concentration is a primary determinant in the fish's decision to locate the bait, once scented.

The odor concentration behind the leading edge of the plume decreases (Fig. 10) so that fish swimming to the bait encounter decreasing odor concentration. This decrease is due to an exponential decline in odor production by the bait and to horizontal and vertical diffusion during downstream propagation of the odor plume (Sainte-Marie and Hargrave 1987). The concentration behind the plume edge may fall below the sablefish response threshold, depending on the feeding regimen. Odor concentrations for longer distances and times are below the response threshold for sablefish deprived of food for 1 day; all odor concentrations are above the response threshold for sablefish deprived of food for 4 days (Fig. 10).

Active space, the volume where the odor concentration is present in superthreshold quantities (Bossert and Wilson 1963), may shrink with time. For odor released at 1 h, the maximum length of the active space is 925 m, for 2 h is 793 m, and for 6 h is 654 m (0.08 $m \cdot s^{-1}$ current, sablefish deprived of food for 1 day (Løkkeborg et al. 1995, their table 3)). The active space may shrink, but the scent level remains above the detection threshold of sablefish over a relatively large volume; the maximum length of the active space for odor released at 6 h was 654 m. Therefore, sufficient scent remains to attract sablefish from a wide area, but eventually, only fish whose movements bring them into contact with the active space will be attracted to the gear. Whether the active space shrinks depends on feeding regimen. The active space stops expanding after 4–5 h for sablefish de-

© 2000 NRC Canada

Fig. 6. Observed (○) capture times and cumulative captures at off-bottom time (+) versus position along longline. Only a subset of the hook timer data is displayed for brevity.

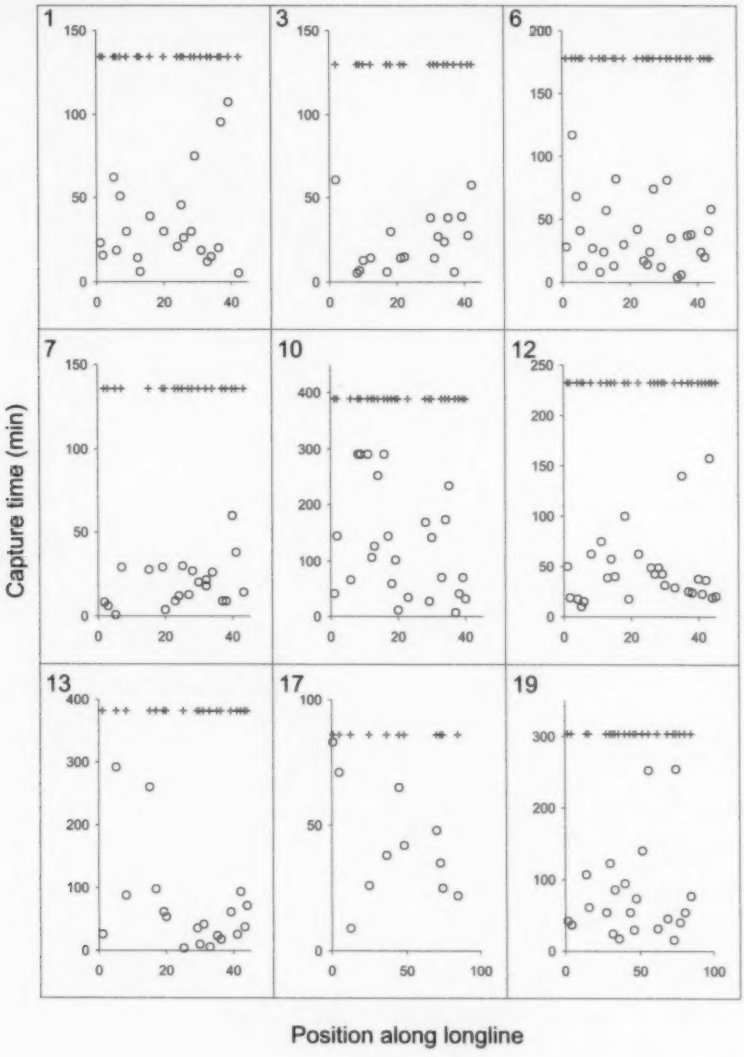

prived of food for 1 day and continues expanding for sablefish deprived of food for 4 days (Fig. 10).

Bait location probability

Sablefish are adept at locating available baits. In the hook timer experiments, the capture rate decreased slowly until as few as 20–30% of the baits remained, and the estimated bait location probability did not begin to decrease until only 50% of the baits remained. In the hook pattern experiments, the decrease in catch rate due to widely spaced and narrowly spaced baits was small, only about 8% from 12- to 42-m gaps. A 42-m gap between single baits is equivalent to only about 5% of the baits remaining for the standard survey skate with 2-m spacing. Thus, sablefish can locate widely spaced baits. This bait location ability implies that gear saturation has little effect on the capture of sablefish, potentially until few baits remain.

Sablefish are good bait predators, probably because they are acutely sensitive to odor. A sablefish deprived of food for 1 day can detect bait odor 300–1200 m downstream of a bait soaked 1 h, depending on current; the response threshold for sablefish deprived of food for 4 days is among the lowest reported for fish (Løkkeborg et al. 1995). Adult sablefish may be this sensitive because they inhabit deep water, typically 150–1000 m, where locating prey depends on smell rather than sight. Because they are good bait predators, sablefish may behave like Atlantic cod, which Løkkeborg and Fernö (1999) observed to swim upstream directly to a baited line and then swim along the line for 100 m or more after locating the baited line. A fish with this searching be-

© 2000 NRC Canada

Table 2. Experiment, treatment, sablefish catch (number) per metre of line and per hook, baits retrieved per hook, and spiny dogfish catch per hook for seven experiments.

Experiment	Treatment	Sablefish catch per metre of line	Sablefish catch per hook	Baits retrieved per hook	Spiny dogfish catch per hook
Hook density, 1986 (n = 10 sets)	0.25 hook·m^{-1}	0.114	0.478	0.084	0.000
	0.5 hook·m^{-1}	0.176	0.367	0.230	0.000
	1.0 hook·m^{-1}	0.246	0.257	0.418	0.000
Hook pattern, 1990 (n = 18 sets)	4-m gap	0.040	0.158	0.032	0.259
	8-m gap	0.041	0.164	0.016	0.233
	24-m gap	0.043	0.172	0.047	0.255
Hook pattern, 1998 (n = 15 sets)	12-m gap	0.095	0.379	0.142	0.000
	22-m gap	0.092	0.367	0.165	0.000
	32-m gap	0.091	0.365	0.164	0.000
	42-m gap	0.087	0.346	0.166	0.000
Soak time, May 1986 (n = 6 sets)	3 h	0.188	0.377	0.169	0.000
	7 h	0.218	0.436	0.039	0.000
Soak time, June 1986 (n = 12 sets)	3 h	0.140	0.281	0.213	0.000
	7 h	0.163	0.326	0.036	0.000
Soak time, 1987 (n = 24 sets)	3 h	0.093	0.186	0.319	0.000
	7 h	0.097	0.194	0.092	0.000
Soak time, 1988 (n = 32 sets)	3 h, herring	0.114	0.228	0.247	0.000
	7 h, herring	0.143	0.285	0.072	0.000
	3 h, squid	0.129	0.258	0.473	0.000
	7 h, squid	0.154	0.307	0.284	0.000

Note: The treatment labels are self-explanatory except for the hook pattern experiments. The hook patterns are all hooks spaced 4 m apart, three hooks spaced 2 m apart, 8 m of bare line, etc., five hooks spaced 2 m apart, 12 m of bare line, etc., 10 hooks spaced 2 m apart, 22 m of bare line, etc., 11 hooks spaced 2 m apart, 24 m of bare line, etc., 15 hooks spaced 2 m apart, 32 m of bare line, etc., and 20 hooks spaced 2 m apart, 42 m of bare line, etc. The hook patterns are denoted by the length of bare line between hook clusters, e.g., 12-m gap denotes five hooks spaced 2 m apart, 12 m of bare line, etc.

Fig. 7. Observed (○) and expected (line) 7-h catch rate versus 3-h catch rate for the soak time experiments.

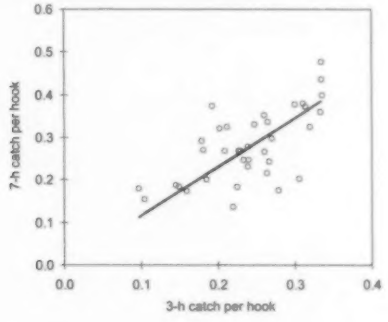

Fig. 8. Observed (○) (Løkkeborg 1990, his table 1) and expected (line) rate of release of amino acids from mackerel bait, expressed as a percentage of the initial value measured at 0 h of exposure to running seawater. The equation that I used to estimate expected release rate is shown in the Appendix.

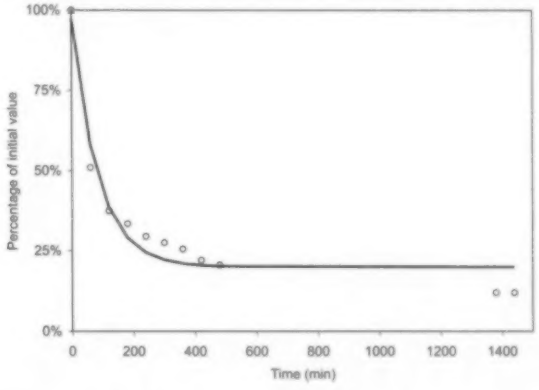

havior would probably locate an available bait unless large sections of line were occupied. Searching the line also makes biological sense as a natural food-seeking behavior. This searching behavior also implies that encounter rate is more important than locating bait.

Models relating longline catch rate to fish abundance have been developed that correct longline catch rates for gear saturation (Murphy 1960; Rothschild 1967). These early models, as well as a more recent one (Somerton and Kikkawa 1995), share two assumptions: (*i*) encounters to the gear are random, independent, and occur at a constant rate through time and (*ii*) the probability of catching fish, the bait location probability, decreases linearly with the number of baits remaining. For example, Murphy (1960) expressed the rate of change of the number of hooked fish as a linear function of the number of baits remaining. I estimated the bait location probability for sablefish, rather than assuming that this probability follows a particular form. The improved fit implies that for sablefish, bait location probability is not proportional to the number of baits available; instead, bait location probability remains constant, at least initially, for a wide range of available baits, probably because sablefish are

© 2000 NRC Canada

Fig. 9. Odor concentration (Sainte-Marie and Hargrave 1987; Løkkeborg et al. 1995) at bait (×) and at the odor plume edge (broken line) and encounter rate at bait (○) expressed as a percentage of values after 1 h on bottom. The calculation equation for odor concentration is shown in the Appendix and was computed assuming a current of 0.08 $m \cdot s^{-1}$ and the estimated decline in odor release rates (Fig. 8). The encounter rate was computed using the average r estimated from the hook timer experiments (Table 1) and the exponential model.

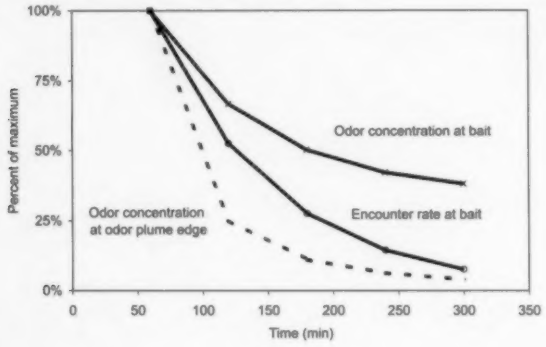

Fig. 10. Concentration profiles of bait odor by distance from the bait and on-bottom time (Sainte-Marie and Hargrave 1987; Løkkeborg et al. 1995) assuming a current of 0.08 $m \cdot s^{-1}$ and the estimated decline in odor release rates (Fig. 8). The calculation equation for odor concentration is shown in the Appendix. For example, after 3 h on bottom, the leading edge of the plume is about 800 m from the bait and the odor concentration there is about 0.000 000 4 $mol \cdot m^{-3}$, whereas the odor concentration 500 m from the bait is less, e.g., about 0.000 000 2 $mol \cdot m^{-3}$. The arrows indicate the response threshold for sablefish deprived of food for 1 day and sablefish deprived of food for 4 days (Løkkeborg et al. 1995, their table 3).

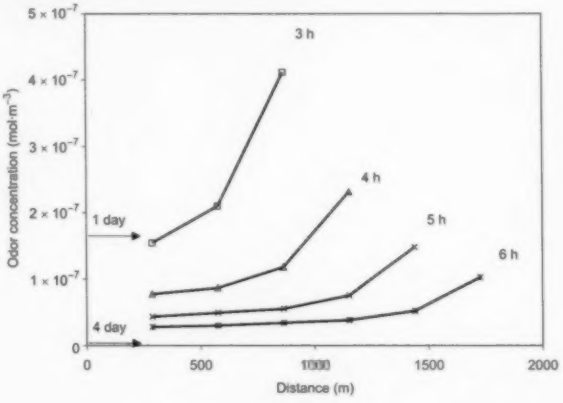

good bait predators. Different species were modeled previously: yellowfin tuna (*Thunnus albacares*) by Murphy (1960) and Rothschild (1967) and pelagic armorhead (*Pseudopentaceros wheeleri*) by Somerton and Kikkawa (1995). The bait location probability may differ by species and gear configuration, but I suspect that most species readily locate baited hooks, even when few remain. If so, gear saturation of longlines may be less important than previously considered.

Hooking fraction

Sablefish encountering the gear may interact, but any interaction appears inconsequential. The random distribution of sablefish captures along the line implies that initial captures do not affect subsequent captures, so that hooking fraction appears unaffected by interaction between individuals. The information supporting this conclusion is indirect because hooking fraction, like encounter rate and bait location probability, was not directly observed. For other species, interaction between individuals has been shown to both enhance and reduce captures. Captures of Pacific halibut (*Hippoglossus stenolepis*) tended to be clustered based on the observed frequency of adjacent captures (Skud and Hamley 1978). Cuing on captured fish or a contagious distribution of fish while free-swimming may cause clustering. Fernö et al. (1986) observed that aggressive interactions occurred when several whiting were in the vicinity of the line. Løkkeborg and Bjordal (1992) observed large Atlantic cod frightening smaller Atlantic cod away from baited hooks and torsk chasing smaller fish away from baited hooks. Interspecific interactions can also increase the hooking fraction. Responses by Atlantic cod were often initiated by a struggling haddock that had just been hooked (Løkkeborg et al. 1989). In addition, behavioral interactions may increase feeding success. Foraging success of ephemeral food patches is enhanced in groups of juvenile walleye pollock (*Theragra chalcogramma*) compared with isolated fish (Baird et al. 1991). Schooling chum salmon (*Oncorhynchus keta*) juveniles gain information by interpreting conspecific behavior (Ryer and Olla 1991).

Interaction between individual sablefish appears inconsequential, but other factors such as season, fish density, and food abundance may affect sablefish hooking fraction and thus the proportion of fish caught. Observed hooking fractions for Atlantic cod and haddock were higher in September than in December, possibly due to seasonal variation in feeding activity; feeding activity is reduced during the spawning period, which includes December (Løkkeborg et al. 1989). Fish density also may affect hooking fraction. The initiation of Atlantic cod responses by struggling haddock (Løkkeborg et al. 1989) implies that captures may serve to motivate fish to locate and attack baits even when few baits remain. Greater numbers of responding and hooked fish increase the probability of intensified responses by other fish through social facilitation and may counteract reduced bait location probability due to fewer available baits. Food abundance may vary annually or be reduced by high fish density and also may affect hooking fraction. Reduced food abundance may lead to increased feeding motivation (sablefish response to bait odor was influenced by feeding frequency (Løkkeborg et al. 1995)), intensified responses towards the baits, and increased hooking fraction.

Hooking fraction may differ between sizes of sablefish. For example, large Atlantic cod frightened smaller Atlantic cod away from baited hooks, torsk chased smaller fish away from baited hooks (Løkkeborg and Bjordal 1992), and larger fish may be attracted to the baits from farther away. As a result, longline gear may not provide accurate estimates of all

© 2000 NRC Canada

size-classes due to size-based differences in the proportion caught. However, the probability that an individual fish will be caught once in contact with the sampling gear varies with size for most species and gear types (Gunderson 1993).

Hook density

Hook density and spacing were varied in the hook density experiments, whereas in the hook pattern experiments, hook spacing was varied, but overall hook density was constant. Sablefish catch per metre of line increased with hook density but remained nearly constant with hook pattern. The lack of a substantial pattern effect implies that the greater number of hooks, not their closer spacing, increased sablefish catch in the hook density experiments.

A larger active space is probably responsible for the relationship between catch and hook density. A higher hook density increases odor concentrations within the odor plume formed downstream of the gear. A denser odor plume enlarges the active space and therefore attracts more fish. A denser odor plume may also increase the hooking fraction. Scent concentration affects sablefish response intensity (Løkkeborg et al. 1995) and thus may increase the feeding motivation.

Varying hook spacings from 2.7 to 12.8 m also affected Pacific halibut catches (Skud and Hamley 1978). As with sablefish, higher hook densities resulted in significantly increased catch per unit of line and decreased catch per hook of Pacific halibut (Skud and Hamley 1978). They addressed the differences in "catch per hook" and suggested that these differences are due to competition between hooks for the available fish: if more than one hook falls within a Pacific halibut's range, these hooks "compete" for the capture of that fish, and the closer they are spaced, the lower the catch per hook is; on the other hand, if the hooks are so far apart that each Pacific halibut encounters no more than one hook, then the hooks fish independently and their efficiency is at its maximum, so that catch per hook no longer increases with hook spacing. Eggers et al. (1982) developed this concept to describe a quantitative method for estimating the effective radius of a baited hook or pot, assuming that each device has on average a capturing field of fixed size and that the capturing field is a circle centered at the baited hook or pot. They applied this method to three species, including Pacific halibut and sablefish. Both methods (Skud and Hamley 1978; Eggers et al. 1982) assume that the capture field per hook is constant. Skud and Hamley (1978, p. 20) phrased this assumption as "...assuming a concentration of bait [does not] attract halibut beyond their normal feeding ranges...." However, "catch per meter of line" increased for halibut and sablefish, implying that the capture field per hook was not constant, but rather, increased with hook density. The capture field per hook may increase because odor plumes from adjacent baits overlap, increasing the downstream odor concentrations and intensifying fish response. If so, the capture field is not constant as Skud and Hamley (1978) and Eggers et al. (1982) assumed, and their measuring the capture field of a hook by experimentally varying hook spacing is not valid.

Conceptualization of sablefish capture by longline and implications for longline survey design

Encounter rate, not bait location probability, appears to control sablefish capture by longline. Sablefish encounter the gear at a decreasing rate with on-bottom time. The encounter rate decreases, but not their ability to locate baits. Sablefish locate baits even as the number of available baits decreases substantially. The bait location probability is constant, at least for a substantial range of available baits, and is not a linear function of the number of available baits, as assumed by the models of Murphy (1960) and Rothschild (1967).

Encounter rate decreases with time, presumably in response to decreasing odor concentration. Odor concentration is highest at the leading edge of the odor plume and decreases behind the leading edge. Odor concentration at the leading edge of the odor plume, the concentration first encountered by the fish, appears to control the encounter rate. The relationship of encounter rate and odor concentration is modulated by fish behavior. The odor concentration decreases rapidly with time, both at and behind the leading edge of the odor plume, yet response intensity and catch rate do not exhibit the same range as odor concentration. Physical constraints or energetic considerations may limit the response range of individual fish. The proportion of the fish responding to the bait odor may approach a limit asymptotically.

Hooking fraction appeared unaffected by interactions between individual sablefish but was not observed directly and may vary in other situations. Hooking fraction has been shown to be influenced by interaction between individuals, season, and conceivably fish density. Other factors such as temperature and food availability also could vary between years and influence the proportion of fish that are caught.

The value of power function parameter β_1 estimated from the capture times can be compared with the slope parameter relating sablefish response intensity and odor concentration estimated by Løkkeborg et al. (1995), who found that the slope parameter value was related to feeding regimen and was 0.397 and 0.163 for 1 and 4 days of feeding deprivation. The value of β_1 estimated from the capture times of the hook timer experiments was 0.105, implying that sablefish in the study areas had not fed for more than 4 days or an equivalent feeding regimen.

Survey catch rates likely provide an accurate linear index of relative abundance over a wide range of sablefish density because sablefish appear adept at locating available baits and because the encounter rate decreases with time. Capture rate slows and most sablefish are caught within the survey's minimum soak time of 3 h; the survey soak time varies from 3 to 10 h because of the length of time required to retrieve the gear. This slowing appears due to reduced encounter rate rather than an inability to locate the decreasing number of baits remaining. This slowing also appears insensitive to sablefish density; catches for longer soak times are similar to the 3-h catch because of the slowed encounter rate. The weak link between catch rate and abundance is the unknown extent that hooking fraction and other factors such as temperature and food availability vary and influence the proportion of fish caught.

Findings of these experiments imply that longline surveys can be designed for a linear relationship between survey catch rate and abundance over a wide range of fish density. The gear should be on bottom long enough that the encoun-

© 2000 NRC Canada

ter rate has slowed sufficiently for most fish to be caught. This minimum on-bottom time can be determined by a series of soak time experiments to learn how catch rate varies with soak time. In addition, the bait density should be high enough that some baits remain after the maximum soak time, so that an available bait can still be located. This bait density can be determined by increasing hook density if "few" baits are left at the maximum soak time to ensure that the decrease in catch rate with soak time is due to decreased encounter rate rather than too few baits remaining. A well-designed longline survey will have enough soak time to include most captures and enough baits for some to remain at the end.

Acknowledgments

Jeff Fujioka, Vincent Gallucci, Ana Parma, Jerry Pella, and Terrance Quinn, II provided substantial advice. Svein Løkkeborg, Jerry Pella, Jon Heifetz, and Phil Rigby and three anonymous referees reviewed the manuscript. This research was supported in part by the U.S. Department of Commerce Pioneer Fund.

References

Baird, T.A., Ryer, C.H., and Olla, B.L. 1991. Social enhancement of foraging on an ephemeral food source in juvenile walleye pollock, *Theragra chalcogramma*. Environ. Biol. Fishes, **31**: 307–311.

Bannerot, S.P., and Austin, C.B. 1983. Using frequency distributions of catch per unit effort to measure fish-stock abundance. Trans. Am. Fish. Soc. **112**: 608–617.

Beverton, R.J.H., and Holt, S.J. 1957. On the dynamics of exploited fish populations. Chapman and Hall, New York.

Bossert, W.H., and Wilson, E.O. 1963. The analysis of olfactory communication among animals. J. Theor. Biol. **5**: 443–469.

Eggers, D.M., Rickard, N.A., Chapman, D.G., and Whitney, R.R. 1982. A methodology for estimating area fished for baited hooks and traps along a ground line. Can. J. Fish. Aquat. Sci. **39**: 448–453.

Fernö, A., Solemdal, P., and Tilseth, S. 1986. Field studies on the behaviour of whiting (*Gadus merlangus* L.) towards baited hooks. FiskeriDir. Skr. Ser. HavUnders. **18**: 83–95.

Gunderson, D.R. 1993. Surveys of fisheries resources. John Wiley & Sons, Inc., New York.

Hilborn, R., and Mangel, M. 1997. The ecological detective: confronting models with data. Princeton University Press, Princeton, N.J.

Løkkeborg, S. 1990. Rate of release of potential feeding attractants from natural and artificial bait. Fish. Res. **8**: 253–261.

Løkkeborg, S., and Bjordal, Å. 1992. Species and size selectivity in longline fishing: a review. Fish. Res. **13**: 311–322.

Løkkeborg, S., and Fernö, A. 1999. Diel activity pattern and food search behaviour in cod, *Gadus morhua*. Environ. Biol. Fishes, **54**: 345–353.

Løkkeborg, S., and Johannessen, T. 1992. The importance of chemical stimuli in bait fishing — fishing trials with presoaked bait. Fish. Res. **14**: 21–29.

Løkkeborg, S., Bjordal, Å., and Fernö, A. 1989. Responses of cod (*Gadus morhua*) and haddock (*Melanogrammus aeglefinus*) to baited hooks in the natural environment. Can. J. Fish. Aquat. Sci. **46**: 1478–1483.

Løkkeborg, S., Olla, B.L., Pearson, W.H., and Davis, M.W. 1995. Behavioural responses of sablefish, *Anoplopoma fimbria*, to bait odour. J. Fish Biol. **46**: 142–155.

Murphy, G.I. 1960. Estimating abundance from longline catches. J. Fish. Res. Board Can. **17**: 33–40.

Ratkowsky, D.A. 1983. Nonlinear regression modeling. Marcel Dekker, Inc., New York.

Richards, L.J., and Schnute, J.T. 1986. An experimental and statistical approach to the question: is CPUE an index of abundance? Can. J. Fish. Aquat. Sci. **43**: 1214–1227.

Rothschild, B.J. 1967. Competition for gear in a multiple-species fishery. J. Cons. Perm. Int. Explor. Mer, **31**: 102–110.

Ryer, C.H., and Olla, B.L. 1991. Agonistic behavior in a schooling fish: form, function and ontogeny. Environ. Biol. Fishes, **31**: 355–363.

Sainte-Marie, B., and Hargrave, B.T. 1987. Estimation of scavenger abundance and distance of attraction to bait. Mar. Biol. **94**: 431–443.

Sasaki, T. 1985. Studies on the sablefish resources in the North Pacific Ocean. Far Seas Fish. Res. Lab. Bull. No. 22.

Sigler, M.F. 1994. An electronic measuring board with bar codes. Trans. Am. Fish. Soc. **123**: 115–117.

Sigler, M.F., and Fujioka, J.T. 1988. Evaluation of variability in sablefish, *Anoplopoma fimbria*, abundance indices in the Gulf of Alaska using the bootstrap method. Fish. Bull. U.S. **86**: 445–452.

Sigler, M.F., and Zenger, H.H. 1989. Assessment of Gulf of Alaska sablefish and other groundfish based on the domestic longline survey, 1987. NOAA Tech. Memo. NMFS F/NWC-169.

Skud, B.E., and Hamley, J.M. 1978. Factors affecting longline catch and effort. I. General review. II. Hook-spacing. III. Bait loss and competition. Int. Pac. Halibut Comm. Sci. Rep. No. 64.

Somerton, D.A., and Kikkawa, B.S. 1995. A stock survey technique using the time to capture individual fish on longlines. Can. J. Fish. Aquat. Sci. **52**: 260–267.

Appendix

The power encounter rate model combines three functions: sablefish response intensity as a function of odor concentration, the odor concentration at the leading edge of the odor plume, and the length of time to travel from the leading edge to the bait. Løkkeborg et al. (1995) measured sablefish response intensity, RI (number and frequency of turns), to different odor concentrations, C (molar), in a laboratory and found that $\log_{10}\mathrm{RI} = \beta_0 + \beta_1 \log_{10} C$; the values of the regression coefficients depended on the feeding regimen.

Odor concentration, derived from the active-space equation in Sainte-Marie and Hargrave (1987) and Løkkeborg et al. (1995), is

$$C = \frac{QU}{x^2 2\pi B_y B_z}$$

where Q is the release rate of the odor source (moles per second), U is the current (metres per second), x is downstream distance (metres), and B_y and B_z are the horizontal and vertical dispersion velocities (metres per second). I used the same values of the dispersion velocities, i.e., $B_y = 10^{-3}$ m·s^{-1} and $B_z = 10^{-5}$ m·s^{-1}, as Sainte-Marie and Hargrave (1987) and Løkkeborg et al. (1995) and similarly assumed that the relationship between horizontal and vertical standard deviations and downstream distance was linear. An equation for the release rate of the odor source is shown in the last paragraph of the Appendix.

The downstream propagation of the odor plume depends on advection (Sainte-Marie and Hargrave 1987), and its length at time t is the product of current v and time, i.e., $x(t) = vt$. However, fish arriving at bait at t are probably at-

© 2000 NRC Canada

tracted from much shorter distances because they also must swim upstream to the bait after contacting the plume. The actual distance of attraction at t is $x_A(t) = U(S - U)t/S$ (Sainte-Marie and Hargrave 1987), where x_A is the attraction distance and S is fish swimming speed (metres per second). The swimming speed must be greater than current if the fish is to reach the gear (the equation applies only if $S > U$).

I combined these three equations to form an expression for the response intensity of fish arriving at the bait at time t:

$$\mathrm{RI}(t) = 10^{\left(\beta_0 + \beta_1 \log_{10} \frac{QU}{(U(S-U))^2 2\pi B_y B_z}\right)} 10^{\beta_1 \log \frac{1}{t^2}}$$

Fish swimming speed and feeding regimen and current are unknown and cannot be estimated separately from the experimental data, so I combined the first part of the equation, the part that is not time dependent, into a single parameter:

$$\mathrm{RI}(t) = \beta_2 10^{\beta_1 \log \frac{1}{t^2}}$$

Assuming that encounter rate is proportional to response intensity:

$$\lambda(t) = \lambda_0 \beta_2 10^{\beta_1 \log \frac{1}{t^2}}$$

where λ_0 is the initial encounter rate. The initial encounter rate and β_2 cannot be estimated separately from the experimental data, so a single parameter $\beta_3 = \lambda_0 \beta_2$ is estimated. The parameter β_3 is proportional to the initial encounter rate and t represents capture time for the hook timer experiments. The parameter β_1 is one of the coefficients of the response intensity regression estimated by Løkkeborg et al. (1995), who found that its value was a function of sablefish feeding regimen.

An exponential model was used to represent the release rate of the odor source:

$$R_u = R_0 e^{\psi u} + \Omega$$

where R_u is the release rate of amino acids at time u (minutes), ψ is a parameter that describes the decline of the release rate, and Ω is a parameter that describes the y asymptote. Observations of the rate of release of amino acids from mackerel bait (Løkkeborg 1990, his table 1), expressed as a percentage of the initial value measured at 0 h of exposure to running seawater, were used to estimate model parameters using nonlinear least squares and assuming additive error. The observed rate was averaged from the two analytical techniques used. The rate of decline of amino acid release for mackerel bait $\psi = 0.012$. The amino acid release rate reached an asymptote ($\Omega = 19.9\%$ of the initial release rate), indicating that the bait continues to release amino acids for a long time, at least 24 h. The lengthy release period may be due to the thickness of the bait, with odor continuing to diffuse from the interior of the bait to be released.

Appendix references

Løkkeborg, S. 1990. Rate of release of potential feeding attractants from natural and artificial bait. Fish. Res. **8**: 253–261.

Løkkeborg, S., Olla, B.L., Pearson, W.H., and Davis, M.W. 1995. Behavioural responses of sablefish, *Anoplopoma fimbria*, to bait odour. J. Fish Biol. **46**: 142–155.

Sainte-Marie, B., and Hargrave, B.T. 1987. Estimation of scavenger abundance and distance of attraction to bait. Mar. Biol. **94**: 431–443.

© 2000 NRC Canada

Changes in sediment viral and bacterial abundances with hypolimnetic oxygen depletion in a shallow eutrophic Lac Brome (Quebec, Canada)

Mahaut Ricciardi-Rigault, David F. Bird, and Yves T. Prairie

Abstract: Two studies were conducted to examine changes in sediment viral and bacterial abundances following hypolimnetic oxygen depletion. Both studies, a spatiotemporal field study and a core incubation experiment set under controlled conditions, demonstrated that bacterial and viral abundances decreased significantly (43–48% for bacteria and 36–38% for viruses) and in a nearly identical pattern when submitted to changes in the oxygen status of their milieu. The consistency of the results strongly suggests that the shift in both population densities is essentially caused by the onset of anoxia, either directly or indirectly. We suggest that the decline in abundance is due to the disappearance of strictly aerobic bacteria and their associated viruses and not due to stress-induced viral lysis. We also show that the P content of the lysed microbial community can represent an important source of P released from the sediments.

Résumé : Deux études ont été menées afin d'examiner les changements dans les abondances virales et bactériennes des sédiments suite à une réduction de l'oxygène dans l'hypolimnion. Les deux études, l'une d'ordre spatio-temporelle et l'autre d'ordre temporelle sous conditions contrôlées, démontrent que les abondances bactériennes et virales ont diminuées significativement (43–48% pour les bactéries et 36–38% pour les virus) et qu'elles suivent un même patron lorsque les populations sont soumises à des changements d'état d'oxygénation de leur milieu. L'uniformité des résultats suggère fortement que le changement de densité des populations bactérienne et virale est essentiellement causé par la mise en place de l'anoxie, soit directement ou indirectement. Nous suggérons que le déclin dans les abondances est relié à la disparition des bactéries aérobies strictes et des virus associés et non par l'induction du cycle lytique des virus par un agent stresseur. Nous démontrons aussi que le contenu en P de la communauté microbienne lysée peut représenter une source importante du P relargué des sédiments.

Introduction

Aquatic bacteriophages can play an important role in the biogeochemical cycling of nutrients through control over planktonic populations (Middelboe et al. 1996; Gobler et al. 1997; Fuhrman 1999). Bacteriophage abundance is associated with that of bacteria (Proctor et al. 1993), and both of their abundances can be positively correlated with high bacterial activity and productivity (Maranger et al. 1994; Maranger and Bird 1996). In anoxic hypolimnetic environments, Weinbauer and Hoefle (1998) found that about 90% of the bacterial mortality was due to viral lysis in an active bacterium–virus loop. Much less is known, however, about the interaction of viruses and their bacterial hosts within sediments, where their numerical abundances are much higher. Both viruses and bacteria are 100- to 1000-fold more abundant in sediments than in the water column (Maranger and Bird 1996). Maranger and Bird (1996) showed that the greatest viral abundances occurred at the water–sediment interface of well-oxygenated littoral zones, rich in organic matter.

As obligate parasites, viruses are functionally linked to bacteria. Surprisingly, however, Maranger and Bird (1996) found no significant statistical relationship between viral and bacterial abundances in the sediments of Lac Gilbert. On the other hand, Lammers (1988) showed that over 80% of the bacteria isolated from the sediments of New River contained lysogenic bacteriophages, suggesting a potentially tight coupling. The factors that trigger or modulate viral lysis in the sediment environment are unstudied, although environmental stresses are believed to play a key role in inducing viral lysis in nature (Bergh et al. 1989).

Boström et al. (1988, 1989) demonstrated that rapid changes in oxygen conditions tend to induce bacterial cell lysis, which contributes to the release of nutrients (P in particular) from the sediments to the water column. In a study of Lac Cromwell, de Montigny and Prairie (1993) demonstrated that almost all P released by sediments could be explained by cell lysis. Moreover, the massive release of sediment P observed in the small hypolimnion of shallow eutrophic lakes has been shown to be strongly related to bacterial activity (Fleisher 1978; Boström et al. 1985; Brunberg and Boström 1992; Prairie et al. 2000). Bacterial cell lysis is thought to be a possible mechanism explaining P concentration peaks occurring at the onset of anoxia during summer stratification of such lakes (Bates and Neafus 1980; Eckerrot and Petterson 1993; Gächter and Meyer 1993). It is not

Received August 20, 1999. Accepted March 10, 2000.
J15322

M. Ricciardi-Rigault, D.F. Bird, and Y.T. Prairie.[1]
Département des Sciences biologiques, Université du Québec à Montréal, C.P. 8888, Succursale Centre-Ville, Montréal, QC H3C 3P8, Canada.

[1]Author to whom all correspondence should be addressed.
e-mail: prairie.yves@uqam.ca

© 2000 NRC Canada

Fig. 1. Location of the sampling stations on (A) Lac Brome along (B) a transect crossing the oxycline of the lake (schematic cross section).

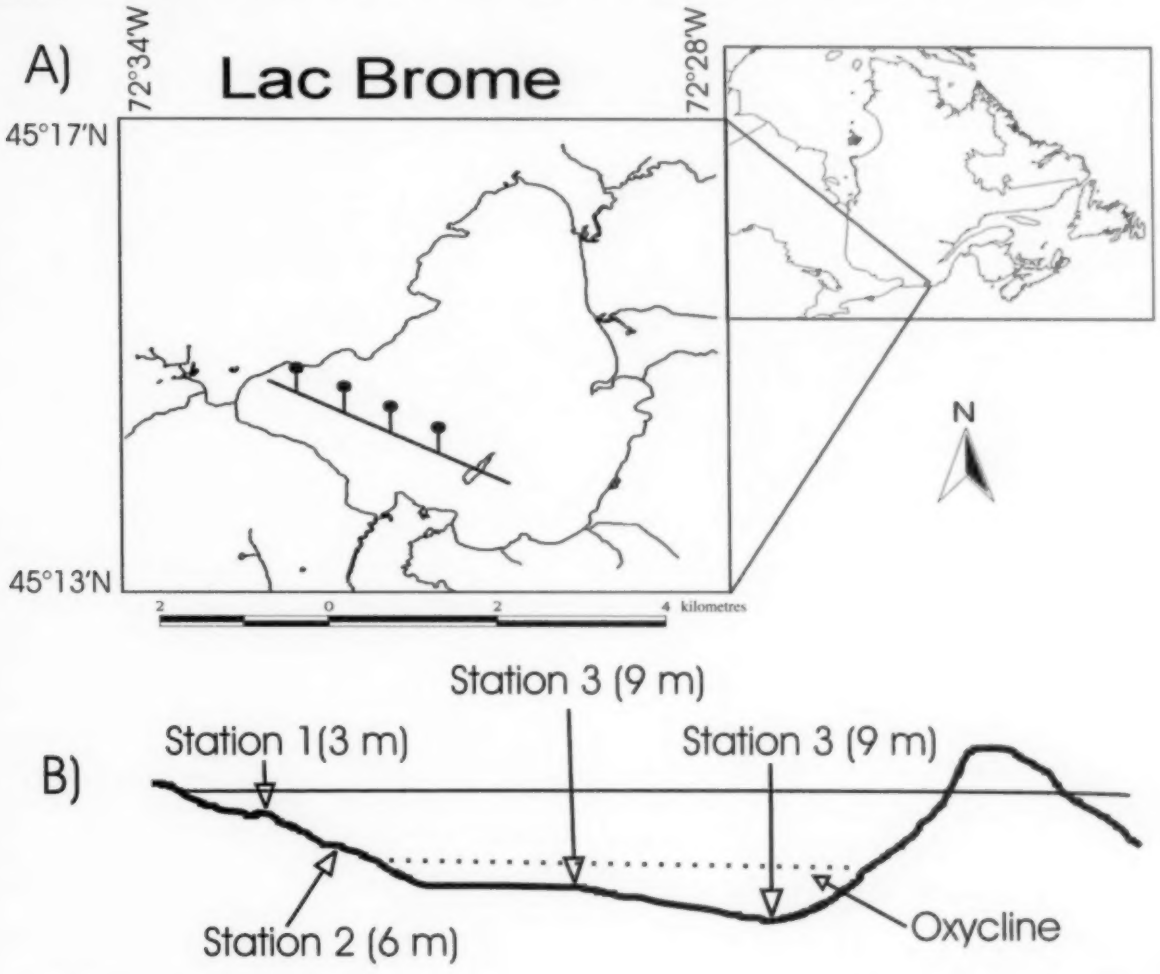

known, however, whether lysis occurs spontaneously or through viral action.

The main objective of this study was to test whether sudden changes in the oxygen state of sediment surfaces alter the abundances of sediment bacteria and viruses. Two approaches were taken. First, we followed the temporal evolution of both sediment viral and bacterial abundances at four stations along a transect crossing the oxycline in Lac Brome (two above and two below the oxycline). Second, we incubated, in the laboratory, several sediment cores collected prior to anoxia and followed abundances as the sediments became anoxic. As a secondary objective, we examined the possible importance of these changes on the release of P from the sediments.

Materials and methods

Study site

Sampling took place in the shallow eutrophic Lac Brome, located in the Eastern Townships of Quebec, Canada (45°15′N, 72°30′W) (Fig. 1). The mean depth of the lake is 4 m and its maximum depth is 12 m. The mean total P and chlorophyll contents and the mean total N to total P ratio are 20 $\mu g \cdot L^{-1}$, 10 $\mu g \cdot L^{-1}$, and 18, respectively (Y.T. Prairie, unpublished data). Because of the lake's size (14.5 km^2), wind action mixes the water column completely except in the deepest basin (12 m) where a small hypolimnion develops with a weak thermal stratification. The warm hypolimnion (18°C) creates a highly metabolic environment supporting areal oxygen consumption rates of >500 mg $O_2 \cdot m^{-2} \cdot day^{-1}$ and a P release rate of 4–5 mg $P \cdot m^{-2} \cdot day^{-1}$ (Prairie et al. 2000).

Sampling

For the field study, sampling was performed weekly from early June to late September 1996. Duplicate sediment samples were collected with a Kajak–Brinkhurst gravity corer at the water–sediment interface (0–1 cm) of four stations along a transect crossing the oxycline of the lake (Fig. 1B). Stations 1 and 2 (3 and 6 m deep, respectively) were well oxygenated throughout the study period whereas stations 3 and 4 (9 and 12 m deep, respectively) became anoxic after thermal stratification. Dissolved oxygen profiles

© 2000 NRC Canada

Table 1. Mean bacterial and viral abundances and VBR according to oxygen conditions for the field study and the core incubation study before and after the onset of anoxia in the sediments.

	Field study			Core incubation study		
	Bacteria (cells·mL^{-1})	Viruses (particles·mL^{-1})	VBR	Bacteria (cells·mL^{-1})	Viruses (particles·mL^{-1})	VBR
Oxic conditions	6.79×10^9 (n = 31)	7.14×10^9 (n = 31)	1.07	6.47×10^9 (n = 5)	4.81×10^9 (n = 5)	0.7
Anoxic conditions	4.69×10^9 (n = 15)	5.39×10^9 (n = 15)	1.24	3.39×10^9 (n = 7)	3.08×10^9 (n = 7)	0.9

Fig. 2. Temporal changes in oxygen concentrations at station 1 (●), station 2 (▲), station 3 (▼), and station 4 (■). The vertical broken line indicates the start of thermal stratification.

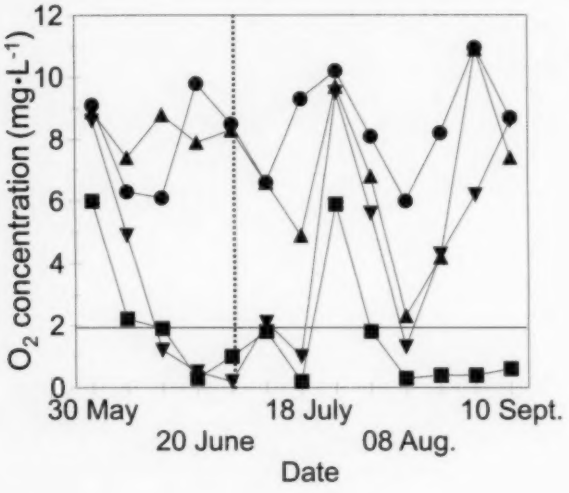

and the organic matter content at the water–sediment interface were measured for each station at each sampling.

For the core incubation study, 24 sediment cores were collected by divers in late May 1997 before thermal stratification at the water–sediment interface of a well-oxygenated zone located at 9 m depth (equivalent to station 3 of the field study). The volume of water overlying the sediments in each core was 0.8 L. The cores were sealed and covered with aluminium foil in order to minimize light penetration. The cores were incubated at constant temperature (in situ temperature of 14.5°C) for 7 days. Given the rate of oxygen consumption and the small overlying volume, the cores became anoxic within about 3 days. Duplicate cores were sacrificed twice daily for a period of 1 week and sampled at the water–sediment interface.

All virus and bacteria samples from both studies were immediately fixed after collection in 10 times their volume of a 3.7% formalin solution. They were then kept at 4°C in the dark for further manipulations. All samples were taken in duplicate.

Desorption method

Samples (1 mL) were first diluted to a final dilution of 1000-fold. Aggregates were dissociated by using a rotating pestle for 1.5 min following the protocol of Lindahl and Bakken (1995). Samples were then left to incubate for 1 h in solution with 0.01 M pyrophosphate ($Na_4P_2O_7$) in order to break the ionic bonds between the microorganisms and the particles. Finally, samples were gently sonicated (Sonic 300 dismembrator, Artek Syst. Corp., New York) at medium-low intensity (30%) for 30 s.

Staining method

Aliquots (0.2 mL) of the samples were filtered and rinsed through a 0.2-μm pore size membrane filter (Anodisc 25, Whatman) under a vacuum of less than 2.5 kPa. The filters were then stained with the nucleic acid stain YO-PRO (4-(3-methyl-2,3-dihydro(benzo-1,3-oxazole)-2-methylmethyledene)-1-(3′-trimethylammoniumpropyl)-quinolinium diiodide); Molecular Probes, Eugene, Oreg.) for examination in an epifluorescence microscope (Leitz DMRB, Leica, Germany) following the method of Hennes and Suttle (1995) adapted to formalin-fixed samples by Xenopoulos and Bird (1997). Using this technique, viruses and bacteria are distinguished on the basis of size and relative brightness. A minimum of 200 cells were counted in over 20 fields of view per slide using a Whipple grid and under a total magnification of 1000×. All abundances are expressed as cells per millilitre of wet sediments.

The organic matter content of each sample was measured as loss of dry mass on ignition from dry sediments burned at 550°C for 2 h.

Results

Oxygen depletion

In 1996, Lac Brome was thermally stratified from 13 June to 10 September (Fig. 2). Before stratification, all stations were oxygenated. After stratification, however (at 7 m), hypolimnetic stations 3 and 4 quickly became anoxic. We considered the sediment–water interface to be anoxic when the oxygen level was less than 2.0 mg·L^{-1} at 1 m above sediments, a criterion successfully used by Marsden (1989). On 25 July, a storm eroded the thermocline and temporally brought oxygen to the hypolimnion, completely reoxygenating station 3 and partially so for the deeper station 4. Slightly elevated oxygen concentrations remained for about 2 weeks at these stations. However, after 8 August, the thermocline deepened further such that only station 4 remained anoxic. Because of the changing oxygen state of some stations through time, we divided the data into oxic and anoxic sites/dates for all further analyses unless otherwise stated.

Temporal changes in microbial abundances

Average bacterial and viral abundances for Lac Brome sediments were similar at 6.07×10^9 and 6.54×10^9 cells·mL^{-1}, respectively (see Table 1 for means according to oxygen status). Although these densities fall within the range of expected abundances for nutrient-rich lakes, they exhibited considerable variability (nearly one order of magnitude) in both space and time. There is a highly significant and strong positive relationship between bacterial and viral abundances within the sediments (all dates and stations combined, r^2 = 0.69, $p < 0.0001$, n = 47) (Fig. 3). An ANCOVA showed that the same relationship holds true in both oxic and anoxic conditions ($p > 0.05$) (see density ellipses in Fig. 3).

Separating the sites/dates into oxic and anoxic conditions shows that there is a large and highly significant difference in the abundance of both bacteria (t test, $p < 0.0001$) and vi-

© 2000 NRC Canada

Fig. 3. Log–log relationship between bacterial and viral abundances for field study samples with density ellipses (90%) distinguishing oxic and anoxic sites/dates.

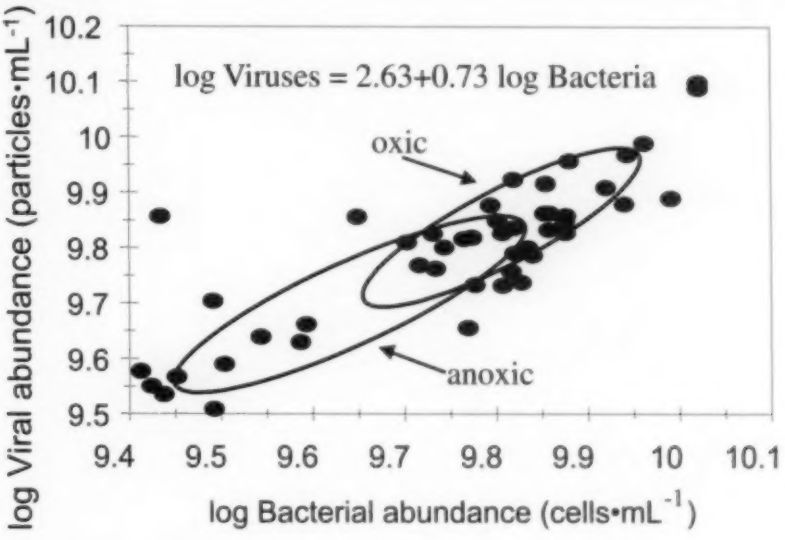

ruses (t test, $p < 0.0001$). Both microbial communities are much more impoverished in anoxic conditions relative to the oxic sites/dates. This pattern is discernible not only among all sites/dates but also within sites undergoing changes in their oxygen status. At stations 3 and 4, bacterial and viral densities were both significantly greater on oxic relative to anoxic dates (t test, $p < 0.05$). Thus, the trend is consistent in both space (among sites of different oxygen status) and time (within a site through time). Overall losses in anoxic conditions during the whole stratified period were 31 and 25% for bacteria and viruses, respectively.

The viruses to bacteria ratio (VBR) was low (generally near 1) and similar to the results for nearby Lac Gilbert (Maranger and Bird 1996). There was a weak but significant negative relationship between VBR and bacterial abundance ($r^2 = 0.34$, $p < 0.001$, $n = 47$) (Fig. 4). We also found a significant relationship between oxygen status and VBR ($p < 0.05$). However, no significant relationship was found between the quantity of organic matter available (0.15–0.22 g dry weight·cm^{-3}) and either viral abundance, bacterial abundance, or VBR.

Core incubations

This controlled experiment was designed to provide a more detailed view of viral and bacterial behavior before, during, and after the onset of anoxia. Given accelerated oxygen depletion, sampling was performed twice daily to closely follow short-term bacterial dynamics.

The results were strikingly similar to those obtained in the field study, although initial abundances were lower presumably because of the lower initial oxygen concentration (3.2 mg·L^{-1}). The relationship between bacterial and viral abundance was positive ($r^2 = 0.75$, $p < 0.0003$, $n = 12$) (Fig. 5) and very similar to that found in the lake the previous year. There was a significant positive relationship between oxygen concentration and bacterial abundance ($r^2 = 0.55$, $p < 0.01$, $n = 12$) as well as between oxygen concentration and viral abundance ($r^2 = 0.46$, $p < 0.05$, $n = 12$). The relationship between VBR and bacterial abundance was slightly negative, although not significant, and unlike the field study, no significant correlation was found between oxygen conditions and VBR.

Mean bacterial abundance in both oxic and anoxic environments in the cores was similar and not significantly different from that of the field study (t test, $p = 0.43$ and $p = 0.16$, respectively) (Table 1). This was not the case for mean viral abundance (t test, $p = 0.002$ and $p = 0.0015$, respectively) where initial abundance was lower than that of the field study. Decline of numbers following anoxia was found to be greater for bacteria than for viruses, with losses of 47.6 and 36.0%, respectively.

Discussion

The relationship between sediment bacterial and viral abundance observed in Lac Brome is consistent with analogous patterns found in the water columns of freshwater systems (Paul et al. 1991; Thingstad et al. 1993; Maranger and Bird 1995). It is, however, different from the conclusion of Maranger and Bird (1996) in their study of the sediments of nearby Lac Gilbert where they did not find any significant trend. This may be attributable to the fact that on their single sampling date, the range in bacterial abundance was much smaller than in Lac Brome, therefore reducing their ability to detect such a relationship.

Both observational and experimental studies of microbial dynamics in Lac Brome demonstrated not only that bacterial and viral abundances are similar in absolute counts, but that they follow a nearly identical pattern when subject to changes in the oxic state of their environment. Maranger and Bird (1996) also found a decline in the abundance of viruses in anoxic sites. The consistency of the results strongly sug-

© 2000 NRC Canada

Fig. 4. Log–log relationship between bacterial abundance and VBR for field study samples.

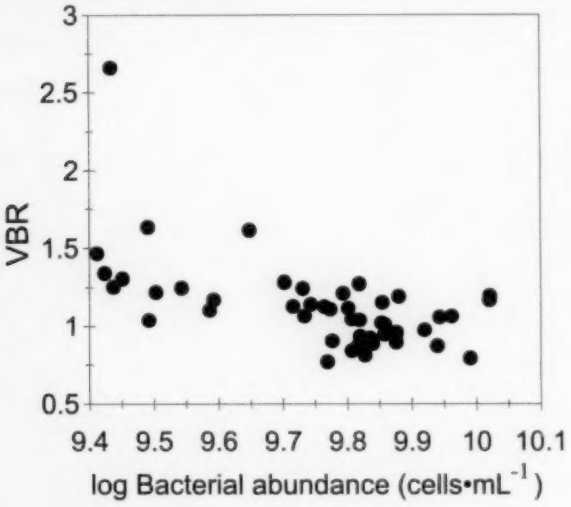

Fig. 5. Log–log relationship between bacterial and viral abundances for core incubation samples (all cores combined).

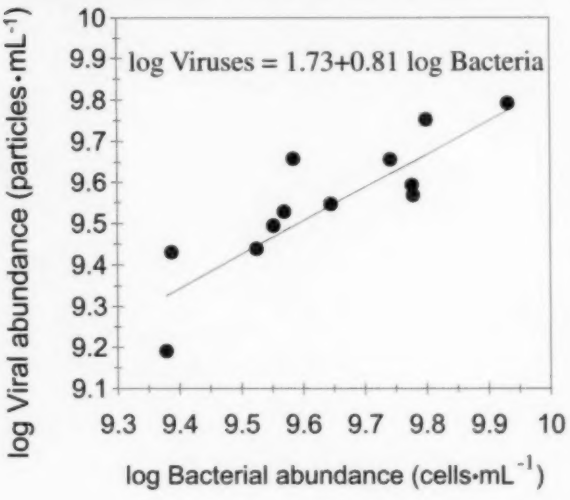

gests that a shift in the densities of both communities is attributable to the onset of anoxia, either directly or indirectly.

Processes of bacterial removal in the sediments are not well understood. The general microbial decline might be interpreted as the viral-induced bacterial lysis following an environmental stress. Rapid changes in oxygen conditions are known to induce strictly aerobic bacteria to lyse (Boström et al. 1988, 1989). However, our data suggest that viruses play a relatively minor role in bacterial mortality in Lac Brome. Intense viral lysis would be expected to produce much increased viral densities relative to bacteria after the viruses have completed their lytic cycle. Instead, VBR was only slightly increased in anoxic conditions. This was most clearly shown in the incubation study where the microbial communities were followed very closely in time. There were no significant changes in VBR and we did not even find a temporary increase in VBR following anoxia. Although viral-induced cell lysis cannot be completely ruled out, we suggest that this is probably not quantatively important. At best, it may significantly affect small subpopulations of bacteria, which would require specific probes to be detected. This apparent lack of viral-induced bacterial mortality may be associated with the very low viral burden (VBR near 1) that the sediment bacteria have to contend with compared with bacterial assemblages from the water column (VBR = 20–25 in freshwater systems, Maranger and Bird 1995).

Our results are more consistent with a restriction of metabolic pathways involving the loss of strictly aerobic bacteria. First, the fact that the relationship between viruses and bacteria is the same in oxic and anoxic environments suggests that viral abundance depends on the density of their hosts more than the converse. Second, a massive bacterial mortality due to viral-induced lysis would be expected to be short-lived as anaerobic bacteria replace the loss of strictly aerobic bacteria. However, we did not observe a recovery in the bacterial abundance in either study. Since the supply of organic C does not change after the onset of anoxia, we suggest that bacterial abundance declines in these conditions because they become limited by the availability of alternative respiratory terminal electron acceptors such as nitrates, sulfates, and particularly ferric iron, known to be controlled by the amount of reducible Fe in the sediments (Prairie et al. 2000). In short, our data suggest that the effect of anoxia on viruses is best explained as an indirect effect of the reduction in the bacterial host abundance. A similar phenomenon has been observed in soil microbial communities (Lawson et al. 1987).

Implication for P release

Whatever the biological mechanism leading to the reduction in microbial abundance, we can calculate a maximum estimate of the P potentially released from the sediments originating from the release of viral and bacterial content. In our calculations, we assumed that bacterial and viral P contents were 5.04 fg·bacterium^{-1} (Turc et al. 1992) and 0.008 fg·viral particle^{-1} (Matthews et al. 1983, cited in Børsheim et al. 1990) and also that only the first centimetre of the water–sediment interface is affected by the change in oxygen status. From initial bacterial and viral abundances of 7.27×10^9 and 7.24×10^9·mL^{-1}, respectively, in the well-oxygenated environment, and using the observed mean bacterial and viral losses of 45 and 35%, respectively, the mass of P liberated is

$$P_{max} = (3.27 \times 10^9 \cdot mL^{-1} \times 5.04 \times 10^{-15}\ g) + (2.53 \times 10^9 \cdot mL^{-1} \times 0.008 \times 10^{-15}\ g) = 16.5\ \mu g \cdot cm^{-2} \text{ or } 165\ mg \cdot m^{-2}$$

First, this calculation shows that the potential contribution of viruses is minimal to the microbial P release. Second, Prairie and del Giorgio (1995) estimated from hypolimnetic P accumulation and porewater P profiles that during the anoxic period, an average of about 4 mg P·m^{-2}·day^{-1} is released from the sediments of Lac Brome. Depending on the diffusion and mineralization rates of this freshly produced organic substrate (the lysed bacterial and viral contents), the

© 2000 NRC Canada

release of P can extend over a long period even if the lysis itself is sudden. Nevertheless, the estimated P loss from bacteria and virus decay is sufficient to sustain the observed rate over 40 days, representing about 70% of the stratified period. Thus, even if a portion of the lysed microbial P content is readsorbed onto particles or assimilated by other organisms (Uehlinger 1986), the observed microbial mortality can help explain the very high P concentration in the interstitial waters of the surface sediments overlain with anoxic waters and possibly even the surge in P release often observed at the beginning of anoxia. The generality of this phenomenon clearly needs further testing.

In summary, two different approaches showed that the transition between an oxic and an anoxic environment produces consistent and large changes in the abundance of both bacterial and viral communities. Viral-induced lysis does not appear to be a major mortality factor for sediment bacteria. Instead, we suggest that the viral population decreased as a result of the decreased abundance in the aerobic bacterial hosts. Simple mass-balance calculations showed that the observed microbial mortality is sufficient to produce a substantial P release.

Acknowledgments

This research is a contribution to the GREAU (Groupe de Recherche en Écologie Aquatique de l'Université du Québec à Montréal) and the GRIL (Groupe de Recherche Interuniversitaire en Limnologie) and was funded by an operating grant to Y.T.P. from the Natural Sciences and Engineering Research Council of Canada. We thank the City of Lac Brome for technical support during sampling. C.M. Duarte and S.K. Juniper made valuable comments on the manuscript.

References

Bates, M., and Neafus, N.J.E. 1980. Phosphorus release from sediments from Lake Carl, Blackwell, Oklahoma. Water Res. **14**: 1477–1481.

Bergh, Ø., Børsheim, K.Y., Bratbak, G., and Heldal, M. 1989. High abundance of viruses found in aquatic environments. Nature (Lond.), **340**: 467–468.

Børsheim, K.Y., Bratbak, G., and Heldal, M. 1990. Enumeration and biomass estimation of planktonic bacteria and viruses by transmission electron microscopy. Appl. Environ. Microbiol. **56**: 352–366.

Boström, B., Ahlgren, I., and Bell, R.T. 1985. Internal nutrient loading in a shallow eutrophic lake, reflected in seasonal variations of some sediment parameters. Verh. Int. Ver. Limnol. **22**: 3335–3339.

Boström, B., Andersen, J.M., Fleisher, S., and, Jansson, M. 1988. Exchange of phosphorus across the sediment–water interface. Hydrobiologia, **170**: 229–244.

Boström, B., Pettersson, A.-K., and Ahlgren, I. 1989. Seasonal dynamics of a cyanobacteria-dominated microbial community in surface sediments of a shallow eutrophic lake. Aquat. Sci. **51**: 153–178.

Brunberg, A.-K., and Boström, B. 1992. Coupling between benthic biomass of *Microcystis* and phosphorus release from the sediments of a highly eutrophic lake. Hydrobiologia, **235/236**: 375–385.

de Montigny, C., and Prairie, Y.T. 1993. The relative importance of biological and chemical processes in the release of phosphorus from a highly organic sediment. Hydrobiologia, **253**: 141–150.

Eckerrot, Ä., and Pettersson, K. 1993. Pore water phosphorus and iron concentrations in a shallow, eutrophic lake — indication of bacterial regulation. Hydrobiologia, **253**: 165–177.

Fleisher, S. 1978. Evidence for the anaerobic release of phosphorus from lake sediments as a biological process. Naturwissenschaften, **65**: 109–110.

Fuhrman, J. 1999. Marine viruses and their biogeochemical and ecological effects. Nature (Lond.), **399**: 541–548.

Gächter, R., and Meyer, J.S. 1993. The role of microorganisms in mobilization and fixation of phosphorus in sediments. Hydrobiologia, **253**: 103–121.

Gobler, C.J., Hutchins, D.A., Fisher, N.S., Cosper, E.M., and Sanudo-Wilhelmy, S.A. 1997. Release and bioavailability of C, N, P, Se, and Fe following viral lysis of a marine chrysophyte. Limnol. Oceanogr. **42**: 1492–1504.

Hennes, K.P., and Suttle, C. 1995. Direct counts of viruses in natural waters and laboratory cultures by epifluorescence microscopy. Limnol. Oceanogr. **40**: 1050–1055.

Lammers, W.T. 1988. Yearly flux of virus-like particles and humic acid in river sediment. Verh. Int. Ver. Limnol. **23**: 1219–1223.

Lawson, K.A., Barnett, Y.M., and McGilchrist, C.A. 1987. Environmental factors influencing numbers of *Rhizobium leguminosarum* biovar *trifolii* and its bacteriophages in two field soils. Appl. Environ. Microbiol. **53**: 1125–1131.

Lindahl, V., and Bakken, L.R. 1995. Evaluation of methods for extraction of bacteria from soil. FEMS Microbiol. Ecol. **16**: 135–142.

Maranger, R., and Bird, D.F. 1995. Viral abundance in aquatic systems: a comparison between marine and fresh waters. Mar. Ecol. Prog. Ser. **121**: 217–226.

Maranger, R., and Bird, D.F. 1996. High concentrations of viruses in the sediments of Lac Gilbert, Québec. Microb. Ecol. **31**: 141–151.

Maranger, R., Bird, D.F., and Juniper, S.K. 1994. Viral and bacterial dynamics in Artic Sea ice during the spring algal bloom near Resolute, N.W.T., Canada. Mar. Ecol. Prog. Ser. **111**: 121–127.

Marsden, M.W. 1989. Lake restoration by reducing external phosphorus loading: the influence of sediment phosphorus release. Freshwater Biol. **21**: 139–162.

Matthews, C.K., Kutter, E.M., Mosig, G., and Berget, P.B. (*Editors*). 1983. Bacteriophage T4. American Society for Microbiology, Washington, D.C.

Middelboe, M., Jorgensen, N.O.G., and Kroer, N. 1996. Effects of viruses on nutrient turnover and growth efficiency of noninfected marine bacterioplankton. Appl. Environ. Microbiol. **62**: 1991–1997.

Paul, J.H., Jiang, S.C., and Rose, J.B. 1991. Concentration of viruses and dissolved DNA from aquatic environments by vortex flow filtration. Appl. Environ. Microbiol. **57**: 2197–2204.

Prairie, Y.T., and del Giorgio, P.A. 1995. Lake Brome project 1995. Final report. Ville de Lac Brome, Que.

Prairie, Y.T., de Montigny, C., and del Giorgio, P. 2000. Phosphorus release from anoxic sediments: a paradigm revisited. Verh. Int. Ver. Limnol. In press.

Proctor, L.M., Okubo, A., and Fuhrman, J.A. 1993. Calibrating estimates of phage-induced mortality in marine bacteria: ultrastructural studies of marine bacteriophage development from one-step growth experiments. Microb. Ecol. **25**: 161–182.

Thingstad, T.F., Heldal, M., Brabtak, G., and Dundas, I. 1993. Are viruses important partners in pelagic foodwebs? Trends Ecol. Evol. **6**: 209–213.

© 2000 NRC Canada

Turc, V., Rehnstam, A.-S., Lundberg, E., and Hagström, Å. 1992. Release of bacterial DNA by marine nanoflagellates, an intermediate step in phosphorus regeneration. Appl. Environ. Microbiol. **58**: 3744–3750.

Uehlinger, U. 1986. Bacteria and phosphorus regeneration in lakes. An experimental study. Hydrobiologia, **135**: 197–206.

Weinbauer, M.G., and Hoefle, M.G. 1998. Significance of viral lysis and flagellate grazing as factors controlling bacterioplankton production in a eutrophic Lake Plussee. Appl. Environ. Microbiol. **64**: 431–438.

Xenopoulos, M.A., and Bird, D.F. 1997. Virus à la sauce YO-PRO: microwave enhanced staining for enumerating virus natural water by epifluorescence microscopy. Limnol. Oceanogr. **42**: 1648–1650.

© 2000 NRC Canada

Comparison of techniques of back-calculation of growth and settlement marks from the otoliths of three species of *Diplodus* from the Mediterranean Sea

Laurent Vigliola, Mireille Harmelin-Vivien, and Mark G. Meekan

Abstract: We developed a model of back-calculation of fish size from otoliths that could accommodate both changes in the relationship between otolith and somatic growth that occur through time and variation in growth rates among individuals. We used this model to back-calculate estimates of size and growth from otoliths of three species of *Diplodus* from the Mediterranean Sea. The outcomes of our model were compared with those of three other models and with growth curves estimated directly from populations of fish in the field. We found that our new model produced estimates of size-at-age that were closer to those observed in the field than the biological intercept, time-varying growth, and body proportional models. Comparison of profiles of increment width from otoliths of newly settled and juvenile *Diplodus puntazzo* and *Diplodus vulgaris* showed that these species formed a settlement mark, where increment width declined at settlement. In contrast, a settlement mark was not evident in the otoliths of *Diplodus sargus*. However, settlement of all species coincided with a sharp decline in somatic growth rate. Thus, growth rate may provide a means of estimating the timing of settlement in species that do not display a marked change in increment width.

Résumé : Nous avons élaboré un modèle de rétrocalcul de la taille des poissons à partir des otolithes qui pourrait prendre en compte à la fois les modifications du rapport entre la croissance d'après les otolithes et la croissance somatique sur une période donnée, et la variation du taux de croissance d'un individu à l'autre. Nous avons utilisé ce modèle pour effectuer un rétrocalcul des estimations de la taille et de la croissance à partir d'otolithes de trois espèces de *Diplodus* de la Méditerranée. Nous avons comparé les résultats de notre modèle à ceux de trois autres modèles et aux courbes de croissance établies directement à partir de populations de poisson dans le milieu naturel. Notre nouveau modèle permet d'obtenir des estimations de la taille en fonction de l'âge qui s'approchent plus des données observées sur le terrain que les données fournies par le modèle biologique des points d'intersection, celui de la croissance variant dans le temps et celui des proportions corporelles. La comparaison des profils de la grandeur de l'espacement des anneaux de croissance sur les otolithes de *Diplodus puntazzo* et de *D. vulgaris* juvéniles et nouvellement installés sur le fond a montré l'apparition d'une marque d'établissement, la grandeur de l'espacement diminuant au moment de l'établissement sur le fond. Par contraste, la présence d'une marque d'établissement n'était pas évidente sur les otolithes de *D. sargus*. Toutefois, l'établissement sur le fond, chez toutes les espèces, a coïncidé avec une diminution nette du taux de croissance somatique. Par conséquent, le taux de croissance serait un moyen d'estimer le moment de l'établissement sur le fond des espèces chez lesquelles on n'observe aucune variation prononcée de la grandeur de l'espacement.

[Traduit par la Rédaction]

Introduction

Otolith analysis has become a standard technique in fisheries science and provides a great deal of information about the life histories of young fish at both the population and individual levels. Counts of increments in otoliths have enabled ages to be determined on a daily basis (Pannella 1971; Campana and Jones 1992). In species where there is a strong relationship between otolith and somatic growth of the fish, individual longitudinal records of growth can be back-calculated from sequential measurements of the width of increments (Francis 1990; Campana and Jones 1992).

All models of back-calculation of growth from otoliths rely on two major assumptions. Firstly, it is assumed that the rate of deposition of increments within the otolith does not vary. Experimental studies have validated this assumption for numerous species (Geffen 1992). Secondly, models assume that there is proportionality between the growth of the otolith and somatic growth of the fish. Evidence for this phenomenon is usually derived from strong correlations between size of the otolith and body size of fish.

Relatively few studies have been able to demonstrate a complete lack of proportionality between otolith and fish size. Some of those that have done so have been confounded

Received August 24, 1999. Accepted March 1, 2000.
J15331

L. Vigliola[1] **and M. Harmelin-Vivien.** Centre d'Océanologie de Marseille, Université de la Méditerranée, CNRS UMR 6540, Station Marine d'Endoume, 13007 Marseille, France.
M.G. Meekan. Australian Institute of Marine Science, P.O. Box 264, Dampier, WA 6713, Australia.

[1]Author to whom all correspondence should be addressed.
e-mail: l.vigliola@aims.gov.au

© 2000 NRC Canada

by problems in regression analysis and sample selection (Meekan et al. 1998). However, changes in the otolith size – fish size relationship among ontogenetic stages appear to be commonplace in many species (Secor and Dean 1992; Hare and Cowen 1995; Sirois et al. 1998). Furthermore, otolith size may be dependent on absolute growth rate, so that otoliths from fast-growing fish are smaller than those of slow-growing fish of the same size. This has been termed a growth effect (Secor and Dean 1992; Sirois et al. 1998).

Some models of back-calculation have been developed that explicitly address these problems. For example, the biological intercept (BI) method (Campana 1990; Campana and Jones 1992) constrains models of back-calculation to known intercepts of otolith and fish size in order to account for growth effects. However, the model still assumes that the same linear relationship between otolith and fish size is maintained over the period for which sizes are back-calculated and thus remains vulnerable to changes in otolith size – fish size relationships that occur over time (Campana 1990; Secor and Dean 1992). Sirois et al. (1998) dealt with this latter problem by proposing a time-varying growth (TVG) model. Effectively, this model retains a constant linear relationship between otolith and fish size throughout life history stages by weighting the contribution of individual increments in a length back-calculation.

The BI and TVG models represent only one approach to solving the problems inherent in back-calculation of growth histories from otoliths. Both effectively assume that the underlying relationship between fish and otolith size is isometric. The BI model can only be used for back-calculation when this assumption is valid, while the TVG model provides a means of transforming an allometric relationship between otolith and fish size into isometry. However, a number of models have been proposed that do not require the assumption of isometry in order to back-calculate size measurements (Francis 1990). To date, there have been few attempts to examine the use of such models.

Here, we develop a model for back-calculation of growth from otoliths that is capable of dealing with the problem of allometry between otolith and fish size and is not vulnerable to growth effects. This is applied to the back-calculation of growth of three species of *Diplodus* from the Mediterranean Sea. The outcomes of our model are compared with those of three other models of back-calculation and with growth curves estimated directly from populations of fish in the field. Finally, we use our model to determine if a settlement mark corresponding to the transition between planktonic and benthic environments exists in the otoliths of *Diplodus* and if this was associated with a change in somatic growth.

Materials and methods

Selection and development of a back-calculation model

A model for back-calculation must clearly define the form of the relationship between otolith and fish growth. We assumed that there was proportionality between the relative growth rates of the fish and the otolith:

$$(1) \qquad \mathrm{d}(L-a)((L-a)\mathrm{d}t)^{-1} = c\mathrm{d}R(R\mathrm{d}t)^{-1}$$

where L and R are fish length and otolith radius, respectively, at time t, a is the body length of an individual at otolith formation (Fraser 1916; Lee 1920), and c is the proportionality coefficient. Solution of this differential equation results in the well-known formula for an allometric relationship between two dimensions of an organism (eq. 2) (Ricker 1975, 1979) or a linear relationship (eq. 3) in the case of isometry (i.e., where $c = 1$):

$$(2) \qquad L = a + bR^c$$

$$(3) \qquad L = a + bR$$

where b is the slope of the L–R relationship and $a > 0$ (Francis 1990).

The choice between these two formulae was made on the basis of their fit to the shape of the relationship between otolith and fish size. In order to avoid growth effects (Campana 1990), we included a biological intercept (R_{0p}, L_{0p}) in back-calculation eqs. 2 and 3 prior to fitting them to data sets so that they became, respectively,

$$(4) \qquad L = L_{0p} - bR_{0p}^c + bR^c$$

$$(5) \qquad L = L_{0p} - bR_{0p} + bR$$

Where the linear eq. 5 provided the best fit to the shape of the relationship between otolith and fish size, the model of Campana (1990) and the body proportional hypothesis (BPH) model of Francis (1990) (with $c = 1$) were appropriate for back-calculation (Table 1). Where the allometric eq. 4 provided the best fit to the otolith size – fish size data set, the model of Fry (1943), the TVG model of Sirois et al. (1998), and the BPH model of Francis (1990) were appropriate for back-calculation. While a variety of other models have been developed for back-calculation (see review by Francis 1990; also see Tremblay and Giguère 1992; Watanabe and Kuroki 1997), these do not clearly state the form of the relationship between otolith and fish growth. For this reason, such models were not included in our study.

Despite the suitability of Fry's model, it does not possess a biological intercept and is thus vulnerable to growth effects. This problem was corrected by incorporating a biological intercept and by using eq. 4 to calculate a (body length at otolith formation), where $a = L_{0p} - bR_{0p}^c$. This modified version of Fry's model possessed the required characteristics of an allometric relationship between fish and otolith size and invulnerability to growth effects. As eq. 4 could be fitted using R or L as the independent variable, two values of a could be derived. The average of these estimates was used in this back-calculation model (Table 1).

Study organisms

Our study examined three sparid fishes of the genus *Diplodus* during the months immediately following their settlement into a nursery habitat of shallow (0–7 m) slopes of sand, pebbles, or boulders in sheltered bays (Garcia-Rubies and Macpherson 1995; Harmelin-Vivien et al. 1995). *Diplodus puntazzo* (Cetti) settled from October to the beginning of November, while *Diplodus sargus* (Linnaeus) settled from late May until late June. *Diplodus vulgaris* (Geoffroy Saint-Hilaire) settled in two distinct peaks, the first in early November and the second from January to March (Garcia-Rubies and Macpherson 1995; Vigliola et al. 1998). *Diplodus puntazzo* and *D. vulgaris* departed the nursery habitat from May to June, while *D. sargus* departed in September (Macpherson 1998).

Sampling

Young *D. sargus*, *D. vulgaris*, and *D. puntazzo* were collected with hand nets near Marseille, France (43°10′N, 5°20′E), from November 1993 to June 1996. Sampling focused on the weeks following settlement and the month immediately prior to the departure of fish from the nursery habitat. A few individuals of a variety of sizes were also captured at regular intervals in order to provide a

© 2000 NRC Canada

Table 1. Summary of the four back-calculation models examined in this study: biological intercept (BI) (Campana 1990), modified Fry (1943) (see Materials and methods), time-varying growth (TVG) (Sirois et al. 1998), and body proportional hypothesis (BPH) (Francis 1990).

	Back-calculation models
BI	$L_i = L_{cpt} + (R_i - R_{cpt})(L_{cpt} - L_{0p})(R_{cpt} - R_{0p})^{-1}$
	L_i obtained directly from R_i
Modified Fry	$L_i = a + \exp(\ln(L_{0p} - a) + (\ln(L_{cpt} - a) - \ln(L_{0p} - a))(\ln(R_i) - \ln(R_{0p}))(\ln(R_{cpt}) - \ln(R_{0p}))^{-1})$
	$a = (a_1 + a_2)/2$
	$a_1 = L_{0p} - b_1 R_{0p}^{c_1}$; b_1 and c_1 estimated from the regression of $L = L_{0p} - b_1 R_{0p}^{c_1} + b_1 R^{c_1}$
	$a_2 = L_{0p} - b_2 R_{0p}^{c_2}$; b_2 and c_2 estimated from the regression of $R = ((L - L_{0p} + b_2 R_{0p}^{c_2}) b_2^{-1})^{-c_2}$
TVG	$L_i = L_{0p} + \sum_{i=1}^{t} (W_i + G_e(W_i - W))(L_{cpt} - L_{0p})(R_{cpt} - R_{0p})^{-1}$
	Growth effect G_e estimated as in Sirois et al. (1998)
BPH	$L_i = g(R_i)(g(R_{cpt}))^{-1} L_{cpt}$ with $g(R) = L = a + bR^c$
	a, b, and c estimated from the regression of $L = g(R)$; in the case of isometry, $c = 1$ in the model

Note: L, fish length; R, otolith radius; L_{0p}, fish length at biological intercept; L_i, length at age i; L_{cpt}, length at capture; R_{0p}, otolith radius at biological intercept; R_i, radius at age i; R_{cpt}, radius at capture; W, mean increment width during each developmental stage; W_i, increment width at age i.

growth series of fish. During the course of the study, a total of 1033 *D. sargus* ranging from 6.3 to 158 mm standard length (SL), 1318 *D. vulgaris* ranging from 8.7 to 155 mm SL, and 525 *D. puntazzo* ranging from 7.4 to 153 mm SL were collected. Fish were immediately preserved in 70% ethyl alcohol after capture and standard and total lengths measured using callipers. Measurement error ranged from ±0.2 mm for smaller individuals to ±1 mm for larger individuals.

For otolith analysis, fish smaller than 80 mm SL were divided into 1-mm size-classes and two fish then selected from each size-class where possible. Six fish ranging from 80 to 160 mm SL were also selected from collections of each species. Together, these fish represented a complete ontogenetic series of individuals from settlement to sexual maturity, which occurs at a size of 15–17 cm and an age of 2 years in *Diplodus* (Fisher et al. 1987). In addition, 40 newly settled fish from the 1994–1995 year-class and 40 juveniles from each of the 1994–1995 and 1995–1996 year-classes were also selected for otolith analysis. Juvenile fish were collected during the month prior to their exit from the nursery habitat (Table 2).

Growth of young *Diplodus* was estimated visually by SCUBA divers at four sites near the habitat where fish were collected. Four replicate counts were made along 40 × 3 m transects at each site at weekly intervals during each of the 1994–1995 and 1995–1996 seasons. Counts recorded the number of fish and their total lengths by comparison with silhouettes (5-mm scale) on a plastic sheet (Planes et al. 1999). The error associated with estimating size by this method was determined by comparing visual estimates with the actual sizes of fish after capture and was always <3.5 mm (Macpherson 1998) (Table 2). Final data were reduced to a mean total length for each species at each sampling time using the method of Planes et al. (1999).

Otolith analysis

Sagittae were dissected from fish using a binocular microscope. Otoliths from individuals selected in the ontogenetic series were placed on a slide and treated with a clearing agent (camomile essence) to enhance visibility of the core. The radii of right and left otoliths from each fish were measured along the dorsal axis from the core to the edge of the sagitta. As radii from left and right otoliths were not significantly different (t test, $p > 0.05$), the average of the two measures was taken as the otolith radius of an individual.

One otolith from each of the fish from the remaining subsamples (40 settlers from the 1994–1995 year-class and 40 juveniles from each of the two consecutive year-classes) was selected and embedded in resin. A transverse section containing the core of the otolith was removed and polished until increments could be easily observed using a compound microscope (Vigliola 1997). The radius and width of each increment were measured three times along the same dorsal axis of each sectioned otolith using an image analysis system.

Vigliola (1997) validated the daily pattern of increment formation in postsettlement *Diplodus*. In the present study, we assumed that increments were also deposited daily during the presettlement phase, as is the case in many species, (e.g., Jones 1986) including other sparids (Tsuji and Aoyama 1982). We also assumed that the first increment in the otolith was formed at hatching (Tsuji and Aoyama 1982).

Application of back-calculation models

Average length at hatching (L_{0p}) of the three *Diplodus* species was 2.5 mm SL (Divanach 1985). Otolith radii at hatching (R_0) were averaged from all sectioned otoliths ($n = 120$) for each of the three species to obtain a mean value (R_{0p}). Estimates of R_{0p} were 9.7, 9.8, and 9.4 µm for *D. sargus*, *D. vulgaris*, and *D. puntazzo*, respectively. These values were included in back-calculation eqs. 4 and 5, which were then fitted to otolith size – fish size data sets by nonlinear regression using the least squares method and the quasi-Newton algorithm (Gill and Murray 1972). Residuals were plotted and their normality examined using Kolmogorov–Smirnov (K-S) tests. Finally, longitudinal records of size were back-calculated for each individual using the models listed in Table 1. To calculate the TVG model, the life history of *Diplodus* was divided into planktonic larval and benthic juvenile stages. An average age at settlement was estimated for each *Diplodus* species from increment counts of otoliths of fish collected in the days immediately following settlement.

Comparison of back-calculation models

Growth curves obtained from size back-calculations were compared with curves derived from visual census. Visual census data sets from each of the four sites were averaged for each sampling occasion to obtain a growth curve for each *Diplodus* species. Curves were extrapolated using published values for length-at-age of larvae (Divanach 1985) to include the planktonic stage of the life history of the three species.

© 2000 NRC Canada

Table 2. Summary of sampling of *Diplodus*.

Sample	Species	Sampling period	*n*	Length (mm) Mean (SD)	Range
Ontogenetic series	*D. sargus*	May 1994 – Nov. 1996	114	44.3 (29.23)	6.3–158
	D. vulgaris	Nov. 1994 – Nov. 1996	93	37.0 (27.43)	8.7–155
	D. puntazzo	Oct. 1994 – Nov. 1996	86	39.9 (27.67)	7.4–153
Settlers	*D. sargus*	25 May 1994	40	8.2 (0.87)	6.2–9.8
	D. vulgaris	9 Jan. 1995	40	11.4 (0.77)	9.9–12.9
	D. puntazzo	27 Oct. 1994	40	10.0 (0.57)	8.9–11.1
Juveniles	*D. sargus*	Sept. 1994	40	48.7 (6.89)	39–68
		Oct. 1995	40	50.2 (7.14)	39–70
	D. vulgaris	June–July 1995	40	43.4 (7.96)	31–62
		June 1996	40	34.4 (3.40)	26–40
	D. puntazzo	May–June 1995	40	40.1 (4.74)	27–47
		May–June 1996	40	37.3 (4.65)	27–49
Visual censuses	*D. sargus*	June 1994 – Sept. 1994	54	37.1 (13.92)	15.0–57.5
		May 1995 – Sept. 1995	60	35.1 (16.65)	12.5–66.4
	D.vulgaris	Oct. 1994 – June 1995	90	21.4 (8.53)	12.5–47.4
		Oct. 1995 – June 1996	54	26.6 (11.68)	12.5–51.8
	D. puntazzo	Oct. 1994 – June 1995	100	26.7 (9.54)	12.5–47.1
		Oct. 1995 – June 1996	71	27.3 (10.37)	12.5–59.0

Note: Mean standard lengths are shown for samples of ontogenetic series, settlers, and juveniles. Mean total lengths are shown for visual censuses. Standard deviations are given for all means. *n* denotes number of fish collected in the samples of ontogenetic series, settlers, and juveniles and the number of visual censuses.

In order to compare growth curves obtained by visual census (time, total length) and by back-calculation from otoliths (age, standard length), it was necessary to convert total to standard lengths and times to ages. We used functional regression (Ricker 1973) to estimate the relationship between size variables. In all species, total and standard lengths were strongly correlated, with $r^2 > 0.99$. Conversion of times to ages was done by the following method. Firstly, the average size of all individuals recorded during the last visual census was calculated. An age was then assigned to this size by averaging all increment counts of otoliths from fish of this size. Because the date of sampling for each census was known, ages could then be assigned to average sizes from all preceding censuses.

Accuracy of size estimates provided by the various back-calculation models was assessed by calculating the proportion of the total variation in the growth curve derived from visual census that could be explained by the back-calculated growth curves. These percentages of explained variation were computed as the coefficient of determination (r^2) of linear regressions (Zar 1984).

Examination of settlement mark

Abrupt changes in regular patterns of increment width can occur when fishes pass from pelagic to benthic habitats (e.g., Wilson and McCormick 1997). We investigated the presence of these settlement marks in the otoliths of *Diplodus* by comparing profiles of otolith increment width and growth of individuals captured during the week following their settlement with those of fish collected at the end of the 1994–1995 recruitment season (Table 2). Size-at-age was calculated from otoliths using the modified Fry model (Table 1). Growth rate at age i (G_i) (sensu Ricker 1975, 1979) was then calculated using the formula

$$(6) \qquad G_i = (\mathrm{d}L(L\mathrm{d}t)^{-1})_i = (L_{i+1} - L_i)L_i^{-1}$$

where L is the back-calculated length of an individual at ages i and $i + 1$.

Results

Back-calculation length

The relationship between otolith radius and standard length of *Diplodus* was allometric (Table 3; Fig. 1). Although the linear eq. 5 explained a considerable portion of variability (86–91%), an allometric eq. 4 gave the best fit to the data set (97–99% of variability). Residuals derived from the linear formula were not normally distributed (K-S, $p < 0.01$), implying that this equation systematically overestimated the size of small fish and underestimated the size of large fish (Fig. 1). When an allometric formula was fitted, residuals were normally distributed (K-S, $p > 0.05$) and no heteroscedasticity was evident in the plot of otolith radius versus standard length (Fig. 1). The relationship between otolith radius and fish size was positively allometric (c ranging from 1.39 to 1.57) for all the three species, suggesting that an increase in otolith radius corresponded to a larger increase in body length for older fish than for younger individuals.

Estimates of body length at otolith formation varied little (range/mean < 0.8%) irrespective of whether R or L was taken as independent variable in eq. 4. Thus, results of length back-calculations using the modified Fry model were not biased by the variable used to estimate this parameter. Average values of body length at otolith formation were 2.39, 2.42, and 2.45 mm for *D. sargus*, *D. vulgaris*, and *D. puntazzo*, respectively.

Diplodus puntazzo and *D. vulgaris* settled in autumn and winter and grew at half the rate of *D. sargus*, which settled throughout spring and summer. The former two species attained a size of 35 mm at an age of 225–235 days, while the latter species attained a size of 35 mm 90–95 days after hatching (Fig. 2). Despite this variation in size-at-age among species, growth curves generated by our back-calculation

© 2000 NRC Canada

Table 3. Summary of allometric and linear regression analyses of otolith radius and fish length of *Diplodus*.

Model	Species	*b*	*c*	*n*	r^2	*d*	*p*
Allometric	*D. sargus*	0.00466	1.39	114	0.97	0.109	ns
	D. vulgaris	0.00279	1.45	93	0.99	0.111	ns
	D. puntazzo	0.00138	1.57	86	0.97	0.109	ns
Linear	*D. sargus*	0.0687		114	0.91	0.191	**
	D. vulgaris	0.0616		93	0.89	0.275	**
	D. puntazzo	0.0672		86	0.86	0.255	**

Note: Normality of residuals from the regression was tested using the K-S procedure. *n*, number of individuals analysed; *d*, K-S distance; *p*, K-S probability: ns, not significant ($p \geq 0.05$); **$p < 0.01$.

Fig. 1. Relationships between otolith radius and standard length of (*a*) *D. sargus*, (*b*) *D. vulgaris*, and (*c*) *D. puntazzo*. Linear (1) and allometric (2) relationships fitted to these data sets by regression (see Table 3) are shown.

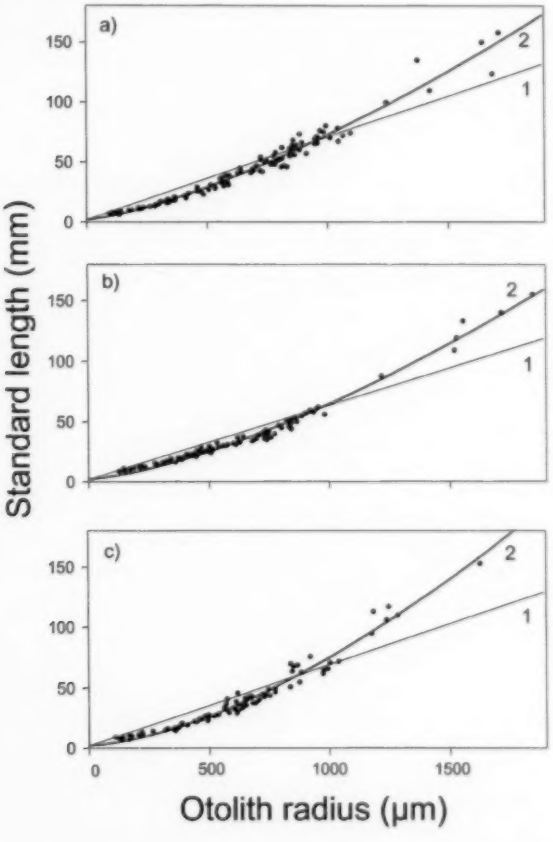

models explained 80–99% of the variation in growth curves directly estimated by visual census (Table 4).

Comparison of the results of the different back-calculation models showed that growth curves generated by the modified Fry model gave a better fit to curves derived from visual census than those generated by the BI and TVG models (Table 4; Fig. 2). This result was consistent for the three species and for growth curves generated from both years of the study. Estimates derived from the BI and TVG models were almost identical and the most distant from visually estimated growth curves (Table 4). Both overestimated body size throughout the early life history of *Diplodus* (Fig. 2). The results of the modified Fry model were very similar to those of the BPH model in both years. These models explained similar amounts of variability of the growth curve generated from the visual censuses (Table 4). However, the BPH model provided estimates of sizes at younger ages of the three species that were larger than those of all other models (Fig. 2).

Settlement marks

Mean increment widths of newly settled *D. vulgaris* and *D. puntazzo* peaked 25 and 22 days after hatching, respectively (Figs. 3*c* and 3*e*). Peaks in increment width occurred slightly later in samples of juvenile fish of these species (30 and 26 days, respectively). In contrast with these species, the profile of increment width of *D. sargus* increased rapidly and remained at high levels for a period of approximately 3 months, after which it gradually declined (Fig. 3*a*).

While patterns of otolith growth differed among species, all displayed similar profiles of somatic growth (Figs. 3*b*, 3*d*, and 3*f*). Growth rates increased rapidly from $<2\%\cdot day^{-1}$ at hatching to $3.5–5.5\%\cdot day^{-1}$ at 20–23 days of age and then quickly declined to $<2\%\cdot day^{-1}$. Peaks in growth of newly settled fish occurred at an age of 20 days after hatching for *D. sargus*, 23 days for *D. vulgaris*, and 21 days for *D. puntazzo*. In contrast, growth profiles derived from samples of juvenile fish showed peaks at 22, 27, and 25 days after hatching, respectively, for these species.

The mean age of the 40 newly settled *D. sargus* examined by our study was 28 days. Thus, the average settler of this species was captured 8 days after the peak in somatic growth, with the youngest individual captured 1 day after this time (Fig. 3*b*). Similarly, the average settler of *D. vulgaris* was captured 16–18 days after otolith and somatic growth peaked. The youngest individual of this species was captured 5–7 days after the peak observed in otolith and somatic growth (Figs. 3*c* and 3*d*). Newly settled *D. puntazzo* were captured on average 4–5 days after the peak in otolith and somatic growth, with the youngest individual collected 0–1 day after this time (Figs. 3*e* and 3*f*).

Discussion

Comparison of back-calculation models

We used an allometric formula to describe the relationship between otolith size and standard length of *Diplodus*. This formula was then used to develop a model for back-calculation of growth histories from the otoliths of these species. While allometric relationships between otolith and fish

© 2000 NRC Canada

Fig. 2. Growth curves back-calculated from otoliths and estimated directly from populations of fish in the field for (*a*) *D. sargus*, (*b*) *D. vulgaris*, and (*c*) *D. puntazzo*. Size-at-age data for field populations are shown as points with error bars of fixed size (±3.5 mm). These bars correspond to the maximum amount of error when fish sizes were estimated underwater by divers (see Materials and methods). Curves were extrapolated to the planktonic larval stage using data provided by Divanach (1985), and these points are shown without error bars. Size-at-age data estimated directly from field populations in both seasons are shown. For each census date, data were averaged among sites. Four models of back-calculation were used to generate growth curves from otoliths collected in each of the two seasons of the study: the modified Fry, biological intercept (BI), time-varying growth (TVG), and body proportional hypothesis (BPH) models (Table 4). Here, data sets from each of the two seasons were pooled and a single curve produced using each of the models.

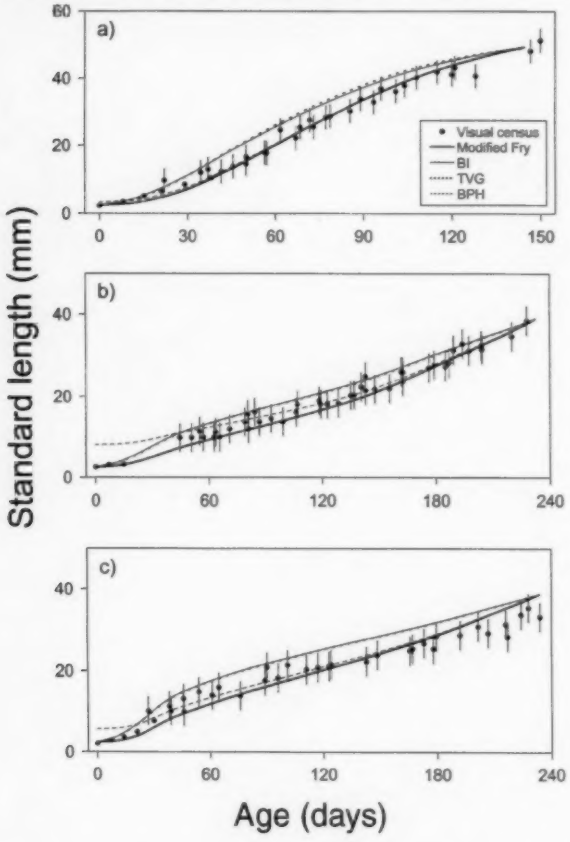

size appear to be common in many species (e.g., Lombarte and Lleonart 1993; Sirois et al. 1998), most previous studies have back-calculated growth using models that assume a linear relationship between these variables. In many cases, the use of linear models may only be appropriate because studies have back-calculated size over a relatively narrow range of ages. For example, Tremblay and Giguère (1992) found that the *L–R* relationship of Atlantic salmon (*Salmo salar*) was allometric over the entire life history but linear if only adult fish were used in the analysis. In some cases where studies have examined a number of ontogenetic stages, the problem of allometry has been overcome by fitting a different linear model to each life history stage (e.g., Ozawa and Penaflor 1990; Wright and Bailey 1996).

The existence of an allometric relationship between otolith and fish size indicated that the Fry model was theoretically the most appropriate for back-calculation of size from the otoliths of *Diplodus*. Prior to use, we constrained the model to biological intercepts. The model thus had the desired characteristics of insensitivity to growth effects and the ability to produce accurate estimates of size, given an allometric relationship between radius of the otolith and body length of the fish.

Our study suggested that the modified Fry model produced the most accurate estimates of size-at-age of *Diplodus*. This model produced growth curves that were the most similar to those generated by the visual census technique in both years of the study. While the BPH and modified Fry models generated curves that were close to those produced by the visual census, the former model gave unrealistic estimates of size-at-age of very young fish. This result was expected, since models derived by proportionality techniques cannot be constrained to go through a biological intercept and are thus vulnerable to growth effects. The BI and TVG models calculated curves that consistently overestimated size-at-age in comparison with visual census curves. This systematic error in length estimates may have important implications for studies of size-selective mortality in young fish (M.G. Meekan and L. Vigliola, unpublished data).

Given that we found an allometric relationship between otolith and fish size in *Diplodus*, we expected that the TVG and modified Fry models would provide the best estimates of size-at-age of our study species. This was not the case; we found that the TVG model produced estimates of size that were virtually identical to those of the BI model and that the modified Fry model produced estimates of size that were closer to those of the visual census technique than the TVG model. In a study of rainbow smelt (*Osmerus mordax*) larvae, Sirois et al. (1998) noted that the outcomes of the BI and TVG models were very similar when there was little variation in growth rate of fish over time. This may account for the similarity of results from these models in the present study, since the visual census technique suggested that there were no major inflexions in the growth curves of *Diplodus* after settlement. Further comparison of the outcomes of modified Fry and TVG models are required in situations where the growth rates of populations are highly variable over time.

Our comparisons assumed that differences among curves generated from otoliths and visual censuses were solely due to errors introduced by the various models of back-calculation. In reality, such differences might also be due to a number of other factors, such as size-selective mortality of juvenile *Diplodus*, nonrepresentative sampling of fish selected for otolith analysis or visual census, and (or) error in estimating average age from a field census. If strong size-selective mortality had occurred in the nursery habitat, the individuals selected for otolith analysis would have been fast growing, since these were older fish collected at the end of the season. In contrast, visual censuses would have included both slow- and fast-growing fish at the start of the season

© 2000 NRC Canada

Table 4. Comparison of growth curves generated from otoliths with size-at-age data derived from visual census of populations of *Diplodus* in the field.

Species	Year	*n*	Modified fry	BI	TVG	BPH
D. sargus	1994	19	0.97	0.95	0.94	0.97
	1995	22	0.99	0.92	0.90	0.99
	1994–1995	33	0.98	0.90	0.88	0.98
D. vulgaris	1994–1995	31	0.96	0.85	0.86	0.94
	1995–1996	16	0.97	0.97	0.97	0.93
	1994–1996	45	0.96	0.91	0.92	0.95
D. puntazzo	1994–1995	20	0.91	0.82	0.83	0.92
	1995–1996	21	0.96	0.89	0.89	0.96
	1994–1996	37	0.91	0.80	0.81	0.92

Note: Size-at-age data were averaged among sites on a given census date. The proportion of variability in size-at-age data sets accounted for by each of the back-calculation models (modified Fry, biological intercept (BI), time-varying growth (TVG), and body proportional hypothesis (BPH)) is shown for each season and for the data sets pooled between seasons. *n*, sample size.

Fig. 3. Profiles of increment width (top panels) and growth (bottom panels) of (*a* and *b*) *D. sargus*, (*c* and *d*) *D. vulgaris*, and (*e* and *f*) *D. puntazzo*. Increment widths and somatic growth are shown for newly settled (settlers) and juvenile fish. Age of the youngest individual collected by the study is indicated by a broken line.

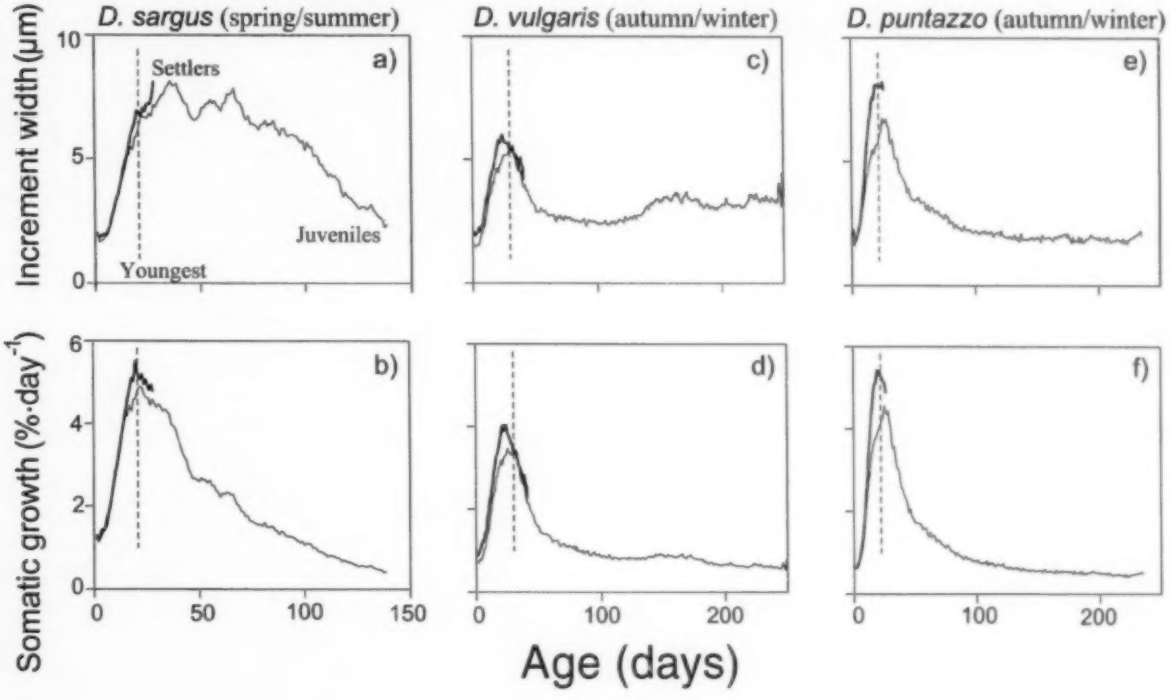

and fast-growing fish late in the season as smaller, slow-growing fish were progressively removed from cohorts. Consequently, we would have expected curves generated from otoliths to produce estimates of size-at-age of recently settled individuals that were greater than those of the visual census technique and curves produced by both techniques to gradually converge over time. This did not occur in our study. Both the BI and TVG models produced curves that consistently overestimated size-at-age, while the modified Fry and BHP models produced curves that tended to underestimate size-at-age of young fish, relative to the curve produced by the visual census technique.

The repeated measurement of reared or tagged fish could have provided data for a direct validation of back-calculation models. This would have allowed growth to be accurately documented on both a population and an individual basis (e.g., Meekan et al. 1998; Sirois et al. 1998). However, such techniques are expensive and can be logistically difficult, particularly when we wanted to follow the growth of *Diplodus* during the entire juvenile stage, which lasted up to

© 2000 NRC Canada

8 months. Consequently, we chose to compare back-calculation models with visual census data, a technique that, while likely to be less accurate than rearing or tagging methods, was relatively simple to accomplish in the field.

Settlement marks

Where species adopt a more benthic habitat at the end of larval life, settlement from the plankton to the benthos may be marked by a rapid change in the width of daily increments. These transition zones (sensu Secor et al. 1995) or settlement marks allow the duration of planktonic life and the timing of settlement to be estimated (e.g., Wellington and Victor 1989; Wilson and McCormick 1997). However, as changes in increment width can be influenced by a wide range of factors, such as water temperature or food (Molony 1996; Radtke and Fey 1996), it is important that the coincidence of timing of mark formation and the transition between planktonic and benthic environments is confirmed. To date, only three studies have attempted to validate the timing of settlement marks (Victor 1982; Pitcher 1988; Wilson and McCormick 1997).

Ideally, the timing of formation of settlement marks would be validated by comparing the increment width profiles of fish collected in the days just prior to their settlement with those of individuals collected at and after settlement. This approach has been used in tropical regions where sampling techniques have been developed that target the pelagic larvae of reef fish immediately prior to their settlement on the reef (Doherty 1987; Wilson and McCormick 1997). Unfortunately, the late-stage larvae of *Diplodus* are not susceptible to such sampling methods (S. Planes, EPHE, 66860 Perpignan, France, personal communication). Consequently, we investigated settlement marks by comparing profiles of mean increment width of fish collected in the first few days after settlement with those of fish collected just prior to their departure from the nursery habitat, up to 8 months after settlement.

Abrupt declines in the width of successive increments that appeared to coincide with settlement were evident in the otoliths of the slow-growing species *D. vulgaris* and *D. puntazzo*. In contrast, there was no decline in the increment widths of *D. sargus* until juveniles were 2–3 months old, which made the timing of settlement difficult to determine using the increment width method. Despite this pattern, settlement of all species was marked by a sharp decline in somatic growth rate. Thus, growth rate may provide a means of estimating the timing of settlement in fish, even in species that do not display a marked change in increment width.

Acknowledgements

The authors thank Robert Marquet, Yolaine Calvisi, and Thomas Webb for excellent technical assistance. Helpful comments on the manuscript were provided by anonymous reviewers. This research was funded by the European Commission (DG XIV, MED/92/007).

References

Campana, S.E. 1990. How reliable are growth back-calculations based on otoliths? Can. J. Fish. Aquat. Sci. **47**: 2219–2227.

Campana, S.E., and Jones, C.M. 1992. Analysis of otolith microstructure data. *In* Otolith microstructure examination and analysis. *Edited by* D.K. Stevenson and S.E. Campana. Can. Spec. Publ. Fish. Aquat. Sci. No. 117. pp. 73–100.

Divanach, P. 1985. Contribution à la connaissance de la biologie et de l'élevage de 6 sparidés méditerranéens: *Sparus aurata*, *Diplodus sargus*, *Diplodus vulgaris*, *Diplodus annularis*, *Lithognathus mormyrus*, *Puntazzo puntazzo* (poissons téléostéens). Ph.D. thesis, Université des Sciences et Techniques du Languedoc, France.

Doherty, P.J. 1987. Light-traps: selective but useful devices for quantifying the distributions and abundances of larval fishes. Bull. Mar. Sci. **41**: 423–431.

Fisher, W., Bauchot, M.L., and Schneider, M. 1987. Fiches FAO d'identification des espèces pour les besoins de la pêche (révision I). Méditerranée et Mer Noire. Zone de pêche 37. Vertebrés. FAO, Rome.

Francis, R.I.C.C. 1990. Back-calculation of fish length: a critical review. J. Fish Biol. **36**: 883–902.

Fraser, C.McL. 1916. Growth of the spring salmon. Trans. Pac. Fish. Soc. **1915**: 29–39.

Fry, F.E.J. 1943. A method for the calculation of the growth of fishes from scale measurements. Publ. Ont. Fish. Res. Lab. No. 61. pp. 5–18.

Garcia-Rubies, A., and Macpherson, E. 1995. Substrate use and temporal pattern of recruitment in juvenile fishes of the Mediterranean littoral. Mar. Biol. **124**: 35–42.

Geffen, A.J. 1992. Validation of otolith increment deposition rate. *In* Otolith microstructure examination and analysis. *Edited by* D.K. Stevenson and S.E. Campana. Can. Spec. Publ. Fish. Aquat. Sci. No. 117. pp. 101–113.

Gill, P.E., and Murray, W. 1972. Quasi-Newton methods for unconstrained optimisation. J. Inst. Math. Appl. **9**: 91–108.

Hare, J.A., and Cowen, R.K. 1995. Effect of age, growth rate, and ontogeny on the otolith size – fish size relationship in bluefish, *Potamus saltatrix*, and the implications for back-calculation of size in fish early life history stages. Can. J. Fish. Aquat. Sci. **52**: 1909–1922.

Harmelin-Vivien, M.L., Harmelin, J.G., and Leboulleux, V. 1995. Microhabitat requirements for settlement of juvenile sparid fishes on Mediterranean rocky shores. Hydrobiologia, **300/301**: 309–320.

Jones, C. 1986. Determining age of larval fish with the otolith increment technique. Fish. Bull. U.S. **84**: 91–103.

Lee, R.M. 1920. A review of the methods of age and growth determination in fishes by means of scales. Fish. Invest. Lond. Ser. **24**(2): 1–32.

Lombarte, A., and Lleonart, J. 1993. Otolith size changes related with body growth, habitat depth and temperature. Environ. Biol. Fishes, **37**: 297–306.

Macpherson, E. 1998. Ontogenetic shifts in habitat use and aggregation in juvenile sparid fishes. J. Exp. Mar. Biol. Ecol. **220**: 127–150.

Meekan, M.G., Dodson, J.J., Good, S.P., and Ryan, D.A.J. 1998. Otolith and fish size relationships, measurement error, and size selective mortality during the early life of Atlantic salmon (*Salmo salar*). Can. J. Fish. Aquat. Sci. **55**: 1666–1673.

Molony, B.W. 1996. Episodes of starvation are recorded in the otoliths of juvenile *Ambassis vachelli* (Chantidae), a tropical estuarine fish. Mar. Biol. **125**: 439–446.

Ozawa, T., and Penaflor, G.C. 1990. Otolith microstructure and early ontogeny of a myctophid species *Benthosema pterotum*. Nippon Suisan Gakkaishi, **56**: 1987–1995.

Pannella, G. 1971. Fish otoliths: daily growth layers and periodical patterns. Science (Washington, D.C.), **173**: 1124–1126.

© 2000 NRC Canada

Pitcher, C.R. 1988. Validation of a technique for reconstructing daily patterns in the recruitment of coral reef damselfish. Coral Reefs, **7**: 105–111.

Planes, S., Macpherson, E., Biagi, F., Garcia-Rubies, A., Harmelin, J., Harmelin-Vivien, M., Jouvenel, J.Y., Tunesi, L., Vigliola, L., and Galzin, R. 1999. Spatio-temporal variability in growth of juvenile sparid fishes from the Mediterranean littoral zone. J. Mar. Biol. Assoc. U.K. **79**: 137–143.

Radtke, R., and Fey, D.P. 1996. Environmental effects on primary increment formation in the otoliths of newly-hatched Arctic charr. J. Fish Biol. **48**: 1238–1255.

Ricker, W.E. 1973. Linear regressions in fishery research. J. Fish. Res. Board Can. **30**: 409–434.

Ricker, W.E. 1975. Computation and interpretation of biological statistics of fish populations. Bull. Fish. Res. Board Can. No. 191.

Ricker, W.E. 1979. Growth rates and models. *In* Fish physiology. Vol. 8. *Edited by* W.S. Hoar, D.J. Randall, and J.R. Brett. Academic Press, Inc., Orlando, Fla. pp. 677–743.

Secor, D.H., and Dean, J.M. 1992. Comparison of otolith-based back-calculation methods to determine individual growth histories of larval striped bass, *Morone saxatilis*. Can. J. Fish. Aquat. Sci. **49**: 1439–1454.

Secor, D.H., Dean, J.M., and Campana, S.E. 1995. Recent developments in fish otolith research. Belle W. Baruch Libr. Mar. Sci. 19, University of South Carolina Press, Columbia, S.C.

Sirois, P., Lecomte, F., and Dodson, J.J. 1998. An otolith-based back-calculation method to account for time-varying growth rate in rainbow smelt (*Osmerus mordax*) larvae. Can. J. Fish. Aquat. Sci. **55**: 2662–2671.

Tremblay, G., and Giguère, L.A. 1992. Relation longueur/écaille allométrique chez le saumon atlantique (*Salmo salar*) durant la phase marine. Can. J. Fish. Aquat. Sci. **49**: 46–51.

Tsuji, S., and Aoyama, T. 1982. Daily growth increments observed in otoliths of the larvae of Japanese red sea bream *Pagrus major* (Temminch et Schlegel). Bull. Jpn. Soc. Sci. Fish. **48**: 1559–1562.

Victor, B.C. 1982. Daily otolith increments and recruitment in two coral-reef wrasses, *Thalassoma bifasciatum* and *Halichoeres bivittatus*. Mar. Biol. **71**: 203–208.

Vigliola, L. 1997. Validation of daily increment formation in otoliths for three *Diplodus* species in the Mediterranean Sea. J. Fish Biol. **51**: 349–360.

Vigliola, L., Harmelin-Vivien, M.L., Biagi, F., Galzin, R., Garcia-Rubies, A., Harmelin, J.G., Jouvenel, J.Y., Le Direach-Boursier, L., Macpherson, E., and Tunesi, L. 1998. Spatial and temporal patterns of settlement among *Diplodus* sparid fishes in the northwestern Mediterranean. Mar. Ecol. Prog. Ser. **168**: 45–56.

Watanabe, Y., and Kuroki, T. 1997. Asymptotic growth trajectories of larval sardine (*Sardinops melanostictus*) in the coastal waters off western Japan. Mar. Biol. **127**: 369–378.

Wellington, G.M., and Victor, B.C. 1989. Planktonic larval duration of one hundred species of Pacific and Atlantic damselfishes (Pomacentridae). Mar. Biol. **101**: 557–567.

Wilson, D.T., and McCormick, M.I. 1997. Spatial and temporal validation of settlement-marks in the otoliths of tropical reef fishes. Mar. Ecol. Prog. Ser. **153**: 259–271.

Wright, P.J., and Bailey, M.C. 1996. Timing of hatching in *Ammodytes marinus* from Shetland waters and its significance to early growth and survivorship. Mar. Biol. **126**: 143–152.

Zar, J.H. 1984. Biostatistical analysis. Prentice Hall, Englewood Cliffs, N.J.

© 2000 NRC Canada

Extreme life history change of white-spotted char (*Salvelinus leucomaenis*) after damming

Kentaro Morita, Shoichiro Yamamoto, and Noboru Hoshino

Abstract: Dam construction has serious consequences for anadromous fishes. We examined the effects of migration barriers formed following dam construction on the migratory behavior of white-spotted char (*Salvelinus leucomaenis*) by comparing migrants in accessible below-dam river sections with migrants in inaccessible above-dam river sections. The frequency of smolts (i.e., potential migrant) was higher for the below-dam sections than for the above-dam sections, and in contrast, the frequency of residents was higher for the above-dam sections. Above-dam sections had lower fry (age 0+) densities and consequently had higher growth rates compared with below-dam sections. A transplant experiment revealed that the majority of the below-dam fish adopted a resident strategy, as well as above-dam fish, when both had experienced the above-dam environment. We conclude that high growth as a result of low density promotes residency in the above-dam sections.

Résumé : La construction des barrages a des conséquences graves pour les poissons anadromes. Nous avons examiné les effets des obstacles à la migration apparus à la suite de la construction d'un barrage sur le comportement de l'omble à taches blanches (*Salvelinus leucomaenis*) en comparant les migrants présents dans les sections accessibles en aval du barrage aux migrants présents dans les sections inaccessibles en amont du barrage. La fréquence des smolts (migrants potentiels) était plus élevée pour les sections d'aval que pour les sections d'amont; par contre, la fréquence des résidents était plus élevée pour les sections d'amont. Les sections d'amont présentaient des densités d'alevins (0+) plus faibles, et donc des taux de croissance plus élevés par rapport aux sections d'aval. Une expérience de transplantation a révélé que la majorité des poissons d'aval adoptait une stratégie de résidence, aussi bien que les poissons d'amont, quand les deux avaient connu le milieu d'amont. Nous en concluons que la forte croissance causée par une faible densité favorise la résidence dans les sections d'amont.

[Traduit par la Rédaction]

Introduction

Ontogenetic habitat shifts between freshwater and marine environments are a common feature of salmonid fishes, but not all salmonids are migratory (reviewed by Thorpe 1987). Salmonid fishes have inherently alternative reproductive strategies of "migrant" (maturing after migration toward productive habitat such as the sea, a lake, or a large river) or "resident" (maturing without migration), and different sympatric forms belong to the same gene pool (Nordeng 1983; Hindar et al. 1991; Jones et al. 1997).

Interpopulational variations in proportions of residents or migrants have been explained by both genetic (e.g., Jonsson 1982; Näslund 1993) and environmental factors (e.g., Myers et al. 1986; L'Abée-Lund et al. 1990). Improved juvenile feeding tends to increase the proportion of residents (reviewed by Jonsson and Jonsson 1993). Therefore, riverine growth conditions could have a strong influence on migratory behavior besides genotype, i.e., the salmonid life history strategy (migration or residence) is a conditional strategy depending on individual growth conditions.

Barriers such as waterfalls and dams have serious consequences for salmonid fishes. Because these barriers are impassable to ascending fish, upstream salmonid habitats are frequently lost (Shimoda et al. 1993; Reyes-Gávilan et al. 1996). Some salmonid populations above such barriers, however, survive as landlocked forms showing little migratory behavior (e.g., masu salmon (*Oncorhynchus masou*), Sano 1968; rainbow trout (*Oncorhynchus mykiss*), Northcote 1981; brown trout (*Salmo trutta*), Jonsson 1982; Atlantic salmon (*Salmo salar*), Vuorinen and Berg 1989; white-spotted char (*Salvelinus leucomaenis*), Shimoda 1992; Dolly Varden (*Salvelinus malma*), Maekawa et al. 1993).

The marked differences in migratory behavior between populations above and below waterfalls have been explained by genotypic specialization due to long-term "knife-edge" selection that has occurred over a few thousand years (Northcote 1981; Jonsson 1982; Vuorinen and Berg 1989; Hindar et al. 1991). However, landlocked populations of white-spotted char live above human-made dams that were constructed only 20 years ago, i.e., less than six generations (Shimoda 1992). This life history change is too drastic to be explained by genotypic specialization only.

This study was designed to investigate the underlying mechanisms contributing to the short-term change in the migratory behavior of white-spotted char populations after

Received July 9, 1999. Accepted January 27, 2000.
J15242

K. Morita.[1] Laboratory of Marine Ecology, Faculty of Fisheries, Hokkaido University, Hakodate 041-8611, Japan.
S. Yamamoto. University Forests, Hokkaido University, Sapporo 060-8589, Japan.
N. Hoshino. Resource Management Division, Hokkaido Wakkanai Fisheries Experiment Station, Wakkanai 097-0001, Japan.

[1]Author to whom all correspondence should be addressed.
e-mail: morita@fish.hokudai.ac.jp

© 2000 NRC Canada

Fig. 1. Map of the study areas including above-dam (*a*) and below-dam (*b*) sections. The asterisk represents the transplant site. The dams on the map are the first impassable dams, i.e., dams with a fishway or located above the first impassable dam are not illustrated. Open arrows indicate the direction of flow.

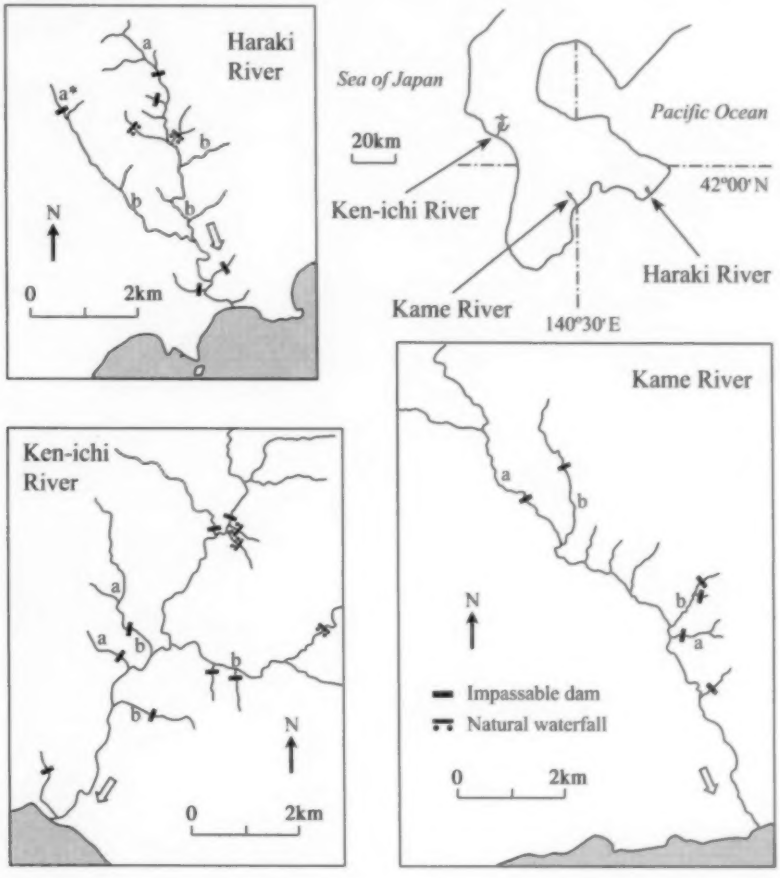

damming. We examined several life history traits of white-spotted char living above dams constructed 20–30 years ago by comparing them with those of white-spotted char living below dams. We also undertook a transplant experiment to compare them under similar environmental conditions.

Materials and methods

Study area

This study was conducted in three rivers, the Haraki (16 km^2 in catchment area), Kame (28 km^2 in catchment area), and Ken-ichi (80 km^2 in catchment area) in southern Hokkaido, Japan (Fig. 1). These rivers have several small dams (height 2–4 m) constructed 20–30 years ago to control erosion. These dams have no impounding areas. Downstream fish cannot access areas upstream of a dam, but upstream fish can access areas downstream of a dam. The study areas were chosen in typical char biotopes from both above-dam and below-dam sections. Hydrological features varied among rivers and tributaries within rivers, but those of the two sections overlapped broadly (Table 1). Although above-dam sections were more upstream, both above-dam and below-dam sections were close to the sea (less than 10 km). Because no association was observed between distance to the sea and life history traits in undammed sites of 1–10 km (K. Morita, unpublished data), we assumed that below-dam sections were a presituation of above-dam sections.

Study fish

White-spotted char have a complex and iteroparous life cycle. Char generally spend 2–5 years in rivers at the parr stage (Yamamoto et al. 1999*a*). Subsequent to the parr stage, some char descend to the sea after smoltification, while other char mature without migration (Yamamoto et al. 1999*a*). The age of smolts varies between 2+ and 6+ years, but wild smolts are chiefly (80%) 2+ or 3+ years old in southern Hokkaido (Yamamoto et al. 1999*b*). Smolting periods in southern Hokkaido occur during April and May, and no smolts occur at other periods of the year (S. Yamamoto, unpublished data). Reproduction occurs in rivers during September and October by both stream residents and returning sea-run migrants, and no reproductive barriers exist between the forms (Ishigaki 1984). Migrants descend again to the sea after reproduction (Takami 1995), but most residents cannot descend to the sea because maturation physiologically inhibits smoltification (e.g., Thorpe 1987; Staurnes et al. 1994).

Fish collection

We chose three sampling periods, April–May (smolting season), July, and September–October (breeding season), but sampling during the smolting season in the Ken-ichi River could not be made

© 2000 NRC Canada

Fig. 2. Fork length distributions (age >1+) of white-spotted char in the (*a*) above-dam and (*b*) below-dam sections during the smolting season. Solid bars represent smolts and open bars represent nonsmolts, i.e., parr plus residents.

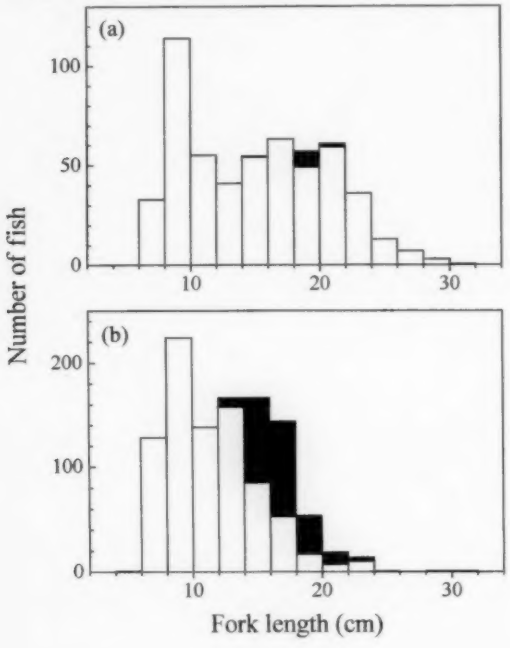

Table 1. Hydrological features of above-dam and below-dam sections in three rivers.

	Section	Site	Stream width (m)	Water depth (cm)
Haraki River	Above dam	1	3.5±0.8	24.1±8.1
		2*	2.4±0.6	20.2±8.4
	Below dam	1	4.4±0.8	31.5±17.2
		2	3.3±0.6	23.6±16.1
		3	1.9±0.3	14.4±5.8
Kame River	Above dam	1	4.1±0.7	24.7±9.0
		2	2.0±0.7	18.2±7.5
	Below dam	1	3.1±0.6	25.5±12.1
		2	2.4±0.5	16.6±7.3
Ken-ichi River	Above dam	1	4.2±0.8	47.2±13.2
		2	2.0±0.5	23.3±6.7
	Below dam	1	5.0±2.1	35.4±9.4
		2	4.5±1.0	35.3±12.0
		3	2.2±0.5	24.7±11.0

Note: The asterisk indicates the transplant site.

because of high flows caused by snowmelt. Fish were collected using several sampling methods, including an electrofishing unit, angling gear, cast net, and hand net, from the Haraki River (n = 449 above-dam fish, n = 1616 below-dam fish) in 1994, 1996, and 1997 and from the Kame River (n = 594 above-dam fish, n = 622 below-dam fish) and the Ken-ichi River (n = 243 above-dam fish, n = 187 below-dam fish) in 1996 and 1997. We also made equal effort removals in each section in the Haraki and Kame rivers in June by electrofishing to evaluate the abundance of newly emerged fry. To eliminate the effect of other fishes on char abundance, the char density was evaluated in char-dominant areas of each section.

Fig. 3. Fork length distributions (age >1+) of white-spotted char in the (*a*) above-dam and (*b*) below-dam sections during the breeding season. Open bars represent parr, gray bars represent residents, and solid bars represent migrants.

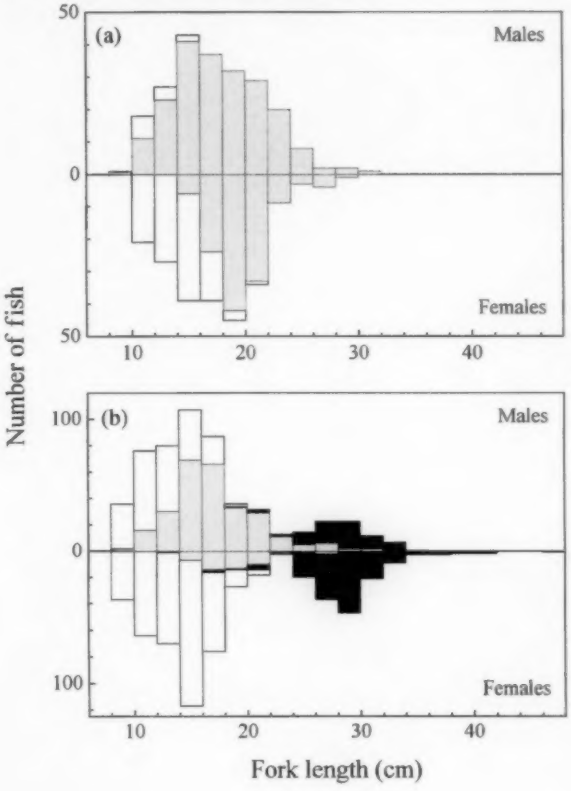

Measurement

Fish were measured for fork length to the nearest 0.1 cm. In the smolting season (April–May), fish were identified as smolts by their coloration and body shape (Ishigaki 1984). In the breeding season (September–October), fish were classified into three categories by their sexual maturity, coloration, and scale patterns (Ishigaki 1984). These categories were parr (juvenile fish), resident fish (maturing without migration), and migrant (fish after seaward migration). Fish were also sexed and aged by otolith analysis (Yamamoto et al. 1992). We used the terminology of age determination established by Elliott (1994).

To evaluate the migrants' contribution to the below-dam populations, the percentage of egg number deposited by migrants (PM) was estimated as

$$PM = 100 \sum EM_i / \left(\sum EM_i + \sum ER_i \right)$$

where EM_i and ER_i are the egg number of each migrant and resident, respectively, estimated from a regression equation of egg number on fork length (Morita and Takashima 1998).

Transplant experiment

To compare growth and maturation patterns of above-dam and below-dam individuals under similar environmental conditions, we

© 2000 NRC Canada

Table 2. Mixed-model two-way ANOVA of the effect of section (fixed), river (random), and their interaction on fork length of female and male resident white-spotted char.

	Female resident				Male resident			
	df	SS	*F*	*P*	df	SS	*F*	*P*
Section	1	0.012	0.65	0.425	1	0.016	0.34	0.555
River	2	0.168	4.38	0.014	2	1.056	11.32	<0.001
Section × river	2	0.083	2.15	0.120	2	0.254	2.72	0.067
Error	170	3.266			571	26.643		

Fig. 4. Maturity rate on age of (*a*) male and (*b*) female white-spotted char. Solid circles represent the above-dam section and open circles represent the below-dam section. Squares represent coincident values.

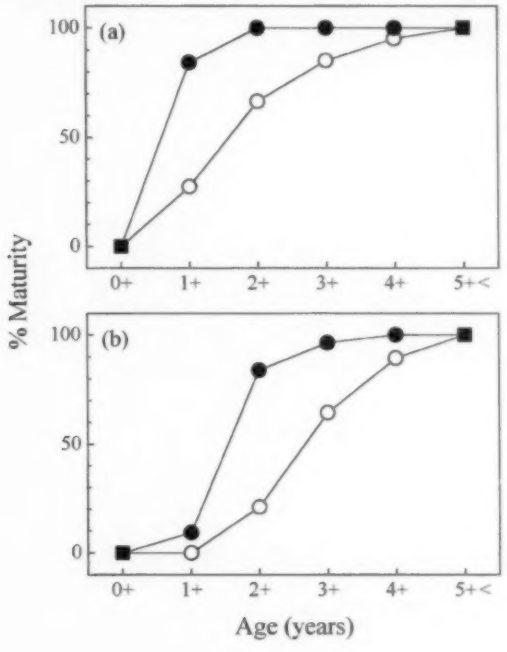

Fig. 5. Abundance of white-spotted char fry (age 0+) in the above-dam and below-dam sections evaluated from the char-dominant area. Error bars indicate standard deviations.

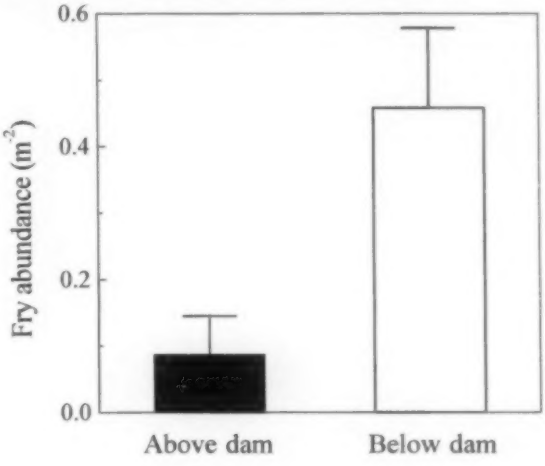

conducted a transplant experiment in the Haraki River using fish of the same river. The transplant site was above a dam (Fig. 1) where fish did not occur. A total of 104 and 96 fry (age 0+) were captured in the above-dam and below-dam sections, respectively, in July 1997. Fry were sampled in reaches of over 1 km to include several families. Captured fry of each section were measured for fork length, marked with an adipose fin clip (below-dam fish only), and immediately released in the transplant site. A total of 34 fish of above-dam origin and 32 fish of below-dam origin were recaptured in October 1997, 34 fish of above-dam origin and 33 fish of below-dam origin were recaptured in October 1998, and 38 fish of above-dam origin and 35 fish of below-dam origin were recaptured in October 1999. Recaptured fish were measured for fork length again and their sexual maturity determined. To capture the smolts completely, we set a trap net (Maekawa 1977) across the stream at the lowermost part of the transplant section from April to May 1999.

Statistical analyses

We homogenized metric data (fork length, abundance) by natural logarithmic transformation and tested the metric data using analysis of variance (ANOVA). In this study, the factor "river" was considered a random factor. We focused on the primary factor "section" (above the dam or below the dam) and therefore used mixed-model ANOVAs. We tested frequency data (frequency of smolts, frequency of residents, frequency of mature fish) using the likelihood ratio test, including logistic regression analysis. The *G* Statistic was used to designate duplicate log-likelihood ratios.

Results

Contrast between above- and below-dam sections

In the smolting season, smolts were scarce in the above-dam section and were common in the below-dam section (Fig. 2). Frequencies of smolts between 12 and 24 cm were 4% in the above-dam section and 42% in the below-dam section. This difference was markedly significant (G = 181.4, $P < 0.001$).

In the breeding season, only small residents populated the above-dam section compared with the below-dam section, which was populated by both large migrants and small residents (Fig. 3). The percentage of the egg number deposited by migrants in the below-dam sections was estimated at 87%, indicating that migrants contributed most of the offspring in the below-dam sections. There was no effect of section on fork length of residents for either sex (Table 2). However, logistic regression analysis showed that the above-dam section had a significantly higher frequency of residents than the below-dam section for both sexes for all fork lengths (males: G = 74.4, $P < 0.001$; females: G = 47.8, $P < 0.001$).

Fish in the above-dam section had a conspicuously youn-

© 2000 NRC Canada

Fig. 6. Fork length on age of above-dam and below-dam white-spotted char (*a*) in each section and (*b*) in a transplant site. Solid circles represent the above-dam fish and open circles represent the below-dam fish. Error bars indicate standard deviations. Maturity rate (including both sexes) at age 1+ is given in parentheses.

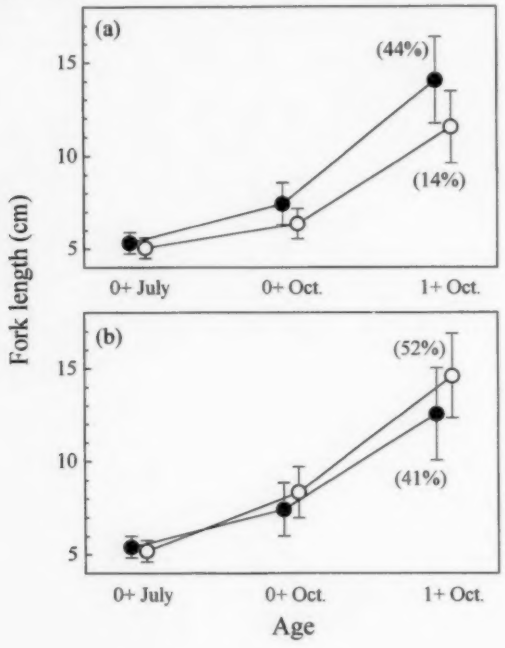

ger age at maturity than fish in the below-dam section (Fig. 4). Logistic regression analysis identified significant differences between sections for both sexes (males: G = 181.6, $P < 0.001$; females: G = 114.5, $P < 0.001$). Most males and females in the above-dam section first reached sexual maturity at age 1+ and age 2+, respectively. In contrast, most males and females in the below-dam section matured by age 3+ and age 4+, respectively.

Fry (age 0+) abundance was much lower for the above-dam sections than for the below-dam sections (Fig. 5). Mixed-model two-way ANOVA identified a significant effect of section on fry abundance (Table 3). Fry density generally reflected egg density, indicating that the spawning biomass in the above-dam section was much lower than that in the below-dam section.

To examine riverine growth, we compared the mean fork length of age <2+ individuals (i.e., before seaward migration) between sections (Fig. 6*a*). Mixed-model three-way ANOVA identified a significant interaction between section and age (Table 4), suggesting that above-dam fish had a higher growth rate than below-dam fish in the parr stage.

Transplant experiment

Figure 6*b* shows the growth trajectories of above-dam and below-dam fish under similar environmental conditions (above-dam environment). Two-way ANOVA identified a significant interaction between origin and age (Table 5). This suggests that the growth rate of char differed depending on origin, even though both above-dam and below-dam fish were pooled into similar above-dam environmental conditions. Contrary to the original growth pattern, below-dam fish had higher growth rates than above-dam fish.

Table 3. Mixed-model two-way ANOVA of the effect of section (fixed), river (random), and their interaction on white-spotted char fry abundance.

	df	SS	F	P
Section	1	0.424	113.26	<0.001
River	1	0.027	6.79	0.019
Section × river	1	<0.001	<1	0.982
Error	16	0.064		

Table 4. Mixed model three-way ANOVA of the effect of section (fixed), age (fixed), river (random), and their interactions on fork length of white-spotted char.

	df	SS	F	P
Section	1	2.179	113.15	<0.001
Age	2	93.704	171.81	<0.001
River	2	0.138	3.59	0.028
Section × age	2	0.355	9.17	<0.001
Section × river	2	0.027	0.72	0.489
Age × river	4	1.091	14.15	<0.001
Section × age × river	4	0.154	1.99	0.094
Error	1174	22.623		

Table 5. Model I two-way ANOVA of the effect of origin (fixed), age (fixed), and their interaction on fork length of white-spotted char in the transplant experiment.

	df	SS	F	P
Origin	1	0.393	19.84	<0.001
Age	2	44.195	1115.01	<0.001
Origin × age	2	0.661	16.66	<0.001
Error	327	6.481		

Maturity rates at age 1+ of above-dam and below-dam origins were 41 and 52% (including both sexes), respectively, and this difference was not statistically significant (G = 0.71, P = 0.40). At age 2+, however, most individuals attained sexual maturity without seaward migration. Maturity rates at age 2+ of above-dam and below-dam origins were 92 and 86%, respectively, and this difference was also not statistically significant (G = 0.72, P = 0.40). We captured only one smolt (age 2+) of below-dam origin with the trap net. Although we did not quantify the frequency of smolts because of very low frequency, the smolting rate would not differ between origins because the recapture ratio of above-dam to below-dam individuals did not differ throughout the experiments (G = 0.04, P = 0.85).

Discussion

A dramatic life history change occurred in white-spotted char populations during the 20–30 years following dam construction. In above-dam sections, the growth rate was higher and most fish matured without migration (resident strategy). In below-dam sections, the growth rate was lower and many

© 2000 NRC Canada

fish matured after seaward migration (migrant strategy). However, as evidenced by the transplant experiment, the majority of below-dam fish adopted a resident strategy like above-dam fish, when both shared above-dam environmental conditions. This suggests that the observed differences in migratory behavior between above-dam and below-dam sections were largely phenotypic rather than genotypic.

Differences in riverine growth rate of fish between above-dam and below-dam sections could have been due to differences in density, the so-called "self-thinning rule" (e.g., Bohlin et al. 1994; Jenkins et al. 1999). Alternatively, the environmental gradient along watercourses (e.g., temperature, dissolved oxygen) might also induce differences in growth rate of fish between the two sections. However, the two sections were adjacent in a relatively short watercourse. Whereas we recognize the potential importance of many environmental factors affecting growth rate, it seems reasonable to assume that the differences in growth rate of fish between the two sections were largely attributed to a density-dependent factor.

Many studies have documented that superior development promotes residency, i.e., early maturation without smolting (e.g., Nordeng 1983; Thorpe 1987; L'Abée-Lund et al. 1990). Our results are consistent with these studies. Thorpe (1994) and Thorpe and Metcalfe (1998) suggested that smolting was a negative developmental decision taken by fish that had failed to mature. Thus, migration to the sea would occur when sufficient energy for maturation could not be obtained. We infer that superior development due to low density promoted a residency in the above-dam sections. Juvenile growth rate that is subject to population density could influence the residency, and therefore, the residency would also be subject to population density. This interpretation is supported by evidence that smolting rate was positively correlated with population density at the within-population level in masu salmon (Sugiwaka and Kojima 1984) and sockeye salmon (*Oncorhynchus nerka*) (Kaeriyama 1996). Kaeriyama (1996) argued this salmonid life history strategy by introducing the idea that fish can conditionally adopt a strategy of residence. According to this scenario, fish adopt residency if sufficient resources such as food and habitat are obtained, and fish migrate if resource demands are not met.

We deduce life history strategies of char in above-dam and below-dam sections as follows. In above-dam sections, most fish grew rapidly and matured early as residents because of low density. In below-dam sections, the growth rate was limited by the population density, and therefore, many fish migrated to the sea and matured late as migrants. Differences in initial population density between sections could be attributed to each breeding population structure (Fig. 2). In contrast with the below-dam sections, which were mostly populated by large migrants, the above-dam sections were populated only by small residents. In brown trout, a long-term study showed that a resident population above a waterfall had a much lower density than that of a neighboring anadromous population from egg through 500 days after hatching (Elliott 1994). The difference in initial population density would be responsible for the difference in reproductive strategies (migrant versus resident) and vice versa. Consequently, a new life history strategy could have been established in above-dam sections without genetic change occurring.

The Kamchatkan sockeye salmon populations show a similar feature (summarized in Thorpe 1986, 1994). In parallel with a numerical decline in migrant salmon stocks resulting from massive fishing pressure in the ocean, both juvenile growth rate and the proportion of resident salmon have increased markedly. These changes are presumably related to each other. With salmonid life history strategies (migrant versus resident), phenotypic change might advance rapidly, even though genetic differentiation is practically absent because the decline in migrants leads not only to a decline in population density, but also to an increase in freshwater growth rate that results in an increase in residents.

For several freshwater fishes, considerable evidence has accumulated in recent years to document that genetic change occurs following isolation above artificial dams (e.g., Lusková et al. 1997; Hansen and Mensberg 1998). Although both growth rate and maturity rate without migration are heritable traits (e.g., Thorpe and Morgan 1978; Nordeng 1983), our transplant experiment results are inconsistent with the idea that above-dam populations have a genetically higher growth rate and (or) higher maturity rate without migration. An interesting finding of this study is that short-term change in migratory behavior after damming can be largely explained by the influence of intraspecific population density rather than genetic differentiation. However, genetic factors influencing the change in migratory behavior should not be ruled out; genetic change has accounted for some of the long-term change in migratory behavior (summarized in Elliott 1994).

Above-dam fish grew faster in the parr stage than below-dam fish, but the reverse occurred when two groups were reared under identical environmental conditions. This would imply that above-dam fish have a genetically lower growth rate. In an analogous study, above-waterfall rainbow trout were found to have a genetically lower growth rate than below-waterfall rainbow trout (Northcote 1981). In general, isolated populations above waterfalls or dams have lower genetic diversity because of the founder effect and (or) random genetic drift (e.g., Vuorinen and Berg 1989; Hindar et al. 1991; Hansen and Mensberg 1998). Above-dam white-spotted char populations also had lower genetic diversity than below-dam populations (S. Yamamoto et al., unpublished data). There has a considerable accumulation of evidence that loss of genetic diversity leads to deleterious effects on fishes, such as decreasing survival and growth rate and increasing developmental instability and frequency of deformities (e.g., Kincaid 1983; Leary et al. 1984; Quattro and Vrijenhoek 1989). Therefore, loss of genetic diversity due to isolation and decreasing population size may be a cause of genetically lower growth of above-dam fish.

In conclusion, short-term change in migratory behavior in white-spotted char populations living above human-made dams was intrinsic to the biological system and was not caused by rapid evolution. Our study shows that the life history strategy of white-spotted char is very flexible and this plasticity can have an important role in preventing local extinction.

Acknowledgments

We thank Y. Kanno, K. Nishimura, and T. Matsuishi for support and invaluable suggestions, T. Kuwahara, Y. Taka-

© 2000 NRC Canada

shima, E. Arai, H. Kurachi, M. Hosono, K. Orito, M. Hukaya, T. Suzuki, T. Undo, M. Nakaya, and S. Hotta for help in the fieldwork, J.R. Bower for critical readings of an earlier version of the manuscript, and two anonymous referees for insightful and critical comments on previous versions of the manuscript.

References

Bohlin, T., Dellefors, C., Faremo, U., and Johlander, A. 1994. The energetic equivalence hypothesis and the relation between population density and body size in stream-living salmonids. Am. Nat. **143**: 478–493.

Elliott, J.M. 1994. Quantitative ecology and the brown trout. Oxford University Press, Oxford, U.K.

Hansen, M.M., and Mensberg, K.-L.D. 1998. Genetic differentiation and relationship between genetic and geographical distance in Danish sea trout (*Salmo trutta* L.) populations. Heredity, **81**: 493–504.

Hindar, K., Jonsson, B., Ryman, N., and Ståhl, G. 1991. Genetic relationships among landlocked, resident, and anadromous brown trout, *Salmo trutta* L. Heredity, **66**: 83–91.

Ishigaki, K. 1984. Exploring the mystery of charrs. Iwanami-shoten, Tokyo, Japan. (In Japanese.)

Jenkins, T.M., Jr., Diehl, S., Kratz, K.W., and Cooper, S.D. 1999. Effect of population density on individual growth of brown trout in streams. Ecology, **80**: 941–956.

Jones, M.W., Danzmann, R.G., and Clay, D. 1997. Genetic relationships among populations of wild resident, and wild and hatchery anadromous brook charr. J. Fish Biol. **51**: 29–40.

Jonsson, B. 1982. Diadromous and resident trout *Salmo trutta*: is their difference due to genetics? Oikos, **38**: 297–300.

Jonsson, B., and Jonsson, N. 1993. Partial migration: niche shift versus sexual maturation in fishes. Rev. Fish Biol. Fish. **3**: 348–365.

Kaeriyama, M. 1996. Effects of population density and habitat environment on life history strategy and migration of juvenile sockeye (*Oncorhynchus nerka*) and chum salmon (*O. keta*). Sci. Rep. Hokkaido Salmon Hatchery, **50**: 101–111.

Kincaid, H.L. 1983. Inbreeding in fish populations used for aquaculture. Aquaculture, **33**: 215–227.

L'Abée-Lund, J.H., Jensen, A.J., and Johnsen, B.O. 1990. Interpopulation variation in male parr maturation of anadromous brown trout (*Salmo trutta*) in Norway. Can. J. Zool. **68**: 1983–1987.

Leary, R.F., Allendorf, F.W., and Knudsen, K.L. 1984. Superior developmental stability of heterozygotes at enzyme loci in salmonid fishes. Am. Nat. **124**: 540–551.

Lusková, V., Šlechtová, V., Povž, M., Šlechta, V., and Lusk, S. 1997. Genetic variability of *Chondrostoma nasus* populations in rivers of the Black Sea and the Baltic Sea drainage systems. Folia Zool. **46**(Suppl. 1): 27–36.

Maekawa, K. 1977. Studies on the variability of the land-locked Miyabe char, *Salvelinus malma miyabei* Oshima. 1. Development and early life history. Jpn. J. Ecol. **27**: 91–102. (In Japanese with English summary.)

Maekawa, K., Hino, T., Nakano, S., and Smoker, W.W. 1993. Mate preference in anadromous and landlocked Dolly Varden (*Salvelinus malma*) females in two Alaskan streams. Can. J. Fish. Aquat. Sci. **50**: 2375–2379.

Morita, K., and Takashima, Y. 1998. Effect of female size on fecundity and egg size in white-spotted charr: comparison between sea-run and resident forms. J. Fish Biol. **53**: 1140–1142.

Myers, R.A., Hutchings, J.A., and Gibson, R.J. 1986. Variation in male parr maturation within and among populations of Atlantic salmon, *Salmo salar*. Can. J. Fish. Aquat. Sci. **43**: 1242–1248.

Näslund, I. 1993. Migratory behaviour of brown trout, *Salmo trutta* L.: importance of genetic and environmental influences. Ecol. Freshwater Fish, **2**: 51–57.

Nordeng, H. 1983. Solution to the "char problem" based on Arctic char (*Salvelinus alpinus*) in Norway. Can. J. Fish. Aquat. Sci. **40**: 1372–1387.

Northcote, T.G. 1981. Juvenile current response, growth and maturity of above and below waterfall stocks of rainbow trout, *Salmo gairdneri*. J. Fish Biol. **18**: 741–751.

Quattro, J.M., and Vrijenhoek, R.C. 1989. Fitness differences among remnant populations of endangered Sonoran topminnow. Science (Washington, D.C.), **245**: 976–978.

Reyes-Gavilán, F.G., Garrido, R., Nicieza, A.G., Toledo, M.M., and Braña, F. 1996. Fish community variation along physical gradients in short streams of northern Spain and the disruptive effect of dams. Hydrobiologia, **321**: 155–163.

Sano, S. 1968. A record of fluvial masu salmon in the Raruishi River. Fish and Eggs, **128**: 28–29. (In Japanese.)

Shimoda, K. 1992. Effect of dam and fishway on distribution of freshwater fish fauna. Master's thesis, Hokkaido University, Sapporo, Japan. (In Japanese.)

Shimoda, K., Nakano, S., Kitano, S., Inoue, M., and Ono, Y. 1993. Present condition of stream fish assemblage in the Shiretoko Peninsula with special reference to human impacts. Hokkaido Univ. Bull. Grad. School Environ. Sci. **6**: 17–27. (In Japanese with English summary.)

Staurnes, M., Sigholt, T., Gulseth, O.A., and Eliassen, R. 1994. Effect of maturation on seawater tolerance of anadromous Arctic char. Trans. Am. Fish. Soc. **123**: 402–407.

Sugiwaka, K., and Kojima, H. 1984. Influence of individual density on smoltification in wild juvenile masu salmon (*Oncorhynchus masou*) in the Atsuta River. Sci. Rep. Hokkaido Fish Hatchery, **39**: 19–37. (In Japanese with English summary.)

Takami, T. 1995. Migration of anadromous white-spotted charr, *Salvelinus leucomaenis*, in southwestern Hokkaido, Japan. Nord. J. Freshwater Res. **71**: 432–437.

Thorpe, J.E. 1986. Age at first maturity in Atlantic salmon, *Salmo salar*: freshwater period influences and conflicts with smolting. Can. Spec. Publ. Fish. Aquat. Sci. No. 89. pp. 7–14.

Thorpe, J.E. 1987. Smolting versus residency: developmental conflict in salmonids. *In* Common strategies of anadromous and catadromous fishes. *Edited by* M.J. Dadswell, R.J. Klauda, C.M. Moffitt, R.L. Saunders, R.A. Rulifson, and J.E. Cooper. American Fisheries Society, Bethesda, Md. pp. 244–252.

Thorpe, J.E. 1994. An alternative view of smolting in salmonids. Aquaculture, **121**: 105–113.

Thorpe, J.E., and Metcalfe, N.B. 1998. Is smolting a positive or a negative developmental decision? Aquaculture, **168**: 95–103.

Thorpe, J.E., and Morgan, R.I.G. 1978. Parental influence on growth rate, smolting rate and survival in hatchery reared juvenile Atlantic salmon, *Salmo salar* L. J. Fish Biol. **13**: 549–556.

Vuorinen, J., and Berg, O.K. 1989. Genetic divergence of anadromous and nonanadromous Atlantic salmon (*Salmo salar*) in the River Namsen, Norway. Can. J. Fish. Aquat. Sci. **46**: 406–409.

Yamamoto, S., Nakano, S., and Tokuda, Y. 1992. Variation and divergence of the life-history of Japanese charr *Salvelinus leucomaenis* in an artificial lake-inlet stream system. Jpn. J. Ecol. **42**: 149–157. (In Japanese with English summary.)

Yamamoto, S., Morita, K., and Goto, A. 1999*a*. Geographic variations in life history characteristics of white-spotted charr (*Salvelinus leucomaenis*). Can. J. Zool. **77**: 871–878.

Yamamoto, S., Morita, K., and Goto, A. 1999*b*. Marine growth and survival of white-spotted charr, *Salvelinus leucomaenis*, in relation to smolt size. Ichthyol. Res. **46**: 85–92.

© 2000 NRC Canada

A bioeconomic model of marine sanctuaries on Georges Bank

Daniel S. Holland

Abstract: An empirically estimated fleet dynamics model for New England trawlers is integrated with spatial, age-structured models of primary groundfish species on Georges Banks, southern New England, and the Gulf of Maine. This bioeconomic model is used to explore how permanent marine sanctuaries on Georges Bank might affect catches, revenues, and spawning stock of principal groundfish species in New England. The simulations explore how the location of sanctuaries relative to major ports and their orientation relative to seasonal movement patterns of fish stocks impact their effectiveness and the distribution of benefits across groups of fishers from different ports. The simulation results also demonstrate that the impacts of sanctuaries can vary greatly across species, sometimes increasing yields for some while decreasing yields for others. While the specific results from the simulations reflect the characteristics of the New England groundfish fishery, the modeling methodology and some general conclusions are applicable to other fisheries.

Résumé : Nous avons intégré à un modèle fondé sur des estimations empiriques de la dynamique de la flottille de chalutiers de Nouvelle-Angleterre des modèles spatiaux de la structure par âge des principales espèces de poisson de fond présentes sur le banc Georges, dans le sud de la Nouvelle-Angleterre et dans le golfe du Maine. Ce modèle bioéconomique sert à explorer la façon dont la présence de réserves marines permanentes sur le banc Georges pourrait affecter les captures, les revenus et le stock reproducteur des principales espèces de poisson de fond en Nouvelle-Angleterre. Les simulations examinent dans quelle mesure l'emplacement des réserves par rapport aux principaux ports et leur orientation par rapport aux régimes saisonniers de déplacement des stocks de poisson ont un effet sur leur efficacité et sur la répartition des profits entre les groupes de pêcheurs des différents ports. Les résultats de ces simulations montrent aussi que l'impact des réserves peut varier fortement d'une espèce à l'autre, la production pouvant augmenter pour certaines et diminuer pour d'autres. Si les résultats des simulations correspondent aux caractéristiques de la pêche du poisson de fond en Nouvelle-Angleterre, la méthodologie de modélisation et certaines des conclusions générales peuvent s'appliquer à d'autres pêches.

[Traduit par la Rédaction]

Introduction

Despite great advances in scientists' understanding of fisheries and the development and application of a wide variety of fishery management strategies, depletion and collapse of fisheries is common throughout the world (OECD 1997). Management failures are frequently the result of the inability of regulators to impose sufficient restrictions on fishing effort or catch. The collapse in the 1990s of key groundfish stocks on Georges Bank is a prime example. Natural variability of recruitment and a lack of accurate information about catch rates and the state of fish stocks make management of fisheries difficult even in the best of circumstances. In the Code of Conduct for Responsible Fisheries, the FAO (1996) has endorsed a precautionary approach to fisheries management that calls for greater use of management strategies that reduce the risk of management failures even if they do not result in the maximum production or profits from the fishery.

There is increasing interest in the use of marine sanctuaries as fisheries management tools to protect habitat and reduce the risk of fishery depletion and as a tool for rebuilding depleted fisheries. For example, in response to the collapse of important groundfish stocks on Georges Bank, the New England Fishery Management Council (NEFMC) in 1993 implemented large year-round area closures that create de facto marine sanctuaries on Georges Bank and in southern New England (NEFMC 1996). Marine sanctuaries are expected to act as a natural hatchery and nursery in which reproduction and growth are not impeded. The population inside the reserve contributes to the surrounding fishery through emigration of adult fish and increased recruitment. Marine sanctuaries may enable the maintenance of significantly higher levels of spawning stock biomass (SSB) at minimal cost in foregone revenues. Maintaining target levels of SSB is sometimes used as an objective of management (Goodyear 1989) to insure against recruitment overfishing and collapse of the fishery. As Lauck et al. (1998) showed, when catch rates vary stochastically, marine sanctuaries can reduce the probability of SSB falling below some critical level at less cost in forgone harvest than reductions in mean catch rates. Sanctuaries may also reduce the risk of fishery collapse by maintaining a more diverse age structure and genetic base. Trippel (1995) noted that the reproductive capability and resiliency to environmental fluctuations of heavily fished populations may be reduced as the average age and average age of maturity are reduced. Additional benefits may be provided through protection of critical habitat such

Received February 25, 1999. Accepted February 11, 2000. J15036

D.S. Holland. National Oceanic and Atmospheric Administration, National Marine Fisheries Service, Alaska Fisheries Science Center, 7600 Sand Point Way NE, Seattle, WA 98115, U.S.A. e-mail: dan.holland@noaa.gov

© 2000 NRC Canada

as nursery grounds favored by juvenile groundfish. Fogarty and Murawski (1998) noted that current closed areas on Georges Bank are serving this purpose.

Although they have been used in many fisheries (Rowley 1994), the impacts of marine sanctuaries are not well understood. A study of the use of time and area closures in over 50 fisheries in 11 countries produced little clear evidence of improved resource conservation (OECD 1997). A study of the effects of areas closed to trawling gear off Cape Cod was also inconclusive (Cadrin et al. 1995). There is evidence that Georges Bank groundfish stocks are now rebuilding (Neilson and Cadrin 1998; Brown 1999; O'Brien and Cadrin 1999), but it is difficult to determine the extent to which this rebuilding is due to the year-round area closures implemented in 1993 versus other effort control measures that were implemented simultaneously.

The lack of empirical evidence has motivated the use of computer modeling to explore the effects of closed areas. Building upon a model developed by Beverton and Holt (1957), Polacheck (1990) developed a model of closed areas for the Georges Bank Atlantic cod (*Gadus morhua*) stock. His results suggested that area closures were not likely to improve yields but that they might increase SSB substantially with only small reductions in yield. Polacheck and subsequent modelers have left open several important questions relevant to assessment of area closures management including how changes in recruitment resulting from increased SSB impact long-run fishery yields, how the impacts of area closures will vary for different species and stocks fished by the same fleets, and how the location and shape of area closures will impact outcomes.

A primary objective of this research is to explore how interaction of the human and biological systems influences the results of alternative area closures. As Sanchirico and Wilen (1999) demonstrated, incorporating integrated and explicitly spatial interaction of the biological and economic systems can be critical to understanding how a spatial management policy will work. Just as spatial heterogeneity in the distribution of the resource will affect the distribution of fishing effort, the distribution of fishing effort may in turn significantly alter the patterns of resource distribution that emerge. It is important to understand how the response of fishers in redistributing their fishing effort after closures will impact fish stocks in other areas and the overall productivity of the fishery.

The questions posed above are explored with a bioeconomic simulation model of the New England multispecies groundfish fishery. Unlike previous models of marine sanctuaries, the model is explicitly spatial with the distribution of fishing effort determined endogenously by an empirically estimated fleet dynamics model. The simulations are used to assess how sanctuaries of different sizes, shapes, and locations on Georges Bank might affect catches, revenues, and spawning stock of principal groundfish species throughout New England. In particular the paper explores the effect of the spatial orientation of the area closure relative to fishing ports and the seasonal movement of the fish stocks. Modeling of fishers' location choice is at the individual vessel level, which allows for the identification of heterogeneous impacts of sanctuaries on geographically dispersed fleets. The methodology used for modeling fleet dynamics also contributes to the broader question of managing biologically separate fish stocks that are fished by overlapping groups of fishers. Although the model is calibrated to a New England fishery, it provides useful insights applicable to other fisheries for which marine sanctuaries might be considered.

Methods

Simulation design

Age-structured models of Georges Bank cod, haddock (*Melanogrammus aeglefinus*), and yellowtail flounder (*Pleuronectes ferrugineus*), southern New England yellowtail flounder, and Gulf of Maine cod were developed from available information (SARC 1997) and integrated with an empirically estimated fleet dynamics model that determines the spatial distribution of a fixed level of nominal effort. Unlike previous age-structured models of these stocks (Overholtz et al. 1995), these model are spatial and use a short time step. Georges Bank is represented by a grid of 16 equal-sized areas to allow for closures of various shapes, sizes, and locations. southern New England is divided into two areas and the Gulf of Maine is divided into four. Figure 1 shows the spatial layout for the simulated fisheries. Fish move between areas within each zone but not between zones. A time step of 5 days is used to correspond to the average length of a fishing trip. Throughout the year, at each time step, individual fish grow according to von Bertalanffy weight-at-age functions (Table 1) estimated directly from weight-at-age data for these stocks (SARC 1997).

The structure (although not the parameters) of the biological models is the same for all species. To avoid superfluous subscripting, the generic model applicable to all species is discussed below. Holland (1998) provided a more detailed description of how the model is constructed including the MATLAB code used to program the simulations. To facilitate presentation, the approximate instantaneous rates of mortality and fish movement are cited in the text and tables. In the simulations, the instantaneous rates are adjusted to reflect the 5-day time step by dividing by 73, the number of periods in a year. For each cohort in each area, survival is calculated from a negative exponential relationship as

$$(1) \qquad N_{1,i,j} = N_{0,i,j} e^{-Z_{i,j}}$$

where $N_{1,i,j}$ is the number of fish in the ith cohort and jth area after each 5-day period and $Z_{i,j}$ is the total instantaneous mortality rate comprising instantaneous natural mortality M_i and instantaneous fishing mortality $F_{i,j}$. Instantaneous natural mortality for all species in all areas is set at 0.2.

Cohort-specific fishing mortality is calculated as

$$(2) \qquad F_{i,j} = q\rho_i E_j$$

where q (Table 1) is the catchability coefficient for the species (Kinani 1997), ρ_i is the age- and weight-specific partial recruitment for the ith cohort at that point in the year, and E_j is the nominal effort level in vessel days fished in the jth area. The effort E_j actually applied to a particular area is the product of the number of vessels that choose to fish there, trip length (5 days), and the proportion of time spent steaming versus fishing, which is determined by historical averages by area and month. The number of vessels that fish each area is determined by the fleet dynamics model, which is discussed below. The models assume joint production for different species within a given area so that the relative species mix of catch produced by a unit of nominal effort is determined solely by the relative stock densities of the species in that area. Squires (1987) tested for and could not reject joint production for this fleet.

The Baranov catch equation is used to calculate catch as

$$(3) \qquad C_{i,j} = N_{i,j} \frac{F_{i,j}}{Z_{i,j}} (1 - e^{-Z_{i,j}})$$

© 2000 NRC Canada

Table 1. Growth and recruitment parameters and catchability coefficients for Georges Bank, Gulf of Maine, and southern New England groundfish species.

	Weight at age t (kg) $W_t = W_\infty(1 - e^{-K(t-t_0)})^b$				Recruitment (millions); SSB (kt) $R = [(a \times \text{SSB})/(c + \text{SSB})]e^{(\sigma^2/2)}$			
Species	W_∞	K	t_0	b	a	c	σ^2	Catchability coefficient q
Georges Bank cod	142.280	0.047	−2.973	3.052	37.745	95.827	0.240	0.00160
Georges Bank haddock	4.840	0.229	−1.322	3.065	17.106	39.738	1.873	0.00090
Georges Bank yellowtail flounder	1.909	0.311	0.593	3.233	50.090	10.737	0.420	0.00314
Gulf of Maine cod	142.000	0.039	−3.917	3.052	5.594	2.543	0.682	0.00078
Southern New England yellowtail flounder	1.909	0.128	−3.914	3.233	21.851	1.422	1.178	0.00222

Note: Catchability coefficients are proportionate to those estimated by Kinani (1997) but are normalized on an arbitrary value chosen for Georges Bank cod. The level chosen for cod was determined by the fishing power of our simulated vessels relative to the standard effort unit used by Kinani (1997). These proportionate coefficients were then multiplied by the number of areas that the species occupies in the simulation. In the case where fish and fishers are evenly spread across the areas, overall catchability is the same as would be for a single-area model.

Fig. 1. Spatial layout of simulated New England groundfish fisheries.

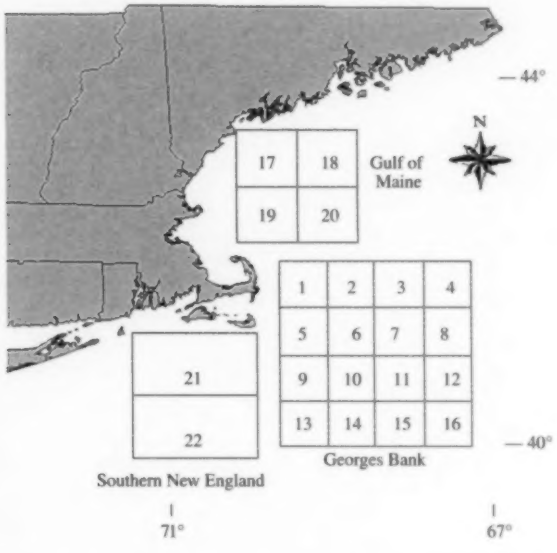

where $C_{i,j}$ is the catch in numbers from the ith cohort in the jth area. Harvest biomass from each cohort for each area is calculated by multiplying numbers of individuals caught by their age-specific weights estimated from the weight-at-age function. Total revenues for each area are calculated by summing over cohorts the product of the cohort- and species-specific harvest biomass from each area and per-kilogram prices that vary by species and fish size. Prices for each species are determined endogenously using demand relationships previously estimated for this fishery (NEFMC 1996).

At the end of each 5-day time step, fish migrations occur and the numbers of individuals in each cohort in each area are adjusted according to

$$(4) \qquad N_{1,i,j} = N_{0,i,j}\left[1 - \sum_{\forall k \neq j}(d_{j,k} + \text{sm}_{j,k})\right] + \sum_{\forall k \neq j} N_{0,i,k}(d_{k,j} + \text{sm}_{k,j})$$

where $d_{j,k}$ and $\text{sm}_{j,k}$ are the rates of diffusion and seasonal movement from area j to area k. Diffusion rates between all contiguous squares are equal for each cohort, although they may differ by species. This simply implies that an equal proportion of the fish population in each square will migrate to each contiguous square. Ignoring seasonal movement, the net flow of fish between two areas will be zero if the fish populations in each are of equal size. The seasonal movement component allows for a directional component to fish movement in addition to the random component of movement modeled as diffusion. The proportion $\text{sm}_{j,k}$ of fish in area j will move to area k in addition to and independent of whatever movement occurs as a result of diffusion. Diffusion and seasonal movement rates between noncontiguous squares and in directions other than the current direction of seasonal movement are zero.

There is not sufficient empirical information available to permit accurate modeling of seasonal movement. The seasonal movement patterns used are a stylized representation of those believed to exist and are useful in demonstrating the impacts of directional movement of fish relative to the shape and location of marine sanctuaries. The seasonal movement parameter for all species other than Georges Bank yellowtail flounder is set such that the density of the fish stocks at one end of the migratory route will be approximately two times the density at the far end at the apex of the cycle. This approximates observed relative densities for cod on Georges Bank and is achieved by setting the instantaneous seasonal movement rate at 1.46. The seasonal movement for Georges Bank yellowtail flounder is assumed to be zero, although diffusion still occurs for that stock. Seasonal movement for Georges Bank cod and haddock is modeled as an east–west movement with stocks moving east for the 6 months prior to the peak spawning period and west for the following 6 months. The Gulf of Maine stocks follow the opposite pattern, moving inshore (west) for spawning. The southern New England yellowtail flounder stock also moves inshore (north) for the 6 months prior to spawning and offshore (south) thereafter.

At the end of each year, recruitment (the number of age-1 fish at the beginning of the year) is calculated using deterministic Beverton and Holt stock–recruitment functions (SARC 1997) as

$$(5) \qquad R = \frac{a \times \text{SSB}}{c + \text{SSB}} e^{\sigma^2/2}$$

where SSB is overall SSB for each species at the peak spawning period and a and c are species-specific parameters. The estimated variance of the stock–recruitment function is σ^2, and $\sigma^2/2$ is the expected value of the multiplicative residual of the stock–recruitment function. The expected value of recruitment is the product of this residual and the stock–recruitment function (SARC 1997). The parameters for the recruitment functions are shown in Table 1. Recruitment for each species in each zone is a function of the entire spawning stock in the zone.

The number of fish that recruit to each of j areas within the zone is assumed to be an equal fraction of the entire number of recruits:

© 2000 NRC Canada

Fig. 2. Fishing grounds in New England and three-digit statistical area divisions used to designate location choices for estimating the fleet dynamics model.

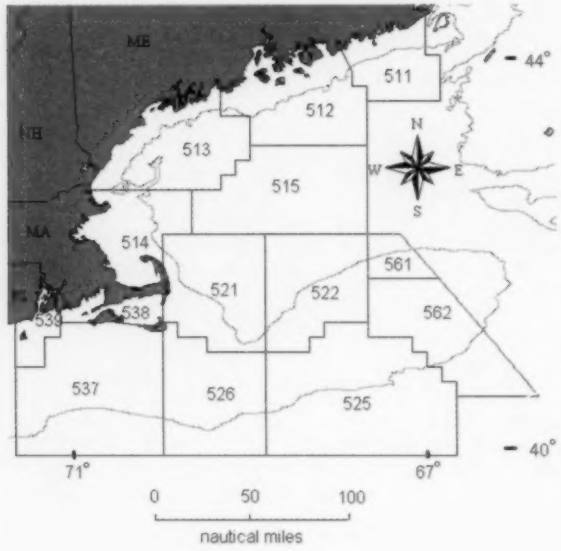

$$(6) \qquad N_{1,j} = \frac{R}{J}$$

Also, at the end of each year, all fish in cohorts age 1 and older are moved to the next cohort, and the fish movement, growth, and mortality loop for the year begins anew. Although an age-1 fish suddenly becomes an age-2 fish at the end of the year, its weight is only incremented slightly, since individual weights of fish in each cohort are increased over the year according to the fitted weight-at-age function. Cohorts are tracked through age 15 after which the survival rate is assumed to be zero.

With the exception of the yellow flounder stock in the Gulf of Maine, the biological models for these stocks are parameterized using data published in the 24th Northeast Regional Stock Assessment Workshop (SARC 1997). The flounder stock for the Gulf of Maine is actually based on the biological characteristics of the Georges Bank yellowtail flounder stock and is used as a proxy for multiple flounder stocks in the Gulf of Maine for which there were insufficient data to construct biological models.

Fleet dynamics submodel

An important goal of this study is to examine the impact on revenues, harvests, and SSB of changes in the spatial distribution of fishing effort when area closures are imposed. To that end, an empirically estimated fleet dynamics model is integrated with the biological fishery models to determine the spatial distribution of fishing effort through time. Following Holland and Sutinen (2000), a discrete choice random utility model was used to estimate an indirect utility function that explains observed location choices of New England trawlers among several discrete alternative fishing areas. The utility function was estimated with a nested logit specification (McFadden 1981) that assumes a hierarchy of decisions: first, a zone choice (e.g., Georges Bank, Gulf of Maine, or southern New England) and then an area choice within the larger zone. This utility function is used to predict location choices of individual vessels on a trip-by-trip basis using information generated internally by the simulation. The model allows for four distinct fleets from Rhode Island, Southern Massachusetts, northern Massachusetts, and Maine. The relative size of these fleets is assumed to be proportionate to their share of groundfish revenues in the 1989–1993 period.

Areas used in the statistical estimation of the fleet dynamics model are the three-digit statistical areas used by the National Marine Fisheries Service to record locations of fishing trips (Fig. 2). The spatial resolution used in estimating the utility function is coarser than that used in the simulations of Georges Bank. However, this does not pose a serious problem, since the utility function is used to evaluate the relative attractiveness of different alternatives based on a separable function of characteristics of the alternatives that are tracked for each location by the simulation. Neither the absolute levels nor the distribution of effort is tied to the historical distribution of fishing effort used in estimating the model, only to the behavioral model implied by the observed location choices. The only real difficulty presented by the finer spatial resolution for Georges Bank relates to the inclusive value parameters that, in effect, scale relative probabilities of choosing zones to account for correlation in choices within a zone. The inclusive value parameter for Georges Bank is adjusted downward to account for the fact that the number of location choices available on Georges Bank is increased in the simulations. This parameter is tuned to achieve a distribution of fishing effort across zones that matches the observed distribution of these fleets in the 1990–1993 period.

The fleet dynamics model assumes that location choices are based on the individual's evaluation of the expected profitability of alternative location choices. Expectations of profitability for a particular area are based partly, but not exclusively, on the average revenue rates of the vessels that fished in that area in the past. This information enters the predictive model as lagged average revenue per day on the grounds (i.e., net of steam time) for all vessels that landed fish from that area. Average revenues per day from both recent trips and trips the same time the prior year are included as explanatory variables. Steam time from the port of landing to the fishing area divided by expected trip length is included as a separate variable to account for the implicit opportunity cost of time spent steaming rather than fishing on a given trip. For an individual vessel, operating costs per day are assumed to be equal across alternatives and are ignored in the decision model. This does not necessarily imply that costs are assumed to be identical for different vessels, since the estimation of the model's parameters is based on comparisons of the alternatives available to each individual. The past behavior of the skipper enters the model as a dummy variable that takes a value of 1 for alternatives that were chosen on prior trips (either in the last 10 days or at the same time the prior year). Previous choices enter the decision model at both the zone choice and area choice levels of the location decision model. The model also includes lagged total effort and the surface area of each fishing area.

The fleet dynamics model described above is used to distribute a fixed quantity of nominal effort (measured in vessel days) between areas open to fishing. Total nominal effort is fixed by specifying number of vessels (150 in the simulations discussed here), the average fishing power of vessels, and the proportion of time that they spend at sea versus in port. Actual fishing time can vary, since the time at sea is divided between time spent steaming and time spent fishing, which depends on the endogenously determined location choices.

Vessels are modeled individually with a location choice (any of the numbered areas in Fig. 1) for each vessel determined each 5-day period (the time step used for the biological models) as follows. All of the variables for the utility function described above are tracked by the simulation. Average revenue per day for each area is determined by the simulation at each time step by dividing the total lagged revenue from each area by the lagged total vessel days (net of steam time) applied to that area. For both average revenue per day and total effort, two sets of lag variables are created

© 2000 NRC Canada

Table 2. Coefficients from the nested logit location choice model used to parameterize the fleet dynamics model in the Georges Bank and multizone simulations.

	Parameter	SE
Individual choice-specific coefficients		
Same area past 10 days	1.48	0.03
Same area last year	1.01	0.03
Same zone past 10 days	0.23	0.05
Same zone last year	0.31	0.05
Steam time/average trip length	–7.96	0.15
Choice-specific coefficients		
Fleet average revenues per day past 10 days	0.35	0.03
Fleet average revenues per day last year	0.51	0.05
Total effort past 10 days	0.08	0.01
Total effort last year	—	—
Surface area (1000s of km^2)	0.22	0.02
Inclusive value parameters		
Southern New England groundfish	2.01	0.05
Georges Bank groundfish	1.57	0.03
Inshore Gulf of Maine groundfish	1.35	0.03
Offshore Gulf of Maine groundfish	1.00	Fixed
Log likelihood function	–22 254	
Restricted log likelihood	–41 489	
Psuedo R^2	0.44	

Note: Pseudo R^2 calculated as 1 minus the ratio of the unrestricted and the restricted (with zero parameters) log likelihood functions.

and incorporated into the vector of explanatory variables. Recent lags are based on effort and revenues in the last two time periods (i.e., past 10 days), and year lags are based on the six periods surrounding the start date of the trip the prior year (i.e., a 30-day period). Both the average revenue and effort variables are normalized on the mean value across alternatives. The individual vessels' prior location choices, both recent and the prior year, are also tracked by the model and enter the utility function as dummy variables as described above. As with the revenue and effort variables, the "habit" variables are based on trips within the past 10 days or in the surrounding 30-day period the prior year. The variable vector for each individual and location also includes the ratio of steam time to trip length as well as the size of the area. The ratio of steam time to trip length is calculated by dividing round-trip steam time from the vessel's home port to the center of the particular area (based on a rate of 10 kn) by average historical trip lengths for each fleet for each area and month.

A utility score is calculated for each location choice for each individual. As described in Holland and Sutinen (1999), the probability of choosing a given alternative is determined by the relative utility scores of the different alternatives available to that individual. For each vessel, the model yields a set of positive probabilities (which sum to 1.0) for each of the area choices in the simulation. A fishing location for each vessel is randomly chosen according to the probability distribution calculated for that vessel. The probability of a layover (not fishing at all that 5-day period) is set at 50%, which corresponds roughly to the average proportion of time that large trawlers spent in port during the 1990–1993 period. Whether a particular vessel takes a layover or not is determined randomly by the model and is uncorrelated with location choice. The nominal effort used in eq. 2 is calculated by summing trip days for the number of vessels that choose each area and adjusting for the time that the vessels would spend steaming to and from port.

As parameters of the statistical fleet dynamics model (Table 2) indicate, location choices are strongly influenced by an individual's past location choices and the distance of the area from the landing port. However, the probabilities of choosing a particular area also increase as lagged average revenues and lagged total effort increase. It is useful to keep in mind some of the implications that these characteristics of the fleet dynamics model have for the distribution of fishing effort in the simulations. Because of the importance of steam time, vessels are more likely to choose areas closer to ports. This can allow large differences in catch rates across areas to persist. While higher average revenues per day will tend to draw vessels to areas with higher catch rates, individuals' fidelity to prior location choices and the tendency to gravitate toward areas where other vessels have been fishing slow the redistribution of effort toward higher-revenue areas. Since individuals are heavily influenced by choices made in the same period the prior year, seasonal patterns of fishing effort emerge that reflect the regular seasonal movement patterns of the fish.

Fig. 3. Diagrams of the areas of the Georges Bank grid closed for alternative area closure simulations. In the simulations, the shaded areas are closed to fishing.

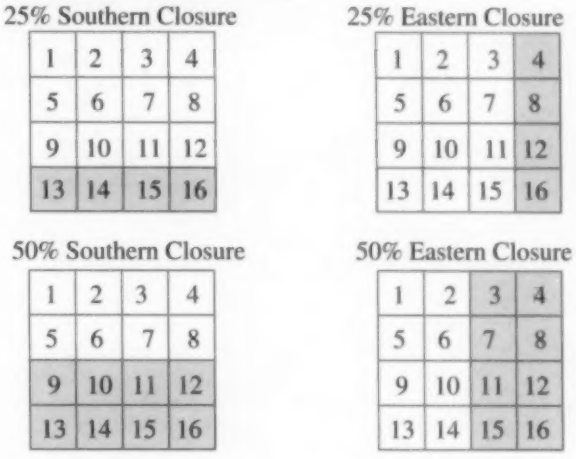

Experimental design

The bioeconomic model discussed above is used to explore the impacts of alternative marine sanctuaries on Georges Bank under varying assumptions about rates of fish movement and levels of nominal effort. For each scenario the effects of different area closures on cumulative discounted revenues are compared with the levels achieved with no closure. Cumulative revenues are in present value terms discounted at a rate of 7%, which is the rate used by the NEFMC in evaluating different rebuilding plans for this fishery (NEFMC 1996). It is also useful to consider how sanctuaries impact equilibrium harvest levels. This allows us to differentiate the long-run and short-run impacts of closures. It also helps to distinguish the impacts of time discounting and price changes from changes in revenues that would result solely from changes in equilibrium harvests. Since recruitment and total nominal effort are not stochastic in these simulations, they do not offer the opportunity to directly assess the benefits that maintaining a higher level of SSB might provide in reducing risks of fishery depletion or collapse. However, it is useful to consider how the equilibrium level of SSB varies for different closure options, as it may be an indirect indicator of value provided in the form of insurance against management failures or environmental perturbations. Equilibrium levels of harvest and SSB are the levels at year 30 by which point both have stabilized.

Due to the coarseness of the spatial grid of Georges Bank (only 16 cells) and because of computational expense, only a limited set

© 2000 NRC Canada

Fig. 4. Variation over time of (*a*) CPUE and (*b*) effort for Georges Bank cod in areas 1–4 in a single-species simulation with no area closures in place. Thin dashed line, area 1; thick dashed line, area 2; thick solid line, area 3; thin solid line, area 4.

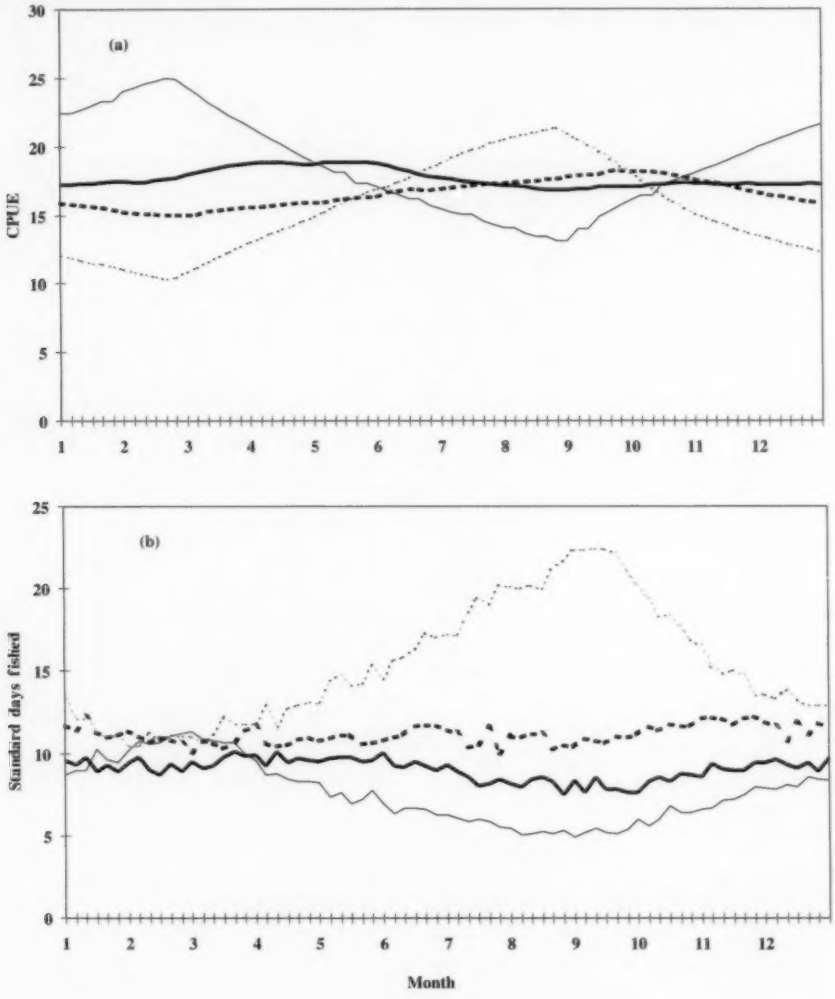

of closure scenarios are explored and no attempt is made to find the "optimal" size or location for a closure. The closure scenarios explored in the simulations proscribe fishing in either a west-to-east or a north-to-south corridor of the spatial grid that represents Georges Bank. For example, a 25% southern closure would close the areas labeled 13, 14, 15, and 16 (Fig. 3), while a 50% eastern closure would close areas 3, 4, 7, 8, 11, 12, 15, and 16.

For each model and each set of closure scenarios, simulations are run with three different levels of nominal effort to demonstrate the relative benefits of sanctuaries with varying levels of fishing intensity. For low-effort scenarios, nominal effort is set at the level that results in a maximum sustainable yield (MSY) level of fishing mortality for Georges Bank cod with no closures in place. For medium-effort scenarios, nominal effort is twice that level, and for high-effort scenarios, effort is set at four times the MSY level for Georges Bank cod. The diffusion rate of fish is believed to be a key element of the model. Since its true magnitude is uncertain, each simulation is run with high and low diffusion (instantaneous diffusion rates used are 1.0 and 0.1) to test the sensitivity of model results to this parameter. Some additional sensitivity analysis varying seasonal migration rates is also discussed.

The level and distribution of fish stocks and the location choice decision variables are initialized by running the simulation at the given level of effort with no area closure long enough to reach a dynamic equilibrium. The area closure is then imposed and harvest, revenue, and SSB levels are tracked for a period of 30 years following the closure, the length of time sufficient to reach a new dynamic equilibrium. Although total nominal effort is fixed, the distribution of effort is stochastic, so each version of the simulation is run multiple times and average results are reported. Models are run a sufficient number of times to allow for the identification of a 1% difference in the levels of harvests, revenues, SSB, and fishing mortality with 95% probability.

Results

Before presenting the results from specific closure scenarios, it is instructive to consider the mechanics behind these

© 2000 NRC Canada

Fig. 5. Changes in cumulative discounted revenues for the combined fleets for simulations with varying levels of nominal effort and diffusion. Diagrams show percent changes in revenues relative to the levels with no area closures for alternative (*a*) 25% area closures and (*b*) 50% area closures.

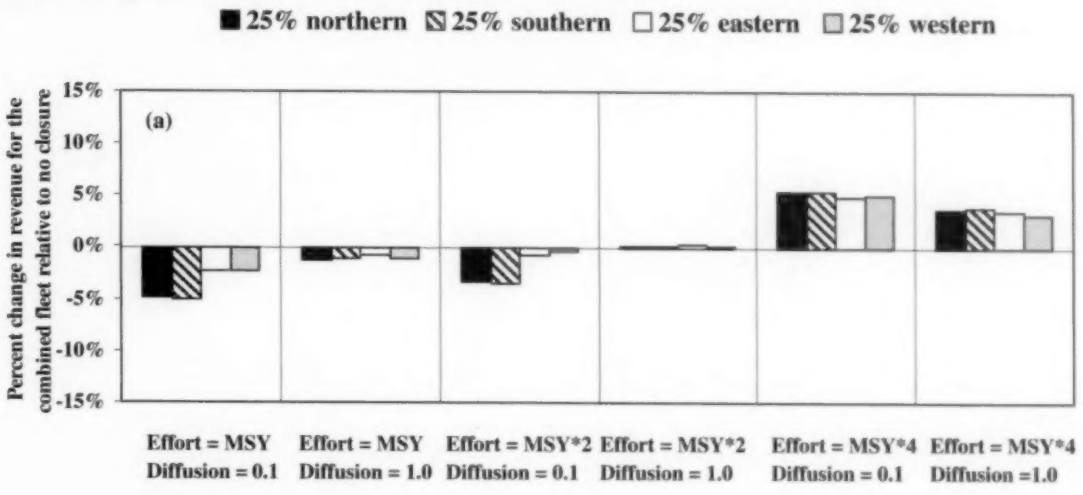

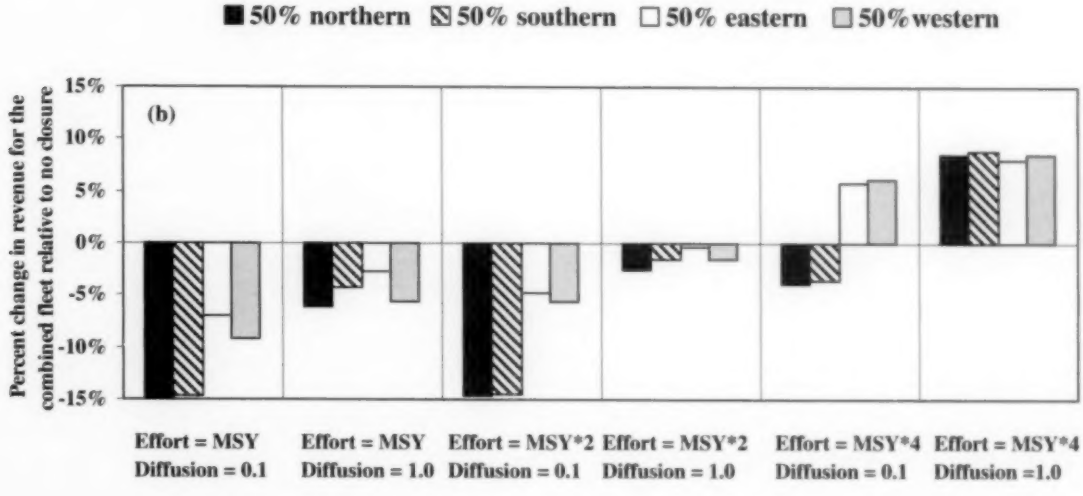

results, particularly how the location and shape of the closures affect outcomes. The geographic orientation of the closure is important because Georges Bank cod and haddock are assumed to follow an east–west seasonal movement pattern moving toward the east for the 6 months of the year prior to the peak spawning period at the end of February and moving west the rest of the year. The migratory patterns of the fish result in shifting patterns of fishing effort through the year as vessels shift effort to areas with higher abundance. This is illustrated by considering how effort is distributed across areas in a simplified simulation of Georges Bank cod only with no closure in place and a single fleet (Fig. 4). The figure shows catch per unit effort (CPUE) and nominal effort for areas 1–4. Although effort tends to concentrate where fish are concentrated, distance from port also affects the distribution of effort. The added steam time to area 4, which is further from port, limits the concentration of effort there during the winter despite the fact that CPUE is considerably higher than in area 1.

These general patterns of fishers concentrating, but not fishing exclusively, in areas where fish are more concentrated carry over to the more complicated multizone, multifleet simulations. When a closure is imposed along the eastern or western edge of Georges Bank perpendicular to the seasonal movement of cod and haddock, the productivity of fishing effort is decreased immediately because many

© 2000 NRC Canada

Fig. 6. Changes in cumulative discounted revenues for the combined fleets and for each of the regional fleets resulting from alternative area closures for simulations with effort at the medium level and alternative diffusion rates set at (*a*) 0.1 and (*b*) 1.0. Diagrams show percent changes relative to the levels with no area closures. Solid bars, 25% northern closure; hatched bars, 25% southern closure; open bars, 25% eastern closure; shaded bars, 25% western closure.

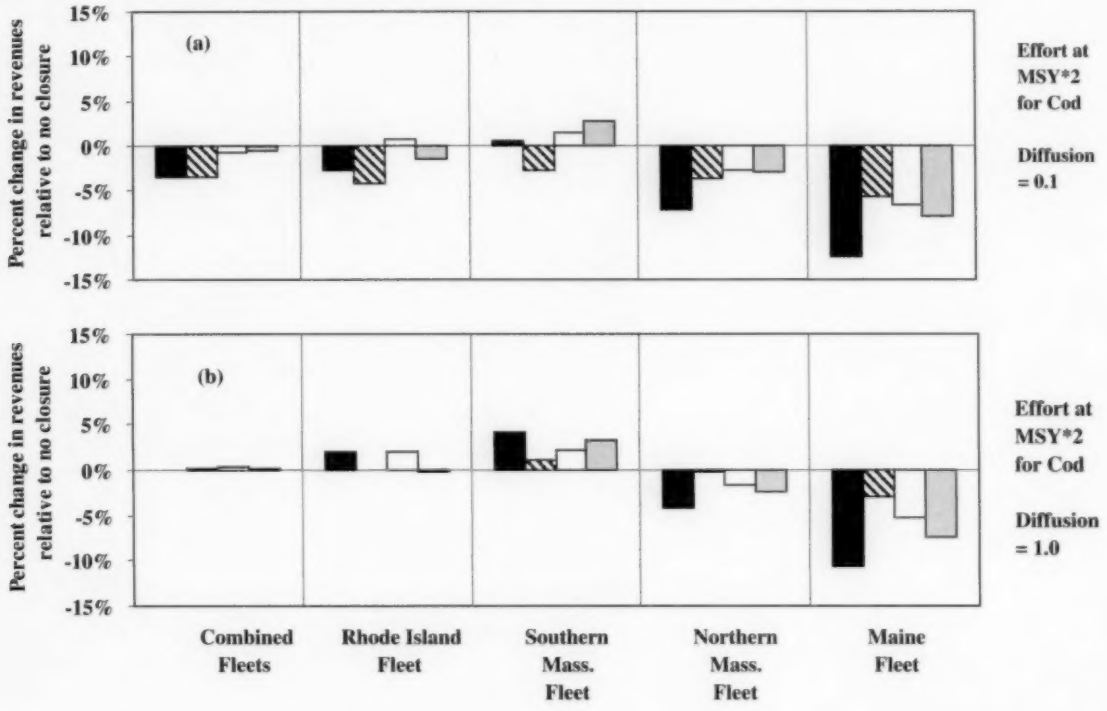

fishers that continue to fish Georges Bank are precluded from fishing in high-CPUE areas where fish aggregate seasonally. Even if nominal effort on Georges Bank remains constant, fishing mortality for Georges Bank cod and haddock drops immediately because the average efficiency of a unit of fishing effort decreases. Fishing mortality for all Georges Banks stocks declines further if effort is displaced from Georges Bank. However, these closures provide little year-round refuge for cod and haddock, since there is a high probability that any individual fish will move outside the closed area during part of the year and be caught. Thus, eastern and western edge closures work much like any other measure that reduces the efficiency or nominal level of fishing effort.

The results of southern or northern closures parallel to the seasonal movement of cod and haddock are quite different. When the closure is imposed, the east-to-west distribution of effort and the productivity of fishing effort on Georges Bank are changed little. Any immediate decline in fishing mortality for Georges Bank cod and haddock results from displacement of nominal effort off Georges Bank to other zones. However, since the closure provides protection all along the migratory range of the fish, resident fish stocks begin to build up inside the area closure, and consequently, the fishing mortality on the overall stock eventually declines considerably. Fishing effort also becomes more concentrated adjacent to the area closure because CPUE in those areas is increased by fish migrating out of the closed area. Southern or northern closures, particularly if the diffusion rate is low, allow relatively older and larger spawning stocks of Georges Bank cod and haddock to build up than do eastern or western closures of equal size.

Simulations were conducted with 25 and 50% area closures along the eastern, western, northern, or southern edge of Georges Bank. Each closure scenario was run with both high and low diffusion rates and a range of effort levels, as discussed under the Experimental design section. Discounted cumulative revenues for the overall fleet were significantly increased by area closures only in the simulations where nominal effort was set at the highest level (four times the MSY level for Georges Bank cod) (Fig. 5). With effort at the highest level, various area closures increase cumulative discounted revenues by 3–8%, with the greatest gains coming from closures of 50% of Georges Bank. All of the closure scenarios with low effort result in present value losses to the overall fleet. When nominal fishing effort is at the medium level and the diffusion rate of fish is set at 1.0, there are a number of closure options that maintain the combined fleet's discounted revenues at essentially the same level as with no closure (Fig. 5). There are also a number of closure scenarios, even with effort at the lower level, that result in only small reductions in revenues, particularly if diffusion is high (i.e., set at 1.0).

The impacts of area closures on different fleets can vary considerably from overall outcomes, however (Fig. 6). The

© 2000 NRC Canada

Fig. 7. Changes in annual harvests at year 30 by species resulting from alternative area closures for simulations with effort at the medium level and alternative diffusion rates set at (*a*) 0.1 and (*b*) 1.0. Diagrams show percent changes relative to the levels with no area closures. Solid bars, 25% northern closure; hatched bars, 25% southern closure; open bars, 25% eastern closure; shaded bars, 25% western closure. GB, Georges Bank; GOM, Gulf of Maine; SNE, southern New England.

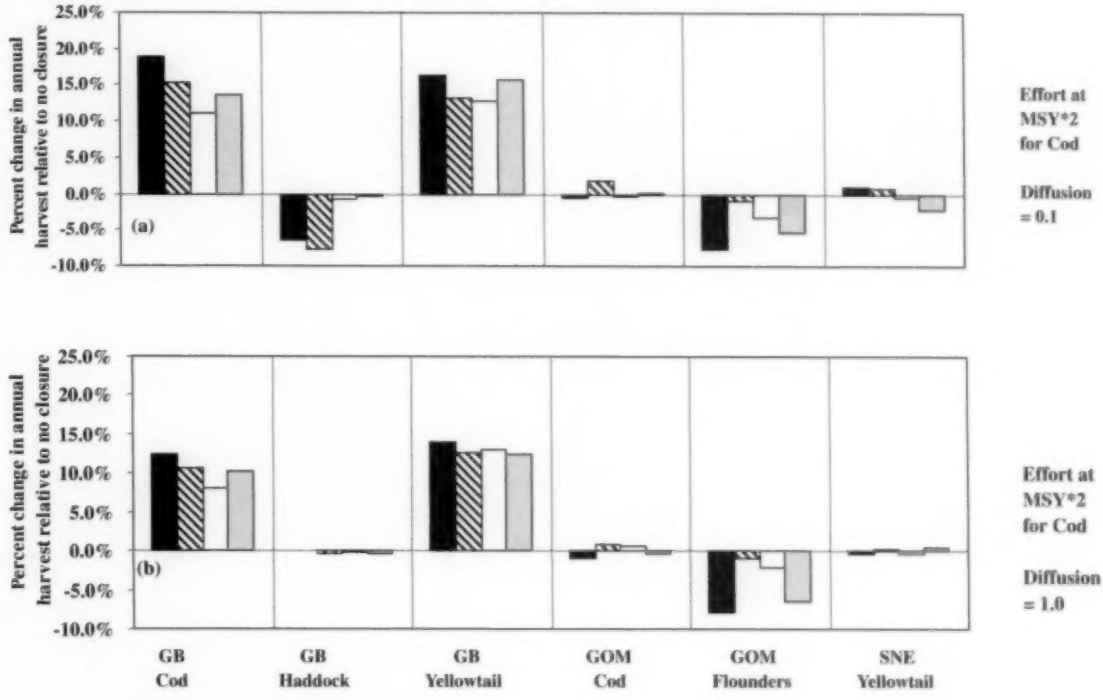

fleet from southern Massachusetts tends to gain most from area closures, often benefiting from closures that reduce revenues for the overall fleet. Revenues for the southern Massachusetts fleet increase under a variety of closure scenarios even with effort at the lower level. In contrast, the fleets from northern Massachusetts and Maine tend to suffer from closures even when the other fleets benefit from them.

These results might seem counterintuitive at first, since it is the fleet from southern Massachusetts that most heavily fishes Georges Bank in the absence of area closures and is therefore most directly affected by them. To understand the reasons for this result, consider the results of a 25% closure along the northern edge of Georges Bank under the assumptions of medium levels of effort and high diffusion. Total effort is initially displaced from Georges Bank to the Gulf of Maine and southern New England, with effort on Georges Bank falling by 14% in the year following the closure and effort in the Gulf of Maine and southern New England rising by 26 and 17%, respectively. As conditions improve on Georges Bank, some of that effort returns, but Georges Bank's share of total nominal effort returns to only 94% of preclosure levels, and effort in the Gulf of Maine and southern New England stabilizes at 112 and 103% of preclosure levels, respectively. For vessels that continue fishing on Georges Bank, revenues per unit of effort begin to rise immediately and reach a dynamic equilibrium 14% above preclosure levels. In equilibrium, average revenues for vessels fishing in the Gulf of Maine decline by 17% as a result of increase fishing pressure, while average revenues in southern New England decline by 8%.

The northern fleets' effort is already concentrated in the Gulf of Maine before the closure, and after the closure, even more of their effort is concentrated there. The average revenue for those vessels that switch from Georges Bank to the Gulf of Maine drops because they are moving to what was already a less profitable area before the area closure was implemented. Average revenues for the northern fleets drop further as catch rates in the Gulf of Maine fall due to the additional effort being applied there with resulting declines in biomass. Average revenues for southern fleet vessels that are displaced also tend to decline but by less than for the northern fleets because most are displaced to southern New England where rates of average revenue are higher than for the Gulf of Maine. Furthermore the southern fleets' fishing effort is concentrated, both before and after the closures on Georges Bank where average revenue rates rise as a result of closures.

Alternative closure locations have heterogeneous effects on the revenues of the different fleets because they displace different groups of vessels to different alternative locations. A 25% southern closure (again assuming medium effort and high diffusion) tends to result in relatively less displacement of the northern fleets into the Gulf of Maine. Consequently, average revenue rates decline less in the Gulf of Maine. Cumulative discounted revenues still decline for the northern fleets but by less than with the northern closure (Fig. 6). The

© 2000 NRC Canada

Fig. 8. Changes in SSB at year 30 by species resulting from alternative area closures for simulations with effort at the medium level and alternative diffusion rates set at (*a*) 0.1 and (*b*) 1.0. Diagrams show percent changes relative to the levels with no area closures. Solid bars, 25% northern closure; hatched bars, 25% southern closure; open bars, 25% eastern closure; shaded bars, 25% western closure. GB, Georges Bank; GOM, Gulf of Maine; SNE, southern New England.

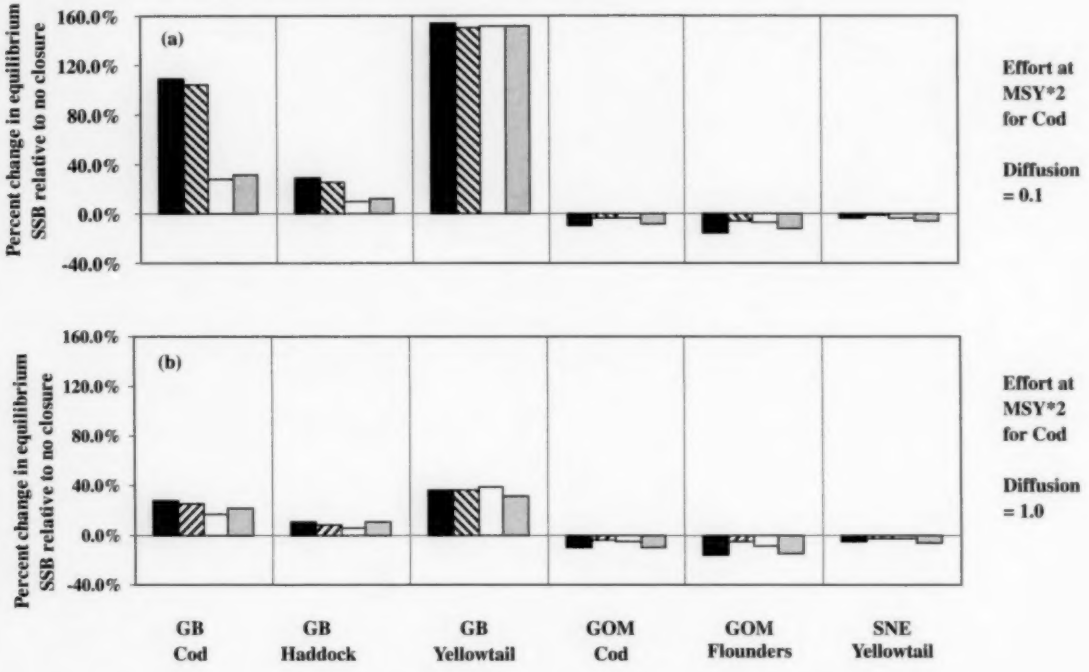

southern closures result in relatively more displacement of the southern fleets, and revenue gains for those fleets are smaller as a result.

Eastern and western closures also have different effects. Eastern closures tend to displace less effort from Georges Bank than do other closure locations, since fewer vessels are fishing in the far eastern areas when no closures are in place. Consequently, the gains for the southern Massachusetts fleet (which gains most when other fleets are displaced from Georges Bank) are smaller than with a western closure. Relative to an eastern closure, western closures result in more displacement of effort both to southern New England and to the Gulf of Maine, which is to the relative disadvantage of the Rhode Island fleets and the two northern fleets but benefits the southern Massachusetts fleet.

The percent increase (decrease) in discounted cumulative revenues resulting from area closures is always smaller (larger) than the increase (decrease) in equilibrium annual revenues, since area closures initially reduce annual harvest and revenues before they eventually rise. In fact, all of the 25% area closure scenarios and many of the 50% area closures with medium effort levels increase equilibrium revenue for the overall fleet. When effort is at the lower level and diffusion is set at the higher level, equilibrium revenues are unchanged by any of the 25% area closures but do fall significantly with larger closures.

These simulations used prices for fish that were determined by empirically estimated price models with downward sloping demand curves. Thus, prices tend to rise when harvests initially decline after area closures are imposed, but prices later fall below preclosure levels if harvests rise above preclosure levels. These two effects largely cancel each other out. When the results of these simulations were compared with simulations that assumed constant (or perfectly elastic) prices, the results of the simulation were not substantially changed.

Sanctuaries have quite varied effects on different species. While a variety of closures at medium effort levels increase equilibrium harvests of Georges Bank cod and yellowtail flounder, these same closures often decrease harvests of other species such as Georges Bank haddock and Gulf of Maine flounders (Fig. 7). For Georges Bank haddock, this is primarily due to the difference in catchability coefficients between haddock and the other species of groundfish on Georges Bank. Because catchability of haddock is relatively low, fishing mortality in the absence of a closure is much lower than for cod and yellowtail flounder. For medium-effort scenarios, Georges Bank cod and yellowtail flounder equilibrium harvests rise as a result of area closures because fishing mortality declines to a level closer to the MSY level, while haddock harvests decline in some cases because fishing mortality falls to a level below that required to achieve MSY for haddock.

Since the area closures result in redistributions of fishing effort among zones, they also affect equilibrium harvests of species off Georges Bank. In southern New England and the Gulf of Maine, which absorb displaced effort, harvests initially rise, although catch rates and average revenue rates de-

© 2000 NRC Canada

cline. If effort is already at or above the MSY level, the added effort can lead to a decrease in equilibrium harvest in these zones. The impact on equilibrium harvests for the stocks in southern New England and the Gulf of Maine depends on whether the increased fishing effort brings fishing mortality closer to or further from the MSY level of the particular stock. With effort at the medium level, the equilibrium effects of effort displacement on southern New England yellowtail flounder harvests and Gulf of Maine cod tend to be relatively minor, since preclosure fishing mortality is close to the MSY level for those stocks and the yield curve is rather flat. However, northern and western closures that result in substantial effort displacement into the Gulf of Maine tend to reduce equilibrium flounder harvests in the Gulf of Maine.

Because of net shift of effort from Georges Bank to the other zones resulting from area closures, SSB for stocks in those zones always decrease, while SSB of Georges Bank stocks increase (Fig. 8). The percent increase of SSB for Georges Bank stocks varies greatly by species and depends on the location of the closure, nominal effort levels, and assumptions about diffusion. Closures that result in relatively more displacement of effort from Georges Bank to other areas yield relatively greater gains in SSB of Georges Bank stocks and greater declines of the other stocks. Gains are greater for yellowtail flounder than for cod, and haddock SSB increases the least of the Georges Bank species. Increases in SSB are naturally greater when diffusion is low, as this increases the level of protection that a given sanctuary affords. For cod and haddock, which have seasonal movement patterns, area closures parallel to seasonal movement tend to lead to greater increases in SSB, again because these sanctuaries provide greater protection to the stock in the long run.

One of the parameters in the model that is poorly understood is the rate of seasonal movement. To test the sensitivity of the results to this parameter, simulations were run with the seasonal movement rate halved and doubled. Increasing the seasonal movement rate tends to increase the productivity of fishing effort, since it results in greater geographic concentration of fish stocks and thus greater susceptibility to spatially targeted fishing effort. Consequently, in cases where fishing effort is above the MSY level, harvests and revenues are lower with a higher seasonal movement rate regardless of whether a closure is implemented. The opposite is true if effort is below the MSY level. However, the adjustments to this parameter do not have significant effects on the impact of alternative area closures relative to the baseline case with no closure. Discounted cumulative revenues (overall and for the different fleets) of alternative closures relative to no closures are changed less than 1%.

Discussion

These simulations should not be regarded as predictions of the impacts of the area closures actually implemented on Georges Bank in 1993. They do not reflect the actual status of stocks at that time or the locations and sizes of those closures. Furthermore, because a number of simplifying assumptions were required to make the model tractable, and the models do not reflect the constantly changing suite of regulations imposed in these fisheries, we should not expect them to accurately predict the absolute impacts that alternative closures will have on fish stocks, harvests, or revenues. Nevertheless, they provide considerable insights into the mechanics of how marine sanctuaries might be expected to work under various conditions and are useful in identifying critical parameters that drive the results. Identification of key parameters provides a focus point for future empirical work. The results also illustrate how fishers' behavior in response to area closures of different sizes and locations can impact the results of these closures.

These simulations show that the primary impact of marine sanctuaries is to decrease the efficiency of nominal effort by prohibiting fishing in areas where stocks have aggregated densely. When fish exhibit seasonal movement and tend to aggregate at different areas at different times of year, the location and shape of the area closures may have profound effects on how they work, although the long-run impacts may be similar in some cases. Closures of the areas where fish tend to aggregate seasonally may result in quick reductions in fishing mortality even when nominal effort remains constant. Such area closures effectively reduce the efficiency of fishing effort by displacing fishers to areas where fish stocks are less dense and CPUE lower. By contrast, closures that provide partial protection throughout the migratory range of a stock may have less effect on overall fishing mortality in the short run but may reduce it considerably once a resident stock of fish builds up inside the boundaries of the area closure. In equilibrium, particularly when diffusion rates are low, an area closure that encompasses the seasonal movement patterns of a resident subpopulation will result in a greater reduction in effective fishing effort and fishing mortality than will an area closure of equal size that provides a refuge for dense aggregations of fish but little year-round protection. Although area closures do affect the age structure of the fish population, the effect appears to differ little from that of simply reducing fishing mortality on the overall stock.

If fish migration out of such sanctuaries is very low, they may reduce harvest substantially, even in the long run. In the simulations, the rate of diffusion was an assumption of the model as opposed to a control variable. However, the effective rate of diffusion of fish across reserve boundaries can be controlled to some degree by the design of the reserve. If true migrations rates are believed to be too low to provide sufficient spillover from the closed areas, a few smaller area closures may be more effective than one large one.

Although these simulation results indicate that marine sanctuaries may be useful in increasing equilibrium harvests and SSB for heavily fished stocks, they show less promise for increasing the value derived from the fishery. Sanctuaries initially result in harvest declines that, in present value terms, weigh more heavily than revenue increases that may occur once a new equilibrium is reached. In addition, increases in harvests and revenues from stocks that receive protection from the sanctuary may be offset by reduction in harvests and revenues from stocks that absorb displaced effort if those stocks are already fully utilized.

The simulations demonstrate that sanctuaries will have heterogeneous impacts on individuals and on user groups from different ports. Even when the sanctuary results in little change in overall revenues, there can be winners and losers,

© 2000 NRC Canada

and the distribution of gains and losses may not be intuitively obvious. Just as it affects who is displaced, the location of the area closure will impact where effort is displaced to. Fishers in areas to which effort is displaced will almost certainly suffer reduced profits due to declines in catch rates. Due to heterogeneity among fishers, fishing effort may not adjust spatially to equate marginal revenue rates among fishers. However, if area closures significantly change the relative profitability of different fisheries and areas, they may, in the long run, lead to declines in the fleets of some ports and increases in others, which might tend to moderate differences in incomes among fishers in different areas.

The results from these simulations demonstrate the difficulty of managing multiple species that are jointly fished by the same fleet. Even when nominal effort can be controlled, differences in catchability across jointly targeted species may make it impossible to reach the optimal level of fishing mortality for all species. Use of area closure further complicates things because the spatial dynamics and hence the effects of the closures are likely to vary across species.

The simulations highlight the need to consider effects on fish stocks other than those directly affected by sanctuaries when evaluating management measures. In many fisheries, fishers have the flexibility to redirect their effort to other stocks and other species as their relative profitabilities change. Management measures that result in increases in harvest or revenues from one stock or fishery may come at the expense of the health of other stocks. The experience with the Gulf of Maine cod stock is an excellent example. Effort displaced from Georges Bank caused a severe decline in Gulf of Maine cod stocks leading National Marine Fisheries Service scientists to recommend a halt of all directed fishing for cod in the Gulf of Maine (SARC 1998). Although the simulation considered only movements of vessels to alternative groundfish stocks, there has clearly been redirection of effort from groundfish toward other species in New England.

Conclusions

In conclusion, these simulations of marine sanctuaries on Georges Bank suggest that properly designed area closures can maintain and in some cases increase fishery revenues and harvests when fishing effort is excessive prior to the closure. Increased revenues and harvests result primarily from decreasing the efficiency of nominal effort. From an economic standpoint, one must question whether policies geared expressly toward decreasing efficiency of effort are the best choice. Increases in harvests and revenues that result from area closures might also be accomplished by controlling nominal fishing effort or by directly controlling total catch. Greater increases in profit might be realized in this way due to costs savings resulting from fewer vessels fishing fewer days. Furthermore, reliance on indirect controls on fishing effort to maintain the appropriate level of effective fishing effort can be risky. Unless nominal effort is tightly controlled, increases in revenues that result from area closures may be dissipated if effort expands in response to higher average revenues. Even when the number of participants and the time that they are allowed to fish are strictly controlled, effective effort may be increased by improvements to vessels and gear.

However, a direct means of controlling effort or catch is not always feasible for practical or political reasons, and area closures may well be the best alternative available in some cases. In addition, marine sanctuaries may provide other benefits that were not quantified monetarily in these simulations. By providing protection of critical habitat and allowing maintenance of higher levels of SSB, sanctuaries may significantly reduce the risks of depletion and collapse of the fishery. They may also maintain greater biodiversity.

The effects of a marine sanctuary will depend on factors such as seasonal movement patterns of fish and locations relative to fishing ports that will almost certainly vary from one fishery to the next. Consequently, the value of trying to develop general rules of thumb for design of marine sanctuaries may be limited. Considerable research on the behavior of both fish and fishers in a given fishery will be required before area closures can be designed effectively for that fishery. Arbitrary designation of areas as marine sanctuaries may result in significant reductions in fisheries revenues and may have quite unequal and unintended impacts on different groups of fishers. Fisheries managers must also guard against overfishing of other stocks toward which effort may be redirected as a result of area closures. Furthermore, the concentration of fishing effort in smaller areas open to fishing could lead to habitat degradation in those areas.

Acknowledgements

Any opinions expressed in this manuscript are those of the author alone and should not be attributed to the National Marine Fisheries Service. Research for this paper was supported by the Rhode Island Sea Grant Program and by the Medical Foundation for Human Health and the Environment. I would also like to thank Jon Sutinen, James Anderson, Jeremy Collie, and three anonymous referees for helpful comments during the research and on earlier drafts of this manuscript.

References

Beverton, R.J.H., and Holt, S.J. 1957. On the dynamics of exploited fish populations. Fish. Invest. Ser. 2. Vol. 19. U.K. Ministry of Agriculture and Fisheries, London, U.K.

Brown, R.W. 1999. 1998 assessment of Georges Bank haddock. Northeast Fish. Sci. Cent. Ref. Doc. 99-07.

Cadrin, S.X., Howe, A.B., Correia, S.J., and Currier, T.P. 1995. Evaluating the effects of two coastal mobile gear fishing closures on finfish abundance off Cape Cod. N. Am. J. Fish. Manage. **15**: 300–315.

Fogarty, M.J., and Murawski, S. 1998. Large-scale disturbance and the structure of marine systems: fishery impacts on Georges Bank. Ecol. Appl. **8**(Suppl.): s6–s22.

Food and Agriculture Organization of the United Nations (FAO). 1996. Precautionary approach to capture fisheries and species introductions. FAO Technical Guidelines for Responsible Fisheries No. 2. FAO, Rome.

Goodyear, C.P. 1989. Spawning stock biomass per recruit: the biological basis for a fisheries management tool. ICCAT Working Doc. SCRS/89/82.

Holland, D. 1998. The use of year-round closed areas for the management of New England trawl fisheries. Ph.D. thesis, University of Rhode Island, Kingston, R.I.

© 2000 NRC Canada

Holland, D., and Sutinen, J. 1999. An empirical model of fleet dynamics. Can. J. Fish. Aquat. Sci. **56**: 253–264.

Holland, D., and Sutinen, J. 2000. Location choice in New England trawl fisheries: old habits die hard. Land Econ. **76**(1): 133–149.

Kinani, A. 1997. Catchability of fishing gears used in the New England groundfish fishery. M.S. thesis, University of Rhode Island, Kingston, R.I.

Lauck, T., Clark, C.W., Mangel, M., and Munroe, G. 1998. Implementing the precautionary principal in fisheries management through marine reserves. Ecol. Appl. **8**(Suppl.): s72–s78.

McFadden, D. 1981. Econometric models of probabilistic choice. *In* Structural analysis of discrete data with econometric applications. *Edited by* C.F. Manski and D. McFadden. MIT Press, Cambridge, Mass.

Neilson, J.D., and Cadrin, S.X. 1998. 1998 assessment of Georges Bank yellowtail flounder. Can. Stock Assess. Secretariat Res. Doc. 98/67.

New England Fishery Management Council (NEFMC). 1996. Final amendment No. 7 to the northeast multispecies fishery management plan. Append. 10. February 7, 1996. NEFMC in consultation with NMFS. NEFMC, Saugus, Mass.

O'Brien, L., and Cadrin, S.X. 1999. 1998 Assessment of the Georges Bank cod stock. Northeast Fish. Sci. Cent. Ref. Doc. 99-03.

Organization for Economic Cooperation and Development (OECD). 1997. Toward sustainable fisheries: economic aspects of the management of living marine resources. OECD, Paris, France.

Overholtz, W.J., Edwards, S.F., and Brodziak, J.K.T. 1995. Effort control in the New England groundfish fishery: a bioeconomic perspective. Can. J. Fish. Aquat. Sci. **52**: 1944–1957.

Polacheck, T. 1990. Year round closed areas as a management tool. Nat. Resour. Model. **4**: 327–353.

Rowley, R.J. 1994. Case studies and reviews: marine reserves in fisheries management. Aquat. Cons. Mar. Freshwater Ecosyst. **4**: 233–254.

Sanchirico, J.N., and Wilen, J.E. 1999. Bioeconomics of spatial exploitation in a patch environment. J. Environ. Econ. Manage. **37**: 129–150.

Squires, D. 1987. Fishing effort: its testing, specification, and internal structure in fisheries economics and management. J. Environ. Econ. Manage. **14**: 268–282.

Stock Assessment and Review Committee (SARC). 1997. Draft report of the 24th Northeast Regional Stock Assessment Workshop. Stock Assessment and Review Committee, Woods Hole, Mass.

Stock Assessment and Review Committee (SARC). 1998. Draft report of the 25th Northeast Regional Stock Assessment Workshop. Stock Assessment and Review Committee, Woods Hole, Mass.

Trippel, E.A. 1995. Age at maturity as a stress indicator in fisheries. BioScience, **45**: 759–771.

© 2000 NRC Canada

ASSIGNMENT OF COPYRIGHT

Ms. No. _____

To: NATIONAL RESEARCH COUNCIL OF CANADA ("NRC") Research Press

From: _____

_____

_____

_____

(name and address of author signing this form)

This refers to the manuscript entitled: _____

_____

written by myself and the following additional author(s): _____

_____

for publication in: _____

1. I declare that the list of authors fairly conforms to academic conventions about who should be listed. I declare that the manuscript, or its equivalent, has not been submitted for publication elsewhere. If it is accepted for publication by the National Research Council of Canada, I will ensure that it, or its equivalent, is not submitted for publication elsewhere.

2. I declare that I am (check ONE):

☐ (a)	the sole owner of the copyright relating to the manuscript,	and → I **assign** to NRC the entire copyright.
☐ (b)	a part owner of the copyright, in conjunction with interests held by co-authors or their employers,	and → I **assign** to NRC my entire interest in the copyright, and I expect the co-authors to also sign a form like this one.
☐ (c)	an agent of my employer with authority to assign the copyright owned by the employer, who is: _____,	and → I **assign** to NRC, on behalf of my employer, my employer's entire interest in the copyright relating to the manuscript, and I expect the co-authors to also sign a form like this one.
☐ (d)	a public servant in Canada (federal, provincial or territorial) or the United Kingdom, so that the copyright is owned by Her Majesty,	and → I have obtained the approval of my employer, according to the terms of my employment, to grant NRC **non-exclusive permission** to publish the manuscript and administer the copyright.
☐ (e)	a public servant of the United States of America, and subject to the law that creates no U.S. copyright for the manuscript,	and → I **assign** to NRC, on behalf of my employer, my employer's entire interest in any copyright that may exist outside the U.S., and I expect the co-authors to sign a form like this one.

3. I understand that my submission of this document does not guarantee publication, and that publication will not occur until **all authors** have provided a copyright transfer. If the manuscript is not published within 2 years after I sign this, the assignment is revoked.

Signed at _____ on _____

(City and Province/State) (Date)

_____

(Signature)

[Standard NRC form; alterations not acceptable.]

Comments on Copyright Transfer
(with extracts from the *Copyright Act*, Revised Statutes of Canada 1985, chapter C-42, as amended)

The publisher is not permitted to publish the manuscript without permission or an assignment of ownership of copyright. For greatest flexibility, and to be prepared to deal with future uses of the published material, the publisher requires ownership.

The owner may assign the right, but that assignment must be in writing:

13.(4) The owner of the copyright in any work may assign the right, either wholly or partially, and either generally or subject to territorial limitations, and either for the whole term of the copyright or for any other part thereof, and may grant any interest in the right by licence, but no assignment or grant is valid unless it is in writing signed by the owner of the right in respect of which the assignment or grant is made, or by his duly authorized agent.

The owner may be the author, but in many cases, the owner is the author's employer:

13.(3) Where the author of a work was in the employment of some other person under a contract of service or apprenticeship and the work was made in the course of his employment by that person, the person by whom the author was employed shall, in the absence of any agreement to the contrary, be the first owner of the copyright, but where the work is an article or other contribution to a newspaper, magazine or similar periodical, there shall, in the absence of any agreement to the contrary, be deemed to be reserved to the author a right to restrain the publication of the work, otherwise than as part of a newspaper, magazine or similar periodical.

The only exception to taking ownership arises when the manuscript is covered by Crown copyright owned by a Canadian government.

12. Without prejudice to any rights or privileges of the Crown, where any work is, or has been, prepared or published by or under the direction or control of Her Majesty or any government department, the copyright in the work shall, subject to any agreement with the author, belong to Her Majesty and in that case shall continue for the remainder of the calendar year of the first publication of the work and for a period of fifty years following the end of that calendar year.

Governments, and in particular the federal government, do not have a simple mechanism for assigning ownership of this particular type of Crown asset. Therefore, when an author is a public servant so that there is Crown copyright in the manuscript, a simple permission to use is acceptable to the publisher, if it is granted by a person with appropriate authority.

CESSION DU DROIT D'AUTEUR

Document n° _____

Au : CONSEIL NATIONAL DE RECHERCHES DU CANADA («CNRC») - Presses scientifiques
De : _____
_____
_____
_____
(nom et adresse de l'auteur qui signe le présent formulaire)

La présente cession porte sur le document intitulé : _____
_____

rédigé par moi, en collaboration avec l'auteur/les auteurs suivant(s) : _____
_____

aux fins de publication dans : _____

1. Je déclare que la liste des auteurs ci-dessus respecte les pratiques usuelles de rédaction savante quant aux personnes dont le nom doit être cité. Je déclare que le document ou son équivalent n'a pas été soumis à quelque autre organisme aux fins de publication. Si le CNRC accepte de publier le document, je m'assurerai que celui-ci ou son équivalent n'est soumis à aucun autre organisme aux fins de publication sans en obtenir la permission préalable du CNRC.

2. Je déclare être (UN SEUL choix) :

☐	(a) le seul titulaire de droit d'auteur afférent au document,	et →	je **cède** le droit d'auteur intégral au CNRC.
☐	(b) un titulaire partite du droit d'auteur, de concert avec des coauteurs ou leurs employeurs,	et →	je **cède** ma part du droit d'auteur au CNRC et m'attends à ce que les coauteurs signent une entente comparable.
☐	(c) un agent de mon employeur ayant l'autorité de céder le droit d'auteur appartenant à l'employeur, nommément : _____,	et →	je **cède** au CNRC, au nom de mon employeur, la part entière du droit d'auteur afférent au document appartenant à mon employeur, et m'attends à ce que les coauteurs signent une entente comparable.
☐	(d) un fonctionnaire du Canada (fédéral, provincial ou territorial) ou du Royaume-Uni, donc le droit d'auteur appartient à Sa Majesté,	et →	j'ai obtenu de mon employeur, en vertu de mes conditions d'emploi, l'autorisation d'accorder au CNRC la **permission non exclusive** de publier le document et de gérer le droit d'auteur.
☐	(e) un fonctionnaire des États-Unis d'Amérique, donc sujet à la loi qui n'associe aucun droit d'auteur américain au document,	et →	je **cède** au CNRC, au nom de mon employeur, la part entière de quelque droit d'auteur en vigueur ailleurs qu'aux É.-U. appartenant à mon employeur, et m'attends à ce que les coauteurs signent une entente comparable.

3. Je comprends que la soumission du document ne garantit aucunement sa publication et que la publication ne pourra être réalisée tant que **tous les auteurs** n'auront pas signé une cession du droit d'auteur. Si le document n'est pas publié dans les deux années suivant ma signature des présentes, la cession sera automatiquement révoquée.

Signé à _____, le _____
(ville et province/état) (date)

_____
(signature)

[Formulaire normalisé du CNRC; aucune modification permise.]

Commentaires sur la cession du droit d'auteur
(accompagnés d'extraits de la *Loi sur le droit d'auteur*, Lois révisées du Canada 1985, chapitre C-42 modifié)

L'éditeur ne peut publier un document sans la permission ou une cession du droit d'auteur. Pour des raisons de souplesse et en vue de l'utilisation future du document publié, l'éditeur doit devenir titulaire du droit d'auteur.

Le titulaire peut céder le droit, mais cette cession doit être faite par écrit :

13.(4) Le titulaire du droit d'auteur sur une oeuvre peut céder ce droit, en totalité ou en partie, d'une façon générale, ou avec des restrictions territoriales, pour la durée complète ou partielle de la protection; il peut également concéder, par une licence, un intérêt quelconque dans ce droit; mais la cession ou la concession n'est valable que si elle est rédigée par écrit et signée par le titulaire du droit qui en fait l'objet, ou par son agent dûment autorisé.

Le titulaire peut être l'auteur, mais dans plusieurs cas, le titulaire est l'employeur de l'auteur:

13.(3) Lorsque l'auteur est employé par une autre personne en vertu d'un contrat de louage de service ou d'apprentissage, et que l'oeuvre est exécutée dans l'exercice de cet emploi, l'employeur est, à moins de stipulation contraire, le premier titulaire du droit d'auteur; mais lorsque l'oeuvre est un article ou un autre contribution, à un journal, à une revue ou à un périodique du même genre, l'auteur, en l'absence de convention contraire, est réputé posséder le droit d'interdire la publication de cette oeuvre ailleurs que dans un journal, une revue ou un périodique semblable.

La seule exception dans la cession du droit d'auteur est lorsque le document est associé au droit d'auteur de la Couronne, qui appartient au gouvernement du Canada .

12. Sous réserve de tous les droits ou privilèges de la Couronne, le droit d'auteur sur les oeuvres préparées ou publiées par l'entremise, sous la direction ou la surveillance de Sa Majesté ou d'un ministère du gouvernement, appartient, sauf stipulation conclue avec l'auteur, à Sa Majesté et, dans ce cas, il subsiste jusqu'à la fin de la cinquantième année suivant celle de la première publication de l'oeuvre.

Les gouvernements, en particulier le gouvernement fédéral, ne disposent pas d'un mécanisme simple de cession de droit d'auteur pour ce genre de biens de la Couronne. C'est pourquoi lorsqu'un auteur est un fonctionnaire et que, par conséquent, le droit d'auteur appartient à la Couronne, une simple permission d'usage est suffisante pour l'éditeur, pour autant que celle-ci ait été octroyée par une personne jouissant de l'autorité nécessaire pour ce faire.

WWW.CFBS.ORG

43RD ANNUAL MEETING / 43e CONGRÈS ANNUEL
CANADIAN FEDERATION OF BIOLOGICAL SOCIETIES
FÉDÉRATION CANADIENNE DESSOCIÉTÉS DE BIOLOGIE

OTTAWA CONGRESS CENTRE
OTTAWA, ONTARIO
JUNE 22 - 25, 2000

THEME I – APOPTOSIS AND SIGNAL TRANSDUCTION

PLENARY LECTURER
Dr. Gerard Evan, University of California, San Francisco, USA
Oncogene Induced Apoptosis in Cancer: If, How, When and Where?

SYMPOSIA:
Regulation of Apoptosis
Signaling in Apoptosis
Apoptosis and Neurodegenerative Diseases
Apoptosis and Cancer

THEME II – NUTRACEUTICALS AND FUNCTIONAL FOODS

PLENARY LECTURER
Dr. John Milner, Pennsylvania State University, PA
A Food-Based Approach to Disease Risk Reduction: Benefits, Risks and Biomarkers

SYMPOSIA:
The History of Vegetable Oils and their Human Health Effects
Functional Foods and the Evaluation of Health Outcomes
Interfaces Between Science and the Public: Education, Communication and Policies on Functional Foods and Nutraceuticals

GORDIN KAPLAN AWARD
Dr. Michael Smith
University of British Columbia, Vancouver, BC

OTHER
Skeletal Muscle Workshop
Society Award Lectures
Poster Presentations

MINI-SYMPOSIA
To be determined from abstract submissions

CFBS OPEN SCIENCE POLICY FORUM

Abstract's Deadline:
March 15, 2000

For Further Information:
Pour Plus D'information:

Canadian Federation of Biological Societies
215 - 1750 Courtwood Cres., Ottawa, Ontario K2C 2B5
Tel.: (613) 225-8889 Fax.: (613) 225-9621
E-Mail: wantonious@cfbs.org
www.cfbs.org

Danny K. Tanner, John C. Brazner, and Valerie J. Brady	**1243–1251**	Factors influencing carbon, nitrogen, and phosphorus content of fish from a Lake Superior coastal wetland
Yolanda Morbey	**1252–1257**	Protandry in Pacific salmon
Linda M. Campbell, David W. Schindler, Derek C.G. Muir, David B. Donald, and Karen A. Kidd	**1258–1269**	Organochlorine transfer in the food web of subalpine Bow Lake, Banff National Park
Michael F. Sigler	**1270–1283**	Abundance estimation and capture of sablefish (*Anoplopoma fimbria*) by longline gear
Mahaut Ricciardi-Rigault, David F. Bird, and Yves T. Prairie	**1284–1290**	Changes in sediment viral and bacterial abundances with hypolimnetic oxygen depletion in a shallow eutrophic Lac Brome (Quebec, Canada)
Laurent Vigliola, Mireille Harmelin-Vivien, and Mark G. Meekan	**1291–1299**	Comparison of techniques of back-calculation of growth and settlement marks from the otoliths of three species of *Diplodus* from the Mediterranean Sea
Kentaro Morita, Shoichiro Yamamoto, and Noboru Hoshino	**1300–1306**	Extreme life history change of white-spotted char (*Salvelinus leucomaenis*) after damming
Daniel S. Holland	**1307–1319**	A bioeconomic model of marine sanctuaries on Georges Bank

National Research Council Canada
Ottawa, Canada K1A 0R6

Conseil national de recherches Canada
Ottawa, Canada K1A 0R6

Postage paid at Ottawa
Publications mail
Registration No. 1240579

Port payé à Ottawa
Poste-publication
Enregistrement n° 1240579

Canadian Journal of Fisheries and Aquatic Sciences

Volume 57, Number 6, June 2000

Journal canadien des sciences halieutiques et aquatiques

Volume 57, numéro 6, juin 2000

James C. Smoot and Robert H. Findlay **1113–1119** Digestive enzyme and gut surfactant activity of detritivorous gizzard shad (*Dorosoma cepedianum*)

Michel Lapointe, Brett Eaton, Steve Driscoll, and Christian Latulippe **1120–1130** Modelling the probability of salmonid egg pocket scour due to floods

Gregory W. Whitledge and Robert S. Hayward **1131–1138** Determining sampling date interval for precise in situ estimates of cumulative food consumption by fishes

Juan C. Colombo, Claudio Bilos, Mauricio Remes Lenicov, Dario Colautti, Patricia Landoni, and Charles Brochu **1139–1150** Detritivorous fish contamination in the Río de la Plata estuary: a critical accumulation pathway in the cycle of anthropogenic compounds

Morag M. Campbell, Keith N. White, Ravin Jugdaohsingh, Jonathan J. Powell, and Catherine R. McCrohan **1151–1159** Effect of aluminum and silicic acid on the behaviour of the freshwater snail *Lymnaea stagnalis*

Olof Berglund, Per Larsson, Göran Ewald, and Lennart Okla **1160–1168** Bioaccumulation and differential partitioning of polychlorinated biphenyls in freshwater, planktonic food webs

Franz J. Mueter and Brenda L. Norcross **1169–1180** Changes in species composition of the demersal fish community in nearshore waters of Kodiak Island, Alaska

Kevin D. Friedland and David G. Reddin **1181–1189** Growth patterns of Labrador Sea Atlantic salmon postsmolts and the temporal scale of recruitment synchrony for North American salmon stocks

B.L. Kerans, Peter L. Chesson, and Roy A. Stein **1190–1199** Assessing density-dependent establishment and dispersal: an example using caddisfly larvae

Paul D. Winger, Pingguo He, and Stephen J. Walsh **1200–1207** Factors affecting the swimming endurance and catchability of Atlantic cod (*Gadus morhua*)

Marten Scheffer, Sergio Rinaldi, and Yuri A. Kuznetsov **1208–1219** Effects of fish on plankton dynamics: a theoretical analysis

Andrew J. Paul, John R. Post, George L. Sterling, and Carl Hunt **1220–1231** Density-dependent intercohort interactions and recruitment dynamics: models and a bull trout (*Salvelinus confluentus*) time series

Simon R. Thorrold and Stephen Shuttleworth **1232–1242** In situ analysis of trace elements and isotope ratios in fish otoliths using laser ablation sector field inductively coupled plasma mass spectrometry

Continued on inside back cover / Suite au verso

Canada

Printed in Canada by / Imprimé au Canada par
INTRA MÉDIA INC./datamark systems
Typesetting by / Typographie par
NRC Research Press / Presses scientifiques du CNRC

0706-652X(200006)57:6;1-C